MEASUREMENT OF ORDINARY HETEROTROPH ORGANISM ANOXIC YIELD IN ANOXIC-AEROBIC ACTIVATED SLUDGE SYSTEMS

by

Ashley Muller
B.Eng. (Bio/Chem.) Thayer School of Engineering
BA (Eng. Sci.) Dartmouth College

Thesis submitted in partial fulfillment of the requirements
for the degree of Master of Science in Engineering at the
University of Cape Town

Department of Civil Engineering
University of Cape Town

April 2003

DECLARATION BY CANDIDATE

I, ASHLEY WALTER MULLER, hereby declare that this thesis is my own work and it has not been submitted for a degree at another University.

signature removed

April 2003

SYNOPSIS

1. BACKGROUND

Integral to the biological nutrient removal (BNR) activated sludge system is the biologically mediated process of denitrification. Not only does this process reduce the N load to the environment, but it also has the advantages of alkalinity recovery and reducing the oxygen demand. Further, the denitrification protects the biological excess P removal (BEPR), if included, from the deleterious effect of recycling nitrate to the anaerobic reactor (Wentzel *et al.*, 1990). Accordingly, quantifying the potential denitrification is fundamental to the design and operation of the BNR activated sludge system. Biological denitrification has been explicitly incorporated into the steady-state design (e.g., WRC, 1984; Wentzel *et al.*, 1990; Maurer and Gujer, 1994) and kinetic simulation (Van Haandel *et al.*, 1981; Henze *et al.*, 1987, 1995; Dold *et al.*, 1980, 1991; Wentzel *et al.*, 1992; Barker and Dold, 1997; Murnleitner *et al.*, 1997; Gujer *et al.*, 1999) models developed as aids to the design and operation of BNR activated sludge systems. In both sets of models, critical as input to quantify the denitrification is the value for the ordinary heterotrophic organism (OHO) anoxic cell yield coefficient ($Y_{H,NO}$).

In terms of the models, the heterotrophic cell yield coefficient, Y_H, is the fraction of substrate electrons that are used to synthesize new cell mass, while the remainder, $1 - Y_H$, are passed to the terminal electron acceptor to generate energy. Hence, the value of Y_H, designated here $Y_{H,NO}$ for anoxic conditions and $Y_{H,AE}$ for aerobic, determines both the mass of electron acceptor utilized and the new cell biomass produced. In activated sludge systems treating municipal wastewaters, the effect of $Y_{H,NO}$ on sludge production typically is small, since the mass of sludge produced under anoxic conditions is small compared to that produced under aerobic conditions, due to the relatively low influent TKN/COD ratios (Barker and Dold, 1997). In contrast, the effect of $Y_{H,NO}$ on the amount of denitrification achievable (and hence, on system design and operation) is quite significant.

In the IWA Task Group models for activated sludge systems, ASM1 (Henze *et al.*, 1987), ASM2 (Henze *et al.*, 1995) and ASM2d (Henze et al., 1999), and similar (e.g. Dold *et al.*, 1991; Wentzel *et al.*, 1992), the heterotrophic yield coefficient is assumed to have the same value under anoxic as under aerobic conditions. However, when nitrate serves as terminal electron acceptor, ideally only 2 ATP are formed per pair of electrons (e^-) transferred to nitrate as compared to 3 ATP when the transfer is to oxygen (Payne 1981, WRC 1984, Kuba *et al.* 1993, Casey *et al.* 1999, Wentzel *et al.* 2001). This difference reduces the energy captured by the organism when nitrate serves as electron acceptor (versus oxygen) in biological oxidation of organic substrate. Correspondingly, therefore, the cell yield under anoxic conditions ($Y_{H,NO}$) should be reduced relative to its aerobic value ($Y_{H,AE}$).

Based on thermodynamic and bioenergetic principles, it is shown (*Appendix A*) that the theoretical anoxic cell yield coefficient ($Y_{H,NO}$) is about 83% of its aerobic value ($Y_{H,AE}$), or 0.35 mgVSS/mgCOD (0.5 mgCOD/mgCOD) compared to the aerobic yield of 0.42 mgVSS/mgCOD (0.6 mgCOD/mgCOD). Similarly, Orhon *et al.* (1996) theoretically quantified the anoxic to aerobic yield ratio for four organic substrates based on bioenergetic principles set out by McCarty (1971, 1972, 1975). For municipal wastewater, protein, lactate and carbohydrate substrates, they obtained the following anoxic:aerobic yield ratios,

respectively: 0.79, 0.80, 0.80, and 0.85. Accepting the standard aerobic heterotrophic yield value of 0.67 mgCOD/mgCOD used in ASM1 and similar models, this gives an anoxic yield of 0.53 mgCOD/mgCOD for municipal-type wastewaters as substrate.

Although limited, several studies reported in the literature provide direct and indirect experimental evidence supporting the theoretical assessment that the anoxic cell yield should be reduced relative to its aerobic counterpart (see Chapter 2). For these studies an average anoxic:aerobic cell yield ratio was calculated as 0.81 ± 0.035, or about 0.54 mgCOD/mgCOD (range 0.52 – 0.57) with respect to the standard aerobic yield of 0.67 mgCOD/mgCOD. This substantiates the theoretical evaluations above that the anoxic yield should be reduced relative to its aerobic value.

2. RESEARCH OBJECTIVES

While a reduced heterotrophic yield under anoxic conditions is apparent from bioenergetic theory and supported by experimental measurements recorded in the literature, no direct experimental measurement with real municipal sewage could be found. Most of the studies identified above were performed with defined substrates, hydrolysates, and/or mixtures of various domestic and industrial wastewaters, and focussed mainly on estimating specific denitrification rates. Consequently, few provide information directly relating nitrate and corresponding substrate utilizations necessary to estimate the yield. Furthermore, some studies were performed with mixed polyphosphate accumulating organism (PAO) sludges from nitrification-denitrification biological excess phosphorous removal (NDBEPR) activated sludge systems, which introduces unquantifiable uncertainty into observed yield measurements. ***Thus, lacking in the current body of research on $Y_{H,NO}$, are any studies and experiments to directly quantify or measure $Y_{H,NO}$ using sewage as substrate.***

The principal aim in this research is to investigate and quantify the ordinary heterotrophic organism (OHO) cell yield under anoxic conditions relative to its value under aerobic conditions for municipal sewage.

In this regard, three primary objectives were identified:

1. Determine the ratio $Y_{H,NO}$:$Y_{H,AE}$ for real sewage in terms of electron acceptor (i.e. nitrate and oxygen respectively) utilization.

2. Measure $Y_{H,NO}$ and $Y_{H,AE}$ directly for known concentrations of readily biodegradable (RB)COD utilized.

3. Compare experimental results with other, independent studies on real sewage.

3. RESEARCH APPROACH

In the research approach adopted to achieve these objectives, it was recognised that the equations quantifying the concentration of soluble substrate utilized in aerobic and anoxic respiration (Chapter 1), in terms of the cell yield and electron acceptor utilization, could be equated if the respective soluble substrate concentrations utilized are the same. Thus, if the oxygen and nitrate utilized (OU and NU respectively) in consumption of the same readily

biodegradable (RB)COD under respective aerobic and anoxic conditions can be quantified, then $Y_{H,NO}$ can be determined as a function of $Y_{H,AE}$. On this basis, "parallel" anoxic and aerobic batch tests containing the same concentration of RBCOD and acclimatised mixed-liquor from the same source were performed. In the corresponding aerobic and anoxic batch tests the OU and NU (respectively) were measured, and used to determine estimates for $Y_{H,NO}$ as a function of $Y_{H,AE}$ (Objective 1). In this approach, since OU and NU are related to *complete* utilization of RBCOD rather than its *rate* of utilization (Ekama *et al.*, 1986), exact definition of the OHO biomass is not essential. What is required is that the initial RBCOD concentration in the two corresponding batch tests is the same and that all the RBCOD is utilized. This is evident from established discussions on loading rate effects in aerobic batch tests (e.g. Ekama *et al.*, 1986; Dold *et al.*, 1991; Mbewe *et al.*, 1995).

In addition, anoxic and aerobic batch tests were also performed containing known concentrations of the artificial RBCOD, acetate, so that $Y_{H,NO}$ and $Y_{H,AE}$ could be determined directly and independently from the respective NU and OU responses (Objective 2).

Further, as an assessment of the estimates determined above, experimental data from independent investigations in the literature were re-interpreted to derive values for the $Y_{H,NO}$:$Y_{H,AE}$ ratio, or for the individual coefficients, and compared with the values obtained in this investigation (Objective 3).

The difficulties and complications in measuring OHO denitrification and associated yields arising from the presence of PAOs, was recognised in this study. Accordingly, to eliminate these, in all the experiments sludges from N removal only (i.e. no BEPR) plants were used. The mixed-liquor for the batch tests initially was obtained from two laboratory scale MLE activated sludge systems operated in a parallel investigation. However, these systems could not provide the quantities of mixed-liquor required. Accordingly, the mixed-liquor source for the batch tests was switched to the Mitchells Plain Wastewater Treatment Plant (MPWWTP). However, the concentration and OHO active biomass fraction of this mixed-liquor varied so that determination of the correct loading rate in the batch tests (to obtain quantifiable OU and NU) was difficult. Thus, a laboratory-scale MLE activated sludge system was set-up and operated, dedicated to providing mixed-liquor for the batch tests.

Since RBCOD is eliminated as a variable by equating aerobic and anoxic respirometry, the concentration of RBCOD is not required to estimate $Y_{H,NO}$, provided $Y_{H,AE}$ is known. However, this requires that the standard $Y_{H,AE}$ (0.67 mgCOD/mgCOD) be accepted in this study. As an independent assessment of this value (and $Y_{H,NO}$ estimates as well), RBCOD recovery in the batch tests (Ekama *et al.*, 1986; Mbewe *et al.*, 1995) was performed, by: (i) independent measurement of the RBCOD concentration in the wastewater added to the batch tests, and (ii) adding known concentrations of the artificial RBCOD, acetate, to the batch tests.

For (i) above, initially the wastewater RBCOD fraction was estimated by the simple direct flocculation-filtration method (Mbewe *et al.*, 1995), using the f_{us} (fraction unbiodegradable soluble COD) obtained in a long sludge University of Cape Town (UCT) activated sludge system operated concurrently on the same sewage. This RBCOD was then compared with the RBCOD concentration calculated with the method of Ekama *et al.* (1986) from the corresponding aerobic batch test OUR profiles accepting the standard $Y_{H,AE}$ of 0.67 mgCOD/mgCOD. If close correspondence was obtained, this would indicate that the value

for $Y_{H,AE}$ is reasonable, and hence $Y_{H,NO}$ also. However, during the course of the investigation floc-filtered RBCOD estimates gave poor recoveries compared with RBCOD values obtained from the batch tests. Accordingly, it was subsequently decided to operate a dedicated square-wave (SQW) fed activated sludge system (Ekama *et al.*, 1986) to estimate the wastewater RBCOD by the original method of Ekama *et al.* (1978). On this basis, independent measurement of the RBCOD in the wastewater was achieved for evaluation of batch test determined $Y_{H,AE}$ and $Y_{H,NO}$ estimates.

For the artificial RBCOD (acetate) experiments, (ii) above, known volumes of a concentrated sodium acetate standard solution were added to aerobic and anoxic batch tests, and $Y_{H,AE}$ and $Y_{H,NO}$ determined directly from the measured OU and NU responses, respectively.

4. CONTINUOUS FLOW-THROUGH EXPERIMENTAL SYSTEMS

The steady-state laboratory-scale activated sludge systems operated in this investigation were:

- Long sludge age University of Cape Town (UCT) BNR activated sludge (AS) system – this system was operated simply to provide an estimate of f_{us} from the filtered effluent COD, required for the flocculation-filtration method to determine RBCOD; consequently details of operation are not reported.

- Long sludge age Modified Ludzack-Ettinger (MLE) AS system – used to provide the source of sludge for the batch tests and estimates of the unbiodegradable soluble COD fraction (f_{us}) with respect to total COD in the wastewater.

- Short sludge age square-wave (SQW) fed AS system – used to quantify RBCOD respirometrically according to the original method of Ekama *et al.* (1978).

4.1 General Overview

The MLE laboratory-scale activated sludge system was operated simply to supply equivalent biomass for corresponding aerobic and anoxic batch tests utilizing the same RBCOD; similarly, the SQW system was operated mainly to characterize the RBCOD fraction in the wastewater. The sewage used to feed the systems was collected in batches from the MPWWTP approximately every 2 weeks (to prevent degradation under storage). This study included a total of 25 sewage batches over a period of 395 days, during which 40 aerobic and 42 denitrifying (anoxic) batch tests (ABT and DBT respectively) were performed.

4.2 Steady-State Periods

Each sewage batch (SB) was accepted as a steady-state period. For each sewage batch (SB), data outside the range mean ± 1.96*sample standard deviation (95% confidence interval), were rejected. All remaining data were considered valid and averaged to represent the "average" response of the system for that sewage batch (steady-state) period.

Average ratios (fractions) of process characteristics (e.g. f_{us}), were calculated from the ratio of the steady-state averages.

4.3 MLE System Performance

The MLE system (Chapter 3) consisted of an anoxic reactor (25% of total system volume), an aerobic reactor (75% of total system volume) and a secondary settling tank (SST), all in series with an underflow recycle (s-recycle) from the SST to the anoxic reactor of 1:1 and from the aerobic to the anoxic reactor (a-recycle) of 1:1, all recycle ratios with respect to influent flow (Q_i).

Unbiodegradable Soluble COD Fraction (f_{us})

The unbiodegradable soluble COD fraction of the influent wastewater (f_{us}) for each sewage batch period was calculated from corresponding influent and filtered effluent COD averages (Ekama *et al.*, 1986). Excluding outliers, the average f_{us} data are normally distributed with a mean f_{us} of 0.096 ± 0.005 for the Mitchells Plain raw wastewater. This average falls within the range of typical values expected of South African domestic sewage (0.04 – 0.10, WRC, 1984), and compares favourably with values observed by other researchers who also used Mitchells Plain raw wastewater: Cronje (2000), f_{us} = 0.085, Ubisi *et al.* (1997a,b), f_{us} = 0.09, and Mbewe *et al.* (1995), f_{us} = 0.074.

Floc-Filtered RBCOD Fraction ($f_{ts,FF}$)

The influent wastewater RBCOD concentrations estimated by the floc-filtration (FF) method of Mbewe *et al.* (1995), were averaged for each sewage batch and the fraction of total COD determined ($f_{ts,FF}$). The average $f_{ts,FF}$ were evaluated for outliers and analysed statistically. Although no outliers were identified, the sewage batch average $f_{ts,FF}$ values did not exhibit a good fit to the true normal distribution. For an improved assessment of the wastewater $f_{ts,FF}$, daily estimates were analysed in a linearized probability graph. The daily data displays a good fit to the true normal distribution, and rejecting two outliers gives a mean $f_{ts,FF}$ = 0.15 ± 0.022 (range 0.098 – 0.196). This compares reasonably well with the average $f_{ts,FF}$ = 0.18 ± 0.02 (range 0.14 – 0.23) determined by Mbewe *et al.* (1995) for the same wastewater.

4.4 SQW System Performance

To quantify the sewage RBCOD concentration, following the method of Ekama *et al.* (1986), a single reactor square-wave (SQW) fed activated sludge system was operated at a short sludge age (Chapter 3). The SQW system comprised a single reactor and SST, with a total system volume (V_p) of 6.7ℓ. A short sludge age of 3 days was maintained. The SQW system was operated in a 12h-ON/12h-OFF feed pattern, with an effective influent flowrate (Q_i) of 18ℓ/0.5d = 36 ℓ/d. The system was operated with a 1:1 recycle ratio with respect to the influent flow, which was also terminated when feed pumping stopped at the end of the 12h feed period.

Unbiodegradable Soluble COD Fraction (f_{us})

For each sewage batch period, the average f_{us} was calculated from corresponding influent and 0.45 μm membrane filtered effluent COD averages (Marais and Ekama, 1976; Ekama *et al.*, 1986). The average sewage batch f_{us} were evaluated for outliers and analysed statistically in a linearized probability graph. No outliers were identified and the linear fit to the data is quite good, indicating that the data are normally distributed. The mean f_{us} is

0.111 ± 0.006. This average lies above the upper limit of the typical range of 0.04 – 0.10 expected of South African domestic sewage (WRC, 1984), and is slightly higher than the f_{us} of 0.096 obtained in the parallel MLE system in this study; this difference is statistically significant at the 95% confidence interval. That the f_{us} of the SQW system is higher than that of the MLE system more than likely is due to the short sludge age (~3 days). Thus, the f_{us} for the SQW system was not used in the flocculation-filtration (FF) method for RBCOD, but the MLE system f_{us} was.

Square-wave (SQW) Fed System RBCOD Fraction ($f_{ts,S}$)

Ekama *et al.* (1986) describe the original "standard" method (Ekama and Marais, 1978) of measuring wastewater RBCOD from the precipitous OUR drop (ΔOUR) occurring at feed termination in a short sludge age square-wave (SQW) fed activated sludge system, see Chapter 3. This method was followed here also to determine RBCOD, as a fraction of the total influent wastewater COD, $f_{ts,S}$. For each sewage batch, the average RBCOD fraction ($f_{ts,S}$) was calculated from the respective sewage batch average feed flowrate (Q_S), total COD and ΔOUR. The average $f_{ts,S}$ values were evaluated for outliers and analysed statistically in a linearized probability graph. The data are normally distributed and give an average $f_{ts,S} = 0.14 \pm 0.03$. Although this value compares well with the SQW average f_{ts} = 0.16 obtained by Ekama and Marais (1978), as well as with the floc-filtered average $f_{ts,FF}$ = 0.15 obtained in this study, it is lower than the average SQW f_{ts} = 0.19 and floc-filtered f_{ts} = 0.18 of Mbewe *et al.* (1995), all for wastewater from the same source.

4.5 Continuous Flow-Through Systems Performance Summary

In summary, this investigation used a total of 25 sewage batches of unsettled municipal wastewater from Mitchell's Plain, Cape Town, and covered a period of 395 days. While a UCT system was used initially to characterize wastewater f_{us} for floc-filtered RBCOD estimation, MLE and SQW continuous-flow systems were subsequently operated to provide a consistent source of OHO biomass for batch tests, and to characterize the wastewater RBCOD by the standard method, respectively. From the results obtained for these systems:

- MLE system performance was generally stable, producing an average unbiodegradable soluble COD fraction with respect to total COD (f_{us}) of 0.096, which falls within the typical range of 0.04 – 0.1 expected for South African domestic sewage (WRC, 1984). Furthermore, it is consistent with values observed by other researchers for wastewater from the same source: Cronje (2000), 0.085; Ubisi *et al.* (1997a,b), 0.09; Mbewe *et al.* (1995), 0.074.

- Floc-filtered estimates of the wastewater RBCOD fraction with respect to total COD ($f_{ts,FF}$) averaged 0.15, which compares favourably with the floc-filter average of 0.18 (range 0.14 – 0.23) obtained by Mbewe *et al.* (1995) for wastewater from the same source.

- The SQW system performance was generally stable, and produced an average f_{us} = 0.111. This f_{us} is higher than the 0.096 obtained in the parallel MLE system. This is not unexpected as the very short sludge age (3d) of the SQW system will influence the f_{us} determination. Accordingly, the SQW system f_{us} values were not used to determine the RBCOD in the flocculation-filtration method.

- The SQW system gave an average wastewater RBCOD fraction ($f_{ts,S}$) of 0.14, which compares well with the SQW average of 0.16 obtained by Ekama and Marais (1978), as well as with the floc-filtered average of 0.15 with f_{us} determined by the MLE system in this study. However, it is substantially lower than the 0.18 – 0.19 average obtained by Mbewe *et al.* (1995) on wastewater from the same source.

5. AEROBIC AND ANOXIC BATCH TESTS

5.1 Batch Test Procedure

The experimental methods and procedures for performing the aerobic and anoxic batch tests are detailed in Chapter 4. In brief, aerobic and anoxic batch tests were performed using domestic wastewater from the Mitchells Plain Wastewater Treatment Plant (MPWWTP), and biomass obtained from laboratory-scale Modified Ludzack-Ettinger (MLE) systems fed wastewater from this plant, as well as from the MPWWTP. In each batch test, defined volumes of wastewater and mixed-liquor were combined in a continuously stirred batch reactor. In the aerobic batch tests (ABT), the oxygen utilization rate (OUR) with time was measured automatically (Randall *et al.*, 1991), while in the denitrification (anoxic) batch tests (DBT), the nitrate utilization rate (NUR) was determined from the nitrate concentration versus time profile for samples drawn manually at specific time intervals during the test. The batch experiments performed were grouped into three chronological Periods:

Period	Dates	Sewage Batch	ABT	DBT
I	17/1/02 – 4/6/02	4 – 13	1 – 22	1 – 19
II	26/8/02 – 10/10/02	18 – 21	23 – 34	20 – 29
III	11/10/02 – 16/12/02	22 – 23	35 – 40	30 – 42

5.2 Batch Test Results: Period I

Estimation of $Y_{H,NO}$ in terms of $Y_{H,AE}$ Using Wastewater RBCOD

In Period I, sewage batches (SB) 4 – 13 were used and 22 aerobic and 19 anoxic batch tests were performed (see Chapter 5). Aerobic and anoxic (denitrification) batch tests (ABT and DBT respectively) in Period I were performed in parallel, with mixtures of the same volumes of wastewater (V_{WW}) and mixed-liquor (V_{ML}), abstracted from the same samples of wastewater and activated sludge, respectively.

For the parallel aerobic and anoxic batch tests, from the respective OU and NU, $Y_{H,NO}$ values as a function of $Y_{H,AE}$ were determined. All the $Y_{H,NO}$ estimates corresponding to $Y_{H,AE}$ = 0.67 mgCOD/mgCOD determined in Period I (16 estimates) were evaluated for outliers and analysed statistically in a linearized probability graph. No outliers were identified and the data exhibits a reasonable fit to the linear true normal line, indicating a normal distribution for the $Y_{H,NO}$ estimates corresponding to $Y_{H,AE}$ = 0.67 mgCOD/mgCOD. The mean $Y_{H,NO}$ for Period I is 0.534 ± 0.041 (range 0.493 – 0.575) mgCOD/mgCOD with respect to $Y_{H,AE}$ = 0.67 mgCOD/mgCOD, or equivalently an anoxic:aerobic yield ratio of 0.797. This compares well with the theoretical prediction of $Y_{H,NO}$:$Y_{H,AE}$ = 0.83, as well as with the average $Y_{H,NO}$ = 0.54, or yield ratio 0.81 ± 0.035, with respect to $Y_{H,AE}$ = 0.67 mgCOD/mgCOD, determined for the experimental investigations in the literature (see Chapter 2).

Evaluation of $Y_{H,AE}$ Using Independent RBCOD Estimation

In the analysis above to determine a value for $Y_{H,NO}$ from corresponding OU-NU combinations, the "standard" value for $Y_{H,AE}$ = 0.67 mgCOD/mgCOD had to be accepted. This standard $Y_{H,AE}$ was evaluated as follows: The wastewater RBCOD concentrations in the respective aerobic and anoxic batch tests (i.e. $RBCOD_{BT,AE}$ and $RBCOD_{BT,NO}$ respectively) were calculated from the respective batch test (BT) respirometries (Ekama *et al.*, 1986) using the standard $Y_{H,AE}$ = 0.67 and corresponding average $Y_{H,NO}$ = 0.534 mgCOD/mgCOD determined above, together with the respective OU and NU measurements; by dividing the $RBCOD_{BT}$ by the total wastewater COD concentration in the batch test ($S_{ti,BT}$), an estimate of the RBCOD fraction (f_{ts}) in the wastewater was obtained. These batch test respirometry estimates for f_{ts} were then compared with the steady-state averages determined independently for each sewage batch; good correspondence between the two estimates would indicate substantiation of the accepted yield value.

The aerobic and anoxic batch test respirometric f_{ts} estimates were analysed for outliers and plotted in linearized probability graphs. No outliers were identified for the aerobic batch test f_{ts} estimations ("$f_{ts,OU}$"), and the data exhibits a reasonable fit to the linear true normal line, giving a mean $f_{ts,OU}$ = 0.064 ± 0.008 (range 0.056 – 0.072). Similarly, for the f_{ts} estimations by anoxic batch test respirometry ("$f_{ts,NU}$"), no outliers were identified and the data also exhibits a reasonable fit to the linear true normal line, giving a mean $f_{ts,NU}$ = 0.065 ± 0.009 (range 0.056 – 0.074).

From these results, it is evident that the aerobic and anoxic batch test estimates for RBCOD are consistent (f_{ts} = 0.064 and 0.065 respectively). This is not unexpected since the value for $Y_{H,NO}$ used to calculate the anoxic batch test RBCOD is determined based on the assumption that equal concentrations of RBCOD are consumed in the respective aerobic and anoxic batch tests. However, the aerobic and anoxic batch test determined RBCOD concentrations are significantly lower than the corresponding values determined

independently with the flocculation-filtration (FF) method; 39.3 and 39.9% of the FF determined values respectively. One possible explanation for this anomaly is that in the batch tests, the RBCOD was not completely consumed when the precipitous drop in OUR was observed in the aerobic batch tests, or, correspondingly, when the denitrification rate dropped from the RBCOD+SBCOD utilization (i.e. K_1+K_2) to SBCOD only utilization (i.e. K_2 only) in the anoxic batch tests. To evaluate this possibility, several aerobic batch tests were subsequently performed in which the COD of floc-filtered samples taken from the batch test at specific time intervals, were compared with the OUR profile obtained in the test. This verified that all the biodegradable soluble COD present in the batch tests, was completely taken up at the time the precipitous drop in OUR occurred in the aerobic batch tests. Consequently, it was suspected that the low f_{ts} recoveries observed in the batch tests, were due to uncertainty in the flocculation-filtration method applied to measure RBCOD. Subsequently, dedicated Modified Ludzack-Ettinger (MLE) and square-wave (SQW) fed activated sludge systems were operated to, respectively, supply consistent biomass and estimate the wastewater RBCOD by the original method of Ekama *et al.* (1978) for the remainder of the investigation (Periods II and III).

5.3 Batch Test Results: Period II

Estimation of $Y_{H,NO}$ in terms of $Y_{H,AE}$ Using Wastewater RBCOD

In Period II, sewage batches (SB) 18 – 21 were used and 12 aerobic and 10 anoxic batch tests were performed. Corresponding aerobic and anoxic (denitrification) batch tests (ABT and DBT respectively) were performed with mixtures of the same volumes of wastewater (V_{WW}) and activated sludge mixed-liquor (V_{ML}).

As for Period I, from the respective OU and NU $Y_{H,NO}$ values as a function of $Y_{H,AE}$ were determined. All the $Y_{H,NO}$ estimates corresponding to $Y_{H,AE}$ = 0.67 mgCOD/mgCOD determined in Period II (11 estimates) were evaluated for outliers and analysed statistically in a linearized probability graph. Two outliers were identified and excluded from further analyses. The data exhibits a reasonable fit to the linear true normal line, with slight deviation noticeable for larger values. The mean $Y_{H,NO}$ = 0.563 ± 0.054 (range 0.51 – 0.62) mgCOD/mgCOD, or equivalently a yield ratio of 0.84, with respect to $Y_{H,AE}$ = 0.67 mgCOD/mgCOD, is consistent with the theoretical prediction of $Y_{H,NO}$:$Y_{H,AE}$ = 0.83, and the average $Y_{H,NO}$ = 0.54 mgCOD/mgCOD (yield ratio 0.81 ± 0.035) corresponding with $Y_{H,AE}$ = 0.67 mgCOD/mgCOD determined for experimental data in the literature.

Verification of $Y_{H,NO}$ Estimation by Independent RBCOD Measurement

In Period I, an inconsistency in the data was evident in that the RBCOD concentrations estimated from the batch test OU and NU determinations (accepting $Y_{H,AE}$ = 0.67 mgCOD/mgCOD and the experimentally determined corresponding $Y_{H,NO}$), were consistently significantly lower than the corresponding concentrations determined with the flocculation-filtration method. A possible cause identified for this inconsistency was the flocculation-filtration method. Accordingly, in Period II independent measurement of the wastewater RBCOD fraction (f_{ts}) was changed to that of using the OUR response of a short sludge age square-wave (SQW) fed continuous flow-through activated sludge system.

Following the procedures set out above for Period I, the RBCOD as a fraction of total COD (f_{ts}) values were determined from the aerobic and anoxic batch test respirometries ($f_{ts,BT}$). These f_{ts} estimates were evaluated for outliers and analysed statistically in linearized probability graphs.

No outliers were identified for the f_{ts} estimations determined by aerobic batch test respirometry, i.e. "$f_{ts,OU}$", although the data exhibits a poor fit to the linear true normal line. This indicates that the $f_{ts,OU}$ estimates are not normally distributed, and consequently the mean $f_{ts,OU}$ = 0.0612 should be rejected for further analysis. However, the results do indicate under-recovery of RBCOD compared with the SQW determined RBCOD concentration, at 45.0%.

For the f_{ts} estimations by anoxic batch test respirometry, i.e. "$f_{ts,NU}$", one outlier was identified and excluded. The data exhibits a reasonable fit to the linear true normal line, indicating a normal distribution for the $f_{ts,NU}$ estimates. The mean $f_{ts,NU} = 0.055 \pm 0.005$ is significantly lower than the steady-state average $f_{ts,S}$ = 0.136 determined for the Mitchells Plain raw wastewater by the SQW system, amounting to only a 40.4% RBCOD recovery. This recovery is consistent with the 39.9% obtained in Period I, leaving a substantial amount of RBCOD still unaccounted for in the respirometric responses of the respective batch tests.

As in Period I, floc-filtered COD measurements were taken at specific time intervals during several aerobic and anoxic batch tests, as a physical check as to whether all the biodegradable soluble COD present in the test, was depleted at approximately the same time as the precipitous drop in OUR, or, correspondingly, the change from the K_1+K_2 to K_2 only denitrification rates. The comparison between the timed floc-filtered COD measurements and the NUR profiles for the anoxic batch tests were not clear however, since only a few floc-filtered samples could be taken in addition to the number of samples necessary for nitrate and nitrite analyses for estimating the NUR profile of the test. Aerobic batch tests were not subject to the same constraint, and good correspondence was observed between the precipitous drop in OUR and plateauing of floc-filtered COD concentrations in the same batch test. Accordingly it could be accepted that all the biodegradable soluble COD was consumed at the time the precipitous drop in OUR occurred. However, although the method for independently measuring the RBCOD was changed from the flocculation-filtration one to the "standard" SQW short sludge age one, the RBCOD recoveries in the batch tests remained approximately 40%. No possible cause for the unaccounted RBCOD could be identified, and so it was decided to add a known mass of the artificial RBCOD, acetate, to aerobic batch tests, and to estimate $Y_{H,AE}$ directly from the observed OU response.

Direct Estimation of $Y_{H,AE}$ Using Known Mass of Acetate in Aerobic Batch Tests

In Period II, known masses of the artificial RBCOD, sodium acetate, were added to several aerobic batch tests. From the known acetate concentration and the observed OU in its consumption, values for $Y_{H,AE}$ could be determined. These values (20 estimates) were evaluated for outliers and analysed statistically in a linearized probability plot. One outlier was identified and excluded. The data exhibits a good fit to the linear true normal line, indicating a normal distribution for the $Y_{H,AE}$ estimates. The mean $Y_{H,AE}$ of 0.687 ± 0.027 (range 0.66 – 0.714) mgCOD/mgCOD for utilization of the artificial RBCOD, acetate, is very close to the conventionally accepted $Y_{H,AE}$ = 0.67 mgCOD/mgCOD for domestic wastewater, with only a 1.7% difference. Therefore, acceptance of the standard $Y_{H,AE}$ = 0.67 mgCOD/mgCOD in this investigation is substantiated.

However, despite the agreement between the acetate determined $Y_{H,AE}$ and the accepted standard value, the apparent low wastewater RBCOD recoveries observed in the aerobic

and anoxic batch tests presented earlier, remain unexplained. This was not of major concern, however, since exact determination of the RBCOD concentration in the corresponding aerobic and anoxic batch tests is not essential for estimating $Y_{H,NO}$, provided $Y_{H,AE}$ is known. As is evident from the above, the standard value for $Y_{H,AE}$ of 0.67 mgCOD/mgCOD can be accepted, and this value substantiated relatively simply under defined conditions by addition of acetate. Since quantifying wastewater RBCOD is not the focus of this research project, comparison of batch test respirometric RBCOD estimations with independent measurement of the wastewater RBCOD was discontinued. However, this aspect does warrant further investigation.

5.4 Batch Test Results: Period III

Estimation of $Y_{H,NO}$ in terms of $Y_{H,AE}$ Using Wastewater RBCOD

In Period III, sewage batches (SB) 22 and 23 were used and 6 aerobic and 14 anoxic batch tests were performed. Corresponding aerobic and anoxic (denitrification) batch tests (ABT and DBT respectively) were performed with the same volumes of wastewater (V_{WW}) and activated sludge mixed-liquor (V_{ML}). Additionally, anoxic batch tests were performed using only a known mass of the artificial RBCOD, acetate ("Ac"), for direct estimation of $Y_{H,NO}$ from the resultant NU response (see Chapter 5).

As for Periods I and II above, from the respective OU and NU $Y_{H,NO}$ values as a function of $Y_{H,AE}$ were determined. All the $Y_{H,NO}$ estimates corresponding to $Y_{H,AE}$ = 0.67 mgCOD/mgCOD determined in Period III (6 estimates) were evaluated for outliers and analysed statistically in a linearized probability graph. No outliers were identified, and the $Y_{H,NO}$ estimates for Period III exhibit a reasonable fit to the linear true normal line. The mean $Y_{H,NO}$ = 0.485 ± 0.088 (range 0.397 – 0.573) mgCOD/mgCOD, or equivalently a yield ratio of 0.724, with respect to $Y_{H,AE}$ = 0.67 mgCOD/mgCOD, is noticeably lower than the theoretical prediction of $Y_{H,NO}$:$Y_{H,AE}$ = 0.83. Further, both the average $Y_{H,NO}$ and yield ratio are lower than the average $Y_{H,NO}$ = 0.54 and yield ratio of 0.81 ± 0.035 respectively, corresponding to $Y_{H,AE}$ = 0.67 mgCOD/mgCOD, as determined for the experimental investigations in the literature.

Direct Estimation of $Y_{H,AE}$ Using Acetate RBCOD

As described above for Period II, in Period III several aerobic batch tests were performed with addition of known amounts of the artificial RBCOD, acetate, to estimate $Y_{H,AE}$ directly from the observed OU response and corresponding concentration of acetate (as mgCOD/ℓ) in the test. The estimated values for $Y_{H,AE}$ (9 estimates) were evaluated for outliers and analysed statistically in a linearized probability plot. No outliers were identified for the $Y_{H,AE}$ estimates, which exhibit a reasonable fit to the linear true normal line indicating a normal distribution for $Y_{H,AE}$ using acetate. The mean $Y_{H,AE}$ of 0.665 ± 0.044 (range 0.621 – 0.709) mgCOD/mgCOD for utilization of the artificial RBCOD, acetate, is in very good agreement with the conventionally accepted $Y_{H,AE}$ = 0.67 mgCOD/mgCOD for domestic wastewater, exhibiting only a 0.75% difference from the standard $Y_{H,AE}$; thus, the acceptance of the standard $Y_{H,AE}$ = 0.67 mgCOD/mgCOD in this study is further substantiated.

Estimation of $Y_{H,NO}$ Using Acetate RBCOD

Following the success achieved with aerobic acetate addition batch tests, several anoxic batch tests were performed with addition of known amounts of the artificial RBCOD, acetate, to estimate $Y_{H,NO}$ directly from the observed NU response.

The acetate was added at the start of the anoxic batch tests, which contained only mixed-liquor and no wastewater. Further, the procedures for the last 4 tests differed from the others in the following respects: (i) DBT 40 was performed using two successive acetate additions ("a" and "b") in the same test; and (ii) DBTs 40b to 42 were aerated for about 2 hours after completion of the respective anoxic acetate tests, and a known mass of acetate added and an aerobic acetate batch test performed in the same reactor.

The estimated values for $Y_{H,NO}$ (6 estimates) were evaluated for outliers and analysed statistically in a linearized probability plot. No outliers were identified for the anoxic acetate $Y_{H,NO}$ estimates, and the data exhibits a good fit to the linear true normal line, indicating normal distribution of the data. The mean $Y_{H,NO}$ is 0.598 ± 0.041 (range 0.557 – 0.639) mgCOD/mgCOD, or equivalently a yield ratio of 0.893, with respect to $Y_{H,AE}$ = 0.67 mgCOD/mgCOD. The yield ratio is somewhat higher than the theoretical prediction of $Y_{H,NO}$:$Y_{H,AE}$ = 0.83, and the directly determined $Y_{H,NO}$ also is higher than the literature experimental average $Y_{H,NO}$ = 0.54. Interestingly, the average $Y_{H,AE}$ = 0.735 ± 0.036 mgCOD/mgCOD estimated from the three anoxic-aerobic acetate batch tests in which acetate was added first anoxically and then aerobically in the same test (DBT 40b – 42), is also noticeably higher than both the aerobic acetate average of $Y_{H,AE}$ = 0.665 ± 0.044 obtained earlier (see above), and the accepted standard value of $Y_{H,AE}$ = 0.67 mgCOD/mgCOD. Hence, the average ratio of the two corresponding anoxic-aerobic yields obtained in the same acetate batch tests (DBT 40b – 42), of $Y_{H,NO}$:$Y_{H,AE}$ = 0.84 ± 0.021, is in good agreement with the theoretically predicted $Y_{H,NO}$:$Y_{H,AE}$ = 0.83 and the literature experimental average of 0.81.

6. YIELD ESTIMATIONS USING EXPERIMENTAL DATA OF OTHER INVESTIGATIONS

6.1 Yield Estimation Using Experimental Data of Wilson (1976)

Wilson (1976) investigated the adsorption phase in biological denitrification using raw domestic sewage from the Cape Flats Wastewater Treatment Plant (CFWWTP) fed to a continuous flow-through steady-state activated sludge system consisting of: (1) a primary anoxic (plug-flow) reactor connected in series to (2) an aeration reactor; no inter-reactor recycles were employed and the settled sludge from the secondary settling tank was returned ("r-recycle") to the primary anoxic reactor. Accepting the average f_{ts} = 0.086 determined by Ekama *et al.* (1984) for raw CFWWTP wastewater, and noting that the r-recycle ratio was 5:1 with respect to the influent flow (Q_i), the average RBCOD concentrations corresponding to the denitrification (NUR) profiles observed by Wilson (1976) were estimated from the operating data provided, and the data re-analysed to estimate values for $Y_{H,NO}$ (*Appendix E*).

The estimated values for $Y_{H,NO}$ (10 estimates) were evaluated for outliers and analysed statistically in a linearized probability graph. No outliers were identified and the $Y_{H,NO}$ estimates exhibit a reasonable fit to the linear true normal line, with only slight deviation at the upper extreme. The mean $Y_{H,NO}$ is 0.458 ± 0.168 (range 0.29 – 0.626), giving a yield ratio of 0.684 with respect to $Y_{H,AE}$ = 0.67 mgCOD/mgCOD. This yield ratio is substantially lower than the theoretical prediction of $Y_{H,NO}$:$Y_{H,AE}$ = 0.83, as is the $Y_{H,NO}$ with respect to the experimental average $Y_{H,NO}$ = 0.54 calculated for the data in the

literature. The data of Wilson, however, is subject to wide variation. This is likely due to the considerable uncertainty in estimation of the K_2 denitrification rate lines (Chapter 5).

6.2 Yield Estimation Using Experimental Data of Ketley *et al.* (1991)

As part of an experimental investigation into the effect of fully anoxic and anoxic-aerobic conditions on low F/M (later "AA") filaments in nitrogen removal systems, Ketley *et al.* (1991) performed corresponding aerobic and anoxic batch tests using sludge from two laboratory-scale fully anoxic continuous flow-through systems ("ANOX2" and "ANOX3" respectively), fed the same raw domestic sewage from the MPWWTP. On day 42 of the study, two parallel anoxic batch tests ("ANBT1" and "ANBT2" respectively) were performed using sludge from the respective systems; at the end of the anoxic tests, the mixed-liquor in the respective batch tests were aerated for two hours and two corresponding aerobic batch tests ("ABT2" and "ABT3" respectively) were performed in each. Since the mixed-liquor used in the respective tests came from parallel systems fed the same sewage and under the same conditions, and the same volume of the same sewage was added to the corresponding anoxic and aerobic batch tests, it is accepted that each batch test contained the same mass of RBCOD and sludge from the same source. On this basis, the corresponding ANBT-ABT data of Ketley *et al.* (1991) were reassessed to determine corresponding NU and OU values for the respective batch tests, and, thus, estimate $Y_{H,NO}$ in terms of $Y_{H,AE}$ (Chapter 5, *Appendix E*).

Using the corresponding OU and NU estimations, the data (4 estimates) gives an average $Y_{H,NO} = 0.603 \pm 0.05$ (range 0.553 – 0.653), or an equivalent yield ratio of 0.90%, with respect to $Y_{H,AE} = 0.67$ mgCOD/mgCOD. The yield ratio is noticeably higher than the theoretically predicted $Y_{H,NO}$:$Y_{H,AE} = 0.83$, and both $Y_{H,NO}$ and the yield ratio are higher than the literature determined experimental average $Y_{H,NO} = 0.54$ and yield ratio 0.81 ± 0.035, respectively, with respect to $Y_{H,AE} = 0.67$ mgCOD/mgCOD.

6.3 Yield Estimation Using Experimental Data of Ekama *et al.* (1996)

To investigate the effect of feeding conditions on filamentous bulking, Ekama *et al.* (1996) operated two single reactor activated sludge systems in parallel, one as an intermittently fed fill and draw (IFFD, also called sequencing batch reactor, SBR), and the other as continuously fed completely mixed (CFCM). In all other respects, the operating conditions for both systems were the same, including the influent feed of settled sewage from the MPWWTP. Alternating anoxic-aerobic conditions were imposed on both systems by alternating periods of aeration with non-aeration over a 4h cycle (3h aeration on and 1h aeration off). The feed to the CFCM system was continuous and with the aeration/non-aeration cycle, the sludge was exposed to the influent RBCOD under both anoxic and aerobic conditions. The IFFD system was batch fed once daily and, in order to expose the sludge to influent RBCOD under both aerobic and anoxic conditions, as in the CFCM system, the time of the daily feed was alternated with the aeration/non-aeration cycle imposed on the system: On one day, the system was fed at the start of the aerobic cycle and on the next day at the start of the anoxic cycle, i.e. 1h earlier.

During the 10 day (i.e. a single sewage batch) period between days 60 and 70 of the study, 5 aerobic and 3 anoxic *in situ* OUR and NUR (respectively) profile tests were performed on the IFFD system, during the two hour period immediately following feed addition; for the anoxic profile tests the anoxic period following feed addition was extended from 1 to 2

hours. It was accepted that the initial RBCOD concentration in the reactor immediately following addition of the batch feed was the same in both the anoxic and aerobic profile tests, since the same wastewater batch was used in all the tests at the same loading rate (see Ekama *et al.*, 1996). On this basis, the experimental data of Ekama *et al.* (1996) was reassessed to estimate $Y_{H,NO}$ in terms of $Y_{H,AE}$, from different combinations of the OU and NU determined from the respective aerobic and anoxic profile tests.

The $Y_{H,NO}$ estimates (15 estimates) corresponding to $Y_{H,AE}$ = 0.67 mgCOD/mgCOD were evaluated for outliers and plotted in a linearized probability graph. One outlier was identified and excluded from subsequent analyses. The $Y_{H,NO}$ estimates exhibit a reasonable fit to the linear true normal line, and gives a mean $Y_{H,NO} = 0.538 \pm 0.068$ (range 0.47 – 0.606) mgCOD/mgCOD, or an equivalent yield ratio of 0.803%, with respect to $Y_{H,AE}$ = 0.67 mgCOD/mgCOD. The yield ratio and $Y_{H,NO}$ estimate compare very well with (respectively) the theoretically predicted $Y_{H,NO}:Y_{H,AE}$ = 0.83, and the calculated literature experimental average $Y_{H,NO}$ = 0.54 (yield ratio 81 ± 3.5%), with respect to $Y_{H,AE}$ = 0.67 mgCOD/mgCOD.

7. YIELD VALUES: SUMMARY

7.1 Wastewater Yield Values

By weighting the respective averages with the corresponding number of samples (N), overall weighted averages of $Y_{H,NO}$ = 0.534 and 0.519 mgCOD/mgCOD were determined for $Y_{H,AE}$ = 0.67 mgCOD/mgCOD, for the batch test analyses using wastewater RBCOD in this investigation, and by re-evaluation of independent experimental data observed by other researchers, respectively.

The weighted average $Y_{H,NO}$ for wastewater determined in this investigation (0.534 mgCOD/mgCOD) is remarkably similar to the value (0.519 mgCOD/mgCOD) calculated from data presented by other investigators. Further, both values are in good agreement with the average $Y_{H,NO}$ = 0.54 mgCOD/mgCOD calculated from the data of a wide range of experimental investigations in the literature. The similarity between the $Y_{H,NO}$ from this investigation and that determined from the data of other investigations suggested that the two data sets could be pooled.

To analyse the pooled data statistically, the $Y_{H,NO}$ averages with respect to $Y_{H,AE}$ = 0.67 mgCOD/mgCOD, were evaluated for outliers and plotted in a linearized probability graph. No outliers were identified, and the $Y_{H,NO}$ estimates exhibit a reasonable fit to the linear true normal line, indicating normal distribution of the data. The mean $Y_{H,NO} = 0.531 \pm 0.048$ (range 0.483 – 0.579), or an equivalent yield ratio of 0.793, with respect to $Y_{H,AE}$ = 0.67 mgCOD/mgCOD, compares very favourably with the calculated literature experimental average of 0.54, or yield ratio of 0.81 ± 0.035, with respect to $Y_{H,AE}$ = 0.67 mgCOD/mgCOD (Chapter 2), and is in reasonable agreement with the theoretically predicted $Y_{H,NO}:Y_{H,AE}$ = 0.83.

Considering only the experimental data for Mitchells Plain wastewater, i.e. excluding the data of Wilson (1976), the $Y_{H,NO}$ estimates were evaluated for outliers and plotted in a linearized probability graph. No outliers were identified, and the $Y_{H,NO}$ estimates exhibit a reasonable fit to the linear true normal line, indicating normal distribution of the data. The

mean $Y_{H,NO}$ = 0.545 ± 0.039 (range 0.506 – 0.584), or an equivalent yield ratio of 0.813, with respect to $Y_{H,AE}$ = 0.67 mgCOD/mgCOD, is virtually identical to the literature experimental average of 0.54, or yield ratio 0.81 ± 0.035, with respect to $Y_{H,AE}$ = 0.67 mgCOD/mgCOD. It also compares very well with the theoretically predicted ratio of $Y_{H,NO}$:$Y_{H,AE}$ = 0.83.

Overall, therefore, this investigation indicates the average value for $Y_{H,NO}$, using Mitchells Plain wastewater, to be 0.545 ± 0.039 (range 0.506 – 0.584), or an equivalent yield ratio of 0.813, with respect to the conventionally accepted $Y_{H,AE}$ = 0.67 mgCOD/mgCOD. This is in very good agreement with both theoretical predictions and experimental determinations by other researchers in the field.

7.2 Acetate Yield Values

Average $Y_{H,AE}$ Estimations from Acetate Addition

For the aerobic batch tests with known concentrations of the artificial RBCOD, acetate, by weighting the respective $Y_{H,AE}$ averages determined in Periods II and III with the corresponding number of samples (N), an overall weighted average of $Y_{H,AE}$ = 0.680 mgCOD/mgCOD was determined. This weighted average is remarkably close to the conventionally accepted $Y_{H,AE}$ = 0.67 mgCOD/mgCOD, with only a 1.5% difference. The similarity between the Periods II and III acetate $Y_{H,AE}$ estimates suggested that the two data sets could be pooled. To analyse the pooled data statistically, the acetate $Y_{H,AE}$ estimates were evaluated for outliers and plotted in a linearized probability graph. Two outliers were identified and excluded from further analysis. The remaining data exhibit a good fit to the linear true normal line, indicating a normal distribution. The mean $Y_{H,AE}$ = 0.684 ± 0.028 (range 0.656 – 0.712) compares very well with the conventionally accepted ("standard") $Y_{H,AE}$ = 0.67 mgCOD/mgCOD, with only a 2% difference. This substantiates acceptance of the standard $Y_{H,AE}$ in this investigation.

Average $Y_{H,NO}$ Estimations from Acetate Addition

Since acetate $Y_{H,NO}$ values were only determined in a single period (Period III), all the $Y_{H,NO}$ acetate estimates were analysed together. The $Y_{H,NO}$ estimates are normally distributed and give a mean value of approximately 0.598 ± 0.041 (range 0.557 – 0.639) mgCOD/mgCOD, or equivalently a yield ratio of 0.893, with respect to $Y_{H,AE}$ = 0.67 mgCOD/mgCOD. The yield ratio is somewhat higher than the theoretical prediction of $Y_{H,NO}$:$Y_{H,AE}$ = 0.83, and the directly determined $Y_{H,NO}$ also is higher than the literature experimental average $Y_{H,NO}$ = 0.54. Interestingly, the average $Y_{H,AE}$ = 0.735 ± 0.036 mgCOD/mgCOD estimated from the three anoxic-aerobic acetate batch tests in which acetate was added first anoxically and then aerobically in the same test, is also noticeably higher than both the aerobic acetate average of $Y_{H,AE}$ = 0.684 ± 0.028 obtained above, and the accepted standard value of $Y_{H,AE}$ = 0.67 mgCOD/mgCOD. Hence, for the two corresponding anoxic-aerobic yields obtained in the same acetate batch tests, the average ratio of $Y_{H,NO}$:$Y_{H,AE}$ = 0.84 ± 0.021 is in good agreement with the theoretically predicted $Y_{H,NO}$:$Y_{H,AE}$ = 0.83 and the literature experimental average of 0.81.

8.0 BATCH TEST RESULTS SUMMARY

Overall, therefore, this investigation indicates the average value for $Y_{H,NO}$, using Mitchells Plain wastewater, to be 0.545 ± 0.039 (range 0.506 – 0.584), or an equivalent yield ratio of 0.813, with respect to the conventionally accepted $Y_{H,AE}$ = 0.67 mgCOD/mgCOD. This is in very good agreement with both theoretical predictions and experimental determinations by other researchers in the field.

Further, $Y_{H,AE}$ values estimated directly from known concentrations of acetate in aerobic batch tests average 0.684 ± 0.028 (range 0.656 – 0.712) mgCOD/mgCOD. This average compares very well with the conventionally accepted ("standard") $Y_{H,AE}$ = 0.67 mgCOD/mgCOD, with only a 2% difference. This substantiates acceptance of the standard $Y_{H,AE}$ in this investigation.

Acetate $Y_{H,NO}$ values average 0.598 ± 0.041 (range 0.557 – 0.639) mgCOD/mgCOD, or equivalently a yield ratio of 0.893, with respect to $Y_{H,AE}$ = 0.67 mgCOD/mgCOD. Both the $Y_{H,NO}$ and yield ratio are higher than expected values. Interestingly, an average $Y_{H,AE}$ = 0.735 ± 0.036 mgCOD/mgCOD was estimated in three anoxic-aerobic acetate batch tests, in which acetate was added first anoxically and then aerobically in the same test. Although this is also noticeably higher than expected, it gives an average ratio for the corresponding anoxic yields obtained in the same batch tests of $Y_{H,NO}$:$Y_{H,AE}$ = 0.84 ± 0.021, which is in good agreement with the theoretically predicted $Y_{H,NO}$:$Y_{H,AE}$ = 0.83 and the literature experimental average of 0.81.

9. REVISION OF THE STEADY-STATE DESIGN MODEL

The finding in this investigation, in agreement with theoretical considerations and other investigations, that the OHO anoxic yield is reduced relative to the aerobic value, necessitated that the steady-state theory for design of nitrification-denitrification activated sludge (NDAS) systems (WRC, 1984) be revised, since this theory is based on a single OHO yield value. Identified for revision were formulations for denitrification potential (D_{pp}), specific denitrification rate constant on SBCOD (K_{2T}) and OHO active biomass (X_a).

9.1 Denitrification Potential

The formulation for the system denitrification potential (D_{pp}) was modified, to take account of the reduced OHO anoxic yield (Chapter 6). This proved possible by introducing a parameter f_{anox}, which is the fraction of biodegradable substrate that is utilized anoxically by the OHOs.

9.2 K_{2T} Specific Denitrification Rate Constant

In the expression for the total denitrification potential of the process (D_{pp}, see Chapter 6), the OHO specific denitrification rate constant, K_{2T}, is defined as the slope of the experimentally observed nitrate concentration-time profile for SBCOD utilization, divided by the concentration of active OHO biomass (X_a) present (see WRC, 1984). From extensive experimental investigations, Marais and co-workers (Stern and Marais, 1974; van Haandel *et al.*, 1981; WRC, 1984) determined an average "constant" $K_{2T} = 0.1008*(1.08)^{T-20}$ mgN/ℓ/mgAVSS/d for the specific denitrification rate for SBCOD utilization. This value has been accepted in current activated sludge steady-state design theory, although it is based on a single OHO (i.e. X_a) yield value for both anoxic and aerobic growth. Accepting from the research presented here that the value for the heterotrophic yield (Y_H) under anoxic ($Y_{H,NO}$) conditions is reduced relative to its value under aerobic ($Y_{H,AE}$) conditions (see Chapter 5), the value for K_{2T} needed to be revised to take into account a separate and different anoxic yield.

Accepting the average $Y_{H,NO}$ = 81.3% with respect to the standard $Y_{H,AE}$ = 0.67 mgCOD/mgCOD determined in this investigation, and the experimental data of van Haandel *et al.* (1981) used to determine the original K_{2T}, the revised $K_{2T,NO}$ was estimated to be 0.111 mgN/mgAVSS/d (T = 20 °C). As expected, the revised $K_{2T,NO}$ = 0.111 is greater than the K_{2T} = 0.1008 mgN/mgAVSS/d determined by van Haandel *et al.* (1981) based on a single OHO yield value – the reduced anoxic yield causes a reduced OHO active biomass concentration which causes the $K_{2T,NO}$ to increase (see Chapter 6).

9.3 OHO Active Biomass

From the discussions above, it is evident that the OHO active biomass concentration (X_a) also will change when taking into account a different cell yield coefficient for anoxic ($Y_{H,NO}$) growth as compared with aerobic ($Y_{H,AE}$) growth. By defining f_{anox} as the fraction of total influent biodegradable substrate (S_{bi}) utilized anoxically, the existing (WRC, 1984) expression for OHO active mass (MX_a) was modified to take into account a separate and different anoxic yield (Chapter 6). The calculation procedure for the remaining activated sludge mixed liquor fractions, endogenous residue and inert material, as set out in the existing design theory (WRC, 1984), remain unmodified when a reduced OHO anoxic yield is introduced. However, since the OHO active biomass concentration and mass do change, the values for the endogenous residue concentration and mass will correspondingly change, since these two mixed liquor fractions are linked.

9.4 Impact of the Modified Steady-State Design Theory

The inclusion of a separate and different yield for anoxic OHO growth in the steady-state design theory, results in a significant change in the predicted performance of NDAS systems compared with the current steady-state predictions. To illustrate this effect, design parameters for a model system were evaluated with the current design theory (WRC, 1984) and compared with their corresponding values determined by the modified theory, accepting the reduced anoxic yield determined in this investigation and the revised $K_{2T,NO}$ rate above. The modified theory predicts overall (Chapter 6):

- a 37% increase in the denitrification with RBCOD as substrate ($D_{p,\alpha}$); this increase is expected since the denitrification with RBCOD is essentially stoichiometric;
- a negligible change in denitrification with SBCOD as substrate ($D_{p,K2T}$), which confirms correct revision of the $K_{2T,NO}$ value – the $D_{p,K2T}$ must remain constant as this is based on experimental observations;
- the two effects above combine to give a 10 – 15 % increase in system denitrification achievable (D_{pp});
- the increased denitrification potential above gives a 63% reduction (9.9 to 3.6 mgN/ℓ, T = 14 °C) in effluent nitrate concentration (N_{ne});
- a 5 – 6% reduction in the mass of volatile suspended solids (MX_V, mgVSS) formed.

The effect of a reduced OHO anoxic yield on the system VSS mass (MX_V) is relatively small, at 5 – 6%. Thus, the influence on system volume requirements will be similarly small (WRC, 1984). This indicates that the most significant effect of the reduced yield is on the predicted N removal performance of an MLE-type system. This will have a significant impact on the system design, in selection of anoxic mass fractions and a-recycle ratios.

10. CONCLUSIONS

In this research project, the ordinary heterotrophic organism (OHO) cell yield under anoxic conditions relative to its value under aerobic conditions for municipal sewage, was investigated. From this investigation, the following conclusions can be drawn:

- For Mitchells Plain raw wastewater, a weighted average $Y_{H,NO}$ of 0.534 ± 0.058 was determined with respect to the conventional standard $Y_{H,AE}$ of 0.67 mgCOD/mgCOD, which gives a corresponding $Y_{H,NO}$:$Y_{H,AE}$ ratio of 0.797. This value compares well with the theoretical ratio of $Y_{H,NO}$:$Y_{H,AE}$ = 0.83, as well as with the experimental average $Y_{H,NO}$:$Y_{H,AE}$ = 0.813 ± 0.035 calculated for the data in the literature (Chapter 2).

- Three previous investigations in the UCT laboratory with municipal wastewater were identified in which sufficient data were available to calculate $Y_{H,NO}$ values of 0.458 ± 0.168, 0.603 ± 0.05 and 0.538 ± 0.068 mgCOD/mgCOD, respectively. These data gave a weighted average $Y_{H,NO}$ = 0.519 ± 0.101 with respect to the standard $Y_{H,AE}$ = 0.67 mgCOD/mgCOD, giving a corresponding $Y_{H,NO}$:$Y_{H,AE}$ ratio of 0.775. Again these values compare reasonably favourably with both the theoretical and literature experimental values.

- Combining the estimations above for Mitchells Plain wastewater, a weighted average $Y_{H,NO}$ = 0.545 ± 0.039 with respect to $Y_{H,AE}$ = 0.67 mgCOD/mgCOD was obtained, which gives a corresponding $Y_{H,NO}$:$Y_{H,AE}$ ratio of 0.813. This latter value compares remarkably well with the theoretical ratio of 0.83 and the experimental average ratio of 0.813 calculated for the data in the literature.

- For the batch tests using the artificial RBCOD, acetate, averages of $Y_{H,NO}$ = 0.598 ± 0.041 and $Y_{H,AE}$ = 0.687 ± 0.027 mgCOD/mgCOD were determined, which correspond to a $Y_{H,NO}$:$Y_{H,AE}$ ratio of 0.87. The average $Y_{H,AE}$ = 0.687 is in good agreement with the conventionally accepted $Y_{H,AE}$ = 0.67 mgCOD/mgCOD, and substantiates its acceptance in this investigation also. However, the average $Y_{H,NO}$ of 0.598 is higher than the theoretically predicted 0.50 mgCOD/mgCOD (*Appendix A*), and the experimental average of 0.54 mgCOD/mgCOD calculated for the data in the literature (Chapter 2), as well as the $Y_{H,NO}$ = 0.545 determined for Mitchells Plain wastewater above. Correspondingly, the average ratio $Y_{H,NO}$:$Y_{H,AE}$ = 0.87 determined for acetate, is higher than that expected for domestic sewage. However, sequential anoxic then aerobic acetate additions in the same batch test gave $Y_{H,NO}$:$Y_{H,AE}$ = 0.84 ± 0.021; this is in close agreement with the values obtained above for municipal sewage, and with both the theoretical and literature experimental values.

- In the long sludge age laboratory-scale activated sludge systems operated in this investigation, it appeared that the fraction of unbiodegradable soluble COD (f_{us}) was inversely influenced by the influent feed COD concentration; a lower f_{us} was obtained for a higher influent feed COD concentration in the laboratory systems (see Chapter 3). Other researchers in the UCT laboratory have similarly observed this effect (Lee, 2002). A consequence of this is the uncertainty it introduces into RBCOD measurement using physical techniques, e.g. the flocculation-filtration methods of Mamais *et al.* (1993) and Mbewe *et al.* (1995), see below.

- Comparison of the wastewater RBCOD fraction (f_{ts}) estimated by batch test respirometry (Ekama *et al.*, 1986), using the standard $Y_{H,AE}$ and the experimentally determined average $Y_{H,NO}$, with the average steady-state value determined independently for each sewage batch, gave consistently low recoveries (≤40%). By comparing the COD concentrations of timed floc-filtered samples in aerobic batch tests with the OUR profile for the same test, it was demonstrated that all the biodegradable soluble COD present in the test was taken up at the same time the precipitous drop in OUR occurred. Since the steady-state f_{ts} averages were initially determined by flocculation-filtration using the f_{us} of a long sludge age UCT system, it was suspected that initial poor recoveries were due to the uncertainties in f_{us} determination, as discussed above. However, despite changing the RBCOD measurement method to the original (standard) square-wave fed continuous flow-through method described by Ekama *et al.* (1986), low recovery of RBCOD in the batch tests remained. It was suspected that this may be due to incorrect acceptance of the conventional standard value of $Y_{H,AE}$ = 0.67 mgCOD/mgCOD. However, aerobic batch tests conducted with known concentrations of acetate gave an average $Y_{H,AE}$ = 0.687 ± 0.027 mgCOD/mgCOD (see above), which is close to the standard value, so that continued acceptance of $Y_{H,AE}$ = 0.67 mgCOD/mgCOD was substantiated. Consequently, the low RBCOD recoveries observed in the batch tests remains unexplained. This was not significant to this investigation, however, since the

RBCOD concentrations in the corresponding aerobic and anoxic batch tests were not required for estimating $Y_{H,NO}$ in terms of known $Y_{H,AE}$, provided the concentrations are equal. It does, however, introduce inconsistency, and accordingly merits further investigation.

From the above, there is a remarkable consistency in the OHO yield data derived from a variety of sources. This provides substantive evidence that the OHO yield is reduced under anoxic conditions compared with aerobic conditions.

Accepting the average value determined for $Y_{H,NO}$ in this study, the steady-state design theory (WRC, 1984) was modified (see Chapter 6) to incorporate individual anoxic and aerobic yield coefficients in the equations for: (1) the OHO active biomass concentration (X_a), and (2) the total system denitrification potential (D_{pp}). The modified theory was applied to the experimental data of van Haandel *et al.* (1981), to revise the specific denitrification rate constant for slowly biodegradable (SB)COD (K_{2T}) to take into account the reduced $Y_{H,NO}$ with respect to $Y_{H,AE}$. By defining "f_{anox}" as the fraction of total biodegradable COD (S_{bi}) utilized anoxically, and recognising that the experimentally observed SBCOD denitrification profile must remain constant, the value of K_{2T} was changed from K_{2T} = 0.1008 mgN/mgAVSS/d based on a single OHO yield constant (van Haandel *et al.*, 1981) to $K_{2T,NO}$ = 0.111 mgN/mgAVSS/d for the reduced OHO anoxic yield, both values at T = 20 °C.

The effect of an anoxic yield reduced relative to its aerobic value was examined by comparing the performance of a nitrogen (N) removal activated sludge system, predicted with the current (WRC, 1984) and modified (Chapter 6) steady-state theories (Chapter 6). This comparison indicated:

- a 37% increase in the denitrification with RBCOD as substrate ($D_{p,\alpha}$); this increase is expected since the denitrification with RBCOD is essentially stoichiometric;
- a negligible change in denitrification with SBCOD as substrate ($D_{p,K2T}$), which confirms correct revision of the $K_{2T,NO}$ value – the $D_{p,K2T}$ must remain constant as this is based on experimental observations;
- the two effects above combine to give a 10 – 15 % increase in system denitrification achievable (D_{pp});
- the increased denitrification potential above gives a 63% reduction (9.9 to 3.6 mgN/ℓ, T = 14 °C) in effluent nitrate concentration (N_{ne}); and
- a 5 – 6% reduction in the mass of volatile suspended solids (MX_V, mgVSS) formed.

The concepts incorporated into the modified theory can be readily extended to biological nutrient removal (BNR) systems if required, although additional studies will be required (see below).

11. RECOMMENDATIONS

Extension of the Modified Steady-State Theory to BEPR Systems

As mentioned above, the steady-state theory modified for nitrogen removal activated sludge systems (Chapter 6), needs to be extended to nitrification-denitrification (ND) biological excess phosphorus removal (BEPR) systems. In this regard, the following issues would need to be addressed:

(i) In extending the modified steady-state theory to NDBEPR systems, due account must be taken of the increased K_{2T} observed for NDBEPR systems (Clayton *et al.*, 1991).

(ii) It would need to be assessed whether or not the $Y_{H,NO}$:$Y_{H,AE}$ ratio determined here remains the same for both the OHO and polyphosphate accumulating organism (PAO) biomasses in NDBEPR systems.

Further Evaluation of Wastewater RBCOD Measurement

In measuring the RBCOD concentration in this investigation, a number of inconsistencies became apparent that require further investigation:

(i) The apparent inverse influence of the influent feed COD concentration on f_{us} determinations in laboratory-scale activated sludge systems.

(ii) Further evaluation of the physical flocculation-filtration method in measuring wastewater RBCOD, as compared with the biological respirometric batch test and square-wave fed continuous flow-through methods.

(iii) Possible changes in the kinetic behaviour of activated sludge biomass taken from continuous flow-through systems (i.e. substrate limiting) and placed in batch test conditions (i.e. substrate saturation).

ACKNOWLEDGEMENTS

Mark Wentzel, Associate Professor and Thesis Supervisor – for his constant encouragement, untiring patience, expert direction and thoughtful advice.

Professor GA Ekama – for his experienced guidance, keen insight and consistent support throughout the experimental investigation.

Mr. MT Lakay, Laboratory Manager – for lending his vast knowledge and experience so generously to the successful operation and maintenance of the laboratory research systems.

Mr. H Mafungwa, Technical Assistant – for his dedication and assistance with the daily analyses and functioning in the laboratory.

Fellow students – BJ Lee, A Tsai, N Ristow and S Sötemann for their willing cooperation and assisting in running the units when needed.

My parents, brother and wife, without whose sacrifices this journey could not have been completed.

My sincere thanks to the University of Cape Town, the National Research Foundation and Ondeo for their funding and sponsorship of this research.

TABLE OF CONTENTS

LIST OF SYMBOLS

$[Ac]_{BT}$	Acetate concentration in the batch test (mg/ℓ)
AA	Anoxic-aerobic
ABT	Aerobic batch test
A_c	Acetate, sodium acetate (CH_3COONa)
AE	Aerobic
AS, A/S	Activated sludge
ASM	Activated Sludge Model
AVG	Average
AVSS	active volatile suspended solids
AX	anoxic
BEPR	Biological excess phosporus removal
b_{HT}	Specific endogenous mass loss rate at temperature T (1/d)
BNR	Biological nutrient removal
BT	Batch test
CFCM	Continuous fed complete mixed (activated sludge system)
CFWWTP	Cape Flats Wastewater Treatment Plant
CO_2	Carbon dioxide
COD	Chemical oxygen demand
COD_{FF}	COD concentration of floc-filtered filtrate (mgCOD/ℓ)
d	Day
Δ	Indicates a change in parameter value
DBT	Denitrification (anoxic) batch test
Deg. f	Degrees of freedom
ΔOUR	Change in OUR (mgO/ℓ/h)
$D_{p,\alpha}$	Denitrification potential for RBCOD as substrate (mgN/ℓ)
$D_{p,K2T}$	Denitrification potential for SBCOD as substrate (mgN/ℓ)
D_{pp}	Total system denitrification potential (mgN/ℓ)
DSVI	Dilute sludge volume index (mℓ/gTSS)
f	Fraction of (unbiodegradable) endogenous residue
f_{anox}	Fraction of biodegradable COD that is utilized anoxically
f_{av}	Active fraction of the volatile suspended solids (AVSS/VSS)
f_{cv}	COD to VSS ratio of the mixed liquor (COD/VSS)
FF	Floc-filtered
FFE	Floc-filtered effluent
FFI	Floc-filtered influent
f_i	VSS to TSS ratio of the mixed liquor (mgVSS/mgTSS)
f_n	Nitrogen to VSS ratio of the mixed liquor (mgN/mgVSS)
f_{na}	Free and saline ammonia to TKN ratio of the influent wastewater
FSA	Free and saline ammonia (mgN/ℓ)
f_{ts}	RBCOD fraction with respect to total in influent wastewater
$f_{ts,BT}$	RBCOD fraction with respect to total, determined by batch test respirometry
$f_{ts,FF}$	RBCOD fraction with respect to total, determined by floc-filtration

	method
f_{up}	Fraction of unbiodegradable particulate (with respect to total) COD in the influent wastewater
f_{us}	Fraction of unbiodegradable soluble (with respect to total) COD in the influent wastewater
h	Hour
IC	Ion chromatography
IFFD	Intermittent fed fill and draw (activated sludge system)
K_{1T}	Specific denitrification rate with RBCOD as substrate (mgN/mgAVSS/d), at temperature T
K_{2T}	Specific denitrification rate with SBCOD as substrate (mgN/mgAVSS/d), at temperature T
K_{3T}	Specific denitrification rate with endogenous generated SBCOD as substrate (mgN/mgAVSS/d), at temperature T
ℓ	Litres
LR	Loading rate (mgCOD/mgVSS)
mg	Milligram
min	Minute
ML	Mixed liquor
MLE	Modified Ludzack-Ettinger (activated sludge system)
mm	Millimetres
MPP, MPWWTP	Mitchells Plain Wastewater Treatment Plant
$MS_{ti,R}$	Mass of total COD concentration of raw, undiluted wastewater (mgCOD)
mV	Millivolt
MX_a	Mass of active biomass (mgAVSS)
MX_V	Mass of volatile suspended solids (mgVSS)
N	Elemental nitrogen
N	Number of data
N_2	Molecular dinitrogen
ND	Nitrification-denitrification
NDBEPR	Nitrification-denitrification-biological-excess P removal
NO_2	Nitrite
NO_3	Nitrate
NO_x	Nitrate and nitrite
NU	Nitrate utilized (mgN/ℓ)
NUR	Nitrate utilization rate (mgN/ℓ/h)
O	Elemental oxygen
O_2	Molecular oxygen
OHO	Ordinary heterotroph organism
OU	Oxygen utilized (mgO/ℓ)
OUR	Oxygen utilization rate (mgO/ℓ/h)
PAO	Polyphosphate accumulating organism
Q_i	Influent wastewater flowrate (ℓ/d)
Q_S	Influent flowrate for the SQW fed activated sludge system (ℓ/d)
RBCOD	Readily biodegradable COD (mgCOD/ℓ)
SB	Sewage batch
SBCOD	Slowly biodegradable COD (mgCOD/ℓ)
S_{bi}	Biodegradable COD in the influent wastewater (mgCOD/ℓ)

S_{bs}	Readily biodegradable (soluble) COD (mgCOD/ℓ)
SCFA	Short-chain fatty acids
sec	Second
SQW	Square-wave (fed activated sludge system)
S_s	Soluble substrate (biodegradable)
SSD	Sample standard deviation
S_{ti}	Total COD concentration of the influent wastewater (mgCOD/ℓ)
$S_{ti,R}$	Total COD concentration of the raw, undiluted wastewater (mgCOD/ℓ)
S_{upi}	Unbiodegradeble particulate COD concentration of the influent wastewater (mgCOD/ℓ)
S_{use}	Unbiodegradable soluble COD concentration of the system effluent (mgCOD/ℓ)
S_{usi}	Unbiodegradable soluble COD concentration of the influent wastewater (mgCOD/ℓ)
T	Temperature (°C)
TAA	Technicon Auto-analyzer
TKN	Total kjeldhal nitrogen concentration (mgN/ℓ)
TSS	Total suspended solids
UCT	University of Cape Town
V	Volume
V_{BT}	Batch test volume
V_{ML}	Volume of activated sludge mixed liquor added in batch test
V_p	Total volume of the system (process)
VSS	Volatile suspended solids
V_{WW}	Volume of wastewater added in batch test
WW	Wastewater
X_a	Active biomass concentration (mgAVSS/ℓ)
X_V	Volatile suspended solids concentration (mgVSS/ℓ)
Y_H	Ordinary heterotrophic cell yield coefficient
$Y_{H,AE}$	Ordinary heterotrophic cell yield coefficient under aerobic conditions
$Y_{H,NO}$	Ordinary heterotrophic cell yield coefficient under anoxic conditions

CHAPTER 1

INTRODUCTION

1.1 BACKGROUND

South Africa is a water-scarce country rapidly approaching the maximum economical exploitation of conventional water resources: South Africa experiences very low (average ~465mm per year) and highly seasonal rainfall, and is frequently subject to droughts and floods. Of the rainfall, less than 10% ultimately ends up in streams and dams. In addition, potential evaporation is substantially in excess of rainfall, by up to twelve times as much in the western parts of the country. Accordingly, protection of fresh water resources and water quality has long been a national priority, resulting in increasingly more stringent legislation controlling pollutant discharges to waterbodies (Sötemann, 2000; van Niekerk, 2000). This has (and will continue to) placed significant demands on existing (aging) and new wastewater treatment plants to limit, in particular, the nutrient (nitrogen, N and/or phosphorus, P) loads in their treated effluents that are required by law to be returned to source catchments. As a consequence, the activated sludge system for biological nutrient removal (BNR) has become the preferred technology for wastewater treatment in South Africa. This type of system also has been widely implemented around the world.

Integral to the BNR activated sludge system is the biologically mediated process of denitrification. Not only does this process reduce the N load to the environment, but it also has the advantages of alkalinity recovery and reducing the oxygen demand. Further, the denitrification protects the biological excess P removal (BEPR), if included, from the deleterious effect of recycling nitrate to the anaerobic reactor (Wentzel *et al.*, 1990). Accordingly, quantifying the potential denitrification is fundamental to the design and operation of the BNR activated sludge system. Biological denitrification has been explicitly incorporated into the steady-state design (e.g., WRC, 1984; Wentzel *et al.*, 1990; Maurer and Gujer, 1994) and kinetic simulation (Van Haandel *et al.*, 1981; Henze *et al.*, 1987, 1995; Dold *et al.*, 1980, 1991; Wentzel *et al.*, 1992; Barker and Dold, 1997; Murnleitner *et al.*, 1997; Gujer *et al.*, 1999) models developed as aids to the design and operation of BNR activated sludge systems. In both sets of models, critical as input to quantify the denitrification is the value for the ordinary heterotrophic organism (OHO) anoxic cell yield coefficient ($Y_{H,NO}$).

In brief, heterotrophic organisms derive the molecular building blocks for synthesizing new cell matter from organic substrates (S). This requires energy, which is obtained by oxidising organic substrates in a complex series of biologically mediated redox reactions (Lehninger, 1973; WRC, 1984; James and Matthews, 1991; Casey, 1993; Wentzel *et al.* 2001): Electrons from substrate molecules are transferred in a sequence (or "chain") of successive electron donors and acceptors called the "Electron Transport Chain" (ETC), ultimately being passed to a terminal electron acceptor; oxygen for aerobic respiration and nitrate for anoxic. In terms of the models, the heterotrophic cell yield coefficient, Y_H, is the fraction of substrate

electrons that are used to synthesize new cell mass, while the remainder, $1 - Y_H$, is passed to the terminal electron acceptor to generate energy. This is shown schematically in Fig. 1.1, after Marais and Ekama (1976), WRC (1984), and Copp and Dold (1998). Hence, the value of Y_H, designated here $Y_{H,NO}$ for anoxic conditions and $Y_{H,AE}$ for aerobic, determines both the mass of electron acceptor utilized and the new cell biomass produced. In particular, the value for the anoxic yield ($Y_{H,NO}$) will influence both the mass of denitrification possible, and the sludge production.

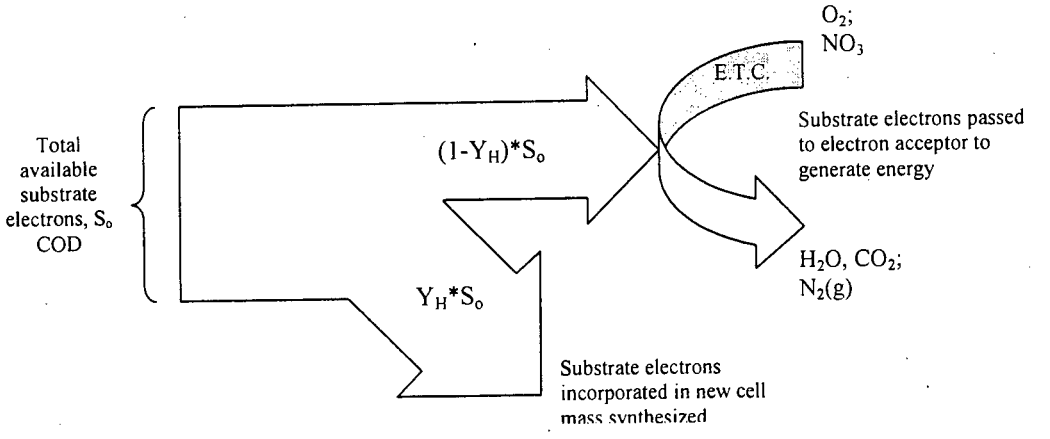

Fig. 1.1: Major fractionation of substrate electron utilization in biological oxidation of organic substrate with oxygen and nitrate as electron acceptors.

In activated sludge systems treating municipal wastewaters, however, the effect of $Y_{H,NO}$ on sludge production typically is small, since the mass of sludge produced under anoxic conditions is small compared to that produced under aerobic conditions, due to the relatively low influent TKN/COD ratios (Barker and Dold, 1997). In contrast, the effect of $Y_{H,NO}$ on the amount of denitrification achievable (and hence, on system design and operation) is quite significant.

1.2 SIGNIFICANCE OF ANOXIC YIELD IN DESIGN AND SIMULATION

The effect of $Y_{H,NO}$ on the denitrification achievable (termed denitrification potential) can be illustrated by examining the stoichiometry of substrate utilization incorporated in the models. Consider, for example, an inoculation of a completely soluble substrate, such as glucose, with bacteria under aerobic conditions. Accepting the COD (chemical oxygen demand) as a measure of the electron donating capacity of a substance (WRC, 1984), conservation of electrons holds that the decrease in soluble COD of the medium must be reflected in a corresponding increase in the COD of the bacterial mass and consumption of the terminal electron acceptor, oxygen (WRC 1984, Wentzel *et al.* 2001):

$$\Delta COD_{sol} = \Delta COD_{bacteria} + \Delta O_{2,utilized} \qquad (1.1)$$

From extensive bacteriological work reviewed by Payne (1971), as referenced in WRC (1984), the fraction of ΔCOD_{sol} appearing as $\Delta COD_{bacteria}$ is approximately

constant. Typically expressed as a ratio, this fraction defines the specific cell yield coefficient in terms of COD (Y_Z, Y_{COD})[1]; i.e.:

$$Y_H = \frac{\text{mass of protoplasm formed}}{\text{mass of substrate oxidized}} \equiv Y_{COD} = \frac{\Delta COD_{sol}}{\Delta COD_{bacteria}} \qquad (1.2)$$

Combining Eq.(1.1) and (1.2) and rewriting in terms of the oxygen utilized (OU, $\Delta O_{2,utilized}$):

$$\Rightarrow OU \equiv \Delta O_{2,utilized} = (1 - Y_{COD})*\Delta COD_{sol} \qquad (1.3)$$

Similarly, by applying the stoichiometric equivalence of the electron accepting capacities of oxygen and nitrate, i.e. 1 mgO = 2.86 mgNO_3-N (WRC, 1984; Moser-Engeler *et al.*, 1998), Eq.(1.3) can be written in terms of nitrate utilized (NU, ΔNO_3-$N_{utilized}$) for anoxic conditions:

$$2.86*NU = OU = (1 - Y_{COD})*\Delta COD_{sol} \qquad (1.4)$$

$$\Rightarrow NU = \frac{(1 - Y_{COD})*\Delta COD_{sol}}{2.86} \qquad (1.5)$$

Now, accepting that the anoxic yield value ($Y_{H,NO}$) equals the "standard" aerobic yield value of $Y_{H,AE}$ = 0.67 mgCOD/mgCOD, as conventionally adopted by ASM1 (Henze *et al.*, 1987) and similar models, the amount of nitrate utilized in consumption of one unit (mg/ℓ) of substrate COD is:

$$\Rightarrow NU = \frac{\Delta COD*(1 - Y_{H,NO})}{2.86} = \frac{(1)*(1-0.67)}{2.86} = 0.115\ {}^{mgNO_3\text{-}N}\!/_{\ell} \qquad (1.6)$$

With $Y_{H,NO}$ reduced to 0.54 mgCOD/mgCOD, similarly the amount of NU denitrified per unit (mg/ℓ) substrate COD consumed is:

$$\Rightarrow NU = \frac{\Delta COD*(1 - Y_{H,NO})}{2.86} = \frac{(1)*(1-0.54)}{2.86} = 0.161\ {}^{mgNO_3\text{-}N}\!/_{\ell} \qquad (1.7)$$

This amounts to a 40% increase in denitrification potential with the reduced yield.

---

[1] The change in bacterial mass generated per substrate consumed in the synthesis reaction is traditionally expressed in terms of volatile solids units (VSS), i.e. as "Y_H"; therefore to use Eq.(1.3) with VSS units a conversion factor is required between Y_{COD} and Y_H. This factor is commonly expressed as the ratio between new cell mass synthesized in VSS units (i.e. ΔX_H) versus the same in COD units (i.e. $\Delta COD_{bacteria}$), and is designated f_{cv}, where:

$$f_{cv} = \frac{\Delta COD_{bacteria}}{\Delta X_H} \equiv \frac{COD}{VSS} \qquad \Rightarrow Y_{COD} \equiv Y_Z = f_{cv}*Y_H$$

The value of f_{cv} is approximately constant and theoretically is 1.42 mgCOD/mgVSS (see *Appendix A*). Experimentally, Marais and Ekama (1976) found f_{cv} = 1.48 mgCOD/mgVSS for activated sludge systems (presented as 1.43 but subsequently increased to 1.48 with the inclusion of additional data).

Therefore, for most anoxic/aerobic (AX/AE) sequencing systems (MLE-type), in which the influent readily biodegradable (RB)COD is typically completely utilized under anoxic conditions, the reduced anoxic yield will result in a substantial increase in the denitrification potential (D_p) with RBCOD substrate, which results in a corresponding increase in the total denitrification potential of the system. Additionally, the increased denitrification potential of the system will ultimately improve (reduce) the steady-state effluent nitrate concentration (N_{ne}) of the system. This can be illustrated by modifying the steady-state theory of Marais and Ekama (1976) and WRC (1984). In terms of this theory, a single heterotroph yield value for both anoxic and aerobic conditions is accepted, and the total denitrification potential of the process (D_{pp}) and the steady-state effluent nitrate concentration of the system are defined, respectively, as:

$$D_{pp} = (1 - f_{us} - f_{up}) * S_{ti} * [\alpha + K_{2T} * f_{xl} * \frac{Y_H * R_s}{(1 + b_{HT} * R_s)}] \quad (1.8)$$

$$N_{ne} = N_c - D_{pp} + a * \frac{O_a}{2.86} + s * \frac{O_s}{2.86} \quad (1.9)$$

where:

$$\alpha = \frac{f_{bs} * (1 - f_{cv} * Y_H)}{2.86} \quad (1.10)$$

$$K_{2T} = 0.1008 * (1.08)^{T-20} \quad (1.11)$$

$$b_{HT} = 0.24 * (1.029)^{T-20} \quad (1.12)$$

and:

D_{pp}	Total denitrification potential of the process, mgNO3-N/ℓ influent
S_{ti}	Total influent COD, mgCOD/ℓ
f_{us}	Fraction of influent unbiodegradable soluble COD w.r.t. S_{ti}
f_{up}	Fraction of influent unbiodegradable particulate COD w.r.t. S_{ti}
f_{bs}	Fraction of influent RBCOD w.r.t. total influent biodegradable COD (S_{bi})
2.86	Equivalent oxygen demand of NO3-N as electron acceptor, mgO/mgNO3-N
SST	Secondary settling tank
α	Fraction of nitrate removed by the initial rapid phase of denitrification
Q_i	The influent flowrate to the system, ℓ/d
f_{cv}	COD value of sludge mixed liquor VSS; f_{cv} = 1.48 mgCOD/mgVSS
K_{2T}	Specific denitrification rate constant with SBCOD as substrate, mgN/mgAVSS/time
f_{xl}	Fraction of total sludge mass in the system that is unaerated (anoxic in this case)
Y_H	OHO cell yield coefficient, mgAVSS/mg substrate COD
b_{HT}	Nett specific endogenous respiration rate, mgAVSS/mgAVSS/d
R_s	The sludge age of the system, d
N_{ne}	The effluent nitrate-nitrogen concentration, mgNO3-N/ℓ
N_c	The nitrification capacity of the system, mgNO3-N/ℓ
a	The recycle rate from the AE reactor/zone to the AX reactor/zone, as ratio w.r.t. Q_i
O_a	The dissolved oxygen (DO) concentration in the a-recycle, mgO/ℓ
s	The recycle rate from the SST to the AX reactor/zone, as ratio w.r.t. Q_i
O_s	The dissolved oxygen (DO) concentration in the s-recycle, mgO/ℓ

Accepting a possible difference in the values for the anoxic and aerobic heterotrophic yields, Eqs.(1.8), (1.9) and (1.10) can be modified to give[2]:

$$D_{pp} = (1 - f_{us} - f_{up}) * S_{ti} * \left[\alpha + K_{2T} * f_{x1} * \left\{ f_{anox} * \frac{Y_{H,NO} * R_s}{(1 + b_{HT} * R_s)} + (1 - f_{anox}) * \frac{Y_{H,AE} * R_s}{(1 + b_{HT} * R_s)} \right\} \right] \quad (1.13)$$

where:

$$\alpha = \frac{f_{bs} * (1 - f_{cv} * Y_{H,NO})}{2.86} \quad (1.14)$$

f_{anox} = the proportion of total biodegradable substrate utilized anoxically,

$$= \frac{\left\{ \frac{D_{pp} * 2.86}{(1 - f_{cv} * Y_{H,NO})} \right\}}{(1 - f_{us} - f_{up}) * S_{ti}} \quad (1.15)$$

In Eq.(1.13) the two components making the D_{pp} can be identified: (1) denitrification with RBCOD as substrate (i.e. the α term, "$D_{p,\alpha}$"), and (2) denitrification with slowly biodegradable (SB)COD as substrate (i.e. the K_{2T} term, "$D_{p,K2T}$"). For the (1) RBCOD term ($D_{p,\alpha}$), since it is accepted that the RBCOD is completely utilized anoxically, its rate of utilization is of no consequence and the RBCOD contribution to D_{PP} is simply stoichiometric. For the (2) SBCOD term ($D_{p,K2T}$), the contribution to D_{PP} is rate dependant via the specific denitrification rate constant, K_{2T}. Since the value for K_{2T} has been derived from experimentally observed denitrification profiles (van Haandel *et al.*, 1981; WRC, 1984), converted to specific rates with a single yield constant ($Y_{H,AE}$), the contribution of $D_{p,K2T}$ to D_{PP} must be kept constant when the different anoxic yield ($Y_{H,NO}$) is incorporated – this can be seen from Fig. 1.2: the theoretically predicted SBCOD denitrification profiles must equal those observed experimentally (i.e. $D_{p,K2T}$ must = the experimentally observed $\Delta NO_{3,K2T}$) and, hence, must remain constant[3].

---

[2] The theory is modified on the basis that usually *all* growth on RBCOD occurs in the anoxic reactor (i.e. the reactor is sufficiently large that all the RBCOD is utilized anoxically), $\Rightarrow$ 100% of the α term is at $Y_{H,NO}$; whereas only a part of growth on SBCOD occurs in the anoxic reactor (i.e. only a fraction of the K_{2T} term is at $Y_{H,NO}$); see Chapter 6 for a detailed analysis.

[3] The theoretically predicted SBCOD denitrification profiles must equal the experimentally observed denitrification profiles resulting from SBCOD utilization (see Fig.1.2); this is achieved by adjusting (revising) the value of K_{2T} corresponding to $Y_{H,NO}$ in Eq.(1.13); see Chapter 6 for details.

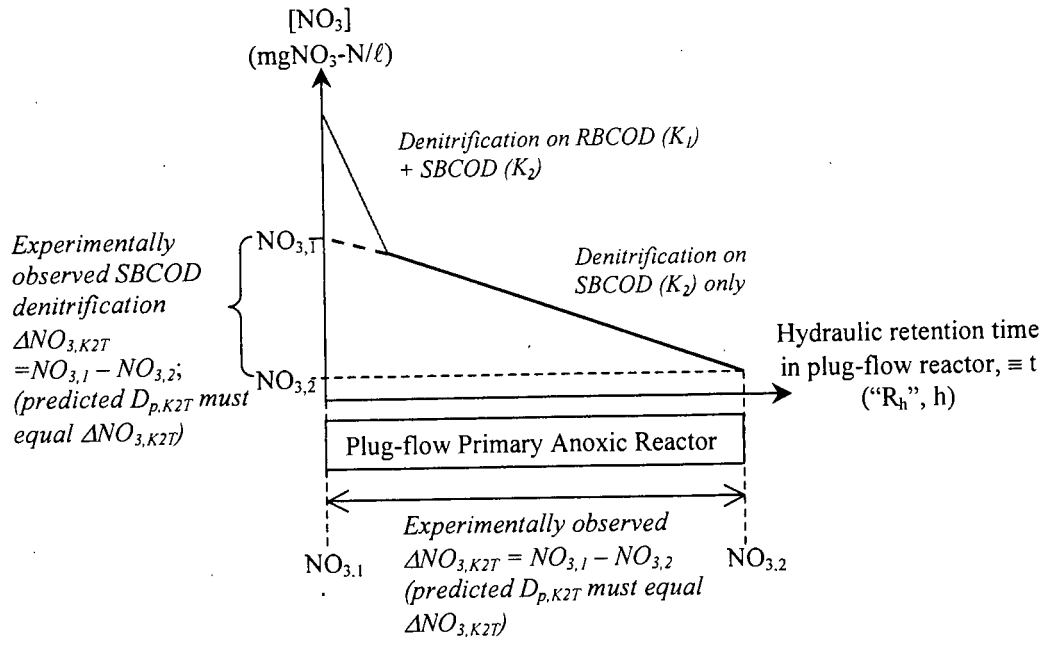

Fig. 1.2: Schematic of a typical denitrification profile resulting from SBCOD utilization, as observed experimentally in the plug-flow primary anoxic reactors by Marais and co-workers (van Haandel *et al.*, 1981; WRC, 1984).

Therefore, accepting that the denitrification contribution of the SBCOD term ($D_{p,K2T}$) remains constant in the D_{pp} equation for both cases $Y_{H,NO} = Y_{H,AE}$ and $Y_{H,NO} \neq Y_{H,AE}$, then by plotting Eqs.(1.13) and (1.9) against $Y_{H,NO}$ and D_{pp} respectively (Fig. 1.3 and 1.4, respectively), it can be seen that the D_{pp} increases and N_{ne} decreases with decreasing $Y_{H,NO}$. Specific D_{pp} values for $Y_{H,NO}$ = 0.45 mgVSS/mgCOD (i.e. same as $Y_{H,AE}$) and 0.37 mgVSS/mgCOD are summarised in Table 1.2 for 14 and 22 °C. At both temperatures, reducing the anoxic yield results in a significant increase in system D_{pp} of 12 – 15%, due to the increase in denitrification with RBCOD ($D_{p,\alpha}$ Table 1.1) of 35%. This increase in D_{pp} causes a corresponding reduction in effluent nitrate concentration (Table 1.1). Clearly, in the steady-state models the value for $Y_{H,NO}$ has a significant impact on predicted denitrification and hence on BNR activated sludge system design and predicted performance. (This aspect is dealt with in more detail in Chapter 6).

Table 1.1: Effect of reduced anoxic yield on denitrification potential and effluent nitrate concentration at high (22 °C) and low (14 °C) temperature.

Temperature	14 °C			22 °C		
$Y_{H,NO}$ (mgVSS/mgCOD)	0.45	0.37	Δ	0.45	0.37	Δ
$D_{p,\alpha}$	17.1	23.1	+35%	17.1	23.1	+35%
$D_{p,K2T}$	23.8	23.8	0%	36.4	36.4	0%
D_{pp}	40.9	47.0	+15%	53.5	59.5	+11%
N_{ne}	9.9	3.88	-61%	0	0	0

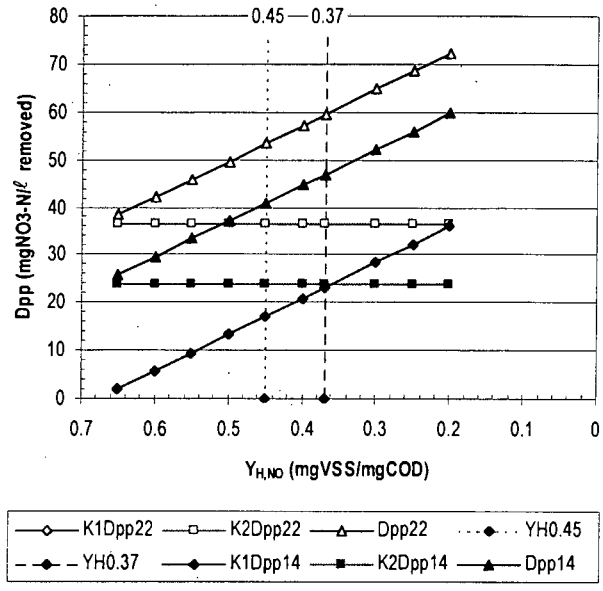

Fig. 1.3: Process denitrification potential (D_{pp}) vs. anoxic cell yield ($Y_{H,NO}$) at 22 °C (solid symbols) and 14 °C (open symbols) temperatures.

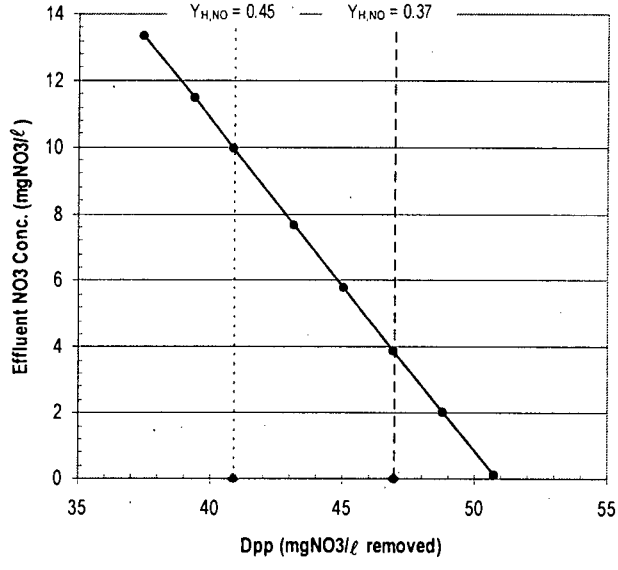

Fig. 1.4: Effluent nitrate concentration (N_{ne}) decrease with increasing process denitrification potential (D_{pp}): N_{ne} decreases from ~10 to 4 mgN/ℓ for a corresponding increase in D_{pp} from 41 to 47 mgN/ℓ removed at 14 °C; i.e. for a corresponding decrease in $Y_{H,NO}$ from 0.45 to 0.37 mgVSS/mgCOD.

In the activated sludge kinetic simulation models, the rates of substrate (both RBCOD and SBCOD) utilization, and associated organism growth and electron acceptor

consumption, are explicitly formulated. Noting that for most activated sludge systems the anoxic reactor is sufficiently large to ensure complete RBCOD utilization for denitrification (provided an anaerobic reactor for BEPR is not included), then the change in denitrification potential with change in $Y_{H,NO}$ for RBCOD, illustrated above for the steady-state model, will apply to the kinetic models also. Considering SBCOD as substrate, the rate limiting process in the sequence of anoxic SBCOD utilisation, whether via hydrolysis and direct utilization (Dold *et al.*, 1991), or via conversion first to RBCOD (ASM1, Henze *et al.*, 1987), or via conversion to RBCOD and subsequent substrate storage (ASM3, Gujer *et al.*, 1999), is usually calibrated from observed denitrification rates. Hence, calibration of the particular SBCOD (hydrolysis/conversion/storage etc.) utilization rate must compensate for the reduced $Y_{H,NO}$ to ensure that the model predicted denitrification rate equals that observed experimentally. This means that the reduced anoxic yield must have little influence on the denitrification potential with SBCOD as substrate in calibration of the kinetic models, as shown above for the steady-state model.

Additionally, in ASM1 (Henze *et al.*, 1987) and similar activated sludge kinetic simulation models, the aerobic rates of growth on RBCOD and hydrolysis of SBCOD are also applied to anoxic conditions, but adjusted by correction factors, η_g for RBCOD and η_h for SBCOD. In ASM3 (Gujer *et al.*, 1999), the aerobic storage of COD and subsequent growth on the stored COD also are applied under anoxic conditions, but both rates are multiplied by the correction factor η_{NO}; the SBCOD hydrolysis rate remains unchanged under anoxic compared to aerobic conditions. Thus, if the anoxic yield is in error, effectively η_g and η_h in ASM1 (Orhon *et al.*, 1996) and η_{NO} in ASM3 will similarly be in error.

Furthermore, for both types of substrates, if anoxic respirometric procedures (i.e. monitoring terminal electron acceptor, NO_3, utilization) are used to calibrate substrate utilisation rates (e.g. van Haandel *et al.*, 1981; Orhon *et al.*, 1996; Sözen *et al.*, 1998), or to characterize wastewater RBCOD (e.g. Ekama *et al.*, 1986; Orhon *et al.*, 1996; Ubay Çokgör *et al.*, 1998; Wentzel *et al.*, 1999), and the anoxic yield value is in error, then the applied measurement similarly will be in error (Orhon *et al.*, 1996; Ubay Çokgör *et al.*, 1998). This is particularly significant with respect to RBCOD characterisation, since it has been identified to be of fundamental importance in design and operation of N (van Haandel *et al.*, 1982) and N and P (Siebritz *et al.*, 1983; Wentzel *et al.*, 1990; Clayton *et al.*, 1991; Wentzel *et al.*, 1992) removal systems. According to Ubay Çokgör *et al.* (1998), "the correct assessment of the readily biodegradable COD in wastewaters (S_{SI}) is of great theoretical and practical significance" because it is directly related to growth kinetics in current models (e.g. ASM3), and is required for determination of the SBCOD fraction (Wentzel *et al.*, 1995) which is the bulk influent biodegradable substrate critical for modelling and design of activated sludge systems.

From the above, it can be seen that ***the correct value for the anoxic yield is essential in the design and simulation of activated sludge wastewater treatment plants, and in anoxic respirometric wastewater RBCOD characterisation.*** As stated by Orhon *et al.* (1998), "it is a parameter of capital importance in setting the necessary stoichiometric relationships for the design and operation of activated sludge systems".

1.3 VALUE FOR HETEROTROPH ANOXIC YIELD

In the IWA Task Group models for activated sludge systems, ASM1 (Henze *et al.*, 1987), ASM2 (Henze *et al.*, 1995) and ASM2d (Henze et al., 1999), and similar (e.g. Dold *et al.*, 1991; Wentzel *et al.*, 1992), the heterotrophic yield coefficient is assumed to have the same value under anoxic as under aerobic conditions. However, when nitrate serves as terminal electron acceptor, ideally only 2 mol ATP are formed per pair of electrons (e^-) transferred to nitrate as compared to 3 mol ATP when the transfer is to oxygen (Payne 1981, WRC 1984, Kuba *et al.* 1993, Casey *et al.* 1999, Wentzel *et al.* 2001). This difference reduces the energy captured by the organism when nitrate serves as electron acceptor (versus oxygen) in biological oxidation of organic substrate. Correspondingly, therefore, the cell yield under anoxic conditions ($Y_{H,NO}$) should be reduced relative to its aerobic value ($Y_{H,AE}$).

A detailed presentation is made in *Appendix A* of a theoretical estimation of the reduced anoxic yield based on thermodynamic and bioenergetic principles developed from WRC (1984) and Wentzel *et al.* (2001). By assuming a molecular cell composition of $C_5H_7O_2N$, it is shown that the theoretical anoxic cell yield coefficient ($Y_{H,NO}$) is about 83% of its aerobic value ($Y_{H,AE}$), or 0.35 mgVSS/mgCOD (0.5 mgCOD/mgCOD) compared to the aerobic yield of 0.42 mgVSS/mgCOD (0.6 mgCOD/mgCOD).

Orhon *et al.* (1996) similarly accepted the difference in ATP formation between anoxic and aerobic metabolism, and theoretically quantified the anoxic to aerobic yield ratio for four organic substrates based on bioenergetic principles set out by McCarty (1971, 1972, 1975). For municipal wastewater, protein, lactate and carbohydrate substrates, they obtained the following anoxic:aerobic yield ratios, respectively: 0.79, 0.80, 0.80, and 0.85. Accepting the standard aerobic heterotrophic yield value of 0.67 mgCOD/mgCOD used in ASM1 and similar models, this gives an anoxic yield of 0.53 mgCOD/mgCOD for municipal-type wastewaters as substrate.

The requirement for a reduced anoxic yield relative to its aerobic value has been recognized in the development of kinetic simulation models for activated sludge systems. In implementation of the kinetic model by Barker and Dold (1997) as the BIOWIN computer program (Envirosim, 2001), an anoxic yield value of 0.54 mgCOD/mgCOD was ultimately adopted, which gives an anoxic:aerobic yield ratio of 0.806 for the standard aerobic yield of 0.67 mgCOD/mgCOD. Similarly, a reduced anoxic yield was also included in ASM3 (Gujer et al., 1999; Henze et al., 2000), with net aerobic and anoxic yields of 0.54 and 0.43 mgCOD/mgCOD respectively. This gives a corresponding net anoxic:aerobic yield ratio of 0.80, which, similarly to that of BIOWIN, compares favourably with theoretical estimates (*Appendix A*, Orhon *et al.* 1996).

Although limited, several studies do provide direct and indirect experimental evidence supporting the theoretical assessment that the anoxic cell yield should be reduced relative to its aerobic counterpart (see Table 1.2 and Chapter 2). Specifically, excluding the values obtained by McClintock *et al.* (1988), for these studies an average anoxic cell yield coefficient can be calculated as approximately 81 ± 3.5% of its corresponding aerobic value, or about 0.54 mgCOD/mgCOD (range 0.52 – 0.57) with respect to the standard aerobic yield of 0.67 mgCOD/mgCOD. This

substantiates the theoretical evaluations above that the anoxic yield should be reduced relative to the aerobic value (*Appendix A*, Orhon *et al.*, 1996).

Table 1.2: Summary table of estimated reduced anoxic cell yield coefficients with respect to its corresponding value under aerobic conditions.

Source	Substrate	Biomass	Y_{AX}	Y_{AE}	Unit	Ratio
Appendix A	acetate, glucose	-	0.35	0.42	1	*(0.80)*
(Theoretical)	*(same)*	-	0.50	0.60	2	*(0.80)*
Orhon *et al.* (1996)	Municipal WW	-	*(0.53)*	*(0.67)*	2	0.79
(Theoretical)	Protein	-				0.80
	Lactate	-				0.80
	Carbohydrate	-				0.85
McClintock *et al.* (1988)	Bacto-peptone	AE/AX	0.272	0.503	1	0.54
	(adj., endog. residue)		*(0.35)*	*(0.55)*	1	*(0.64)*
Kuba *et al.* (1993)	acetate, other	NDBEPR	*(0.50)*	*(0.67)*	2	0.74
Isaacs and Henze (1995)	acetate	NDBEPR	0.51	*(0.67)*	2	*(0.76)*
Cöpp and Dold (1998)	citrate *(P.denitrif.)*	Pure cultr.	0.575	*(0.67)*	2	*(0.86)*
Ubay Çokgör *et al.* (1998)	defined, various	AE/AX	0.37	0.45	1	0.82
	(accepting f_{cv} = 1.42)		*(0.53)*	*(0.64)*	2	*(0.83)*
Moser-Engeler *et al.* (1998)	fermented PS	NDBEPR	0.57	*(0.67)*	2	*(0.85)*
Sperandio *et al.* (1999)	acetate	AE/AX	0.45	0.54	3	0.83
	glucose		0.57	0.67	3	0.85
	acetic acid/starch		0.51	0.66	3	0.77
ASM3 (1999, 2000)	*(Model)*	-	0.43	0.54	2	0.80
Biowin (2001)	*(Model)*	-	0.54	*(0.67)*	2	*(0.81)*

Note: Values without parentheses are reported/derived values directly from sources, while values in parentheses are obtained from subsequent calculations based on assumed/accepted quantities, e.g. the standard aerobic yield of 0.67 mgCOD/mgCOD. Also, unit designations are: 1 = mgVSS/mgCOD; 2 = mgCOD/mgCOD; 3 = gC/gC.

1.4 RESEARCH OBJECTIVES

While a reduced heterotrophic yield under anoxic conditions is apparent from bioenergetic theory and supported by experimental measurements recorded in the literature, no direct experimental measurement with real municipal sewage could be found: Most of the studies identified above were performed with defined substrates, hydrolysates, and/or mixtures of various domestic and industrial wastewaters, and focussed mainly on estimating specific denitrification rates. Consequently, few provide information directly relating nitrate and corresponding substrate utilizations necessary to estimate the yield. Furthermore, some studies were performed with mixed polyphosphate accumulating organism (PAO) sludges from nitrification-denitrification biological excess phosphorous removal (NDBEPR) activated sludge systems, which introduces unquantifiable uncertainty into observed yield measurements, as a result of (i) variably increased inorganic content of the NDBEPR biomass, (ii) losses of RBCOD due to anoxic sequestration by the PAO biomass unable to denitrify (Clayton *et al.*, 1991; Wentzel *et al.*, 1992) and (iii) contribution of PAOs to denitrification (Hu *et al.*, 2000, 2002; Vermande *et al.*, 2002) possibly on stored substrate. ***Thus, lacking in the current body of research on $Y_{H,NO}$, are any studies and experiments to directly quantify or measure $Y_{H,NO}$ using sewage as substrate.***

The principal aim in this research is to investigate and quantify the ordinary heterotrophic organism (OHO) cell yield under anoxic conditions relative to its value under aerobic conditions for municipal sewage.

Three primary objectives were identified in this regard:

1. Determine the ratio $Y_{H,NO}$:$Y_{H,AE}$ for real sewage in terms of electron acceptor (OU vs. NU) utilization.

2. Measure $Y_{H,NO}$ and $Y_{H,AE}$ directly for known concentration of RBCOD utilized.

3. Compare experimental results with other, independent studies on real sewage.

1.5 RESEARCH APPROACH

For the investigation, the difficulties and complications noted above in measuring OHO denitrification and associated yields arising from the presence of PAOs was recognised. Accordingly, to eliminate these, in all investigations sludges from N removal only (i.e. no BEPR) plants were used. Since the relative contribution of PAOs to denitrification is small (Hu *et al.*, 2000), the information obtained with N removal sludges can be applied directly to BEPR sludges with little error.

The basis for the research approach derives from Fig. 1.1, in that oxygen (aerobic, AE) and nitrate (anoxic, AX) electron acceptor utilizations (OU and NU, respectively) are stoichiometrically related for the same soluble substrate COD (RBCOD, S_s, S_{bs}) utilized. That is, the equations quantifying RBCOD utilization in terms of OU and NU, i.e. Eq.(1.16) and (1.17) respectively, can be equated if the same mass of RBCOD is utilized, to give Eq.(1.18):

$$RBCOD_{AE} = \frac{OU}{(1 - Y_{H,AE})} \tag{1.16}$$

$$RBCOD_{AX} = \frac{2.86 * NU}{(1 - Y_{H,NO})} \tag{1.17}$$

$\Rightarrow$ for $RBCOD_{AE} = RBCOD_{AX}$:

$$\boxed{\Rightarrow \frac{OU}{(1 - Y_{H,AE})} = RBCOD \equiv S_s = \frac{2.86 * NU}{(1 - Y_{H,NO})}} \tag{1.18}$$

Therefore, for the same concentration of RBCOD utilized, $Y_{H,NO}$ can be expressed in terms of OU, NU and the aerobic cell yield coefficient, $Y_{H,AE}$:

$$\boxed{\therefore Y_{H,NO} = 1 - \frac{2.86 * NU}{OU} * (1 - Y_{H,AE})} \tag{1.19}$$

Thus, by measuring the OU and NU for the same RBCOD utilized, a plot of Eq.(1.19) can be developed giving $Y_{H,NO}$ for various $Y_{H,AE}$. This will enable the ratio of the two yields to be calculated, as in Objective 1 above. Further, if the widely accepted value for $Y_{H,AE}$ = 0.67 mgCOD/mgCOD is accepted here also, then Eq.(1.19) reduces to:

$$\boxed{Y_{H,NO} = 1 - 0.944 * \frac{NU}{OU}} \qquad (1.20)$$

On this basis, values for $Y_{H,NO}$ can be estimated by measuring the OU and NU in identical aerobic and anoxic batch tests respectively, containing the same concentration of wastewater RBCOD and biomass from the same source, provided the value of $Y_{H,AE}$ is known.

The critical criterion in this approach is that the RBCOD concentration in the corresponding aerobic and anoxic batch tests is the same in order for Eqs.(1.16) to (1.20) to remain valid. Furthermore, because OU and NU are related to *complete* utilization of RBCOD rather than its *rate* of utilization (Ekama *et al.*, 1986), specific definition of the biomass used is not necessary. In fact, all that is required is that the same concentration of wastewater RBCOD be utilized by the same biomass (i.e. in a consistent manner) regardless of its concentration in the test: From, for example, Ekama *et al.* (1986), Dold *et al.* (1991) and Mbewe *et al.* (1995), OUR profiles for the same concentration of RBCOD utilized, but with different active biomass concentrations, will have the *same area* reflected in the RBCOD utilization part of the curve (OUR_{Ss}) but with *different shapes* in each case; the test with less active biomass will have an OUR_{Ss} profile that is relatively short and wide, while the test with more active biomass will have a profile that is tall and narrow (Figs. 1.4a,b). Similarly, for anoxic batch tests with the same RBCOD concentration, the NU of the RBCOD utilization part of the curve will be the same although the *rate* of utilization will differ depending on the concentration of active biomass present (Figs. 1.4c,d). On this basis, therefore, although the same biomass is required to compare corresponding OU and NU responses of respective aerobic and anoxic batch tests utilizing the same RBCOD, specific characterization of the biomass is actually not required. Consequently, complete definition of the parent systems producing the biomass for these batch experiments was not required or performed.

In the approach above, since RBCOD is eliminated as a variable by equating aerobic and anoxic respirometry [Eq.(1.18)], the concentration of RBCOD is also not required to estimate $Y_{H,NO}$, provided $Y_{H,AE}$ is known. However, this requires that the "standard" $Y_{H,AE}$ (0.67 mgCOD/mgCOD) be accepted in this study. As an independent assessment of the validity of this value, direct estimation of $Y_{H,AE}$ and $Y_{H,NO}$ need to be performed; Objective 2 above. This was to be done by:

(i) Measuring the RBCOD concentration of the wastewater added to the batch tests.
(ii) Adding known concentrations of an artificial substrate to the batch tests.

For (i) above, the wastewater RBCOD fraction was to be estimated by the simple direct flocculation-filtration method (Mbewe *et al.*, 1995) using the fraction

unbiodegradable soluble COD (f_{us}) obtained in a long sludge age UCT-system operated concurrently on the same sewage. This RBCOD would then be compared with the RBCOD concentration calculated with the method of Ekama *et al.* (1986) from the corresponding aerobic batch test OUR profiles accepting the standard $Y_{H,AE}$ of 0.67 mgCOD/mgCOD. If close correspondence is obtained, this indicates that the value for $Y_{H,AE}$ is reasonable, and hence $Y_{H,NO}$ also.

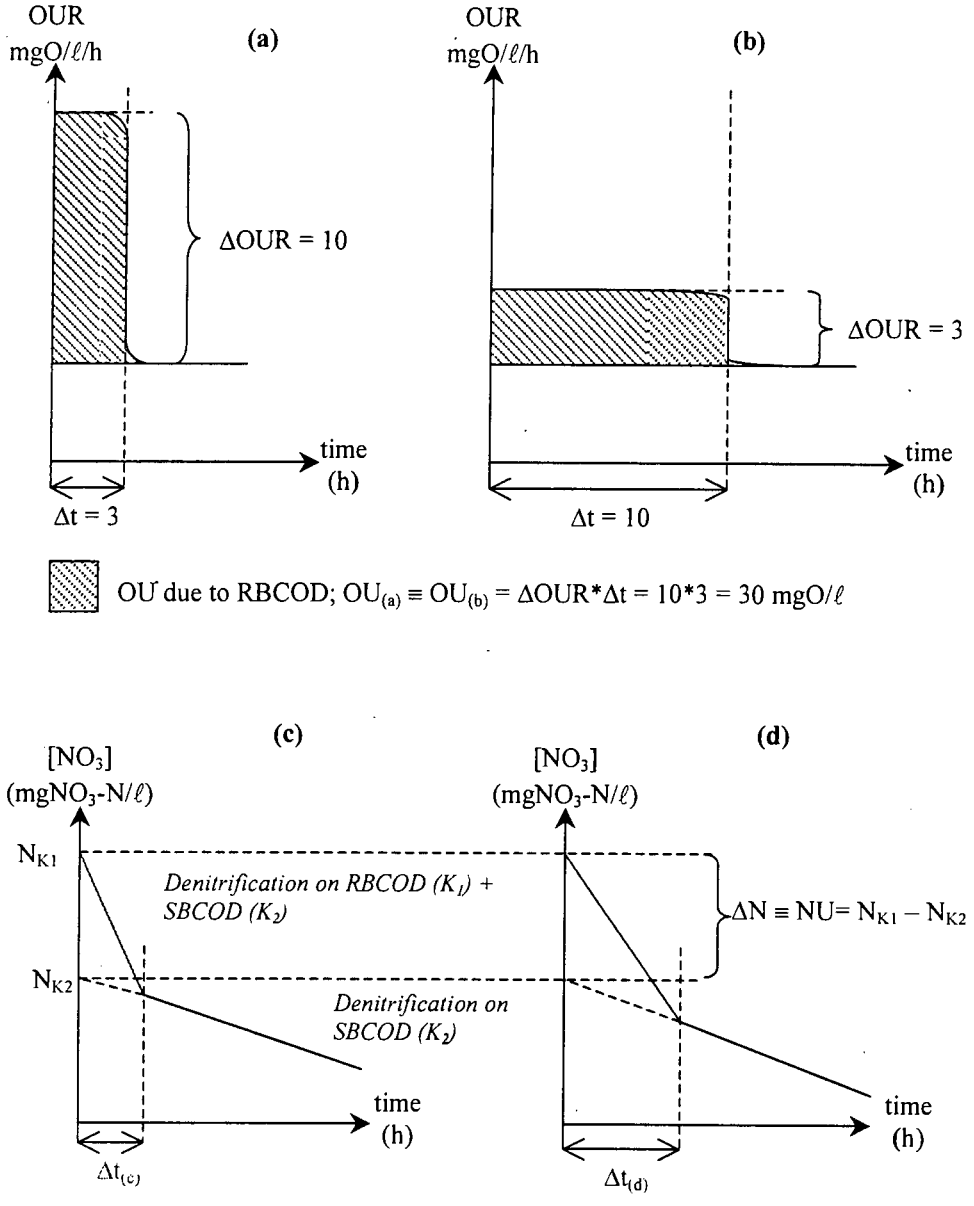

Fig. 1.4: Schematic representation of typical OUR and NUR patterns for aerobic (a and b) and anoxic (c and d) respiration in batch tests with the same RBCOD but different concentrations of active biomass, respectively. Curves (a) and (c) depict oxygen and nitrate utilizations, respectively, with more biomass present, while (b) and (d) are corresponding curves with less biomass present (after WRC, 1984; Ekama *et al.*, 1986).

However, during the course of the investigation floc-filtered RBCOD estimates gave poor recoveries compared with RBCOD values obtained from the batch tests, and it was subsequently decided to operate dedicated Modified Ludzack-Ettinger (MLE) and square-wave (SQW) fed activated sludge systems (Ekama *et al.*, 1986) to, respectively, produce consistent biomass and estimate wastewater RBCOD by the original method of Ekama *et al.* (1978). On this basis, independent measurement of the RBCOD in the wastewater was achieved for evaluation of batch test determined $Y_{H,AE}$ and $Y_{H,NO}$ estimates.

For the artificial substrate investigations, (ii) above, known concentrations of the RBCOD sodium acetate would be added to aerobic and anoxic batch tests, and $Y_{H,AE}$ and $Y_{H,NO}$ determined directly from the respective measured OU and NU, via Eqs.(1.16) and (1.17) respectively.

In summary, for the experimental investigation the OU and NU were measured in corresponding aerobic and anoxic batch tests, respectively, containing the same concentration of wastewater RBCOD and acclimatised biomass from the same mixed liquor source. The domestic sewage used in the experiments was obtained from the Mitchells Plain Wastewater Treatment Plant (MPWWTP) while the biomass was obtained from laboratory-scale MLE systems fed wastewater from this plant, as well as from the MPWWTP. Wastewater RBCOD was estimated both physically and respirometrically, by: (1) a floc-filtered method (Mamais *et al.*, 1993; Mbewe *et al.*, 1995); (2) batch test respirometry (Mbewe *et al.*, 1995; Wentzel *et al.*, 1999); and (3) a continuous flow-through short sludge age activated sludge system (Ekama *et al.* 1986; Mbewe *et al.* 1995). Additionally, aerobic and anoxic batch tests were also performed with known masses of the artificial substrate, acetate, to directly measure $Y_{H,AE}$ and $Y_{H,NO}$ from resultant OU and NU profiles, respectively.

To assess the experimental investigation and data collected above, experimental data in the literature from which it may be possible to derive values for the $Y_{H,NO}$:$Y_{H,AE}$ ratio, or for the individual coefficients, was to be identified and compared with those values obtained here; Objective 3 above.

CHAPTER 2

LITERATURE REVIEW

2.1 INTRODUCTION

In Chapter 1, for the design and simulation models for BNR activated sludge systems, the importance of the value for the ordinary heterotrophic organism (OHO) anoxic yield ($Y_{H,NO}$) was demonstrated. The principle aim in this research project is to quantify this stoichiometric coefficient. In this Chapter, theoretical and experimental investigations into this aspect in the literature are reviewed.

2.2 THEORETICAL BASIS FOR REDUCED ANOXIC CELL YIELD

As presented in Chapter 1, reduced energy capture with nitrate as electron acceptor, as compared with oxygen, suggests that the OHO cell yield coefficient for anoxic conditions ($Y_{H,NO}$) should be reduced relative to its value under aerobic conditions ($Y_{H,AE}$). Based on thermodynamic and bioenergetic principles it is shown theoretically in *Appendix A* that $Y_{H,NO}$ should be about 83% of $Y_{H,AE}$, or approximately 0.35 mgVSS/mgCOD (0.5 mgCOD/mgCOD), as compared with the theoretical $Y_{H,AE}$ of 0.42 mgVSS/mgCOD (0.60 mgCOD/mgCOD). This analysis is developed from postgraduate lecture notes, *"Bioenergetics"* and *"Chapter One: Fundamentals of Biological Behaviour"*, by Wentzel *et al.* (2001).

In brief, accepting an approximate molecular composition for cell protoplasm of $C_5H_7O_2N$ (molecular weight 113 g/mol), and simplifying anabolism to occur in two steps, i.e.: (1) formation of protoplasm, and (2) oxidation of substrate, it is shown that 10 mol NAD_{red} (energy transport molecule) are required to synthesize 1 mol $C_5H_7O_2N$, and that 0.83 mol of glucose are required to supply the necessary CO_2, NH_3, e^- and H^+ for the reaction. Anabolism requires energy, however, which is estimated as the Gibbs free energy of reaction (ΔG_R) for protoplasm formation, of 110.6 kcal/mol $C_5H_7O_2N$ formed. But energy transfer is not 100% efficient, however; therefore, assuming an efficiency of 55% (same as in catabolism) the energy required for anabolism is 201 kcal/mol. Catabolism provides this energy via a complex series of biologically mediated coupled redox exchanges in which the energy released is captured in the biological energy carrier molecule ATP. Accepting that each ATP molecule has an available free energy ~10 kcal/mol ATP, $\Rightarrow$ 201/10 = 20.1 mol ATP needs to be generated to synthesize 1 mol of protoplasm. Further, accepting the electron equivalence of oxygen, i.e. 4 mol e^- equivalent (e^- eq.) accepted per mol oxygen utilized, and that ideally 3 mol ATP are formed per pair of e^- transferred to oxygen versus 2 mol ATP with transfer to nitrate, it is shown that the total energy required to synthesize 1 mol protoplasm is 33.4 e^- eq. aerobically, and 40.1 e^- eq. anoxically. On this basis, theoretically:

$$Y_{H,AE} = (113 \text{ g/mol protoplasm})/(33.4 \text{ e}^- \text{ eq. required/mol protoplasm})$$
$$= (3.38 \text{ gVSS/e}^- \text{ eq.})/(8 \text{ gO/e}^- \text{ eq.}) = \underline{0.42 \text{ gVSS/gTh.COD}}$$

and:

$$Y_{H,NO} = (113 \text{ g/mol protoplasm})/(40.1 \text{ e}^- \text{ eq. required/mol protoplasm})$$
$$= (2.82 \text{ gVSS/e}^- \text{ eq.})/(8 \text{ gO/e}^- \text{ eq.}) = \underline{0.35 \text{ gVSS/gTh.COD}}$$

$$\Rightarrow \text{a theoretical } Y_{H,NO}:Y_{H,AE} \text{ ratio} = 0.35/0.42 = \underline{0.833}.$$

Orhon *et al.* (1996), in investigating the correction factor (η_g) commonly applied to aerobic heterotrophic growth rates for anoxic conditions (e.g. Henze *et al.*, 1987; Dold *et al.*, 1991; Gujer *et al.*, 1999), performed theoretical estimations of anoxic and aerobic yields for four substrates based on the bioenergetic principles set out by McCarty (1971, 1972, 1975). Similarly recognising reduced energy capture with nitrate as electron acceptor versus that with oxygen, and accepting the electron equivalent (e^- eq.) as a unit of biomass or substrate, they calculated the free energy (ΔG) required for biomass synthesis from pyruvate and ammonia as 7.5 kcal/e^- eq., noting that the free energy required for synthesis depends on the energy level of the carbon source. Accepting that energy transfer efficiency may vary from 0.4 – 0.8 they used an average of 0.6 (McCarty, 1972), and determined OHO theoretical yield values for the following organic (wastewater) substrates:

Table 2.1: Theoretical estimates of reduced anoxic yield relative to its aerobic value for four organic substrates (Orhon *et al.*, 1996).

Substrate	$Y_{H,AE}$ (e^-/e^-)	$Y_{H,NO}$ (e^-/e^-)	Ratio ($Y_{H,NO}/Y_{H,AE}$)
Domestic sewage	0.63	0.50	0.79
Proteinaceous (Meat processing)	0.64	0.51	0.80
Lactate (Dairy)	0.65	0.52	0.80
Carbohydrate (Confectionary)	0.72	0.61	0.85

Accepting the standard OHO aerobic yield ($Y_{H,AE}$) value of 0.67 mgCOD/mgCOD (used in ASM1 and similar models), this gives an anoxic yield ($Y_{H,NO}$) value of 0.79*0.67 = 0.53 mgCOD/mgCOD for municipal-type wastewater substrates. This is consistent with the theoretical estimates presented in *Appendix A*.

2.3 EXPERIMENTAL EVIDENCE FOR A REDUCED ANOXIC YIELD

McClintock *et al.* (1988) operated two parallel bench-scale continuous-flow aerobic and anoxic (nitrate fed) artificial substrate (Bacto-peptone) fed systems over a range of sludge ages (1.5 – 15 days) to investigate reduced sludge production under anoxic as compared with aerobic conditions. At four of the sludge ages (1.5, 3, 6 and 15 days) the sludge production in the anoxic system was less than that in the corresponding aerobic system. McClintock *et al.* used the activated sludge model of Lawrence and McCarty (1970) to derive an anoxic yield value of 0.272 mgVSS/mgCOD and a corresponding aerobic yield of 0.503 mgVSS/mgCOD, which gives an anoxic:aerobic yield ratio of 0.54. They also noted that (in terms of the model of Lawrence and McCarty) the anoxic specific endogenous respiration rate (0.057 d^{-1}) was significantly less than the aerobic value (0.111 d^{-1}); both values also are lower than the generally accepted value of 0.24 d^{-1} (WRC, 1984). However, the

Lawrence and McCarty model does not include endogenous residue generation (Marais and Ekama, 1976), which would have a significant impact on the estimations for the yields (and specific endogenous respiration rates); endogenous residue generation is fundamental to the more recently proposed activated sludge models, including the IWA Task Group models. Accordingly, the theory of Marais and Ekama (1976), which includes endogenous residue generation, was applied to McClintock *et al.'s* data; see Figs. 2.1 (a) and (b) for anoxic and aerobic conditions respectively. This gave a revised anoxic yield value of 0.35 mgVSS/mgCOD, with a corresponding aerobic yield of 0.55 mgVSS/mgCOD giving an anoxic:aerobic yield ratio of 0.64; in both cases a specific endogenous respiration rate of 0.24 d^{-1} is determined, equal to the standard value (WRC, 1984) (different anoxic and aerobic decay rates do not provide good fit to the experimental data, contrary to the observations of Siegrist *et al.*, 1999). The anoxic:aerobic yield ratio is significantly lower than that determined theoretically (*Appendix A*, Orhon *et al.* 1996), and may be due to the poor COD mass balances for the anoxic systems (Barker and Dold, 1997).

(a)

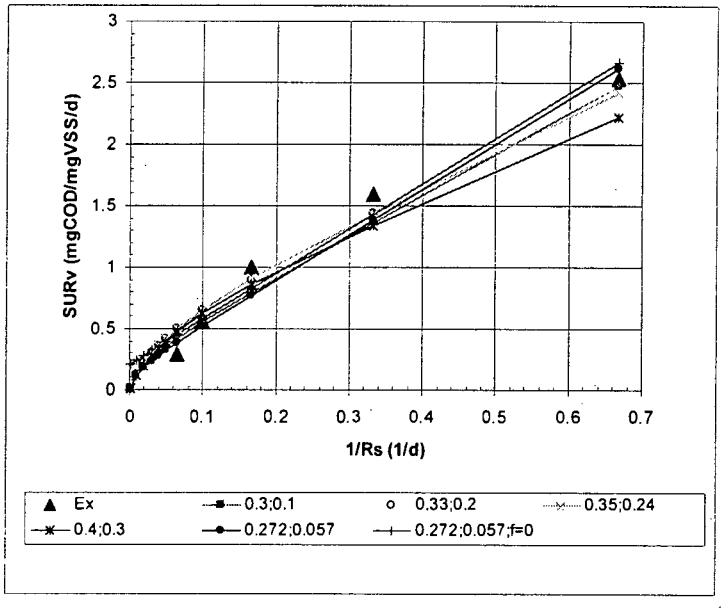

(b)

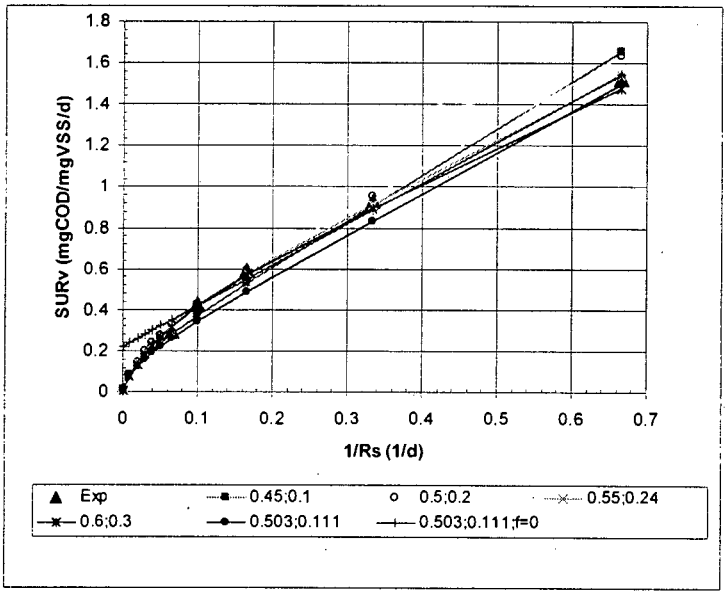

Fig. 2.1: Relative substrate utilization rate (SUR_v) versus reciprocal sludge age (1/Rs) for McClintock *et al.'s* (1988). Curves fitted to experimental data predicted using the model of Marais and Ekama (1976) for (a) aerobic and (b) anoxic conditions; values for yield and specific endogenous respiration rate for each curve listed in legends.

Kuba *et al.* (1993) operated two parallel sequencing batch reactors (SBR's) fed synthetic wastewater (acetate and phosphorous based) to investigate the possibility of anoxic phosphorous (P) uptake in BNR systems. Both systems comprised enhanced cultures of polyphosphate accumulating organisms (PAO's), one operated in an anaerobic-anoxic (A_2) sequence and the other in an anaerobic-aerobic (A/O) sequence. Overall, Kuba *et al.* reports a reduced sludge yield in the A_2 system relative to the A/O system, of 0.25 – 0.3 versus 0.35 – 0.4 gSS/gCOD, respectively. Since the two systems were identical except for the terminal electron acceptor, this gives an average anoxic:aerobic yield ratio of 0.74, which, although less than that determined theoretically (*Appendix A*, Orhon *et al.* 1996), nonetheless supports the view that the anoxic yield should be reduced relative to its aerobic counterpart. The lower yield ratio may have arisen in part from the complexities introduced by using BEPR sludges, see Section 1.4, Chapter 1.

Isaacs and Henze (1995) investigated the effect of controlled carbon source addition on the rate of denitrification in BNR processes by performing anoxic batch tests and pilot plant experiments with acetate and hydrolysate substrates. Of these, there is sufficient data presented to use three ("A", "B" and "C") of the six acetate batch tests reported to calculate anoxic yield values. For the hydrolysate batch tests, since calculating an anoxic yield with hydrolysate would require accepting an underlying assumption that all of it is RBCOD when in fact some soluble COD might not be readily biodegradable, the hydrolysate tests were not considered for this review. By graphical interpretation, the three acetate batch tests utilised 1.42, 2.0 and 9.0 mgNO_3-N/ℓ for respective substrate concentrations of 5.4, 13 and 52.4 mgCOD/ℓ in the batch reactors. By applying Eq.(1.5), this gives corresponding $Y_{H,NO}$ values of 0.25, 0.56 and 0.51 mgCOD/mgCOD, respectively. Of these tests, however, the authors note that due to the low sampling frequency in the batch tests, precise determination of the denitrification profiles were difficult in some cases. In particular, with respect to denitrification batch tests A and B, a transition was expected between the initial, rapid ("K_1") and the second slower, endogenous ("K_3") denitrification rates. However, due to the low sampling frequency, this transition could not be precisely identified so that improved estimations of the linear fits to the denitrification profiles were not possible. In the calculation of the yield value, this is important since it determines the NU for RBCOD utilization. Therefore, only batch test C was retained and batch tests A and B were rejected. On this basis, the estimated $Y_{H,NO}$ with acetate is 0.51 mgCOD/mgCOD, which compares well with that determined theoretically in *Appendix A* and by Orhon *et al.* (1996), and gives an anoxic:aerobic yield ratio of 0.76 with respect to the conventionally accepted aerobic value of 0.67 mgCOD/mgCOD.

Copp and Dold (1998), in investigating reduced sludge production under anoxic versus aerobic conditions, performed aerobic and anoxic batch tests using various defined, fully soluble substrates with pure cultures of *Pseudomonas denitrificans* as

well as with activated sludge mixed liquor from full-scale treatment plants. In the mixed liquor batch tests, 60 mℓ of mixed liquor was combined with 1040 mℓ substrate medium for a final batch test volume of 1.1ℓ. In the *P. denitrificans* tests, 200 mℓ of culture medium was first inoculated with a colony from an agar plate, placed in a reciprocating shaker and incubated at room temperature (~22 °C) for 12 – 48 hours before the tests. After this period, the 200 mℓ of grown culture was transferred to the batch test apparatus and brought up to the final volume of 1.1ℓ with fresh substrate medium. The batch reactors were relatively complex, and comprised three-necked round bottom flasks stoppered at each neck with accesses only for pH, DO and ORP probes, and gas pressure measurement. pH was controlled automatically with a 3% phosphoric acid solution, and maintained at ~7.5. From the graphical presentation of "one typical example" of an anoxic batch test with *P. denitrificans* on citrate substrate, the data suggest that the soluble substrate concentration (S_s) in the reactor is ~616.7 mgCOD/ℓ, and that the nitrate utilised (NU) ~91.7 mgNO_3-N/ℓ. Applying Eq.(1.5), this gives $Y_{H,NO}$ = 1 – 2.86*(91.7)/616.7 = 1 – 0.425 = 0.575 mgCOD/mgCOD, which gives an anoxic:aerobic yield ratio of 0.86 with respect to the conventional aerobic yield of 0.67 mgCOD/mgCOD; both of these values are reasonably close to the theoretical estimates (*Appendix A*, Orhon *et al.* 1996). Unfortunately, the raw data for the remaining tests are not available for similar examination.

Ubay Çokgör *et al.* (1998) performed parallel anoxic and aerobic batch tests to investigate oxygen utilisation rate (OUR) and nitrate utilisation rate (NUR) measurements in characterising the RBCOD content of various substrates. Synthetic substrates and mixtures of different municipal and industrial wastewaters were used. For the various substrates, they performed anoxic and aerobic 1ℓ batch tests with biomass previously acclimatised to the same substrate in a fill-and-draw (F/D) reactor operated in an anoxic-aerobic sequence (pH 7-8) at a sludge age (R_s) of 7 – 10 days. They report a total of 16 batch tests, and noted that the RBCOD concentrations determined by NUR measurements were consistently higher than those calculated by the OUR, giving an average NUR to OUR determined RBCOD ratio of 1.14 using the same "standard" yield coefficient of 0.45 gVSS/gCOD for both anoxic and aerobic batch tests. Accepting that the RBCOD concentration in each test was the same, they concluded that the yield coefficient must be less in the anoxic tests compared with the corresponding aerobic tests, and derived a value for $Y_{H,NO}$ = 0.37 mgVSS/mgCOD for the accepted $Y_{H,AE}$ = 0.45 mgVSS/mgCOD. Using a value of f_{cv} = 1.42 mgCOD/mgVSS, they determined equivalent anoxic and aerobic yields of 0.53 and 0.64 mgCOD/mgCOD, respectively. This gives an anoxic:aerobic yield ratio of 0.83, which compares well with the theoretical estimates (*Appendix A*, Orhon *et al.* 1996).

Moser-Engeler *et al.* (1998) performed anoxic batch tests to investigate the use of readily biodegradable substrates, particularly defined short chain fatty acids (SCFA) and dissolved fermentation products from mixed waste and primary sludges, to increase denitrification rates in a BNR process. In the study, they determined an average anoxic yield of 0.57 mgCOD/mgCOD for dissolved fermentation products, which gives a corresponding anoxic:aerobic yield ratio = 0.85 with the accepted standard $Y_{H,AE}$ = 0.67 mgCOD/mgCOD. This compares well with the theoretical estimations (*Appendix A*, Orhon *et al.* 1996).

Sperandio *et al.* (1999) developed a method in which the carbon dioxide evolution rate (CER) was measured by infrared analysis and used in conjunction with a modelling technique, to investigate characterisation of OHO biomass under anoxic conditions. In the study, with this method yield coefficients were determined in anoxic and aerobic batch tests (pH controlled to ~7.2) with acetate, glucose and acetic acid/starch synthetic substrates. Biomass for the aerobic tests was obtained from a full-scale wastewater treatment plant, while mixed anoxic-aerobic tests were performed with biomass from a denitrifying two-stage pilot plant. For the three types of synthetic substrates, they determined anoxic yields (weighted average) of: 0.45, 0.57 and 0.51 gC/gC, respectively. Corresponding aerobic values (weighted average) were: 0.54, 0.67 and 0.663 gC/gC, respectively. This gives respective anoxic:aerobic yield ratios of: 0.83, 0.85 and 0.77 for acetate, glucose and acetic acid/starch substrates. With the exception of the acetic acid/starch mixed substrate, these ratios compare well with the theoretical values determined in *Appendix A* and by Orhon *et al.* (1996)

2.4 VALUE FOR ANOXIC YIELD IN ACTIVATED SLUDGE MODELS

In the current steady-state design models for N removal (WRC, 1984) and N and P removal (e.g. Wentzel et al., 1990; Maurer and Gujer, 1994), the heterotroph aerobic and anoxic yield coefficients are assumed to have the same value. Similarly, in the IWA Task Group models for activated sludge systems, ASM1 (Henze *et al.*, 1987), ASM2 (Henze *et al.*, 1995) and ASM2d (Henze et al., 1999), and similar (e.g. Dold *et al.*, 1991; Wentzel *et al.*, 1992), the heterotrophic yield coefficient is assumed to have the same value under anoxic as under aerobic conditions.

More recently, the requirement for a reduced anoxic yield relative to its aerobic counterpart has been recognized in the development of kinetic simulation models for activated sludge systems. Barker and Dold (1997) presented a kinetic model for BNR activated sludge systems which incorporated separate values for the aerobic and anoxic yield coefficients. Initially the two parameters were assigned the same value (0.666 mgCOD/mgCOD), but subsequently this was changed in implementation of the model as the BIOWIN computer program (Envirosim, 2001). The anoxic value was first 0.403 mgCOD/mgCOD, but ultimately changed to 0.54. This latter value gives an anoxic:aerobic yield ratio of 0.806 for the conventionally accepted standard aerobic yield of 0.67 mgCOD/mgCOD, which compares favourably with the theoretical estimates (*Appendix A*, Orhon *et al.*, 1996).

Similarly, the necessity for a reduced anoxic yield was also recognised and included in ASM3 (Gujer et al., 1999; Henze et al., 2000). In this model all substrate utilization proceeds via intracellular COD storage, with the stored substrate product serving as the COD source for heterotrophic growth. Both storage and growth processes have individual yield values, both of which differ for anoxic versus aerobic conditions. For the storage processes the aerobic and anoxic yield values are, respectively, 0.85 and 0.80 mgCOD/mgCOD, and for the growth processes 0.63 and 0.54 mgCOD/mgCOD, respectively. This gives net aerobic and anoxic yield values of 0.54 and 0.43 mgCOD/mgCOD respectively, with a corresponding net anoxic:aerobic yield ratio of 0.80. No guidance is given on the source of these values, however, except that it is accepted that the anoxic:aerobic energy yield ratio is 0.70.

It is stated that these "values (and values for ASM3 constants in general) are provided as examples and are not part of ASM3" (Gujer *et al.*, 1999). Nonetheless, the net anoxic:aerobic yield ratio (0.80) obtained from the given values compares favourably with that predicted theoretically (*Appendix A*, Orhon *et al.* 1996).

2.5. SUMMARY

In summary, several studies lend support to theoretical predictions that the ordinary heterotrophic cell yield is reduced under anoxic conditions as compared to aerobic conditions (Table 2.2). From this experimental data, excluding the values obtained by McClintock *et al.* (1988), the average anoxic cell yield coefficient can be calculated as approximately 81 ± 3.5% of its corresponding aerobic value, or about 0.54 mgCOD/mgCOD (range 0.52 – 0.57) with respect to the conventionally accepted standard aerobic yield of 0.67 mgCOD/mgCOD.

However, these studies contain several limitations. Only a few of the studies specifically focussed on measuring $Y_{H,NO}$ with respect to $Y_{H,AE}$ (e.g. Copp and Dold, 1998; Sperandio *et al.*, 1999); some addressed anoxic correction factors commonly applied in activated sludge modelling (e.g. Orhon et al., 1996), or addition of external carbon sources to accelerate denitrification rates (e.g. Isaacs and Henze, 1995; Moser-Engeler *et al.*, 1998), or characterisation of wastewater RBCOD (e.g. Ubay Çokgör *et al.*, 1998). Furthermore, most studies were performed with artificial (synthetic) substrates (e.g. Isaacs and Henze, 1995; Sperandio *et al.*, 1999) and/or mixed industrial-domestic wastewaters (e.g. Ubay Çokgör *et al.*, 1998). In addition, some studies were performed with pure cultures of a specific strain of denitrifying organism (Copp and Dold, 1998) or with NDBEPR mixed cultures (e.g. Isaacs and Henze, 1995; Moser-Engeler , 1998). The former introduces uncertainty on the repeatability for a different pre-selected organism, while the latter introduces unquantifiable uncertainty because of (i) the relatively high inorganic content of the sludge biomass, and (ii) possible loss of RBCOD due to sequestration (rather than utilization) by non-denitrifying PAO's in anoxic environments (Barker and Dold, 1996), or (iii) contribution of PAO's to denitrification (e.g. Hu *et al.*, 2000, 2002) possibly on stored substrate. Furthermore, the studies focussing primarily on the rates of denitrification typically do not report on the relative utilizations of nitrate and substrate COD necessary to calculate the observed biomass yield; thus, while instructive on denitrification kinetics, they do not lend experimental data useful to the examination of reduced OHO yield under anoxic conditions. Though the more recent models do make provision for reduced heterotroph anoxic yield values, the actual values find their origins more in the theoretical estimations than direct substantive experimental evidence. ***Thus, lacking in the current body of research on $Y_{H,NO}$, are any studies and experiments to directly quantify or measure $Y_{H,NO}$ using sewage as substrate.***

Accordingly, the principle aim of this study is to investigate and quantify the ordinary heterotrophic organism (OHO) cell yield under anoxic conditions relative to its value under aerobic conditions with municipal sewage as substrate. In terms of this aim, specific objectives identified are:

1. Determine the ratio $Y_{H,NO}$:$Y_{H,AE}$ for real sewage in terms of electron acceptor (i.e. nitrate and oxygen respectively) utilization.

2. Measure $Y_{H,NO}$ and $Y_{H,AE}$ directly for known concentration of readily biodegradable (RB)COD utilized.

3. Compare experimental results with other, independent studies on real wastewater.

To eliminate the complexities arising from sludges from BEPR activated sludge systems, the investigation will be restricted to N removal sludges; projection of the information generated to BEPR sludges will be evaluated in the conclusions.

Table 2.2. Summary table of estimated reduced anoxic cell yield coefficients with respect to its corresponding value under aerobic conditions.

Source	Substrate	Biomass	Y_{AX}	Y_{AE}	Unit	Ratio
Appendix A	acetate, glucose	-	0.35	0.42	1	*(0.80)*
(Theoretical)	*(same)*	-	0.50	0.60	2	*(0.80)*
Orhon *et al.* (1996)	Municipal WW	-	*(0.53)*	*(0.67)*	2	0.79
(Theoretical)	Protein	-				0.80
	Lactate	-				0.80
	Carbohydrate	-				0.85
McClintock *et al.* (1988)	Bacto-peptone	AE/AX	0.272	0.503	1	0.54
	(adj., endog. residue)		*(0.35)*	*(0.55)*	1	*(0.64)*
Kuba *et al.* (1993)	acetate, other	NDBEPR	*(0.50)*	*(0.67)*	2	0.74
Isaacs and Henze (1995)	acetate	NDBEPR	0.51	*(0.67)*	2	*(0.76)*
Copp and Dold (1998)	citrate *(P.denitrif.)*	Pure cultr.	0.575	*(0.67)*	2	*(0.86)*
Ubay Çokgör *et al.* (1998)	defined, various	AE/AX	0.37	0.45	1	0.82
	(accepting f_{cv} = 1.42)		*(0.53)*	*(0.64)*	2	*(0.83)*
Moser-Engeler *et al.* (1998)	fermented PS	NDBEPR	0.57	*(0.67)*	2	*(0.85)*
Sperandio *et al.* (1999)	acetate	AE/AX	0.45	0.54	3	0.83
	glucose		0.57	0.67	3	0.85
	acetic acid/starch		0.51	0.66	3	0.77
ASM3 (1999, 2000)	*(Model)*	-	0.43	0.54	2	0.80
Biowin (2001)	*(Model)*	-	0.54	*(0.67)*	2	*(0.81)*

Note: Values without parentheses are reported/derived values directly from sources, while values in parentheses are obtained from subsequent calculations based on assumed/accepted quantities, e.g. the standard aerobic yield of 0.67 mgCOD/mgCOD. Also, unit designations are: 1 = mgVSS/mgCOD; 2 = mgCOD/mgCOD; 3 = gC/gC.

CHAPTER 3

MODIFIED LUDZACK-ETTINGER AND SQUARE-WAVE FED ACTIVATED SLUDGE SYSTEMS

3.1 INTRODUCTION

As described in Chapters 1 and 2, there is a theoretical basis to suggest that the ordinary heterotrophic organism (OHO) anoxic cell yield should be reduced relative to its value under aerobic conditions. However, available research on this relationship with real wastewater and activated sludge OHO biomass is limited. While the available studies do present evidence of a reduced OHO yield under anoxic conditions, most studies were performed with synthetic and/or mixed industrial-domestic wastewater substrates. Additionally, some used mixed NDBEPR sludges or pure culture strains of *Pseudomonas denitrificans*. In view of these limitations, the aim of this research is to investigate and quantify the reduced OHO anoxic yield by means of anoxic and aerobic batch tests using domestic wastewater and OHO biomass. To supply the OHO biomass for the tests and characterise the wastewater RBCOD, Modified Ludzack-Ettinger (MLE) and square-wave (SQW) fed continuous-flow systems were operated, respectively. This Chapter describes the operation and performance of these systems.

3.1.1 Research Approach

The basic research approach adopted was to run "parallel" anoxic and aerobic batch tests with the same concentration of sewage substrate and mixed-liquor from the same source. In the batch tests, the nitrate utilized (NU) and oxygen utilized (OU), respectively, were measured. From Chapter 1, Fig. 1.1, aerobic (AE) and anoxic (AX) respiration are stoichiometrically related for the same soluble substrate COD (RBCOD, S_s, S_{bs}) utilized. That is, equations quantifying RBCOD consumption in terms of OU and NU can be equated if the same RBCOD is utilized:

$$\frac{OU}{(1-Y_{H,AE})} = RBCOD \equiv S_s = \frac{2.86 * NU}{(1-Y_{H,NO})} \tag{3.1}$$

Rearranging Eq.(3.1), $Y_{H,NO}$ can be expressed in terms of OU, NU and the aerobic cell yield coefficient, $Y_{H,AE}$:

$$\therefore Y_{H,NO} = 1 - \frac{2.86 * NU}{OU} * (1-Y_{H,AE}) \tag{3.2}$$

On this basis, values for $Y_{H,NO}$ can be estimated by measuring the OU and NU in corresponding (respective) aerobic and anoxic batch tests, containing the same biomass and RBCOD concentration from the same source, provided the value for $Y_{H,AE}$ is known.

In the approach above, since OU and NU are related to *complete* utilization of RBCOD rather than its *rate* of utilization (Ekama *et al.*, 1986), exact definition of the OHO biomass is not essential. What is required is that the initial RBCOD concentration in the two corresponding batch tests is the same and that all the RBCOD is utilized. This is evident from established discussions on loading rate effects in aerobic batch tests (e.g. Ekama *et al.*, 1986; Dold *et al.*, 1991; Mbewe *et al.*, 1995): OUR profiles for the same concentration of RBCOD utilized but with different active biomass concentrations, will have the *same area* reflected in the RBCOD utilization part of the curve (OUR_{Ss}) except with *different shapes* in each case; the test with less active biomass will have an OUR_{Ss} profile that is relatively short and wide, while the test with more active biomass will have a profile that is tall and narrow (see Fig. 1.4a,b in Chapter 1). Similarly, for anoxic batch tests with the same RBCOD concentration, the NU of the RBCOD utilization part of the curve will be the same although the *rate* of utilization will differ depending on the concentration of active biomass present (see Fig. 1.4c,d in Chapter 1). Therefore, although the same biomass is required to compare corresponding OU and NU responses of respective aerobic and anoxic batch tests utilizing the same RBCOD, specific characterization of the biomass is actually not required. Consequently, complete definition of the parent systems producing the biomass for these batch experiments was not required nor performed.

In the investigation, the mixed-liquor for the batch tests initially was obtained from two laboratory scale MLE activated sludge systems operated in a parallel investigation. However, these systems could not provide the quantities of mixed-liquor required. Accordingly, the mixed-liquor source for the batch tests was switched to the Mitchells Plain Wastewater Treatment Plant (MPWWTP). However, the concentration and OHO active biomass fraction of this mixed-liquor varied considerably so that determination of the correct loading rate in the batch tests (to obtain quantifiable OU and NU) was difficult. Thus, a laboratory-scale MLE activated sludge system was set-up and operated, dedicated to providing mixed-liquor for the batch tests. Operation of this system is described in this Chapter.

Since RBCOD is eliminated as a variable by equating aerobic and anoxic respirometry [Eq.(3.1)], the concentration of RBCOD is not required to estimate $Y_{H,NO}$, provided $Y_{H,AE}$ is known (see Eq.(1.17), Chapter 1). However, this requires that the "standard" $Y_{H,AE}$ (0.67 mgCOD/mgCOD) be accepted in this study. As an independent assessment of the validity of this value, direct estimation of $Y_{H,AE}$ and $Y_{H,NO}$ needed to be performed. This was to be done by: (i) Measuring the RBCOD concentration of the wastewater added to the batch tests, and (ii) Adding known concentrations of an artificial substrate to the batch tests.

For (i) above, the wastewater RBCOD fraction was to be estimated by the simple direct flocculation-filtration method (Mbewe *et al.*, 1995) using the f_{us} (fraction unbiodegradable soluble COD) obtained in a long sludge UCT-system operated concurrently on the same sewage. This RBCOD would then be compared with the RBCOD concentration calculated with the method of Ekama *et al.* (1986) from the corresponding aerobic batch test OUR profiles accepting the standard $Y_{H,AE}$ of 0.67 mgCOD/mgCOD. If close correspondence is obtained, this indicates that the value for $Y_{H,AE}$ is reasonable, and hence $Y_{H,NO}$ also. However, during the course of the

investigation floc-filtered RBCOD estimates gave poor recoveries compared with RBCOD values obtained from the batch tests, and it was subsequently decided to operate a dedicated square-wave (SQW) fed activated sludge system (Ekama *et al.*, 1986) to estimate the wastewater RBCOD by the original method of Ekama *et al.* (1978). On this basis, independent measurement of the RBCOD in the wastewater was accepted, and evaluation of batch test determined $Y_{H,AE}$ and $Y_{H,NO}$ estimates verified.

For the artificial substrate investigations, (ii) above, known concentrations of the RBCOD sodium acetate would be added to aerobic and anoxic batch tests, and $Y_{H,AE}$ and $Y_{H,NO}$ determined from the measured OU and NU, respectively.

3.1.2 Activated Sludge Systems Operated

Thus, the steady-state laboratory-scale activated sludge systems operated in this investigation were:

- Long sludge age UCT – this system was operated simply to provide an estimate of f_{us} from the filtered effluent COD, required for the flocculation-filtration method to determine RBCOD; consequently details of operation are not reported.
- Long sludge age MLE – used to provide the source of sludge for the batch tests and estimates of f_{us}.
- Short sludge age SQW – used to quantify RBCOD biologically.

Details on the latter two systems are reported in this Chapter.

3.2 MODIFIED LUDZACK-ETTINGER (MLE) SYSTEM DESCRIPTION

An MLE activated sludge system was operated at laboratory-scale to provide the source mixed-liquor for the anoxic and aerobic batch tests. Schematic layout and configuration of the MLE system is shown in Figs. 3.1 and 3.2. The MLE system consisted of an anoxic reactor (25% of the total system volume), an aerobic reactor (75% of the total system volume) and a secondary settling tank (SST), all in series with an underflow recycle (s-recycle) from the SST to the anoxic reactor of 1:1 and from the aerobic reactor to the anoxic reactor (a-recycle) of 1:1. All the recycle ratios are given with respect to the influent flow (Q_i).

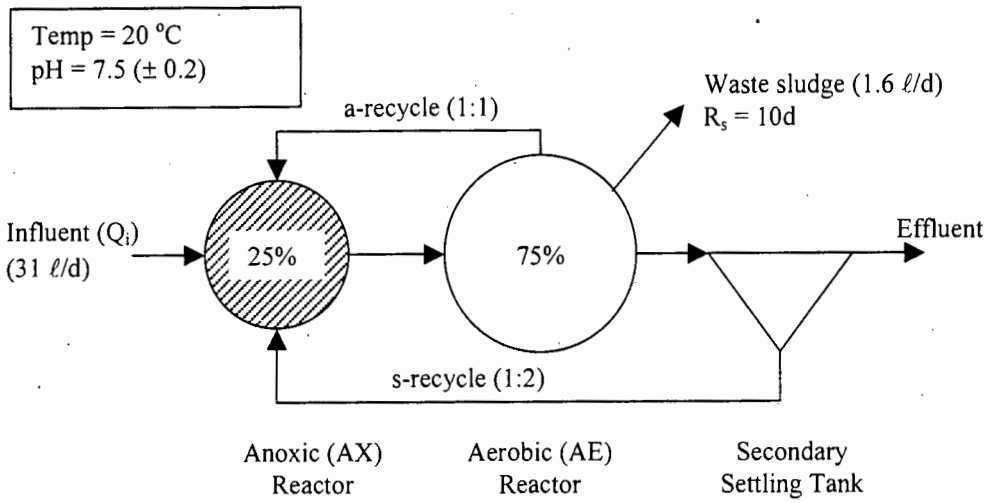

Fig. 3.1: Schematic layout of parent laboratory-scale Modified Ludzack-Ettinger (MLE) anoxic/aerobic activated sludge system.

As detailed by Clayton *et al.* (1989), all process vessels used in the system were constructed of clear cylindrical Perspex (~5 cm thick), with approximate dimensions (ht. x dia.): anoxic reactor, 41 x 19; aerobic reactor, 47 x 21; and SST, 45 x 6 cm. The contents of the anoxic and aerobic reactors were completely mixed by means of a motor driven paddle mixer (~100 rpm), mounted centrally on the lid of the reactor. To prevent hydraulic short-circuiting, each reactor was equipped with a pair of vertical side wall baffles situated opposite each other and extending about 2 cm into the bulk solution. The aerobic reactor had two paddles fitted to the mixing shaft, one situated at the bottom and one ~1 cm above it. They were positioned to ensure complete suspension of the reactor contents while avoiding turbulence at the liquid surface to minimise air entrainment into the bulk solution. The anoxic reactor had a smaller process volume and was fitted with a single paddle located at the bottom of the mixing shaft. In addition, hollow spherical balls were floated on its liquid surface to prevent oxygen exchange at the air/liquid interface. The lid to each reactor was equipped with two small (~5 cm dia.) circular access holes to allow for placement of a DO probe and in-situ sample retrieval. The second access was also used for routine brushing of the inside walls of the reactor to return any attached particulates to the bulk solution. Each reactor had a single inlet and outlet situated about 10 cm apart on its bottom plate. The process volume was maintained in each reactor by placing the outlet overflow tube at a desired overflow level on an adjustable vertical slide attached to the outside wall of the reactor. Aeration in the aerobic reactor was provided by low-pressure compressed air entering the reactor through a small bore Perspex tube that terminated in a small-bubble diffuser at the bottom of the tank. The air flowrate was controlled manually by throttling the air supply valve and adjusting a hose-clamp on the air-line entering the reactor. The dissolved oxygen concentration in the aerobic reactor was maintained at ~4.5 – 6.5 mgO/l, and was checked regularly with a YSI Model 5739 DO probe and HiTech Microsystems OUR meter (Randall *et al.*, 1991).

The SST was a vertically inclined tube at 60° to the horizontal, fitted with a motor driven (~1 rpm) wiper blade rotating ¼ turn every minute to reduce attached growth on the inside wall and release any nitrogen gas from possible denitrification in the settled sludge. Secondary sludge from the aerobic reactor entered the SST at the bottom to facilitate settling, while clarified effluent overflowed at the top and was collected in an effluent bucket. The s-recycle was drawn from the bottom of the SST and pumped to the anoxic reactor. All pumped flows in the system were by means of a multiple channel peristaltic pump, with flow rate controlled by timers switching the pump on and off to maintain a constant average daily flowrate (for further details, see Burke *et al.*, 1986). Unit processes in the system were connected by soft PVC or silicone tubing (~5 – 15 cm dia.).

The process volume (V_p) for the MLE system totalled 16ℓ, and was divided into 4ℓ anoxic and 12ℓ aerobic to give an unaerated mass fraction (f_x) of 4/16 = 0.25. The system was operated at a sludge age (R_s) of 10 days by maintaining a wasting rate (Q_w) of 1.6 ℓ/d. Waste sludge was removed once per day (batchwise) from the aerobic reactor at the end of the daily feed cycle. The influent COD load to the system was at a flowrate (Q_i) of 31 ℓ/d with target COD concentration (S_{ti}) of 500 mgCOD/ℓ, to give a target mass loading rate of 15500 mgCOD/d.

3.3 SQUARE-WAVE (SQW) FED SYSTEM DESCRIPTION

To quantify the sewage RBCOD concentration, following the method of Ekama *et al.* (1986), a single reactor square-wave (SQW) fed activated sludge system was operated at short sludge ages. A schematic layout of the SQW system is shown in Fig. 3.3. The SQW system comprised a single reactor and SST constructed and equipped in the same way as for the MLE system (above). The reactor dimensions were approximately (ht. x dia.) 40 x 18 cm, with a total system process volume V_p = 6.7ℓ. A short sludge age of 3 days was maintained by wasting batchwise 2.2 ℓ/d from the reactor at the end of each day's feed cycle.

Unlike the MLE system, however, the SQW system was operated in a 12h-ON/12h-OFF feed pattern, with an effective influent flowrate (Q_i) of 18ℓ/0.5d = 36 ℓ/d. The flowrate was measured by feeding a total of 20 ℓ/d day and subtracting the volume remaining after the 12h feed cycle from the 20ℓ initially fed; the difference constituted the actual volume fed during the 12h-ON period. Besides measuring the RBCOD fraction in the influent wastewater, the SQW system was also intended as a possible source of mixed-liquor for the batch tests, and therefore had an anoxic (unaerated) condition imposed on it for the first 4 hours after the start of the feed cycle each day. To avoid nitrate limitation, excess nitrate was added as 40 mℓ of a concentrated KNO_3 solution (38 gKNO_3/ℓ, ~5.2 mgNO_3-N/mℓ) directly to the reactor at the start of the feed cycle. The influent COD load to the system was at an effective Q_i = 18 ℓ/0.5d = 36 ℓ/d and target COD concentration (S_{ti}) of 500 mgCOD/ℓ, for a target mass loading of 18000 mgCOD/d. The system was operated with a 1:1 recycle ratio with respect to the influent flow, which was also terminated when feed pumping stopped at the end of the 12h feed period

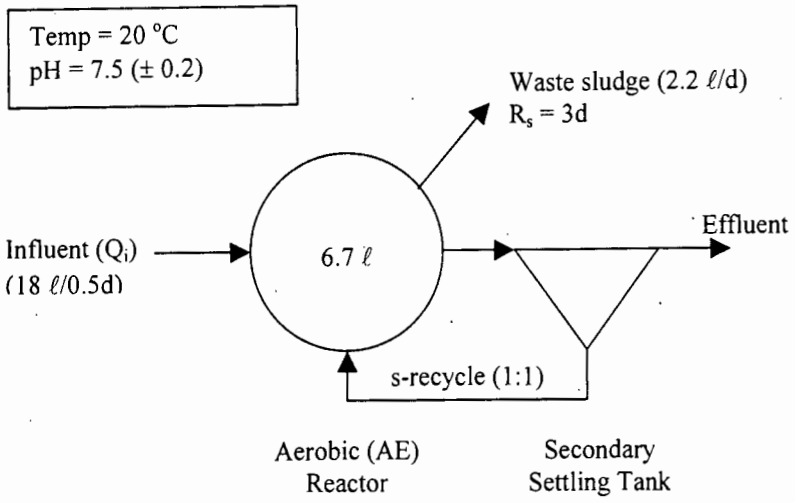

Fig. 3.2: Schematic layout of square-wave (SQW) fed flow-through activated sludge system for measuring wastewater RBCOD fraction.

The oxygen utilization rate (OUR) in the reactor was measured continually and automatically using the technique detailed by Randall *et al.* (1991): A DO probe (YSI Model 5739) was placed in the activated sludge mixed liquor and connected to an automatic DO meter/OUR data logger (HiTech Microsystems), which controlled reactor aeration between high and low DO setpoints via a solenoid valve. When the DO content in the mixed-liquor reached the low setpoint (≤2.5 mgO/l), the solenoid valve was opened and the reactor contents aerated. When the DO in the bulk solution reached the high setpoint (≥5.0 mgO/ℓ) the air was switched off automatically and the decrease in DO with time was monitored. When the DO reached the low setpoint again, the aeration was automatically switched on and the cycle repeated. During each air-off period in the cycle, the slope of the DO-time data was calculated by linear regression to give the OUR at that time index, which, along with the correlation coefficient, temperature and time, was stored in the meter. The OUR results for each day's feed cycle were downloaded from the DO meter to a PC the following day. The data was imported into a spreadsheet program where it was plotted and the RBCOD fraction of the wastewater calculated. The DO meter and probe were routinely calibrated.

3.4 WASTEWATER COLLECTION AND STORAGE

The influent wastewater used in the study was raw (unsettled) sewage from the Mitchells Plain Wastewater Treatment Plant (MPWWTP) in Cape Town, South Africa. This wastewater is mainly domestic with a small (<25%) industrial component. The wastewater was collected in approximately 2000ℓ batches from the main inlet channel at the head of the works, just upstream of the influent screw lift pumps and before screening (coarse and fine) and grit removal. The collected wastewater was brought to the laboratory by tanker-truck and, while being agitated

with high-pressure compressed air, was dispensed by gravity through an in-line macerator into individual 400ℓ stainless steel tanks in the laboratory's 4 °C cold room. The sewage batch was stored in this way for approximately 10 – 14 days after which it was discarded and a new sewage batch collected. Experience in the UCT laboratory has shown that storage of sewage for longer than 3 weeks led to septicity (hydrogen sulphide accumulation) in the cold room tanks and non-representative changes in the sewage characteristics. Immediately after storage in the cold room, a COD test was done on the new sewage to determine the necessary dilution for feed preparation for experimental systems operated in the laboratory. Typically, undiluted raw sewage COD from MPWWTP ranges between 1000 – 1500 mgCOD/ℓ.

3.5 FEED PREPARATION

The target total influent COD (S_{ti}) for the MLE and SQW systems were identical at 500 mgCOD/ℓ. Knowing the total COD of the raw sewage batch, daily feed batches at the target influent COD concentration were prepared by dilution of the raw sewage with tap water. For example, if the daily feed volumes for the MLE and SQW systems were 20 and 31ℓ (51ℓ total) respectively, and the raw sewage batch COD was 1000 mgCOD/ℓ, then the required dilution would be 500/1000 = 0.5, ⇒ the required feed volume mix would be 0.5*(51) = 25.5ℓ raw sewage + 25.5ℓ tap water.

Raw sewage was drawn from the tanks in the cold room via a valved outlet pipe at the bottom of each tank. Before dispensing the daily volume of raw sewage, the contents of the tank were vigorously stirred to resuspend settled particulates. The wastewater was drawn through the valved outlet pipe and passed over a coarse (1mm) sieve to trap large bits of debris that could clog the plastic tubing of the laboratory systems. An excess volume was usually drawn to allow for abstraction of a 1ℓ sample for floc-filtered analysis for RBCOD estimation (see later). Then, slightly more than the required volume (e.g. 25.5ℓ) raw wastewater was measured out in a graduated bucket to allow for retrieval of a small (~200mℓ) sample for later analysis. The wastewater was then poured into a 100ℓ plastic drum where it was mixed with a tablespoon of sodium bicarbonate (to increase alkalinity) and the required volume of tap water (also measured by a graduated bucket).

3.6 FEEDING THE SYSTEMS

Once the common feed mix had been prepared, 20ℓ were removed and added to the daily feed tank of the SQW system, from which a small (~200mℓ) sample was drawn for subsequent analysis. The remainder of the feed mix was poured into the feed tank of the MLE system after a small sample (~200mℓ) had also been taken. The feed tanks for the MLE and SQW systems were relatively small (~30ℓ), cylindrical PVC buckets maintained upright in a chest refrigerator at ~4 – 8 °C to minimise biological activity in the sewage during the daily feed cycle. The contents were continuously stirred at ~10 rpm by paddle mixers to keep particulates in suspension and the sewage completely mixed, but minimize air entrainment. The diluted wastewater was pumped through an outlet at the bottom of each feed tank via narrow plastic tubing to

the respective systems. The pump flowrate was intermittent and regulated by an ON/OFF timer to ensure that all the feed contents were discharged at a constant average rate over the 24h period. The feed tanks were cleaned daily with boiling water at the end of each feed cycle to remove and minimise slime growth on the inside walls of the tank. Additionally, feed tubes were cleaned regularly to eliminate blockages and prevent the growth of the filamentous organism, *S. natans*, on the inside walls of system tubing (a common occurrence with systems operated in the UCT laboratory). The feed pump was calibrated by measuring the time it took to discharge 50 mℓ of water when pumping continuously. An average of 10 measurements were converted into a pump flowrate capacity in mℓ/sec and compared with the desired daily flowrate in mℓ/min. This ratio gave the required number of seconds that the pump would need to be ON during each minute in order to achieve the desired daily rate. In this way the required ON/OFF pump timer settings were set. Although the pump flowrate was checked by ensuring that all the feed tank contents were discharged by the same time each day (e.g. 8:30am), calibration checks were also routinely performed. When it was noticed that the pump flowrate was either greater or less than that required in 24h, the timer setpoints were adjusted to decrease or increase, respectively, the number of seconds per minute that the pump would be ON. If the desired improvement did not occur, then all process vessels and tubing in the system was cleaned with boiling water (occasionally with dilute solution of sodium hypochlorite as well) and the pump recalibrated.

3.7 SAMPLING AND MEASUREMENTS

To evaluate process performance of the MLE and SQW systems, the following routine samples were taken (shown schematically in Fig. 3.3).

Undiluted Raw and Floc-Filtered Sewage Samples:
For feed preparation, an excess volume of raw wastewater was drawn from the storage tanks in the cold room, from which 1ℓ and ~200mℓ samples were taken. The 1ℓ sample was briefly (5 mins) but rapidly mixed with 10 mℓ of stock aluminium sulphate solution (50 g/ℓ $Al(SO_4)_3 \bullet 15H_2O$), allowed to flocculate for 20 minutes with slow stirring (25 rpm) and then to settle for a minimum of 30 minutes, after which the clarified supernatant was filtered through a 0.45 μm membrane filter (see Section 3.8.1 for detailed description of the procedure). The filtered sample was immediately preserved with 1 drop of mercuric chloride solution (8.6 g/ℓ $HgCl_2$) and, together with the 200mℓ sample, placed in the 4 °C cold room for later analysis.

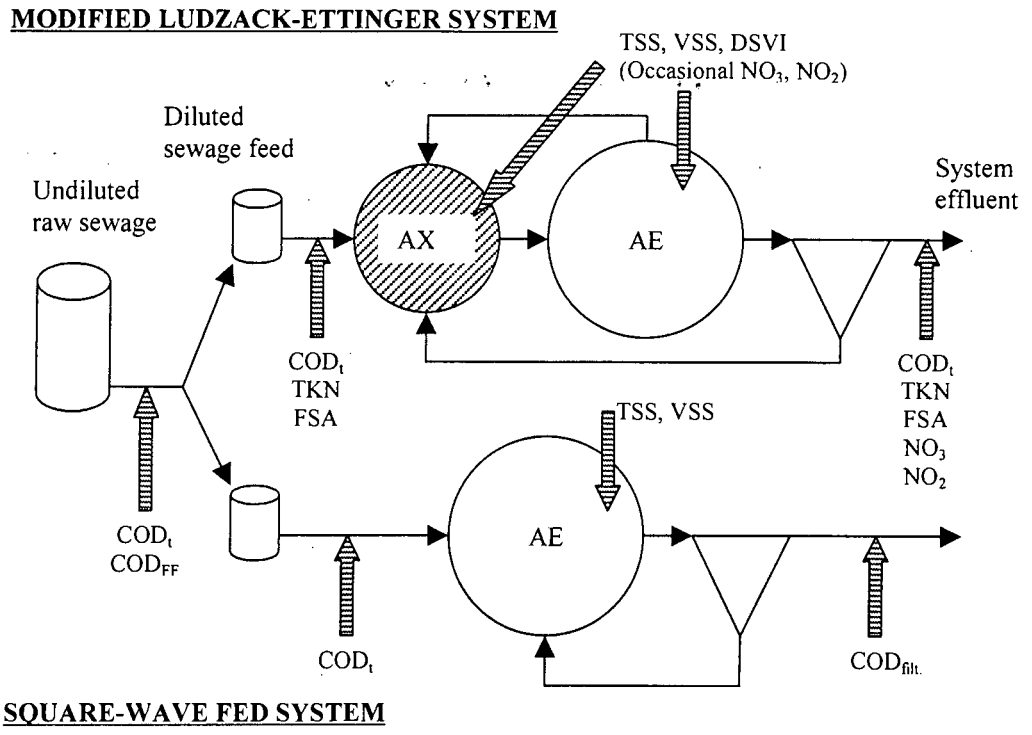

Fig. 3.3: Schematic representation of routine sampling of Modified Ludzack-Ettinger (MLE) and square-wave (SQW) fed systems.

Influent Feed Samples:

The raw sewage drawn from the cold room was diluted with tap water to achieve a target influent COD concentration of 500 mgCOD/ℓ in a total volume of 51ℓ. A tablespoon of sodium bicarbonate ($NaHCO_3$) was added to the diluted feed to add buffer and achieve a pH of ~7 – 8, and the solution was thoroughly mixed. 20ℓ of the common feed mix was dispensed into the feed bucket of the SQW system, from which a ~200mℓ sample was taken. The remaining volume was poured into the MLE feed bucket and another ~200mℓ sample taken. Both samples were then placed in the 4 °C cold room for later analysis.

Reactor Mixed-Liquor Samples:

For the MLE system, just before the end of each day's feed cycle, one 50 mℓ sample and 2 x 50 mℓ samples were taken from the anoxic and aerobic reactors, respectively. One 50 mℓ sample from each reactor was placed in 50 mℓ centrifuge tubes and centrifuged at 3500 rpm for 10 minutes. The supernatant was filtered through a 0.45 µm membrane filter and immediately preserved with 1 drop of mercuric chloride solution for later nitrate and nitrite analyses. The solids pellet in each tube was washed into ceramic crucibles for total and volatile suspended solids (TSS and VSS respectively) analyses. The remaining 50 mℓ aerobic reactor sample was placed in a 500 mℓ volumetric flask and diluted up to 500 mℓ (1:10). The mixture was poured into a domestic blender and homogenised for approximately 1 minute. The resultant solution was then analysed for COD. Additionally, a 500 mℓ sample of mixed-liquor was drawn from the aerobic reactor and diluted with secondary effluent up to 1ℓ in a graduated cylinder to measure dilute sludge volume index (DSVI, Ekama and Marais,

1984b). After sealing the top and inverting the cylinder several times, it was allowed to settle quiescently for 30 minutes after which the settled volume was read. This value (DSV_{30}) was divided by the TSS concentration of the mixed-liquor in the measuring cylinder to give the system DSVI in mℓ/g; i.e., an estimation of the volume occupied by 1g of sludge. Duplicate 50 mℓ samples were similarly taken from the SQW reactor for TSS and VSS analyses.

Effluent Samples:
At the end of the day's feed cycle, a sample of secondary effluent was drawn from the effluent bucket of each system. The samples were filtered through a 0.45 µm membrane filter and analysed for COD. Additionally, the MLE filtered effluent sample was preserved with 1 drop mercuric chloride solution and stored in the cold room for subsequent TKN, FSA, NO_3 and NO_2 analyses.

Summary:
In summary, the following analyses were routinely performed on system samples (shown in Table 3.1). Although all analyses refer to Standard Methods (1989), some have been adapted to suit the requirements in the UCT wastewater treatment laboratory; a detailed description is obtainable from the laboratory manager.

1. COD — Chemical oxygen demand, open reflux method; 5220(B)
2. TKN — Total organic nitrogen (kjeldahl), micro-kjeldahl method; 4500-N_{org}(C)
3. FSA — Ammonia nitrogen, titrimetric method; 4500-NH_3(B), (E)
4. NO_3 — Hydrazine reduction (Technicon Auto-Analyser); 4500-NO_3^-(H)
5. NO_2 — Hydrazine reduction (Technicon Auto-Analyser); 4500-NO_2^-(H)
6. TSS — Total suspended solids dried at 103-105 °C; 2540(D)
7. VSS — Volatile suspended solids ignited at 600 °C; 2540(E)
8. ISS — Inert (fixed) suspended solids ignited at 600 °C; 2540(E)
9. DSVI — Dilute sludge volume index; (Ekama and Marais, 1984b), 2710(D)
10. OUR — Oxygen utilization rate; automated (Randall *et al.*, 1991), 2710(B)
11. pH — pH meter, Hanna Instruments model HI9023; 4500-H^+(B)

Table 3.1: Summary of routine sampling and analysis performed on MLE and SQW continuous-flow systems.

Analysis	Undil. Raw	MLE Inf.	MLE AX	MLE AE	MLE Eff.	SQW Inf.	SQW AE	SQW Eff.
COD	■ ❑	■		■	○	■		○
TKN		■			○			
FSA		○			○			
Nitrate			(○)	(○)	○			
Nitrite			(○)	(○)	○			
TSS			▲	▲			▲	
VSS			▲	▲			▲	
ISS			▲	▲			▲	
DSVI				●				
OUR							◆	
pH	◆	◆	◆	◆	◆	◆	◆	◆

■ Total ❑ Floc-filtered ▲ Centrifuged pellet ◆ In-situ reading
(○) Occasional ● Direct measurement ○ Membrane (0.45 µm) filtered

3.8 RBCOD MEASUREMENT

As discussed previously, RBCOD is an essential parameter in this research. Although not explicitly required to estimate $Y_{H,NO}$ from equivalent aerobic and anoxic batch tests provided $Y_{H,AE}$ is known, the RBCOD concentration is required to determine $Y_{H,NO}$ and $Y_{H,AE}$ directly and independantly. The wastwater RBCOD fraction was measured independently by both flocculation-filtration and a short sludge age square-wave (SQW) fed activated sludge system (Fig. 3.3). These methods are described below.

3.8.1 Flocculation-Filtration Method

The flocculation-filtration method to measure RBCOD used in this investigation is based on the modified method by Mbewe *et al.* (1995). Noting its critical role in activated sludge theory and design, Mbewe *et al.* conducted a comprehensive evaluation of different methods to quantify wastewater RBCOD. In particular, the original flocculation-filtration method of Mamais *et al.* (1993) was successfully modified by Mbewe *et al.* to use aluminium sulphate ("alum", 50 g/ℓ $Al(SO_4)_3 \bullet 15H_2O$) instead of zinc sulphate for flocculating the larger, colloidal molecules in the wastewater; i.e., to enable subsequent separation from truly soluble constituents by 0.45 μm membrane filtration. It was shown that pH adjustment was no longer necessary since addition of the alum reduced the solution pH to ~6.0 – 6.3 which is close to the optimum for alum flocculation. A COD analysis of the floc-filtered (FF) filtrate provided an estimate of the soluble COD (biodegradable + unbiodegradable) in the wastewater. The RBCOD fraction was obtained by substracting the unbiodegradable soluble COD of the wastewater, as determined in a long sludge age activated sludge system (Marais *et al.*, 1976), from the flocculated filtered COD.

Floc-filtered (FF) samples of raw, undiluted sewage were analysed daily for each sewage batch, as well as for wastewater used in the batch tests. As previously described, an excess volume of raw wastewater was drawn from the storage tanks in the cold room, from which 1ℓ was measured in a graduated cylinder. The sewage was transferred to a glass beaker and 10 mℓ alum stock solution (50 g/ℓ $Al(SO_4)_3 \bullet 15H_2O$) added. A magnetic stir-bar was placed in the beaker and the 1ℓ sample rapidly mixed (~250 rpm) for 5 minutes on a magnetic stirrer. The mixing speed was then reduced to ~25 rpm to flocculate for 20 minutes, after which it was stopped completely and allowed to settle for a minimum of 30 minutes. The supernatant was then filtered through a 0.45 μm membrane filter and the COD measured shortly thereafter, or immediately preserved with 1 drop of mercuric chloride and placed in the cold room for later COD analysis. The RBCOD concentration in the undiluted raw wastewater was estimated as follows:

$$RBCOD_{FF} = COD_{total\ soluble} - COD_{unbiod.\ soluble} = COD_{FF} - f_{us} * S_{ti,R} \qquad (3.6)$$

which, expressed as a fraction of the total COD is:

$$f_{ts,FF} = \frac{RBCOD_R}{S_{ti,R}} \qquad (3.7)$$

where:

$f_{ts,FF}$ = fraction of RBCOD with respect to total COD by floc-filtered method; COD/COD

$RBCOD_{FF}$ = RBCOD concentration in undiluted raw wastewater estimated by floc-filtration; mgCOD/ℓ

COD_{FF} = measured total soluble COD (floc-filtered filtrate) of the raw, undiluted wastewater; mgCOD/ℓ

$S_{ti,R}$ = measured total COD of raw, undiluted sewage; mgCOD/ℓ

f_{us} = S_{use}/S_{ti}, fraction unbiodegradable soluble COD in the sewage; COD/COD

S_{use} = measured COD of the filtered effluent of a long sludge age activated sludge system; mgCOD/ℓ

S_{ti} = measured total COD of (diluted) influent feed to the system; mgCOD/ℓ

3.8.2 Square-wave Fed Activated Sludge System

The short sludge age square-wave (SQW) fed system used in this study is based on the conventional "standard" method developed by Ekama and Marais (1978) to measure RBCOD. As described previously, the SQW system comprised a single aerobic completely mixed tank activated sludge system operated at a sludge age of 3 days (Fig. 3.3). Since it was initially envisaged that this system would provide source sludge for the batch tests, it was conditioned to denitrify by imposing an unaerated environment with excess nitrate for 4 hours at the start of each feed cycle, after which aeration was automatically initiated for the remainder of the day. The oxygen utilization rate (OUR) was measured continually and automatically using the technique detailed by Randall *et al.* (1991), see Section 3.3.

A schematic of a typical OUR profile for a SQW activated sludge system with a 12h-ON/12h-OFF feed pattern is shown in Fig. 3.5. The essential feature of this pattern is the precipitous drop in OUR at the end of the feed period. In terms of the UCT model (Dold *et al.*, 1980), this step change occurs as a result of cessation of OHO growth on RBCOD supplied to the system, but continued (maximum) OHO growth on SBCOD accumulated during the feed period (Ekama *et al.*, 1986). Basically, utilization of RBCOD is so rapid that practically all of it is consumed immediately upon entry into the reactor. In contrast, SBCOD utilization, although also occurring at its maximum rate, is slower than the rate of supply so that SBCOD accumulates in the system during the feed period.† When the feed flowrate is stopped, the OUR drops immediately (due to termination of the RBCOD supply) to the level of maximum

† Nitrification, if present, also occurs at its maximum rate which is less than the rate of ammonia supplied to the system (both as free and saline ammonia, and via ammonification of organic nitrogen); consequently, the OUR due to nitrification is constant and of longer duration than RBCOD utilization, so that it forms a constant background throughout the OUR step change at feed termination (see Dold *et al.*, 1991), and can be ignored in RBCOD evaluation.

utilization of SBCOD accumulated in the system. This level is sustained for a period until all the accumulated SBCOD is utilized, after which the OUR decreases noticeably to reflect only nitrification and endogenous utilization. Consequently, the ΔOUR associated with the step change at feed termination is related to the RBCOD fraction in the influent wastewater (Dold *et al.*, 1980).

From Ekama *et al.* (1986), the RBCOD in the influent is estimated as:

$$RBCOD = \frac{\Delta OUR}{(1 - Y_{H,AE})} * V_p * \left(\frac{24}{Q}\right) \qquad (3.8)$$

where:

RBCOD = RBCOD concentration in the feed; mgCOD/ℓ
ΔOUR = difference in (average) OUR plateaus defining the step change; mgO/ℓ/h
$Y_{H,AE}$ = aerobic OHO cell yield; accept standard 0.67 mgCOD/mgCOD
V_p = process volume of SQW system; 6.7ℓ
Q = effective daily flow; target 18 ℓ/0.5d ≡ 36 ℓ/d
24 = converts days to hours; h/d

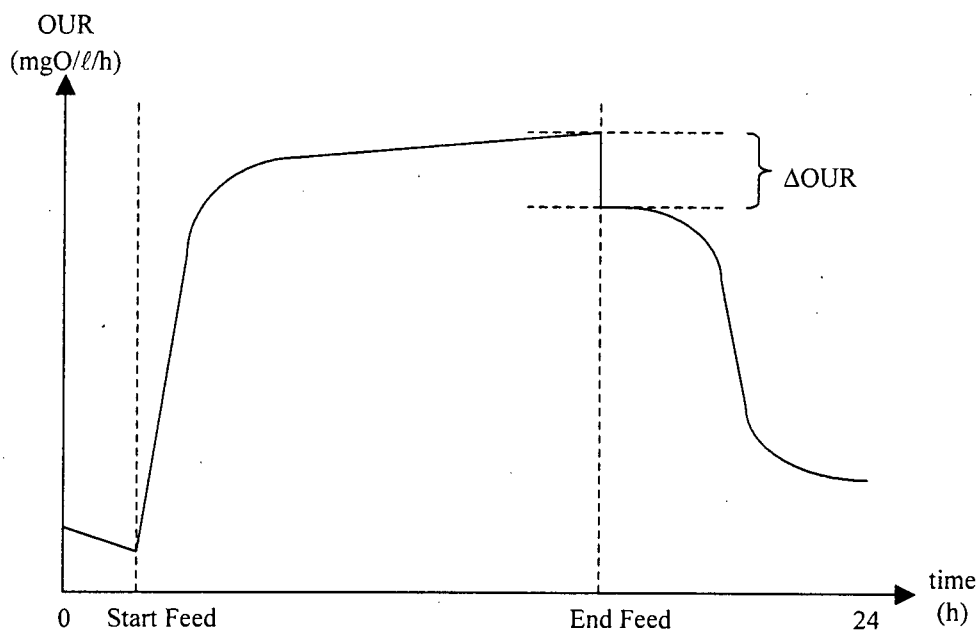

Fig. 3.5: Schematic representation of a typical feed cycle OUR profile in a short sludge age square-wave fed activated sludge system (after Ekama *et al.*, 1986).

3.8.3 Typical RBCOD Values for Mitchells Plain Wastewater

As part of an investigation on characterizing wastewater carbonaceous content, Mbewe *et al.* (1995) developed extensive estimates of the MPWWTP raw wastewater RBCOD fraction of the total COD (f_{ts}) by three different methods: (1) a square-wave (SQW) fed activated sludge system, (2) aerobic batch test respirometry, and (3) flocculation-filtration. By evaluating the sewage batch steady-state averages for outliers and analysing the remaining data on a linearized probability plot, the average f_{ts} obtained by Mbewe *et al.* (1995) for all the methods, was determined as 0.18 – 0.19 (Table 3.2):

Table 3.2: Average RBCOD as a fraction of total COD (f_{ts}) for MPWWTP raw sewage developed from Mbewe *et al.* (1995); SSD = sample standard deviation, N = number of samples where each sample is the average of a number of measurements on one batch of sewage.

Method	Average	SSD	N
SQW system	0.19	0.01	19
Aerobic Batch Test	0.19	0.02	22
Floc-filtration	0.18	0.02	19

In another study, Ekama and Marais (1978) conducted several tests with a short sludge age SQW system to validate a dynamic kinetic model for the aerobic activated sludge system, including nitrification. Of these, five tests (Table 3.3) were performed with raw Mitchells Plain sewage, with reactor conditions: $V_p = 6.73\ell$, Q = 18ℓ/0.5d, pH ~7, temperature ~20 °C, and influent COD ~500 mgCOD/ℓ. For these five tests, an average f_{ts} = 0.16 (range 0.11 – 0.21) with sample standard deviation of 0.042 was obtained.

Table 3.3: RBCOD fraction (f_{ts}) for MPWWTP raw sewage developed from Ekama and Marais (1978); S_{ti} = total COD concentration, ΔOUR is the drop in OUR on feed termination and S_{bsi} = RBCOD concentration.

Test	S_{ti} (mgCOD/ℓ)	ΔOUR (mgO/ℓ/h)	S_{bsi} (mgCOD/ℓ)	f_{ts}
L1	570	8.1	108.8	0.191
L2	535	4.5	60.7	0.113
L3	550	8.8	117.8	0.214
L4	515	5.6	75.2	0.146
L6	490	4.8	64.5	0.132

3.9 SYSTEM CONDITIONS AND STEADY-STATE PERIODS

3.9.1 Experimental Overview

As noted earlier, the MLE laboratory-scale activated sludge system was operated simply to supply equivalent biomass for corresponding aerobic and anoxic batch tests utilizing the same RBCOD; similarly, the SQW system was operated mainly to characterize the RBCOD fraction in the wastewater. Furthermore, it was shown that as long as the biomasses used in the corresponding batch tests were the same, precise definition of the conditions present in the MLE activated sludge system was not necessary. Also, to quantify RBCOD in the SQW system, the system does not have to be precisely defined (Ekama *et al.*, 1986). Accordingly, process parameters for the two systems were assessed only to monitor general process stability during the course of the investigation; these are described below. Details of the systems' configuration and operation have been described in Sections 3.2 and 3.3 (above) respectively.

The sewage used to feed the systems was collected in batches from the MPWWTP and was changed approximately every 2 weeks to prevent degradation under storage. As detailed in Table 3.4, this study included a total of 25 sewage batches over a period of 395 days, during which 40 aerobic and 42 denitrifying (anoxic) batch tests (ABT and DBT respectively) were performed. The batch test methods used were adapted from Ekama *et al.* (1986), Dold *et al.* (1991) and Mbewe *et al.* (1995), and are described in Chapter 4. During periods of absence by the writer, no testing was done on the systems, but they were maintained by postgraduate colleagues and technical staff in the Water Research Laboratory.

In the initial stages of the investigation (sewage batches 1 – 13), the wastewater RBCOD fraction was estimated by the floc-filtered method only, with the required f_{us} determined in a long sludge age UCT system operating concurrently in the laboratory on the same wastewater. Similarly, mixed liquor biomass samples for the batch tests prior to sewage batch 18 were obtained from the waste sludge of 10 and 20 day sludge age MLE systems also operating concurrently in the laboratory on the same wastewater, as well as from the MPWWTP. As will be discussed later, however, indeterminate batch test responses during these periods, including poor RBCOD recovery, motivated the subsequent decision to operate independent MLE and SQW systems dedicated to the objectives of this investigation. Only these systems are described here.

3.9.2 Steady-state Periods

Daily results for the MLE and SQW activated sludge systems are presented in *Appendix B*. As mentioned earlier, the research approach adopted did not require precise characterization of the SQW and MLE systems, so routine sampling and analyses were performed simply to monitor process performance and quantify the wastewater RBCOD fraction. Each sewage batch was accepted as a steady-state period based on the fundamental requirement that no accumulation occurs within the system at steady state; i.e. all rates and concentrations in the system should remain fairly constant with time (Davis and Cornwell, 1985; Tchobanoglous and Schroeder,

1987). System data was analysed for day-to-day consistency by evaluating each day's data within the 95% confidence interval. Each value outside this interval, i.e. outside the range mean ± 1.96*sample standard deviation, was rejected as non-representative of steady-state performance during that sewage batch (steady-state period). All remaining measurements were considered valid and averaged to represent the "average" response of the system for that sewage batch. Average fractions, e.g. f_{us}, f_i and f_{ts}, for each sewage batch were calculated as the ratio of the steady-state averages of valid daily measurements. These averages, corresponding sample standard deviations (SSD) and number of data points (N), used to characterize the general performance of the MLE and SQW systems are presented in the Sections below.

Table 3.4: Sewage batch (SB) periods and corresponding operation of long sludge age (LSA) laboratory-scale activated sludge systems to characterize wastewater unbiodegradable soluble COD fraction (f_{us}) and RBCOD for aerobic and denitrification batch tests (ABT and DBT respectively).

SB No.	Generic SB	Date		Day No.	LSA System	RBCOD Method	ABT No.	DBT No.
		From	To					
1	19/01	19/11/01	29/11/01	1-12	UCT	FF		
2	20/01	30/11/01	18/12/01	13-31	UCT	FF		
3	21/01	19/12/01	5/1/02	32-49	UCT	FF		
4	01/02	6/1/02	22/1/02	50-66	UCT	FF	1-2	1-2
5	02/02	23/1/02	13/2/02	67-88	UCT	FF		
6	03/02	14/2/02	9/3/02	89-112	UCT	FF	3-7	3-7
7	04/02	10/3/02	16/3/02	113-118	UCT	FF		
8	05/02	17/3/02	27/3/02	119-129	UCT	FF		
9	06/02	28/3/02	13/4/02	130-146	UCT	FF	8-9	8-9
10	07/02	14/4/02	29/4/02	147-162	UCT	FF	10-13	10-13
11	08/02	30/4/02	16/5/02	163-179	UCT	FF	14-19	14-19
12	09/02	17/5/02	31/5/02	180-194	UCT	FF	20	
13	10/02	1/6/02	14/6/02	195-208	UCT	FF	21-22	
14	11/02	15/6/02	2/7/02	209-226	UCT	FF/SQW		
15	12/02	3/7/02	17/7/02	227-241	UCT	FF/SQW		
16	13/02	18/7/02	1/8/02	242-256	UCT	FF/SQW		
17	14/02	2/8/02	15/8/02	257-270	UCT	FF/SQW		
18	15/02	16/8/02	30/8/02	271-285	MLE	FF/SQW	23-24	20
19	16/02	31/8/02	15/9/02	286-301	MLE	FF/SQW	25	
20	17/02	16/9/02	29/9/02	302-315	MLE	FF/SQW	26-29	21-23
21	18/02	30/9/02	16/10/02	316-332	MLE	FF/SQW	30-34	24-33
22	19/02	17/10/02	1/11/02	333-348	MLE	FF/SQW	35-37	34
23	20/02	2/11/02	20/11/02	349-367	MLE	FF/SQW	38-40	35-37
24	21/02	21/11/02	6/12/02	368-383	MLE	FF/SQW		
25	22/02	7/12/02	18/12/02	384-395	MLE	FF/SQW		38-42

3.10 MLE SYSTEM PERFORMANCE

A comprehensive listing of daily data for the MLE system is contained in *Appendix B1*, while average steady-state performance is detailed in Tables 3.5 to 3.10 below.

Table 3.5: Sewage batch (SB) average (AVG) undiluted and flocculated-filtered raw sewage COD concentrations ($S_{ti,R}$ and FFI_R, respectively), and RBCOD determined by floc-filtration method as a concentration and fraction of total COD ($Sbsi_{FF}$ and fts_{FF} respectively); also shown are sample standard deviations (SSD) and number of samples (N).

	Sti_R (mgCOD/ℓ)			FFI_R (mgCOD/ℓ)			$Sbsi_{FF}$ (mgCOD/ℓ)	fts_{FF}
SB	AVG	SSD	N	AVG	SSD	N	AVG	AVG
18	1157.6	41.0	13	256.6	17.4	12	188.5	0.163
19	1036.9	36.3	7	237.5	24.1	7	144.3	0.139
20	1094.7	58.5	12	281.1	9.2	11	184.3	0.168
21	1128.3	49.3	12	272.3	12.3	9	157.8	0.140
22	1106.7	43.4	11	270.6	9.1	8	155.9	0.141
23	1079.9	67.1	15	249.1	30.2	12	145.6	0.135
24	1092.7	64.3	14	259.1	42.3	8	160.8	0.147
25	1101.0	58.6	9	278.3	22.3	8	167.3	0.152

Table 3.6: MLE System: Sewage batch (SB) average influent (S_{ti}), aerobic reactor (AE), 0.45 μm filtered effluent (FE), and fraction unbiodegradable soluble with respect to total, (f_{us}) COD; also shown are sample standard deviations (SSD) and number of samples (N).

	Sti (mgCOD/ℓ)			AE (mgCOD/ℓ)			FE (mgCOD/ℓ)			f_{us}
SB	AVG	SSD	N	AVG	SSD	N	AVG	SSD	N	AVG
18	498.6	13.0	12				33.2	7.9	12	0.067
19	507.3	29.0	16				45.6	7.7	15	0.090
20	493.3	11.1	11				43.6	6.1	12	0.088
21	493.6	31.7	13	2857.6	170.5	5	50.1	11.9	13	0.101
22	516.1	14.3	13	2176.4	407.5	6	53.5	6.5	11	0.104
23	500.9	24.9	14	2553.9	107.7	7	48	5.3	11	0.096
24	491.5	17.8	10	2817.0	262.6	6	44.2	8.3	10	0.090
25	509.0	30.4	9				51.3	9.6	8	0.101

Table 3.7: MLE System: Sewage batch (SB) average influent (I) and 0.45 μm filtered effluent (FE) TKN and FSA concentrations; also shown are sample standard deviations (SSD) and number of samples (N).

	TKN (mgN/ℓ)						FSA (mgN/ℓ)					
	I			FE			I			FE		
SB	AVG	SSD	N	AVG	SSD	N	AVG	SSD	N	AVG	SSD	N
18	46.09	3.2	10	4.30	0.5	10	35.45	3.5	10	2.85	0.443	9
19	39.69	2.2	8	2.98	0.6	8	32.26	2.5	8	2.36	0.700	8
20	48.53	7.3	9	3.64	0.7	8	34.36	0.9	8	2.65	0.652	8
21	37.28	1.4	8	2.42	0.4	8	24.28	0.6	7	1.16	0.224	7
22	40.04	1.9	7	2.43	0.7	8	30.10	0.9	8	1.45	0.211	8
23	37.24	2.7	6	2.48	0.3	7	25.75	1.3	7	2.28	0.359	7
24	50.52	3.1	7	3.18	0.4	7	38.92	1.6	7	2.78	0.474	7
25	42.93	2.1	6	3.80	0.7	6	34.86	1.7	6	3.27	0.927	6

Table 3.8: MLE System: Sewage batch (SB) average 0.45 μm filtered effluent nitrate (NO_3) and nitrite (NO_2) concentrations; also shown are sample standard deviations (SSD) and number of samples (N).

	NO3 (mgN/ℓ)			NO2 (mgN/ℓ)		
SB	AVG	SSD	N	AVG	SSD	N
18	7.58	0.68	10	0.09	0.078	9
19						
20	14.32	1.18	9	0.00	0.000	9
21	9.98	0.35	8	0.00	0.000	8
22	14.47	1.31	9	0.16	0.1	9
23	13.25	1.11	6	0.03	0.052	6
24	20.8	0.23	9	0.00	0.000	9
25	12.77	0.41	6	0.06	0.063	6

Table 3.9: MLE System: Sewage batch (SB) average aerobic (AE) and anoxic (AX) reactor total and volatile suspended solids concentrations (mg/ℓ).

	Total Suspended Solids (mgTSS/ℓ)						Volatile Suspended Solids (mgVSS/ℓ)					
	AE			AX			AE			AX		
SB	AVG	SSD	N	AVG	SSD	N	AVG	SSD	N	AVG	SSD	N
18	2723	132	7	3080	323	7	2267	102	7	2576	208	7
19	2260	201	2	2886	127	2	1957	174	2	2502	113	2
20	2062	94	5	2595	219	5	1797	80	5	2260	203	5
21	2246	69	8	2618	253	9	1908	50	8	2238	212	9
22	1620	245	7	2029	199	8	1384	209	7	1745	162	8
23	1953	114	10	2393	140	10	1676	94	11	2052	121	9
24	2317	115	8	2667	89	7	1969	92	8	2277	73	7
25	2323	86	4	2547	124	4	1945	75	4	2143	96	4

Table 3.10: MLE System: System average total and volatile suspended solids concentrations (mg/ℓ; TSS, VSS respectively)†, and VSS/TSS (f_i) and COD/VSS (f_{cv}) ratios.

	TSS			VSS			f_i	f_{cv}
SB	AVG	SSD	N	AVG	SSD	N		
18	2812	133	7	2344	104	7	0.833	
19	2416	182	2	2093	159	2	0.866	
20	2195	109	5	1912	98	5	0.871	
21	2390	54	8	2033	39	8	0.850	1.50
22	1719	231	7	1472	195	7	0.856	1.57
23	2051	115	10	1737	130	10	0.847	1.52
24	2418	115	8	2057	91	8	0.851	1.43
25	2379	84	4	1995	73	4	0.839	

† The average solids concentration in the MLE system for each sewage batch is the average of the total mass of solids in the system divided by the total system volume; i.e., the total mass of solids in the system is the sum of the solids concentration in each reactor multiplied by its respective volume (4ℓ AX, 12ℓ AE), and the total process volume of the system is Vp = 16ℓ. The average f_{cv} ratio is determined from the average COD and VSS concentrations of the AE reactor for each sewage batch.

3.10.1 Unbiodegradable Soluble COD Fraction (f_{us})

The unbiodegradable soluble COD fraction of the influent wastewater (f_{us}) was determined from the MLE system using the method of Ekama *et al.* (1986). According to Marais and Ekama (1976), for long sludge age activated sludge systems, the unbiodegradable soluble COD in the influent wastewater (S_{usi}) is equivalent to the unbiodegradable soluble COD in the effluent (S_{use}), which is given by the COD analysis of the system filtered effluent. As a fraction of the total influent COD (S_{ti}), the S_{usi} ($\equiv S_{use}$) is, therefore, defined by the ratio:

$$f_{us} = S_{use}/S_{ti} \qquad (3.9)$$

Using Eq.(3.9), the average f_{us} for each sewage batch period was calculated from corresponding influent and filtered effluent COD averages (Table 3.6). The average f_{us} data were plotted in a linearized probability graph to check for normality (Fig. 3.6; see *Appendix F* for interpretation). One outlier was identified (sewage batch 18, f_{us} = 0.067) and rejected. Rejecting this point, the data were replotted in Fig. 3.7. Although the data exhibits slight curvature, the linear fit is reasonable indicating normality, and gives a mean f_{us} = 0.096 and sample standard deviation of 0.005 for Mitchells Plain raw wastewater. This average falls within the range of typical values expected of South African domestic sewage (0.04 – 0.10, WRC, 1984), and compares favourably with values observed by other researchers who also used Mitchells Plain raw wastewater: Cronje (2000), f_{us} = 0.085, Ubisi *et al.* (1997a,b), f_{us} = 0.09, and Mbewe *et al.* (1995), f_{us} = 0.074.

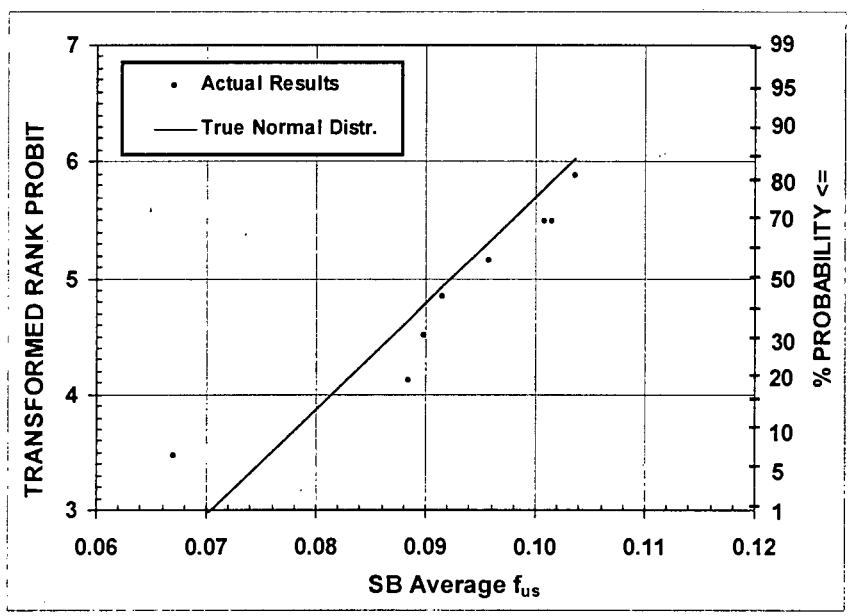

Fig. 3.6: MLE System: Linearized probability plot of sewage batch (SB) average (steady-state) unbiodegradable soluble COD fraction (f_{us}) in influent wastewater.

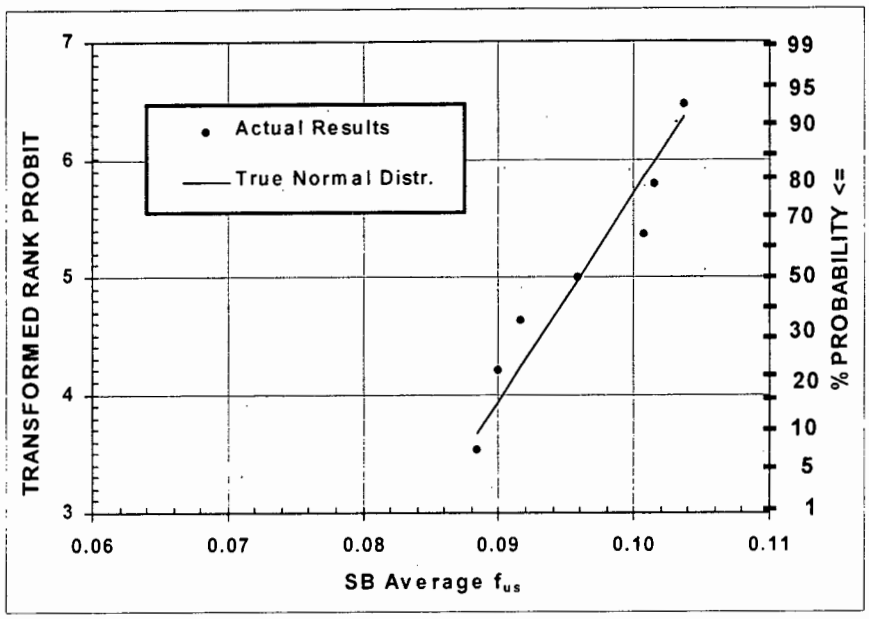

Fig. 3.7: MLE System: Revised (excluding outliers) probability plot of sewage batch (SB) average (steady-state) influent unbiodegradable soluble COD fraction (f_{us}).

3.10.2 Floc-Filtered RBCOD Fraction ($f_{ts,FF}$):

As previously discussed, Mbewe *et al.* (1995) showed that flocculation of undiluted raw wastewater with a 1:10 dose of aluminium sulphate (50 g/ℓ $Al(SO_4)_3 \bullet 15H2O$), followed by quiescent settling and subsequent membrane (0.45 μm) filtration of the supernatant, effectively separates out the truly soluble constituents of the raw wastewater. Hence, the COD of the floc-filtered (FF) filtrate (COD_{FF}, COD_{sol}) measures the total soluble COD in the influent wastewater, including unbiodegradable soluble COD. Therefore, the fraction of RBCOD in the influent wastewater can be estimated by subtracting the unbiodegradable soluble COD from the floc-filtered COD. In this manner, the average RBCOD fraction ($f_{ts,FF}$) for each sewage batch was calculated by applying the average f_{us} from the MLE system (Table 3.6) to the total and floc-filtered COD of the undiluted raw wastewater (Table 3.5). In equation form:

$$RBCOD_{FF} = COD_{FF} - f_{us}*S_{ti,R} \quad (3.10)$$

$$\Rightarrow f_{ts,FF} = RBCOD_{FF}/S_{ti,R} \quad (3.11)$$

The sewage batch average $f_{ts,FF}$ data were plotted in a linearized probability graph to check for normality (Fig. 3.8). Although no outliers were identified, the sewage batch average $f_{ts,FF}$ values do not exhibit a good fit to the true normal distribution, however, so that the mean of approximately $f_{ts,FF} = 0.148$ and sample standard deviation = 0.011 contains considerable uncertainty.

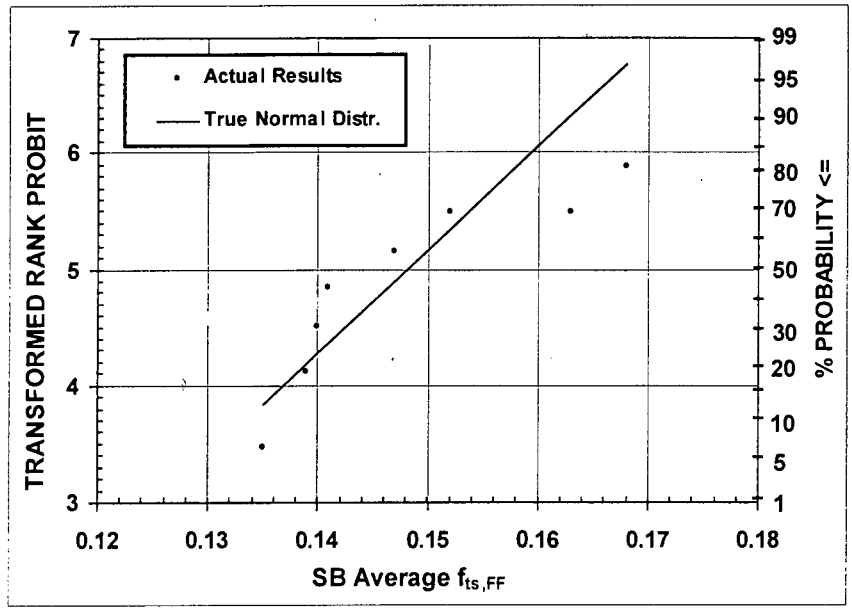

Fig. 3.8: MLE System: Statistical plot of sewage batch (SB) average wastewater $RBCOD_{FF}$ determined by flocculation-filtration, as a fraction of the total COD ($f_{ts,FF}$).

To develop an improved assessment of wastewater $f_{ts,FF}$, daily estimates (*Appendix B*, Table B1-8) were analysed on the linearized probability graph and are plotted in Fig. 3.9. The data displays a good fit to the true normal distribution, but includes two apparent outliers (0.033, 7-Oct; 0.228, 21-Oct). Analysing the data for outliers confirmed these two data as such, and they were subsequently rejected. A revised plot of the corrected data is presented in Fig. 3.10. The data retains its good fit to the true normal line, and gives a mean $f_{ts,FF} = 0.15$ and sample standard deviation = 0.022 (range 0.098 – 0.196). This compares reasonably well with the average $f_{ts,FF} = 0.18 \pm 0.02$ (range 0.14 – 0.23) determined by Mbewe *et al.* (1995) for the same wastewater.

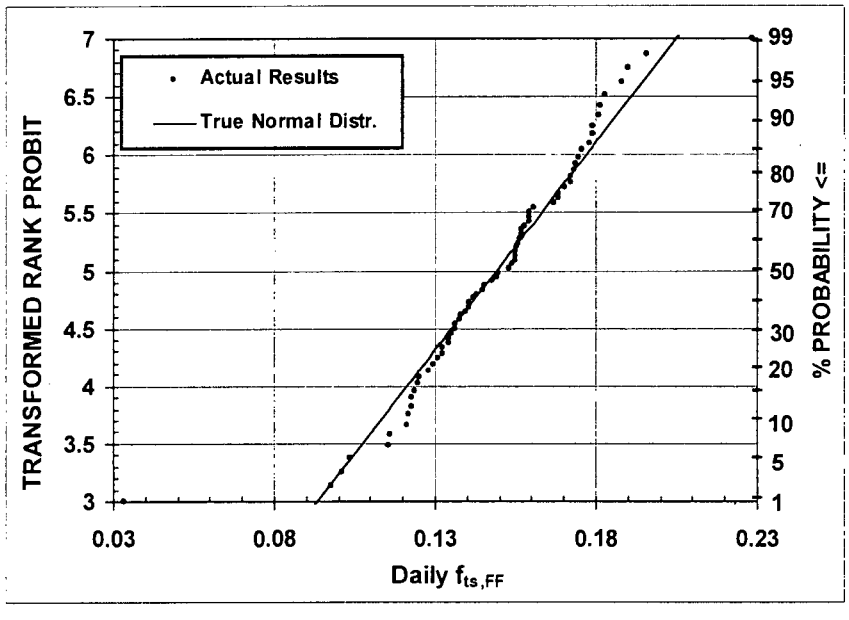

Fig. 3.9: MLE System: Statistical plot of daily estimates of undiluted raw wastewater $RBCOD_{FF}$ as a fraction of total COD ($f_{ts,FF}$).

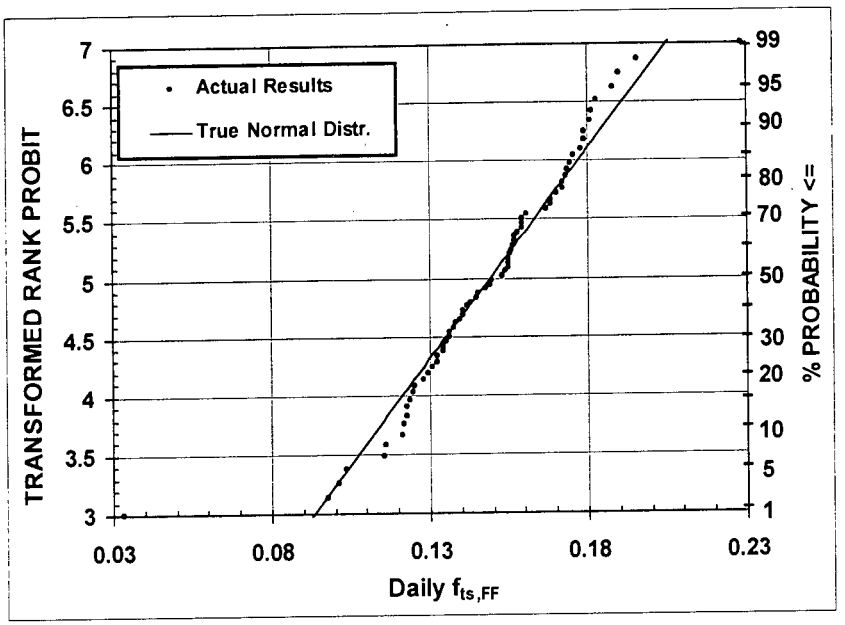

Fig. 3.10: MLE System: Revised statistical plot of daily wastewater $RBCOD_{FF}$ as a fraction of total COD ($f_{ts,FF}$), excluding 2 outliers (7-Oct, 0.033; 21-Oct, 0.228).

3.10.3 Unbiodegradable Particulate COD Fraction

Since this study was only focussed on RBCOD utilization, specific characterization of the influent wastewater unbiodegradable particulate COD fraction (f_{up}) was not required. However, since sufficient data are available, the following calculation is provided to illustrate the procedure. Using the steady-state model of Marais and Ekama (1976), the average f_{up} can be determined from the average f_{us}, f_{cv} and VSS (X_v) for each sewage batch (Tables 3.6 and 3.10) by the following equation:

$$MX_v = \frac{MS_{ti} * (1 - f_{us} - f_{up}) * Y_H * R_s}{(1 + b_H * R_s)} * (1 + f * b_H * R_s) + \left(\frac{f_{up} * MS_{ti}}{f_{cv}} \right) * R_s \qquad (3.12)$$

where:

MX_v = mass of volatile solids in the system (mgVSS)
= $X_v * V_p$

X_v = mixed liquor volatile solids concentration (mgVSS/ℓ)
= steady-state average of daily measurements (*Table 3.8*)

V_p = system process volume (ℓ)
= 16ℓ (4ℓ anoxic, 12ℓ aerobic)

Y_H = aerobic OHO biomass yield coefficient (in VSS units)
= 0.45 mgVSS/mgCOD (accept standard for steady-state f_{up} estimate)

R_s = sludge age (d) = 10 days

b_H = net specific endogenous mass loss rate coefficient (WRC, 1984)
= 0.24/d at 20 °C
f = fraction of endogenous residue generated = 0.2
f_{cv} = COD/VSS ratio of activated sludge mixed liquor
= average calculated for each sewage batch period (*Table 3.8*)
MS_{ti} = mass of influent COD fed to the system each day (mgCOD/d)
= $Q_i * S_{ti}$
Q_i = influent flowrate (ℓ/d) = 31 ℓ/d
S_{ti} = influent wastewater total COD concentration (mgCOD/ℓ)
= steady-state average of daily measurements (*Table 3.4*)

For each sewage batch, successive values for f_{up} are substituted into Eq.(3.12) until equality is obtained between the mass of VSS (MX_V) measured in the system and that theoretically predicted by Eq.(3.12); the f_{up} for which this is true is accepted as the average f_{up} for that sewage batch. The average f_{up} values calculated in this manner for each sewage batch are presented below (Table 3.11):

Table 3.11: MLE System: Sewage batch (SB) average influent wastewater unbiodegradable COD fraction (f_{up}).

SB	18	19	20	21	22	23	24	25
f_{up}	0.125	0.072	0.045	0.077	(-0.065)	0.004	0.075	0.05

The data exhibits considerable variability with four values (highlighted) lying outside the typical range of 0.07 – 0.2 expected for South African wastewaters (WRC, 1984), and one f_{up} <0! Excluding this latter value, the data are plotted with respect to a true normal distribution in Fig. 3.11; it is evident that insufficient data are available to determine f_{up} accurately. However, as noted above, the value for f_{up} is not of consequence in this research.

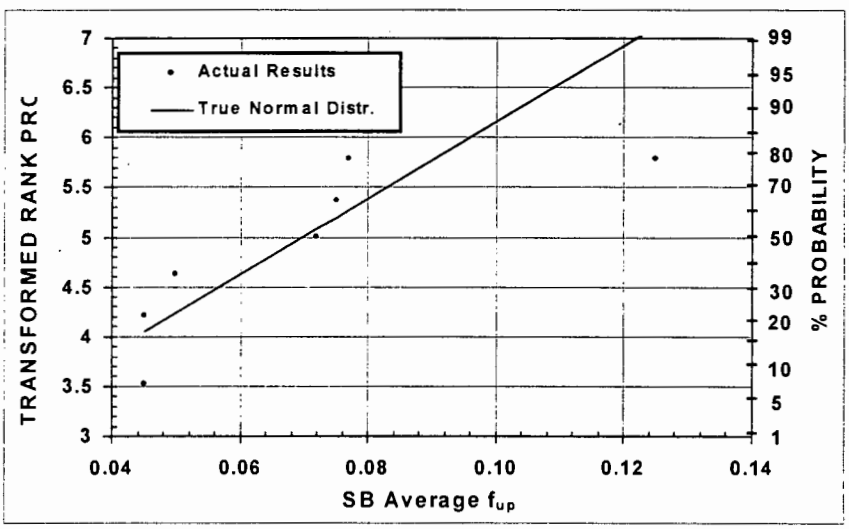

Fig. 3.11: MLE System: Data spread of average unbiodegradable particulate COD fraction (f_{up}) with respect to true normal distribution.

3.10.4 Sludge Settleablity

The sludge settleablity of the system was monitored by means of the dilute sludge volume index (DSVI), as a basic assessment of the general performance of the activated sludge process, and is presented in *Appendix B*, Table B1-6. The DSVI trend during the investigation is presented in Fig. 3.12. The DSVI remained relatively low throughout the study period and varied between 82 – 153 mℓ/g. No incidence of bulking nor effluent sludge loss occurred.

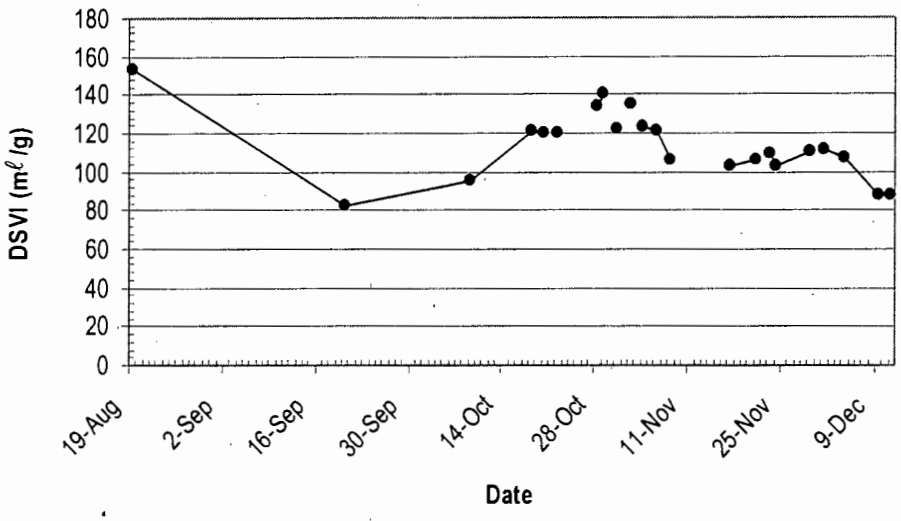

Fig. 3.12: MLE System: General trend of diluted sludge volume index (DSVI) during the study.

3.11 SQW SYSTEM PERFORMANCE

A comprehensive listing of daily data for the SQW system is contained in *Appendix B2*, while average steady-state performance is detailed in Tables 3.12 to 3.14 below.

Table 3.12: SQW System: Sewage batch (SB) average influent total (S_{ti}), 0.45 μm filtered effluent (FE), and fraction unbiodegradable soluble, with respect to total, (f_{us}) COD; also shown are sample standard deviations (SSD) and number of samples (N).

	Sti			FE			f_{us}
SB	AVG	SSD	N	AVG	SSD	N	
18	489.5	19.2	13	48.9	8.9	12	0.100
19	498.8	30.8	6	55.0	13.5	6	0.110
20	477.8	26.6	12	54.0	9.3	12	0.113
21	487.5	22.2	15	56.5	1.8	12	0.116
22	509.0	17.8	13	58.1	5.4	10	0.114
23	486.9	25.2	17	53.9	6.6	14	0.111
24	487.6	25.6	15	50.7	8.6	14	0.104
25	510.7	19.1	11	61.6	9.4	10	0.121

Table 3.13: SQW System: Sewage batch (SB) average influent flow rate (Q_s), ΔOUR, RBCOD concentration ($S_{bsi,S}$, mgCOD/ℓ) and fraction ($f_{ts,S}$) with respect to total influent COD ($S_{ti,S}$, mgCOD/ℓ); also shown are sample standard deviations (SSD) and number of samples (N).

	Q_s (ℓ/d)			ΔOUR (mgO/ℓ/h)			Sti_S	$Sbsi_S$	fts_S
SB	AVG	SSD	N	AVG	SSD	N	AVG	AVG	AVG
18	36.14	0.7	12	4.07	0.8	13	489.5	54.8	0.112
19	35.82	0.7	16	3.73	0.7	7	498.8	50.7	0.102
20	35.33	1.0	14	4.85	0.6	13	477.8	66.9	0.140
21	35.99	1.7	13	4.5	0.6	11	487.5	60.9	0.125
22	36.31	1.1	11	6.47	1.0	10	509.0	86.8	0.171
23	35.76	0.4	17	5.19	0.7	16	486.9	70.8	0.145
24	35.91	1.1	14	4.74	0.5	14	487.6	64.4	0.132
25	35.04	1.6	11	7.16	0.9	10	510.7	99.6	0.195

Table 3.14: SQW System: Sewage batch (SB) average mixed-liquor total and volatile suspended solids concentrations (mg/ℓ; TSS, VSS respectively) and VSS/TSS ratio (f_i); also shown are sample standard deviations (SSD) and number of samples (N).

	TSS			VSS			f_i
SB	AVG	SSD	N	AVG	SSD	N	AVG
18	1308	117	7	1131	106	7	0.864
19	1274	110	2	1108	89	2	0.869
20	1170	159	4	1014	130	4	0.867
21	1152	199	5	971	159	5	0.842
22	1290	45	5	1107	37	5	0.858
23	1253	57	6	1086	60	6	0.867
24	1372	92	7	1172	79	7	0.854
25	1256	9	3	1057	8	3	0.842

3.11.1 Unbiodegradable Soluble COD Fraction (f_{us}):

As with the MLE system, the filtered effluent COD of the SQW system is a measure of the unbiodegradable soluble COD in the influent wastewater ($S_{usi} \equiv S_{use}$). Similarly, using Eq.(3.9), the average f_{us} for each sewage batch period was calculated from corresponding influent and filtered effluent COD averages (Table 3.12), and are plotted in a linearized probability graph to check for normality (Fig. 3.13).

No outliers were identified and the linear fit to the data is quite good, indicating that the data are normally distributed. The mean is f_{us} = 0.111 with sample standard deviation = 0.006. This average lies above the upper limit of the typical range of 0.04 – 0.10 expected of South African domestic sewage (WRC, 1984), and is slightly higher than the f_{us} of 0.096 obtained in the parallel MLE system in this study; Note: this difference is statistically significant at the 95% confidence interval. That the f_{us} of the SQW system is higher than that of the MLE system more than likely is due to

the short sludge age (~3 days). Thus, the f_{us} for the SQW system was not used in the flocculation-filtration test for RBCOD, but the MLE system f_{us} was.

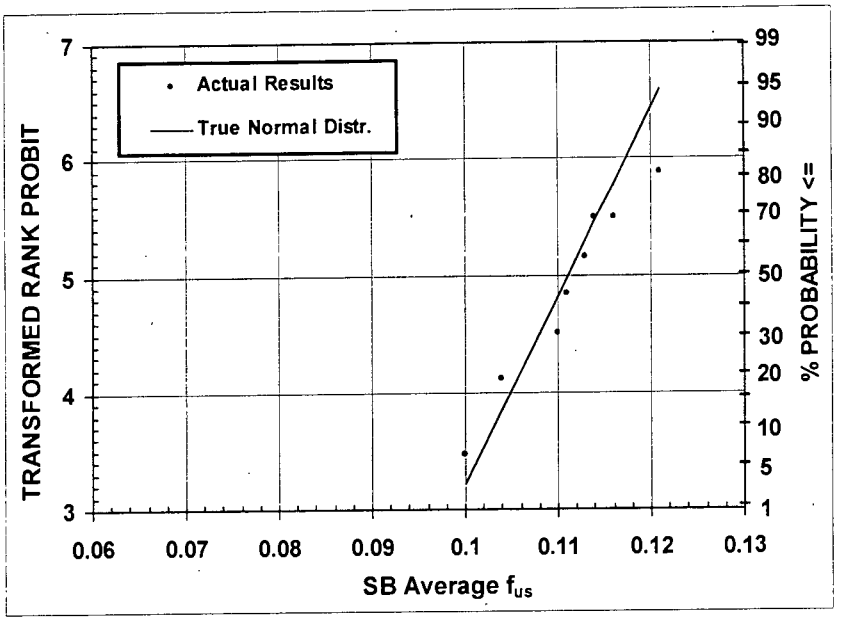

Fig. 3.13: SQW System: Linearized probability plot of sewage batch (SB) average (steady-state) unbiodegradable soluble COD fraction (f_{us}) in influent wastewater.

3.11.2 Square-wave (SQW) Fed System RBCOD Fraction ($f_{ts,S}$):

As previously discussed, Ekama *et al.* (1986) describes the original "standard" method (Ekama and Marais, 1978) of measuring wastewater RBCOD by the precipitous OUR drop occurring at feed termination in a short sludge age square-wave (SQW) fed activated sludge system. As described in Section 3.8.2, this method is based on the bisubstrate nature of municipal wastewater (Dold *et al.*, 1980), and relates the magnitude of the precipitous OUR drop (due to the abrupt change at feed termination from maximum growth on RBCOD+SBCOD to SBCOD only) to the relative concentration of RBCOD in the influent wastewater. Recall from Section 3.8.2:

$$RBCOD_S = \frac{\Delta OUR}{(1 - Y_{H,AE})} * V_p * \left(\frac{24}{Q_S}\right) \qquad (3.13)$$

where:

$RBCOD_S$ = RBCOD concentration in the influent feed to the SQW process; mgCOD/ℓ

ΔOUR = difference in (average) OUR plateaus defining the step change; mgO/ℓ/h

$Y_{H,AE}$ = aerobic heterotroph cell yield; accept standard 0.67 mgCOD/mgCOD

V_p = process volume of SQW system; 6.7ℓ
Q_S = effective daily flowrate in SQW system; target 18 ℓ/0.5d ≡ 36 ℓ/d
24 = converts days to hours

As a fraction of the total influent wastewater COD ($S_{ti,S}$), the RBCOD$_S$ ($S_{bsi,S}$, S_{si}) is defined by the ratio ($f_{ts,S}$), where:

$$f_{ts,S} = RBCOD_S/S_{ti,S} \quad (3.14)$$

Using Eqs.(3.13) and (3.14), the average RBCOD fraction ($f_{ts,S}$) for each sewage batch was calculated from the respective sewage batch average feed flowrate (Q_S) and ΔOUR (Table 3.13), and plotted in a linearized probability graph to check for normality (Fig. 3.14).

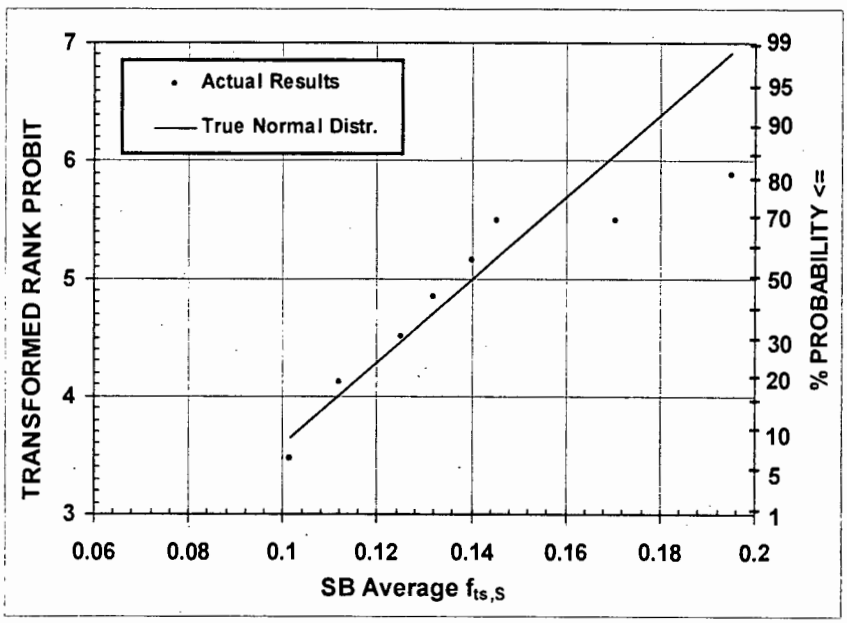

Fig. 3.14: SQW System: Statistical plot of sewage batch (SB) average (steady-state) RBCOD fraction with respect to total COD ($f_{ts,S}$) in influent wastewater.

Although no outliers were identified, the data exhibits deviation from the true normal line for the two highest values in the range; sewage batches 22 (0.17) and 25 (0.19), respectively. Despite these deviations, however, the remaining points display a good fit to the true normal and give an average $f_{ts,S}$ = 0.14 with sample standard deviation = 0.03. Although this value compares well with the SQW average f_{ts} = 0.16 obtained by Ekama and Marais (1978), as well as with the floc-filtered average $f_{ts,FF}$ = 0.15 obtained in this study, it is lower than the average SQW f_{ts} = 0.19 and floc-filtered f_{ts} = 0.18 of Mbewe *et al.* (1995) for wastewater from the same source.

As an additional assessment of the average wastewater $f_{ts,S}$, daily estimates (*Appendix B*, Table B1-8) were plotted in the linearized probability graph, see Fig. 3.15. Four outliers at the 95% confidence interval (18-Oct, 0.208; 19-Oct, 0.2; 12-Dec, 0.172; 13-Dec, 0.185) were identified and excluded from the analysis. Again, although the data displays good linearity over most of its range, it does exhibit marked deviation for the two highest values (9-Dec, 0.232 and 10-Dec, 0.239). The average $f_{ts,S} = 0.136$ with a sample standard deviation of 0.03. By comparison, this value is the same as determined for the sewage batch average data of 0.14 above, and is consistent with the steady-state 0.14 and 0.15 (MLE daily) floc-filtered averages determined in this study, as well as with the 0.16 by Ekama and Marais (1978). It is, however, substantially lower than the 0.18 floc-filtered and 0.19 SQW and aerobic batch test averages from Mbewe *et al.* (1995).

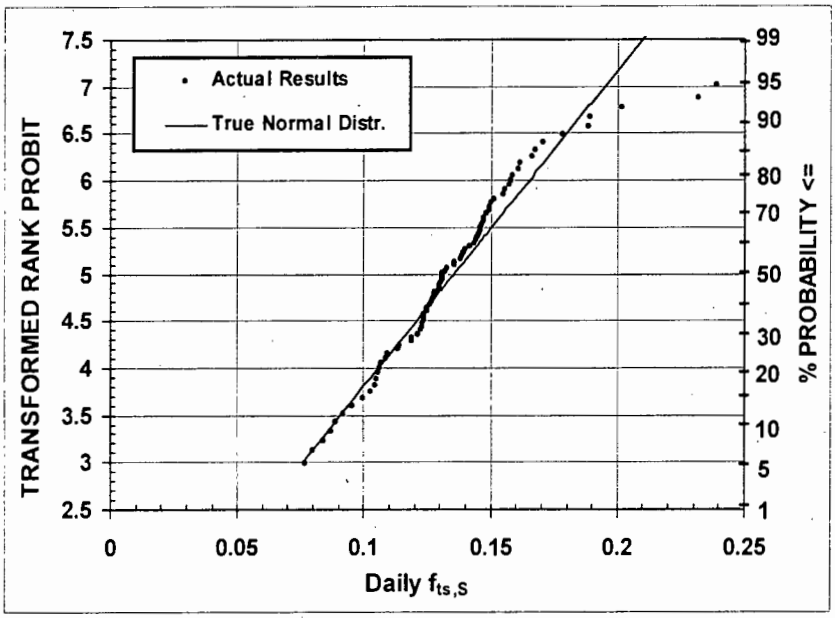

Fig. 3.15: SQW System: Statistical plot of daily estimates of RBCOD fraction ($f_{ts,S}$) in influent wastewater.

3.12 OPERATIONAL PROBLEMS

Besides routine pipe blockages and bulking sludge, several operational problems were encountered during the course of the study due to demolition and reconstruction of portions of the Water Research Laboratory between April and July 2002. Construction related problems resulted in frequent, unplanned interruptions of electrical, air and water services that affected ambient temperature control, sewage and sample refrigeration, and chemical analyses. Specifically, service failures created uncertainty in steady-state evaluation of the UCT system by elevating laboratory temperatures above 20 °C (~24 – 27 °C), cold room storage temperatures above 4 °C (~8 – 10 °C), feed refrigeration temperatures above 7 °C, and disrupted in-progress analyses for COD, TKN, FSA, TSS and VSS, as well as operation of the feed pump, reactor mixers, DO control and aeration cycles, and deletion of stored OUR data from the DO meter. Although generally intermittent, these disruptions were on occasion

sustained for several days at a time. When possible, service interruptions were resolved immediately by resetting electrical service breakers and restarting pumps, mixers, the air compressor, ambient air conditioning, aeration and OUR measurement. However, when interruptions occurred during the night or were of extended duration, experimental testing was not performed and steady-state operation for that period rejected. The greatest impact these problems had on this period of the study, was introducing uncertainty in stored wastewater feed characteristics and the f_{us} obtained from the UCT system used to determine the influent RBCOD fraction in the flocculation-filtration method.

Operation of the MLE and SQW systems were generally free of facility-related problems, but remained subject to occasional pipeline blockages (e.g. Days 337, 343) caused by lumps of sludge settling in connecting piping. When this happened, reactor volumes would accumulate due to ongoing feeding and ultimately overflow the reactor vessels resulting in sludge loss from the system. During the day following a sludge spillage, the reactors were drained and the mixed liquor was screened through the 1 mm sieve to break-up or remove sludge lumps. All pipelines were removed, cleaned and replaced and no testing was done on the system for that day. The volume of sludge wasted for that day was also decreased to account for the lost sludge. Such occurrences were significantly reduced, however, by the large headspace in the anoxic and aerobic reactors (MLE system), which allowed the sludge to accumulate in the system rather than overflow the reactor vessels. In this case, the blockage was released and the excess sludge captured in graduated cylinders. The sludge was settled in the cylinders and the supernatant drained off. The settled sludge was visually assessed for density and diluted with unfiltered effluent if too compact. The sludge was then returned to the aerobic reactor.

In addition, the SQW system was particularly prone to occasional freezing of the narrow feed tube extending from the feed bucket to the pump (e.g. Days 374, 384). The ice would reduce or completely block the feed flowrate to the reactor during the feed cycle, resulting in a non-representative feed cycle in the process. No testing was performed on these days. Freezing problems were mitigated by placing the refrigerator power supply on a timer to reduce the cooling frequency, and by positioning the feed tube away from the inside walls of the refrigerator.

As noted previously, however, the MLE and SQW continuous-flow systems in this study were operated simply to provide an equivalent biomass and to characterize wastewater RBCOD for corresponding aerobic and anoxic batch tests, respectively. Therefore, although daily operation of the MLE system sought reliable process stability, it was not essential for the batch tests. Furthermore, for the SQW system, daily OUR profiles for days with obvious operational disturbances were rejected as non-representative of steady-state characterization of the average RBCOD concentration in the influent feed. The short sludge of the SQW system, however, benefited rapid recovery of the biomass from any major process upset, so RBCOD characterization was generally consistent.

3.13 CLOSURE

In summary, this investigation used a total of 25 sewage batches of unsettled municipal wastewater from Mitchell's Plain, Cape Town, and covered a period of 395 days from 19/11/01 to 18/12/02. While a UCT system was used initially to characterize wastewater f_{us} for floc-filtered RBCOD estimation, MLE and SQW continuous-flow systems were subsequently operated to provide a consistent source of OHO biomass for batch tests, and to characterize the wastewater RBCOD by the standard method, respectively. From the results obtained for these systems:

- MLE system performance was generally stable, producing an average unbiodegradable soluble COD fraction with respect to total COD (f_{us}) of 0.096, which falls within the typical range of 0.04 – 0.1 expected for South African domestic sewage (WRC, 1984). Furthermore, it is consistent with similar values observed by other researchers for the wastewater from the same source: Cronje (2000), 0.085; Ubisi *et al.* (1997a,b), 0.09; Mbewe *et al.* (1995), 0.074.

- Floc-filtered estimates of the wastewater RBCOD fraction with respect to total COD ($f_{ts,FF}$) averaged 0.15, which compares favourably with the floc-filter average of 0.18 (range 0.14 – 0.23) obtained by Mbewe *et al.* (1995) for wastewater from the same source.

- Similarly, the SQW system performance was generally stable, and produced an average f_{us} = 0.111. This f_{us} is slightly higher than the 0.096 obtained in the parallel MLE system. This is not unexpected as the very short sludge age (3d) of the SQW system will influence the f_{us} determination. Accordingly, the SQW system fus value was not used to determine the RBCOD in the flocculation-filtration method.

- The SQW system gave an average wastewater RBCOD fraction ($f_{ts,S}$) of 0.14; which compares well with the SQW average of 0.16 obtained by Ekama and Marais (1978), as well as with the floc-filtered average of 0.15 with f_{us} determined by the MLE system in this study. However, it is substantially lower than the 0.18 – 0.19 average obtained by Mbewe *et al.* (1995) on wastewater from the same source.

- Routine operational problems such as pipe blockages, for example, occurred throughout the course of the study, and were relatively easily resolved. However, substantial disruption was experienced during the period April – July 2002, when sections of the laboratory was demolished and reconstructed.

CHAPTER 4

AEROBIC AND ANOXIC BATCH TEST CONDITIONS AND PROCEDURES

4.1 INTRODUCTION

In Chapters 1 and 2 it was shown that while a reduced heterotrophic yield under anoxic conditions ($Y_{H,NO}$) is apparent from bioenergetic theory and supported by experimental measurements recorded in the literature, no direct experimental measurement with real municipal sewage could be found: Most of the studies were performed with defined substrates, hydrolysates, and/or mixtures of various domestic and industrial wastewaters, and focussed primarily on estimating specific denitrification rates. Consequently, few provide information directly relating nitrate and corresponding substrate utilizations, which is necessary to estimate the yield. Furthermore, some studies were performed with mixed polyphosphate accumulating organism (PAO) sludges from nitrification-denitrification biological excess phosphorous removal (NDBEPR) activated sludge systems, which introduces unquantifiable uncertainty into observed yield measurements. As a result, in the current body of research there is a dearth of studies and experiments to directly quantify or measure $Y_{H,NO}$ using sewage as substrate.

Hence, the principal aim in this study is to investigate and quantify the ordinary heterotrophic organism (OHO) cell yield under anoxic conditions relative to its value under aerobic conditions ($Y_{H,AE}$) for domestic sewage. The three primary objectives identified in this regard are:

1. Determine the ratio $Y_{H,NO}$:$Y_{H,AE}$ for real sewage in terms of electron acceptor (OU vs. NU) utilization.

2. Measure $Y_{H,NO}$ and $Y_{H,AE}$ directly for known concentration of RBCOD utilized.

3. Compare experimental results with other, independent studies on real sewage.

In developing a research approach to address these objectives, in Section 1.5, Chapter 1, it was shown that the expressions quantifying RBCOD consumption in terms of the oxygen and nitrate utilized (OU and NU, for aerobic and anoxic respiration respectively) can be equated if the same mass and type of RBCOD is consumed; i.e.:

$$\frac{OU}{(1-Y_{H,AE})} = RBCOD = \frac{2.86 * NU}{(1-Y_{H,NO})} \tag{4.1}$$

$$\boxed{\Rightarrow Y_{H,NO} = 1 - \frac{2.86 * NU}{OU} * (1-Y_{H,AE})} \tag{4.2}$$

Thus, from E.(4.2) if the NU and OU can be experimentally quantified and a value for $Y_{H,AE}$ is known, then $Y_{H,NO}$ can be determined. To find a value for $Y_{H,AE}$ two approaches can be followed.

(1) The widely accepted value for $Y_{H,AE}$ = 0.67 mgCOD/mgCOD can be accepted here also, in which case Eq.(4.2) reduces to:

$$\boxed{Y_{H,NO} = 1 - 0.944 * \frac{NU}{OU}} \qquad (4.3)$$

Thus, by measuring the OU and NU in identical aerobic and anoxic batch tests respectively, containing the same concentration of RBCOD and biomass from the same source, and accepting the "standard" value for $Y_{H,AE}$, values for $Y_{H,NO}$, and the ratio $Y_{H,NO}$:$Y_{H,AE}$ (Objectives 1 and 2) can be estimated. This approach was followed in this investigation.

(2) The value for $Y_{H,AE}$, and similarly $Y_{H,NO}$, can be experimentally determined by adding a known concentration of RBCOD to the two batch tests described above, and calculating the respective yields via Eq.(4.1). This known RBCOD addition can be achieved via real wastewater in which the RBCOD has been independently quantified, or via addition of a known mass of artificial substrate RBCOD. In this investigation both approaches were followed. The concentration of the RBCOD in the real wastewater added to the batch tests was quantified by flocculation-filtration (Mbewe *et al.*, 1995) and the OUR (aerobic) response of a short sludge age square-wave (SQW) fed activated sludge system (Ekama *et al.*, 1986), see Chapter 3. Also, known quantities of the artificial RBCOD acetate were added to selected batch tests.

Thus, the fundamental experimental approach was to perform sets of anoxic and aerobic batch tests identical in all respects (mixed-liquor, RBCOD) except electron acceptor conditions. To these paired sets of batch tests, either real wastewater for which the RBCOD concentration had been independently quantified, or the artificial RBCOD acetate were added, and electron acceptor (O_2 or NO_3) utilization monitored. This Chapter describes these aerobic and anoxic batch test experiments. Results from the batch tests and interpretation of the experimental data are presented in Chapter 5.

4.2 GENERAL BATCH TEST METHODOLOGY

The general procedure followed for the aerobic and anoxic batch experiments performed in this study was based on the methods described by Ekama *et al.* (1986), Ubisi *et al.* (1997a), Mbewe *et al.* (1995), Wentzel *et al.* (1995) and Wentzel *et al.* (1999).

4.2.1 Sewage Addition Batch Tests

Corresponding aerobic and anoxic batch tests were performed using the same defined volumes and concentrations of domestic wastewater (V_{WW}) and activated sludge mixed-liquor (V_{ML}), in single tank continuously stirred batch reactors maintained at

20 °C. For each batch test where real wastewater was added, an excess volume of raw wastewater was drawn from the storage tanks in the 4 °C cold room and the following abstractions made:

(i) 200 mℓ for determining total COD of the wastewater,
(ii) 1ℓ for determining the floc-filtered COD of the wastewater (Section 3.8, Chapter 3), and
(iii) 2ℓ for use in the batch test (V_{WW}).

The 2ℓ (V_{WW}) sample was placed in a hot water bath and heated to ambient temperature (20 °C, ~5 – 10 minutes). Simultaneously, an excess volume of activated sludge (also at ambient temperature) was settled (concentrated) to ~1.12ℓ of which 100 mℓ was abstracted for total and volatile suspended solids (TSS and VSS respectively) analyses (Standard Methods, 1989); 1ℓ of the remaining volume of mixed-liquor was measured in a graduated cylinder for use in the batch test (V_{ML}). The V_{WW} = 2ℓ and V_{ML} = 1ℓ were then combined in the batch reactor to form the 3ℓ batch test volume (V_{BT}), and the particular batch test performed. The pH in the batch tests was monitored continually, and manually controlled to ~7.5 ± 0.2 by appropriate addition (dropwise) of concentrated NaOH and/or HCl solutions to raise or lower (respectively) the reactor pH.

The batch test apparatus was constructed of the same material and comprised the same equipment as that described in Sections 3.2 and 3.3, Chapter 3. Specifically, the batch test set-up consisted of a pair of identical cylindrical Perspex reactors of roughly 30 x 13 cm (ht. x. dia.) dimensions, each equipped with a motor driven paddle mixer mounted centrally to the lid of the reactor. The mixing shaft extended into a small recess at the bottom of the reactor and was fitted with two sets of Perspex paddles, one (with inclined vanes) at the bottom of the shaft and the other (with flat, vertical vanes) approximately 1 cm above it. The lid of the reactor had a semi-circular opening for retrieval of samples and insertion of pH and dissolved oxygen (DO) probes into the bulk solution. A schematic description of a typical set-up configured for an aerobic batch test is shown in Fig. 4.1.

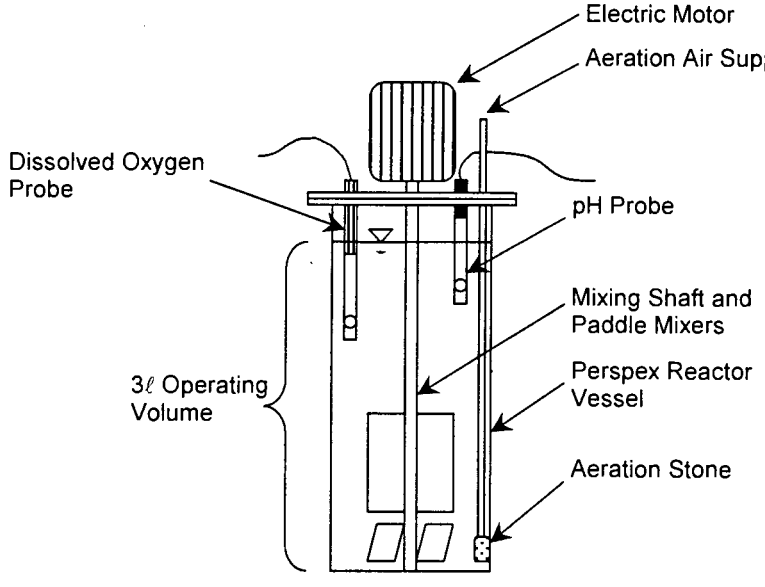

Fig. 4.1: Schematic of a typical set-up for an aerobic batch test; the set-up is identical for anoxic batch tests, except that the air is replaced by nitrogen gas and DO measurement by nitrate sampling.

In the aerobic batch tests, aeration was provided by low-pressure compressed air that entered the reactor through a small bore Perspex tube, which terminated in an aeration stone at the bottom of the reactor vessel. The air flowrate was regulated by throttling a ball valve on the main air supply line and adjusting a hose-clamp on the tube entering the reactor. The DO concentration, and concomitantly, oxygen utilization rate (OUR), was measured continuously and automatically using a YSI Model 5739 DO probe and HiTech MicroSystems DO meter in the automated technique described by Randall *et al.* (1991); see Section 3.3, Chapter 3. The inside walls of the reactor were routinely brushed during aeration cycles to prevent mixed-liquor particles (brought to the surface by fine bubbles) from adhering to the reactor walls above the liquid surface. The effect of this phenomenon was negligible, however, since the accumulated particulates formed an insignificant fraction of the total biomass present in the bulk solution.

Anoxic (denitrification) batch tests were performed identically to corresponding aerobic ones, except that an oxygen-free environment was maintained throughout the test and excess nitrate added at the start of the test to measure the nitrate utilization rate (NUR) instead of the OUR. At the start of the test, nitrate was added directly to the reactor as a small volume (5 – 40 mℓ) of concentrated potassium nitrate solution (38 – 140 gKNO_3/ℓ), sufficient to ensure that nitrate was present for the entire test period. To eliminate oxygen ingress, nitrogen (N_2) gas was gently bubbled through the reactor contents. Hence, anoxic conditions were maintained throughout the test. Grab samples were taken manually at specific time intervals during the test; the sampling intervals (in minutes) per hourly period during the test are summarised in Table 4.1.

Table 4.1: Anoxic (denitrification) batch test sample time intervals (in minutes) per test hourly period.

Sample Interval (minutes)	Test Period (t = hour no.)
5	0 – 1
10	1 – 2
15	2 – 4
30	4 – 12

Sample volumes taken from batch tests were generally kept small (~25 mℓ) to ensure that the liquid level in the particular batch test did not fall below 2ℓ; at levels <2ℓ the mixing paddles would be sufficiently close to the liquid surface and possibly induce air entrainment into the bulk solution, which would distort the OUR and NUR

measurements in the respective tests. All sampling and analytical techniques used in the batch experiments were identical to those detailed in Section 3.7, Chapter 3.

4.2.2 Acetate Addition Batch Tests

The basic procedures described above were followed also for the acetate addition batch tests. The acetate was added to the appropriate batch, either:

(1) At the start of the test, in which case the acetate was the only external substrate; or,
(2) Following on from the sewage addition batch tests described above, after complete utilization of the sewage RBCOD.

For both types of tests, a concentrated stock solution of sodium acetate (CH_3COONa) was prepared by dissolving 3.908g of sodium acetate in 1ℓ of distilled, deionized water, to achieve a target theoretical COD ("COD_{Th}") concentration of 3000 mgCOD/ℓ, see *Appendix D*. The concentrated stock solutions of sodium acetate were stored in the cold room at 4 ^{o}C to inhibit biological contamination. The actual COD concentration of the stock solution ("Ac_{COD}") was measured whenever samples were used in the batch tests, as well as routinely to monitor the COD degradation in the stock solution over time. Degradation was not a significant factor in performance of the tests, however, since the stock solution was replaced every week and the actual COD of the solution was determined each time it was used in a batch test, for use in subsequent calculations.

For aerobic batch tests using acetate, the basic procedure was to measure out the desired volume of acetate (V_{Ac}) in a volumetric flask (25, 50 or 25 + 50 = 75 mℓ). The aerobic batch tests with sewage addition described above were then started. The OUR was monitored continually to observe when the precipitous drop on OUR occurred, i.e. the sewage RBCOD was depleted. Once the OUR had dropped and stabilised at the second lower plateau (see Section 4.4), ~0.5 – 1 hour later, the known volume of concentrated acetate solution (V_{Ac}) was added directly to the batch reactor during an aeration cycle and OUR monitoring continued. At the end of the aeration cycle during which the acetate was added, the liquid level in the batch reactor was marked on the side of the vessel. At the end of the test, the reactor vessel was emptied and reassembled exactly as during the test; i.e. with the mixer and probes in place. The reactor was then filled with tap water to the level marked on the reactor, and the water decanted into graduated cylinders to determine the volume in the reactor in to which the known volume and, hence, mass of acetate had been dosed ("$V_{BT,Ac}$"). Thus, the concentration of acetate in the batch test, in mgCOD/ℓ ("$[Ac_{COD}]_{BT}$"), was calculated as the mass of COD added (i.e. MAc = V_{Ac}*Ac_{COD}) divided by the corresponding batch test volume ($V_{BT,Ac}$) in which it was dissolved, i.e.: $[Ac_{COD}]_{BT}$ = $MAc/V_{BT,Ac}$. Using the known concentration of acetate-RBCOD in the batch test and the corresponding OU determined from the area under the appropriate portion of the OUR curve (see Section 4.4 below), $Y_{H,AE}$ could be estimated from the left hand side of Eq.(4.1).

The same sodium acetate solution and basic procedure used for the aerobic batch tests above, were used also for the anoxic batch tests. However, whereas in the aerobic

batch tests the acetate could be added following depletion of the sewage RBCOD, because this depletion could be detected in real-time by observing the precipitous drop in OUR on the DO meter, in the anoxic batch tests sewage RBCOD depletion could not be detected in real-time so that the acetate had to be added at the start of the anoxic batch tests – hence, no other source of RBCOD was present in the anoxic batch test except for the acetate. Anoxic batch tests with acetate were composed of 2ℓ MLE mixed-liquor diluted up to approximately 3.12ℓ with unfiltered secondary effluent from the MLE system; 100mℓ was abstracted from this mixture for TSS and VSS analyses, and the remaining volume used to measure out exactly 3ℓ (V_{ML}) for performing the batch test. Typically, 25 or 50 mℓ of acetate stock solution (V_{Ac}) was combined directly with the 3ℓ V_{ML} at the start of the test, and grab samples taken with time for nitrate and nitrite analyses according to the method described in Section 4.3.1. Since the anoxic batch tests with acetate contained no wastewater, the NU for acetate consumption was determined by the difference in y-intercepts from the K_1 (due to utilization of the artificial RBCOD acetate) and K_3 (due to utilization of endogenously generated SBCOD; see WRC 1984 and van Haandel *et al.*, 1981) rates. Further, because only a relatively small amount of RBCOD substrate was present in the tests, the duration of the K_1 period was reduced substantially, and the sample intervals had to be shortened to obtain sufficient data points for adequate definition of the K_1 and K_3 rate lines to estimate NU accurately. Accordingly, the sample intervals in anoxic acetate tests were modified to 5 minutes apart for the first 2 hours and 10 minutes apart until the end of the test, typically 1 – 2 hours afterwards (3 to 4 hours total).

4.3 EXPERIMENTAL OVERVIEW

The aerobic and anoxic (denitrification) batch test experiments are described below and detailed in *Appendix C*. As presented in Section 3.9, Chapter 3, this study used a total of 25 sewage batches over a period of 395 days, and a total of 40 aerobic and 42 anoxic (denitrification) batch tests were performed, identified as "ABT" and "DBT" respectively. The batch test experiments were conducted on real wastewater RBCOD as well as on the artificial RBCOD acetate. The batch tests have been grouped into three chronological periods, generally defined by the method of estimating the wastewater RBCOD fraction, the source of mixed-liquor used in the tests and initiation of anoxic batch tests using the artificial RBCOD acetate (Table 4.2).

Table 4.2: Experimental Periods for aerobic and anoxic (denitrification) batch test experiments, labelled "ABT" and DBT" respectively.

Period	Dates	ABT	DBT
I	17/1/02 – 4/6/02	1 – 22	1 – 19
II	26/8/02 – 10/10/02	23 – 34	20 – 29
III	11/10/02 – 16/12/02	35 – 40	30 – 42

A comprehensive summary of all aerobic and anoxic (denitrification) batch tests performed, including the respective batch test number ("ABT" and "DBT"), the

sewage batch (SB) used, dates of the tests and source of mixed-liquor (ML), are presented in Table 4.3 below.

Table 4.3: Summary of all aerobic and denitrification batch tests (ABT and DBT respectively), corresponding sewage batches (SB) used, dates of the tests, source of mixed-liquor (ML) and analyses performed.

Period	SB	Dates 2002	Aerobic Batch Tests					Denitrification Batch Tests			
			ML	No.	FF	Ac	NOx	ML	No.	FF	Ac
I	4	17/1 - 22/1	LML	1-2				LML	1-2		
	6	24/2 - 7/3	LML	3-7				LML	3-7		
	9	4/4 - 17/4	LML	8-11				LML	8-11		
	10	24/4 - 26/4	LML	12-13				LML	12-13		
	11	29/4 - 5/5	MPP	14-18			◆	MPP	14-18		
	NS	11/5	MPP	19	◆			MPP	19	◆	
	12	16/5	MPP	20							
	13	3/6 - 4/6	MPP	21-22	◆						
II	18	26/8 - 28/8	SQW	23-24		◆		MLE	20		
	19	13/9	MLE	25	◆	◆					
	20	15/9 - 22/9	MLE	26-27	◆	◆					
		25/9 - 29/9	SQW	28-29	◆	◆		MLE	21-23	◆	
	21	1/10 - 10/10	MLE	30-34	◆	◆		MLE	24-29	◆	
III	21	11/10 - 14/10						MLE	30-33		◆
	22	24/10 - 27/10	MLE	35-37		◆		MLE	34		
	23	4/11 - 17/11	MLE	38-40		◆		MLE	35-37		
	25	7/12 - 16/12						MLE	38-42	◆	❖

ML = Mixed-liquor
LML = ML from concurrent lab-system
MPP = ML from Mitchells Plain Plant
MLE = ML from dedicated MLE system
SQW = ML from square-wave fed system

FF = Floc-filtered analyses performed during test
Ac = Tests with artificial RBCOD actetate performed
NOx = Nitrate and nitrite analyses performed during test
NS = "New sewage"; not from sewage batch.
❖ = Same batch test; first anoxic then aerobic

4.3.1 Period I:

In Period I, sewage batches (SB) 4 – 13 were used over the period 17/1/02 – 4/6/02, and 22 aerobic and 19 anoxic batch tests were performed: ABT 1 – 22 and DBT 1 – 19 respectively. In this period all batch tests were with wastewater only as substrate (Table 4.3), following the general procedure set out in Section 4.2.1. The wastewater RBCOD fraction was estimated by the flocculation-filtration method, using the unbiodegradable soluble COD fraction (f_{us}) obtained from a long sludge age laboratory-scale UCT system fed the same sewage (see Section 3.9, Chapter 3 for details).

As discussed in Section 1.4, Chapter 1, the specific quality of the biomass used in the batch tests is irrelevant (provided the biomass has had pre-exposure to both aerobic and anoxic conditions) when considering *complete* utilization of the RBCOD, as is the case in this study for determining $Y_{H,NO}$ by Eqs.(4.1) to (4.3). Thus, batch tests performed in Period I initially used waste activated sludge (WAS) from an MLE system operated in a concurrent experiment in the UCT laboratory (designated "LML" in Table 4.3), but later mixed-liquor from the Mitchells Plain Wastewater

Treatment Plant was used (MPWWTP, designated "MPP" in Table 4.3). The aerobic and anoxic batch tests were performed in parallel by splitting common samples of mixed liquor and wastewater equally between the pair of reactors. When the mixed-liquor was drawn from the laboratory scale system, only a small volume of WAS was obtainable each day. Hence, for these tests it became necessary to either dilute batch test mixtures up to the 3ℓ batch test volume, or to store and accumulate sufficient WAS for the tests. Initial results indicated that dilution of the batch test mixture reduced the RBCOD concentration in the test substantially, which led to poorly defined OUR and NUR profiles for the RBCOD utilization portions of the curves. In contrast, batch tests using full strength (undiluted) wastewater and concentrated biomass produced more easily discernable OUR and NUR profiles. Consequently, following SB 6, it was decided to standardize the batch test procedure to V_{WW} = 2ℓ undiluted wastewater and V_{ML} = 1ℓ activated sludge biomass. The WAS mixed-liquor was accumulated in the 4 °C cold room for up to 2 days and on the third day the batch test was performed. Depending on the average mixed-liquor volatile solids (VSS) concentration (X_V) and the total COD of the undiluted raw wastewater, a specific volume of WAS was settled to concentrate the required sludge mass into 1ℓ (to achieve a desired loading rate, see *Appendix C*), which was then combined with 2ℓ of undiluted raw sewage in the batch test. Although this procedure proved successful, the dependency on another experiment's WAS as the mixed-liquor source for the batch tests imposed significant restrictions on the scheduling and consistency of the tests. To alleviate this constraint, from SB 11 (Table 4.3) the mixed-liquor source for the batch tests was switched to sludge obtained from the MPWWTP. Periodically, a mixed-liquor volume (~60ℓ) was drawn from the aeration basin of the MPWWTP. The mixed-liquor was kept under aeration in the 4 °C cold room and the appropriate volumes for performing the batch tests drawn off when required.

Occasionally, batch tests during this period exhibited uncharacteristic OUR and NUR profiles, which suggested possible interferences in the tests. Further, the fraction of wastewater RBCOD recovered in the aerobic batch tests from the area under the RBCOD OUR profile (using $Y_{H,AE}$ = 0.67 mgCOD/mgCOD in the method detailed by Ekama *et al.*, 1986) compared with that estimated by flocculation-filtration (FF) of the original undiluted wastewater added to the test, was generally poor. One possible explanation identified for this inconsistency was incomplete RBCOD utilization when the OUR dropped precipitously. To verify complete utilization of the wastewater RBCOD at the time the precipitous drop in OUR occurred, samples were taken at specific time intervals during certain aerobic batch tests, and the FF COD concentration determined. The sampling procedure was analogous to that described in Section 3.8.1, Chapter 3: At specific time intervals a 150 mℓ sample was pipetted from the reactor and discharged into a 150 mℓ glass beaker; 1.5 mℓ alum solution (50g/ℓ) was added to the beaker and the mixture stirred vigorously for a few seconds after which it was allowed to settle. After a minimum of 30 minutes, the clarified supernatant was filtered through a 0.45 μm membrane filter and immediately preserved with one drop of mercuric chloride solution and placed in the cold room for later COD analysis.

In anoxic batch tests, samples drawn for nitrate (NO_3) and nitrite (NO_2) analyses were also pipetted (~22 mℓ) from the reactor at specific time intervals during the course of the test (Table 4.1). The samples were first filtered through glass fibre filters (GF/C)

to remove mixed-liquor suspended solids, after which the filtrate was passed through a 0.45 μm membrane filter; the membrane filtered sample was preserved with one drop of concentrated mercuric chloride solution and placed in the cold room for later analysis (see Section 4.4).

4.3.2 Period II:

Period II commenced with the operation of the dedicated Modified Ludzack-Ettinger (MLE) and square-wave (SQW) fed continuous-flow systems in this investigation, as described in Chapter 3. Sewage batches (SB) 18 – 21 were used over this period, 26/8/02 – 10/10/02, and 9 aerobic and 10 anoxic batch tests were performed: ABT 23 – 34 and DBT 20 – 29 respectively. Both sewage and acetate addition tests were performed, see Table 4.3.

The procedural difficulties encountered in Period I of irregular availability of mixed-liquor for the batch tests were only marginally alleviated by using the mixed-liquor samples obtained periodically from the MPWWTP. Also, the mixed-liquor samples obtained from the MPWWTP varied considerably in their characteristics (concentration, active fraction etc.); this made predetermination of the correct loading rate to be applied in the batch test to obtain discernable OUR and NUR profiles extremely difficult. Further, the uncertainty surrounding estimation of the wastewater RBCOD fraction by the floc-filtration method using the f_{us} of the UCT system, was also problematic. Therefore, as discussed in Chapter 3, dedicated MLE and SQW activated sludge systems were implemented to provide a reliable source of sufficient, consistent biomass for the batch tests, and to establish a standard measure for the RBCOD fraction in the wastewater. Therefore, in Period II, batch tests were performed with "fresh" mixed-liquor drawn directly from either the MLE or SQW systems, see Table 4.3.

For the wastewater addition batch tests, the wastewater RBCOD fraction was estimated from the OUR response of the 12h-ON/12h-OFF SQW fed activated sludge system, as described by Ekama *et al.* (1986); see Section 3.8, Chapter 3. The general procedure detailed in Section 4.2.1 above was followed. Additionally, the routine (developed in Period I) of taking samples for FF COD analysis at defined time intervals during the batch tests to verify complete RBCOD utilisation, was continued.

Also during Period II, acetate addition batch tests were performed. These batch tests were to independently verify the value for $Y_{H,AE}$, and hence, only aerobic acetate addition batch tests were conducted, following the procedure set out in Section 4.2.2 above. Further, as for the wastewater addition batch tests, samples were drawn at defined intervals for FF COD analysis, to verify complete acetate utilization.

4.3.3 Period III:

Period III is defined by initiation of anoxic batch tests using known quantities of the artificial RBCOD acetate ("Ac") for direct estimation of $Y_{H,NO}$ via the right hand side of Eq.(4.1). Sewage batches (SB) 21 – 25 were used over the period 11/10/02 – 16/12/02, and 6 aerobic and 13 anoxic batch tests were performed: ABT 35 – 40 and

DBT 30 – 42 respectively. As in Period II, batch tests were performed using mixed-liquor from the dedicated MLE system and either wastewater, or acetate, or both added to the batch tests. For the wastewater, the RBCOD fraction was determined by the OUR response of the SQW system (see Section 3.8, Chapter 3).

For the anoxic acetate addition batch test, results from initial tests (DBT 30 – 33) exhibited a general increasing trend in the nitrate concentrations during the endogenous K_3 denitrification period (see *Appendix C*). This suggested the possible occurrence of nitrification in the tests. If true, this would imply ingress of oxygen during the test. To evaluate this possibility, several anoxic batch tests, in which the DO concentration was monitored continually, were performed using only mixed-liquor and secondary effluent from the MLE system. To determine if contamination with air of the N_2 gas used in sparging the anoxic batch tests was the source of the oxygen, N_2 gas was only bubbled through the batch test after a period. The DO concentration in the tests increased from ≤ 0 mgO/ℓ before the start of N_2 gas bubbling to approximately 0.6 ± 0.2 mgO/ℓ during N_2 gas bubbling. Consequently, it was concluded that the N_2 gas supply contained a small amount of oxygen (this was later confirmed by the manufacturer). The effect of this contamination was not evident in the observed K_1 and K_2 denitrification rates of previous anoxic tests (Periods I and II), but was clearly apparent in the observed K_3 rates of the anoxic acetate-only tests. This raised the question of the possible effects of air contamination in the previous anoxic batch tests. However, this is unlikely to be significant since the K_1 and K_2 denitrification rates, and associated substrate utilization rates, are substantially higher than possible oxygen contamination rates. Further, different N_2 gas cylinders were used in previous experiments, and did not exhibit oxygen contamination. However, for surety it was decided to eliminate N_2 gas bubbling during the anoxic batch tests.

To evaluate elimination of N_2 gas bubbling from the anoxic batch test procedure on possible air entrainment in the test, three types of anoxic batch tests composed of only mixed-liquor and secondary effluent from the MLE system were performed. The DO concentration was continually monitored in the following tests:

(i) the reactor headspace above the liquid surface was continually purged with N_2 gas;
(ii) no N_2 gas was used and the liquid surface was isolated from the air in the reactor headspace by small hollow plastic balls floating on the liquid surface; and
(iii) neither hollow balls nor N_2 gas was used.

All three tests were run for at least 6 hours, during which time the observed DO concentration in all tests remained ≤ 0 mgO/ℓ throughout. Thus, it was concluded that an oxygen-free environment could be maintained in the anoxic batch tests without bubbling N_2 gas through the reactor contents. Consequently, in subsequent anoxic batch tests (DBT 34 on) the test procedure was modified, by continually purging the reactor headspace above the liquid surface with N_2 gas, and isolating the air-liquid interface with small hollow balls floating on the liquid surface. Additionally, to further enhance denitrification by the biomass in the test, the sludge biomass was conditioned to "activate" denitrifying metabolic pathways prior to the start of the test, by combining the mixed-liquor and KNO_3 solutions in the batch reactor at least 2 hours before addition of the relevant acetate RBCOD.

The nitrate (NO_3) and nitrite (NO_2) samples in anoxic batch tests in Period III were analysed by two different methods, i.e.:

(i) the usual automated hydrazine reduction method using a Technicon Auto-Analyser (TAA, see Section 3.7, Chapter 3), and
(ii) by ion chromatography (IC) using a DIONEX Ion Chromatograph at a contracted outside laboratory (see Section 4.4).

The reason for the change was because for samples from batch tests conducted during SB 21, the TAA exhibited significant fragmentation and splitting of NO_3 and NO_2 output peaks. Problems were initially ascribed to possible malfunction of the air-bubble separator, degradation of reagent stock solutions and/or interference caused by the mercuric chloride used as sample preservative. However, when the problem remained with replacement of the air-bubble separator and using fresh chemical reagents and identically preserved NO_3 and NO_2 standard solutions, it was determined that the problem was caused by mechanical malfunction of the plotter used to record the output from the TAA. Accordingly, the plotter was replaced in the later stages of Period III; however, in the interim, NO_3 and NO_2 batch test samples for DBT 34 – 37 were analysed by IC at the outside laboratory. NO_3 and NO_2 standards were supplied with the samples for IC analysis as a cross check on accuracy.

4.4 DATA INTERPRETATION

In interpretation of the batch test results, the fundamental information that needs to be extracted from the data is the electron acceptor utilized in the consumption of the RBCOD, oxygen for the aerobic and nitrate/nitrite for the anoxic batch tests. This is irrespective of whether the RBCOD concentration is known or not. Determination of these parameters is detailed in this Section.

4.4.1 Oxygen Utilization (OU) Determination

A typical OUR-time profile for an aerobic batch test with wastewater addition is shown in Fig. 4.2 below.

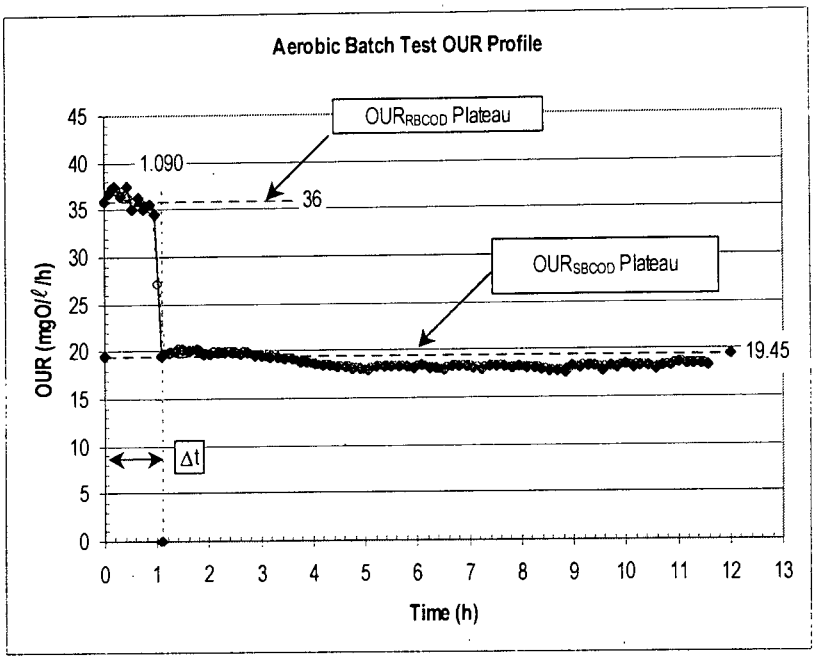

Fig. 4.2: Aerobic batch test number 16 (ABT 16) as a typical example of an OUR profile and area (OU) estimation of the RBCOD utilization portion of the curve; OU = 15.0 mgO/ℓ.

As described in Chapter 1, Section 1.4, the oxygen utilization rate (OUR) in aerobic (AE) batch tests with domestic sewage addition characteristically attains an initial maximum level associated with the utilization of RBCOD+slowly biodegradable (SB)COD, followed by a precipitous drop when the RBCOD is depleted to a second, lower level associated with utilization of SBCOD only; as idealized in Fig. 4.3, after WRC (1984) and Ekama *et al.* (1986). (Nitrification in the batch tests produces a constant background OUR that, while recognised, is not of importance to this discussion). The oxygen utilized (OU, mgO/ℓ-batch volume) in the consumption of the RBCOD is given by the area under the OUR-time curve bounded by the upper (RBCOD+SBCOD) and lower (SBCOD) OUR plateaus.

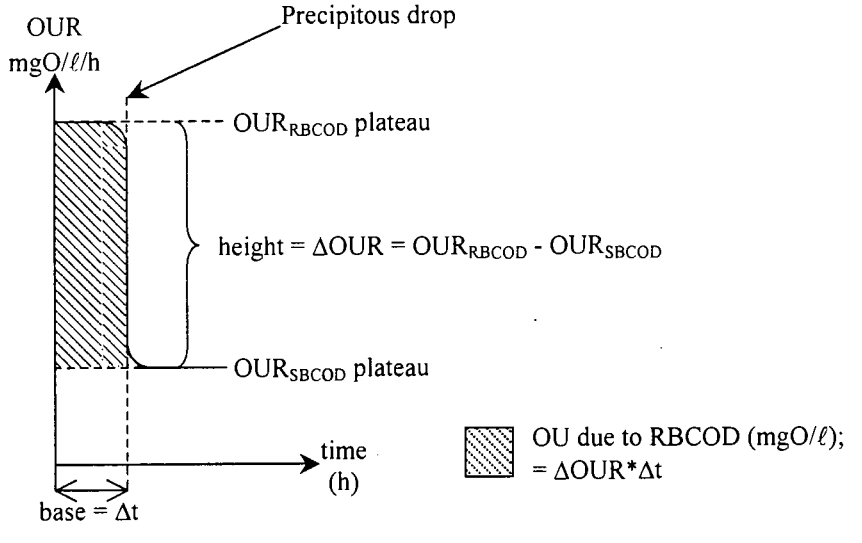

Fig. 4.3: Schematic representation of the characteristic OUR profile for an aerobic batch test with domestic sewage (after WRC, 1984; Ekama *et al.*, 1986).

To determine the OU for the batch tests, at the end of each aerobic batch test, the OUR-time data was downloaded from the DO meter to a PC and imported into a spreadsheet program. An OUR profile for the test was constructed by plotting the OUR measurements as a function of time (Fig. 4.2), and the area under the curve approximated by summing the areas of sequential rectangles (known as "Riemann sums") along the time axis (Swokowski, 1984); see Fig. 4.4:

$$R_P = \sum_{i=1}^{n} f(w_i) * \Delta x_i \qquad (4.4)$$

where:

R_P = The Riemann sum of f on the closed partition (P) [a,b]; i.e., the area of the rectangle under the portion of the curve defined by width = Δx_i and height = $f(w_i)$.

w_i = Some number in the closed subinterval $[x_i,x_{i-1}]$ on P = [a,b], for i = 1, 2, ..., n

$f(w_i)$ = the function $f(x)$ evaluated at $x = w_i$ on the interval $[x_i,x_{i-1}]$; i.e., the height and width of the rectangle, respectively.

[a,b] = a typical partition, illustrated in Fig. 4.3 below:

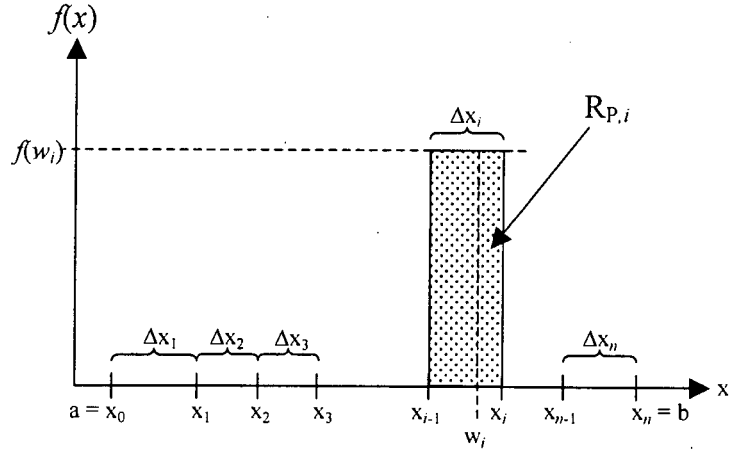

Fig. 4.4: Schematic representation of the rectangular area quantified by the Riemann sum in Eq.(4.4).

This approximation was applied to the OUR(t) plot as follows: The areas of sequential rectangular segments defined by the time interval (Δt_i) between successive OUR measurements (OUR_i and OUR_{i-1} respectively), and the approximate OUR value at the midpoint of the interval, $OUR_{mid,i}$, are summed over the length of the curve; $OUR_{mid,i}$ is estimated by linear interpolation between OUR_i and OUR_{i-1} (see Fig. 4.5).

On this basis, the area of the RBCOD portion of individual rectangles under the curve is given by:

$$Area_{RBCOD,i} \equiv Rp_i = (OUR_{mid,i} - OUR_{SBCOD})^* \Delta t_i \quad (4.5)$$

where:

$$\Delta t_i = t_i - t_{i-1} \ (=\Delta x_i \text{ in Eq.(4.4)}) \quad (4.6)$$

Rp_i = The Riemann sum of the i'th interval on $t = x$, see Eq.(4.4)

The total (net) OU (i.e. area) for complete utilization of the RBCOD, i.e. the OU in Eqs.(4.1 – 4.4), is the sum of all the individual rectangular areas, $Area_{RBCOD,i}$; i.e.:

$$OU = \sum Area_{RBCOD,i} = \sum[\Delta t_i^*(OUR_{mid,i} - OUR_{SBCOD})] \quad (4.7)$$

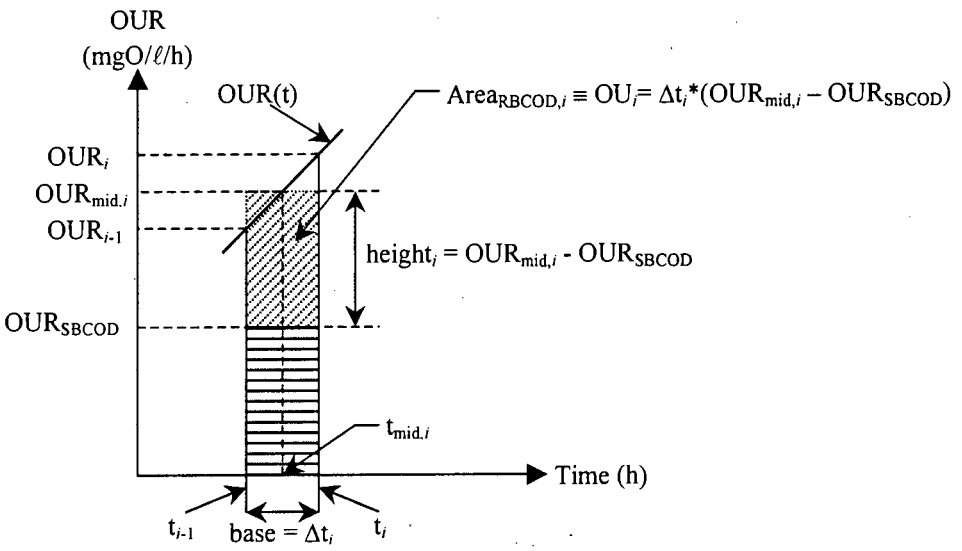

Fig. 4.5: Schematic representation of a Riemann sum (rectangular segment) under the OUR(t) curve in estimating the area (OU) under the RBCOD portion of the curve: $OU = \sum Area_{RBCOD,i} = \sum[\Delta t_i^*(OUR_{mid,i} - OUR_{SBCOD})]$.

This approximation of OU is reasonable because Δt_i is sufficiently small so that the error introduced by linear interpolation of $OUR_{mid,i}$ is negligible. Concomitantly, it is also accepted that only insignificant errors are induced by the implicit assumption that the average OUR_{SBCOD} is linear and remains constant throughout the RBCOD utilization period, and that it equals the average OUR_{SBCOD} plateau immediately following the precipitous drop in OUR. An example of a typical OUR profile and area estimation is shown in Fig. 4.2. Using the procedure above, the OUs for all aerobic batch tests were determined, see *Appendix C*.

4.4.2 Nitrate Utilization (NU) Determination

The anoxic batch tests differ from the aerobic ones in that the NO_3^- and NO_2^- concentrations with time are monitored, and not the utilization rate (as OUR is in aerobic tests). However, as presented in Chapter 1, interpretation of the nitrate/nitrite

concentration-time profile for anoxic batch tests using municipal wastewater is analogous to that of the OUR profile in corresponding aerobic batch tests. That is, two (linear) denitrification rates (slope of the nitrate-time profile) can be identified: (i) an initial rapid rate, associated with the simultaneous utilization of RBCOD and SBCOD, followed by (ii) a second, slower "K_2" rate corresponding to utilization of only SBCOD after the RBCOD is depleted; see Fig. 4.5 (after van Haandel *et al.*, 1981; WRC, 1984; Ekama *et al.*, 1986). Since the K_2 rate corresponds to SBCOD utilization only, and assuming that it remains constant throughout, the denitrification rate for utilization of RBCOD only (K_1) can be obtained by subtracting the back-projection of the K_2 rate (to the y-axis) from the observed initial rapid rate (after van Haandel *et al.*, 1981; WRC, 1984; Ekama *et al.*, 1986). On this basis, the nitrate (and nitrite) samples taken at specific time intervals during anoxic batch tests were plotted and analysed by linear regression to characterize the K_1 and K_2 rates, respectively. The difference between the respective y-intercepts of the linear regression K_1 and K_2 lines (ΔNO_3) gives the NU for RBCOD utilization (see Fig. 4.6).

Some tests exhibited nitrite accumulation during the RBCOD utilization period, which indicated that some of the observed ΔNO_3 did not result from *complete* denitrification (reduction) to nitrogen gas (N_2), but instead from partial denitrification to the intermediate NO_2. This has implications in determining the electron equivalents accepted by the nitrate. This can be seen from the stoichiometric equivalence of the electron accepting (reductive) capacities of oxygen, nitrate and nitrite as illustrated by the following half reactions, respectively (van Haandel *et al.*, 1981):

$$e^- + (1/4)O_2 + H^+ \rightarrow (1/2)H_2O \quad (4.8)$$

$$e^- + (1/5)NO_3 + (6/5)H^+ \rightarrow (1/10)N_2 + (3/5)H_2O \quad (4.9)$$

$$e^- + (1/3)NO_2 + (4/3)H^+ \rightarrow (1/6)N_2 + (2/3)H_2O \quad (4.10)$$

Accepting that there are approximately equal exchanges of free energy per electron transferred regardless of the electron acceptor (O_2, NO_3, NO_2) used (McCarty, 1964)[Υ], the transfer of one electron equivalent (e^-, e^- eq., "one mole of electrons") requires 1/5 mole NO_3 ≡ 1/3 mole NO_2 ≡ 1/4 mole O_2. Stoichiometrically, this means that the reduction of 1 mole NO_3 to N_2 consumes 5 e^- eq. (donated by the organic substrate) as compared with only 3 e^- eq. consumed in the reduction of NO_2 to N_2. Now, since NO_3 utilization is observable, NU measurements are used as an indirect estimate of the amount of substrate electrons used for energy generation versus synthesis of new cell mass in the biological oxidation of organic substrates under anoxic conditions (see Fig. 1.1, Chapter 1 and *Appendix A*). Implicit in the stoichiometric equivalence between OU and NU (i.e. 1 $mgNO_3$-N ≡ 2.86 mgO_2) is the requirement that each mole of NU reflects 5 e^- eq. donated by the RBCOD substrate. Therefore, if denitrification is only partially complete, i.e. NO_3 is denitrified only as far as NO_2 – i.e. nitrite is observed to accumulate in the process, then 3 out of the 5 e^- eq. required to denitrify NO_3 completely to N_2 (i.e. the 3 e^- eq. required to reduce NO_2 to N_2) were in effect not donated by the substrate to NO_3. That is, the apparent decrease in NO_3 (ΔNO_3) does not reflect 5 e^- eq. donated by the RBCOD as assumed. Hence, the observed ΔNO_3 must be reduced by 3/5 of the accumulated NO_2 formed during the RBCOD

[Υ] This is the basis of the COD test as a means for estimating free energy change in terms of oxygen, see Chapter 1 and Appendix A (WRC, 1984).

utilization period, to maintain the electron balance and stoichiometric equivalence between NU and OU in the process; i.e. the validity of Eqs.(4.1 – 4.3).

Specifically, this means that the difference in the K_1 and K_2 y-intercepts (ΔNO3) must be reduced by 3/5 of the NO_2 concentration accumulated at the end of the RBCOD utilization period in the anoxic batch test; i.e. (see Figs. 4.6 and 4.7):

$$NU = \Delta NO_3 - (3/5)*NO_2 = N_{K1} - N_{K2} - (3/5)*NO_2 \qquad (4.11)$$

A schematic of a typical NUR profile for an anoxic (denitrification) batch test containing domestic sewage (after WRC, 1984; Ekama *et al.*, 1986) is shown in Fig. 4.6, and an example of an actual NUR profile (DBT 16) of an anoxic batch test in this investigation is presented in Fig. 4.7. All anoxic batch tests were analysed following the procedures above to determine the equivalent NU.

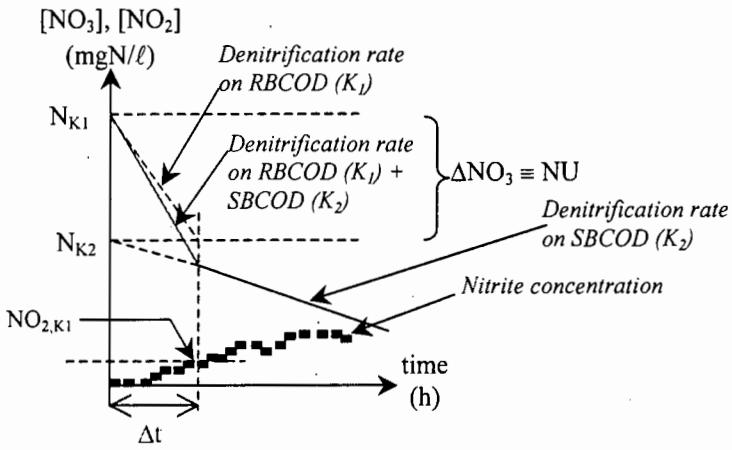

Fig. 4.6: Schematic representation of a typical NUR profile for an anoxic batch test containing domestic sewage (after WRC, 1984; Ekama *et al.*, 1986).

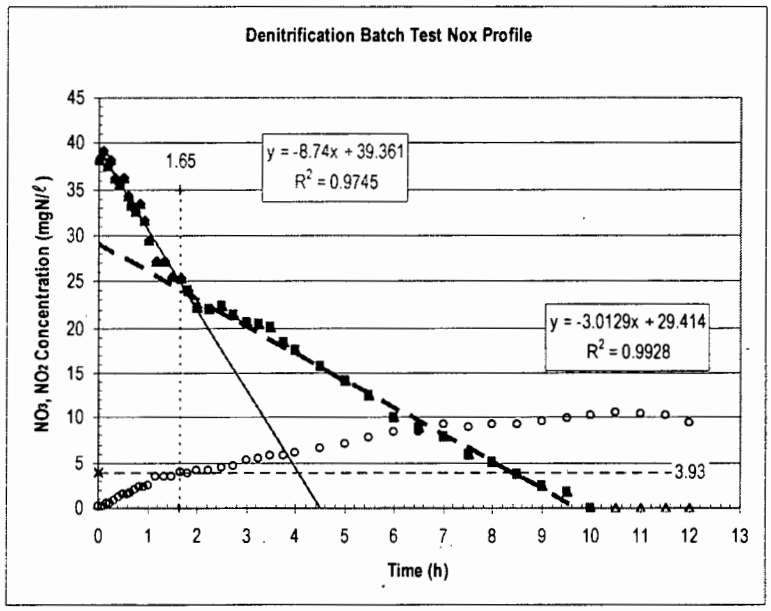

Fig. 4.7: Denitrification (anoxic) batch test number 16 (DBT 16) as a typical example of a NUR profile and NU estimation for RBCOD consumption in the test: $\Delta NO_3 = 39.361 - 29.414 = 9.95$ mgN/ℓ and $NO_2 = 3.93$ mgN/ℓ, $\Rightarrow$ NU = 9.95 – 0.6*3.93 = 7.59 mgN/ℓ.

As discussed in Section 4.3.3, the NO_3 and NO_2 concentrations determined in denitrification batch tests DBT 34 – 37 were analysed by ion chromatography (IC) at an outside (Dept. Geological Sciences, UCT) laboratory and not in the Water Research Laboratory (WRL) by the Technicon Auto-Analyser (TAA) method, as for all other NO_3 and NO_2 analyses performed in this investigation (see Section 3.9, Chapter 3). Preserved samples from anoxic batch tests DBT 34 – 37 were diluted with distilled water (DW) to within the maximum IC analytical range of 20 mgNO_3/ℓ and delivered to the outside laboratory for analysis. As an independent check on the accuracy and precision of the IC analyses, a set of the NO_3 and NO_2 standard solutions normally used in the TAA analyses were included amongst the anoxic batch test samples sent to the outside laboratory. The IC measurements of the standard solutions were almost identical to their known concentrations, but some variation was observed. This variation can be due to variations caused by the preparation and use of eluant, reagents and a mixed-standard (containing $NaNO_3$ and $NaNO_2$) by the outside laboratory in the IC method: Serial dilutions of the mixed-standard are analysed on the ion chromatograph and a linear fit is made to their corresponding peak areas; peak areas of the desired anions, i.e. NO_3 and NO_2, in the unknown samples are then measured and converted via the standard curve (linear fit) to corresponding concentrations, in mgNO_3/ℓ and mgNO_2/ℓ units respectively. To eliminate these uncertainties and variations, it was decided to accept the sets of standards provided by the WRL for IC analysis. To correct the IC results, the IC values determined for the known NO_3 and NO_2 WRL standards (composed of KNO_3 and KNO_2) normally used in the TAA method (Section 3.7, Chapter 3), were plotted against the known concentrations and their respective relationships determined by a linear fit to the data forced through the origin (Figs. 4.7 and 4.8). On this basis, the outside laboratory's IC determined NO_2 and NO_3 concentrations in the batch test samples were converted via Eqs.(4.12) and (4.13), respectively, into "equivalent TAA" values based on the supplied standards:

$$NO_2: \quad TAA\ (mgN/\ell) = 1.1473*IC\ (mgN/\ell) \equiv 0.2591*IC\ (mgNO_2/\ell) \qquad (4.12)$$

$$NO_3: \quad TAA\ (mgN/\ell) = 1.1221*IC\ (mgN/\ell) \equiv 0.2534*IC\ (mgNO_3/\ell) \qquad (4.13)$$

The IC determined values for the known WRL NO_3 and NO_2 standard solution concentrations are presented in Table 4.4 and plotted in Figs. 4.7 and 4.8, respectively.

Table 4.4: Corresponding nitrate (NO_3) and nitrite (NO_2) concentrations determined by ion chromatography (IC) at a contracted outside laboratory, for the Water Research Laboratory's (WRL) standard NO_3 and NO_2 solutions normally used in the Technicon Auto-Analyser (TAA) method (Section 3.7, Chapter 3); excluding one value (shaded) from the linear fit.

TAA (mgN/ℓ)		IC (mgNOx/ℓ)		IC (mgN/ℓ)	
NO_3	NO_2	NO_3	NO_2	NO_3	NO_2
0.25	0.1	1.06	0.04	0.239	0.009
0.5	0.2	1.83	0.91	0.413	0.205
0.75	0.3	2.74	1.07	0.619	0.242
1.0	0.4	3.86	1.49	0.872	0.336
1.25	0.5	7.78	1.86	(1.757)	0.420
1.5	0.6	6.01	2.30	1.357	0.519
1.75	0.7	6.72	2.78	1.517	0.628
2.0	0.8	8.12	4.27	1.834	0.964

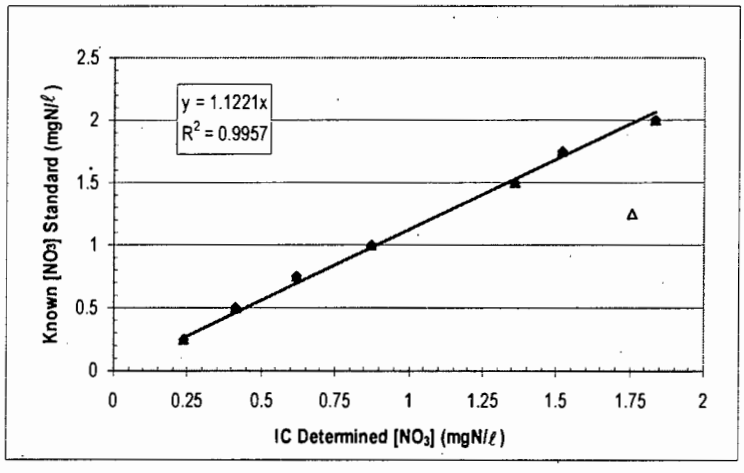

Fig. 4.7: Plot of nitrate concentrations ("[NO_3]") determined by ion chromatography (IC) at an outside laboratory, using a sodium based mixed-standard, for the Water Research Laboratory's (WRL) standard (potassium based) NO_3 solutions normally used in the Technicon Auto-Analyser (TAA) method (Section 3.7, Chapter 3)., in mgN/ℓ; one value is excluded from the linear fit (shaded in Table 4.4).

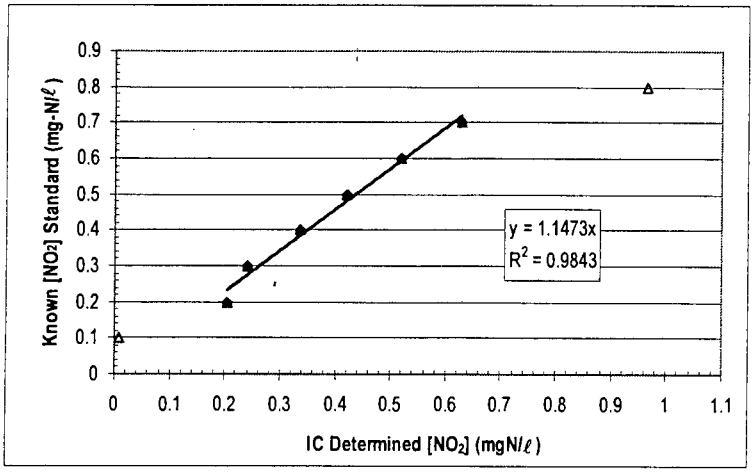

Fig. 4.8: Plot of nitrite concentrations ("$[NO_2]$") determined by ion chromatography (IC) at an outside laboratory, using a sodium based mixed-standard, for the Water Research Laboratory's (WRL) standard (potassium based) NO_2 solutions normally used in the Technicon Auto-Analyser (TAA) method (Section 3.7, Chapter 3)., in mgN/ℓ.

4.5 CLOSURE

In this Chapter, the procedures followed to conduct the aerobic and anoxic batch tests have been described, as well as the calculation procedures to determine OU and NU from the batch test data. In Chapter 5, the results of these batch tests will be presented.

CHAPTER 5

AEROBIC AND ANOXIC BATCH TEST RESULTS

5.1 INTRODUCTION

5.1.1 General Background

In Chapter 1, it was shown that reduced energy capture in biological oxidation of organic substrate with nitrate as electron acceptor (as compared with oxygen), suggests that the ordinary heterotrophic organism (OHO) yield under anoxic conditions ($Y_{H,NO}$) should be reduced relative to its aerobic value ($Y_{H,AE}$). Based on bioenergetic and thermodynamic principles, it is demonstrated in *Appendix A* that the anoxic cell yield ($Y_{H,NO}$) is theoretically about 83% of its aerobic value ($Y_{H,AE}$). Furthermore, several studies reviewed in Chapter 2 suggest an experimentally derived average $Y_{H,NO}$ of approximately 81 ± 3.5% with respect to the corresponding aerobic value ($Y_{H,AE}$), or about 0.54 (range 0.52 – 0.57) with respect to the conventionally accepted $Y_{H,AE}$ of 0.67 mgCOD/mgCOD. However, lacking in the current body of research on $Y_{H,NO}$, are any studies and experiments to directly quantify or measure $Y_{H,NO}$ using domestic sewage as substrate. Thus, the principle aim of this research is to investigate and quantify $Y_{H,NO}$ relative to $Y_{H,AE}$ for domestic sewage. Specific objectives identified are:

1. Determine the ratio $Y_{H,NO}$:$Y_{H,AE}$ for real sewage in terms of electron acceptor (i.e. nitrate and oxygen respectively) utilization.

2. Measure $Y_{H,NO}$ and $Y_{H,AE}$ directly for known concentration of readily biodegradable (RB)COD utilized.

3. Compare experimental results with other, independent studies on real wastewater.

The research approach adopted for the experimental investigation to address the objectives above is detailed in Chapter 1. In summary, the expressions quantifying RBCOD consumption in aerobic (AE) and anoxic (AX) respiration, in terms of the OHO yield and respective oxygen and nitrate utilized (OU and NU respectively), can be equated if the same mass of RBCOD is utilized; i.e.:

$$RBCOD_{AE} = \frac{OU}{(1 - Y_{H,AE})} \tag{5.1}$$

$$RBCOD_{AX} = \frac{2.86 * NU}{(1 - Y_{H,NO})} \tag{5.2}$$

$\Rightarrow$ for $RBCOD_{AE} = RBCOD_{AX}$:

$$\frac{OU}{(1-Y_{H,AE})} = RBCOD \equiv S_s = \frac{2.86*NU}{(1-Y_{H,NO})} \quad (5.3)$$

Therefore, for the same concentration of RBCOD utilized, $Y_{H,NO}$ can be expressed in terms of OU, NU and the aerobic cell yield coefficient, $Y_{H,AE}$:

$$\therefore Y_{H,NO} = 1 - \frac{2.86*NU}{OU}*(1-Y_{H,AE}) \quad (5.4)$$

On this basis, the OU and NU were measured in corresponding aerobic and anoxic batch tests (respectively) containing the same RBCOD, and Eq.(5.4) plotted to give $Y_{H,NO}$ in terms of $Y_{H,AE}$. This enabled the ratio of the two yields to be calculated or $Y_{H,NO}$ to be determined for any selected value of $Y_{H,AE}$ (Objective 1 above). Accepting the standard value of $Y_{H,AE}$ = 0.67 mgCOD/mgCOD, values for $Y_{H,NO}$ were estimated from the measured OU and NU via Eq.(5.4).

An independent assessment of the estimations above was also performed by direct determination of $Y_{H,AE}$ and $Y_{H,NO}$ (Objective 2 above) by: (i) measuring the wastewater RBCOD concentration added to the batch tests (see Chapter 3), and (ii) adding known masses of the artificial RBCOD, acetate, to the batch tests (see Chapter 4). Additionally, experimental data reported by other researchers in the literature, from which it was possible to derive values for the $Y_{H,NO}$:$Y_{H,AE}$ ratio or the individual coefficients, were identified and re-analysed for comparison with the values obtained here (Objective 3 above).

5.1.2 Basic Batch Test Procedure

The experimental methods and procedures for performing the aerobic and anoxic batch tests are detailed in Chapter 4. In summary, the batch tests were performed using domestic wastewater from the Mitchells Plain Wastewater Treatment Plant (MPWWTP), and biomass obtained from laboratory-scale Modified Ludzack-Ettinger (MLE) systems fed wastewater from this plant, as well as from the MPWWTP. In each batch test, defined volumes of wastewater (V_{WW}) and mixed-liquor (V_{ML}) were combined in a continuously stirred batch reactor of 3ℓ total volume (V_{BT}). In the aerobic batch tests (ABT), the oxygen utilization rate (OUR) with time was measured automatically (Randall *et al.*, 1991), while in the denitrification batch tests (DBT), the nitrate utilization rate (NUR) was determined from the nitrate concentration versus time profile for samples drawn manually at specific time intervals during the test. The batch experiments performed were grouped into the three chronological Periods summarised in Table 5.1 below.

Table 5.1: Experimental Periods for aerobic and anoxic (denitrification) batch test experiments, labelled "ABT" and DBT" respectively.

Period	Dates	ABT	DBT
I	17/1/02 – 4/6/02	1 – 22	1 – 19
II	26/8/02 – 10/10/02	23 – 34	20 – 29
III	11/10/02 – 16/12/02	35 – 40	30 – 42

5.2 INDEPENDENT RBCOD ESTIMATION

As discussed previously (Chapters 1, 2 and 3), RBCOD is an important parameter in this research. Although not explicitly required to estimate $Y_{H,NO}$ from equivalent aerobic and anoxic batch tests, provided $Y_{H,AE}$ is known, the RBCOD concentration is required to determine $Y_{H,NO}$ and $Y_{H,AE}$ directly and independantly. Results for RBCOD determination for the research periods are presented in this Section.

5.2.1 Period I

In Period I, independent estimation of the wastewater RBCOD fraction was by the flocculation-filtration (FF) method described in Section 3.8.1, Chapter 3, using the fraction of unbiodegradable soluble COD (f_{us}) obtained from a long sludge age UCT activated sludge system operated concurrently on the same sewage. A detailed analysis of the COD data for the UCT system is presented in *Appendix C*.

Each sewage batch was accepted as a steady-state period, and daily measurements of the UCT system filtered effluent, total influent and floc-filtered (FF) influent COD (S_{use}, S_{ti} and COD_{FF} respectively) were analysed for consistency within the 95% confidence interval; each value outside the interval range mean ± 1.96*sample standard deviation, was rejected as non-representative of steady-state performance during that sewage batch (steady-state) period. The remaining measurements were averaged to represent the respective "average" COD values for that sewage batch. The corresponding average unbiodegradable soluble COD fraction with respect to total COD (f_{us}) in the wastewater, was calculated from the sewage batch averages of valid daily measurements for S_{use} and S_{ti} via Eq.(5.5).

$$f_{us} = S_{use}/S_{ti} \qquad (5.5)$$

Similarly, the average steady-state wastewater RBCOD concentration and as a fraction with respect to total COD (f_{ts}), were calculated from the corresponding sewage batch average for daily COD_{FF} measurements, and the steady-state average f_{us} determined by Eq.(5.5), i.e.:

$$RBCOD_{FF} \equiv S_{bsi,FF} = COD_{FF} - f_{us}*S_{ti} \qquad (5.6)$$

$$\Rightarrow f_{ts,FF} = RBCOD_{FF}/S_{ti} \qquad (5.7)$$

A summary of the f_{us} and f_{ts} sewage batch steady-state averages determined for the UCT system are presented in Table 5.2 below:

Table 5.2: UCT System: Sewage batch (SB) average (AVG) influent (S_{ti}), floc-filtered influent (COD_{FF}), fraction RBCOD (fts_{FF}) and unbiodegradable soluble (f_{us}) COD, and RBCOD concentration ($Sbsi_{FF}$); also shown are sample standard deviations (SSD) and number of samples (N).

	S_{ti} (mgCOD/ℓ)			COD_{FF} (mgCOD/ℓ)			fus	$Sbsi_{FF}$	fts_{FF}
SB	AVG	SSD	N	AVG	SSD	N	AVG	mgCOD/ℓ	AVG
1	663.1	159.4	11				0.056		
2	697.9	55.6	10				0.037		
3	673.1	103.6	7	113.4	8.9	6	0.053	77.7	0.115
4	653.1	63.7	9	164.0	27.7	9	0.060	124.7	0.191
6	690.6	67.8	10	177.1	27.2	10	0.061	134.6	0.195
8	696.8	29.8	7	143.8	15.6	7	0.055	105.5	0.151
9	590.2	47.3	5	116.5	8.5	5	0.060	81.3	0.138
10	735.0	51.6	3	169.9	24.8	2	0.047	135.6	0.184
12	754.9	27.3	2				0.061		

The steady-state average $f_{ts,FF}$ values were evaluated for outliers and analysed statistically in a linearized probability graph, see Fig. 5.1.

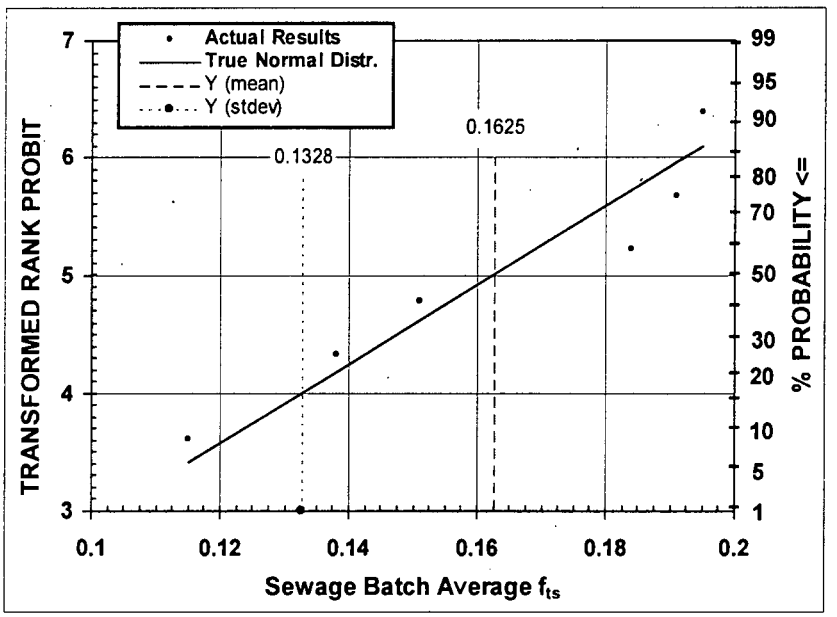

Fig. 5.1: UCT System: Linearized probability plot of average (steady-state) influent wastewater $RBCOD_{FF}$ fraction with respect to total COD ($f_{ts,FF}$).

No outliers were identified for the $f_{ts,FF}$ averages in Fig. 5.1, and the fit to the linear true normal line is reasonable, indicating a normal distribution. On this basis, the mean $f_{ts,FF}$ for Period I is 0.163 with a sample standard deviation of 0.03 (range 0.133 – 0.193). See *Appendix C* for a complete analysis.

5.2.2 Periods II and III

Independent estimation of the wastewater RBCOD fraction in Periods II and III, was achieved via both the flocculation-filtration method as applied to the dedicated MLE system, and the OUR response of the square-wave (SQW) fed short sludge age activated sludge system as described in Chapter 3.

During Periods II and III, the flocculation-filtration method was applied to the MLE system; as described in Section 3.10, Chapter 3, an average f_{ts} = 0.15 0.022 was obtained for sewage batches 18 – 25, see Fig. 3.10.

For the SQW system, a detailed analysis of the system data is presented in Section 3.11, Chapter 3, and is summarised in Table 5.3 below.

Table 5.3: SQW System: Sewage batch (SB) average influent flow rate (Q_s), ΔOUR, RBCOD concentration ($S_{bsi,S}$, mgCOD/ℓ) and fraction ($f_{ts,S}$) with respect to total influent COD ($S_{ti,S}$, mgCOD/ℓ); also shown are sample standard deviations (SSD) and number of samples (N).

	Q_s (ℓ/d)			ΔOUR (mgO/ℓ/h)			Sti_S	$Sbsi_S$	fts_S
SB	AVG	SSD	N	AVG	SSD	N	AVG	AVG	AVG
18	36.14	0.7	12	4.07	0.8	13	489.5	54.8	0.112
19	35.82	0.7	16	3.73	0.7	7	498.8	50.7	0.102
20	35.33	1.0	14	4.85	0.6	13	477.8	66.9	0.140
21	35.99	1.7	13	4.5	0.6	11	487.5	60.9	0.125
22	36.31	1.1	11	6.47	1.0	10	509.0	86.8	0.171
23	35.76	0.4	17	5.19	0.7	16	486.9	70.8	0.145
24	35.91	1.1	14	4.74	0.5	14	487.6	64.4	0.132
25	35.04	1.6	11	7.16	0.9	10	510.7	99.6	0.195

For statistical analysis, the average RBCOD fractions with respect to total COD (f_{ts}) for the respective sewage batch (steady-state) periods, were evaluated for outliers and are plotted in the linearized probability graph Fig. 5.2.

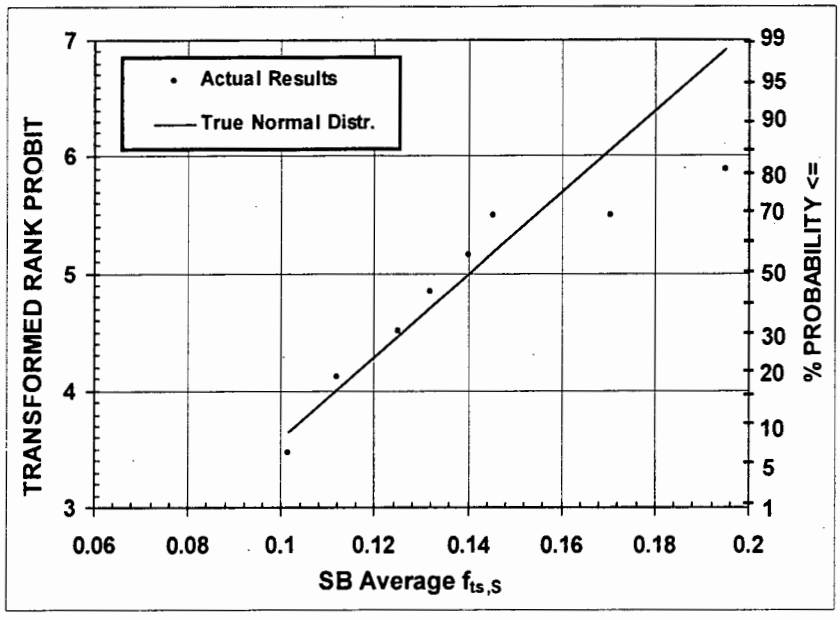

Fig. 5.2: SQW System: Statistical plot of sewage batch (SB) average (steady-state) RBCOD fraction with respect to total COD ($f_{ts,S}$) in influent wastewater.

Although no outliers were identified, the two highest values in the range do exhibit deviation from the true normal line; i.e. sewage batches 22 (0.17) and 25 (0.19), respectively. Despite this deviation, however, the remaining points display a good fit to the true normal line and give an average $f_{ts,S} = 0.14$ with sample standard deviation = 0.03. Although this value compares well with the SQW average $f_{ts} = 0.16$ obtained by Ekama and Marais (1978), as well as with the floc-filtered average $f_{ts,FF} = 0.163$ and $f_{ts,FF} = 0.15$ obtained with the respective UCT (see Section 5.2.1 above) and MLE (see Section 3.10, Chapter 3) systems in this study, it is lower than the average SQW $f_{ts} = 0.19$ and floc-filtered $f_{ts} = 0.18$ of Mbewe *et al.* (1995), all values for wastewater from the same source.

5.3 BATCH TEST RESULTS: PERIOD I

5.3.1 Estimation of $Y_{H,NO}$ in terms of $Y_{H,AE}$ Using Wastewater RBCOD

In Period I, sewage batches (SB) 4 – 13 were used over the period 1/17/02 – 4/6/02, and 22 aerobic and 19 anoxic batch tests were performed, as summarised in Table 5.4 below. Aerobic and anoxic (denitrification) batch tests (ABT and DBT respectively) in Period I were performed in parallel, with mixtures of the same volumes of wastewater (V_{WW}) and mixed-liquor (V_{ML}), abstracted from the same samples of wastewater and activated sludge, respectively. Consequently, the composition (and index number) for the parallel aerobic and anoxic batch tests in Table 5.4 were identical, except for SB 12 and 13 (shaded) which refer only to aerobic batch tests, since no corresponding anoxic batch tests were performed. Detailed results for the batch tests are presented in *Appendix C*.

Table 5.4: Period I: Summary of aerobic and anoxic (denitrification) batch tests (ABT and DBT respectively), showing sewage batch (SB) used, batch test number (No.), mixed-liquor (ML) source, volumes of wastewater (V_{WW}) and mixed-liquor (V_{ML}) added, total COD concentration of the wastewater ($S_{ti,R}$), the mixed-liquor (ML) volatile suspended solids (VSS) concentration (X_V) and the organic loading rate (LR) in the test. "LML" = ML from concurrent MLE laboratory-scale systems; "MPP" = ML from Mitchells Plain Wastewater Treatment Plant.

SB	Date (2002)	ABT/DBT No.	ML	V_{WW} (ℓ)	V_{ML} (ℓ)	Sti_R (mgCOD/ℓ)	X_V (mgVSS/ℓ)	LR (COD/VSS)
4	17/1	1	LML	2.7	0.3	480	3347	1.29
	22/1	2	LML	2.7	0.3	528	3188	1.49
6	24/2	3	LML	2.7	0.3	245	2497	0.88
	25/2	4	LML	2.55	0.45	224	2424	0.52
	26/2	5	LML	0.815	0.685	1072	2505	0.51
	27/2	6	LML	1.63	1.37	980	2587	0.45
	7/3	7	LML	2	1	871	4288	0.41
9	4/4	8	LML	2	1	892.5	4109	0.43
	9/4	9	LML	2	1	917.5	4061	0.45
	15/4	10	LML	2	1	845.3	4153	0.41
	17/4	11	LML	2	1	853.6	4311	0.40
10	24/4	12	LML	2	1	1038.4	4053	0.51
	26/4	13	LML	2	1	1179.4	4034	0.58
11	29/4	14	MPP	2	1	1090.8	3102	0.70
	2/5	15	MPP	2	1	1151.2	2921	0.79
	3/5	16	MPP	2	1	1151.2	2887	0.80
	4/5	17	MPP	2	1	1126.8	2844	0.79
	5/5	18	MPP	2	1	1172	2724	0.86
NS	11/5	19	MPP	2	1	1154	1520	1.52
12	16/5	20	MPP	2	1	1337.2	2529	1.06
13	3/6	21	LML	1.333	0.667	967.2	5468	0.35
	4/6	22	MPP	2	1	1209	2161	1.12

Batch test data were analysed via Eq.(5.4) with the measured OU and NU, to determine values for $Y_{H,NO}$ for corresponding values for $Y_{H,AE}$. In the initial (17/1/02 – 27/2/02, SB 4 – 6, Table 5.4) batch tests, the compositions varied from one test day to the next so that only the OU and NU of a corresponding pair of aerobic and anoxic batch tests could be used in Eq.(5.4) to estimate $Y_{H,NO}$ with respect to $Y_{H,AE}$. Consequently, if either the OU or NU obtained for the aerobic or anoxic batch test pair was invalidated in some way (e.g. OUR readings deleted from the DO meter due to a power failure; disruption of the air supply caused by a compressor malfunction; indistinguishable K_1 and K_2 denitrification profiles due to insufficient NO_3 added at the start of anoxic tests; distortion of NO_3 and NO_2 sample peaks on the Technicon Auto-Analyser), then an estimate for $Y_{H,NO}$ could not be obtained from the particular batch test pair. Subsequently in the investigation it was realized that, since it was found that the individual daily RBCOD measurements on a particular sewage batch are consistent and can be averaged to give the average sewage batch (steady-state) RBCOD fraction with respect to total COD (f_{ts}), it can be accepted that aerobic and anoxic batch tests performed using the same volume of sewage from the same sewage batch, contain the same mass of RBCOD. Furthermore, during a particular sewage

batch the same volume of mixed-liquor from the same source was added to the batch tests, i.e. same quality of mixed-liquor. Accordingly, for batch tests conducted during a specific sewage batch, $Y_{H,NO}$ can be estimated in terms of $Y_{H,AE}$ by Eq.(5.4), from different combinations of all the OU and NU determined in respective aerobic and anoxic batch tests, provided the same V_{WW} from the same sewage batch was added to all the tests. Thus, in the set of batch tests if the data from one test is invalidated, only this test's data need to be excluded from the analysis. Accordingly, from SB 6 batch test compositions were standardized (see Chapter 4 and Table 5.4). In analysis of the batch tests, all the batch tests conducted during one sewage batch were grouped, and all possible combinations of OU and NU values inserted into Eq.(5.4) to determine estimates for $Y_{H,NO}$ for various $Y_{H,AE}$. This procedure was followed for the rest of the investigation.

Excluding invalidated batch tests, estimates of $Y_{H,NO}$ as a function of $Y_{H,AE}$ are plotted in Figs. 5.3, 5.4 and 5.5 for corresponding OU-NU combinations, determined from respective aerobic and anoxic batch tests for SB 4 – 6, 10 and 11 respectively.

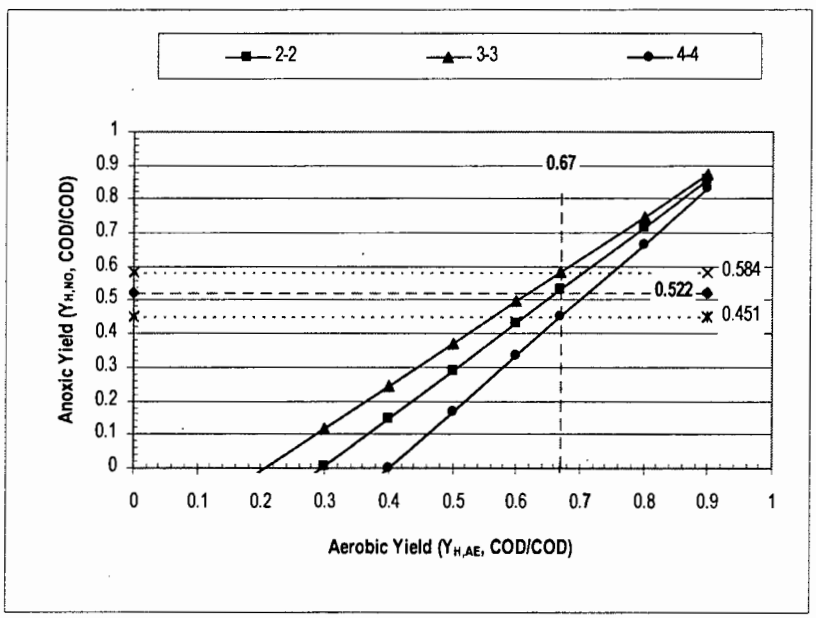

Fig. 5.3: Period I: Plot of $Y_{H,NO}$ in terms of $Y_{H,AE}$ for OU-NU combinations from respective aerobic and anoxic batch tests using sewage batches (SB) 4 – 6; legend key refers to aerobic-anoxic batch test numbers.

For SB 4 – 6, an average $Y_{H,NO} = 0.522 \pm 0.067$ (range 0.455 – 0.589) with respect to $Y_{H,AE} = 0.67$ mgCOD/mgCOD was obtained (Fig. 5.3), which is an anoxic to aerobic yield ratio of 77.9%. Although the ratio $Y_{H,NO}:Y_{H,AE} = 0.779$ is slightly lower (6%) than the theoretically predicted $Y_{H,NO}:Y_{H,AE} = 0.83$, the average $Y_{H,NO} = 0.522$ is very close to the average of 0.54, or yield ratio of 81 ± 3.5%, with respect to $Y_{H,AE} = 0.67$ mgCOD/mgCOD determined for the various experimental investigations reported in the literature (see Chapter 2).

Similarly, for SB 10 plots of $Y_{H,NO}$ estimates with respect to $Y_{H,AE}$ for the various OU-NU combinations obtained in respective aerobic and anoxic batch tests are shown in Fig. 5.4.

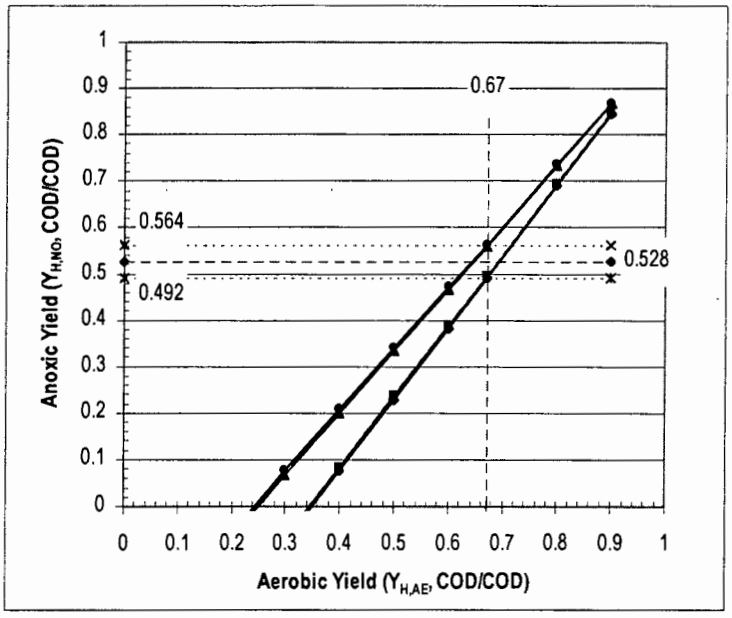

Fig. 5.4: Period I: Plot of $Y_{H,NO}$ in terms of $Y_{H,AE}$ for OU-NU combinations from respective aerobic and anoxic batch tests using sewage batch (SB) 10.

For SB 10, an average $Y_{H,NO} = 0.528 \pm 0.039$ (range 0.489 – 0.567) mgCOD/mgCOD with respect to $Y_{H,AE} = 0.67$ mgCOD/mgCOD was obtained (Fig. 5.4), or equivalently a $Y_{H,NO}$:$Y_{H,AE}$ ratio of 78.8%. As with SB 4 – 6, the average $Y_{H,NO}$:$Y_{H,AE} = 0.788$ is slightly lower (5%) than the theoretically predicted $Y_{H,NO}$:$Y_{H,AE} = 0.83$, and the average $Y_{H,NO} = 0.528$ is close to the average of 0.54, or the yield ratio of 81 ± 3.5%, with respect to $Y_{H,AE} = 0.67$ mgCOD/mgCOD, determined for the various experimental investigations in the literature (Chapter 2).

For SB 11, estimates of $Y_{H,NO}$ as a function of $Y_{H,AE}$ from OU-NU combinations of respective aerobic and anoxic batch tests, are plotted in Fig. 5.5.

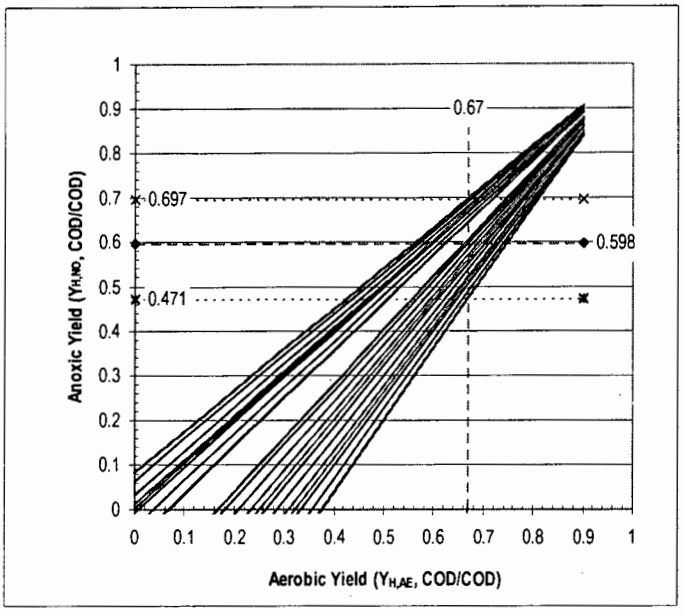

Fig. 5.5: Period I: Plot of $Y_{H,NO}$ in terms of $Y_{H,AE}$ for OU-NU combinations from respective aerobic and anoxic batch tests using sewage batch (SB) 11.

For SB 11 (Fig. 5.5), the $Y_{H,NO}$ estimates give an average $Y_{H,NO}$ = 0.598 ± 0.073 (range 0.525 – 0.671) mgCOD/mgCOD with respect to $Y_{H,AE}$ = 0.67 mgCOD/mgCOD, or equivalently a yield ratio of 89.3%. The average $Y_{H,NO}$ and average $Y_{H,NO}$:$Y_{H,AE}$ ratio are higher (7.6%) than the theoretically predicted $Y_{H,NO}$:$Y_{H,AE}$ = 0.83, as well as the calculated literature experimental average $Y_{H,NO}$ = 0.54, or yield ratio of 81 ± 3.5%, with respect to $Y_{H,AE}$ = 0.67 mgCOD/mgCOD. However, the data in Fig. 5.5 appears to group into two sets, which, if true, will require that they be separated and analysed individually. The two apparent data sets in Fig 5.5 were separated by calculating $Y_{H,NO}$ for each ABT-DBT (i.e. OU and NU respectively) combination, in terms of $Y_{H,AE}$ = 0.67 mgCOD/mgCOD. These $Y_{H,NO}$ estimates were then ranked in ascending order while retaining the corresponding ABT-DBT index for each. By inspection, data set one was selected for all $Y_{H,NO}$ estimates ≤ 0.604 mgCOD/mgCOD, while data set 2 comprised the remainder, i.e. $Y_{H,NO}$ > 0.604 mgCOD/mgCOD; the two data sets, "1" and "2" respectively, are listed in Table 5.6. To determine whether or not the two apparent data sets originate from two different data populations, the Student t-Test was used to compare the means of the two populations (see Table 5.6): if the means are equal, then the two data sets originate from the same population and can be grouped; however, if the means are not equal, then the two data sets originate from different populations and must be treated separately. In the Student t-Test it is assumed that the variances of the two populations are equal; this assumption must be tested using the F-Test. See Underhill and Bradfield (1996) for detailed descriptions of the F- and t-Test methods.

Accordingly, first the F-Test was applied to the two identified sets of $Y_{H,NO}$ values, see *Appendix D*. This indicated that the population variances for the two data sets could not be assumed to be equal. In such cases, the Student t-Test cannot be used. However, an approximate t-Test that does not pool the variances can be used

(Underhill and Bradfield, 1996). Accordingly, the approximate t-Test was applied to the two sets of data (*Appendix D*). This indicated that the two data sets originated from different populations and must, therefore, be analysed separately. Reasons for the differentiation into the two populations were sought.

Table 5.6: Sewage batch (SB) 11 data analysis: Two data sets (1 and 2) separated by ranking $Y_{H,NO}$ estimates for each ABT-DBT (i.e. OU and NU respectively) combination using $Y_{H,AE}$ = 0.67 mgCOD/mgCOD. Also shown are: sample standard deviation (SSD), sample mean, number of data (N) and sample degrees of freedom (Deg. f).

SB 11: DATA SET 1		SB 11: DATA SET 2	
ABT-DBT Combination	**$Y_{H,NO}$ (mgCOD/mgCOD)**	**ABT-DBT Combination**	**$Y_{H,NO}$ (mgCOD/mgCOD)**
16-14	0.471	16-18	0.646
15-14	0.488	15-18	0.657
14-14	0.504	14-18	0.668
17-14	0.513	16-17	0.671
18-14	0.513	17-18	0.674
16-16	0.523	18-18	0.674
15-16	0.538	15-17	0.681
14-16	0.552	14-17	0.691
17-16	0.561	17-17	0.697
18-16	0.561	18-17	0.697
16-15	0.570		
15-15	0.584		
14-15	0.597		
17-15	0.604		
18-15	0.604		
SSD1	0.042484	**SSD2**	0.0167345
N1	15	**N2**	10
Deg. f1	14	**Deg. f2**	9
Mean1	0.546	**Mean2**	0.676

Reviewing the data in Table 5.6, it is apparent that all the $Y_{H,NO}$ estimates in data set 2 are formed by OU-NU combinations corresponding with the NU from DBT 17 and 18. It is reasonable to assume, therefore, that DBT 17 and 18 were each influenced by a single dominant factor, and, therefore, cannot be accepted as representative of the same batch test conditions as the other batch tests also using SB 11. Consequently, DBT 17 and 18 were rejected for further analysis. Also, since the aerobic and anoxic batch tests in Period I were performed in parallel on the same day, composed of the same wastewater and mixed-liquor samples, it was assumed that ABT 17 and 18 were subject to the same influences and conditions as DBT 17 and 18; therefore, the corresponding aerobic batch tests, ABT 17 and 18, were also rejected for further analysis.

On this basis, excluding ABT and DBT 17 and 18, estimates for $Y_{H,NO}$ from corresponding OU-NU combinations of the remaining batch tests using SB 11, are plotted in Fig. 5.6.

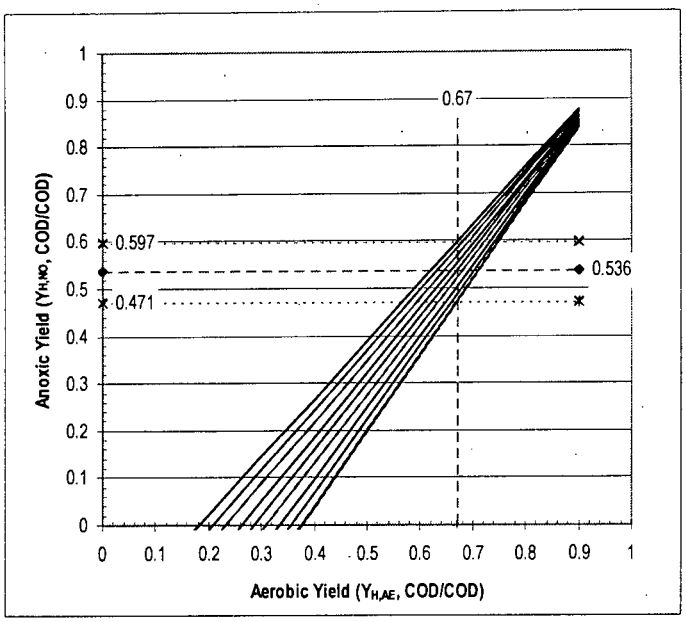

Fig. 5.6: Period I: Revised plot of $Y_{H,NO}$ in terms of $Y_{H,AE}$ for OU-NU combinations from respective aerobic and anoxic batch tests using sewage batch (SB) 11, excluding aerobic and anoxic tests 17 and 18.

The data for SB 11 in Fig. 5.6 gives an average $Y_{H,NO} = 0.536 \pm 0.043$ (range 0.493 – 0.579) mgCOD/mgCOD with respect to $Y_{H,AE} = 0.67$ mgCOD/mgCOD, or equivalently a yield ratio of 80.0%. The $Y_{H,NO}:Y_{H,AE} = 0.80$ is consistent with the theoretically predicted $Y_{H,NO}:Y_{H,AE} = 0.83$, and the average $Y_{H,NO} = 0.536$ is in good agreement with the average of 0.54, or yield ratio of 81 ± 3.5%, with respect to $Y_{H,AE} = 0.67$ mgCOD/mgCOD, determined in Chapter 2 for the experimental investigations in the literature.

To check for normality, the estimates of $Y_{H,NO}$, with respect to $Y_{H,AE} = 0.67$ mgCOD/mgCOD, determined for SB 11 were analysed in the linearized probability plot, Fig. 5.7.

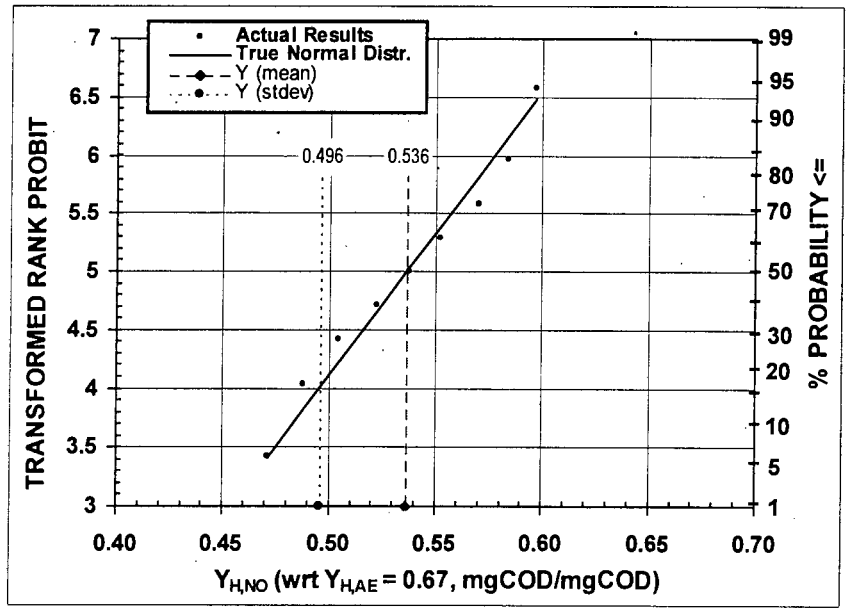

Fig. 5.7: Period I: Statistical plot of $Y_{H,NO}$ in terms of $Y_{H,AE}$ for OU-NU combinations from respective aerobic and anoxic batch tests using sewage batch (SB) 11.

The data for SB 11 in Fig. 5.7 exhibits only slight curvature with respect to the true normal line, indicating that the data are normally distributed – i.e. it is accepted that the influences on the data were small and random, with no single factor exerting dominating influence. The mean $Y_{H,NO}$ is 0.536 ± 0.04 (range 0.496 – 0.576) mgCOD/mgCOD with respect to $Y_{H,AE}$ = 0.67 mgCOD/mgCOD, or equivalently the yield ratio is 80.0%, for the corresponding aerobic and anoxic batch tests using SB 11.

In summary, all the $Y_{H,NO}$ estimates corresponding to $Y_{H,AE}$ = 0.67 mgCOD/mgCOD determined in Period I are presented in Table 5.7; the estimates were analysed for outliers and plotted in the linearized probability graph, Fig. 5.8.

Table 5.7: Period I Summary: All determinations of $Y_{H,NO}$ corresponding to $Y_{H,AE}$ = 0.67 mgCOD/mgCOD for OU-NU combinations from respective aerobic and anoxic batch tests, per sewage batch (SB) in Period I.

Sewage Batch	ABT-DBT Combination	$Y_{H,NO}$ (mgCOD/mgCOD)
4	2-2	0.531
6	3-3	0.584
	4-4	0.451
10	12-12	0.560
	12-13	0.564
	13-12	0.492
	13-13	0.496
11	14-14	0.504
	14-15	0.597
	14-16	0.552
	15-14	0.488
	15-15	0.584
	15-16	0.538
	16-14	0.471
	16-15	0.570
	16-16	0.523

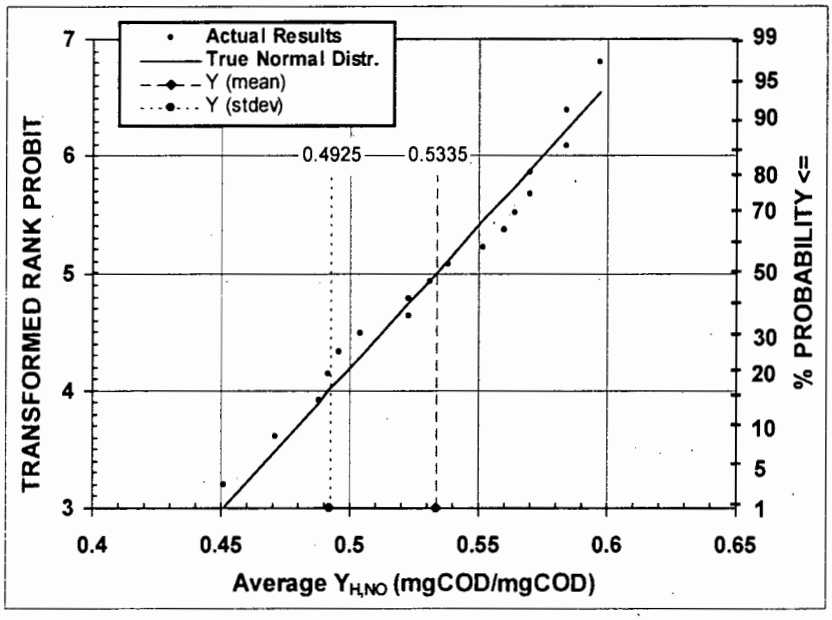

Fig. 5.8: Period I: Statistical plot of all $Y_{H,NO}$ estimates corresponding to $Y_{H,AE}$ = 0.67 mgCOD/mgCOD determined in Period I

No outliers were identified and the data in Fig. 5.8 exhibits a reasonable fit to the linear true normal line, indicating a normal distribution for the $Y_{H,NO}$ estimates corresponding to $Y_{H,AE}$ = 0.67 mgCOD/mgCOD, in Period I. The mean $Y_{H,NO}$ is 0.534 ± 0.041 (range 0.493 – 0.575) mgCOD/mgCOD with respect to $Y_{H,AE}$ = 0.67 mgCOD/mgCOD, or equivalently a yield ratio of 79.7%. This compares well with the theoretical prediction of $Y_{H,NO}$:$Y_{H,AE}$ = 83%, as well as with the average $Y_{H,NO}$ = 0.54,

or yield ratio 81 ± 3.5%, with respect to $Y_{H,AE}$ = 0.67 mgCOD/mgCOD, determined in Chapter 2 for the experimental investigations in the literature.

5.3.2 Evaluation of $Y_{H,AE}$ Using Independent RBCOD Estimation

In the analysis above for the Period I data, the estimate for the $Y_{H,NO}$:$Y_{H,AE}$ ratio could be determined independently of the RBCOD concentration in the batch tests, since complete utilization of RBCOD from the same source occurred in corresponding aerobic and anoxic batch tests (see Section 1.5, Chapter 1). However, to determine a value for $Y_{H,NO}$, the "standard" value for $Y_{H,AE}$ = 0.67 mgCOD/mgCOD had to be accepted. This standard $Y_{H,AE}$ needs to be evaluated. This can be accomplished in two equivalent fashions:

(1) Quantify the RBCOD concentration in an aerobic batch test by an independent technique, insert this concentration in Eq.(5.1) together with OU, and solve for $Y_{H,AE}$.

(2) With the accepted $Y_{H,AE}$ = 0.67 mgCOD/mgCOD, calculate the aerobic batch test determined RBCOD concentration via Eq.(5.1) with the relevant batch test OU and compare this RBCOD concentration with that measured independently.

The two approaches above are effectively equivalent. Approach (2) was followed, since this technique can be readily applied to the anoxic batch tests also, to provide an evaluation for the determined $Y_{H,NO}$. Accordingly, the wastewater RBCOD fraction (f_{ts}) was estimated from the respective batch test (BT) repirometries as follows: The standard $Y_{H,AE}$ = 0.67 and corresponding average $Y_{H,NO}$ = 0.534 mgCOD/mgCOD were inserted in Eqs. (5.1) and (5.2) respectively, together with the relevant OU or NU, and the RBCOD concentrations in the respective aerobic (AE) and anoxic (AX) batch tests (i.e. $RBCOD_{BT,AE}$ and $RBCOD_{BT,NO}$ respectively) calculated. By dividing the respective $RBCOD_{BT}$ by the total wastewater COD concentration in the batch test ($S_{ti,BT}$), an estimate of the RBCOD fraction (f_{ts}) in the wastewater was obtained:

$$f_{ts,BT} = RBCOD_{BT}/S_{ti,BT} \qquad (5.13)$$

where:

$$S_{ti,BT} = (MS_{ti,R}/V_{BT}) = (V_{WW}*S_{ti,R}/V_{BT}) \qquad (5.14)$$

$MS_{ti,R}$ = mass of total wastewater COD added to the batch test, mgCOD

$S_{ti,R}$ = total COD of the wastewater added to the batch test, mgCOD/ℓ

V_{WW} = volume of wastewater added to the batch test, ℓ

V_{BT} = 3ℓ, total volume of the batch test

$f_{ts,BT}$ = wastewater RBCOD fraction estimated by batch test respirometry

The batch test respirometry estimates for f_{ts} were then compared with the steady-state averages determined independently for each sewage batch. As presented in Section 5.2, the average steady-state wastewater RBCOD fraction (f_{ts}) in Period I was independently determined by the floc-filtration method described in Section 3.8, Chapter 3 (Mbewe *et al.*, 1995), using the unbiodegradable soluble COD fraction (f_{us}) obtained in a long sludge age UCT system operated concurrently on the same sewage. A detailed analysis of the COD data for the UCT system is contained in *Appendix C1*.

For Period I, the f_{ts} estimated by aerobic and anoxic batch test respirometry, as well as the respective comparison with the corresponding steady-state average f_{ts} determined independently by the flocculation-filtration method, are presented in Tables 5.8 and 5.9 respectively.

Table 5.8: Period I: Aerobic batch test respirometric estimation of wastewater RBCOD fraction (f_{ts}), accepting $Y_{H,AE}$ = 0.67 mgCOD/mgCOD, compared with the sewage batch (SB) average f_{ts} determined independently by floc-filtration (FF). Also shown: corresponding oxygen utilized (OU), and batch test (BT) RBCOD and total COD concentrations ($RBCOD_{BT}$ and $S_{ti,BT}$ respectively).

SB	SB AVG $f_{ts,FF}$	ABT No.	OU (mgO/ℓ)	$RBCOD_{BT}$ (mgCOD/ℓ)	$S_{ti,BT}$ (mgCOD/ℓ)	$f_{ts,BT}$	f_{ts} Recovered $f_{ts,BT}$:$f_{ts,FF}$
4	0.191	1	7.2	21.6	432.0	0.050	0.261
6	0.195	3	5.1	15.3	220.5	0.069	0.355
		4	4.4	13.2	190.4	0.069	0.355
10	0.184	12	17.8	53.3	692.3	0.077	0.418
		13	15.4	46.1	786.3	0.059	0.319
11	*0.163**	14	16	47.9	727.2	0.066	0.404
		15	15.5	46.4	767.5	0.060	0.371
		16	15	44.9	767.5	0.059	0.359

**Note: No $f_{ts,FF}$ determinations were performed; the accepted average $f_{ts,FF}$ = 0.163 ± 0.04 is used (Section 5.2.2).*

Table 5.9: Period I: Anoxic batch test respirometric estimation of wastewater RBCOD fraction (f_{ts}), accepting $Y_{H,NO}$ = 0.534 with respect to $Y_{H,AE}$ = 0.67 mgCOD/mgCOD, compared with the sewage batch (SB) average f_{ts} determined independently by floc-filtration (FF). Also shown: corresponding oxygen utilized (OU), and batch test (BT) RBCOD and total COD concentrations ($RBCOD_{BT}$ and $S_{ti,BT}$ respectively).

SB	SB AVG $f_{ts,FF}$	DBT No.	NU (mgO/ℓ)	$RBCOD_{BT}$ (mgCOD/ℓ)	$S_{ti,BT}$ (mgCOD/ℓ)	$f_{ts,BT}$	f_{ts} Recovered $f_{ts,BT}$:$f_{ts,FF}$
4	0.191	1	3.578	22.0	432.0	0.051	0.266
6	0.195	3	2.247	13.8	220.5	0.063	0.321
		4	2.558	15.7	190.4	0.082	0.423
10	0.184	12	8.294	50.9	692.3	0.074	0.400
		13	8.219	50.4	786.3	0.064	0.349
11	*0.163**	14	8.403	51.6	727.2	0.071	0.435
		15	6.833	41.9	767.5	0.055	0.335
		16	7.589	46.6	767.5	0.061	0.372

**Note: No $f_{ts,FF}$ determinations were performed; the accepted average $f_{ts,FF}$ = 0.163 ± 0.04 is used (Section 5.2.2).*

The aerobic and anoxic batch test respirometric f_{ts} estimates were analysed for outliers and are plotted in the linearized probability graphs Figs. 5.9 and 5.10 respectively.

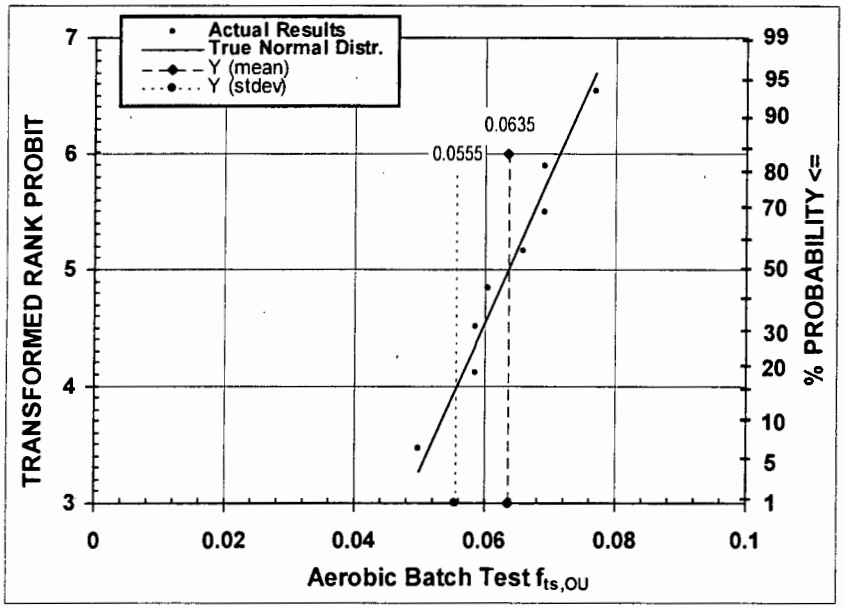

Fig. 5.9: Period I: Statistical plot of the average RBCOD fraction (f_{ts}) determined in aerobic batch tests (i.e. $f_{ts,OU}$).

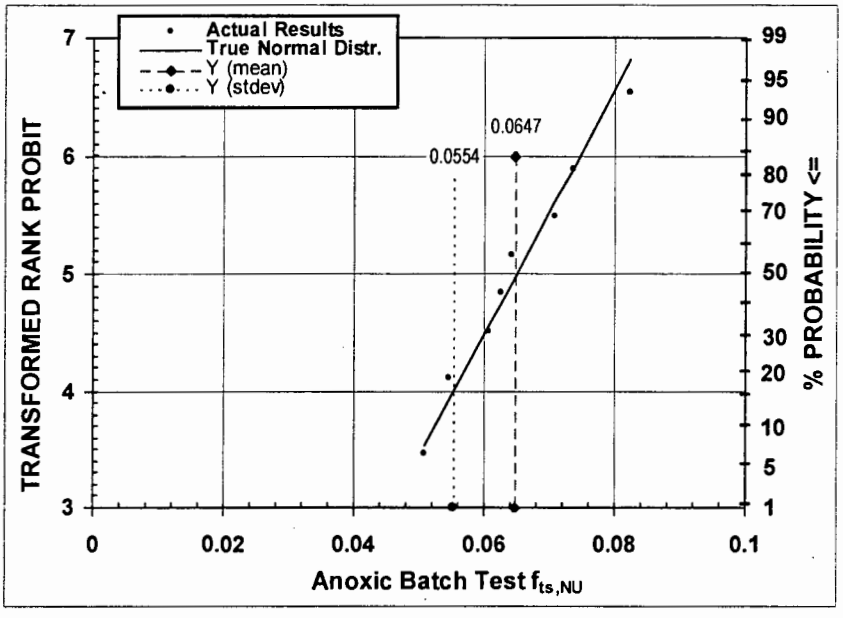

Fig. 5.10: Period I: Statistical plot of the average RBCOD fraction (f_{ts}) determined in anoxic batch tests (i.e. $f_{ts,NU}$).

No outliers were identified for the f_{ts} estimations by aerobic batch test respirometry, labelled "$f_{ts,OU}$" in Fig. 5.9, which exhibits a reasonable fit to the linear true normal line, giving a mean $f_{ts,OU} = 0.064 \pm 0.008$ (range 0.056 – 0.072), or 39.3% of the steady-state average $f_{ts,FF} = 0.163$ independently determined by the flocculation-filtration method, see *Appendix C*.

Similarly, for the f_{ts} estimations by anoxic batch test respirometry (labelled "$f_{ts,NU}$" in Fig. 5.10), no outliers were identified and the data also exhibits a reasonable fit to the

linear true normal line, giving a mean $f_{ts,NU} = 0.065 \pm 0.009$ (range 0.056 – 0.074), or about 39.9% of the independently determined steady-state average $f_{ts,FF} = 0.163$, see Section 5.2.

From the results above, it is evident that the aerobic and anoxic batch test estimates for RBCOD are consistent (f_{ts} = 0.064 and 0.065 respectively). This is not unexpected since the value for $Y_{H,NO}$ used to calculate the anoxic batch test RBCOD is determined based on the assumption that equal concentrations of RBCOD are consumed in the respective aerobic and anoxic batch tests. However, the batch test determined RBCOD concentrations are significantly lower than the corresponding values determined independently with the flocculation-filtration method. One possible explanation for this anomaly is that in the batch tests, the RBCOD was not completely consumed when the precipitous drop in OUR was observed in the aerobic batch tests, or, correspondingly, when the denitrification rate dropped from the K_1+K_2 to K_2 only in the anoxic batch tests.

To evaluate this possibility, several aerobic batch tests were subsequently performed in which the COD of floc-filtered samples taken from the batch test at specific time intervals, were compared with the OUR profile obtained in the test; this served as a physical check on whether all the biodegradable soluble COD was utilized in the batch test.

Floc-filtered COD Profiles in Aerobic Batch Tests

The OUR and floc-filtered COD profiles for aerobic batch test (ABT) number 19 are presented in Figs. 5.11 and 5.12, respectively, as a typical example of an assessment of whether all the biodegradable soluble COD was utilized in the batch tests.

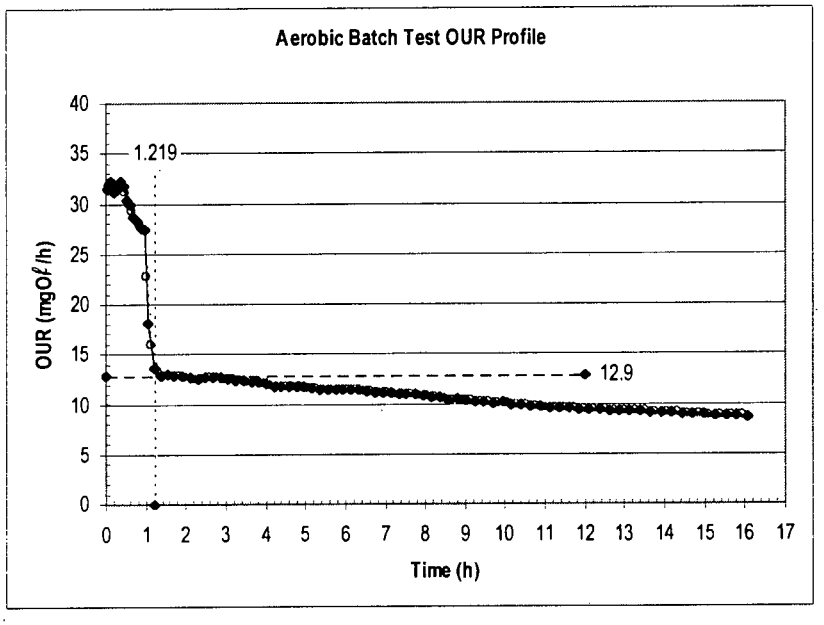

Fig. 5.11: Period I: The OUR profile of aerobic batch test (ABT) 19, to be compared with the floc-filtered COD profile (below) determined in the same test, Fig. 5.12.

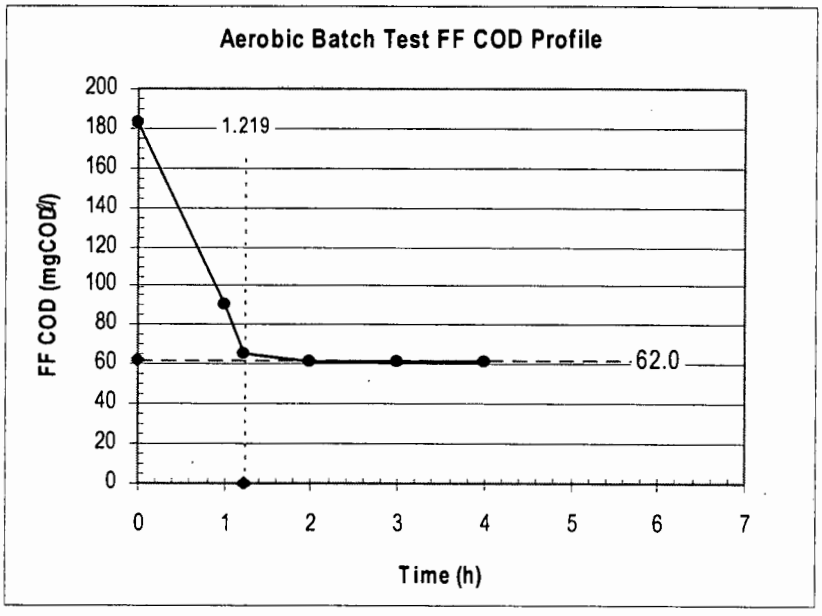

Fig. 5.12: Period I: Floc-filtered COD profile of aerobic batch test (ABT) 19; this is compared with the OUR profile (Fig. 5.11) determined for the same test, as physical check of complete utilization of biodegradable soluble COD present in the batch test.

From Fig. 5.12, initially the floc-filtered (i.e. soluble) COD concentration in the batch test decreased at a rapid rate until approximately t = 1.2h, after which it remained constant; the concentration drop is due to soluble biodegradable COD (S_{bs}) consumption, and the level concentration due to unbiodegradable soluble COD (S_{us}) remaining. Correspondingly, the OUR profile in Fig. 5.11 exhibits the characteristic pattern of an initial maximum rate associated with the utilization of RBCOD+SBCOD, followed by a precipitous drop to the rate associated with SBCOD utilization when the RBCOD present is depleted (Ekama *et al.*, 1986). Comparing the OUR and floc-filtered COD profiles in Figs. 5.11 and 5.12 respectively, it is evident that all the biodegradable soluble COD was consumed at the time the precipitous drop in OUR occurred. On this basis, it was verified that all the biodegradable soluble COD present in the aerobic batch tests, was completely utilized at the time the precipitous drop in OUR occurred.

Consequently, it was suspected that the low f_{ts} recoveries observed in the batch tests with respect to the steady-state average f_{ts} determined for the same wastewater, was due to uncertainty in the flocculation-filtration method applied to independently measure RBCOD, possibly caused by inconsistencies in the f_{us} obtained in the UCT activated sludge system. Consequently, as discussed in Chapter 3, for the remainder of the investigation (Periods II and III) dedicated Modified Ludzack-Ettinger (MLE) and square-wave (SQW) fed activated sludge systems were operated to, respectively, supply consistent biomass and estimate the wastewater RBCOD by the original method of Ekama *et al.* (1978).

5.4 BATCH TEST RESULTS: PERIOD II

5.4.1 Estimation of $Y_{H,NO}$ in terms of $Y_{H,AE}$ Using Wastewater RBCOD

In Period II, sewage batches (SB) 18 – 21 were used over the period 26/8/02 – 10/10/02, and 12 aerobic and 10 anoxic batch tests were performed. Corresponding aerobic and anoxic (denitrification) batch tests (ABT and DBT respectively) were performed with mixtures of the same volumes of wastewater (V_{WW}) and activated sludge mixed-liquor (V_{ML}). The composition and index number for the respective aerobic and anoxic batch tests performed in Period II, are summarised in Tables 5.10 and 5.11 respectively.

Table 5.10: Period II: Aerobic batch test (ABT) compositions, showing the sewage batch (SB) used, mixed-liquor (ML) source, volumes of wastewater (V_{WW}) and ML (V_{ML}) added, total COD concentration of the wastewater ($S_{ti,R}$), the ML volatile suspended solids (VSS) concentration (X_V) and the organic loading rate (LR) in the test.

SB	Date (2002)	ABT No.	ML	V_{WW} (ℓ)	V_{ML} (ℓ)	Sti_R (mgCOD/ℓ)	X_V (mgVSS/ℓ)	LR (COD/VSS)
18	26/8	23	SQW	1.39	1.61	1139.8	1059	0.93
	27/8	24	SQW	2	1	1352	5236	0.52
19	13/9	25	MLE	2	1	1170.2	2199	1.06
20	15/9	26	MLE	2	1	955.2	2505	0.76
	22/9	27	MLE	2	1	1127.2	3751	0.60
	27/9	28	SQW	2	1	1113.2	3076	0.72
	29/9	29	SQW	2	1	1053	2777	0.76
21	2/10	30	MLE	2	1	1165.2	2823	0.83
	4/10	31	MLE	2	1	1187.4	2803	0.85
	7/10	32	MLE	2	1	1158.2	4127	0.56
	8/10	33	MLE	2	1	1162.3	3628	0.64
	10/10	34	MLE	2	1	1150.1	3282	0.70

Table 5.11: Period II: Denitrification batch test (DBT) compositions, showing the sewage batch (SB) used, mixed-liquor (ML) source, volumes of wastewater (V_{WW}) and ML (V_{ML}) added, total COD concentration of the wastewater ($S_{ti,R}$), the ML volatile suspended solids (VSS) concentration (X_V) and the organic loading rate (LR) in the test.

SB	Date (2002)	DBT No.	ML	V_{WW} (ℓ)	V_{ML} (ℓ)	Sti_R (mgCOD/ℓ)	X_V (mgVSS/ℓ)	LR (COD/VSS)
18	28/8	20	MLE	2	1	1206.4	2451	0.98
20	25/9	21	MLE	2	1	1119.1	4120	0.54
	27/9	22	MLE	2	1	1113.2	3503	0.64
	29/9	23	MLE	2	1	1053	3093	0.68
21	1/10	24	MLE	2	1	1177.2	4174	0.56
	3/10	25	MLE	2	1	1185.4	3064	0.77
	5/10	26	MLE	2	1	1149.1	2585	0.89
	6/10	27	MLE	2	1	1141.4	4518	0.51
	8/10	28	MLE	2	1	1162.3	4339	0.54
	10/10	29	MLE	2	1	1150.1	4417	0.52

As detailed for Period I in Section 5.4, $Y_{H,NO}$ was estimated in terms of $Y_{H,AE}$ via Eq.(5.4), from various combinations of the OU and NU determined in respective aerobic and anoxic batch tests composed of the same wastewater volume (V_{WW}) from the same sewage batch (SB).

Excluding invalidated batch tests, estimates for $Y_{H,NO}$ as a function of $Y_{H,AE}$ for corresponding OU-NU combinations determined from respective aerobic and anoxic batch tests, are plotted in Figs. 5.13 and 5.15 for sewage batches (SB) 20 and 21, respectively.

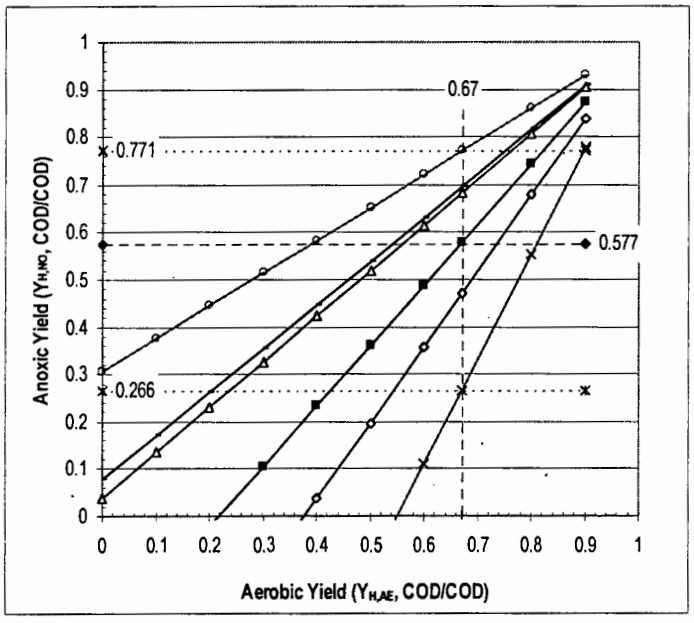

Fig. 5.13: Period II: Plot of $Y_{H,NO}$ in terms of $Y_{H,AE}$ for OU-NU combinations from respective aerobic and anoxic batch tests using sewage batch (SB) 20.

For SB 20, the data in Fig. 5.13 gives an average $Y_{H,NO} = 0.577 \pm 0.185$ (range 0.392 – 0.762) mgCOD/mgCOD, or equivalently a yield ratio of 86.1%, with respect to $Y_{H,AE} = 0.67$ mgCOD/mgCOD. These estimates are slightly higher (about 5%) than the theoretically predicted ratio $Y_{H,NO}:Y_{H,AE} = 0.83$, and the average $Y_{H,NO} = 0.54$ (or yield ratio of 81 ± 3.5%) with respect to $Y_{H,AE} = 0.67$ mgCOD/mgCOD, determined for the experimental investigations in the literature (see Chapter 2). However, the data displays significant variation, as indicated by the relatively high sample standard deviation (i.e. 0.185) and the wide range of possible values. Most likely this was due to poor definition of the K_1 denitrification rates in DBT 21 and 22 (see *Appendix C3*), caused by apparent attenuation of NO_3 and NO_2 sample peaks in the plotted output from the Technicon Auto-Analyser, used for measuring NO_3 and NO_2 concentrations (Section 4.3.3, Chapter 4). Consequently, the NU determinations for DBT 21 and 22 contain some uncertainty. Additionally, the initial (RBCOD utilization) period of the OUR profile in ABT 27 displays some distortion (see *Appendix C2*), which similarly

introduces uncertainty into the OU determination for this batch test. Despite these uncertainties, the average data does not appear unreasonable.

To analyse the data statistically, estimates for $Y_{H,NO}$ corresponding to $Y_{H,AE}$ = 0.67 mgCOD/mgCOD were evaluated for outliers and plotted in the linearized probability graph, Fig. 5.14.

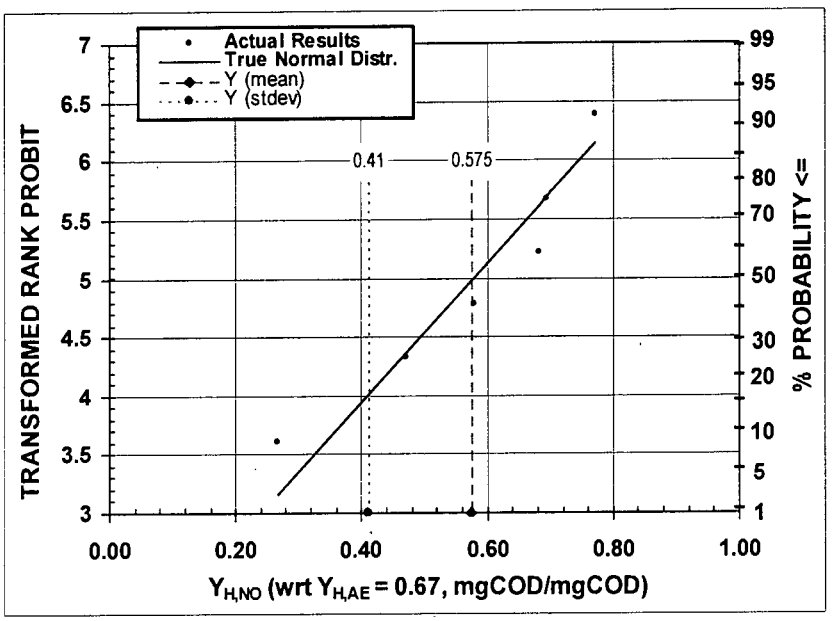

Fig. 5.14: Period II: Statistical plot of $Y_{H,NO}$ in terms of $Y_{H,AE}$ for OU-NU combinations from respective aerobic and anoxic batch tests using sewage batch (SB) 20.

For SB 20, no outliers were identified and Fig. 5.14 exhibits a reasonable fit to the linear true normal line, although curvature is evident. The mean $Y_{H,NO}$ is approximately 0.575 ± 0.165 (range 0.41 – 0.74) mgCOD/mgCOD, or yield ratio 85.8%, with respect to $Y_{H,AE}$ = 0.67 mgCOD/mgCOD. Although this average is only slightly higher than the theoretical prediction of $Y_{H,NO}$:$Y_{H,AE}$ = 83%, as well as with respect to the experimental average $Y_{H,NO}$ = 0.54 (or yield ratio 81 ± 3.5%) with respect to $Y_{H,AE}$ = 0.67 mgCOD/mgCOD, the relatively high standard deviation confirms significant variation in the data.

For SB 21, estimates for $Y_{H,NO}$ as a function of $Y_{H,AE}$ are plotted in Fig. 5.15.

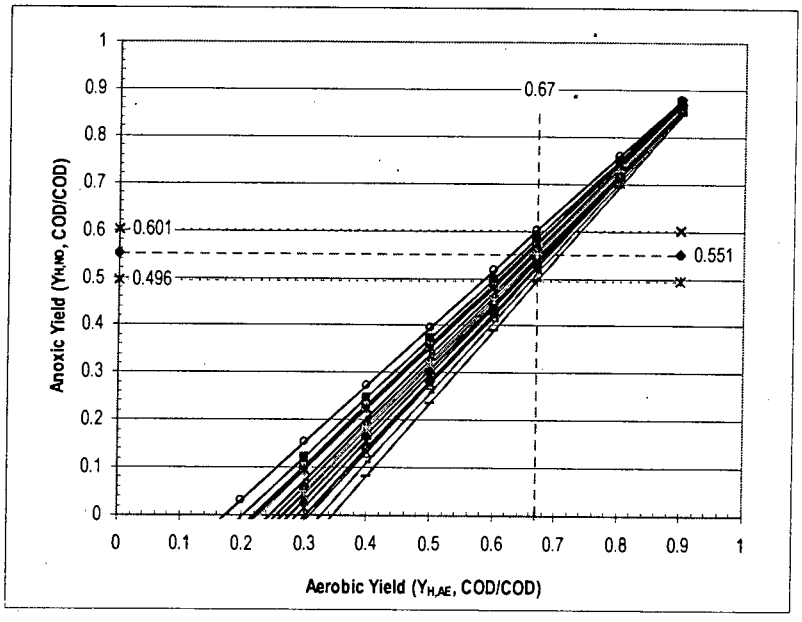

Fig. 5.15: Period II: Plot of $Y_{H,NO}$ in terms of $Y_{H,AE}$ for OU-NU combinations from respective aerobic and anoxic batch tests using sewage batch (SB) 21.

For SB 21, the data in Fig. 5.15 gives an average $Y_{H,NO} = 0.551 \pm 0.029$ (range 0.522 – 0.58) mgCOD/mgCOD with respect to $Y_{H,AE} = 0.67$ mgCOD/mgCOD, or equivalently a yield ratio of 82.2%. The average yield ratio is in good agreement with the theoretically predicted $Y_{H,NO}$:$Y_{H,AE}$ = 83%, and both $Y_{H,NO}$ and the yield ratio compare well with the average $Y_{H,NO} = 0.54$ (or yield ratio $81 \pm 3.5\%$) with respect to $Y_{H,AE} = 0.67$ mgCOD/mgCOD, determined for the experimental investigations in the literature (see Chapter 2).

For statistical analysis, the $Y_{H,NO}$ estimates corresponding to $Y_{H,AE} = 0.67$ mgCOD/mgCOD were evaluated for outliers and are plotted in the linearized probability graph in Fig. 5.16.

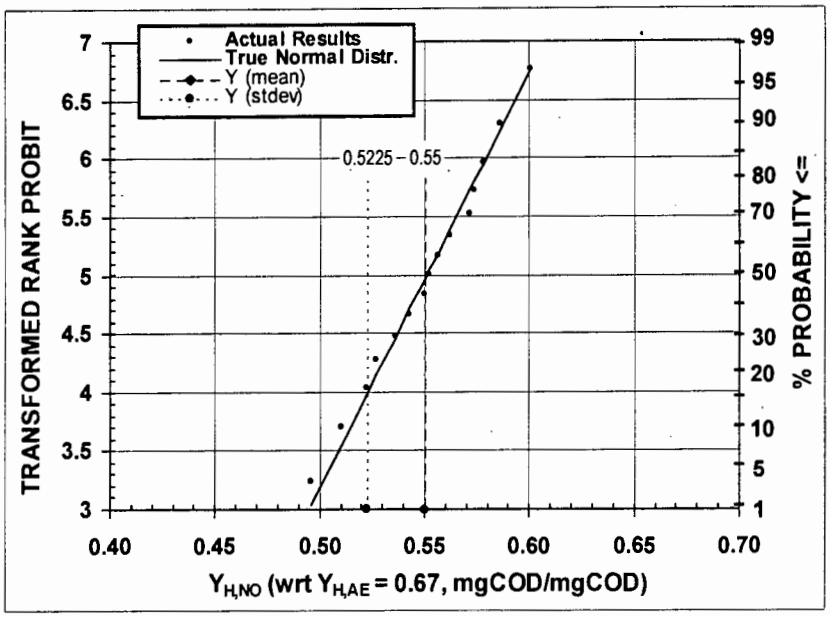

Fig. 5.16: Period II: Statistical plot of $Y_{H,NO}$ in terms of $Y_{H,AE}$ for OU-NU combinations from respective aerobic and anoxic batch tests using sewage batch (SB) 21.

For the SB 21 estimates, no outliers were identified and Fig. 5.16 exhibits a normal distribution for the $Y_{H,NO}$ estimates. The mean $Y_{H,NO}$ = 0.55 ± 0.0275 (range 0.523 – 0.578), is in close agreement with both the theoretical prediction of $Y_{H,NO}$:$Y_{H,AE}$ = 83%, and the experimental average of 0.54 mgCOD/mgCOD (81 ± 3.5%) with respect to $Y_{H,AE}$ = 0.67 mgCOD/mgCOD.

In summary, all the $Y_{H,NO}$ estimates corresponding to $Y_{H,AE}$ = 0.67 mgCOD/mgCOD determined in Period II (Table 5.12), were evaluated for outliers. Two outliers were identified (shaded and bracketed in Table 5.12) and were excluded from further analysis. The remaining data are plotted in the linearized probability graph Fig. 5.17.

Table 5.12: Period II Summary: All determinations of $Y_{H,NO}$ corresponding to $Y_{H,AE}$ = 0.67 mgCOD/mgCOD for OU-NU combinations from respective aerobic and anoxic batch tests, per sewage batch (SB).

Sewage Batch	ABT-DBT Combination	$Y_{H,NO}$ (mgCOD/mgCOD)
20	26-21	0.578
	26-22	0.683
	26-23	(0.266)
	27-21	0.696
	27-22	(0.771)
	27-23	0.470
21	30-27	0.556
	30-28	0.543
	30-29	0.572
	31-27	0.562
	31-28	0.550
	31-29	0.578
	32-27	0.536

	32-28	0.522
	32-29	0.552
	33-27	0.586
	33-28	0.574
	33-29	0.601
	34-27	0.510
	34-28	0.496
	34-29	0.527

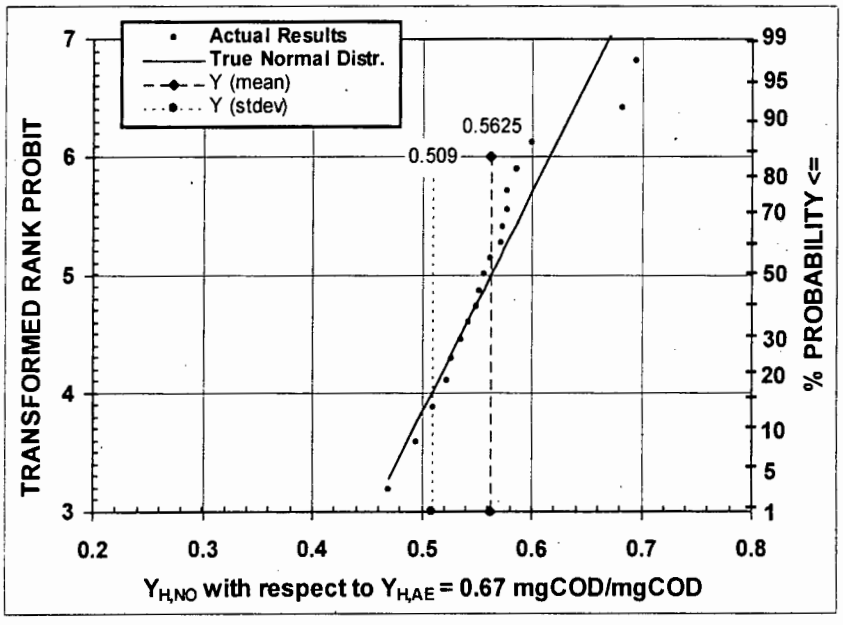

Fig. 5.17: Period II: Statistical plot of all $Y_{H,NO}$ estimates (with respect to $Y_{H,AE}$ = 0.67 mgCOD/mgCOD) determined from OU-NU combinations of corresponding aerobic and anoxic batch tests in Period II, excluding 2 outliers.

For Period II, the $Y_{H,NO}$ estimates in Fig. 5.17 exhibit a reasonable fit to the linear true normal line, with some deviation noticeable for the two largest values. The mean $Y_{H,NO}$ = 0.563 ± 0.054 (range 0.51 – 0.62) mgCOD/mgCOD, or equivalently a yield ratio of 84.0%, with respect to $Y_{H,AE}$ = 0.67 mgCOD/mgCOD, is consistent with the theoretical prediction of $Y_{H,NO}$:$Y_{H,AE}$ = 83%, and the experimental average $Y_{H,NO}$ = 0.54 mgCOD/mgCOD (yield ratio 81 ± 3.5%) corresponding with $Y_{H,AE}$ = 0.67 mgCOD/mgCOD.

5.4.2 Verification of $Y_{H,NO}$ Estimation by Independent RBCOD Measurement

In Period I, an inconsistency in the data was evident in that the RBCOD concentrations estimated from the batch test OU and NU determinations (accepting $Y_{H,AE}$ = 0.67 mgCOD/mgCOD and the experimentally determined corresponding $Y_{H,NO}$), were consistently significantly lower than the corresponding concentrations determined with the flocculation-filtration method. A possible cause identified for this inconsistency was uncertainty in the flocculation-filtration method for measuring RBCOD. Accordingly, in Period II independent measurement of the wastewater

RBCOD fraction (f_{ts}) was changed to that of using the OUR response of a short sludge age square-wave (SQW) fed continuous flow-through activated sludge system (Section 3.8, Chapter 3; Ekama *et al.*, 1986). A detailed analysis of the SQW system data is presented in Chapter 3.

Following the procedures set out in Section 5.4, the f_{ts} values from aerobic and anoxic batch test respirometry ($f_{ts,BT}$), as well as respective comparisons with the corresponding steady-state average f_{ts} determined by the SQW system ($f_{ts,S}$), are presented in Tables 5.13 and 5.14 respectively.

Table 5.13: Period II: Aerobic batch test (ABT) estimation of wastewater RBCOD fraction (f_{ts}), accepting $Y_{H,AE}$ = 0.67 mgCOD/mgCOD, compared with the sewage batch (SB, steady-state) average f_{ts} determined by the OUR response of a square-wave (SQW) fed activated sludge system (Ekama *et al.*, 1986). Also shown: corresponding oxygen utilized (OU), and batch test (BT) RBCOD and total COD concentrations ($RBCOD_{BT}$ and $S_{ti,BT}$ respectively).

SB	SB AVG $f_{ts,S}$	ABT No.	OU (mgO/ℓ)	$RBCOD_{BT}$ (mgCOD/ℓ)	$S_{ti,BT}$ (mgCOD/ℓ)	$f_{ts,BT}$	fts Recovery $f_{ts,BT}$:$f_{ts,S}$
20	0.14	26	15.8	47.9	636.8	0.075	0.537
		27	21.9	66.4	751.5	0.088	0.631
21	0.125	30	13.8	41.8	776.8	0.054	0.431
		31	14	42.4	791.6	0.054	0.429
		32	13.2	40.0	772.1	0.052	0.414
		33	14.8	44.8	774.9	0.058	0.463
		34	12.5	37.9	766.7	0.049	0.395

Table 5.14: Period II: Denitrification batch test (DBT) estimation of wastewater RBCOD fraction (f_{ts}), accepting $Y_{H,NO}$ = 0.563 mgCOD/mgCOD, compared with the sewage batch (SB, steady-state) average f_{ts} determined by the OUR response of a square-wave (SQW) fed activated sludge system (Ekama *et al.*, 1986). Also shown: corresponding nitrate utilized (NU), and batch test (BT) RBCOD and total COD concentrations ($RBCOD_{BT}$ and $S_{ti,BT}$ respectively).

SB	SB AVG $f_{ts,S}$	DBT No.	NU (mgN/ℓ)	$RBCOD_{BT}$ (mgCOD/ℓ)	$S_{ti,BT}$ (mgCOD/ℓ)	$f_{ts,BT}$	fts Recovery $f_{ts,BT}$:$f_{ts,S}$
20	0.14	21	7.06	46.2	746.1	0.062	0.442
		22	5.311	34.8	742.1	0.047	0.335
		23	12.287	80.4	702.0	0.115	0.818
21	0.125	27	6.49	42.5	760.9	0.056	0.447
		28	6.68	43.7	774.9	0.056	0.451
		29	6.263	41.0	766.7	0.053	0.428

The aerobic and anoxic respirometric f_{ts} estimates were evaluated for outliers and analysed statistically in the linearized probability graphs Figs. 5.18 and 5.19 respectively.

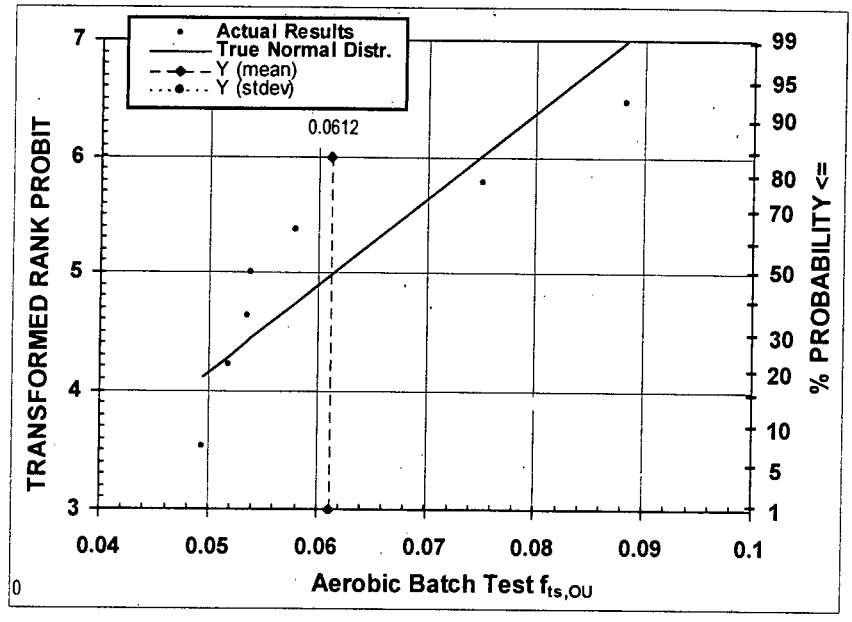

Fig. 5.18: Period II: Statistical plot of the average RBCOD fraction (f_{ts}) determined in aerobic batch tests (i.e. "$f_{ts,OU}$").

No outliers were identified for the f_{ts} estimations determined by aerobic batch test respirometry, i.e. "$f_{ts,OU}$" in Fig. 5.18, although the data exhibits a poor fit to the linear true normal line. This indicates that the $f_{ts,OU}$ estimates are not normally distributed, and consequently the mean $f_{ts,OU}$ = 0.0612 should be rejected for further analysis. However, the results do indicate under-recovery of RBCOD compared with the SQW determined RBCOD concentration, Tables 5.13 and 5.14. Clearly, changing the independent RBCOD measurement method from the flocculation-filtration to the SQW system did not resolve the poor RBCOD recovery difficulties experienced in Period I.

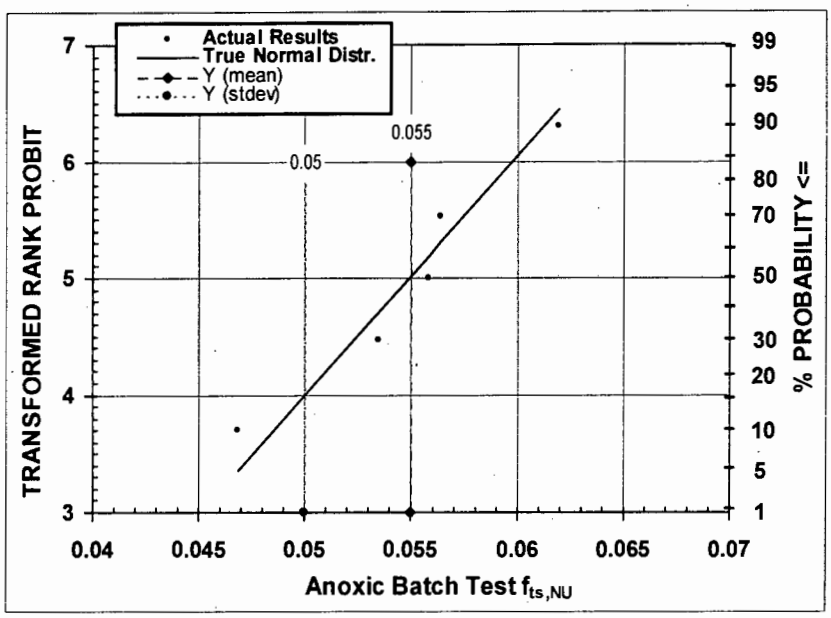

Fig. 5.19: Period II: Statistical plot of the average RBCOD fraction (f_{ts}) determined in anoxic batch tests (i.e. "$f_{ts,NU}$").

For the f_{ts} estimations by anoxic batch test respirometry (i.e. "$f_{ts,NU}$"), one outlier was identified (DBT 23, 0.115) and excluded from the estimates shown in Fig. 5.19. The data exhibits a reasonable fit to the linear true normal line, indicating a normal distribution for the $f_{ts,NU}$ estimates. The mean $f_{ts,NU} = 0.055 \pm 0.005$ is significantly lower than the steady-state average $f_{ts,S} = 0.136$ determined for the Mitchells Plain raw wastewater by the SQW system in Chapter 3, amounting to only a 40.4% RBCOD recovery in the batch tests compared with the steady-state SQW test average. This recovery is consistent with the 39.9% obtained in Period I (Section 5.3.2), leaving a substantial amount of RBCOD still unaccounted for in the respirometric responses of the respective batch tests.

Following from Period I, floc-filtered COD measurements were taken at specific time intervals during several aerobic and anoxic batch tests, as a physical check as to whether all the biodegradable soluble COD present in the test, was depleted at approximately the same time as the precipitous drop in OUR, or, correspondingly, the change from the K_1+K_2 to K_2 only denitrification rates. The comparison between the timed floc-filtered COD measurements and the NUR profiles for the anoxic batch tests were not clear however, since only a few floc-filtered samples could be taken in addition to the number of samples necessary for nitrate and nitrite analyses for estimating the NUR profile of the test. Aerobic batch tests were not subject to the same constraint, and good correspondence was observed between the precipitous drop in OUR and plateauing of floc-filtered COD concentrations in the same batch test. OUR and floc-filtered COD profiles for a typical example of such a test are presented in Figs. 5.20 and 5.21 respectively, for aerobic batch test (ABT) 26 (also shown are subsequent OUR responses corresponding to additions of known mass of acetate, see later).

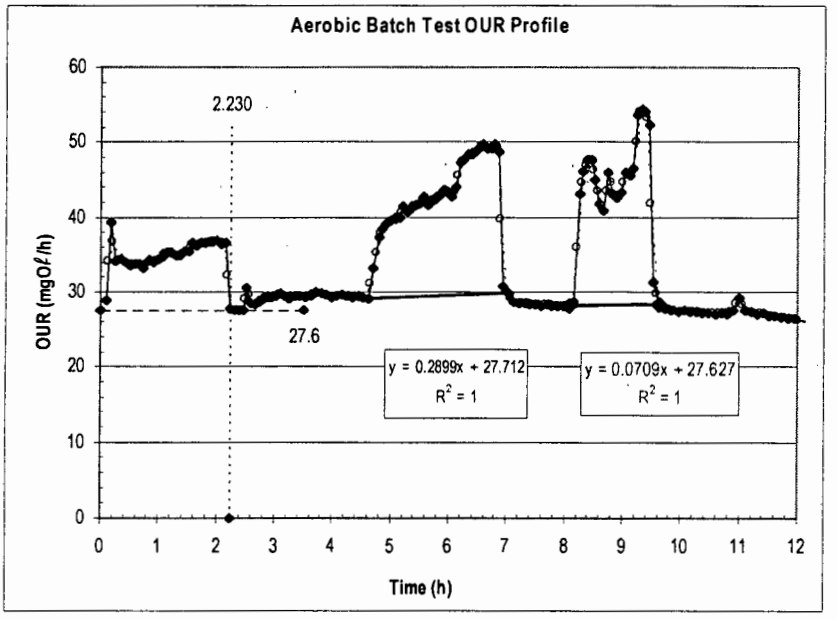

Fig. 5.20: Period II: The OUR profile of aerobic batch test (ABT) 26, to be compared with the corresponding floc-filtered COD profile in Fig. 5.23 obtained in the same test.

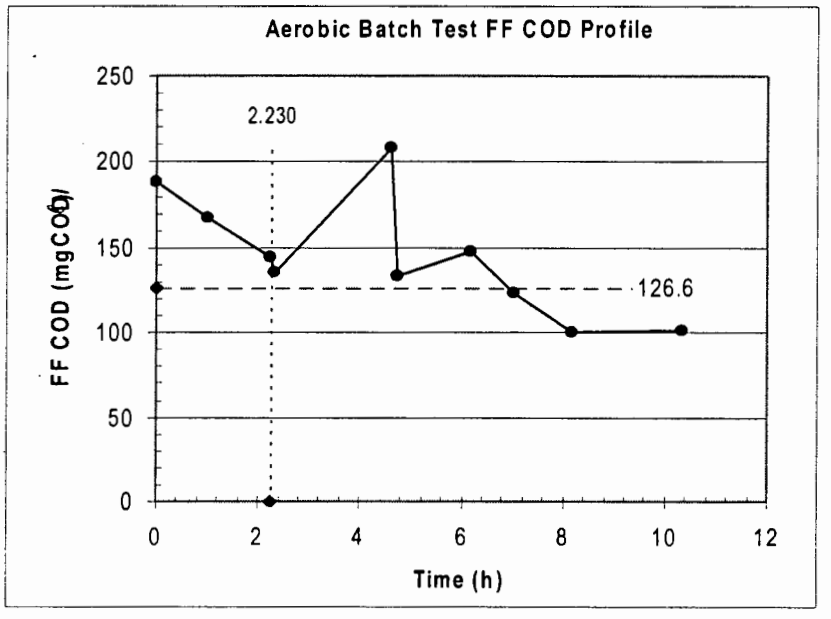

Fig. 5.21: Period II: The floc-filtered COD profile of aerobic batch test (ABT) 26, to be compared with the corresponding OUR profile in Fig. 5.22 obtained in the same test.

From comparing all the OUR and corresponding floc-filtered COD profiles in aerobic batch tests, it was found that the flocculated-filtered COD concentrations levelled off at the same time that the precipitous drop in OUR occurred. Accordingly it could be accepted that all the biodegradable soluble COD was depleted at the time the

precipitous drop in OUR occurred ($t \approx 2.23$h in the example), and, by implication, at the same time the K_1+K_2 denitrification rate changed to K_2 only in the corresponding anoxic batch tests. However, although changing the method for independently measuring the RBCOD from the flocculation-filtration one to the "standard" SQW short sludge age one, the RBCOD recoveries in the batch tests remained poor, at approximately 40%. No possible cause for the unaccounted RBCOD could be identified, and so it was decided to add a known mass of the artificial RBCOD, acetate, to aerobic batch tests, and to estimate $Y_{H,AE}$ directly from the observed OU response.

Direct Estimation of $Y_{H,AE}$ Using Known Mass of Acetate in Aerobic Batch Tests

As detailed in Chapter 4, in Period II stock solutions of a known concentration of sodium acetate were prepared, and used to introduce known masses of this artificial RBCOD into several aerobic batch tests. $Y_{H,AE}$ was then estimated directly from the observed OU response and the known concentration of acetate-RBCOD in the test, by rearranging Eq.(5.1):

$$\Rightarrow Y_{H,AE} = 1 - OU/RBCOD_{BT,AE} \qquad (5.15)$$

The procedures followed for the acetate addition aerobic batch tests have been described in Section 4.2, Chapter 4. Of note is that at the start of the tests wastewater was added (as for the tests described above), and following the precipitous drop in OUR due to wastewater RBCOD depletion, the acetate was added. A typical example of an OUR profile resulting from two such sequential acetate additions in an aerobic batch test, is shown in Fig. 5.20. For the various batch tests, the concentration of acetate in the respective aerobic batch tests (ABT), expressed as mgCOD/ℓ ($[Ac]_{BT}$) for respective sequential additions "1" and "2", and the corresponding OU and $Y_{H,AE}$ determinations, are summarised in Table 5.15.

Table 5.15: Period II: Direct estimation of $Y_{H,AE}$ from known batch test concentrations of Ac ($[Ac]_{BT}$) and corresponding OU responses; also shown are, the sewage batch used (SB), mixed-liquor (ML) source and aerobic batch test (ABT) number. Labels "MLE" and "SQW" refer to ML from the dedicated MLE and SQW systems operated in Period II (Chapter 3).

SB	ABT	ML	$[Ac]_{BT,1}$ (mgCOD/ℓ)	$[Ac]_{BT,2}$ (mgCOD/ℓ)	OU_1 (mgO/ℓ)	OU_2 (mgO/ℓ)	$Y_{H,AE\,1}$ (COD/COD)	$Y_{H,AE\,2}$ (COD/COD)
18	24	SQW	95.12		25.75		0.729	
19	25	MLE	95.24		44.31		0.535	
20	26	MLE	98.63	87.3	31.32	23.61	0.682	0.730
	27	MLE	88.21	57.62	24.66	16.37	0.720	0.716
	28	SQW	87.71	60.89	31.3	19.11	0.643	0.686
	29	SQW	82.34	28.64	25.63	9.26	0.689	0.677
21	30	MLE	54.28	28.41	18.79	9.88	0.654	0.652
	31	MLE	53.55	26.52	18.02	9.36	0.663	0.647
	32	MLE	76.89	50.31	22.91	15.63	0.702	0.689
	33	MLE	80.3	52.52	23.87	16.9	0.703	0.678
	34	MLE	78.26	51.23	24.04	16.03	0.693	0.687

The estimated values for $Y_{H,AE}$ from known additions of acetate, were evaluated for outliers and analysed statistically in a linearized probability plot, Fig. 5.22.

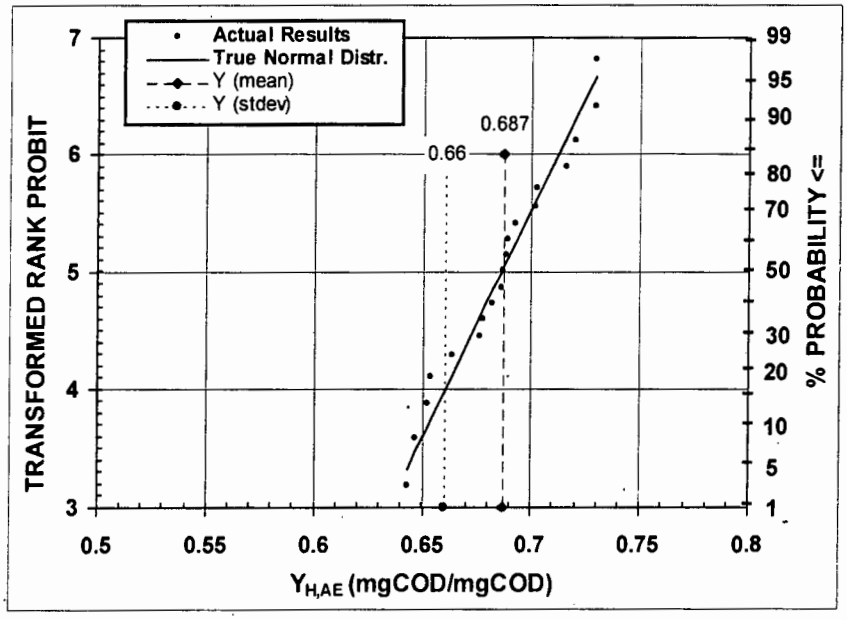

Fig. 5.22: Period II: Statistical plot of the $Y_{H,AE}$ determinations from addition of known concentration of acetate to aerobic batch tests..

One outlier was identified (ABT 25, $Y_{H,AE} = 0.535$) and excluded from the plot in Fig. 5.22. The data exhibits a good fit to the linear true normal line, indicating a normal distribution for the $Y_{H,AE}$ estimates using the artificial RBCOD, acetate. The mean $Y_{H,AE}$ of 0.687 ± 0.027 (range 0.66 – 0.714) mgCOD/mgCOD for utilization of the artificial RBCOD, acetate, is very close to the conventionally accepted $Y_{H,AE} = 0.67$ mgCOD/mgCOD for domestic wastewater, with only a 1.7% difference. Therefore, acceptance of the standard $Y_{H,AE} = 0.67$ mgCOD/mgCOD in this investigation is substantiated.

However, despite the agreement between the acetate determined $Y_{H,AE}$ and the accepted standard value, the apparent low wastewater RBCOD recoveries observed in the aerobic and anoxic batch tests presented earlier, remain unexplained. This is not of major concern in this investigation, however, since, as discussed in Chapter 3, exact determination of the RBCOD concentration in the corresponding aerobic and anoxic batch tests is not essential for estimating $Y_{H,NO}$, provided $Y_{H,AE}$ is known. As is evident from the above, the standard value for $Y_{H,AE}$ of 0.67 mgCOD/mgCOD can be accepted, and this value substantiated relatively simply under defined conditions by addition of acetate. Since quantifying wastewater RBCOD is not the focus of this research project, comparison of batch test respirometric RBCOD estimations with independent measurement of the wastewater RBCOD was discontinued. However, this aspect does warrant future further investigation.

5.5 BATCH TEST RESULTS: PERIOD III

5.5.1 Estimation of $Y_{H,NO}$ in terms of $Y_{H,AE}$ Using Wastewater RBCOD

In Period III, sewage batches (SB) 22 and 23 were used over the period 11/10/02 – 16/12/02, and 6 aerobic and 14 anoxic batch tests were performed. Corresponding aerobic and anoxic (denitrification) batch tests (ABT and DBT respectively) were performed with the same volumes of wastewater (V_{WW}) and activated sludge mixed-liquor (V_{ML}). The composition and index number for the respective aerobic and anoxic batch tests performed in Period III, are summarised in Tables 5.16 and 5.17 respectively; "Ac" refers to anoxic batch tests performed using only a known mass of the artificial RBCOD, acetate (see Chapter 4).

Table 5.16: Period III: Aerobic batch test (ABT) compositions, showing the sewage batch (SB) used, mixed-liquor (ML) source, volumes of wastewater (V_{WW}) and ML (V_{ML}) added, total COD concentration of the wastewater ($S_{ti,R}$), the ML volatile suspended solids (VSS) concentration (X_V) and the organic loading rate (LR) in the test.

SB	Date (2002)	ABT No.	ML	V_{WW} (ℓ)	V_{ML} (ℓ)	Sti_R (mgCOD/ℓ)	X_V (mgVSS/ℓ)	LR (COD/VSS)
22	25/10	35	MLE	2	1	1144.8	2930	0.78
	26/10	36	MLE	2	1	1124.4	3261	0.69
	27/10	37	MLE	2	1	1110	2153	1.03
23	4/11	38	MLE	2	1	1143	3078	0.74
	6/11	39	MLE	2	1	1188.1	3595	0.66
	7/11	40	MLE	2	1	1116.3	2303	0.97

Table 5.17: Period III: Denitrification batch test (DBT) compositions, showing the sewage batch (SB) used, mixed-liquor (ML) source, volumes of wastewater (V_{WW}) and ML (V_{ML}) added, total COD concentration of the wastewater ($S_{ti,R}$), the ML volatile suspended solids (VSS) concentration (X_V) and the organic loading rate (LR) in the test; "Ac" refers to tests performed using only the artificial RBCOD, acetate.

SB	Date (2002)	DBT No.	ML	V_{WW} (ℓ)	V_{ML} (ℓ)	Sti_R (mgCOD/ℓ)	X_V (mgVSS/ℓ)	LR (COD/VSS)
21	11/10	30	MLE	-	-	Ac	-	-
	12/10	31	MLE	2	-	Ac	1932	-
	13/10	32	MLE	2	-	Ac	1938	-
	14/10	33	MLE	2	-	Ac	1926	-
22	24/10	34	MLE	2	1	1118.2	2285	0.98
23	5/11	35	MLE	2	1	1140.9	3450	0.66
	11/11	36	MLE	2	1	1120.4	3920	0.57
	17/11	37	MLE	2	1	971.9	3462	0.56
25	7/12	38	MLE	3	-	Ac	1589	-
	8/12	39	MLE	3	-	Ac	1479	-
	10/12	40	MLE	3	-	Ac	1573	-
	14/12	41	MLE	3	-	Ac	1302	-
	16/12	42	MLE	3	-	Ac	1485	-

As described in Sections 5.3 and 5.4 above, $Y_{H,NO}$ was estimated as a function of $Y_{H,AE}$ via Eq.(5.4), from combinations of the various OU and NU determined in respective aerobic and anoxic batch tests composed of the same volume of wastewater (V_{WW}) from the same sewage batch (SB). Excluding invalidated batch tests (see Section 5.4), estimates for $Y_{H,NO}$ as a function of $Y_{H,AE}$ are plotted in Figs. 5.23 and 5.24, for corresponding OU-NU combinations determined from respective aerobic and anoxic batch tests using sewage batches (SB) 22 and 23, respectively.

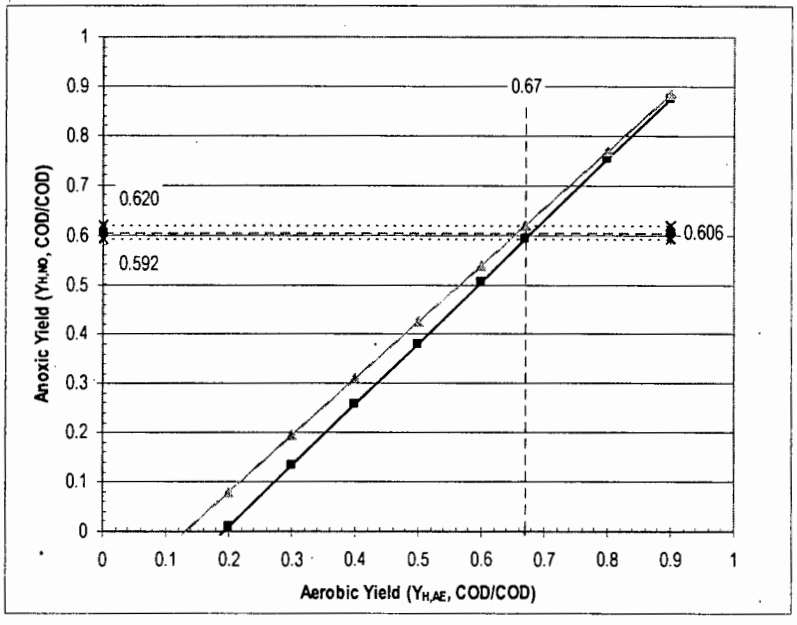

Fig. 5.23: Period III: Plot of $Y_{H,NO}$ in terms of $Y_{H,AE}$ for OU-NU combinations from respective aerobic and anoxic batch tests using sewage batch (SB) 22.

For SB 22, the data in Fig. 5.23 gives an average $Y_{H,NO}$ = 0.606 mgCOD/mgCOD, or an equivalent yield ratio of 90.4%, with respect to $Y_{H,AE}$ = 0.67 mgCOD/mgCOD. The yield ratio is significantly higher than the theoretically predicted ratio $Y_{H,NO}$:$Y_{H,AE}$ = 0.83, as is the average $Y_{H,NO}$ compared with the calculated literature experimental average of $Y_{H,NO}$ = 0.54, or 81 ± 3.5%, with respect to $Y_{H,AE}$ = 0.67 mgCOD/mgCOD. Unfortunately, there are too few data for a statistical analysis, and the average had to be accepted.

For SB 23, estimates of $Y_{H,NO}$ as a function of $Y_{H,AE}$ are plotted in Fig. 5.24 for respective OU-NU combinations of corresponding aerobic and anoxic batch tests.

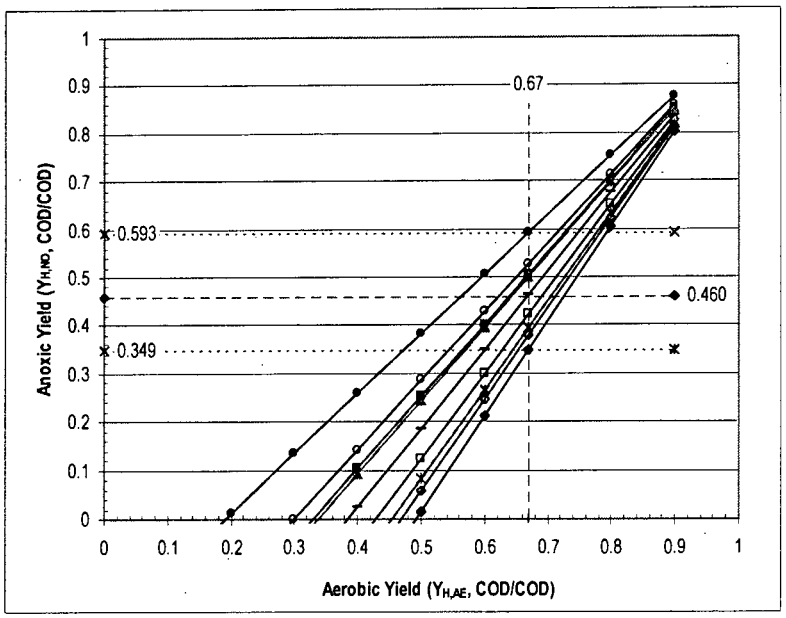

Fig. 5.24: Period III: Plot of $Y_{H,NO}$ in terms of $Y_{H,AE}$ for OU-NU combinations from respective aerobic and anoxic batch tests using sewage batch (SB) 23.

For SB 23, the data in Fig. 5.24 gives an average $Y_{H,NO}$ = 0.460 ± 0.08 (range 0.38 – 0.54) mgCOD/mgCOD, or an equivalent yield ratio of 68.7%, with respect to $Y_{H,AE}$ = 0.67 mgCOD/mgCOD. This estimate is substantially lower than the theoretically predicted ratio $Y_{H,NO}$:$Y_{H,AE}$ = 0.83, as is $Y_{H,NO}$ = 0.460 compared with the calculated literature experimental average $Y_{H,NO}$ = 0.54, or 81 ± 3.5%, with respect to $Y_{H,AE}$ = 0.67 mgCOD/mgCOD.

To analyse the SB 23 data statistically, the estimates of $Y_{H,NO}$ corresponding to $Y_{H,AE}$ = 0.67 mgCOD/mgCOD, were evaluated for outliers and plotted in the linearized probability graph, Fig. 5.25.

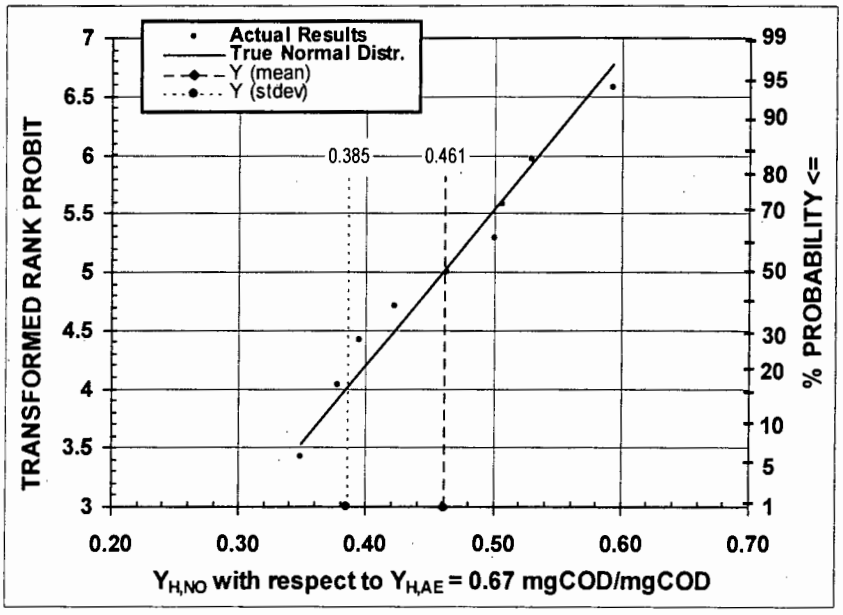

Fig. 5.25: Period III: Statistical plot of $Y_{H,NO}$ in terms of $Y_{H,AE}$ for OU-NU combinations from respective aerobic and anoxic batch tests using sewage batch (SB) 23.

For the SB 23 $Y_{H,NO}$ estimates, no outliers were identified and Fig. 5.25 exhibits a reasonable fit to the linear true normal line, indicating normal distribution of the data. The mean $Y_{H,NO}$ is 0.461 ± 0.076 (range 0.385 – 0.537) mgCOD/mgCOD, or equivalently a yield ratio of 68.8%, with respect to $Y_{H,AE}$ = 0.67 mgCOD/mgCOD. As noted above, this yield ratio is substantially lower than the theoretically predicted $Y_{H,NO}$:$Y_{H,AE}$ = 83%, as well as the average YH,NO compared with the calculated experimental average $Y_{H,NO}$ = 0.54 (81 ± 3.5%) with respect to $Y_{H,AE}$ = 0.67 mgCOD/mgCOD (see Chapter 2).

In summary, for Period III the average estimates determined for $Y_{H,NO}$ corresponding to $Y_{H,AE}$ = 0.67 mgCOD/mgCOD were combined and are presented in Table 5.18 below. The $Y_{H,NO}$ estimates were evaluated for outliers and analysed statistically in the linearized probability graph, Fig. 5.25.

Table 5.18: Period III Summary: All determinations of $Y_{H,NO}$ corresponding to $Y_{H,AE}$ = 0.67 mgCOD/mgCOD for OU-NU combinations from respective aerobic and anoxic batch tests, per sewage batch (SB).

Sewage Batch	ABT-DBT Combination	$Y_{H,NO}$ (mgCOD/mgCOD)
22	35-34	0.592
	36-34	0.620
23	38-35	0.529
	38-36	0.593
	38-37	0.507
	39-35	0.378

	39-36	0.463
	39-37	0.349
	40-35	0.422
	40-36	0.501
	40-37	0.395

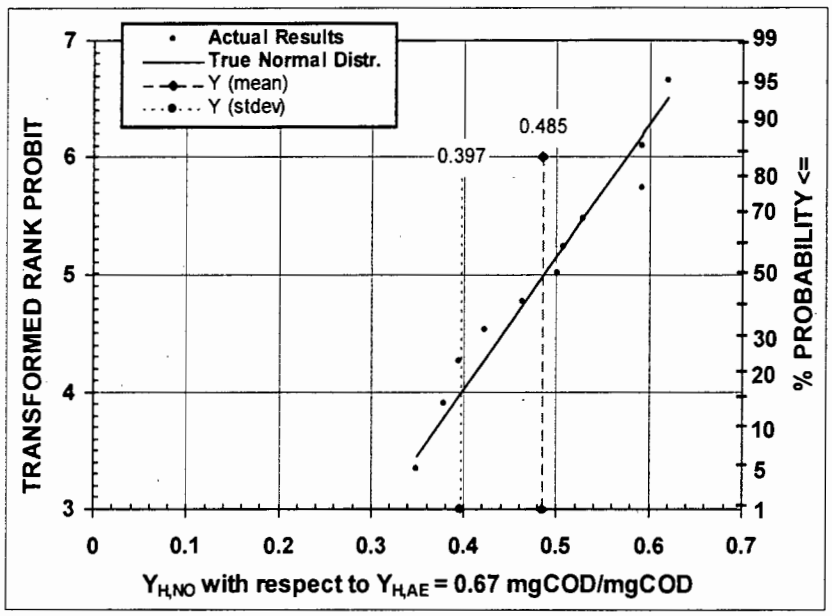

Fig. 5.25: Period III: Statistical plot of all $Y_{H,NO}$ estimates (with respect to $Y_{H,AE}$ = 0.67 mgCOD/mgCOD) determined from OU-NU combinations of corresponding aerobic and anoxic batch tests in Period III.

No outliers were identified, and the $Y_{H,NO}$ estimates for Period III in Fig. 5.25 exhibits a reasonable fit to the linear true normal line. The mean $Y_{H,NO} = 0.485 \pm 0.088$ (range 0.397 – 0.573) mgCOD/mgCOD, or equivalently a yield ratio of 72.4%, with respect to $Y_{H,AE}$ = 0.67 mgCOD/mgCOD, is noticeably lower than the theoretical prediction of $Y_{H,NO}$:$Y_{H,AE}$ = 83%. Further, both the average $Y_{H,NO}$ and yield ratio are lower than the experimental average $Y_{H,NO}$ = 0.54 and yield ratio of 81 ± 3.5% respectively, corresponding to $Y_{H,AE}$ = 0.67 mgCOD/mgCOD, as determined in Chapter 2.

5.5.2 Direct Estimation of $Y_{H,AE}$ Using Acetate RBCOD

As described in Section 5.4 for Period II, in Period III several aerobic batch tests were performed with addition of known amounts of the artificial RBCOD, acetate, to estimate $Y_{H,AE}$ directly via Eq.(5.15), using the observed OU response and corresponding concentration of acetate (as mgCOD/ℓ) in the test. The procedures for acetate addition and determination of the acetate concentration as mgCOD/ℓ in the batch test, were identical to those described in Section 5.4.2; a typical example of an OUR profile for an aerobic batch test with two sequential acetate additions is presented in Fig. 5.20. Similarly, the concentration of acetate in respective aerobic batch tests (ABT), expressed as mgCOD/ℓ ($[Ac]_{BT}$), for respective sequential

additions "1" and "2", and the corresponding OU and $Y_{H,AE}$ determinations, are summarised in Table 5.19.

Table 5.19: Period III: Direct estimation of $Y_{H,AE}$ from known concentration of acetate ($[Ac]_{BT}$) and corresponding OU response; also shown are, the sewage batch used (SB), mixed-liquor (ML) source and aerobic batch test (ABT) number. Labels "MLE" and "SQW" refer to ML from the dedicated MLE and SQW systems operated in Period II (Chapter 3).

SB	ABT	ML	$[Ac]_{BT,1}$ (mgCOD/ℓ)	$[Ac]_{BT,2}$ (mgCOD/ℓ)	OU_1 (mgO/ℓ)	OU_2 (mgO/ℓ)	$Y_{H,AE\,1}$ (COD/COD)	$Y_{H,AE\,2}$ (COD/COD)
22	35	MLE	58.09	38.11	20.82	12.09	0.642	0.683
	36	MLE	58.88	38.63	19.2	12.03	0.674	0.689
	37	MLE	58.18	38.18	21.93	16.25	0.623	0.574
23	39	MLE	76.57	51.05	20.52	15.16	0.732	0.703
	40	MLE	77.98	-	25.93	-	0.667	-

The estimated values for $Y_{H,AE}$ were evaluated for outliers and analysed statistically in the linearized probability plot in Fig. 5.26.

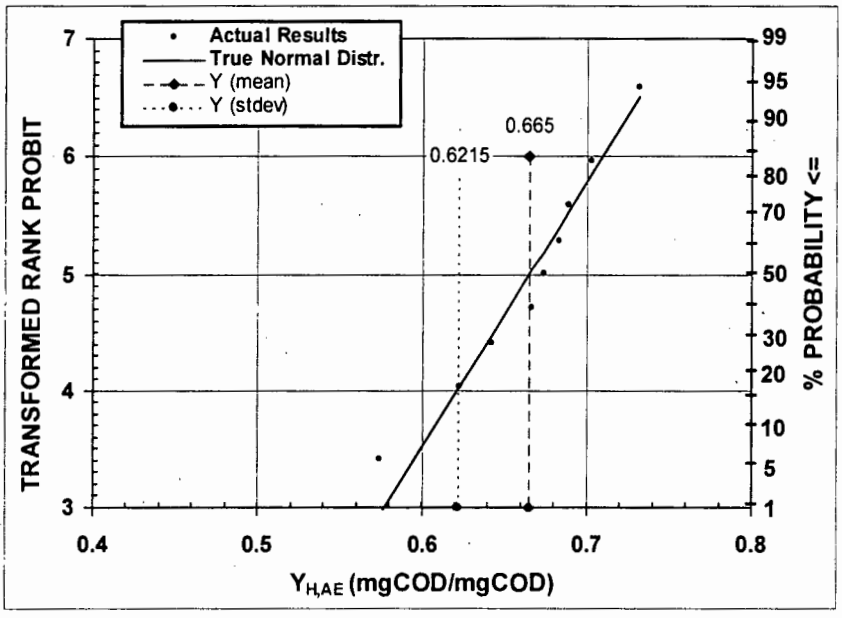

Fig. 5.26: Period III: Statistical plot of the $Y_{H,AE}$ determinations from addition of known concentration of acetate to aerobic batch tests..

No outliers were identified for the $Y_{H,AE}$ estimates in Table 5.19, which exhibit a reasonable fit to the linear true normal line in Fig. 5.26, indicating a normal distribution for $Y_{H,AE}$ using the artificial RBCOD, acetate. The mean $Y_{H,AE}$ of 0.665 ± 0.044 (range 0.621 – 0.709) mgCOD/mgCOD for utilization of the artificial RBCQD, acetate, is in remarkably good agreement with the conventionally accepted $Y_{H,AE}$ = 0.67 mgCOD/mgCOD for domestic wastewater, exhibiting only a 0.75%

difference from the standard $Y_{H,AE}$; thus, the acceptance of the standard $Y_{H,AE}$ = 0.67 mgCOD/mgCOD in this study is further substantiated (see Section 5.4.2).

5.5.3 Estimation of $Y_{H,NO}$ Using Acetate RBCOD

Following the success achieved with aerobic acetate addition batch tests (Sections 5.4.2 and 5.5.2 above), as described in Chapter 3, several anoxic batch tests were performed with addition of known amounts of the artificial RBCOD, acetate, to estimate $Y_{H,NO}$ directly from the observed NU response by rearranging Eq.(5.2):

$$\Rightarrow Y_{H,NO} = 1 - 2.86*NU/RBCOD_{BT,AX} \qquad (5.16)$$

A detailed description of the anoxic batch test procedure using acetate is given in Section 4.2.2., Chapter 4. The methods for acetate addition and estimation of its concentration as mgCOD/ℓ in the anoxic batch tests, were identical to those described in Section 5.4.2 above for similar aerobic batch tests, except that no wastewater was added to the anoxic acetate batch tests (for reasons set out in Section 4.2.2, Chapter 4), but rather the acetate was added at the start of the test. Further, the procedures for the last 4 tests differed from the others in the following respects: (i) DBT 40 was performed using two successive acetate additions ("a" and "b") in the same test; and (ii) DBTs 40b to 42 were aerated for about 2 hours after completion of the respective anoxic acetate tests, and a known mass of acetate added and an aerobic acetate batch test performed in the same reactor. Typical examples of NUR profiles for anoxic batch tests with: (i) a single acetate addition at time = 0 and (ii) a sequential acetate addition, are given in Fig. 5.27 for DBT 39 and in Fig. 5.28 for DBT 40 respectively.

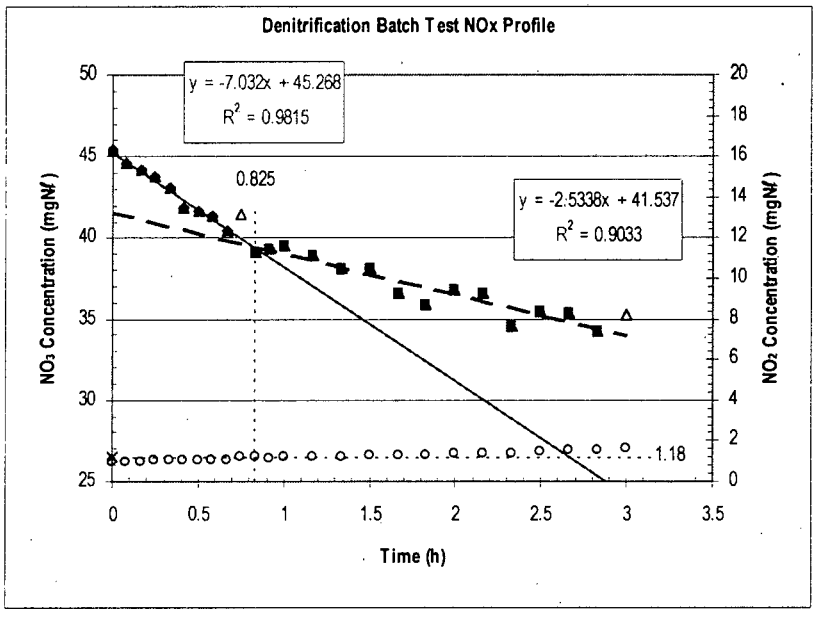

Fig. 5.27: Period III: The NUR profile for anoxic (denitrification) batch test (DBT) 39 as a typical example of an anoxic batch test using only acetate.

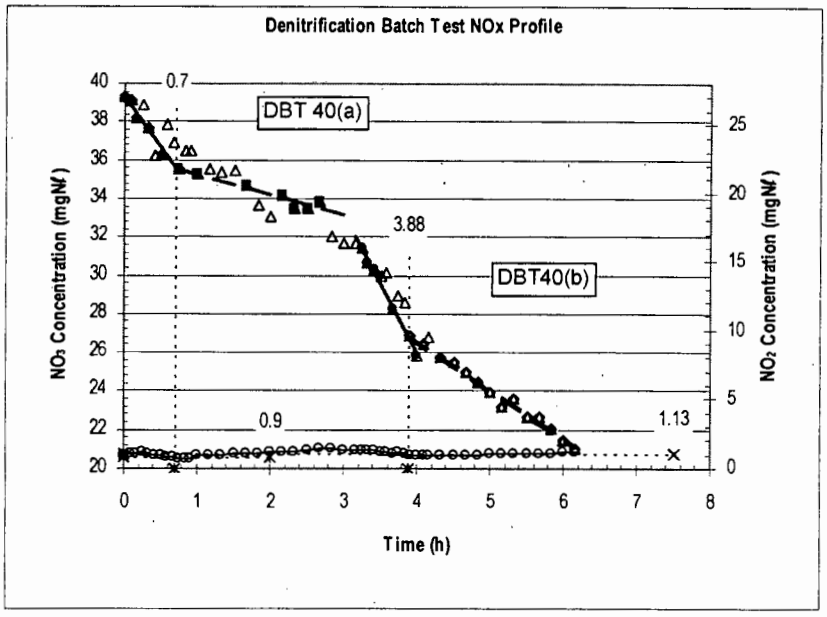

Fig. 5.28: Period III: The NUR profile of anoxic (denitrification) batch test (DBT) 40, showing the denitrification response due to two successive additions of acetate in the same test.

The concentration of acetate, in mgCOD/ℓ ($[Ac]_{BT}$), in the respective anoxic (denitrification) batch tests (DBT) and corresponding NU, $Y_{H,NO}$, OU, $Y_{H,AE}$, and $Y_{H,NO}$:$Y_{H,AE}$ determinations, are summarised in Table 5.20 below[1].

Table 5.20: Period III: Direct estimation of $Y_{H,NO}$ from known concentration of acetate ($[Ac]_{BT}$) and corresponding NU response. Also shown are, the sewage batch (SB), mixed-liquor (ML) source and denitrification batch test (DBT) number; "MLE" refers to ML from the dedicated MLE system described in Chapter 3.

DBT	$[Ac]_{BT,NO}$ (mgCOD/ℓ)	NU (mgN/ℓ)	$Y_{H,NO}$ (COD/COD)	$[Ac]_{BT,AE}$ (mgCOD/ℓ)	OU (mgO/ℓ)	$Y_{H,AE}$ (COD/COD)	$Y_{H,NO}$:$Y_{H,AE}$ (COD/COD)
38	17.1	2.602	0.565				
39	18.7	3.023	0.538				
40a	18.8	2.458	0.626				
40b	22.6	2.623	0.667	28.51	6.55	0.770	0.866
41	21.2	2.90	0.608	25.5	6.70	0.737	0.825
42	21.3	3.07	0.588	25.66	7.72	0.699	0.840

The estimated values for $Y_{H,NO}$ were evaluated for outliers and analysed statistically in the linearized probability plot, Fig. 5.31.

[1] The results of initial anoxic acetate tests, DBT 30 – 33, were invalidated due to air contamination of the nitrogen gas bubbled through the reactor contents, and are excluded from further analysis; see Section 4.3.3., Chapter 4

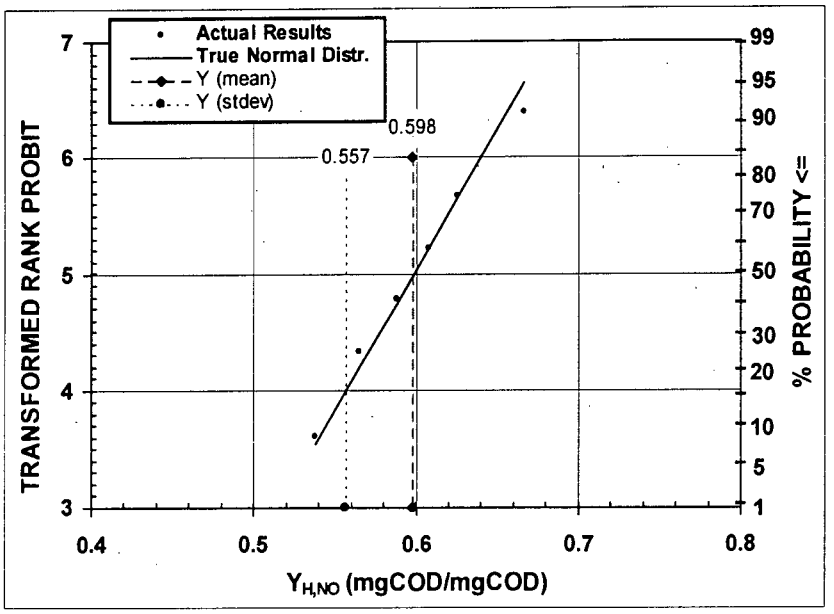

Fig. 5.29: Period III: Statistical plot of the $Y_{H,NO}$ determinations from addition of known concentration of acetate to anoxic batch tests..

No outliers were identified for the anoxic acetate $Y_{H,NO}$ estimates, and Fig. 5.29 exhibits a good fit to the linear true normal line, indicating normal distribution of the data. The mean $Y_{H,NO}$ is approximately 0.598 ± 0.041 (range 0.557 – 0.639) mgCOD/mgCOD, or equivalently a yield ratio of 89.3%, with respect to $Y_{H,AE}$ = 0.67 mgCOD/mgCOD. The yield ratio is somewhat higher than the theoretical prediction of $Y_{H,NO}$:$Y_{H,AE}$ = 83%, and the directly determined $Y_{H,NO}$ also is higher than the literature experimental average $Y_{H,NO}$ = 0.54. Interestingly, the average $Y_{H,AE}$ = 0.735 ± 0.036 mgCOD/mgCOD estimated from the three anoxic-aerobic acetate batch tests in which acetate was added first anoxically and then aerobically in the same test (DBT 40b – 42), is also noticeably higher than both the aerobic acetate average of $Y_{H,AE}$ = 0.665 ± 0.044 obtained earlier (Section 5.5.2), and the accepted standard value of $Y_{H,AE}$ = 0.67 mgCOD/mgCOD. Hence, the average ratio of the two corresponding anoxic-aerobic yields obtained in the same acetate batch tests (DBT 40b – 42), of $Y_{H,NO}$:$Y_{H,AE}$ = 0.84 ± 0.021, is in good agreement with the theoretically predicted $Y_{H,NO}$:$Y_{H,AE}$ = 0.83 and the literature experimental average of 0.81.

5.6 YIELD ESTIMATIONS USING EXPERIMENTAL DATA FROM OTHER INVESTIGATIONS

5.6.1 Yield Estimation Using Experimental Data from Wilson (1976)

As part of experimental research conducted for partial fulfilment of a Master of Science degree at the University of Cape Town, Wilson (1976) investigated the adsorption phase in biological denitrification – i.e. the K_2 denitrification rate – using domestic sewage from the Cape Flats Wastewater Treatment Plant (CFWWTP) in anoxic plug-flow reactors similar to those of Stern and Marais (1974).

In particular, to verify the adsorption theory proposed, Wilson (1976) used unsettled (raw) sewage from the CFWWTP in a continuous flow-through steady-state activated sludge system consisting of: (1) a primary anoxic (plug-flow) reactor connected in series to (2) an aeration reactor; no inter-reactor recycles were employed and the settled sludge from the secondary settling tank was returned ("r-recycle") to the primary anoxic reactor. A typical example of a nitrate concentration-time profile observed by Wilson (1976) is shown in Fig. 5.30 below.

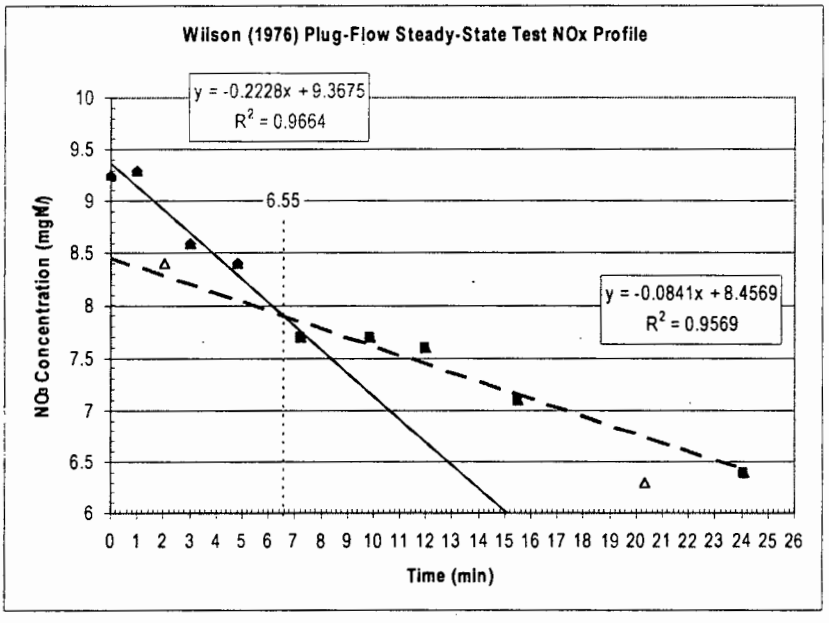

Fig. 5.30: A typical example of a nitrate concentration-time profile observed by Wilson (1976).

By accepting the average f_{ts} = 0.086 determined by Ekama *et al.* (1984) for raw CFWWTP wastewater, and noting that the r-recycle ratio was 5:1 with respect to the influent flow (Q_i), the average RBCOD concentration corresponding to the denitrification (NUR) profiles observed by Wilson (1976) was estimated from the operating data provided. On this basis, the data by Wilson (1976) was re-analysed to estimate values for $Y_{H,NO}$ in the steady-state experiments using Eq.(5.16). A complete analysis of the steady-state experimental observations by Wilson (1976) is presented in *Appendix E* and summarised in Table 5.21 below.

Table 5.21: Estimation of $Y_{H,NO}$ from the experimental data obtained by Wilson (1976), showing the corresponding test number, NU and RBCOD, including the R^2 correlation coefficients for the linear fits of K_1 and K_2 denitrification rates to observed NO_3 concentration data.

Test No.	RBCOD (mgCOD/ℓ)	NU (mgN/ℓ)	$Y_{H,NO}$ (COD/COD)	R^2_{K1}	R^2_{K2}
1	6.88	0.91	0.621	0.9664	0.9569
2	6.12	1.17	0.453	0.9859	0.729
3	6.31	1.74	0.209	0.9481	0.8149
4	6.56	1.71	0.255	0.9827	0.8918
5	6.88	0.63	0.739	0.9482	0.9721
6	6.21	1.37	0.367	0.9526	0.8769
7	6.67	1.19	0.491	0.6431	0.6479
8	6.21	1.29	0.404	0.9953	0.7854
9	6.45	0.61	0.731	0.9972	0.9779
10	6.67	1.52	0.348	0.987	0.2185

The estimated values for $Y_{H,NO}$ were evaluated for outliers and analysed statistically in the linearized probability graph, Fig. 5.31.

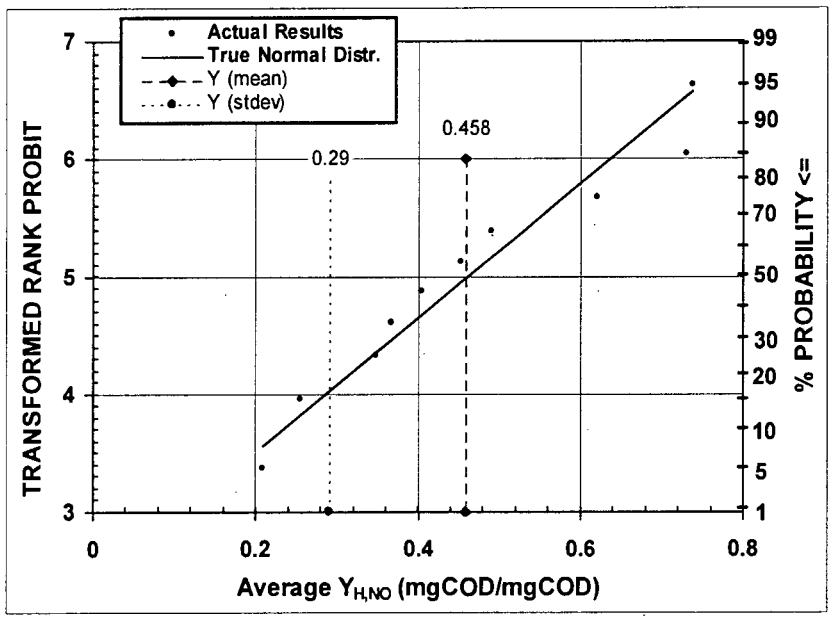

Fig. 5.31: Statistical plot of the $Y_{H,NO}$ values estimated from the experimental data by Wilson (1976).

No outliers were identified for the $Y_{H,NO}$ estimates determined from the experimental data of Wilson (1976), and a reasonable fit to the linear true normal line is exhibited in Fig. 5.31, with only slight deviation at the upper extreme. The mean $Y_{H,NO}$ is 0.458 ± 0.168 (range 0.29 – 0.626), giving a yield ratio of 68.4% with respect to $Y_{H,AE}$ = 0.67 mgCOD/mgCOD. This yield ratio is substantially lower than the theoretical prediction of $Y_{H,NO}$:$Y_{H,AE}$ = 83%, as is the $Y_{H,NO}$ with respect to the experimental

average $Y_{H,NO}$ = 0.54 calculated in the literature, see Chapter 2. The values also are lower than those determined in this experimental investigation. The data, however, is subject to wide variation as evidenced by the broad range of values for $Y_{H,NO}$ and, consequently, the relatively high standard deviation. This is likely due to the considerable uncertainty in estimation of the K_2 denitrification rate lines, as indicated by the generally low correlation coefficients (R^2_{K2}) obtained from the linear fits to the observed data (Table 5.21).

5.6.2 Yield Estimation Using Experimental Data from Ketley *et al.* (1991)

As part of an experimental investigation into the effect of fully anoxic and anoxic-aerobic conditions on low F/M (later "AA") filaments in nitrogen removal systems, Ketley *et al.* (1991) performed corresponding aerobic and anoxic batch tests using sludge from two laboratory-scale fully anoxic continuous flow-through systems ("ANOX2" and "ANOX3" respectively), fed the same raw domestic sewage from the MPWWTP. On day 42 of the study, two parallel anoxic batch tests ("ANBT1" and "ANBT2" respectively) were performed using sludge from the respective systems; at the end of the anoxic tests, the mixed-liquors in the respective batch tests were aerated for two hours and two corresponding aerobic batch tests ("ABT2" and "ABT3" respectively) were performed in each. The basic procedure was: (i) a 2ℓ volume of activated sludge mixed-liquor was combined with 1ℓ raw sewage to form a total 3ℓ batch test volume at the start of each anoxic test; (ii) at the end of the anoxic test, the batch test mixed-liquor was settled out and the supernatant decanted; (iii) the concentrated mixed-liquor was then supplemented with additional mixed-liquor from the steady-state systems to form a 2ℓ volume in the reactor; (iv) 1ℓ raw sewage was then added and the aerobic batch test started.

Since the mixed-liquor used in the respective tests came from parallel systems fed the same sewage and under the same conditions, and the same volume of the same sewage was added to the corresponding anoxic and aerobic batch tests, it could be accepted that each batch test contained the same mass of RBCOD and sludge from the same source. On this basis, the corresponding ANBT-ABT data from Ketley *et al.* (1991) were reassessed to determine corresponding NU and OU values for the respective batch tests, and, thus, estimate $Y_{H,NO}$ in terms of $Y_{H,AE}$ via Eq.(5.4), as demonstrated earlier in Sections 5.3 – 5.5. The corresponding NU and OU values for ANBT 1 and 2, and ABT 3 and 4, respectively, were determined by graphical interpretation of the respective NUR and OUR profiles reported by Ketley *et al.* (1991): The OU was estimated as the area of a simple rectangle under the RBCOD utilization portion of the OUR profile (see Section 4.4.1, Chapter 4), while the NU was estimated as the difference (ΔNO_3) between the NO_3 concentrations corresponding to the y-intercepts of the K_1 ("y-K_1") and the back-projection of the K_2 ("y-K_2") denitrification rate lines – it is accepted that NO_2 formation was negligible, since none was reported (see Section 4.4.2, Chapter 4). A complete analysis of the experimental observations by Ketley *et al.* (1991) is set out in *Appendix E* and summarised in Table 5.22 below.

Table 5.22a: Estimated nitrate utilization (NU) for anoxic batch tests, ANBT 1 and 2, reported by Ketley *et al.* (1991), corresponding to aerobic batch tests ABT 3 and 4 in Table 5.32b below; also shown are the y-intercepts for corresponding K_1 and K_2 denitrification rate lines.

ANBT	y-K_1 (mgNO_3-N/ℓ)	y-K_2 (mgNO_3-N/ℓ)	ΔNO_3 = NU (mgN/ℓ)
1	24.2	17.8	6.4
2	24.33	16.35	7.98

Table 5.22b: Estimated oxygen utilization (OU) for aerobic batch tests, ABT 2 and 3, reported by Ketley *et al.* (1991), corresponding to anoxic batch tests ANBT 1 and 2 in Table 5.32a above; also shown are the estimated RBCOD and SBCOD OUR plateaus, and corresponding time (t) indices for determining OU = $Area_{RBCOD}$ = $\Delta OUR^*\Delta t$ (see Chapter 4).

ABT	OUR Plateau (mgO/ℓ/h)		t (h)		ΔOUR (mgO/l/h)	Δt (h)	OU (mgO/ℓ)
	RBCOD	SBCOD	t_{RBCOD}	t_{SBCOD}			
2	34.0	12.5	2.64	3.45	21.5	0.80	17.2
3	40.7	20.7	2.9	3.75	20	0.85	17.0

Using the corresponding OU and NU estimations determined from the respective aerobic (ABT 3 and 4) and anoxic (ANBT 1 and 2) batch tests shown in Table 5.22, estimates of $Y_{H,NO}$ as a function of $Y_{H,AE}$ were calculated with Eq.(5.4), and are plotted in Fig. 5.32.

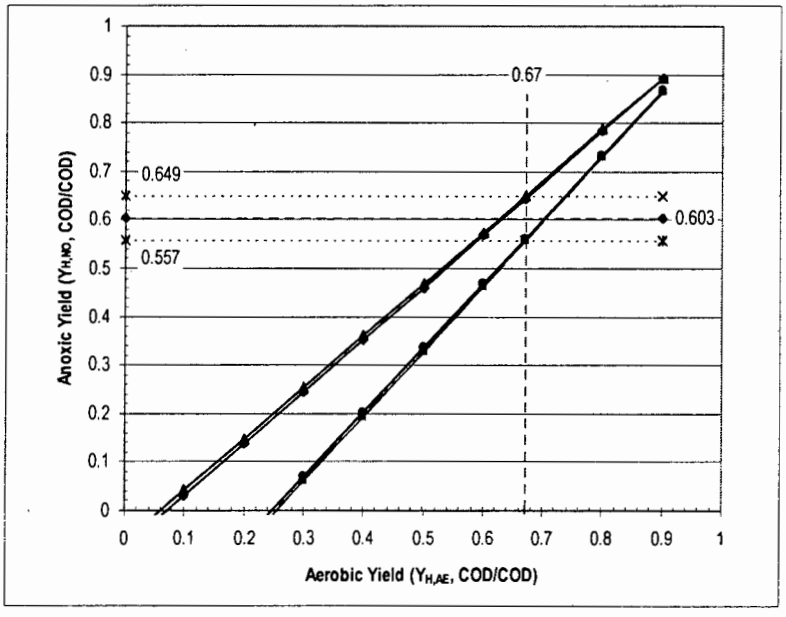

Fig. 5.32: Plot of $Y_{H,NO}$ in terms of $Y_{H,AE}$ for OU-NU combinations estimated from corresponding aerobic and anoxic batch tests containing the same mass of wastewater RBCOD, as reported by Ketley *et al.* (1991).

For the corresponding anoxic-aerobic batch tests reported by Ketley *et al.* (1991), the data in Fig. 5.32 gives an average $Y_{H,NO}$ = 0.603 ± 0.05 (range 0.553 – 0.653), or an equivalent yield ratio of 90.0%, with respect to $Y_{H,AE}$ = 0.67 mgCOD/mgCOD. The yield ratio is noticeably higher than the theoretically predicted $Y_{H,NO}$:$Y_{H,AE}$ = 83%, and both $Y_{H,NO}$ and the yield ratio are higher than the literature determined experimental average $Y_{H,NO}$ = 0.54 and yield ratio 81 ± 3.5%, respectively, with respect to $Y_{H,AE}$ = 0.67 mgCOD/mgCOD.

5.6.3 Yield Estimation Using Experimental Data from Ekama *et al.* (1996)

To investigate the effect of feeding conditions on filamentous bulking, Ekama *et al.* (1996) operated two single reactor activated sludge systems in parallel, one as an intermittently fed fill and draw (IFFD, also called sequencing batch reactor, SBR), and the other as continuously fed completely mixed (CFCM). In all other respects, the operating conditions for both systems were the same, including the influent feed of settled sewage from the MPWWTP. Alternating anoxic-aerobic conditions were imposed on both systems by alternating periods of aeration with non-aeration over a 4h cycle (3h aeration on and 1h aeration off). The feed to the CFCM system was continuous and with the aeration/non-aeration cycle, the sludge was exposed to the influent RBCOD under both anoxic and aerobic conditions. The IFFD system was batch fed once daily and, in order to expose the sludge to influent RBCOD under both aerobic and anoxic conditions, as in the CFCM system, the time of the daily feed was alternated with the aeration/non-aeration cycle imposed on the system: On one day, the system was fed at the start of the aerobic cycle and on the next day at the start of the anoxic cycle, i.e. 1h earlier.

During the 10 day (i.e. a single sewage batch) period between days 60 and 70 of the study, 5 aerobic and 3 anoxic *in situ* OUR and NUR (respectively) profile tests were performed on the IFFD system, during the two hour period immediately following feed addition; for the anoxic profile tests the anoxic period following feed addition was extended from 1 to 2 hours. Examples of typical OUR and nitrate concentration-time profiles obtained in the study are presented below in Figs. 5.33 and 5.34, respectively (Ekama *et al.*, 1996). Note that the *in-situ* nitrate concentration was additionally measured with a nitrate ion-selective electrode.

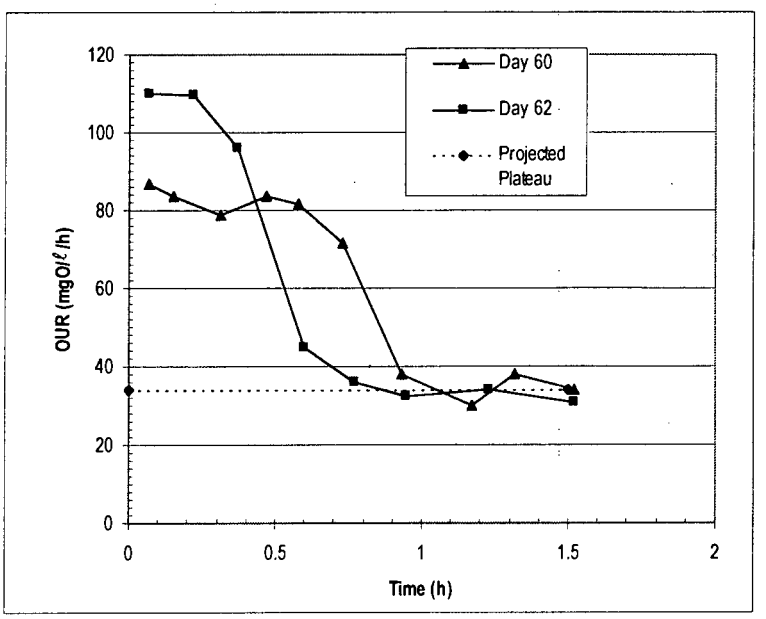

Fig. 5.33: Typical oxygen utilisation rate (OUR) versus time profiles following batch feeding under aerobic conditions of intermittently fed fill and draw (IFFD) activated sludge system.

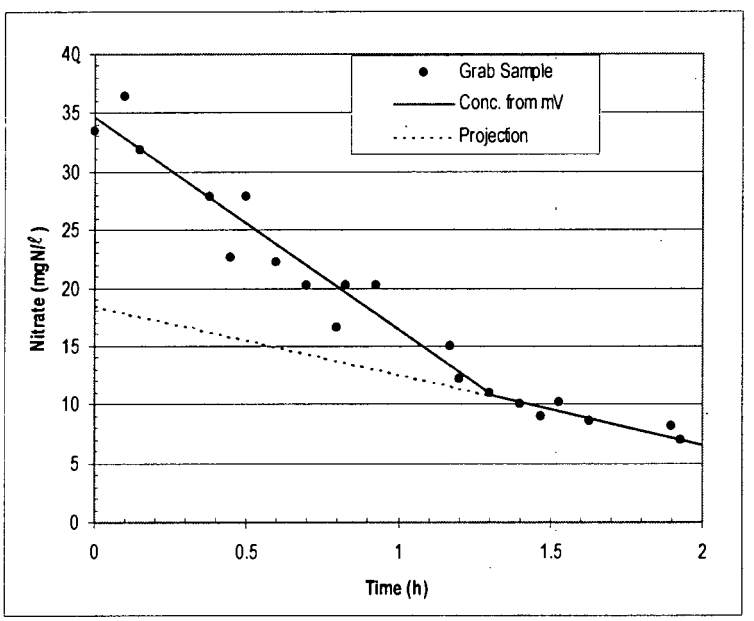

Fig. 5.34: Typical nitrate versus time profiles following batch feeding under anoxic conditions of intermittently fed fill and draw (IFFD) activated sludge system; mV refers to the millivolt reading from a nitrate ion-selective electrode, calibrate to nitrate concentration with the grab samples.

Corresponding OU and NU values were estimated from the respective OUR and nitrate concentration-time profiles, by the same methods as in Section 5.6.2, and are presented in Table 5.23.

Table 5.23: Corresponding oxygen and nitrate utilizations (OU and NU respectively) estimated for the respective aerobic and anoxic profile tests by Ekama *et al.* (1996).

Aerobic Profile	OU (mgO/ℓ)	Anoxic Profile	NU (mgN/ℓ)
1	36.7	1	16
2	37.3	2	22
3	38.7	3	17
4	29.1		
5	41.7		

It is accepted that the initial RBCOD concentration in the reactor immediately following addition of the batch feed is the same in both the anoxic and aerobic profile tests, since the same wastewater batch was used in all the tests at the same loading rate (see Ekama *et al.*, 1996). On this basis, the experimental data of Ekama *et al.* (1996) was reassessed to estimate $Y_{H,NO}$ in terms of $Y_{H,AE}$ via Eq.(5.4), from different combinations of the OU and NU determined from the respective aerobic and anoxic profile tests. A plot of $Y_{H,NO}$ as a function of $Y_{H,AE}$ for the OU-NU combinations formed from Table 5.23 is presented in Fig. 5.35.

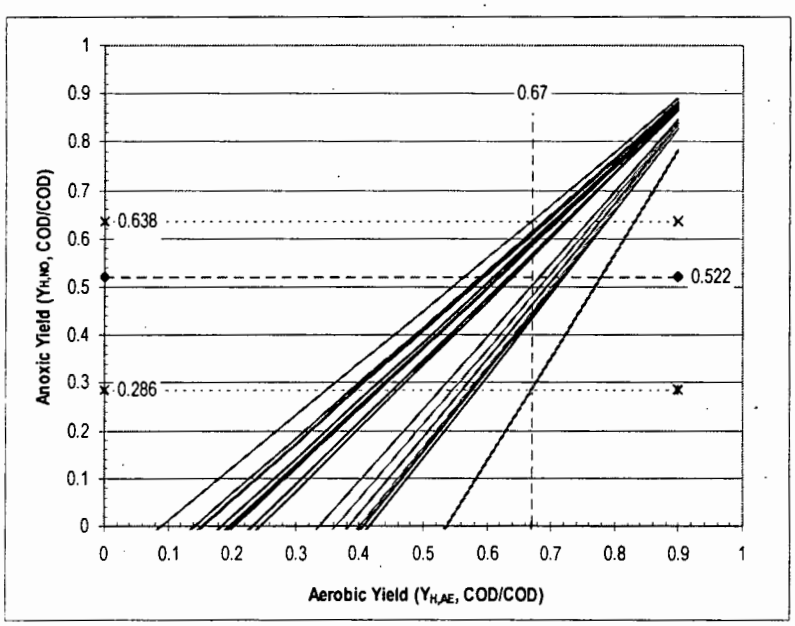

Fig. 5.37: Plot of $Y_{H,NO}$ in terms of $Y_{H,AE}$ for OU-NU combinations estimated from the aerobic and anoxic profiles reported by Ekama *et al.* (1996).

The $Y_{H,NO}$ estimates in Fig. 5.35 give an average $Y_{H,NO} = 0.552 \pm 0.096$ (range 0.456 – 0.648), or an equivalent yield ratio of 82.4%, with respect to $Y_{H,AE} = 0.67$ mgCOD/mgCOD. The yield ratio compares very well with the theoretically predicted $Y_{H,NO}$:$Y_{H,AE} = 0.83$, and both $Y_{H,NO}$ and the yield ratio are in good agreement with the calculated literature experimental average $Y_{H,NO} = 0.54$ and yield ratio of 81 ± 3.5%,

both with respect to $Y_{H,AE}$ = 0.67 mgCOD/mgCOD. However, the data exhibits wide variation and suggests, possibly, the presence of two different data populations, as seen previously in Section 5.3.1.

The $Y_{H,NO}$ estimates corresponding to $Y_{H,AE}$ = 0.67 mgCOD/mgCOD were evaluated for outliers and tested by the Student t-Test to assess if they belong to the same data population (see *Appendix E*). One outlier was identified (OU-NU combination 4-2, $Y_{H,NO}$ = 0.286) and excluded from subsequent analyses, and the result of the t-Test (95% significance level) determined that all the data belong to the same population. Accordingly, excluding the single outlier above, the estimates for $Y_{H,NO}$ as a function of $Y_{H,AE}$ are replotted in Fig. 5.36.

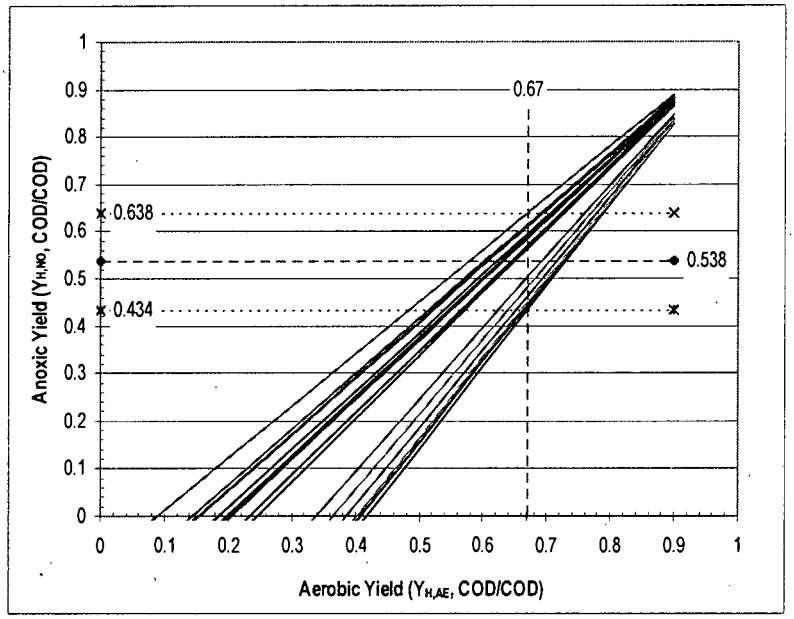

Fig. 5.36: Revised plot of $Y_{H,NO}$ in terms of $Y_{H,AE}$ for OU-NU combinations estimated from the aerobic and anoxic profiles reported by Ekama *et al.* (1996), excluding one outlier (OU-NU combination 4-2).

The replotted $Y_{H,NO}$ estimates in Fig. 5.36 gives an average $Y_{H,NO}$ = 0.538 ± 0.073 (range 0.465 – 0.611), or an equivalent yield ratio of 80.3%, with respect to $Y_{H,AE}$ = 0.67 mgCOD/mgCOD. These values are in very good agreement with the theoretically predicted $Y_{H,NO}$:$Y_{H,AE}$ = 0.83, and the calculated literature experimental average $Y_{H,NO}$ = 0.54 (yield ratio 81 ± 3.5%) with respect to $Y_{H,AE}$ = 0.67 mgCOD/mgCOD. To analyse the data statistically, the estimates for $Y_{H,NO}$ corresponding to $Y_{H,AE}$ = 0.67 mgCOD/mgCOD are plotted in the linearized probability graph, Fig. 5.37.

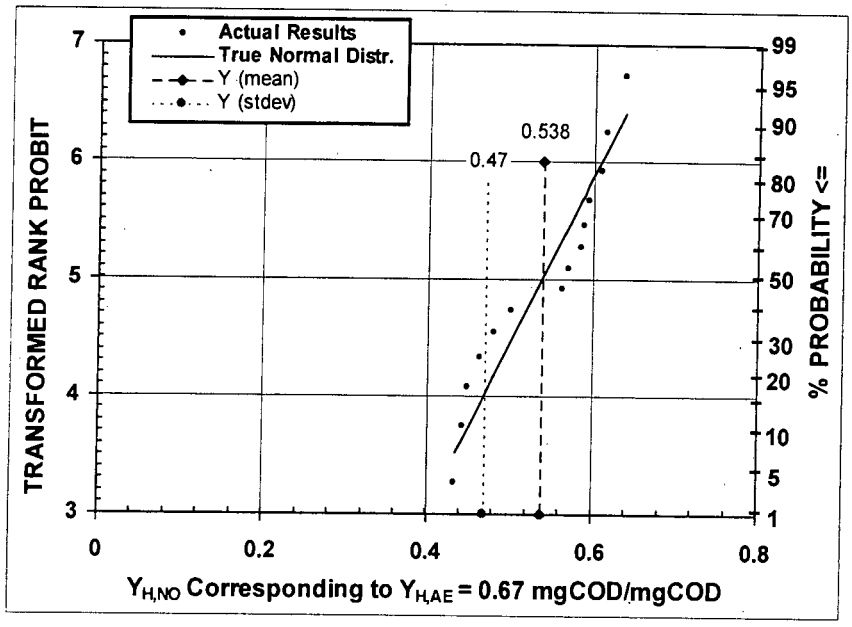

Fig. 5.37: Statistical plot of $Y_{H,NO}$ in terms of $Y_{H,AE}$ for OU-NU combinations estimated from the aerobic and anoxic profiles reported by Ekama *et al.* (1996).

The $Y_{H,NO}$ estimates plotted in Fig. 5.37 exhibit a reasonable fit to the linear true normal line. The mean $Y_{H,NO} = 0.538 \pm 0.068$ (range 0.47 – 0.606) mgCOD/mgCOD, or an equivalent yield ratio of 80.3%, with respect to $Y_{H,AE} = 0.67$ mgCOD/mgCOD, compares very well with the theoretically predicted $Y_{H,NO}$:$Y_{H,AE}$ = 83%, as well as with the calculated literature experimental average $Y_{H,NO} = 0.54$ (yield ratio 81 ± 3.5%), with respect to $Y_{H,AE} = 0.67$ mgCOD/mgCOD.

5.7 SUMMARY ANALYSIS

5.7.1 Wastewater Yield Values

The average estimates for $Y_{H,NO}$ corresponding to $Y_{H,AE} = 0.67$ mgCOD/mgCOD, determined in the previous Sections from corresponding OU-NU combinations of respective aerobic and anoxic batch tests on wastewater, are summarised in Table 5.24.

Table 5.24: Summary of average (AVG) estimates for $Y_{H,NO}$ determined with respect to $Y_{H,AE}$ = 0.67 mgCOD/mgCOD in this investigation; also shown, are the data reference, sample standard deviation (SSD), number of samples (N), weighted average and the sewage used in each case, where "MPWWTP" and "CFWWTP" refer to the Mitchells Plain and Cape Flats Wastewater Treatment Plants respectively.

Data Reference	Thesis Section	Sewage Used	AVG $Y_{H,NO}$ wrt $Y_{H,AE}$ = 0.67 (mgCOD/mgCOD)			Weighted AVG
			AVG	SSD	N	
Period I	5.4	MPWWTP	0.534	0.041	16	0.1857
Period II	5.5	MPWWTP	0.563	0.054	19	0.2325
Period III	5.5	MPWWTP	0.485	0.088	11	0.1160
TOTAL					**46**	**0.534**
Wilson (1976)	5.6.1	CFWWTP	0.458	0.168	10	0.1636
Ketley *et al.* (1991)	5.6.2	MPWWTP	0.603	0.05	4	0.0862
Ekama *et al.* (1996)	5.6.3	MPWWTP	0.538	0.068	14	0.2690
TOTAL					**28**	**0.519**

By weighting the respective averages with the corresponding number of samples (N), overall weighted averages of $Y_{H,NO}$ = 0.534 and 0.519 mgCOD/mgCOD were determined for $Y_{H,AE}$ = 0.67 mgCOD/mgCOD, for the batch test analyses using wastewater RBCOD in this investigation, and by re-evaluation of independent experimental data observed by other researchers, respectively.

The weighted average $Y_{H,NO}$ for wastewater determined in this investigation (0.534) is remarkably similar to the value calculated from the data presented by other investigators (0.519). Further, both values are in good agreement with the average $Y_{H,NO}$ = 0.54 mgCOD/mgCOD calculated from the $Y_{H,NO}$ values of a wide range of experimental investigations in the literature with $Y_{H,AE}$ = 0.67 mgCOD/mgCOD.

The similarity between the $Y_{H,NO}$ from this investigation (0.534 mgCOD/mgCOD) and that determined from the data of other investigations (0.519 mgCOD/mgCOD) suggested that the two data sets could be pooled. To analyse the pooled data statistically, the $Y_{H,NO}$ averages with respect to $Y_{H,AE}$ = 0.67 mgCOD/mgCOD, were evaluated for outliers and plotted in the linearized probability graph, Fig. 5.38.

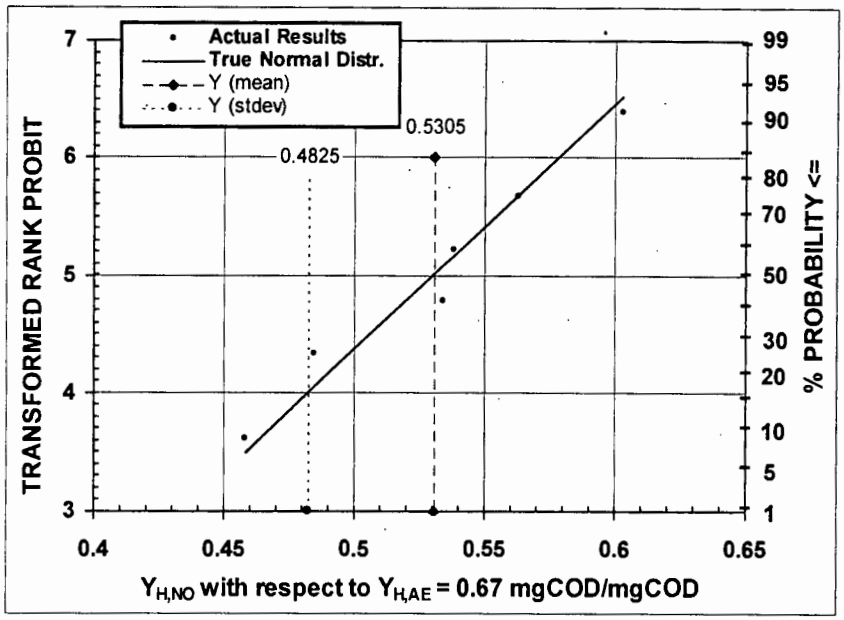

Fig. 5.38: Statistical plot of average $Y_{H,NO}$ estimates relative to $Y_{H,AE}$ = 0.67 mgCOD/mgCOD for experimental data using wastewater RBCOD.

No outliers were identified, and the $Y_{H,NO}$ estimates in Fig. 5.38 exhibit a reasonable fit to the linear true normal line, indicating normal distribution of the data. The mean $Y_{H,NO}$ = 0.531 ± 0.048 (range 0.483 – 0.579), or an equivalent yield ratio of 79.3%, with respect to $Y_{H,AE}$ = 0.67 mgCOD/mgCOD, compares very favourably with the calculated literature experimental average of 0.54, or yield ratio of 81 ± 3.5%, with respect to $Y_{H,AE}$ = 0.67 mgCOD/mgCOD (Chapter 2), and is in reasonable agreement with the theoretically predicted $Y_{H,NO}$:$Y_{H,AE}$ = 83%.

Considering only the experimental data for Mitchells Plain sewage, i.e. excluding the data by Wilson (1976), the corresponding weighted averages for $Y_{H,NO}$ relative to $Y_{H,AE}$ = 0.67 mgCOD/mgCOD were recalculated, and are presented in Table 5.25.

Table 5.25: Summary of average and weighted average (AVG) $Y_{H,NO}$ estimates corresponding to $Y_{H,AE}$ = 0.67 mgCOD/mgCOD for experimental data using sewage from Mitchells Plain Wastewater Treatment Plant (MPWWTP) only; also shown , the data reference, sample standard deviation (SSD) and number of samples (N).

Data Reference	Thesis Section	Sewage Used	AVG $Y_{H,NO}$ wrt $Y_{H,AE}$ = 0.67 (mgCOD/mgCOD)			Weighted AVG
			AVG	SSD	N	
Period I	5.4	MPWWTP	0.534	0.041	16	0.1335
Period II	5.5	MPWWTP	0.563	0.054	19	0.1672
Period III	5.5	MPWWTP	0.485	0.088	11	0.0834
Ketley *et al.* (1991)	5.6.2	MPWWTP	0.603	0.05	4	0.0377
Ekama *et al.* (1996)	5.6.3	MPWWTP	0.538	0.068	14	0.1177
TOTAL					**64**	**0.5395**

An overall weighted average of $Y_{H,NO}$ = 0.5395 ≈ 0.540, or an equivalent yield ratio of 80.6%, corresponding to $Y_{H,AE}$ = 0.67 mgCOD/mgCOD is obtained for Mitchells Plain wastewater. This estimate is near identical to the experimental average of $Y_{H,NO}$ = 0.54, or yield ratio of 81 ± 3.5%, with respect to $Y_{H,AE}$ = 0.67 mgCOD/mgCOD as determined in Chapter 2; it is also in good agreement with the theoretically predicted ratio of $Y_{H,NO}$:$Y_{H,AE}$ = 83%. To analyse the data statistically, the $Y_{H,NO}$ estimates were evaluated for outliers and plotted in the linearized probability graph, Fig. 5.39.

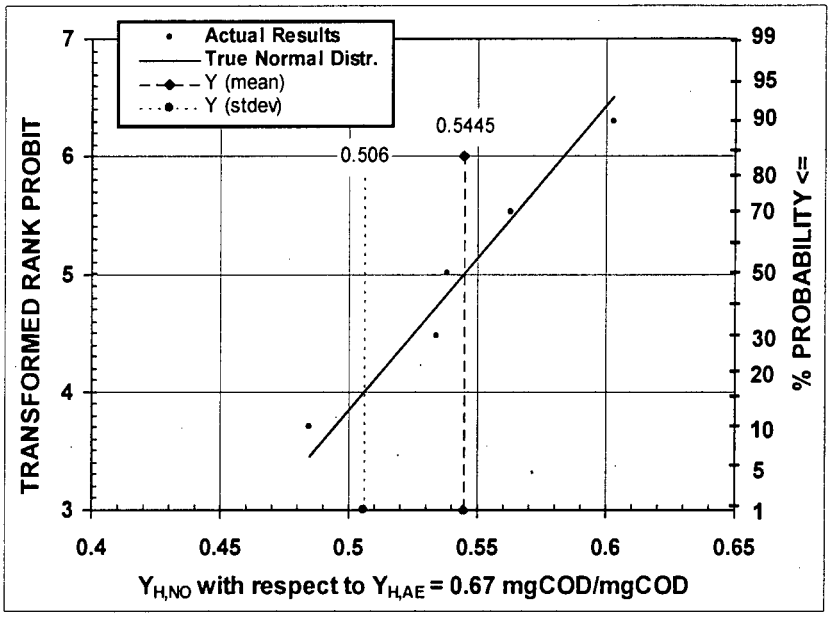

Fig. 5.39: Statistical plot of average $Y_{H,NO}$ estimates relative to $Y_{H,AE}$ = 0.67 mgCOD/mgCOD for experimental data using Mitchells Plain wastewater.

No outliers were identified, and the $Y_{H,NO}$ estimates in Fig. 5.39 exhibit a reasonable fit to the linear true normal line, indicating normal distribution of the data. The mean $Y_{H,NO}$ = 0.545 ± 0.039 (range 0.506 – 0.584), or an equivalent yield ratio of 81.3%, with respect to $Y_{H,AE}$ = 0.67 mgCOD/mgCOD, is virtually identical to the literature experimental average of 0.54, or yield ratio 81 ± 3.5%, with respect to $Y_{H,AE}$ = 0.67 mgCOD/mgCOD as determined in Chapter 2. It also compares very well with the theoretically predicted ratio of $Y_{H,NO}$:$Y_{H,AE}$ = 83%.

Overall, therefore, this investigation indicates the average value for $Y_{H,NO}$, using Mitchells Plain wastewater, to be approximately 0.545 ± 0.039 (range 0.506 – 0.584), or an equivalent yield ratio of 81.3%, with respect to the conventionally accepted $Y_{H,AE}$ = 0.67 mgCOD/mgCOD. This is in very good agreement with both theoretical predictions and experimental determinations by other researchers in the field.

5.7.2 Acetate Yield Values

Average $Y_{H,AE}$ Estimations from Acetate Addition

The average estimates for $Y_{H,AE}$ determined from known additions to aerobic batch tests of the artificial RBCOD, acetate, in Periods II (Fig. 5.22) and III (Fig. 5.26) are summarised in Table 5.26.

Table 5.26: Summary of average (AVG) estimates for $Y_{H,AE}$ determined from known additions of acetate (Ac) in this investigation; also shown, are the data reference, sample standard deviation (SSD), number of samples (N) and the calculated weighted averages of each.

Data Reference	Thesis Section	AVG Acetate $Y_{H,AE}$ (mgCOD/mgCOD)			Weighted AVG
		AVG	SSD	N	
Period II	5.4.2	0.687	0.027	19	0.466
Period III	5.5.2	0.665	0.044	9	0.214
TOTAL				**28**	**0.680**

By weighting the respective averages with the corresponding number of samples (N), an overall weighted average of $Y_{H,AE}$ = 0.680 mgCOD/mgCOD was determined for the aerobic batch tests with known concentrations of the artificial RBCOD, acetate. This weighted average is remarkably close to the conventionally accepted $Y_{H,AE}$ = 0.67 mgCOD/mgCOD, with only a 1.5% difference. The similarity between the two $Y_{H,AE}$ acetate estimates suggests that the two data sets could be pooled.

To analyse the pooled data statistically, the $Y_{H,AE}$ estimates from known acetate additions in Periods II and III, were evaluated for outliers and plotted in the linearized probability graph, Fig. 5.40.

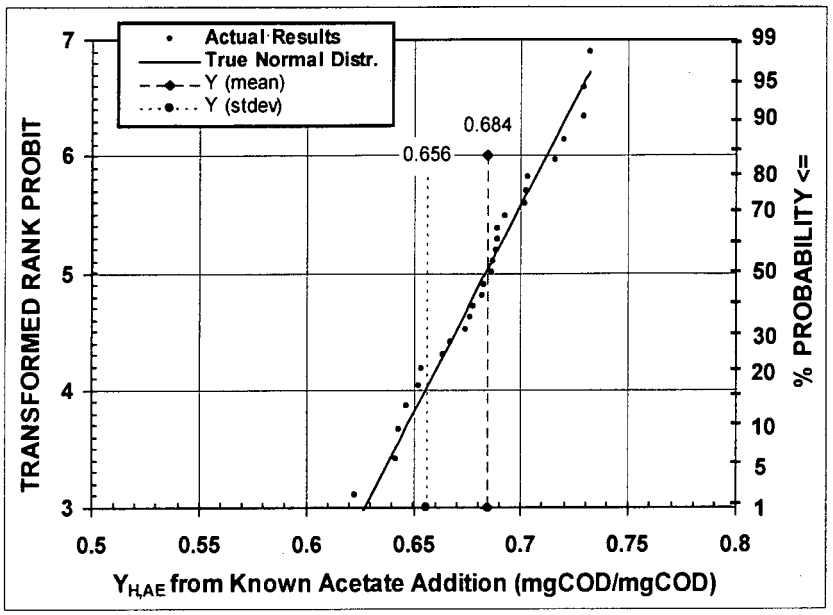

Fig. 5.40: Statistical plot of average $Y_{H,AE}$ estimates from known additions of the artificial RBCOD, acetate, in Periods II and III.

Two outliers were identified (ABT 25, $Y_{H,AE}$ = 0.535 and ABT 37, $Y_{H,AE}$ = 0.574 mgCOD/mgCOD) and excluded from the data plotted in Fig. 5.40. The data exhibit a good fit to the linear true normal line, indicating normal distribution of the data. The mean $Y_{H,AE}$ = 0.684 ± 0.028 (range 0.656 – 0.712) compares very well with the conventionally accepted ("standard") $Y_{H,AE}$ = 0.67 mgCOD/mgCOD, with only a 2% difference. This substantiates acceptance of the standard $Y_{H,AE}$ in this investigation.

Average $Y_{H,NO}$ Estimations from Acetate Addition

Since acetate $Y_{H,NO}$ values were only determined in a single period (Period III), all the $Y_{H,NO}$ acetate estimates were analysed together in Section 5.5.3 above. In summary, the $Y_{H,NO}$ estimates are normally distributed (Fig. 5.29) and give a mean value of approximately 0.598 ± 0.041 (range 0.557 – 0.639) mgCOD/mgCOD, or equivalently a yield ratio of 89.3%, with respect to $Y_{H,AE}$ = 0.67 mgCOD/mgCOD. The yield ratio is somewhat higher than the theoretical prediction of $Y_{H,NO}$:$Y_{H,AE}$ = 83%, and the directly determined $Y_{H,NO}$ also is higher than the literature experimental average $Y_{H,NO}$ = 0.54. Interestingly, the average $Y_{H,AE}$ = 0.735 ± 0.036 mgCOD/mgCOD estimated from the three anoxic-aerobic acetate batch tests in which acetate was added first anoxically and then aerobically in the same test (DBT 40b – 42), is also noticeably higher than both the aerobic acetate average of $Y_{H,AE}$ = 0.665 ± 0.044 obtained earlier (Section 5.5.2), and the accepted standard value of $Y_{H,AE}$ = 0.67 mgCOD/mgCOD. The average ratio of the two corresponding anoxic-aerobic yields obtained in the same acetate batch tests (DBT 40b – 42) is $Y_{H,NO}$:$Y_{H,AE}$ = 0.84 ± 0.021. This is in good agreement with the theoretically predicted $Y_{H,NO}$:$Y_{H,AE}$ = 0.83 and the literature experimental average of 0.81.

5.8 CLOSURE

From this investigation, the average value for $Y_{H,NO}$, using Mitchells Plain wastewater, was found to be 0.545 ± 0.039 (range 0.506 – 0.584), with respect to the conventionally accepted $Y_{H,AE}$ = 0.67 mgCOD/mgCOD, giving an equivalent yield ratio of 81.3%. These values are in very good agreement with both theoretical predictions and experimental determinations by other researchers in the field.

Further, $Y_{H,AE}$ values estimated directly from known concentrations of acetate in aerobic batch tests gave an average of 0.684 ± 0.028 (range 0.656 – 0.712) mgCOD/mgCOD. This average compares very well with the conventionally accepted ("standard") $Y_{H,AE}$ = 0.67 mgCOD/mgCOD, with only a 2% difference. This substantiates acceptance of the standard $Y_{H,AE}$ in this investigation.

Acetate determined $Y_{H,NO}$ values, however, gave an average of 0.598 ± 0.041 (range 0.557 – 0.639) mgCOD/mgCOD, or equivalently a yield ratio of 89.3%, with respect to $Y_{H,AE}$ = 0.67 mgCOD/mgCOD. Both the $Y_{H,NO}$ and yield ratio are higher than the theoretical predictions and experimental determinations by both other researchers and this investigation with sewage. Interestingly, an average $Y_{H,AE}$ = 0.735 ± 0.036 mgCOD/mgCOD was estimated for the three anoxic-aerobic acetate batch tests, in which acetate was added first anoxically and then aerobically in the same test (DBT 40b – 42). Although this $Y_{H,AE}$ is also noticeably higher than expected, it gives an average ratio for the corresponding anoxic yields obtained in the same batch tests (DBT 40b – 42) of $Y_{H,NO}$:$Y_{H,AE}$ = 0.84 ± 0.021. This is in good agreement with the theoretically predicted $Y_{H,NO}$:$Y_{H,AE}$ = 0.83 and the literature experimental average of 0.81.

Thus it can be concluded that this investigation substantiates a reduced OHO yield under anoxic conditions compared with aerobic conditions. For sewage fed systems, a $Y_{H,NO}$ = 0.545 mgCOD/mgCOD for $Y_{H,AE}$ = 0.67 mgCOD/mgCOD would appear to be indicated. The impact of this reduced anoxic yield on nitrification-denitrification (ND) activated sludge system design will be presented in Chapter 6.

CHAPTER 6

MODIFICATION TO THE ACTIVATED SLUDGE STEADY-STATE DESIGN THEORY FOR NITROGEN REMOVAL SYSTEMS

6.1 INTRODUCTION

In Chapter 1, the impact of the reduced ordinary heterotroph organism (OHO) yield for anoxic conditions (relative to its aerobic value) on the denitrification achievable (and, hence, on the effluent nitrate concentration) in typical anoxic/aerobic sequencing (MLE-type) activated sludge systems, has been presented. This proved possible because it was noted that, since the denitrification rate on slowly biodegradable (SB)COD is calibrated against observed nitrate concentration-time profiles, the denitrification potential on SBCOD must remain constant when a reduced anoxic yield is included in the design theory. Hence, the denitrification potential on SBCOD for a selected system could be calculated using the "old" design theory, i.e. based on a single OHO yield constant, and this denitrification potential then used in the modified theory in which the reduced OHO anoxic yield is incorporated. This enabled calculation of the system denitrification potential independently of the specific denitrification rate constant for SBCOD utilization, i.e. K_{2T}. However, for design and general application of the design theory, this calculation procedure is not satisfactory. What is required is that the value for K_{2T} is revised to take into account the reduced anoxic yield, so that a single modified theory can be applied for design. In this Chapter, the value for K_{2T}, as determined by Stern and Marais (1974) and validated by van Haandel *et al.* (1981), will be revised to take into account the reduced anoxic cell yield coefficient ($Y_{H,NO}$) determined in this research (Chapter 5). Also, the reduced OHO anoxic yield must necessarily influence the OHO active biomass concentration and mass, and hence volatile suspended solids (VSS) concentration and mass. In this Chapter, this aspect also will be examined.

6.2 REVISION OF THE K_{2T} DENITRIFICATION RATE CONSTANT

As demonstrated in Chapter 1, for most anoxic/aerobic (AX/AE) sequencing systems (MLE-type), in which the influent readily biodegradable (RB)COD is typically completely utilized under anoxic conditions, the reduced anoxic yield results in a substantial increase in the denitrification potential (D_p) with RBCOD as substrate, which results in a corresponding increase in the total denitrification potential of the system. To accommodate this, the steady-state theory of Marais and Ekama (1976) and WRC (1984) needs to be modified. In terms of this theory, a single heterotroph yield value (Y_H) is accepted for OHO (i.e. X_a) growth under both anoxic and aerobic conditions, and the total denitrification potential of the process (D_{pp}) is defined as:

$$D_{pp} = (1 - f_{us} - f_{up}) * S_{ti} * [\alpha + K_{2T} * f_{xl} * \frac{Y_H * R_s}{(1 + b_{HT} * R_s)}] \qquad (6.1)$$

where:

$$\alpha = \frac{f_{bs} * (1 - f_{cv} * Y_H)}{2.86} \qquad (6.2)$$

$$b_{HT} = 0.24*(1.029)^{T-20} \qquad (6.3)$$

D_{pp}	Total denitrification potential of the process, mgNO3-N/ℓ influent
S_{ti}	Total influent COD, mgCOD/ℓ
f_{us}	Fraction of influent unbiodegradable soluble COD w.r.t. S_{ti}
f_{up}	Fraction of influent unbiodegradable particulate COD w.r.t. S_{ti}
f_{bs}	Fraction of influent RBCOD w.r.t. total influent biodegradable COD (S_{bi})
2.86	Equivalent oxygen demand of NO3-N as electron acceptor, mgO/mgNO3-N
α	Fraction of nitrate removed by the initial rapid phase of denitrification
Q_i	The influent flowrate to the system, ℓ/d
f_{cv}	COD value of sludge mixed liquor VSS; f_{cv} = 1.48 mgCOD/mgVSS
K_{2T}	Specific denitrification rate constant with SBCOD as substrate, mgN/mgAVSS/time
f_{x1}	Fraction of total sludge mass in the system that is unaerated (anoxic in this case)
Y_H	OHO cell yield coefficient, mgAVSS/mg substrate COD
b_{HT}	Nett specific endogenous respiration rate, mgAVSS/mgAVSS/d
R_s	The sludge age of the system, d
T	Temperature, °C

In Eq.(6.1), the specific denitrification rate constant, K_{2T}, is defined as the slope of the experimentally observed nitrate concentration-time profile for SBCOD utilization, divided by the concentration of active OHO biomass (X_a) present (see WRC, 1984), i.e.:

$$K_{2T} = \frac{\left(dNO_3/dt\right)_{SBCOD}}{X_a} = 0.1008*(1.08)^{T-20} \text{ mgN/mgAVSS/d} \qquad (6.4)$$

where:

$$X_a = (1 - f_{us} - f_{up}) * S_{ti} * \frac{Y_H * R_s}{(1 + b_{HT} * R_s)} \qquad (6.5)$$

K_{2T}	Specific denitrification rate constant with SBCOD as substrate, mgN/mgAVSS/time = $0.1008*(1.08)^{T-20}$ mgN/mgAVSS/d (van Haandel *et al.*, 1981; WRC, 1984)
X_a	OHO active biomass concentration, mgAVSS/ℓ
dNO_3/dt	the experimentally observed slope of the nitrate concentration-time profile for SBCOD utilization (see Fig. 6.1), mgN/ℓ/d

From extensive experimental investigations, Marais and co-workers (Stern and Marais, 1974; van Haandel *et al.*, 1981; WRC, 1984) determined an average "constant" $K_{2T} = 0.1008*(1.08)^{T-20}$ mgN/ℓ/mgAVSS/d for the specific denitrification rate for SBCOD utilization. This value has been accepted in current activated sludge steady-state design theory, although, as demonstrated by Eqs.(6.1) to (6.5) above, it is based on a single OHO (i.e. X_a) yield value for both anoxic and aerobic growth. Accepting from the research presented here that the value for the heterotrophic yield under anoxic ($Y_{H,NO}$) conditions is reduced relative to its value under aerobic ($Y_{H,AE}$)

conditions (see Chapter 5), the steady-state formulations for X_a, K_{2T} and D_{pp} need to be revised to take into account a separate and different anoxic yield.

Following from Chapter 1, this can be achieved by defining "f_{anox}" as the fraction of total influent biodegradable COD (S_{bi}) that is utilized anoxically. Accepting that usually all the influent RBCOD is consumed anoxically, the denitrification potential given by Eqs.(6.1) and (6.2) can be appropriately modified to include different anoxic and aerobic cell yield coefficients ($Y_{H,NO}$ and $Y_{H,AE}$ respectively) as follows[1]:

$$D_{pp} = (1 - f_{us} - f_{up}) * S_{ti} * \left[\alpha + K_{2T,NO} * f_{xl} * \left\{ f_{anox} * \frac{Y_{H,NO} * R_s}{(1 + b_{HT} * R_s)} + (1 - f_{anox}) * \frac{Y_{H,AE} * R_s}{(1 + b_{HT} * R_s)} \right\} \right] \quad (6.6$$

where:

$$\alpha = \frac{f_{bs} * (1 - f_{cv} * Y_{H,NO})}{2.86} \quad (6.7)$$

f_{anox} = the proportion of total biodegradable substrate utilized anoxically,

$$= \frac{\left\{ \frac{D_{pp} * 2.86}{(1 - f_{cv} * Y_{H,NO})} \right\}}{(1 - f_{us} - f_{up}) * S_{ti}} \quad (6.8)$$

and:

$K_{2T,NO}$ = the specific denitrification rate constant with SBCOD as substrate, when a separate and different $Y_{H,NO} \neq Y_{H,AE}$ is included, mgN/mgAVSS/time

In Eq.(6.6) the two components making the D_{pp} can be identified: (1) denitrification with RBCOD as substrate (i.e. the α term, "$D_{p,\alpha}$"), and (2) denitrification with slowly biodegradable (SB)COD as substrate (i.e. the $K_{2T,NO}$ term, "$D_{p,K2TNO}$"). For the (1) RBCOD term ($D_{p,\alpha}$), since it is accepted that the RBCOD is completely utilized anoxically (a reasonable assumption given the relatively rapid rate of RBCOD utilization, WRC, 1984), its rate of utilization is of no consequence and the RBCOD contribution to D_{PP} is simply stoichiometric, i.e. via $Y_H = Y_{H,NO}$ in Eq.(6.7). However, for the (2) SBCOD term ($D_{p,K2TNO}$), since SBCOD is not completely utilized anoxically, some OHO (i.e. X_a) growth on SBCOD will occur anoxically at $Y_{H,NO}$ and the remainder aerobically at $Y_{H,AE}$. Thus, incorporating a reduced OHO anoxic yield would imply that the OHO active biomass concentration must be reduced compared with a single OHO yield for both anoxic and aerobic conditions. Since the OHO specific denitrification rate on SBCOD, K_{2T}, is defined as the observed rate divided by the OHO active biomass concentration [Eq.(6.4)], the change in OHO active biomass would necessitate that the value for K_{2T} be revised. However, since the value for K_{2T} given by Eq.(6.4) has been derived from experimentally observed $\Delta NO_3/\Delta t$ nitrate concentration-time profiles (see Fig. 6.1), the amount denitrified by

[1] The theory is modified on the basis that usually *all* growth on RBCOD occurs in the anoxic reactor (i.e. the reactor is sufficiently large that all the RBCOD is utilized anoxically), $\Rightarrow$ 100% of the α term is at $Y_{H,NO}$; whereas only a part of growth on SBCOD occurs in the anoxic reactor (i.e. only a fraction of the K_{2T} term is at $Y_{H,NO}$); see van Haandel *et al.* (1981).

SBCOD utilization, i.e. the contribution of $D_{p,K2T}$ to D_{PP}, must be kept constant when the different anoxic yield ($Y_{H,NO}$) is incorporated. As shown in Fig. 6.1, this means that the theoretically predicted SBCOD denitrification ($D_{p,K2T}$), which equals the experimentally observed $\Delta NO_{3,K2T}$, must remain constant when a single $Y_H = Y_{H,NO} = Y_{H,AE}$ is used, as well as when a separate and different $Y_{H,NO} \neq Y_{H,AE}$ is taken into account. That is, since the experimentally observed slope (dNO_3/dt) must remain constant in Eq.(6.4), the value for K_{2T}, as accepted by van Haandel *et al.* (1981) and others (e.g. Marais and Ekama, 1976; WRC, 1984; Dold *et al.*, 1980 and 1991), must be revised to take into account a separate and different anoxic yield.

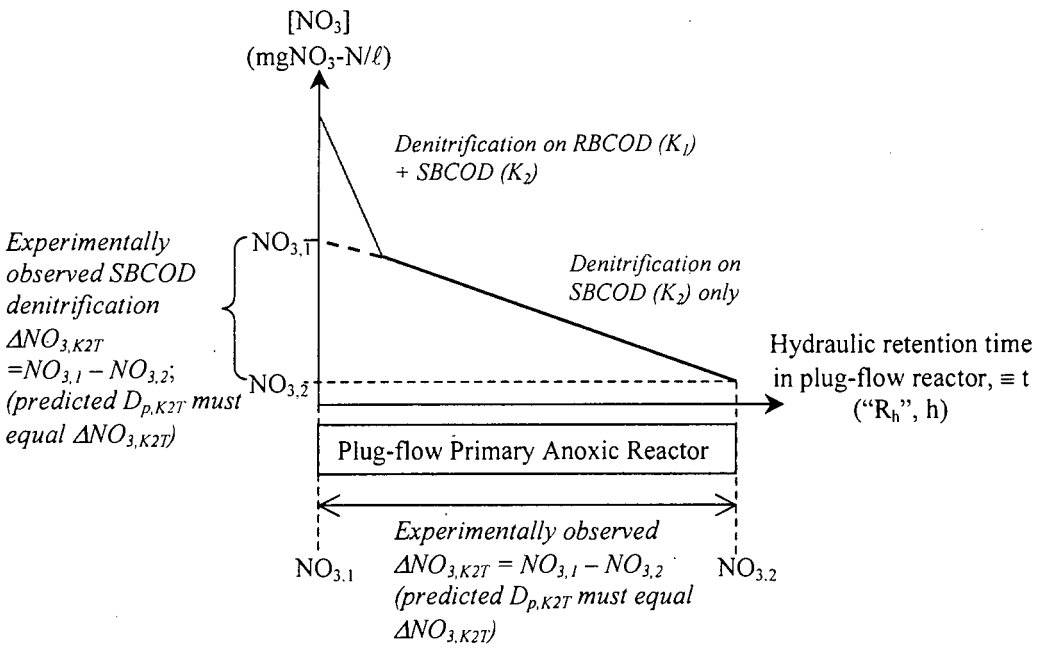

Fig. 6.1: Schematic of a typical denitrification profile resulting from SBCOD utilization, as observed experimentally in the plug-flow primary anoxic reactors by Marais and co-workers (van Haandel *et al.*, 1981; WRC, 1984).

The revised value for the specific denitrification rate constant with SBCOD as substrate, i.e. "$K_{2T,NO}$" in Eq.(6.6), can be determined by equating the corresponding SBCOD utilization terms "$D_{p,K2T}$" and "$D_{p,K2TNO}$" in Eqs.(6.1) and (6.6), respectively, (since the D_p is in effect experimentally observed and must remain constant) and solving for $K_{2T,NO}$:

$$D_{p,K2T} = (1-f_{us}-f_{up})*S_{ti}*K_{2T}*f_{x1}*Y_{H,AE}*R_s/(1+b_{HT}*R_s) \quad (6.9)$$

$$= D_{p,K2TNO}$$

$$= (1-f_{us}-f_{up})*S_{ti}*K_{2T,NO}*f_{x1}*\{f_{anox}*Y_{H,NO}*R_s/(1+b_{HT}*R_s)... \\ ...+ (1-f_{anox})*Y_{H,AE}*R_s/(1+b_{HT}*R_s)\} \quad (6.10)$$

By simplifying and rearranging:

$$K_{2T} * \frac{Y_{H,AE} * R_s}{(1 + b_{HT} * R_s)} = K_{2T,NO} * \left\{ f_{anox} * \frac{Y_{H,NO} * R_s}{(1 + b_{HT} * R_s)} + (1 - f_{anox}) * \frac{Y_{H,AE} * R_s}{(1 + b_{HT} * R_s)} \right\} \quad (6.11)$$

$$\Rightarrow K_{2T,NO} = \frac{K_{2T} * \frac{Y_{H,AE} * R_s}{(1 + b_{HT} * R_s)}}{\left\{ f_{anox} * \frac{Y_{H,NO} * R_s}{(1 + b_{HT} * R_s)} + (1 - f_{anox}) * \frac{Y_{H,AE} * R_s}{(1 + b_{HT} * R_s)} \right\}} \quad (6.12)$$

Therefore, for a given experimental nitrate concentration-time profile with known corresponding wastewater and system characteristics, $K_{2T,NO}$ can be determined by solving the three Eqs.(6.6), (6.8) and (6.12), i.e. D_{pp}, f_{anox} and $K_{2T,NO}$, simultaneously, provided $Y_{H,NO}$ and the corresponding $Y_{H,AE}$ are also known. On this basis, accepting the average $Y_{H,NO}$ = 81.3% with respect to the standard $Y_{H,AE}$ = 0.67 mgCOD/mgCOD (≡ 0.45 mgAVSS/mgCOD, see Chapter 1) determined in Chapter 5, and the experimental data (Table 6.1) of van Haandel *et al.* (1981) used to determine the original K_{2T}, the revised $K_{2T,NO}$ is estimated below.

Table 6.1: Summary of experimental data by van Haandel *et al.* (1981).

S_{ti}	= 600	mgCOD
f_{us}	= 0.05	mgCOD/mgCOD
f_{up}	= 0.13	mgCOD/mgCOD
f_{ts}	= 0.20	mgCOD/mgCOD
f_{bs}	= $f_{ts}/(1-f_{us}-f_{up})$ = 0.24	mgCOD/mgCOD
T	= 20	°C
b_{HT}	= $0.24*(1.029)^{T-20}$ = 0.24	1/d
K_{2T}	= $0.101*(1.08)^{T-20}$ = 0.101	mgN/mgAVSS/d
R_s	= 20	d
f_{xI}	= 0.25	mgAVSS/mgAVSS
f_{cv}	= 1.48	mgCOD/mgAVSS
$Y_{H,AE}$	= 0.45	mgAVSS/mgCOD
$Y_{H,NO}$	= $0.813*Y_{H,AE}$ = 0.366	mgAVSS/mgCOD

By simultaneous solution of Eqs.(6.6), (6.8) and (6.12) using a technique for convergence on f_{anox}, an estimated f_{anox} = 0.488 was determined for the experimental system of van Haandel *et al.* (1981), which gave corresponding $K_{2T,NO}$ = 0.111 mgN/mgAVSS/d (T = 20 °C) and $D_{pp} = D_{p,\alpha} + D_{p,K2TNO}$ = 19.24 + 19.24 = 38.5 mgN/ℓ influent removed, for the $Y_{H,NO}$ = 0.366 with respect to $Y_{H,AE}$ = 0.45 mgAVSS/mgCOD determined in this investigation (Chapter 5). As expected, the revised $K_{2T,NO}$ = 0.111 is greater than the K_{2T} = 0.1008 mgN/mgAVSS/d determined by van Haandel *et al.* (1981) based on a single OHO yield value – the reduced anoxic yield causes a reduced OHO active biomass concentration which causes the $K_{2T,NO}$ to increase [(Eq.(6.4)].

6.3 MODIFICATION OF THE STEADY-STATE DESIGN THEORY OHO ACTIVE BIOMASS

From the equations and discussions above, it is evident that the OHO active biomass concentration (X_a) also will change when taking into account a different cell yield coefficient for anoxic ($Y_{H,NO}$) growth as compared with aerobic ($Y_{H,AE}$) growth. In the current activated sludge design theory (WRC, 1984) which is based on a single OHO yield, the active mass equation is given by:

$$MX_a = (1 - f_{us} - f_{up}) * MS_{ti} * \frac{Y_H * R_s}{(1 + b_{HT} * R_s)} \quad (6.13)$$

where:

"M" denotes a mass quantity, and
a single $Y_H = Y_{H,NO} = Y_{H,AE}$ is accepted.

By defining f_{anox} as the fraction of total influent biodegradable substrate (S_{bi}) utilized anoxically, Eq.(6.13) can be modified to take into account a separate and different anoxic yield as follows:

$$MX_a = (1 - f_{us} - f_{up}) * MS_{ti} * \left\{ f_{anox} * \frac{Y_{H,NO} * R_s}{(1 + b_{HT} * R_s)} + (1 - f_{anox}) * \frac{Y_{H,AE} * R_s}{(1 + b_{HT} * R_s)} \right\} \quad (6.14)$$

where:

f_{anox} = the proportion of total biodegradable substrate utilized anoxically, (see earlier, Section 6.2).

The calculation procedure for the remaining activated sludge mixed liquor fractions, endogenous residue and inert material, as set out in the existing design theory (WRC, 1984), remain unmodified when a reduced OHO anoxic yield is introduced. However, since the OHO active biomass concentration and mass do change, the values for the endogenous residue concentration and mass will correspondingly change, since these two mixed liquor fractions are linked.

6.4 IMPACT OF MODIFIED THEORY

The modifications above, i.e. inclusion of a separate and different yield for anoxic growth, results in a significant change in the predicted performance of nitrogen removal activated sludge systems compared with the current steady-state theory. To illustrate this effect, design parameters for the model system described in Section 1.2, Chapter 1 (summarised in Table 6.2), are evaluated with the current design theory (WRC, 1984) and compared with their corresponding values determined by the modified theory, accepting the reduced anoxic yield determined in Chapter 5 and the revised $K_{2T,NO}$ rate above.

Table 6.2: Summary of the system parameters for the model system in Section 1.2, Chapter 1.

S_{ti}	= 750	mgCOD/ℓ
f_{us}	= 0.07	mgCOD/mgCOD
f_{up}	= 0.15	mgCOD/mgCOD
f_{bs}	= 0.25	mgCOD/mgCOD
N_c	= 40	mgN/ℓ
a	= 15	recycle ratio, a:Q_i
s	= 1	recycle ratio, s:Q_i
O_a	= 2	mgO/ℓ
O_s	= 1	mgO/ℓ
R_s	= 23	d
f_{x1}	= 0.35	mgVSS/mgVSS
f_{cv}	= 1.48	mgCOD/mgVSS

The corresponding values for system performances predicted with the current and modified steady-state design formulations (to account for reduced OHO yield under anoxic conditions, see Section 6.2) are summarised in Table 6.3 below.

Table 6.3: Comparison of design parameters for the model system described in Section 1.2, Chapter 1, (Table 6.2) evaluated with the current and modified steady-state design formulations.

	Existing Theory Single $Y_{H,NO}$ = $Y_{H,AE}$		**Modified Theory Separate $Y_{H,NO}$ = 0.813*$Y_{H,AE}$**		**Percentage Change**	
Temperature, °C	14	22	14	22	14	22
$Y_{H,AE}$, mgVSS/mgCOD	0.45	0.45	0.45	0.45		
$Y_{H,NO}$, mgVSS/mgCOD	0.45	0.45	0.366	0.366		
f_{anox}			0.503	0.627		
b_{HT}, 1/d	0.202	0.254	0.202	0.254		
K_{2T}, mgN/mgVSS/d	0.064	0.118	0.070	0.129		
α, mgN/ℓ influent	0.0292	0.0292	0.0401	0.0401		
$D_{p,\alpha}$, mgN/ℓ influent	17.1	17.1	23.4	23.4	37.3%	37.3%
$D_{p,K2T}$, mgN/ℓ influent	23.8	36.4	23.8	35.4	-0.2%	-2.8%
D_{pp}, mgN/ℓ influent	40.9	53.5	47.2	58.8	15.4%	10.0%
N_{ne}, mgN/ℓ	9.9	-2.6	3.6	-8.0	-63.5%	
MX_a, mgVSS	25720	21230	23300	18741	-9.4%	-11.7%
MX_V, mgVSS	91598	88006	86929	82607	-5.1%	-6.1%

As shown in Table 6.3, the modified theory predicts overall

- a 37% increase in the denitrification with RBCOD as substrate ($D_{p,\alpha}$); this increase is expected since the denitrification with RBCOD is essentially stoichiometric (see Section 6.2 above);
- a negligible change in denitrification with SBCOD as substrate ($D_{p,K2T}$), which confirms correct revision of the $K_{2T,NO}$ value;

- the two effects above combining to give a 10 – 15 % increase in system denitrification achievable (D_{pp});
- the increased denitrification potential above gives a 63% reduction (9.9 to 3.6 mgN/ℓ, T = 14 °C) in effluent nitrate concentration (N_{ne}); and
- a 5 – 6% reduction in the mass of volatile suspended solids (MX_V, mgVSS) formed.

The effect of a reduced OHO anoxic yield on the system VSS mass (MX_V, Table 6.3) is relatively small, at 5 – 6%. Thus, the influence on system volume requirements will be similarly small (WRC, 1984). This indicates that the most significant effect of the reduced yield is on the predicted N removal performance of an MLE-type system. This will have a significant impact on the system design, in selection of anoxic mass fractions and a-recycle ratios.

6.5 CLOSURE

In Chapter 5 it was shown experimentally that the cell yield coefficient for OHO growth under anoxic ($Y_{H,NO}$) conditions is reduced relative to its value under aerobic ($Y_{H,AE}$) conditions; on average, $Y_{H,NO}$ = 0.545, or 81.3%, with respect to the standard $Y_{H,AE}$ = 0.67 mgCOD/mgCOD (≡ 0.45 mgAVSS/mgCOD).

In this Chapter, the current steady-state activated sludge design theory (for nitrogen removal systems) has been modified to take into account the separate and different anoxic cell yield coefficient determined in Chapter 5. In particular, the currently accepted value (e.g. Marais and Ekama, 1976; Dold *et al.*, 1980 and 1991) for the specific denitrification rate for SBCOD utilization (K_{2T}), as determined by Marais and co-workers (Stern and Marais, 1974; van Haandel *et al.*, 1981; WRC, 1984), has been revised from K_{2T} = 0.1008 to $K_{2T,NO}$ = 0.111 mgN/mgAVSS/d for T = 20 °C. Further, the effect of the modified theory on current design predictions for a model nitrogen removal activated sludge system has been demonstrated.

CHAPTER 7

CONCLUSIONS AND RECOMMENDATIONS

7.1 INTRODUCTION

In the IWA Task Group (ASM1, ASM2 and ASM2d, see Chapter 1) and similar (e.g. Dold *et al.*, 1991; Wentzel *et al.*, 1992) activated sludge models, the value for the OHO yield is assumed to be the same under anoxic ($Y_{H,NO}$) as under aerobic ($Y_{H,AE}$) conditions. However, reduced energy capture with nitrate as electron acceptor (versus oxygen), implies that $Y_{H,NO}$ should be reduced relative to $Y_{H,AE}$. Based on bioenergetic and thermodynamic principles, it has been estimated theoretically (*Appendix A*) that $Y_{H,NO}$ is approximately 0.35 mgVSS/mgCOD (0.5 mgCOD/mgCOD), or 83%, with respect to the theoretical $Y_{H,AE}$ of 0.42 mgVSS/mgCOD (0.60 mgCOD/mgCOD). Although limited, experimental evidence in the literature supports this prediction, suggesting an average $Y_{H,NO}$:$Y_{H,AE}$ ratio of approximately 0.81 ± 0.035, or an average $Y_{H,NO}$ of 0.54 with respect to the conventionally accepted "standard" $Y_{H,AE}$ of 0.67 mgCOD/mgCOD. However, lacking in the current body of research on $Y_{H,NO}$, are any studies and experiments to directly quantify or measure $Y_{H,NO}$ using domestic sewage as substrate, and thus substantiate the above prediction.

The principal aim in this research was to investigate and quantify the ordinary heterotrophic organism (OHO) cell yield under anoxic conditions relative to its value under aerobic conditions for municipal sewage. In this regard, three main objectives were identified:

1. Determine the ratio $Y_{H,NO}$:$Y_{H,AE}$ for real sewage in terms of electron acceptor (i.e. nitrate and oxygen respectively) utilization.

2. Measure $Y_{H,NO}$ and $Y_{H,AE}$ directly for known concentration of readily biodegradable (RB)COD utilized.

3. Compare experimental results with other, independent studies on real sewage.

To achieve these objectives, it was recognised that the equations quantifying the concentration of soluble substrate utilized in aerobic and anoxic respiration, i.e. in terms of the cell yield and electron acceptor utilization, could be equated if the respective soluble substrate concentrations are the same. On this basis, an extensive experimental investigation was undertaken in which identical aerobic and anoxic batch tests were performed, containing the same concentration of readily biodegradable (RB)COD and acclimatised mixed-liquor from the same source. Accordingly, from the corresponding oxygen and nitrate utilized (OU and NU respectively) in the respective aerobic and anoxic batch tests, estimates for $Y_{H,NO}$ were determined as a function of $Y_{H,AE}$. Anoxic and aerobic batch tests were also performed containing known concentrations of the artificial RBCOD, acetate, so that

$Y_{H,NO}$ and $Y_{H,AE}$ could be determined directly from the respective NU and OU responses.

The experimental investigation used 25 (raw) sewage batches from the Mitchells Plain Wastewater Treatment Plant and included a total of 40 aerobic and 42 anoxic batch tests over a period of 395 days.

7.2 CONCLUSIONS

From this investigation, the following conclusions can be drawn:

- For Mitchells Plain raw wastewater, a weighted average $Y_{H,NO}$ of 0.534 ± 0.058 was determined with respect to the conventional standard $Y_{H,AE}$ of 0.67 mgCOD/mgCOD, which gives a corresponding $Y_{H,NO}$:$Y_{H,AE}$ ratio of 0.797 for Mitchells Plain raw wastewater. This value compares well with the theoretical ratio of $Y_{H,NO}$:$Y_{H,AE}$ = 0.83, as well as with the experimental average $Y_{H,NO}$:$Y_{H,AE}$ = 0.813 ± 0.035 calculated for the data in the literature (Chapter 2).

- Three previous investigations in the UCT laboratory with municipal wastewater were identified in which sufficient data were available to calculate $Y_{H,NO}$ values of 0.458 ± 0.168, 0.603 ± 0.05 and 0.538 ± 0.068 mgCOD/mgCOD, respectively. These data gave a weighted average $Y_{H,NO}$ = 0.519 ± 0.101 with respect to the standard $Y_{H,AE}$ = 0.67 mgCOD/mgCOD, giving a corresponding $Y_{H,NO}$:$Y_{H,AE}$ ratio of 0.775. Again these values compare reasonably favourably with both the theoretical and literature experimental values.

- Combining the estimations above for Mitchells Plain wastewater, a weighted average $Y_{H,NO}$ = 0.545 ± 0.039 with respect to $Y_{H,AE}$ = 0.67 mgCOD/mgCOD was obtained, which gives a corresponding $Y_{H,NO}$:$Y_{H,AE}$ ratio of 0.813. This latter value compares remarkably well with the theoretical ratio of 0.83 and the experimental average ratio of 0.813 calculated for the data in the literature.

- For the batch tests using the artificial RBCOD, acetate, averages of $Y_{H,NO}$ = 0.598 ± 0.041 and $Y_{H,AE}$ = 0.687 ± 0.027 mgCOD/mgCOD were determined, which correspond to a $Y_{H,NO}$:$Y_{H,AE}$ ratio of 0.87. The average $Y_{H,AE}$ = 0.687 is in good agreement with the conventionally accepted $Y_{H,AE}$ = 0.67 mgCOD/mgCOD, and substantiates its acceptance in this investigation also. However, the average $Y_{H,NO}$ of 0.598 is higher than the theoretically predicted 0.50 mgCOD/mgCOD (*Appendix A*), and the experimental average of 0.54 mgCOD/mgCOD calculated for the data in the literature (Chapter 2), as well as the $Y_{H,NO}$ = 0.545 determined for Mitchells Plain wastewater above. Correspondingly, the average ratio $Y_{H,NO}$:$Y_{H,AE}$ = 0.87 determined for acetate, is higher than that expected for domestic sewage. However, sequential anoxic then aerobic acetate additions in the same batch test gave $Y_{H,NO}$:$Y_{H,AE}$ = 0.84 ± 0.021; this is in close agreement with the values obtained above for municipal sewage, and with both the theoretical and literature experimental values.

- An apparent effect was observed on the fraction of unbiodegradable soluble COD (f_{us}) obtained in the long sludge age laboratory-scale activated sludge systems operated in this investigation. It appeared that the f_{us} was inversely influenced by the influent feed concentration; a lower f_{us} was obtained for a higher influent feed COD concentration in the laboratory systems (see Chapter 3). Other researchers in the UCT laboratory have similarly observed this effect (Lee, 2002). A consequence of this effect is the uncertainty it introduces into RBCOD measurement using physical techniques, e.g. the flocculation-filtration methods of Mamais *et al.* (1993) and Mbewe *et al.* (1995), see below.

- Comparison of the wastewater RBCOD fraction (f_{ts}) estimated by batch test respirometry (Ekama *et al.*, 1986), using the standard $Y_{H,AE}$ and the estimated average $Y_{H,NO}$, with the average steady-state value determined independently for each sewage batch, gave consistently low recoveries (≤40%). By comparing the COD concentrations of timed floc-filtered samples in aerobic batch tests with the OUR profile for the same test, it was demonstrated that all the biodegradable soluble COD present in the test was taken up at the same time the precipitous drop in OUR occurred. Since the steady-state f_{ts} averages were initially determined by flocculation-filtration using the f_{us} of a long sludge age UCT system, it was suspected that initial poor recoveries were due to the uncertainties in f_{us} determination, as discussed above. However, despite changing the RBCOD measurement method to the original (standard) square-wave fed continuous flow-through method described by Ekama *et al.* (1986), low recovery of RBCOD in the batch tests remained. It was suspected that this may be due to incorrect acceptance of the conventional standard value of $Y_{H,AE}$ = 0.67 mgCOD/mgCOD. However, aerobic batch tests conducted with known concentrations of acetate gave an average $Y_{H,AE}$ = 0.687 ± 0.027 mgCOD/mgCOD (see above), which is close to the standard value, so that continued acceptance of $Y_{H,AE}$ = 0.67 mgCOD/mgCOD was substantiated. Consequently, the low RBCOD recoveries observed in the batch tests remains unexplained. This is not significant to this investigation, however, since (as discussed in Chapter 3), the RBCOD concentrations in the corresponding aerobic and anoxic batch tests are not required for estimating $Y_{H,NO}$ in terms of known $Y_{H,AE}$, provided the concentrations are equal. It does, however, introduce inconsistency, and accordingly merits further investigation.

From the above, there is a remarkable consistency in the OHO yield data derived from a variety of sources. This provides substantive evidence that the OHO yield is reduced under anoxic conditions compared with aerobic conditions.

Accepting the average value determined for $Y_{H,NO}$ in this study, the steady-state design theory (WRC, 1984) was modified (see Chapter 6) to incorporate individual anoxic and aerobic yield coefficients in the equations for: (1) the OHO active biomass concentration (X_a), and (2) the total system denitrification potential (D_{pp}). The modified theory was applied to the experimental data of van Haandel *et al.* (1981), to revise the specific denitrification rate constant for slowly biodegradable (SB)COD (K_{2T}) to take into account the reduced $Y_{H,NO}$ with respect to $Y_{H,AE}$. By defining "f_{anox}" as the fraction of total biodegradable COD (S_{bi}) utilized anoxically, and recognising that the experimentally observed SBCOD denitrification profile must remain constant, the value of K_{2T} was changed from K_{2T} = 0.1008 mgN/mgAVSS/d

based on a single OHO yield constant (van Haandel *et al.*, 1981) to $K_{2T,NO}$ = 0.111 mgN/mgAVSS/d for the reduced OHO anoxic yield, both values at T = 20 °C.

The effect of an anoxic yield reduced relative to its aerobic value was examined by comparing the performance of a nitrogen (N) removal activated sludge system, predicted with the current (WRC, 1984) and modified (Chapter 6) steady-state theories (Chapter 6). This comparison indicated:

- a 37% increase in the denitrification with RBCOD as substrate ($D_{p,\alpha}$); this increase is expected since the denitrification with RBCOD is essentially stoichiometric (see Section 6.2 above);
- a negligible change in denitrification with SBCOD as substrate ($D_{p,K2T}$), which confirms correct revision of the $K_{2T,NO}$ value;
- the two effects above combining to give a 10 – 15 % increase in system denitrification achievable (D_{pp});
- the increased denitrification potential above gives a 63% reduction (9.9 to 3.6 mgN/ℓ, T = 14 °C) in effluent nitrate concentration (N_{ne}); and
- a 5 – 6% reduction in the mass of volatile suspended solids (MX_V, mgVSS) formed.

The concepts incorporated into the modified theory can be readily extended to biological nutrient removal (BNR) systems if required, although additional study will be required (see below).

7.3 RECOMMENDATIONS FOR FURTHER STUDY

Extension of the Modified Steady-State Theory to BNR Systems
As mentioned above, the steady-state theory modified for nitrogen removal activated sludge systems (Chapter 6), needs to be extended to biological nutrient removal (BNR) systems. In this regard, the following issues would need to be addressed:

(i) In extending the modified steady-state theory to BNR systems, due account must be taken of the increased K_{2T} observed for NDBEPR systems (Clayton *et al.*, 1991).

(ii) It would need to be assessed whether or not the $Y_{H,NO}$:$Y_{H,AE}$ ratio determined here remains the same for both the OHO and polyphosphate accumulating organism (PAO) biomasses in nitrification-denitrification biological excess phosphorus (P) removal (NDBEPR) systems.

Further Evaluation of Wastewater RBCOD Measurement
In measuring the RBCOD concentration in this investigation, a number of inconsistencies became apparent that require further investigation:

(i) The apparent inverse influence of the influent feed COD concentration on f_{us} determinations in laboratory-scale activated sludge systems

(ii) Further evaluation of the physical flocculation-filtration method in measuring wastewater RBCOD, as compared with the biological respirometric batch test and square-wave fed continuous flow-through methods.

(iii) Possible changes in the kinetic behaviour of activated sludge biomass taken from continuous flow-through systems (i.e. substrate limiting) and placed in batch test conditions (i.e. substrate saturation).

REFERENCES

Alcamo I.E. (1998). *Schaum's outline of theory and problems of microbiology.* McGraw-Hill, San Francisco, California.

Bailey J.E. and Ollis D.F. (1977). *Biochemical engineering fundamentals.* McGraw-Hill, San Francisco, California.

Barker P.S. and Dold P.L. (1997). General model for biological nutrient removal activated - sludge systems: Model presentation. *Water Environment Research* **69**(5), 969- 984.

Barker P.S. and Dold P.L. (1996). Sludge production and oxygen demand in nutrient removal activated sludge systems. *Water Sci. Technol.* **34**(5-6), 43-50.

Berthouex P.M. and Brown L.C. (1994). *Statistics for environmental engineers.* Lewis Publishers, New York.

Burke R.A, Dold P.L. and Marais G.v.R (1986). Biological excess phosporus removal in short sludge age activated sludge systems. *Res. Rept.* W58, Department of Civil Eng., University of Cape Town, Rondebosch 7700, South Africa.

Casey T.G. (1993). Causes and control of low F/M bulking in long sludge age nutrient removal activated sludge systems. Ph.D. Thesis, Dept. Civil Engineering, University of Cape Town, South Africa.

Casey T.G., Wentzel M.C. and Ekama G.A. (1999). Filamentous organism bulking in nutrient removal activated sludge systems. Paper 10: Metabolic behaviour of heterotrophic facultative aerobic organisms under aerated/unaerated conditions. *Water SA* **25**(4), 425-442.

Choi E. and Daehwan R. (2001). NUR and OUR relationship in BNR processes with sewage at different temperatures and its design application. *Water Research* **35**(7), 1748-1756.

Clayton J.A., Ekama G.A., Wentzel M.C. and Marais G.v.R. (1989). Denitrification kinetics in biological nitrogen and phosphorus removal activated sludge systems. *Res. Rept.* W63, Department of Civil Eng., University of Cape Town, Rondebosch 7700, South Africa.

Clayton J.A., Ekama G.A., Wentzel M.C. and Marais G.v.R. (1991). Denitrification kinetics in biological nitrogen and phosphorus removal activated sludge systems treating municipal wastewaters. *Water Sci. Technol.* **23**, 1025-1035.

Copp J.B. and Dold P.L. (1998). Comparing sludge production under aerobic and anoxic conditions. *Water Sci. Technol.* **38**(1), 285-294.

Davis M.L. and Cornwell D.A. (1985). *Introduction to environmental engineering.* PWS Publishers, Statler Building, 20 Park Plaza, Boston, Massachusetts 02116, USA.

Dold P.L., Ekama G.A. and Marais G.v.R. (1980). A general model for the activated sludge process. *Prog. Wat. Tech.* **12**(Tor), 47-77.

Dold P.L., Wentzel M.C., Billing A.E., Ekama G.A. and Marais G.v.R (1991). *Activated sludge simulation programs: Nitrification and nitrification/denitrification systems (Version 1.0).* Water Research Commission, P O Box 824, Pretoria 0001, South Africa. TT 52/91, ISBN 0 947447 19 9.

Ekama G.A., Dold P.L. and Marais G.v.R. (1986). Procedures for determining influent COD fractions and the maximum specific growth rate of heterotrophs in activated sludge systems. *Water Sci. Technol.* **18**(6), 91-114.

Ekama G.A. and Marais G.v.R. (1978). The dynamic behaviour of the activated sludge process. *Res. Rept.* W27, Department of Civil Eng., University of Cape Town, Rondebosch 7700, South Africa.

Ekama G.A. and Marais G.v.R. (1984a). Preliminary investigation for the optimization of the Cape Flats Sewage Purification Works. *Res. Rept.* W50, Department of Civil Eng., University of Cape Town, Rondebosch 7700, South Africa.

Ekama G.A. and Marais G.v.R. (1984b). Two improved sludge settleability parameters. IMIESA, **9**(6), 20.

Ekama G.A., Wentzel M.C., Casey T.G. and Marais G.v.R. (1996). Filamentous organism bulking in nutrient removal activated sludge systems Paper 3 - Stimulation of the selector effect under anoxic conditions. *Water SA* **22**(2), 119-126.

Envirosim (2001) *BIOWIN 32 Process Simulator.* 7 Innovation Drive, Suite 205, Flamborough, Ontario, L9H 7H9, Canada.

Gujer W., Henze M., Mino T. and Van Loosdrecht M.C.M (1999). Activated sludge Model No. 3. *Water Sci. Technol.* **39**(1), 183-193.

Henze M. (1991). Capabilities of biological nitrogen removal processes from wastewater. *Water Sci. Technol.* **23**.

Henze M. (1992). Characterization of wastewater for modelling of activated sludge processes. *Water Sci. Technol.* **25**(6), 1-15.

Henze M., Grady C.P.L. (Jr), Gujer W., Marais G.v.R. and Matsuo T. (1987). *Activated Sludge Model No. 1.* IAWPRC Scientific and Technical Report No. 1, IAWPRC, London.

Henze M., Gujer W., Mino T., Matsuo T., Wentzel M.C. and Marais G.v.R. (1995). *Activated sludge model No.2.* IAWQ Scientific and Technical Report No 3, IAWQ, London.

Henze M., Gujer W., Mino T., Matsuo T., Wentzel M.C., Marais G.v.R. and Van Loosdrecht M.C.M. (1999). Activated sludge model no. 2d. *Water Sci. Technol.* **39**(1), 165-182.

Henze M., Gujer W., Mino T. and Van Loosdrecht M.C.M. (2000). *Activated sludge models ASM1, ASM2, ASM2d and ASM3.* IWA Scientific and Technical Report No 9, IWA, London.

Hu Z., Wentzel M.C. and Ekama G.A. (2002). The significance of denitrifying polyphosphate accumulating organisms in biological nutrient removal activated sludge systems. *Water Sci. Technol.* **46**(1-2), 129-138.

Hu Z., Wentzel M.C. and Ekama G.A. (2000). External nitrification in biological nutrient removal activated sludge systems. *Water SA.* **26**(2), 225-238.

Isaacs S.H. and Henze M. (1995). Controlled carbon source addition to an alternating nitrification-denitrification wastewater treatment process including biological P removal. *Water Sci. Technol.* **29**(1), 77-89.

James D.C. and Matthews G.S. (1991). *Understanding the biochemistry of respiration.* Cambridge University Press, London.

Kappeler J. and Gujer W. (1992). Estimation of kinetic parameters of heterotrophic biomass under aerobic conditions and characterization of wastewater for activated sludge modelling. *Water Sci. Technol.* **25**(6), ???-?39.

Ketley D.A., Casey T.G., Ekama G.A., Wentzel M.C. and Marais G.v.R. (1991). The effect of fully anoxic conditions and frequency of exposure to anoxic and aerobic conditions on the growth of low F/M filaments in nitrogen removal systems. *Res. Rept.* W68, Department of Civil Eng., University of Cape Town, Rondebosch 7700, South Africa.

Koch G., Kühni M., Gujer W. and Siegrist H. (2000). Calibration and validation of Activated Sludge Model No.3 for Swiss municipal wastewater. *Water Research* **34**(14), 3580-3590.

Kristensen G.H., Jørgensen P.E. and Henze M. (1992). Characterization of functional microorganism groups and substrate in activated sludge and wastewater by AUR, NUR and OUR. *Wat. Sci. Technol.* **25**(6), 43-57.

Kuba T., Smolders G.J.F., van Loosdrecht M.C.M. and Heinen J.J. (1993). Biological phosphorus removal from wastewater by anaerobic-anoxic sequencing batch reactor. *Water Sci. Technol.* **27**(5/6), 241-252.

Kuchel P.W. and Ralston G.B. (1998). *Schaum's outline of theory and problems of biochemistry.* McGraw-Hill, San Francisco, California.

Kujawa K. and Klapwijk B. (1999). A method to estimate denitrification potential for predinitrification systems using NUR batch test. *Water Research* **33**(10), 2291-2300.

Lawrence A.W. and McCarty P.L. (1970). Unified basis for biological treatment design and operation. *J. Sanit Eng Div. ASCE* **96**(SA3), 757-778.

Lee B.J. (2002). Batch test for measurement of ordinary heterotrophic organism active biomass in activated sludge mixed liquor. MSc(Eng) Thesis, Dept. Civil Engineering, University of Cape Town, South Africa.

Lehninger A.L. (1973). *Bioenergetics.* Newman/Cummings Publishing Company, Reading, Massachusetts.

Levenspiel O. (1972). *Chemical reaction engineering.* 2nd. Ed., John Wiley and Sons Inc., New York.

Mamais D., Jenkins D. and Pitt P. (1993). A rapid physical-chemical methods for the determination of readily biodegradable soluble COD in municipal wastewater. *Water Research* **27**(1), 195-197.

Marais G.v.R. and Ekama G.A. (1976). The activated sludge process Part 1 – Steady state behaviour. *Water SA* **2**(4), 163-200.

Massidda D. (1991). An investigation into the utilization of slowly biodegradable organic material in activated sludge systems. *Res. Rept.*, Department of Civil Engineering, University of Cape Town, Rondebosch 7700, South Africa.

Maurer M. and Gujer W. (1994). Prediction of the performance of enhanced biological phosphorus removal plants. *Wat. Sci. Technol.* **30**(6), 333-344.

Mbewe A, Wentzel MC and Ekama GA (1995). Characterization of the carbonaceous materials in municipal wastewaters. *Res. Rept.* W84, Department of Civil Engineering, University of Cape Town, Rondebosch 7700, South Africa.

McCarty P.L. (1971). Energetics and bacterial growth. In: *Organic compounds in aquatic enviroments*. Eds Faust SD and Hunter JV, Marcell Dekker, New York, NY, USA.

McCarty PL (1972). Energetics of organic matter degradation. In: *Water pollution microbiology*. Ed Mitchell R, Wiley & Sons, New York, NY, USA.

McCarty P.L. (1975). Stoichiometry of biological reactions. *Prog. Wat. Tech.*7(1), 157-172.

McClintock S.A., Sherrard J.H., Novak J.T. and Randall C.W. (1988). Nitrate versus oxygen respiration in the activated sludge process. *Journal WPCF* **60**(3), 342-350.

Moser-Engeler R., Udert K.M., Wild D. and Siegrist H. (1998). Products from primary sludge fermentation and their suitability for nutrient removal. *Water Sci. Technol.* **38**(1), 265-273.

Muller A., Wentzel M., Loewenthal R. and Ekama G. (2002). Heterotroph anoxic yield in anoxic aerobic activated sludge systems treating municipal wastewater. *Water Sci. Technol.* **38**(1), 265-273.

Murnleitner E., Kuba T., van Loosdrecht M.C.M. and Heinen J.J. (1997). An integrated metabolic model for aerobic and denitrifying biological phosphorus removal. *Biotech & Bioeng* **54**(5), 434-450.

Naidoo V. and Buckley C.A. (2000). WRC Report No. 820/1/00. *Municipal wastewater characterization: Application of denitrification batch tests.* Published by the Water Research Commission, PO Box 824, Pretoria 0001, South Africa.

Nebergall W.H., Holtzclaw H.F.Jr. and Robinson W.R. (1998). *College chemistry with qualitative analysis.* D.C. Heath and Company, Lexington, Massachusetts.

Orhon D., Hanhan O., Görgün E. and Sözen S. (1998). A unified basis for the design of nitrogen removal activated sludge process – The Braunschweig exercise. *Water Sci. Technol.* **38**(1), 227-236.

Orhon D., Sözen S. and Artan N. (1996). The effect of heterotrophic yield on the assessment of the correction factor for anoxic growth. *Water Sci. Technol.* **34** (5-6), 67-74.

Payne W.J. (1981). *Denitrification.* John Wiley and Sons, New York.

Pilson R.A., Ekama G.A., Wentzel M.C. and Casey T.G. (1995). The effect of temperature on denitrification kinetics and biological excess phosphorus removal in nutrient removal activated sludge systems in temperate climates (12 – 20 °C).

Res. Rept. W86, Department of Civil Engineering, University of Cape Town, Rondebosch 7700, South Africa.

Randall EW, Wilkinson A and Ekama GA (1991). An instrument for the direct determination of oxygen utilization rate. *Wat. SA.*, **17** (1), 11-18.

Riggs J.B. (1994). *An introduction to numerical methods for chemical engineers.* 2nd Ed., Texas Tech University Press, Lubbock, Texas 79409-1037, U.S.A. ISBN 0-89672-334-8

Shuler M.L. and Kargi F. (1992). *Bioprocess engineering – basic concepts.* Prentice Hall, Englewood Cliffs, New Jersey 07632.

Siegrist H., Brunner I., Koch G., Linh Con Phan and Van Chieu L.E. (1999). Reduction of biomass decay rate under anoxic and anaerobic conditions. *Water Sci. Technol.* **39**(1), 129-137.

Sneyders M.J., Wentzel M.C. and Ekama G.A. (1998). The effect of dosing unstabilized landfill leachate to a nutrient removal activated sludge sysytem. *Res. Rept.* W95, Department of Civil Engineering, University of Cape Town, Rondebosch 7700, South Africa.

Sollfrank U. and Gujer W. (1991). Characterisation of domestic wastewater for mathematical modelling of the activated sludge process. *Water Sci. Technol.* **23**, 1057-1066.

Sötemann S. (2000). External nitrification in biological nutrient removal activated sludge systems. MSc(Eng) Thesis, Dept. Civil Engineering, University of Cape Town, South Africa.

Sözen S., Ubay Çokgör E., Orhon D. and Henze M. (1998). Respirometric analysis of activated sludge behaviour - II. Heterotrophic growth under aerobic and anoxic conditions. *Water Research* **32**(2), 476-488.

Sperandio M., Urbain V., Audic J-M. and Paul E. (1999). Use of carbon dioxide evolution rate for denitrifying heterotrophic yield and characterizing denitrifying biomass. *Water Sci. Technol.* **39**(1), 139-146.

Standard Methods (1985). *Standard Methods for the examination of water and wastewater* (16th end.) American Public Health Assoc., 1015 15th Str. NW, Washington DC 200005, USA.

Stern L.B. and Marais G.v.R. (1974). Sewage as electron donor in biological denitrification. *Res. Rept.* W7, Department of Civil Eng., University of Cape Town, Rondebosch 7700, South Africa.

Still D.A., Blackbeard J.R., Ekama G.A. and Marais G.v.R. (1986). The effect of feeding patterns on sludge growth rate and sludge settleability. *Interim Report*, to the WRC steering committee for research on sludge bulking and foaming in the activated sludge process (K5/165), Department of Civil Engineering, University of Cape Town, Rondebosch 7700, South Africa.

Swokowski E.W. (1984). *Calculus, with analytic geometry.* Prindle, Weber and Schmidt Publishers, 20 Statler Office Building, Boston, Massachusetts, 02116, USA.

Tchobanoglous G. and Schroeder E. (1987). *Water Quality.* Addison-Wesley Publishing Company, Reading, Massachusetts, USA.

Ubay Çokgör E., Sözen S., Orhon D. and Henze M. (1998). Respirometric analysis of activated sludge behaviour - I. Assessment of the readily biodegradable substrate. *Water Research* **32**(2), 461-475.

Ubisi MF, Wentzel MC and Ekama GA (1997a). Activated sludge mixed liquor heterotrophic active biomass. *Wat. SA.*, **23** (3), 239-248.

Ubisi MF, Wentzel MC and Ekama GA (1997b). Organic and inorganic components of activated sludge mixed liquor. *Res. Rept. W94*, Department of Civil Engineering, University of Cape Town, Rondebosch 7700, South Africa.

Underhill L. and Bradfield D. (1996). 2nd Ed., *IntroSTAT.* Juta and Co. Ltd, PO Box 14373, Kenwyn, 7790 South Africa.

Van Haandel A.C., Ekama G.A. and Marais G.v.R. (1981). The activated sludge process 3 - Single sludge denitrification. *Water Research* **15**(10), 1135-1152.

Van Niekerk A.M. (2000). Technological perspectives on the new South African effluent (waste) discharge standards. Presented at the Water Institute of Southern Africa (WISA) 2000 Biennial Conference, Sun City, South Africa, 28 May – 1 June 2000.

Vermande S.M., Sötemann S, Soriano G.A., Wentzel M.C., Audic J.M. and Ekama G.A. (2002). Comparison of aerobic and anoxic phosphorus uptake in NDBEPR systems (UCT and ENBRAS). *Water Sci. Technol.* **46**(4-5), 201-207.

Wentzel M.C., Ekama G.A., Loewenthal R.E. and Marais G.v.R. (2001). Unpublished draft. Chapter 1: Fundamentals of Biological Behaviour. In: *Theory, Design and Operation of Nutrient Removal Activated Sludge Processes.* 2nd Edition. Published by Water Research Commission, PO Box 824, Pretoria 0001, South Africa.

Wentzel M.C., Ekama G.A. and Marais G.v.R. (1992). Processes and modelling of nitrification denitrification biological excess phosphorus removal systems – A review. *Water Sci. Technol.* **25**(6), 59-82.

Wentzel M.C., Ekama G.A., Dold P.L. and Marais G.v.R (1990). Biological excess phosphorus removal – Steady state process design. *Wat. SA.*, **16**(1), 29-53.

Wentzel M.C., Mbewe A. and Ekama GA (1995). Batch test for measurement of readily biodegradable COD and active organism concentrations in municipal wastewaters. *Wat. SA.*, **21**(2), 117-124.

Wentzel M.C., Mbewe A., Lakay M.T. and Ekama GA (1999). Batch test for characterisation of carbonaceous materials in municipal wastewaters. *Wat. SA.*, **25**(3), 327-335.

Wilson D.E. (1976). The adsorption phase in biological denitrification. MSc(Eng) Thesis, Dept. Civil Engineering, University of Cape Town, South Africa.

WRC (1984). *Theory, Design and Operation of Nutrient Removal Activated Sludge Processes.* Water Research Commission, P O Box 824, Pretoria, RSA.

APPENDIX A

THEORETICAL ESTIMATION OF HETEROTROPHIC CELL YIELD COEFFICIENT (Y_H)

APPENDIX A

THEORETICAL ESTIMATE OF THE HETEROTROPHIC CELL YIELD

The following theoretical estimates for the ordinary heterotrophic organism (OHO) aerobic and anoxic cell yields are developed from procedures detailed in postgraduate lecture notes (CIV508G, 2001) *"Bioenergetics"* and *"Chapter One: Fundamentals of Biological Behaviour"*, by Wentzel *et al.* (2001).

A.1 ANABOLISM (SYNTHESIS OF NEW CELL PROTOPLASM)

Although the formation of new cell mass (anabolism) follows a wide variety of complex pathways (Lehninger, 1973; WRC, 1984; James and Matthews, 1991; Casey, 1993), anabolism can be simplified to occur in two steps:

(1) Formation of protoplasm from CO_2, NH_3 and electrons (and protons)

(2) Oxidation of substrate to supply CO_2 and electrons (and protons) for step 1.

Step 1: Formation of protoplasm from CO_2, NH_3, e^-, H^+

Accepting the approximate molecular composition of cell protoplasm as $C_5H_7O_2N$, (Hoover and Porges 1952, as referenced in WRC 1984), with corresponding molecular weight 113 g/mol (i.e. 53% C, 28% O, 12% N and 6% H; 1% P omitted), then new cell mass is synthesized according to the following stoichiometry:

$$5CO_2 + NH_3 + 20e^- + 20H^+ \rightarrow C_5H_7O_2N + 8H_2O \quad (A.1)$$

(i.e. 1 mol $C_5H_7O_2N$ requires $20e^-$ and $20H^+$ which are supplied by NAD_{red})

$$\text{i.e. } 5CO_2 + NH_3 + (20/2)NAD_{red} \rightarrow C_5H_7O_2N + 8H_2O + (20/2)NAD_{ox} \quad (A.2)$$

(Note: only $10NAD_{red}$ required because 1 NAD_{ox} accepts $2e^- + 2H^+$ to form 1 NAD_{ox})

The above equations (A.1 and A.2) are not intended to suggest that OHO's use CO_2 as a carbon source for anabolism, but rather CO_2, H^+ and e^- represent the datum from which the bioenergetic calculations are made.

Step 2: Oxidation of substrate (e.g. glucose) to provide CO_2, NH_3, e^-, H^+

$$\textit{Oxidation:} \quad C_6H_{12}O_6 + 6H_2O \rightarrow 6CO_2 + 24H^+ + 24e^- \quad (A.3)$$

$$\textit{Reduction:} \quad 24H^+ + 24e^- + 12NAD_{ox} \rightarrow 12NAD_{red} \quad (A.4)$$

$$\textit{Overall:} \quad C_6H_{12}O_6 + 6H_2O + 12NAD_{ox} \rightarrow 6CO_2 + 12NAD_{red} \quad (A.5)$$

$\Rightarrow$ the amount of glucose required to synthesize 1 mol $C_5H_7O_2N$,
= (10 NAD_{red} required/mol protoplasm synthesized)/(12 NAD_{red}/mol glucose)
= 0.83 (moles of glucose)/(mol protoplasm synthesized) required for anabolism

(i.e., 0.83 mol glucose is required to supply the e^-, H^+ and CO_2 for the synthesis of 1 mol new cell mass).

However, the anabolism reaction (A.1) requires energy. Therefore, noting the following standard Gibbs free energies of formation (ΔG_f°):

$$\Delta G_f^\circ(C_5H_7O_2N) \approx +40.6 \text{ kcal/mol}, \text{ and} \quad (A.6)$$

$$\Delta G_f^\circ(NAD_{red} - NAD_{ox}) \approx -5.0 \text{ kcal/mol} \quad (A.7)$$

$\Rightarrow$ the free energy required for the synthesis reaction (A.1) can be calculated as follows:

$$\Delta G_R^\circ = \Delta G_f^\circ(\text{products}) - \Delta G_f^\circ(\text{reactants})$$

$$= \Delta G_f^\circ(C_5H_7O_2N) + \Delta G_f^\circ(H_2O) * 8 - \Delta G_f^\circ(CO_2) * 5 - \Delta G_f^\circ(NAD_{red} - NAD_{ox}) * 10 - \Delta G_f^\circ(NH_3)$$

$$= +40.6 + (-57) * 8 - (-94) * 5 - (-5) * 10 - (-6)$$

$$= +110.6 \text{ kcal/mol} \quad \textit{(Note : + sign indicates energy is required)}$$

But energy transfer is not 100% efficient; therefore, accepting that it is only 55% efficient as in catabolism (Wentzel *et al.* 2001), the energy required for synthesis of protoplasm (anabolism, reaction A.1) is 110.6/0.55 = 201 kcal/mol protoplasm, which is supplied by catabolic reactions.

A.2 CATABOLISM (GENERATION OF ENERGY FOR ANABOLISM)

Catabolism supplies the energy requirements for anabolism via NAD_{ox}-NAD_{red}-ADP-ATP exchanges in a complex series of biologically mediated, coupled redox reactions[1]. Accepting that each ATP molecule has an available free energy of ~10 kcal/mol ATP, $\Rightarrow$ 201/10 = 20.1 mol ATP/mol protoplasm needs to be generated in catabolism to supply the required energy (201 kcal/mol protoplasm synthesized) for anabolism.

Considering the electron equivalence (e^- eq.) of oxygen (A.9 below), i.e. 4 mol of e^- consumed (accepted) per mol of oxygen utilized, and noting that ideally 3 mol ATP are formed/pair of e^- passed to oxygen (Wentzel *et al.* 2001), $\Rightarrow$ (20.1 mol ATP required)/(3 mol ATP formed/2 e^- accepted) = 13.4 e^- eq. are required from the substrate. Now, recalling that oxidation of 1 mol of glucose provides 24 e^- eq. (A.3), this means that (13.4 e^- eq. required)/(24 e^- eq./mol glucose) = 0.56 mol of glucose are required to be oxidised to supply the necessary energy (e^- eq.) for the synthesis of 1 mol protoplasm. Therefore, the total energy required to synthesize 1 mol of protoplasm ($C_5H_7O_2N$) is:

Anabolism	20	e^- eq.
Catabolism	13.4	e^- eq.
Total Energy Required	33.4	e^- eq.

[1] For detailed description of synthesis pathways, see any or all of Lehninger, 1973; WRC, 1984; James and Matthews, 1991; Shuler and Kargi, 1992; Alcamo, 1998; Kuchel and Ralston, 1998; Wentzel *et al.*, 2001.

A.3 HETEROTROPHIC YIELD (AEROBIC)

The heterotrophic cell yield can be defined in several ways to relate the mass of new cell protoplasm formed per mass of substrate oxidised, i.e.:

$$Y = \frac{\text{mass of protoplasm formed}}{\text{mass of substrate oxidised}} \qquad \text{(A.8)}$$

and can be expressed equally as:

- mol protoplasm/mol substrate
- mass (g) protoplasm/mass (g) substrate
- mass (g) protoplasm/e^- eq. of substrate
- mass (g) protoplasm/e^- eq. of oxygen

The latter definition, based on the e- eq. of oxygen, is the most useful because it can be related directly to the COD measure of a substance (see WRC 1984); i.e.:

$$4e^- + 4H^+ + O_2 \rightarrow 2H_2O \qquad \text{(A.9)}$$

$\Rightarrow 4e^-$ eq. $\equiv$ 1 mol oxygen $\equiv$ 32g oxygen

$\Rightarrow 1e^-$ eq. $\equiv$ 8g oxygen $\equiv$ *8g $COD_{(Theoretical)}$*

Consider, for example, oxidation of substrates acetate (CH_3COOH) and glucose ($C_6H_{12}O_6$):

Acetate

$CH_3COOH + 2H_2O \rightarrow 2CO_2 + 8H^+ + 8e^-$

i.e. 1 mol acetate $\rightarrow$ 8 e^- eq.

but recall, 33.4 e^- eq. are required to synthesize 1 mol protoplasm,

$\Rightarrow$ 33.4/8 = 4.17 mol acetate required to synthesize 1 mol protoplasm.

Now, from the molecular weight of protoplasm ($C_5H_7O_2N$), 113 g/mol, the theoretical specific organism yield is:

$\Rightarrow Y = 1/4.17 = 0.24$ mol protoplasm/mol acetate

$\equiv 113/4.17 = 27.1$ g protoplasm/mol acetate

Glucose, similarly:

$C_6H_{12}O_6 + 6H_2O \rightarrow 6CO_2 + 24H^+ + 24e^-$

i.e. 1 mol glucose $\rightarrow$ 24 e^- eq.

but recall, 33.4 e^- eq. are required to synthesize 1 mol protoplasm,

$\Rightarrow$ 33.4/24 = 1.39 mol glucose required to synthesize 1 mol protoplasm.

$\Rightarrow Y = 1/1.39 = 0.72$ mol protoplasm/mol glucose

$\equiv 113/1.39 = 81.3$ g protoplasm/mol glucose

However, since all the constituents of protoplasm ($C_5H_7O_2N$) are organic, its volatile solids mass (VSS) is the same as its molecular weight, i.e. 113 gVSS/mol. Also, because organisms respond to the available free energy (e^- eq.) rather than the type of substrate, it is better to express the cell yield (gVSS) in terms of e^- eq., or equivalently, in terms of COD via the electron equivalence of oxygen, i.e. as "Y_H". On this basis, the theoretical specific organism yield in terms of VSS/COD is:

$$
\begin{aligned}
Y_H &= (113 \text{ g/mol protoplasm})/(33.4 \text{ e}^- \text{ eq. required/mol protoplasm}) \\
&\equiv 3.38 \text{ gVSS/e}^- \text{ eq.} \\
&\equiv (3.38 \text{ gVSS/e}^- \text{ eq.})/(8 \text{ gO/e}^- \text{ eq.}) \\
&= 0.42 \text{ gVSS/gTh.COD} \qquad \text{(A.10)}
\end{aligned}
$$

A.4. HETEROTROPHIC YIELD (ANOXIC)

When nitrate serves as terminal electron acceptor, approximately the same amount of free energy is available (94%) to the organisms as with oxygen (WRC 1984); however, ideally only 2 mol ATP are formed per pair of electrons transferred as compared to 3 with oxygen. Therefore, with nitrate, the catabolic e^- eq. requirement from the substrate is increased from 13.4 e^- eq. with oxygen to = (20.1 ATP required)/(2 ATP formed/2 e^- transferred) = 20.1 e^- eq. required with nitrate. Therefore, since the anabolic energy requirement remains the same, the total energy required to synthesize 1 mol of protoplasm ($C_5H_7O_2N$) with nitrate as electron acceptor is increased to 40.1 e^- eq. as compared to 33.4 with oxygen:

Anabolism	20	e^- eq.
Catabolism	20.1	e^- eq.
Total Energy Required	40.1	e^- eq.

Now, similarly considering the substrates acetate and glucose, $\Rightarrow$ 40.1/8 = 5.0 mol acetate, and 40.1/24 = 1.67 mol glucose are required to synthesize 1 mol of protoplasm with nitrate as electron acceptor, respectively. Correspondingly:

Acetate

$\Rightarrow Y_{H,NO}$ = 1/5 = 0.2 mol protoplasm/mol acetate

$\equiv$ 113/5 = 22.6 g protoplasm/mol acetate

Glucose

$\Rightarrow Y_{H,NO}$ = 1/1.67 = 0.60 mol protoplasm/mol glucose

$\equiv$ 113/1.67 = 67.7 g protoplasm/mol glucose

Therefore, on an e^- eq. basis in terms of oxygen demand and VSS mass units, the theoretical specific organism yield with nitrate as terminal electron acceptor is:

$$
\begin{aligned}
Y_{H,NO} &= (113 \text{ g/mol protoplasm})/(40.1 \text{ e}^- \text{ eq. required/mol protoplasm}) \\
&\equiv 2.82 \text{ gVSS/e}^- \text{ eq.} \\
&\equiv (2.82 \text{ gVSS/e}^- \text{ eq.})/(8 \text{ gO/e}^- \text{ eq.}) \\
&= 0.35 \text{ gVSS/gTh.COD} \qquad \text{(A.11)}
\end{aligned}
$$

On this basis, the theoretical anoxic:aerobic yield ratio = 0.35/0.42 = 0.833 (see later).

A.5 THEORETICAL COD VALUE OF CELL PROTOPLASM

From WRC 1984, if a completely soluble biodegradable substrate (e.g. glucose) is inoculated with bacteria, synthesis of new bacterial mass will occur. Conservation of

electrons (e^- eq.) requires that the decrease in soluble COD (ΔCOD_{sol}) of the medium must be reflected in a corresponding increase in the COD of the bacterial mass ($\Delta COD_{bacteria}$) and the oxygen utilized ($\Delta O_{2,utilized}$) for generating the free energy required for anabolism; i.e.:

$$(\Delta COD_{sol}) = (\Delta COD_{bacteria}) + (\Delta O_{2,utilized}) \tag{A.12}$$

From extensive bacteriological work reviewed by Payne (1971), as referenced in WRC 1984, the fraction ΔCOD_{sol} appearing as $\Delta COD_{bacteria}$ is approximately constant. Typically expressed as a ratio, this fraction defines the specific cell yield coefficient (A.8) in terms of COD, i.e. "Y_{COD}" or "Y_Z":

$$Y_{COD} = \frac{\Delta COD_{sol}}{\Delta COD_{bacteria}} \tag{A.13}$$

Combining A.12 and A.13, and rewriting in terms of oxygen utilized (OU, $\Delta O_{2,utilized}$),

$$\Rightarrow \Delta O_{2,utilized} = (1 - Y_{COD})*\Delta COD_{sol} \tag{A.14}$$

However, the change in bacterial mass generated per substrate consumed in the synthesis reaction is traditionally expressed in terms of volatile solids units (VSS), i.e. as Y_H; therefore, to use A.14 with VSS units a conversion factor is required between Y_{COD} and Y_H. It has become common to express the relationship between new cell mass synthesized in VSS units (i.e. ΔX_H) and in COD units (i.e. $\Delta COD_{bacteria}$) as the ratio of the two parameters, f_{cv}:

$$f_{cv} = \frac{\Delta COD_{bacteria}}{\Delta X_H} \equiv \frac{COD}{VSS} \tag{A.15}$$

$$\Rightarrow Y_{COD} \equiv Y_Z = f_{cv}*Y_H \tag{A.16}$$

On this basis, A.14 is rewritten as:

$$\Rightarrow \Delta O_{2,utilized} = (1 - f_{cv}*Y_H)*\Delta COD_{sol} \tag{A.17}$$

Now, accepting the empirical molecular composition of cell protoplasm as $C_5H_7O_2N$, the theoretical value of f_{cv} can be estimated from the oxidation reaction:

$$C_5H_7O_2N + 5O_2 \rightarrow 5CO_2 + 2H_2O + NH_3 \tag{A.18}$$

$$\Rightarrow 113\ gVSS \rightarrow 160\ gO \equiv 160\ gCOD$$
$$\text{i.e., } 1\ gVSS \rightarrow 1.42\ gCOD$$
$$\therefore f_{cv} = 1.42\ mgVSS/mgCOD \tag{A.19}$$

A.6 SUMMARY

In summary, therefore, the theoretical estimates of aerobic and anoxic cell yields are, respectively:

$$\begin{aligned} Y_H &= 0.42 \text{ mgVSS/mgCOD} \\ &\equiv 0.42*1.42 \text{ mgCOD/mgCOD} \\ &\equiv Y_Z = 0.60 \text{ mgCOD/mgCOD} \end{aligned} \quad \text{(A.20)}$$

$$\begin{aligned} Y_{H,NO} &= 0.35 \text{ mgVSS/mgCOD} \\ &\equiv 0.35*1.42 \text{ mgCOD/mgCOD} \\ &\equiv Y_{Z,NO} = 0.50 \text{ mgCOD/mgCOD} \end{aligned} \quad \text{(A.21)}$$

and their ratio with respect to each other:

$$\Rightarrow Y_{H,NO}/Y_H = (0.35/0.42) \equiv (0.5/0.6) = 0.83 \quad \text{(A.22)}$$

In the bioenergetic calculations above, a number of simplifications and assumptions have been made, for example, synthesis of OHO biomass from CO_2, moles of ATP generated per electron equivalents and efficiency of biological processes; while these simplifications and assumptions influence the individual values calculated for the OHO yields, since they are similarly applied to both the aerobic and anoxic yields their impact on the ratio of the two yields is minimized. It is the theoretical development of this ratio that is of importance in this section.

APPENDIX B

OPERATIONAL DATA FOR MODIFIED LUDZACK-ETTINGER (MLE) AND SQUARE-WAVE (SQW) FED ACTIVATED SLUDGE SYSTEMS

TABLE OF CONTENTS

APPENDIX B-1

LONG SLUDGE AGE MODIFIED LUDZACK-ETTINGER SYSTEM (MLE) DAILY INFLUENT WASTEWATER CHARACTERIZATION

TABLE OF CONTENTS

Table B1-1. Undiluted wastewater average COD data (mgCOD/ℓ).

	UNDILUTED WASTEWATER COD (mgCOD/ℓ)							
	Sti_R			FFI_R			$Sbsi_{FF}$	fts_{FF}
SB	AVG	SSD	N	AVG	SSD	N	AVG	AVG
18	1157.6	41.0	13	265.6	17.4	12	188.5	0.163
19	1036.9	36.3	7*	237.5	24.1	7	144.3	0.139
20	1094.7	58.5	12	281.1	9.2	11	184.3	0.168
21	1128.3	49.3	12	272.3	12.3	9	157.8	0.140
22	1106.7	43.4	11	270.6	9.1	8	155.9	0.141
23	1079.9	67.1	15	249.1	30.2	12	145.6	0.135
24	1092.7	64.3	14	259.1	42.3	8	160.8	0.147
25	1101.0	58.6	9	278.3	22.3	8	167.3	0.152

Table B1-2. MLE System: Average influent, reactor and filtered effluent COD Concentrations.

	MLE SYSTEM AVERAGE COD DATA (mgCOD/ℓ)										ML COD/VSS Ratio			
	Diluted Influent			Aerobic Reactor			Filtered Effluent			f_{us}	AE mgVSS/ℓ			f_{cv}
SB	AVG	SSD	N	AVG	SSD	N	AVG	SSD	N	AVG	AVG	SSD	N	AVG
18	498.6	13.0	12				33.2	7.9	12	0.067	2267	102	7	
19	507.3	29.0	16				45.6	7.7	15	0.090	1957	174	2	
20	493.3	11.1	11				43.6	6.1	12	0.088	1797	80	5	
21	493.6	31.7	13	2857.6	170.5	5	50.1	11.9	13	0.101	1908	50	8	1.50
22	516.1	14.3	13	2176.4	407.5	6	53.5	6.5	11	0.104	1384	209	7	1.57
23	500.9	24.9	14	2553.9	107.7	7	48.0	5.3	11	0.096	1676	94	11	1.52
24	491.5	17.8	10	2817.0	262.6	6	44.2	8.3	10	0.090	1969	92	8	1.43
25	509.0	30.4	9				51.3	9.6	8	0.101	1945	75	4	

Table B1-3. MLE System: Average TKN, FSA and NOx data per sewage batch.

	TKN (mgN/ℓ)						FSA (mgN/ℓ)						Filtered Effluent NOx (mgN/ℓ)					
	Diluted Influent			Filtered Effluent			Diluted Influent			Filtered Effluent			NO3			NO2		
SB	AVG	SSD	N	AVG	SSD	N	AVG	SSD	N	AVG	SSD	N	AVG	SSD	N	AVG	SSD	N
18	46.09	3.2	10	4.30	0.5	10	35.45	3.5	10	2.85	0.443	9	7.58	0.679	10	0.09	0.078	9
19	39.69	2.2	8	2.98	0.6	8	32.26	2.5	8	2.36	0.700	8						
20	48.53	7.3	9	3.64	0.7	8	34.36	0.9	8	2.65	0.652	8	14.32	1.179	9	0.00	0.000	9
21	37.28	1.4	8	2.42	0.4	8	24.28	0.6	7	1.16	0.224	7	9.98	0.345	8	0.00	0.000	8
22	40.04	1.9	7	2.43	0.7	8	30.10	0.9	8	1.45	0.211	8	14.47	1.313	9	0.16	0.101	9
23	37.24	2.7	6	2.48	0.3	7	25.75	1.3	7	2.28	0.359	7	13.25	1.057	6	0.03	0.052	6
24	50.52	3.1	7	3.18	0.4	7	38.92	1.6	7	2.78	0.474	7	20.80	0.229	9	0.00	0.000	9
25	42.93	2.1	6	3.80	0.7	6	34.86	1.7	6	3.27	0.927	6	12.77	0.406	6	0.06	0.063	6

Table B1-4. MLE System: Average reactor total and volatile suspended solids.

	Total Suspended Solids (mgTSS/ℓ)						Volatile Suspended Solids (mgVSS/ℓ)					
	Aerobic (AE)			Anoxic (AX)			Aerobic (AE)			Anoxic (AX)		
SB	AVG	SSD	N	AVG	SSD	N	AVG	SSD	N	AVG	SSD	N
18	2723	132	7	3080	323	7	2267	102	7	2576	280	7
19	2260	201	2	2886	127	2	1957	174	2	2502	113	2
20	2062	94	5	2595	219	5	1797	80	5	2260	203	5
21	2246	69	8	2618	253	9	1908	50	8	2238	212	9
22	1620	245	7	2029	199	8	1384	209	7	1745	162	8
23	1953	114	10	2393	140	10	1676	94	11	2052	121	9
24	2317	115	8	2667	89	7	1969	92	8	2277	73	7
25	2323	86	4	2547	124	4	1945	75	4	2143	96	4

Table B1-5. MLE System: Average system TSS and VSS.

	TSS (mgTSS/ℓ)			VSS (mgVSS/ℓ)			f_i
SB	AVG	SSD	N	AVG	SSD	N	AVG
18	2812	133	7	2344	104	7	0.833
19	2416	182	2	2093	159	2	0.866
20	2195	109	5	1912	98	5	0.871
21	2390	54	8	2033	39	8	0.850
22	1719	231	7	1472	195	7	0.856
23	2051	115	10	1737	130	10	0.847
24	2418	115	8	2057	91	8	0.851
25	2379	84	4	1995	73	4	0.839

Table B1-6. MLE System: DSVI and pH Trend.

SB	Date	DSV30 (mℓ/0.5ℓ)	AE (mgTSS/ℓ)	DSVI (mℓ/g)	System pH			
					I	AX	AE	UE
18	19-Aug	200.0	2612.0	153.1				
20	20-Sep	80.0	1946.0	82.2				
21	09-Oct	110.0	2306.0	95.4				
22	18-Oct	85.0	1404.0	121.1		7.55	7.81	7.80
	20-Oct	110.0	1828.0	120.4		7.65	7.79	7.68
	20-Oct					7.58	7.70	7.77
	22-Oct	120.0	2000.0	120.0		7.60	7.70	7.57
	23-Oct					7.59	7.82	7.66
	28-Oct	90.0	1342.0	134.1	8.32	8.11	8.33	8.20
	29-Oct	100.0	1420.0	140.8	8.16	7.87	8.06	7.88
	30-Oct				8.07	7.89	7.93	7.94
	31-Oct	100.0	1634.0	122.4		7.92	7.96	7.89
	01-Nov					7.78	7.91	7.64
23	02-Nov	105.0	1560.0	134.6	7.53	7.22	7.30	7.29
	03-Nov				7.66	7.37	7.43	7.45
	04-Nov	110.0	1778.0	123.7	7.71	7.38	7.32	7.41
	06-Nov	120.0	1988.0	120.7	7.60	7.21	7.36	7.21
	08-Nov	105.0	1978.0	106.2	7.64	7.24	7.21	7.18
	12-Nov				7.67	7.18	7.22	7.19
	17-Nov	105.0	2038.0	103.0				
24	21-Nov	115.0	2178.0	105.6		7.08	6.98	7.06
	22-Nov				7.93	7.20	7.10	7.07
	23-Nov	115.0	2106.0	109.2				
	24-Nov	125.0	2430.0	102.9				
	29-Nov	130.0	2360.0	110.2				
	30-Nov				7.83	7.23	7.19	7.28
	01-Dec	130.0	2338.0	111.2	7.78	7.12	6.97	7.20
	04-Dec	130.0	2418.0	107.5				
25	09-Dec	105.0	2388.0	87.9				
	11-Dec	105.0	2398.0	87.6				
	Average	113.4	2020.5	113.6	7.83	7.49	7.55	7.52
	Stdev	23.7	374.8	17.7	0.25	0.31	0.39	0.33
	Count	22	22	22	12	20	20	20
	Min	80.0	1342.0	82.2	7.53	7.08	6.97	7.06
	Max	200.0	2612.0	153.1	8.32	8.11	8.33	8.20

Table B1-7. MLE System: Daily solids data (mg/ℓ). *(Note: Outliers boxed).*

SB	Date	TSS_{AE}	VSS_{AE}	TSS_{AX}	VSS_{AX}	TSS_{avg}	VSS_{avg}	f_i
18	17-Aug	2924.0	2354.0	3210.0	2586.0	2995.5	2412.0	0.805
	19-Aug	2612.0	2104.0	2810.0	2276.0	2661.5	2147.0	0.807
	21-Aug	2784.0	2306.0	2928.0	2438.0	2820.0	2339.0	0.829
	23-Aug	2730.0	2268.0	3482.0	2906.0	2918.0	2427.5	0.832
	26-Aug	2802.0	2364.0	3204.0	2718.0	2902.5	2452.5	0.845
	28-Aug	2690.0	2322.0	2570.0	2214.0	2660.0	2295.0	0.863
	30-Aug	2520.3	2148.0	3356.0	2894.0	2729.3	2334.5	0.855
	AVG	*2723.2*	*2266.6*	*3080.0*	*2576.0*	*2812.4*	*2343.9*	*0.834*
	STDEV	*132.2*	*101.9*	*323.0*	*280.0*	*132.8*	*103.8*	*0.022*
	Count	*7*	*7*	*7*	*7*	*7*	*7*	*7*
19	12-Sep	2402.0	2080.0	2976.0	2582.0	2545.5	2205.5	0.866
	13-Sep	2118.0	1834.0	2796.0	2422.0	2287.5	1981.0	0.866
	AVG	*2260.0*	*1957.0*	*2886.0*	*2502.0*	*2416.5*	*2093.2*	*0.866*
	STDEV	*200.8*	*173.9*	*127.3*	*113.1*	*182.4*	*158.7*	*0.000*
	Count	*2*	*2*	*2*	*2*	*2*	*2*	*2*
20	18-Sep	2026.0	1766.0	2734.0	2382.0	2203.0	1920.0	0.872
	20-Sep	1946.0	1710.0	2548.0	2226.0	2096.5	1839.0	0.877
	22-Sep	2146.0	1868.0	2752.0	2412.0	2297.5	2004.0	0.872
	24-Sep	2170.0	1894.0	2710.0	2358.0	2305.0	2010.0	0.872
	29-Sep	2020.0	1746.0	2230.0	1920.0	2072.5	1789.5	0.863
	AVG	*2061.6*	*1796.8*	*2594.8*	*2259.6*	*2194.9*	*1912.5*	*0.871*
	STDEV	*93.9*	*80.0*	*219.4*	*202.7*	*108.8*	*98.1*	*0.005*
	Count	*5*	*5*	*5*	*5*	*5*	*5*	*5*
21	01-Oct	**2516.0**	**2148.0**	2234.0	1904.0	2445.5	2087.0	0.853
	05-Oct	2080.0	1786.0	2292.0	1978.0	**2133.0**	**1834.0**	0.860
	09-Oct	2306.0	1922.0	2954.0	2498.0	2468.0	2066.0	0.837
	11-Oct	2256.0	1926.0	2442.0	2078.0	2302.5	1964.0	0.853
	12-Oct	2280.0	1932.0	2630.0	2244.0	2367.5	2010.0	0.849
	13-Oct	2266.0	1938.0	2658.0	2282.0	2364.0	2024.0	0.856
	14-Oct	2264.0	1926.0	2800.0	2394.0	2398.0	2043.0	0.852
	15-Oct	2254.0	1922.0	2646.0	2280.0	2352.0	2011.5	0.855
	16-Oct	2262.0	1912.0	2902.0	2484.0	2422.0	2055.0	0.848
	AVG	*2246.0*	*1908.0*	*2617.6*	*2238.0*	*2389.9*	*2032.6*	*0.852*
	STDEV	*69.1*	*49.9*	*253.5*	*212.4*	*54.2*	*38.6*	*0.006*
	Count	*8*	*8*	*9*	*9*	*8*	*8*	*9*
22	18-Oct	1404.0	1196.0	1966.0	1698.0	1544.5	1321.5	0.856
	19-Oct			2132.0	1820.0			
	20-Oct	1828.0	1568.0	2112.0	1824.0	1899.0	1632.0	0.859
	22-Oct	2000.0	1710.0	2336.0	1990.0	2084.0	1780.0	0.854
	28-Oct	1342.0	1156.0	1648.0	1430.0	1418.5	1224.5	0.863
	29-Oct	1420.0	1214.0	1936.0	1660.0	1549.0	1325.5	0.856
	30-Oct	1714.0	1454.0	1998.0	1732.0	1785.0	1523.5	0.854
	31-Oct	1634.0	1392.0	2104.0	1806.0	1751.5	1495.5	0.854
	AVG	*1620.3*	*1384.3*	*2029.0*	*1745.0*	*1718.8*	*1471.8*	*0.856*
	STDEV	*245.2*	*208.7*	*198.6*	*162.3*	*231.2*	*195.4*	*0.004*
	Count	*7*	*7*	*8*	*8*	*7*	*7*	*7*

23	02-Nov	**1560.0**	**1336.0**	2280.0	1968.0	**1740.0**	1494.0	0.859
	04-Nov	1778.0	1540.0	2450.0	2112.0	1946.0	1683.0	0.865
	06-Nov	1988.0	1698.0	2680.0	2308.0	2161.0	1850.5	0.856
	07-Nov	1954.0	1696.0	2328.0	2020.0	2047.5	1777.0	0.868
	08-Nov	1978.0	1704.0	2374.0	2056.0	2077.0	1792.0	0.863
	09-Nov	1860.0	1600.0	2508.0		2022.0	**1200.0**	0.593
	11-Nov	1824.0	1554.0	**1804.0**	**1544.0**	1819.0	1551.5	0.853
	13-Nov	1906.0	1640.0	2290.0	1974.0	2002.0	1723.5	0.861
	15-Nov	2062.0	1760.0	2188.0	1888.0	2093.5	1792.0	0.856
	17-Nov	2038.0	1724.0	2356.0	2012.0	2117.5	1796.0	0.848
	19-Nov	2146.0	1844.0	2474.0	2130.0	2228.0	1915.5	0.860
	AVG	*1953.4*	*1676.0*	*2392.8*	*2052.0*	*2051.4*	*1737.5*	*0.835*
	STDEV	*113.7*	*94.1*	*140.1*	*121.4*	*114.7*	*130.1*	*0.080*
	Count	*10*	*11*	*10*	*9*	*10*	*10*	*11*
24	21-Nov	2178.0	1856.0	2600.0	2238.0	2283.5	1951.5	0.855
	23-Nov	2106.0	1802.0	2642.0	2262.0	2240.0	1917.0	0.856
	24-Nov	2430.0	2076.0	2802.0	2390.0	2523.0	2154.5	0.854
	25-Nov	2366.0	1992.0	2772.0	2348.0	2467.5	2081.0	0.843
	29-Nov	2360.0	2000.0	2566.0	2176.0	2411.5	2044.0	0.848
	01-Dec	2338.0	1994.0	2614.0	2232.0	2407.0	2053.5	0.853
	04-Dec	2418.0	2036.0	**3104.0**	**2630.0**	2589.5	2184.5	0.844
	06-Dec	2342.0	1998.0	2670.0	2296.0	2424.0	2072.5	0.855
	AVG	*2317.3*	*1969.3*	*2666.6*	*2277.4*	*2418.3*	*2057.3*	*0.851*
	STDEV	*114.7*	*92.2*	*88.9*	*73.2*	*115.2*	*90.6*	*0.005*
	Count	*8*	*8*	*7*	*7*	*8*	*8*	*8*
25	09-Dec	2388.0	2008.0	2606.0	2194.0	2442.5	2054.5	0.841
	11-Dec	2398.0	2008.0	2642.0	2218.0	2459.0	2060.5	0.838
	14-Dec	2286.0	1906.0	2366.0	2004.0	2306.0	1930.5	0.837
	15-Dec	2218.0	1858.0	2574.0	2156.0	2307.0	1932.5	0.838
	AVG	*2322.5*	*1945.0*	*2547.0*	*2143.0*	*2378.6*	*1994.5*	*0.838*
	STDEV	*86.1*	*75.3*	*123.8*	*96.1*	*83.6*	*72.8*	*0.002*
	Count	*4*	*4*	*4*	*4*	*4*	*4*	*4*

Table B1-8. MLE System: Daily COD, $RBCOD_{FF}$, TKN, FSA and NOx analyses. *(Note: Outliers boxed).*

		UNDILUTED WW mgCOD/ℓ				COD (mgCOD/ℓ)				TKN (mgN/ℓ)		FSA (mgN/ℓ)		NOx (mgN/ℓ)	
SB	Date	Sti_R	FFI_R	$Sbsi_{FFI,R}$	fts_{FFI}	I	AE	FE	fus	I	FE	I	FE	NO3	NO2
18	17-Aug	1167.6	220.2	*161.4*	*0.138*	502.0		25.3	*0.050*	50.96	4.20	34.72	3.08	6.58	0.04
	18-Aug	1137.2	251.5	*197.2*	*0.173*	485.8		23.2	*0.048*	45.36	5.04	30.24	2.94	6.79	0.22
	19-Aug	1124.4	**214.9**	*173.0*	*0.154*	485.9		18.1	*0.037*	46.20	4.62	34.72	**4.20**	7.06	0.04
	20-Aug	1190.8	264.1	*160.0*	*0.134*	517.1		45.2	*0.087*	42.00	3.64	32.48	3.64	8.43	0.03
	21-Aug	1160.6	278.7	*194.1*	*0.167*	499.2		36.4	*0.073*	49.28	4.90	39.48	2.80	7.54	0.03
	22-Aug	1108.6	271.4	*186.8*	*0.168*	504.4		38.5	*0.076*	50.12	4.48	42.00	3.08	7.47	0.02
	23-Aug	1098.2	257.9	*190.8*	*0.174*	476.3		29.1	*0.061*	44.80	3.50	37.80	2.94	7.20	0.17
	24-Aug	1156.4	282.9	*207.0*	*0.179*	507.5		33.3	*0.066*	46.20	4.34	35.84	2.66	8.50	**0.45**
	25-Aug	1123.2	265.2	*176.1*	*0.157*	498.2		39.5	*0.079*	44.52	4.20	34.44	2.10	8.02	0.17
	26-Aug	1139.8	274.6	*196.3*	*0.172*	484.6		33.3	*0.069*	41.44	4.06	32.76	2.38	8.16	0.05
	27-Aug	1229.2	275.6	*150.7*	*0.123*	**532.5**		**54.1**	*0.102*						
	28-Aug	1214.8	262.1	*176.6*	*0.145*	516.9		36.4	*0.070*						
	29-Aug	1198.1	282.9	*189.3*	*0.158*	505.4		39.5	*0.078*						
	AVG	***1157.6***	***265.6***	***181.5***	***0.157***	***498.6***		***33.2***	***0.069***	***46.09***	***4.30***	***35.45***	***2.85***	***7.58***	***0.09***
	STDEV	***41.0***	***17.4***	***16.8***	***0.018***	***13.0***		***7.9***	***0.017***	***3.22***	***0.49***	***3.50***	***0.44***	***0.68***	***0.08***
	Count	***13***	***12***	***13***	***13***	***12***		***12***	***13***	***10***	***10***	***10***	***9***	***10***	***9***
19	31-Aug	**1160.6**	229.9	*117.7*	*0.101*	519.1		50.2	*0.097*	40.88	3.64	33.80	3.50		
	1-Sep					556.2		38.2	*0.069*	36.12	2.80	31.08	1.68		
	2-Sep					520.1		54.2	*0.104*	42.56	3.92	35.28	3.36		
	3-Sep					516.1		48.2	*0.093*	37.24	3.22	28.56	2.24		
	4-Sep					502.0		57.2	*0.114*	38.64	2.24	35.56	1.82		
	5-Sep					487.9		46.2	*0.095*	41.44	2.80	32.48	1.82		
	6-Sep					554.2		44.2	*0.080*	40.04	2.38	30.52	2.10		
	7-Sep					461.8		54.2	*0.117*	40.60	2.80	30.80	2.38		
	8-Sep					522.1		34.1	*0.065*						
	9-Sep	1056.2				513.0		37.1	*0.072*						
	10-Sep	1052.2	235.9	*143.3*	*0.136*	536.1		47.2	*0.088*						
	11-Sep	1000.0	243.0	*156.5*	*0.157*	487.9		42.2	*0.086*						
	12-Sep	987.9	228.9	*153.6*	*0.156*	473.9		36.1	*0.076*						
	13-Sep	1018.1	196.7	*138.8*	*0.136*	464.4		**26.4**	*0.057*						
	14-Sep	1052.5	274.8	*190.9*	*0.181*	482.7		38.5	*0.080*						
	15-Sep	1091.1	253.5	*136.2*	*0.125*	519.2		55.8	*0.107*						
	AVG	***1036.9***	***237.5***	***148.1***	***0.142***	***507.3***		***45.6***	***0.088***	***39.69***	***2.98***	***32.26***	***2.36***		
	STDEV	***36.3***	***24.1***	***22.8***	***0.026***	***29.0***		***7.7***	***0.018***	***2.19***	***0.58***	***2.47***	***0.70***		
	Count	***7***	***7***	***7***	***7***	***16***		***15***	***16***	***8***	***8***	***8***	***8***		
20	16-Sep	1156.0				498.9		51.7	*0.104*						
	17-Sep	1119.5	**237.3**	*145.1*	*0.130*	492.8		40.6	*0.082*	46.50	3.90	35.80	1.70	15.60	0.00
	18-Sep	1141.8	271.8	*183.3*	*0.161*	496.9		38.5	*0.077*	67.80				14.60	0.00
	19-Sep	1164.1	297.1	*196.3*	*0.169*	491.8		42.6	*0.087*	46.20	4.50	35.30	1.70	14.50	0.00
	20-Sep	1100.9	275.7	*197.0*	*0.179*	494.9		35.4	*0.072*	48.20	2.80	34.70	3.20	13.70	0.00
	21-Sep	1056.5	272.7	*165.7*	*0.157*	478.7		48.5	*0.101*	47.00	3.60	33.30	3.20	14.10	0.00
	22-Sep	1016.1	272.7	*184.0*	*0.181*	**462.6**		40.4	*0.087*	44.50	3.80	34.40	2.40	14.90	0.00
	23-Sep		281.8					40.4		44.20	2.80	33.90	3.20	16.10	0.00
	24-Sep	1064.5	290.9	*208.3*	*0.196*	494.9		38.4	*0.078*	45.10	3.20	33.90	3.10	13.00	0.00
	25-Sep	1084.7	286.8	*166.2*	*0.153*	500.0		55.6	*0.111*	47.30	4.50	33.60	2.70	12.40	0.00
	26-Sep	1179.7	287.9	*188.1*	*0.159*	513.1		43.4	*0.085*						
	27-Sep	1047.0	285.3	*178.5*	*0.170*	470.5		48.0	*0.102*						
	28-Sep	1005.0	269.3	*142.8*	*0.142*	493.5		**62.1**	*0.126*						
	29-Sep														
	AVG	***1094.7***	***281.1***	***177.7***	***0.163***	***493.3***		***43.6***	***0.093***	***48.53***	***3.64***	***34.36***	***2.65***	***14.32***	***0.00***
	STDEV	***58.5***	***9.2***	***21.0***	***0.019***	***11.1***		***6.1***	***0.016***	***7.35***	***0.67***	***0.86***	***0.65***	***1.18***	***0.00***
	Count	***12***	***11***	***11***	***11***	***11***		***12***	***12***	***9***	***8***	***8***	***8***	***9***	***9***
21	30-Sep	1189.2													
	1-Oct	1183.2	268.3	*188.4*	*0.159*	488.5		33.0	*0.068*	35.56	2.52	**26.32**	1.12	9.70	0.00
	2-Oct	1159.2	275.3	*179.8*	*0.155*	497.5		41.0	*0.082*	37.52	2.94	24.92	1.26	10.10	0.00
	3-Oct	1133.0	290.3	*198.9*	*0.176*	512.1		41.3	*0.081*	36.40	2.10	23.80	1.12	9.70	0.00
	4-Oct	1155.2	**321.6**	*219.5*	*0.190*	525.2		46.4	*0.088*	38.08	2.24	24.08	0.98	10.30	0.00
	5-Oct	1167.3	280.2			529.2				36.40	2.24	24.64		9.40	0.00
	6-Oct	1149.1	281.2	*154.4*	*0.134*	521.1		57.5	*0.110*	39.76	2.52	24.08	0.84	10.00	0.00
	7-Oct	**1276.1**	262.1	*42.5*	*0.033*	448.6		***77.2***	***0.172***	36.40	1.82	23.52	1.26	10.40	0.00
	8-Oct	1109.5	254.0	*128.2*	*0.116*	528.3	2722.9	59.9	*0.113*	38.08	2.94	24.92	1.54	10.20	0.00
	9-Oct	1101.3	281.4	*151.7*	*0.138*	491.7	3129.3	57.9	*0.118*						
	10-Oct	1085.1	258.1	*132.3*	*0.122*	508.0		58.9	*0.116*						
	13-Oct	1087.1				479.6		49.8	*0.104*						
	14-Oct						2916.0	64.0							
	15-Oct	1020.0				445.0	2730.0	50.0	*0.112*						
	16-Oct	**968.0**				442.0	2790.0	41.0	*0.093*						
	AVG	***1128.3***	***272.3***	***155.1***	***0.136***	***493.6***	***2857.6***	***50.1***	***0.105***	***37.28***	***2.42***	***24.28***	***1.16***	***9.98***	***0.00***
	STDEV	***49.3***	***12.3***	***52.1***	***0.045***	***31.7***	***170.5***	***11.9***	***0.027***	***1.35***	***0.39***	***0.55***	***0.22***	***0.35***	***0.00***
	Count	***12***	***9***	***9***	***9***	***13***	***5***	***13***	***12***	***8***	***8***	***7***	***7***	***8***	***8***

22	17-Oct	1158.0				520.0								11.70	0.29
	18-Oct					509.0	1740.0	41.0	0.081	37.80	2.66	29.12	1.68	15.27	0.03
	19-Oct	1024.0	264.0	126.6	0.124	492.0	2350.0	66.0	0.134	37.80	2.24	29.40	1.26	14.71	0.09
	20-Oct	969.6	274.0	172.7	0.178	536.0	2440.0	56.0	0.104	42.30	2.10	30.20	1.40	14.61	0.09
	21-Oct	1160.0	265.0	265.0	0.228	508.0				39.50	1.82	30.00	1.68	13.06	0.34
	22-Oct	1104.0	260.0	149.4	0.135	519.0	2540.0	52.0	0.100	51.00	3.50	31.40	1.12	14.44	0.16
	23-Oct	1046.5				511.0	2641.9	48.1	0.094	41.70	1.82	30.80	1.40	15.06	0.14
	24-Oct	1118.5	286.7	174.5	0.156	530.4		53.2	0.100	39.20	3.50	29.10	1.40	15.71	0.09
	25-Oct	1108.0				535.6		48.1	0.090	42.00	1.82	30.80	1.68	15.71	0.19
	26-Oct	1144.8	274.4	151.4	0.132	533.5		57.3	0.107						
	27-Oct	1124.4	277.5	148.7	0.132	510.0		58.4	0.115						
	28-Oct	1110.0	263.2	145.5	0.131	501.8	1792.0	53.2	0.106						
	29-Oct	1075.2	229.4	111.1	0.103	502.8	1904.6	55.3	0.110						
	31-Oct						2130.0								
	1-Nov						2089.0								
	AVG	***1106.7***	***270.6***	***160.6***	***0.147***	***516.1***	***2201.2***	***53.5***	***0.104***	***40.04***	***2.43***	***30.10***	***1.45***	***14.47***	***0.16***
	STDEV	***43.4***	***9.1***	***43.9***	***0.037***	***14.3***	***377.8***	***6.5***	***0.014***	***1.95***	***0.72***	***0.86***	***0.21***	***1.31***	***0.10***
	Count	***11***	***8***	***9***	***9***	***13***	***7***	***11***	***11***	***7***	***8***	***8***	***8***	***9***	***9***
23	2-Nov	1149.1				534.5									
	3-Nov	1188.1	267.8	116.2	0.098	498.6	2349.5	63.6	0.128	36.12	2.52	26.16	2.38	12.49	0.00
	4-Nov	1101.9	246.2	127.9	0.116	535.6	2411.1	57.5	0.107	42.56	2.80	28.32	2.80	13.32	0.00
	5-Nov	1089.6	283.2	168.8	0.155	518.1		54.4	0.105	35.84	2.66	25.92	2.52	14.73	0.00
	6-Nov	1140.9	282.2	176.6	0.155	531.5	2688.1	49.2	0.093	37.52	2.38	24.48	2.10	13.91	0.00
	7-Nov	1130.7	252.4	137.4	0.122	474.0	2606.0	48.2	0.102	55.56	2.80	25.68	2.38	11.71	0.10
	8-Nov	1116.3	263.7	166.6	0.149	495.6	2565.0	43.1	0.087	35.56	1.96	24.48	1.68	13.31	0.10
	9-Nov	1106.0	256.5	165.6	0.150	498.6		41.0	0.082	35.84	2.24	25.20	2.10		
	10-Nov					509.9		50.3	0.099						
	11-Nov	1120.4	252.4	156.3	0.139	514.0		44.1	0.086						
	12-Nov	1060.9	255.5	153.6	0.145	491.5	2595.8	47.2	0.096						
	13-Nov	1026.0	238.0	125.8	0.123	468.9	2400.8	51.3	0.109						
	14-Nov														
	15-Nov	973.9	220.9												
	16-Nov	998.0				453.8		41.2	0.091						
	17-Nov	971.9	170.7				2610.4								
23b	18-Nov	1024.1				487.9									
	19-Nov														
	AVG	***1079.9***	***249.1***	***149.5***	***0.135***	***500.9***	***2528.3***	***48.0***	***0.099***	***37.24***	***2.48***	***25.75***	***2.28***	***13.25***	***0.03***
	STDEV	***67.1***	***30.2***	***21.1***	***0.019***	***24.9***	***123.2***	***5.3***	***0.013***	***2.70***	***0.31***	***1.31***	***0.36***	***1.06***	***0.05***
	Count	***15***	***12***	***10***	***10***	***14***	***8***	***11***	***12***	***6***	***7***	***7***	***7***	***6***	***6***
24	21-Nov	1228.9	267.1			531.1	2479.9								
	22-Nov	1048.2	204.8			466.9		47.2	0.101	49.84	2.52	38.64	2.38	21.13	0.00
	23-Nov	1162.2	300.2	202.9	0.175	492.0	2570.2	41.2	0.084	47.88	3.22	36.96	2.66	20.58	0.00
	24-Nov	1054.2	279.1	181.4	0.172	476.9	3052.0	44.2	0.093	47.60	3.64	39.48	3.64	20.91	0.00
	25-Nov	911.6	181.7	114.0	0.125	391.6		29.1	0.074	49.56	3.08	38.92	2.66	21.13	0.00
	26-Nov	1076.5	272.2	151.4	0.141	484.8		54.4	0.112	49.00	3.50	37.80	3.22	20.69	0.00
	27-Nov	1066.5	278.2	169.8	0.159	485.9		49.4	0.102	55.72	2.94	38.64	2.52	20.80	0.00
	28-Nov	1151.1	289.3	216.6	0.188	493.9		31.2	0.063	54.04	3.36	42.00	2.38	20.46	0.00
	29-Nov	997.9				484.8	3024.0	47.4	0.098						
	30-Nov	1050.3				510.0		45.4	0.089					20.80	0.00
	1-Dec	1016.1				488.9	2711.5	52.4	0.107					20.69	0.00
	2-Dec	1066.5													
	3-Dec	1153.2													
	4-Dec	1133.0					3064.3								
	5-Dec	1092.7													
	6-Dec														
	AVG	***1092.7***	***259.1***	***172.7***	***0.160***	***491.5***	***2817.0***	***44.2***	***0.092***	***50.52***	***3.18***	***38.92***	***2.78***	***20.80***	***0.00***
	STDEV	***64.3***	***42.3***	***36.9***	***0.023***	***17.8***	***262.6***	***8.3***	***0.015***	***3.13***	***0.38***	***1.58***	***0.47***	***0.23***	***0.00***
	Count	***14***	***8***	***6***	***6***	***10***	***6***	***10***	***10***	***7***	***7***	***7***	***7***	***9***	***9***
25	7-Dec	1193.5				534.2									
	8-Dec	1155.2	298.4	211.3	0.183	521.1		39.3	0.075	42.84	3.64	31.92	3.50	13.16	0.00
	9-Dec	1096.0	259.0	140.1	0.128	461.0		50.0	0.108	43.68	3.78	36.68	4.76	13.30	0.00
	10-Dec	1000.0	259.0	140.7	0.141	458.0		54.2	0.118	39.48	4.90	34.16	3.64	12.88	0.00
	11-Dec	1154.0	317.0	170.3	0.148	528.0		67.1	0.127	45.92	3.08	35.00	3.08	12.37	0.10
	12-Dec	1068.0	254.0	152.9	0.143	504.0		47.7	0.095	43.40	4.34	35.84	2.38	12.44	0.12
	13-Dec	1098.0	287.0	198.6	0.181	534.0		43.0	0.081	42.28	3.08	35.56	2.24	12.44	0.12
	14-Dec	1082.0	285.0	157.6	0.146	535.0		63.0	0.118						
	15-Dec	1062.0	267.0	170.5	0.161	506.0		46.0	0.091						
	16-Dec														
	17-Dec														
	18-Dec														
	AVG	***1101.0***	***278.3***	***167.7***	***0.154***	***509.0***		***51.3***	***0.102***	***42.93***	***3.80***	***34.86***	***3.27***	***12.77***	***0.06***
	STDEV	***58.6***	***22.3***	***25.9***	***0.020***	***30.4***		***9.6***	***0.019***	***2.10***	***0.72***	***1.67***	***0.93***	***0.41***	***0.06***
	Count	***9***	***8***	***8***	***8***	***9***		***8***	***8***	***6***	***6***	***6***	***6***	***6***	***6***

APPENDIX B-2

SQUARE-WAVE (SQW) FED SHORT SLUDGE AGE ACTIVATED SLUDGE SYSTEM DAILY COD AND SUSPENDED SOLIDS ANALYSES

TABLE OF CONTENTS

Table B2-1. SQW System: Average Influent (I) and Filtered Effluent (FE) COD Concentrations (mgCOD/ℓ).

	Diluted Influent			Filtered Effluent			f_{us}
SB	AVG	SSD	N	AVG	SSD	N	AVG
18	489.5	19.2	13	48.9	8.9	12	0.100
19	498.8	30.8	6	55.0	13.5	6	0.110
20	477.8	26.6	12	54.0	9.3	12	0.113
21	487.5	22.2	15	56.5	10.8	12	0.116
22	509.0	17.8	13	58.1	5.4	10	0.114
23	486.9	25.2	17	53.9	6.6	14	0.111
24	487.6	25.6	15	50.7	8.6	14	0.104
25	510.7	19.1	11	61.6	9.4	10	0.121

Table B2-2. SQW System: Average flow (Q_s), ΔOUR, S_{ti} (mgCOD/ℓ) and S_{bsi} (mgCOD/ℓ) estimation.

	Q_s (ℓ/d)			ΔOUR (mgO/ℓ/h)			Sti_S	$Sbsi_S$	fts_S
SB	AVG	SSD	N	AVG	SSD	N	AVG	AVG	AVG
18	36.14	0.7	12	4.07	0.8	13	489.5	54.8	0.112
19	35.82	0.7	16	3.73	0.7	7	498.8	50.7	0.102
20	35.33	1.0	14	4.85	0.6	13	477.8	66.9	0.140
21	35.99	1.7	13	4.50	0.6	11	487.5	60.9	0.125
22	36.31	1.1	11	6.47	1.0	10	509.0	86.8	0.171
23	35.76	0.4	17	5.19	0.7	16	486.9	70.8	0.145
24	35.91	1.1	14	4.74	0.5	14	487.6	64.4	0.132
25	35.04	1.6	11	7.16	0.9	10	510.7	99.6	0.195

Table B2-3. SQW System: Average system total and volatile suspended solids.

	TSS (mgTSS/ℓ)			VSS (mgVSS/ℓ)			f_i
SB	AVG	SSD	N	AVG	SSD	N	AVG
18	1308	117	7	1131	106	7	0.864
19	1274	110	2	1108	89	2	0.869
20	1170	159	4	1014	130	4	0.867
21	1152	199	5	971	159	5	0.842
22	1290	45	5	1107	37	5	0.858
23	1253	57	6	1086	60	6	0.867
24	1372	92	7	1172	79	7	0.854
25	1256	9	3	1057	8	3	0.842

Table B2-4. SQW System: Buffered influent pH data.

Date	8-Nov	9-Nov	12-Nov	22-Nov	30-Nov	1-Dec	Avg	Stdev	Range	
pH	7.72	7.66	7.73	7.92	7.91	7.8	*7.8*	*0.1*	*7.7*	*7.9*

Table B2-5. SQW System: DSVI check (mℓ/g).

Date	23-Nov	29-Nov	Avg	Stdev
DSVI	101.6	107.5	*104.6*	*4.2*

Table B2-6. SQW System: Daily solids data (mg/ℓ). *(Note: Outliers boxed).*

SB	Date	TSS-1	TSS-2	VSS-1	VSS-2	TSS_{avg}	VSS_{avg}	f_i
18	17-Aug	1374.0	1376.0	1186.0	1184.0	1374.5	1185.5	0.862
	19-Aug	1318.0	1274.0	1128.0	1116.0	1307.0	1125.0	0.861
	21-Aug	1530.0	1478.0	1330.0	1292.0	1517.0	1320.5	0.870
	23-Aug	1158.0	1136.0	988.0	978.0	1152.5	985.5	0.855
	26-Aug	1230.0	1202.0	1066.0	1052.0	1223.0	1062.5	0.869
	27-Aug	1262.0	1250.0	1086.0	1076.0	1259.0	1083.5	0.861
	30-Aug	1326.0	1322.0	1154.0	1144.0	1325.0	1151.5	0.869
	AVG					***1308.3***	***1130.6***	
	STDEV					***117.0***	***106.0***	
	Count					***7***	***7***	
19	12-Sep	1350.0	1360.0	1172.0	1168.0	1352.5	1171.0	0.866
	13-Sep	1198.0	1192.0	1048.0	1034.0	1196.5	1044.5	0.873
	AVG					***1274.5***	***1107.7***	
	STDEV					***110.3***	***89.4***	
	Count					***2***	***2***	
20	18-Sep	1188.0	1152.0	1036.0	1000.0	1179.0	1027.0	0.871
	20-Sep	1328.0	1330.0	1150.0	1150.0	1328.5	1150.0	0.866
	24-Sep	1216.0	1234.0	1038.0	1058.0	1220.5	1043.0	0.855
	29-Sep	944.0	970.0	830.0	856.0	950.5	836.5	0.880
	AVG					***1169.6***	***1014.1***	
	STDEV					***159.1***	***130.4***	
	Count					***4***	***4***	
21	01-Oct	1242.0	1300.0	1074.0	1104.0	1256.5	1081.5	0.861
	07-Oct	1258.0	1192.0	1060.0	1006.0	1241.5	1046.5	0.843
	09-Oct	1348.0	1310.0	1078.0	1082.0	1338.5	1079.0	0.806
	11-Oct	872.0	884.0	746.0	748.0	875.0	746.5	0.853
	13-Oct	1016.0	1004.0	860.0	848.0	1013.0	857.0	0.846
	15-Oct	1296.0	1226.0	1104.0	1044.0	1278.5	1089.0	0.852
	AVG					***1152.3***	***970.6***	
	STDEV					***198.6***	***159.1***	
	Count					***5***	***5***	
22	18-Oct	1276.0	1306.0	1102.0	1132.0	1283.5	1109.5	0.864
	20-Oct	1300.0	1314.0	1118.0	1130.0	1303.5	1121.0	0.860
	22-Oct	824.0	818.0	728.0	718.0	**822.5**	**725.5**	0.882
	25-Oct	1280.0	1340.0	1092.0	1146.0	1295.0	1105.5	0.854
	29-Oct	1228.0	1204.0	1052.0	1038.0	1222.0	1048.5	0.858
	31-Oct	1342.0	1362.0	1148.0	1160.0	1347.0	1151.0	0.854
	AVG					***1290.2***	***1107.1***	
	STDEV					***45.1***	***37.3***	
	Count					***5***	***5***	
23	02-Nov	1320.0	1320.0	1142.0	1334.0	1320.0	1190.0	0.902
	04-Nov	1260.0	1286.0	1090.0	1116.0	1266.5	1096.5	0.866
	09-Nov	1234.0	1214.0	1066.0	1052.0	1229.0	1062.5	0.865
	11-Nov	1228.0	1186.0	1048.0	1012.0	1217.5	1039.0	0.853
	13-Nov	1292.0	1266.0	1110.0	1090.0	1285.5	1105.0	0.860
	15-Nov	1344.0	1328.0	1140.0	1126.0	1340.0	1136.5	0.848
	19-Nov	1196.0	1128.0	1038.0	980.0	1179.0	1023.5	0.868
	AVG					***1252.9***	***1086.1***	
	STDEV					***56.8***	***59.9***	
	Count					***6***	***6***	

24	21-Nov	1358.0	1366.0	1164.0	1174.0	1360.0	1166.5	0.858
	23-Nov	1280.0	1236.0	1094.0	1062.0	1269.0	1086.0	0.856
	25-Nov	1308.0	1340.0	1104.0	1130.0	1316.0	1110.5	0.844
	29-Nov	1474.0	1502.0	1256.0	1284.0	1481.0	1263.0	0.853
	01-Dec	1350.0	1320.0	1176.0	1150.0	1342.5	1169.5	0.871
	04-Dec	1320.0	1318.0	1114.0	1116.0	1319.5	1114.5	0.845
	06-Dec	1518.0	1516.0	1296.0	1286.0	1517.5	1293.5	0.852
	AVG					***1372.2***	***1171.9***	
	STDEV					***91.8***	***79.1***	
	Count					***7***	***7***	
25	09-Dec	1268.0	1260.0	1060.0	1048.0	1266.0	1057.0	0.835
	11-Dec	1250.0	1240.0	1052.0	1042.0	1247.5	1049.5	0.841
	14-Dec	1264.0	1228.0	1076.0	1036.0	1255.0	1066.0	0.849
	AVG					***1256.2***	***1057.5***	
	STDEV					***9.3***	***8.3***	
	Count					***3***	***3***	

Table B2-7. SQW System: Daily influent (I) and filtered effluent (FE) COD (mgCOD/ℓ). *(Note: Outliers are boxed).*

		SQW SYSTEM DAILY COD AND RBCOD ESTIMATION					
SB	Date	I	FE	Q_S	ΔOUR_1	$Sbsi_{OUR}$	fts_{OUR}
18	17-Aug	501.0	44.4	36.70	3.51	*46.0*	*0.092*
	18-Aug	484.8	34.3	36.86	3.95	*51.6*	*0.106*
	19-Aug	457.8	**14.1**	34.96	2.90	*39.9*	*0.087*
	20-Aug	501.0	51.2	36.74	4.90	*64.2*	*0.128*
	21-Aug	490.9	53.0	36.68	4.86	*63.8*	*0.130*
	22-Aug	490.9	42.6	36.32	5.25	*69.6*	*0.142*
	23-Aug	472.2	47.8	**41.20**	5.35		
	24-Aug	463.8	49.9	34.88	3.55	*49.0*	*0.106*
	25-Aug	483.6	48.9	36.16	3.88	*51.7*	*0.107*
	26-Aug	476.3	43.7	36.68	3.79	*49.7*	*0.104*
	27-Aug	523.1	66.6	35.90	4.10	*55.0*	*0.105*
	28-Aug	514.8	41.6	35.92	3.67	*49.2*	*0.096*
	29-Aug	503.4	62.4	35.90	3.15	*42.2*	*0.084*
	AVG	***489.5***	***48.9***	***36.14***	***4.07***	***52.7***	***0.107***
	STDEV	***19.2***	***8.9***	***0.67***	***0.79***	***9.0***	***0.018***
	Count	***13***	***12***	***12***	***13***	***12***	***12***
19	31-Aug	523.1		35.36			
	1-Sep			36.51			
	2-Sep			35.60			
	3-Sep			35.70			
	4-Sep			36.52			
	5-Sep			34.40			
	6-Sep			35.00	3.90	53.6	
	7-Sep			36.40			
	8-Sep			34.80			
	9-Sep			36.20			
	10-Sep		59.2	35.60	3.80	*51.4*	
	11-Sep	475.9	52.2	36.72	2.80	*36.7*	*0.077*
	12-Sep	475.9	38.2	36.76	3.73	*48.9*	*0.103*
	13-Sep	477.6	41.6	36.56	2.90	*38.2*	*0.080*
	14-Sep	490.8	71.0	35.51	3.95	*53.6*	*0.109*
	15-Sep	549.6	67.9	35.53	5.00	*67.8*	*0.123*
	AVG	***498.8***	***55.0***	***35.82***	***3.73***	***50.0***	***0.098***
	STDEV	***30.8***	***13.5***	***0.73***	***0.74***	***10.5***	***0.020***
	Count	***6***	***6***	***16***	***7***	***7***	***5***
20	16-Sep	517.1	50.7	36.16	5.27	*70.2*	*0.136*
	17-Sep	498.9	43.6	36.48	5.42	*71.5*	*0.143*
	18-Sep	497.9	52.7	36.24	4.92	*65.4*	*0.131*
	19-Sep	467.5	52.7	35.70	5.11	*68.9*	*0.147*
	20-Sep	495.9	41.4	36.52	5.20	*68.6*	*0.138*
	21-Sep	479.8	51.5	36.00	4.40	*58.8*	*0.123*
	22-Sep	462.6	47.5	35.64	5.19	*70.1*	*0.152*
	23-Sep		48.5	35.49	5.00	*67.8*	
	24-Sep	472.7	55.6	34.70	5.49	*76.2*	*0.161*
	25-Sep	490.9	66.7	35.04	5.23	*71.9*	*0.146*
	26-Sep	481.8	65.7	35.07	4.50	*61.8*	*0.128*
	27-Sep	452.5	71.1	34.06	4.00	*56.5*	*0.125*
	28-Sep	**415.4**		33.91	**3.22**		
	29-Sep			33.63	3.31	***47.4***	
	AVG	***477.8***	***54.0***	***35.33***	***4.85***	***67.3***	***0.139***
	STDEV	***26.6***	***9.3***	***0.96***	***0.63***	***5.7***	***0.012***
	Count	***12***	***12***	***14***	***13***	***12***	***11***
21	30-Sep	503.5		35.83	4.98	*66.9*	*0.133*
	1-Oct	496.5	44.0	35.21	4.60	*62.9*	*0.127*
	2-Oct	491.5	52.1	34.90	4.99	*68.8*	*0.140*
	3-Oct	501.0	53.4	36.00	4.88	*65.3*	*0.130*
	4-Oct	510.0		36.16	4.55	*60.6*	*0.119*
	5-Oct	518.1		34.31			
	6-Oct	508.0	60.5	36.16	4.53	*60.3*	*0.119*
	7-Oct	472.8	65.0	36.96	4.14	*53.9*	*0.114*
	8-Oct	495.8	73.2	36.74	5.25	*68.8*	*0.139*
	9-Oct	495.8	55.9	37.28	3.42	*44.2*	***0.089***
	10-Oct	445.0	44.7	37.32	3.75	*48.4*	*0.109*
	13-Oct	485.6	75.2	**31.76**	4.39		
	14-Oct	478.5	54.9	32.07			
	15-Oct	464.0	58.0				
	16-Oct	446.0	41.0	38.90	**6.30**		
	AVG	***487.5***	***56.5***	***35.99***	***4.50***	***60.0***	***0.125***
	STDEV	***22.2***	***10.8***	***1.67***	***0.55***	***8.6***	***0.011***
	Count	***15***	***12***	***13***	***11***	***10***	***9***

22	17-Oct	535.0		36.88	6.81	*88.9*	*0.166*
	18-Oct	481.0	50.0	38.56	8.00	*99.9*	*0.208*
	19-Oct	506.0	52.0	36.78	7.75	*101.4*	*0.200*
	20-Oct	514.0	61.0	37.44			
	21-Oct	515.0					
	22-Oct	512.0	63.0	34.57			
	23-Oct	492.5	56.3	**32.80**	6.90		
	24-Oct	522.2	61.4	35.82	6.94	*93.3*	*0.179*
	25-Oct	528.4	53.2	35.87	5.90	*79.2*	*0.150*
	26-Oct	532.5	59.4	36.00	5.87	*78.5*	*0.147*
	27-Oct	490.5	67.6	35.73	5.77	*77.7*	*0.159*
	28-Oct	486.4	**75.8**	35.28	5.20	*71.0*	*0.146*
	29-Oct	501.8	57.3	36.52	5.54	*73.0*	*0.146*
	AVG	***509.0***	***58.1***	***36.31***	***6.47***	***84.8***	***0.167***
	STDEV	***17.8***	***5.4***	***1.09***	***0.95***	***11.4***	***0.024***
	Count	***13***	***10***	***11***	***10***	***9***	***9***
23	2-Nov	513.0		36.54			
	3-Nov	520.2	**74.9**	36.08	6.30	*84.1*	*0.162*
	4-Nov	507.9	67.7	35.66	5.50	*74.3*	*0.146*
	5-Nov	492.5	60.5	35.92	5.30	*71.0*	*0.144*
	6-Nov	521.2	60.5	36.22	4.90	*65.1*	*0.125*
	7-Nov	474.0	55.4	35.96	4.60	*61.6*	*0.130*
	8-Nov	512.0	62.6	35.70	4.70	*63.4*	*0.124*
	9-Nov	472.0	47.2	36.16	5.60	*74.6*	*0.158*
	10-Nov	515.0	48.2	36.10	5.10	*68.0*	*0.132*
	11-Nov	500.7	55.4	35.78	5.80	*78.0*	*0.156*
	12-Nov	481.2	50.3	**34.62**	5.60		
	13-Nov	457.0	47.2	35.40	5.30	*72.1*	*0.158*
	14-Nov	460.8	47.2	35.42	6.40	*87.0*	***0.189***
	15-Nov	468.9	51.2	35.46	4.70	*63.8*	*0.136*
	16-Nov	453.8	50.2	35.56	3.80	*51.4*	*0.113*
	17-Nov	445.8	51.2	35.72	4.10	*55.3*	*0.124*
23b	18-Nov	480.9		35.30	**7.00**		
	19-Nov			34.96	5.40	*74.4*	
	AVG	***486.9***	***53.9***	***35.76***	***5.19***	***69.6***	***0.139***
	STDEV	***25.2***	***6.6***	***0.40***	***0.71***	***9.8***	***0.016***
	Count	***17***	***14***	***17***	***16***	***15***	***13***
24	21-Nov	537.1		35.00	3.90	*53.6*	***0.100***
	22-Nov	450.8	53.2	35.30	4.90	*66.8*	*0.148*
	23-Nov	480.9	35.1	35.32	5.10	*69.5*	*0.145*
	24-Nov	459.8	51.2	34.84	**3.60**		
	25-Nov	**380.5**	42.2	34.54	4.10	*57.1*	*0.150*
	26-Nov	473.8	60.5	34.50	4.20	*58.6*	*0.124*
	27-Nov	462.7	**74.6**				
	28-Nov	506.0	39.3	**32.32**	4.70		
	29-Nov	479.8	59.5	35.78	4.50	*60.5*	*0.126*
	30-Nov	477.8	63.5	36.58	4.40	*57.9*	*0.121*
	1-Dec	463.7	55.4	36.84	5.50	*71.9*	*0.155*
	2-Dec	502.0	40.3	37.34	4.80	*61.9*	*0.123*
	3-Dec	483.8	57.5	37.96	5.00	*63.4*	*0.131*
	4-Dec	491.9	50.4	36.58	5.20	*68.4*	*0.139*
	5-Dec	528.2	49.4	36.20	5.20	*69.2*	*0.131*
	6-Dec	515.1	52.4	35.91	4.90	*65.7*	*0.128*
	AVG	***487.6***	***50.7***	***35.91***	***4.74***	***63.4***	***0.135***
	STDEV	***25.6***	***8.6***	***1.06***	***0.47***	***5.6***	***0.012***
	Count	***15***	***14***	***14***	***14***	***13***	***12***
25	7-Dec	535.2					
	8-Dec	509.0	59.5	32.40	8.80	***130.8***	
	9-Dec	494.0	58.0	34.90	8.30	*114.5*	*0.232*
	10-Dec	**449.0**	82.0	35.40	7.90	*107.4*	*0.239*
	11-Dec	538.0	**88.0**	35.97	7.60	*101.7*	*0.189*
	12-Dec	528.0	72.0	36.06	6.80	*90.8*	*0.172*
	13-Dec	515.0	59.0	34.30	6.80	*95.4*	*0.185*
	14-Dec	519.0	65.0	34.30	6.30	*88.4*	*0.170*
	15-Dec	498.0	60.0	32.60	6.80	*100.4*	*0.202*
	16-Dec	478.0	55.0	34.98			
	17-Dec	491.0	57.0	36.82	6.30	*82.4*	*0.168*
	18-Dec	512.1	48.7	37.68	6.00	*76.7*	*0.150*
	AVG	***510.7***	***61.6***	***35.04***	***7.16***	***98.9***	***0.190***
	STDEV	***19.1***	***9.4***	***1.62***	***0.94***	***16.0***	***0.030***
	Count	***11***	***10***	***11***	***10***	***10***	***9***

APPENDIX B-3

SQUARE-WAVE FED SYSTEM DAILY OXYGEN UTILIZATION RATE (OUR) PROFILES AND RBCOD ESTIMATION

TABLE OF CONTENTS

APPENDIX B-3(a)

Analysis of original OUR data by Ekama et al. (1978) to establish criteria for determining the end of RBCOD utilization following the precipitous drop in OUR.

TABLE OF CONTENTS

Table. B3(a)-1. Estimating the time after the precipitous drop in OUR to the start of the SBCOD plateau for the original data (at similar operating conditions) by Ekama *et al.* (1978).

Test	Drop t (h)	End t(h)	Diff. (Δt)
L1	13.9	14.3	0.4
L2	13.85	14.1	0.25
L3	13.95	14.1	0.15
L4	13.9	14.45	**0.55**
L6	13.85	14.25	0.4
Longest	*13.95*		

Table. B3(a)-2. Estimation of the average RBCOD fraction with respect to total COD (f_{ts}) for the original experimental data by Ekama *et al.* (1978).

Source: [1]				Source: [2]		Calculated Values			
Test (L)	COD	OUR1	OUR2	Vp (L)	Qs (L/0.5d)	Qs (L/d)	ΔOUR	Sbsi	fts
1	570	40.3	32.2	6.73	18	*36*	*8.1*	*108.8*	*0.191*
2	535	34.7	30.2	6.73	18	*36*	*4.5*	*60.7*	*0.113*
3	550	39.1	30.3	6.73	18	*36*	*8.8*	*117.8*	*0.214*
4	515	40.5	34.9	6.73	18	*36*	*5.6*	*75.2*	*0.146*
6	490	25.0	20.2	6.73	18	*36*	*4.8*	*64.5*	*0.132*
								Avg	***0.159***
								Stdev	***0.04199***
								Min	***0.113***
								Max	***0.214***

Note: [1] Square wave experimental values (T=20 degC, pH = 7 tests): W27 Vol3, p.I.11-I.16

[2] System Configuration/Design Parameters: W27 Vol2, p.6.8 Table 6.2, in "Behaviour at 20 degC"

Table. B3(a)-3. Original Sbsi measurements in SQW system with similar operating conditions by Ekama *et al.* (1978): W27 vol.3, pp. I-11 to I-16.

L1			
t (h)	OUR1	tcont.	OUR
0.00	14.60	16.75	31.30
0.25	15.10	17.10	29.40
0.45	15.30	17.45	28.70
0.60	13.80	18.00	28.00
1.00	14.40	18.20	27.20
1.00	15.10	18.50	26.00
1.50	14.00	18.90	23.40
1.80	14.20	19.35	23.00
1.90	15.00	19.75	21.60
2.00	14.40	20.20	20.70
2.15	25.50	20.50	20.20
2.35	29.80	20.90	19.20
2.50	32.10	21.20	18.50
2.70	33.40	21.50	17.40
3.00	35.20	21.75	16.70
3.40	36.50	22.00	16.40
3.90	37.00	22.50	16.30
4.50	37.90	23.00	16.40
4.95	38.40	23.50	15.80
5.60	39.20	23.70	15.00
5.80	38.50	24.00	14.60
6.00	40.00	24.40	15.40
6.35	39.60	25.00	14.50
6.65	40.10	25.50	14.00
7.25	40.50	25.80	14.10
7.70	41.20	26.00	14.30
8.20	40.00		
8.85	40.80		
9.15	38.80		
9.35	40.00		
9.75	39.20		
10.20	40.00		
10.75	40.10		
11.40	40.50		
11.90	40.30		
12.30	40.10		
12.70	40.00		
13.10	40.20		
13.60	40.20		
13.90	**40.50**		
14.10	32.00		
14.30	**32.30**		
14.60	33.50		
14.80	33.80		
15.25	32.70		
15.60	32.40		
16.00	31.70		
16.50	32.00		

L2			
t (h)	OUR2	tcont.	OUR
0.00	15.20	21.70	18.50
0.85	14.60	22.30	16.20
1.00	15.30	23.00	15.60
1.40	14.40	23.45	15.80
1.45	15.40	24.00	15.30
1.85	14.40	24.90	14.80
1.90	15.20	25.35	14.40
2.20	25.20	25.70	14.50
2.40	27.60		
2.65	30.40		
3.00	30.70		
3.20	31.80		
3.50	32.50		
3.90	32.80		
4.50	33.10		
4.90	32.70		
5.35	33.50		
5.90	34.00		
6.45	34.10		
7.00	33.20		
7.50	34.10		
8.15	34.20		
8.75	33.90		
9.20	33.80		
9.80	34.70		
10.50	34.10		
10.95	34.40		
11.75	34.50		
12.15	34.90		
12.80	34.40		
13.10	34.80		
13.65	34.50		
13.85	**35.00**		
14.10	**30.40**		
14.40	30.10		
14.75	30.20		
15.15	28.80		
15.50	29.00		
16.00	27.40		
16.50	27.00		
17.00	26.20		
17.45	25.10		
17.90	24.60		
18.50	23.20		
19.15	21.90		
19.75	21.00		
20.30	20.50		
21.05	19.30		

L3			
t (h)	OUR3	tcont.	OUR
0.45	14.60	19.30	19.10
1.00	14.40	19.80	16.70
1.50	14.30	20.10	17.00
1.70	14.00	20.50	16.50
1.80	15.00	21.00	17.00
1.90	14.80	21.50	16.50
2.20	26.30	21.90	16.30
2.35	30.20	22.60	16.10
2.50	32.50	23.10	14.80
2.70	33.80	23.60	14.80
2.90	34.00	23.90	14.50
3.15	35.60	24.40	14.60
3.50	36.60	25.00	14.40
3.80	37.20	25.60	14.20
4.20	37.40		
4.50	37.70		
5.20	37.80		
5.50	38.20		
6.00	38.00		
6.50	37.80		
7.00	37.20		
7.50	38.00		
8.00	38.70		
8.60	39.60		
9.30	40.30		
9.90	39.00		
10.65	38.60		
11.20	38.00		
11.50	38.40		
12.00	37.30		
12.30	37.40		
13.00	39.60		
13.50	38.40		
13.95	**39.20**		
14.10	**30.40**		
14.30	29.70		
14.50	30.00		
14.70	30.40		
14.80	31.00		
15.25	31.00		
15.50	30.40		
16.00	30.00		
16.45	27.80		
16.70	27.20		
17.30	25.70		
18.00	23.60		
18.60	21.20		
19.00	20.40		

L4	
t (h)	OUR4
0.25	16.40
0.60	17.00
1.00	15.80
1.20	16.40
1.80	15.50
1.95	16.00
2.30	29.50
2.75	32.00
3.30	34.80
3.70	35.60
4.25	36.60
4.90	37.60
5.40	38.40
6.00	37.60
6.50	38.30
7.30	38.40
8.40	38.50
9.50	39.00
10.20	40.30
10.50	39.20
11.40	39.80
12.40	39.80
13.30	40.00
13.65	40.60
13.90	**41.00**
14.45	**34.70**
14.95	35.10
15.45	34.10
16.05	34.50
16.80	34.00
16.95	32.50
17.55	30.40
17.90	29.30
18.40	28.40
19.10	25.30
19.60	22.30
20.35	19.00
21.30	18.10
22.00	17.40
22.60	17.90
23.55	16.60
24.20	16.20
25.05	15.50
25.80	15.40

L6	
t (h)	OUR6
1.00	12.40
1.60	12.60
1.80	11.80
2.40	19.20
2.75	21.30
3.20	23.00
4.00	23.70
4.25	24.10
5.00	24.00
5.50	23.80
6.00	24.10
6.45	24.60
7.00	24.00
7.60	24.10
8.00	23.80
8.70	24.00
9.50	24.20
10.00	23.70
10.75	25.00
11.50	24.90
12.05	24.40
12.70	24.60
13.30	25.00
13.85	**24.70**
14.25	**20.60**
14.75	20.50
15.15	20.60
16.00	19.90
16.40	19.60
16.80	19.20
17.50	17.60
18.00	17.00
18.50	16.00
19.25	15.60
20.00	15.30
21.00	14.60
21.50	14.40
22.00	14.00
23.00	12.60
23.45	12.10
24.00	11.70
24.50	11.30
25.05	11.20
25.85	11.00

Figure B3(a)-1. Original Sbsi measurments in SQW system with similar operating conditions by Ekama *et al.*, 1978: W27, Vol3 p.I.11-16.

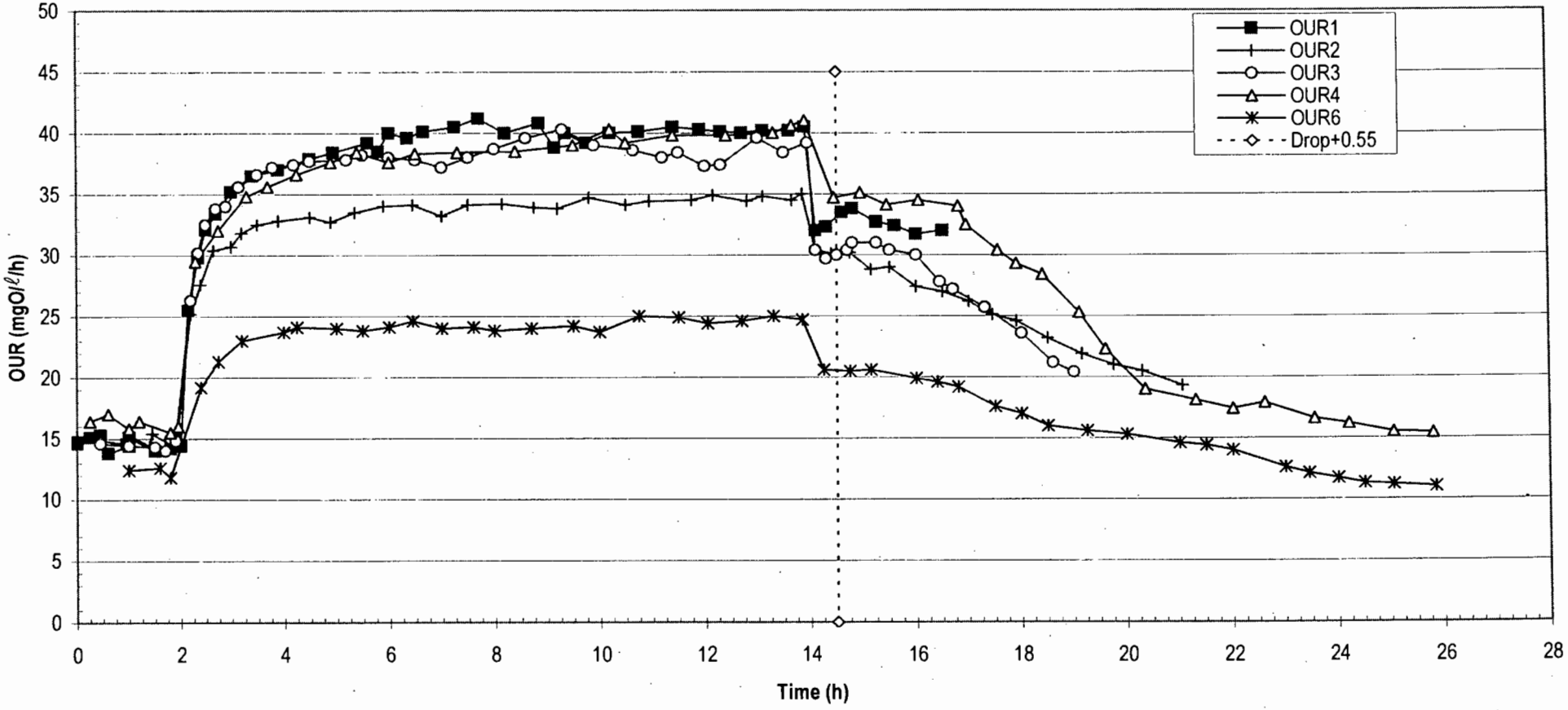

APPENDIX B-3(b)

SQW system daily data for measuring the RBCOD fraction in the influent wastewater. (Note: Data coincides with concurrent MLE operation and introduction of initial 4-hour anoxic period at start of feed cycle).

TABLE OF CONTENTS

Sewage Batch:

SB	Date	Day
18	16.08.02	271

Sbsi Drop (Time): 8.4

System Parameters:

Sti	498.9	mgCOD/ℓ
Suse	42.4	mgCOD/ℓ
Qs	35.73	ℓ/d
Sbsi	*59.3*	mgCOD/ℓ
fus	*0.085*	mgCOD/mgCOD
fts	*0.119*	mgCOD/mgCOD

Plot Sbsi (Max OUR) Plateau:

Sbsi Plat	x-Sbsi
0	20.2
18	20.2

Plot SBCOD OUR Plateau:

SBCOD Plat	x-SBCOD
0	15.8
18	*15.8*

Plot GAE-Sbsi End Criteria:

Sbsi End (Time)	Range
8.95	0
8.95	*23.2*

ΔOUR = *4.4* mgO/ℓ

Figure B3(b)-1. SB 18 SQW System OUR

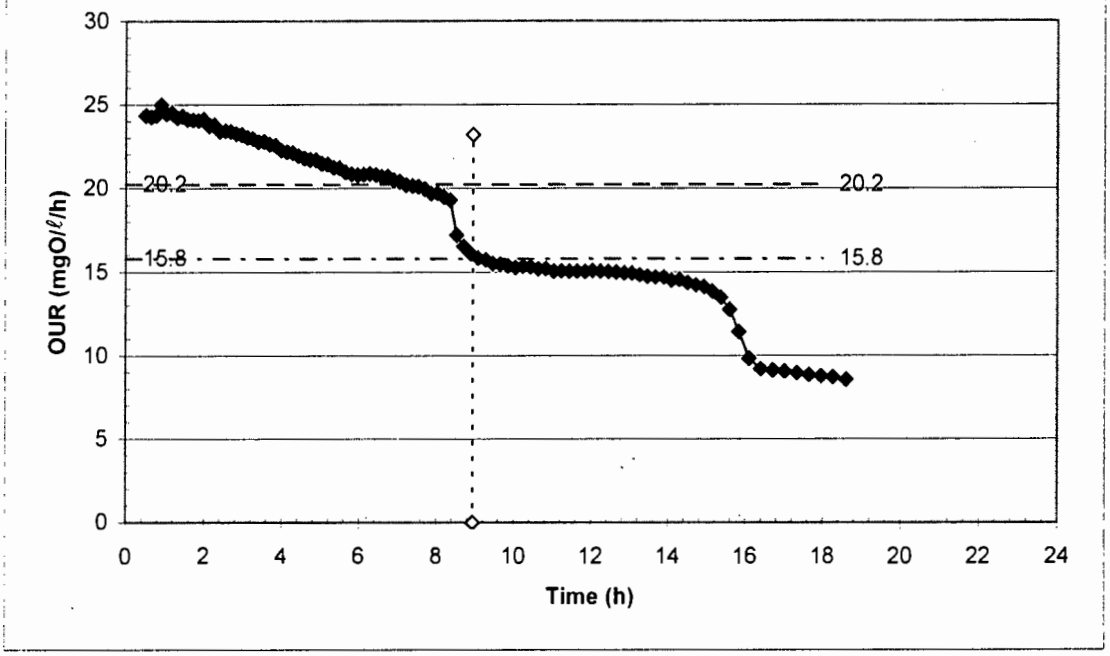

SB	Date	Day
18	17.08.02	272

Sbsi Drop (Time): 8.83

Plot Sbsi (Max OUR) Plateau:

Sbsi Plat	x-Sbsi
0	20
18	*20*

System Parameters:

Sti	501.1	mgCOD/ℓ
Suse	44.4	mgCOD/ℓ
Qs	36.7	ℓ/d
Sbsi	*52.6*	mgCOD/ℓ
fus	*0.089*	mgCOD/mgCOD
fts	*0.105*	mgCOD/mgCOD

Plot SBCOD OUR Plateau:

SBCOD Plat	x-SBCOD
0	15.99
18	*15.99*

Plot GAE-Sbsi End Criteria:

Sbsi End (Time)	Range
9.38	0
9.38	*23*

ΔOUR = *4.0* mgO/ℓ

Figure B3(b)-2. SB 18 SQW System OUR

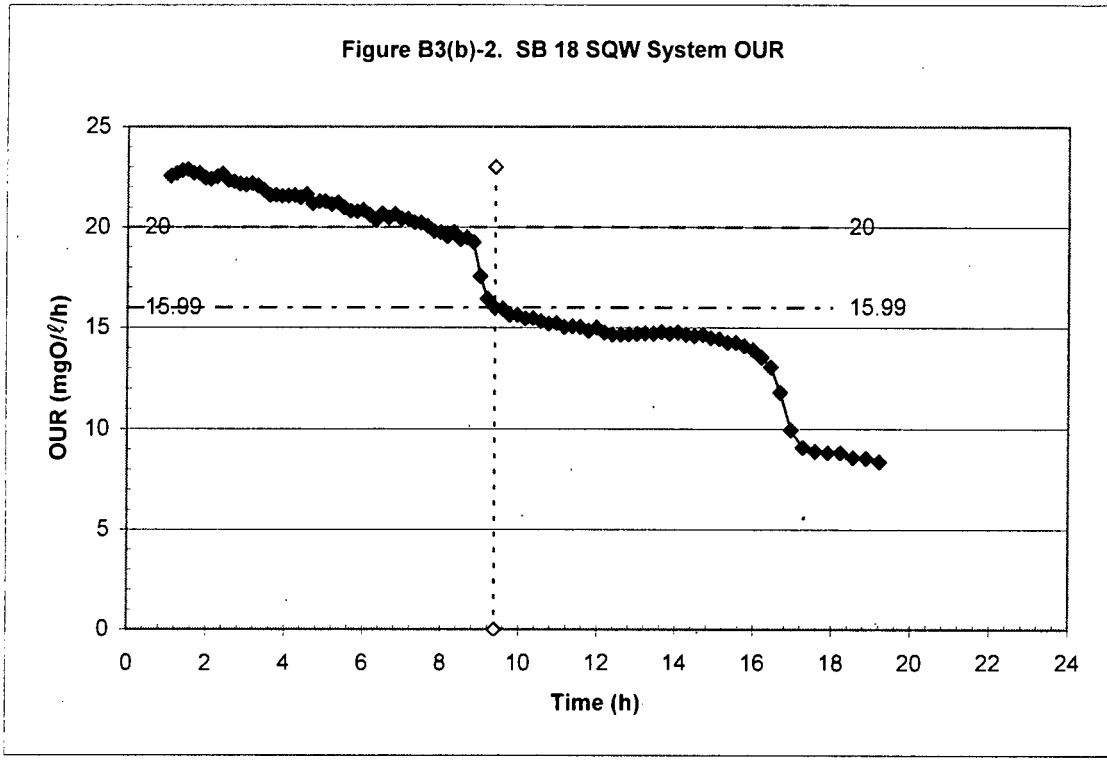

SB	Date	Day
18	18.08.02	273

Sbsi Drop (Time): 8.43

System Parameters:

Sti	484.8	mgCOD/ℓ
Suse	34.3	mgCOD/ℓ
Qs	36.86	ℓ/d
Sbsi	*54.9*	mgCOD/ℓ
fus	*0.071*	mgCOD/mgCOD
fts	*0.113*	mgCOD/mgCOD

Plot Sbsi (Max OUR) Plateau:

Sbsi Plat	x-Sbsi
0	19.6
18	*19.6*

Plot SBCOD OUR Plateau:

SBCOD Plat	x-SBCOD
0	15.4
18	*15.4*

Plot GAE-Sbsi End Criteria:

Sbsi End (Time)	Range
8.98	0
8.98	*22.6*

ΔOUR = 4.2 mgO/ℓ

Figure B3(b)-3. SB 18 SQW System OUR

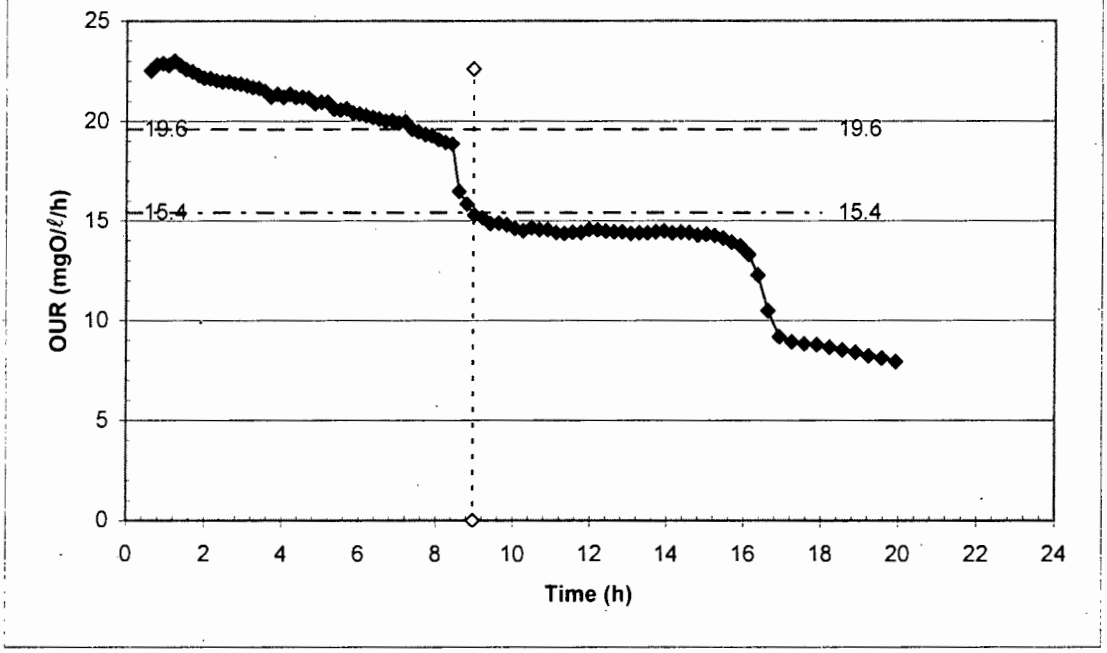

SB	Date	Day
18	19.08.02	274

Sbsi Drop (Time): 8.55

System Parameters:

Sti	457.8	mgCOD/ℓ
Suse	14.1	mgCOD/ℓ
Qs	34.96	ℓ/d
Sbsi	*44.8*	mgCOD/ℓ
fus	*0.031*	mgCOD/mgCOD
fts	*0.098*	mgCOD/mgCOD

Plot Sbsi (Max OUR) Plateau:

Sbsi Plat	x-Sbsi
0	22.65
18	*22.65*

Plot SBCOD OUR Plateau:

SBCOD Plat	x-SBCOD
0	19.4
18	*19.4*

Plot GAE-Sbsi End Criteria:

Sbsi End (Time)	Range
9.1	0
9.1	*25.65*

ΔOUR = *3.3* mgO/ℓ

Figure B3(b)-4. SB 18 SQW System OUR

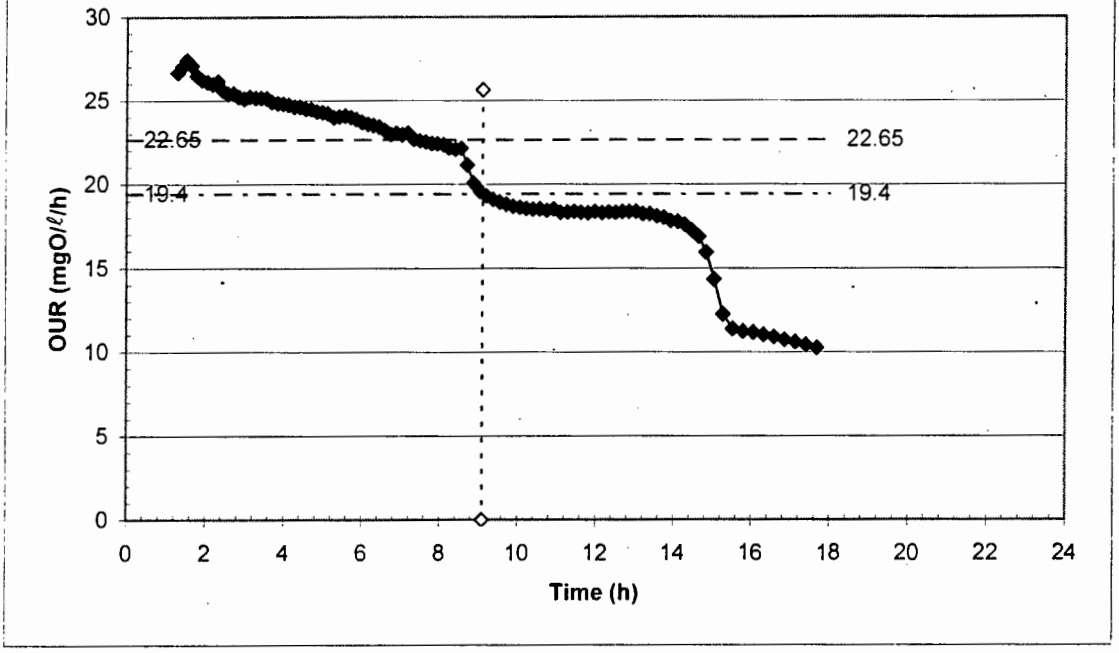

SB	Date	Day
18	20.08.02	275

Sbsi Drop (Time): **8.05**

System Parameters:

Sti	501	mgCOD/ℓ
Suse	51.2	mgCOD/ℓ
Qs	36.74	ℓ/d
Sbsi	*64.1*	mgCOD/ℓ
fus	*0.102*	mgCOD/mgCOD
fts	*0.128*	mgCOD/mgCOD

Plot Sbsi (Max OUR) Plateau:

Sbsi Plat	x-Sbsi
0	**25.56**
18	*25.56*

Plot SBCOD OUR Plateau:

SBCOD Plat	x-SBCOD
0	**20.67**
18	*20.67*

Plot GAE-Sbsi End Criteria:

Sbsi End (Time)	Range
8.6	0
8.6	*28.56*

ΔOUR = *4.9* mgO/ℓ

Figure B3(b)-5. SB 18 SQW System OUR

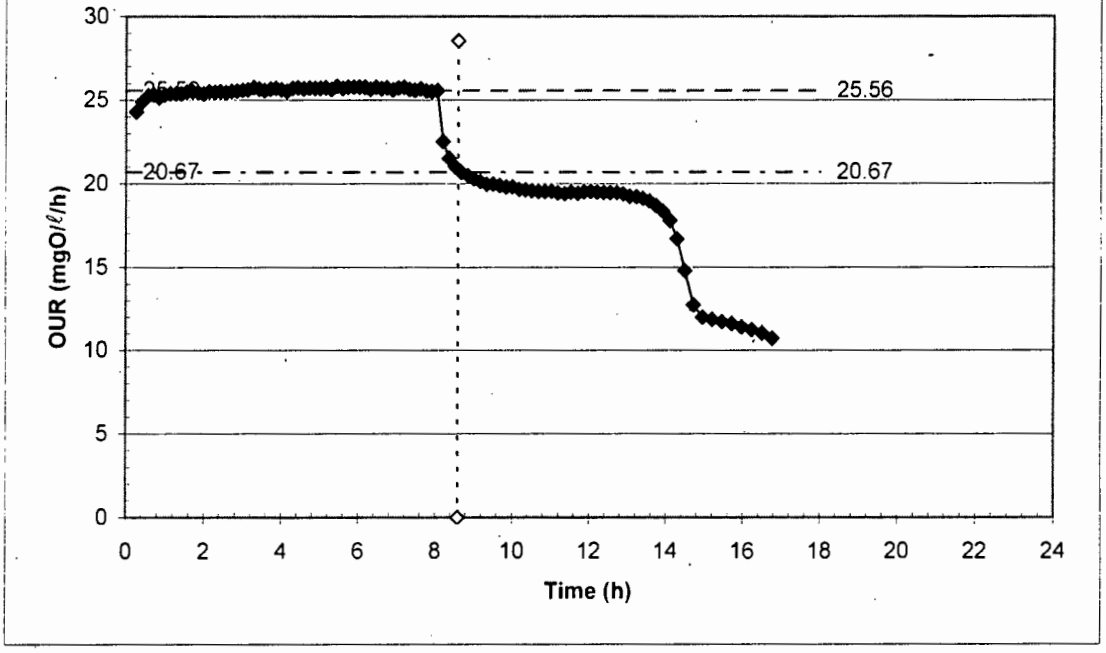

SB	Date	Day
18	21.08.02	276

Sbsi Drop (Time): 8.89

System Parameters:

Sti	490.9	mgCOD/ℓ
Suse	53	mgCOD/ℓ
Qs	36.68	ℓ/d
Sbsi	*58.7*	mgCOD/ℓ
fus	*0.108*	mgCOD/mgCOD
fts	*0.120*	mgCOD/mgCOD

Plot Sbsi (Max OUR) Plateau:

Sbsi Plat	x-Sbsi
0	29.96
18	*29.96*

Plot SBCOD OUR Plateau:

SBCOD Plat	x-SBCOD
0	25.49
18	*25.49*

Plot GAE-Sbsi End Criteria:

Sbsi End (Time)	Range
9.44	0
9.44	*32.96*

ΔOUR = *4.5* mgO/ℓ

Figure B3(b)-6. SB 18 SQW System OUR

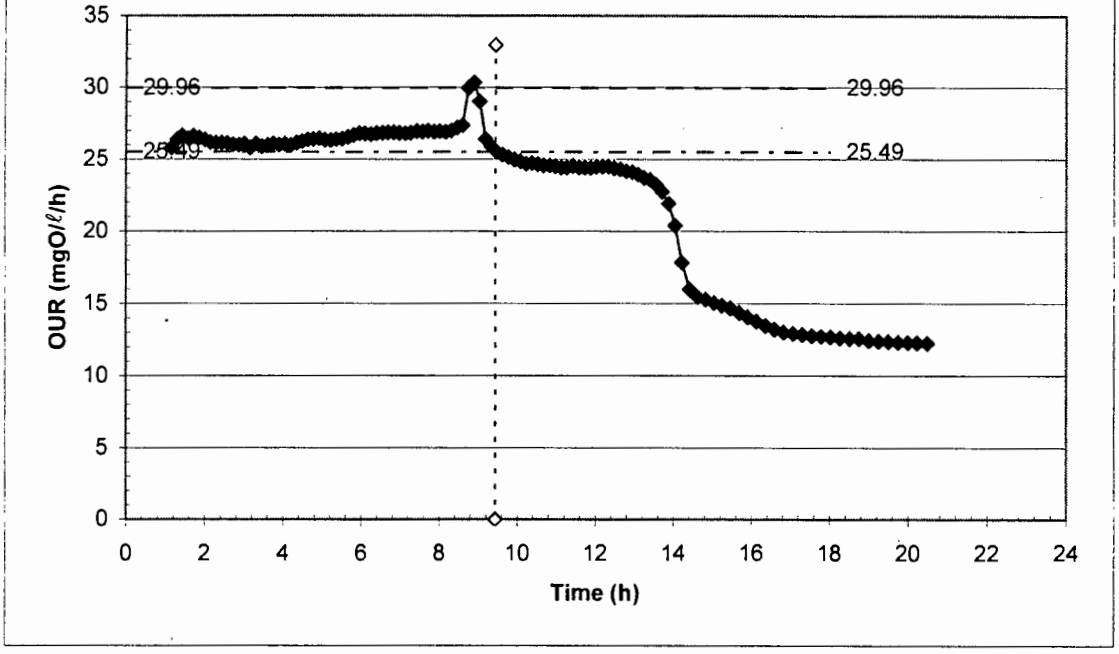

SB	Date	Day
18	22.08.02	277

Sbsi Drop (Time): **8.74**

System Parameters:

Sti	490.9	mgCOD/ℓ
Suse	42.6	mgCOD/ℓ
Qs	36.32	ℓ/d
Sbsi	*71.4*	mgCOD/ℓ
fus	*0.087*	mgCOD/mgCOD
fts	*0.146*	mgCOD/mgCOD

Plot Sbsi (Max OUR) Plateau:

Sbsi Plat	x-Sbsi
0	**27.97**
18	*27.97*

Plot SBCOD OUR Plateau:

SBCOD Plat	x-SBCOD
0	**22.58**
18	*22.58*

Plot GAE-Sbsi End Criteria:

Sbsi End (Time)	Range
9.29	0
9.29	*30.97*

ΔOUR = *5.4* mgO/ℓ

Figure B3(b)-7. SB 18 SQW System OUR

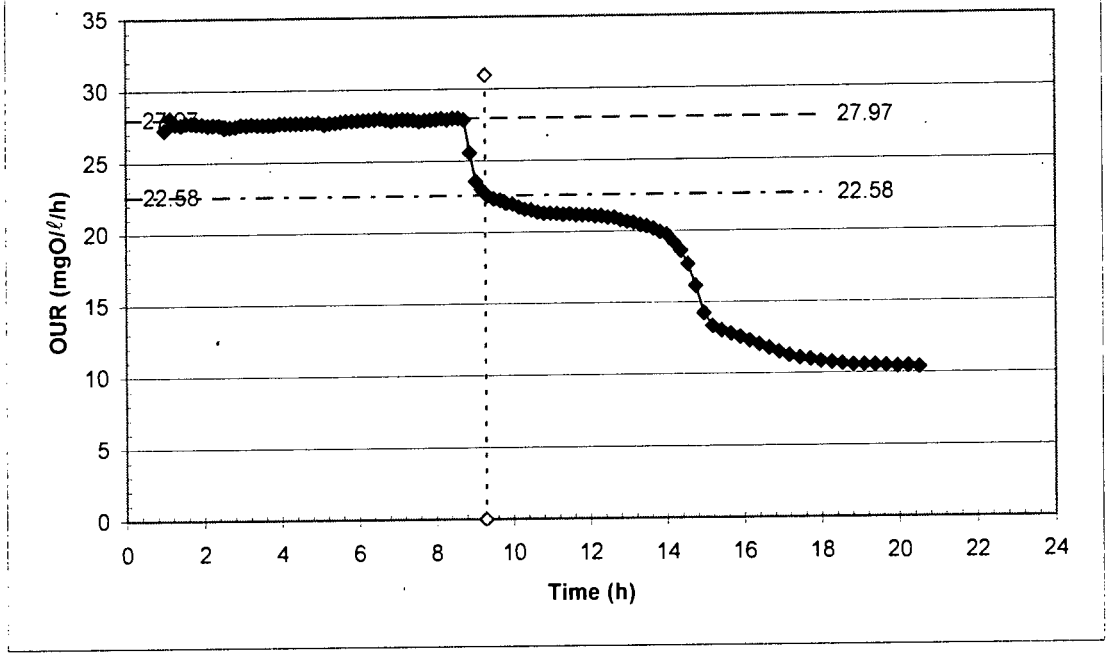

SB	Date	Day
18	23.08.02	278

Sbsi Drop (Time): 8.8

System Parameters:

Sti	472.2	mgCOD/ℓ
Suse	47.8	mgCOD/ℓ
Qs	41.2	ℓ/d
Sbsi	*64.9*	mgCOD/ℓ
fus	*0.101*	mgCOD/mgCOD
fts	*0.137*	mgCOD/mgCOD

Plot Sbsi (Max OUR) Plateau:

Sbsi Plat	x-Sbsi
0	**26.15**
18	*26.15*

Plot SBCOD OUR Plateau:

SBCOD Plat	x-SBCOD
0	**20.6**
18	*20.6*

Plot GAE-Sbsi End Criteria:

Sbsi End (Time)	Range
9.35	0
9.35	*29.15*

ΔOUR = *5.6* mgO/ℓ

Figure B3(b)-8. SB 18 SQW System OUR

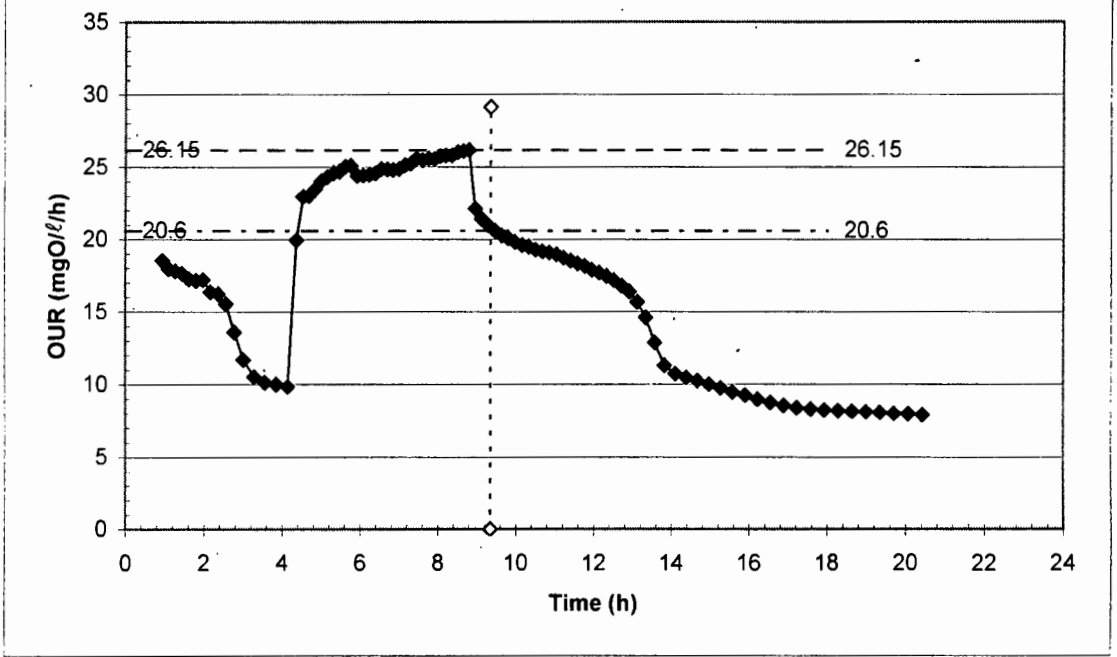

SB	Date	Day
18	24.08.02	279

Sbsi Drop (Time): **14.16**

System Parameters:

Sti	463.8	mgCOD/ℓ
Suse	49.9	mgCOD/ℓ
Qs	34.88	ℓ/d
Sbsi	*50.0*	mgCOD/ℓ
fus	*0.108*	mgCOD/mgCOD
fts	*0.108*	mgCOD/mgCOD

Plot Sbsi (Max OUR) Plateau:

Sbsi Plat	x-Sbsi
0	**22.2**
18	22.2

Plot SBCOD OUR Plateau:

SBCOD Plat	x-SBCOD
0	**18.58**
18	*18.58*

Plot GAE-Sbsi End Criteria:

Sbsi End (Time)	Range
14.71	0
14.71	*25.2*

ΔOUR = *3.6* mgO/ℓ

Figure B3(b)-9. SB 18 SQW System OUR

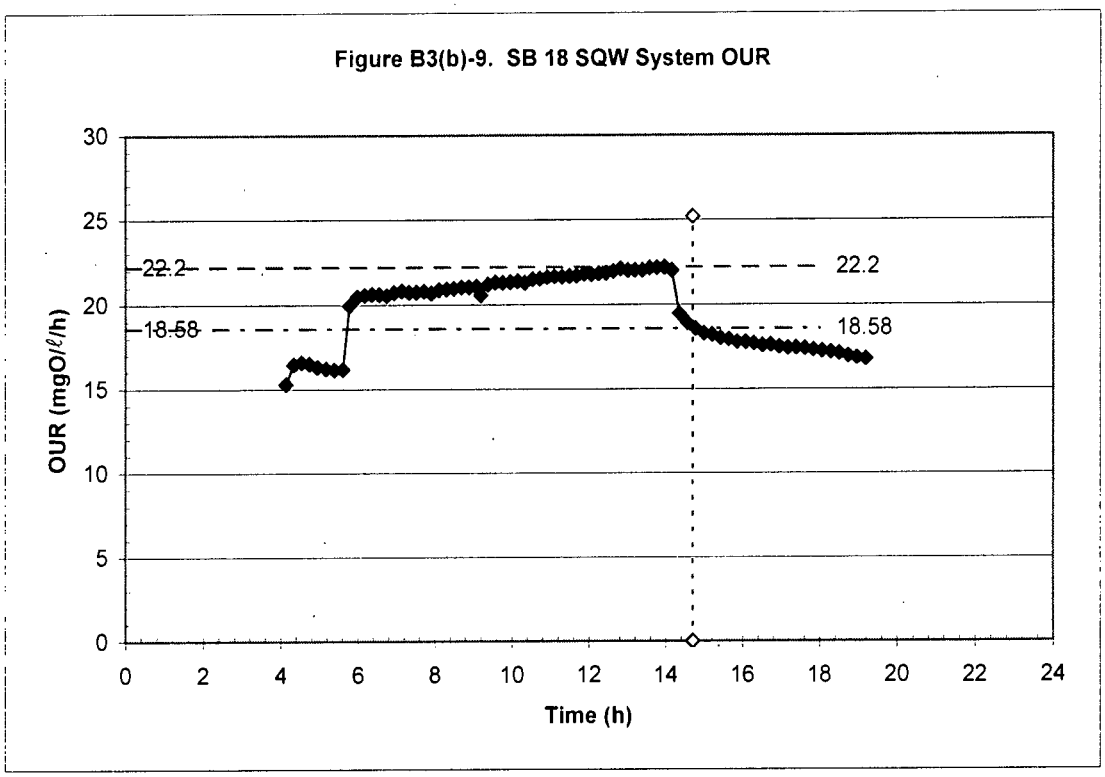

SB	Date	Day
18	25.08.02	280

Sbsi Drop (Time): **8.2**

System Parameters:

Sti	483.6	mgCOD/ℓ
Suse	48.9	mgCOD/ℓ
Qs	36.16	ℓ/d
Sbsi	*57.3*	mgCOD/ℓ
fus	*0.101*	mgCOD/mgCOD
fts	*0.118*	mgCOD/mgCOD

Plot Sbsi (Max OUR) Plateau:

Sbsi Plat	x-Sbsi
0	**26**
18	*26*

Plot SBCOD OUR Plateau:

SBCOD Plat	x-SBCOD
0	**21.7**
18	*21.7*

Plot GAE-Sbsi End Criteria:

Sbsi End (Time)	Range
8.75	0
8.75	*29*

ΔOUR = *4.3* mgO/ℓ

Figure B3(b)-10. SB 18 SQW System OUR

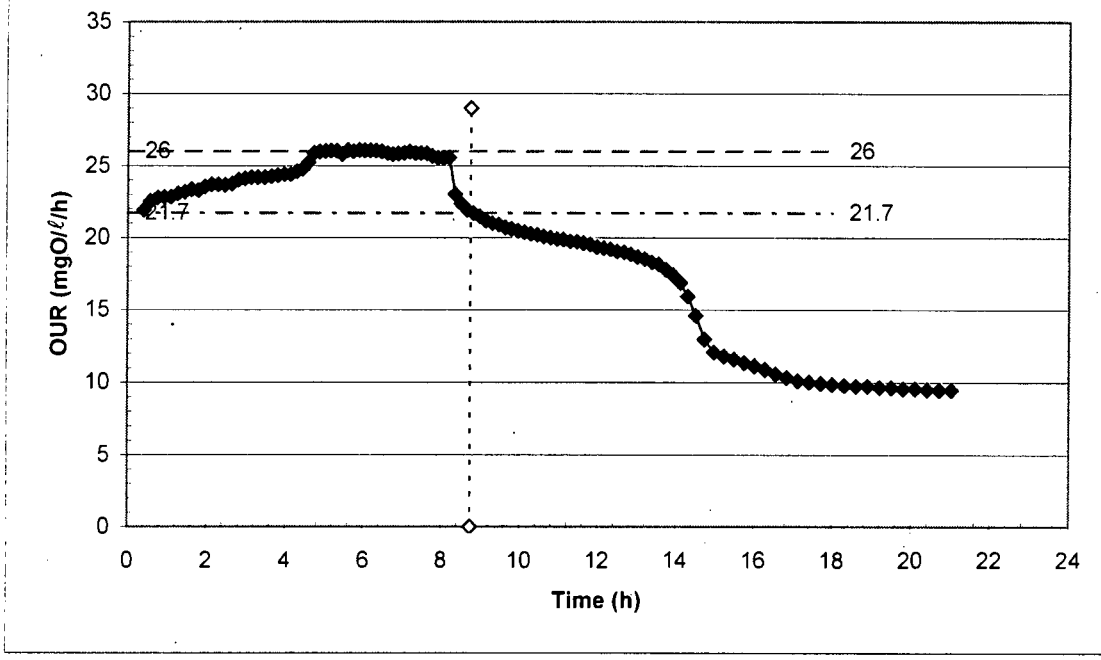

SB	Date	Day
18	26.08.02	281

Sbsi Drop (Time): **9.29**

System Parameters:

Sti	476.3	mgCOD/ℓ
Suse	43.7	mgCOD/ℓ
Qs	36.68	ℓ/d
Sbsi	*58.0*	mgCOD/ℓ
fus	*0.092*	mgCOD/mgCOD
fts	*0.122*	mgCOD/mgCOD

Plot Sbsi (Max OUR) Plateau:

Sbsi Plat	x-Sbsi
0	**24.6**
18	*24.6*

Plot SBCOD OUR Plateau:

SBCOD Plat	x-SBCOD
0	**20.18**
18	*20.18*

Plot GAE-Sbsi End Criteria:

Sbsi End (Time)	Range
9.84	0
9.84	*27.6*

ΔOUR = *4.4* mgO/ℓ

Figure B3(b)-11. SB 18 SQW System OUR

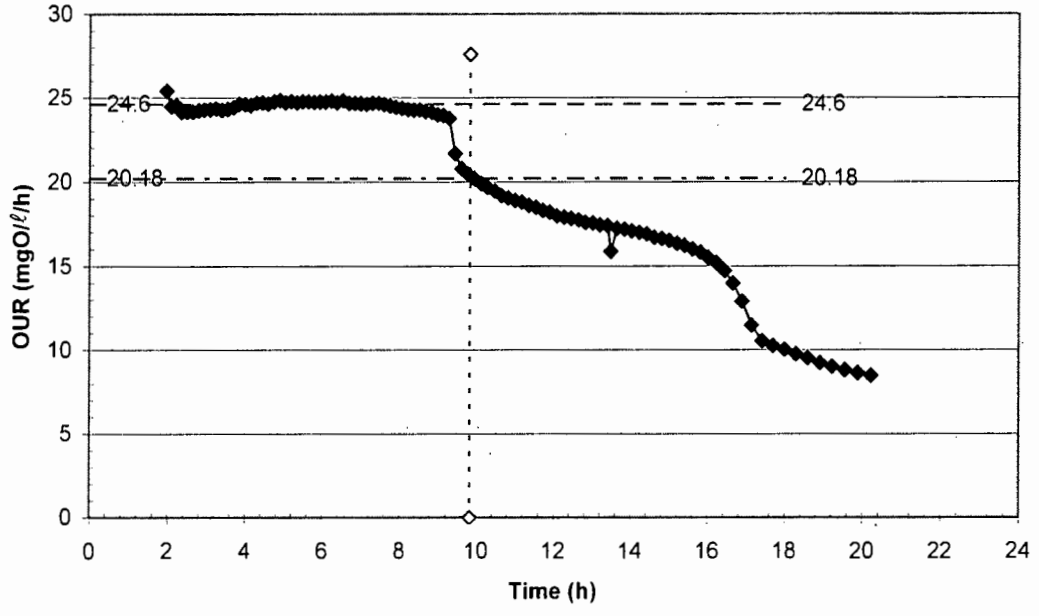

SB	Date	Day
18	27.08.02	282

Sbsi Drop (Time): **8.67**

System Parameters:

Sti	523.1	mgCOD/ℓ
Suse	66.6	mgCOD/ℓ
Qs	35.9	ℓ/d
Sbsi	*56.3*	mgCOD/ℓ
fus	*0.127*	mgCOD/mgCOD
fts	*0.108*	mgCOD/mgCOD

Plot Sbsi (Max OUR) Plateau:

Sbsi Plat	x-Sbsi
0	**25.3**
18	*25.3*

Plot SBCOD OUR Plateau:

SBCOD Plat	x-SBCOD
0	**21.1**
18	*21.1*

Plot GAE-Sbsi End Criteria:

Sbsi End (Time)	Range
9.22	0
9.22	*28.3*

ΔOUR = *4.2* mgO/ℓ

Figure B3(b)-12. SB 18 SQW System OUR

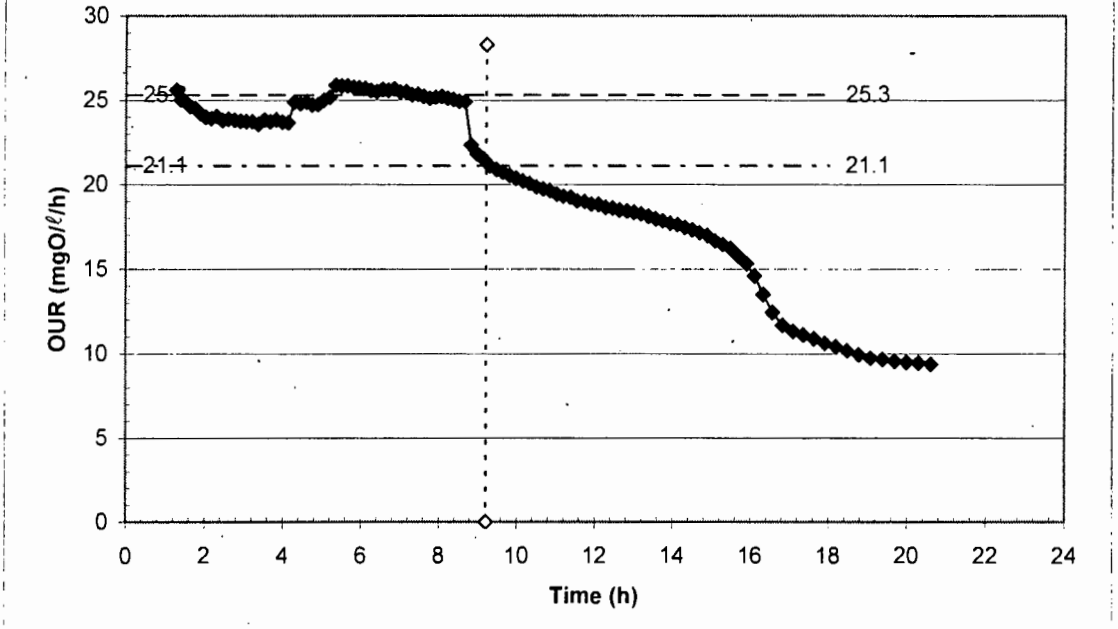

SB	Date	Day
18	28.08.02	283

Sbsi Drop (Time): **9.1**

System Parameters:

Sti	514.8	mgCOD/ℓ
Suse	41.6	mgCOD/ℓ
Qs	35.92	ℓ/d
Sbsi	*57.0*	mgCOD/ℓ
fus	*0.081*	mgCOD/mgCOD
fts	*0.111*	mgCOD/mgCOD

Plot Sbsi (Max OUR) Plateau:

Sbsi Plat	x-Sbsi
0	**23.35**
18	*23.35*

Plot SBCOD OUR Plateau:

SBCOD Plat	x-SBCOD
0	**19.1**
18	*19.1*

Plot GAE-Sbsi End Criteria:

Sbsi End (Time)	Range
9.65	0
9.65	*26.35*

ΔOUR = *4.3* mgO/ℓ

Figure B3(b)-13. SB 18 SQW System OUR

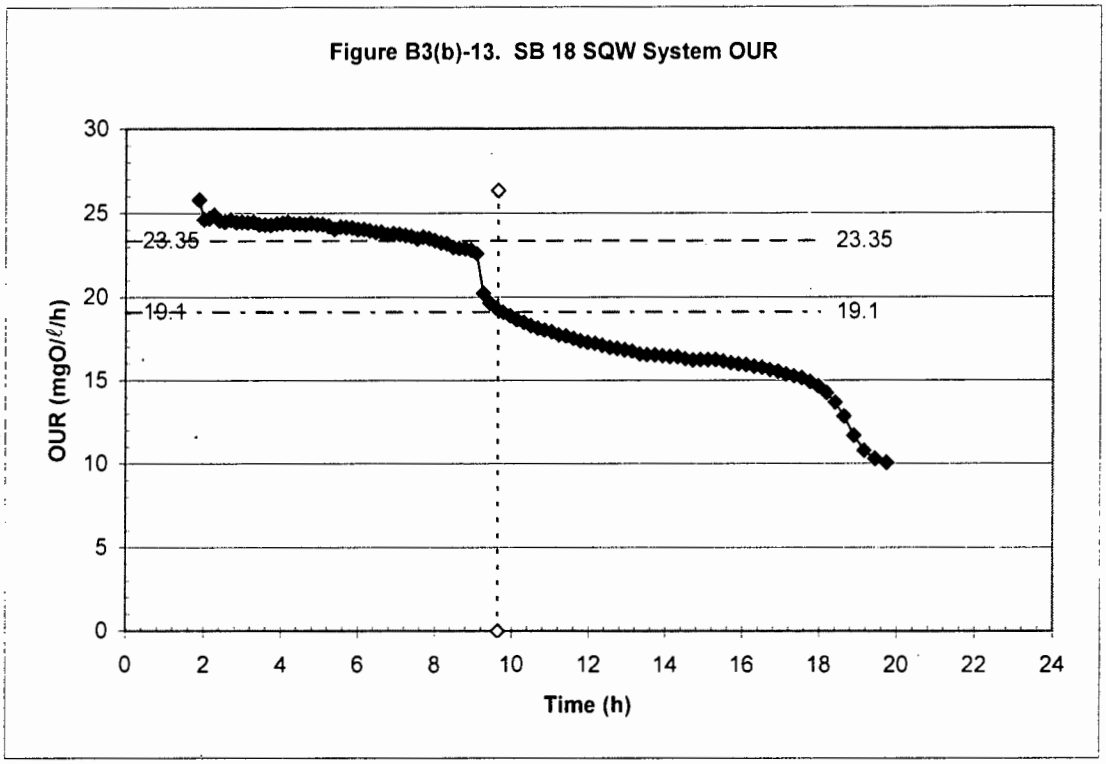

SB	Date	Day
18	29.08.02	284

Sbsi Drop (Time): 7.94

System Parameters:

Sti	503.4	mgCOD/ℓ
Suse	62.4	mgCOD/ℓ
Qs	35.9	ℓ/d
Sbsi	*47.6*	mgCOD/ℓ
fus	*0.124*	mgCOD/mgCOD
fts	*0.095*	mgCOD/mgCOD

Plot Sbsi (Max OUR) Plateau:

Sbsi Plat	x-Sbsi
0	24
18	*24*

Plot SBCOD OUR Plateau:

SBCOD Plat	x-SBCOD
0	20.45
18	*20.45*

Plot GAE-Sbsi End Criteria:

Sbsi End (Time)	Range
8.49	0
8.49	*27*

ΔOUR = *3.6* mgO/ℓ

Figure B3(b)-14. SB 18 SQW System OUR

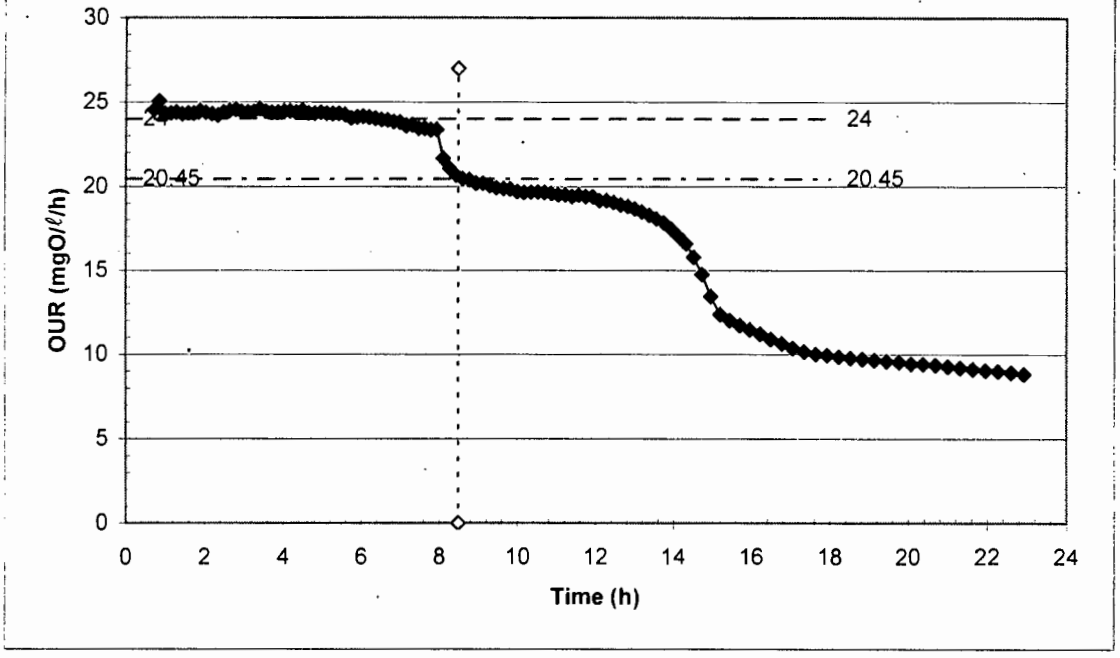

SB	Date	Day
19	06.09.02	292

Sbsi Drop (Time): **8.62**

System Parameters:

Sti	554.2	mgCOD/ℓ
Suse	44.2	mgCOD/ℓ
Qs	35	ℓ/d
Sbsi	*56.4*	mgCOD/ℓ
fus	*0.080*	mgCOD/mgCOD
fts	*0.102*	mgCOD/mgCOD

Plot Sbsi (Max OUR) Plateau:

Sbsi Plat	x-Sbsi
0	**26.4**
18	26.4

Plot SBCOD OUR Plateau:

SBCOD Plat	x-SBCOD
0	**22.3**
18	22.3

Plot GAE-Sbsi End Criteria:

Sbsi End (Time)	Range
9.17	0
9.17	*29.4*

ΔOUR = *4.1* mgO/ℓ

Figure B3(b)-15. SB 19 SQW System OUR

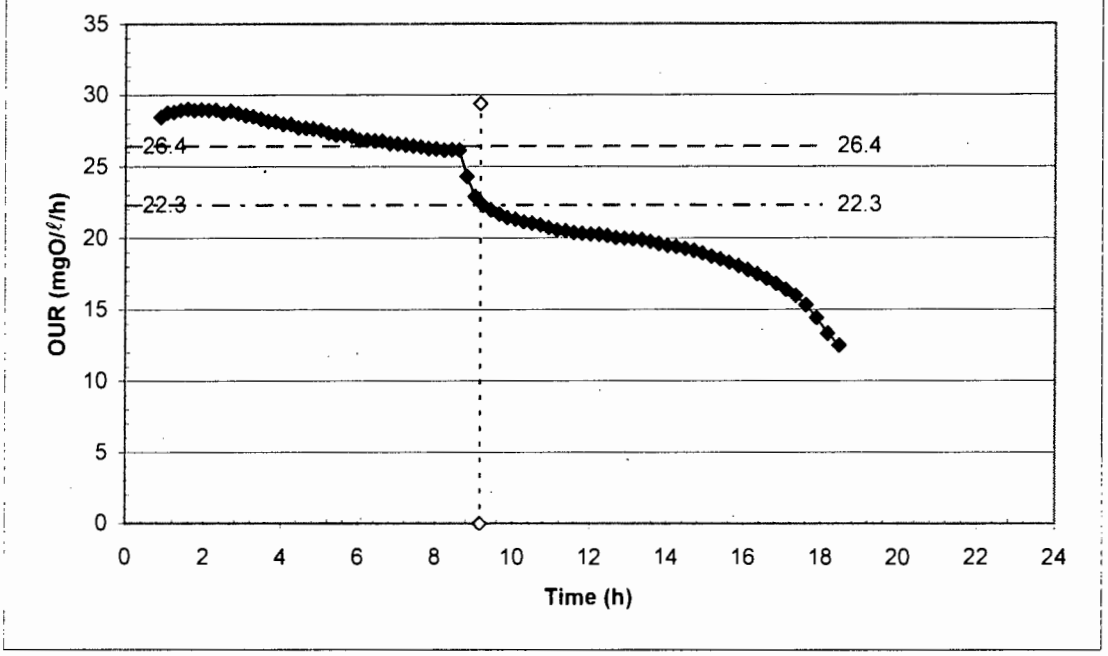

SB	Date	Day
19	10.09.02	296

Sbsi Drop (Time): 8.52

System Parameters:

Sti	513	mgCOD/ℓ
Suse	59.2	mgCOD/ℓ
Qs	35.6	ℓ/d
Sbsi	*55.4*	mgCOD/ℓ
fus	*0.115*	mgCOD/mgCOD
fts	*0.108*	mgCOD/mgCOD

Plot Sbsi (Max OUR) Plateau:

Sbsi Plat	x-Sbsi
0	22.7
18	22.7

Plot SBCOD OUR Plateau:

SBCOD Plat	x-SBCOD
0	18.6
18	*18.6*

Plot GAE-Sbsi End Criteria:

Sbsi End (Time)	Range
9.07	0
9.07	*25.7*

ΔOUR = *4.1* mgO/ℓ

Figure B3(b)-16. SB 19 SQW System OUR

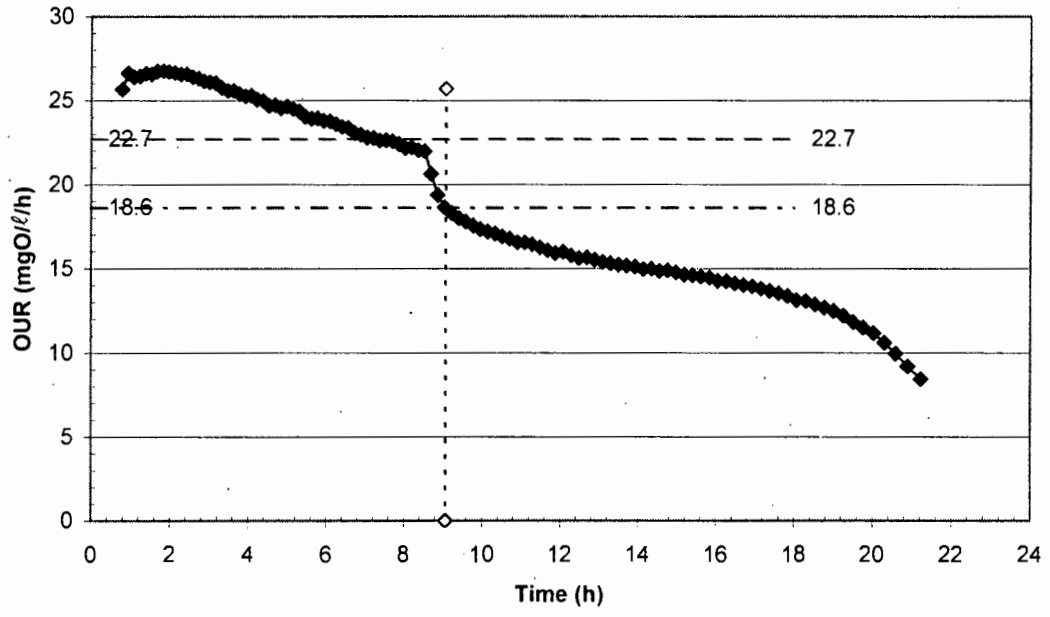

SB	Date	Day
19	11.09.02	297

Sbsi Drop (Time): 4.9

System Parameters:

Sti	475.9	mgCOD/ℓ
Suse	52.2	mgCOD/ℓ
Qs	36.72	ℓ/d
Sbsi	*39.3*	mgCOD/ℓ
fus	*0.110*	mgCOD/mgCOD
fts	*0.083*	mgCOD/mgCOD

Plot Sbsi (Max OUR) Plateau:

Sbsi Plat	x-Sbsi
0	25.6
18	*25.6*

Plot SBCOD OUR Plateau:

SBCOD Plat	x-SBCOD
0	22.6
18	*22.6*

Plot GAE-Sbsi End Criteria:

Sbsi End (Time)	Range
5.45	0
5.45	*28.6*

ΔOUR = *3.0* mgO/ℓ

Figure B3(b)-17. SB 19 SQW System OUR

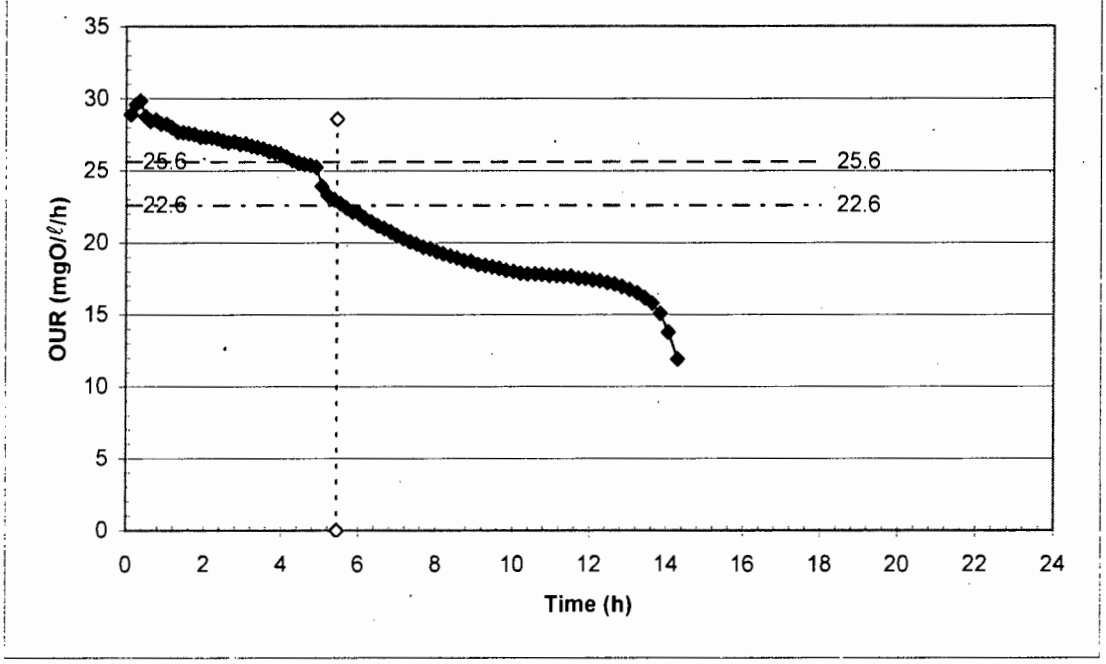

SB	Date	Day
19	12.09.02	298

Sbsi Drop (Time): **8.42**

System Parameters:

Sti	475.9	mgCOD/ℓ
Suse	38.2	mgCOD/ℓ
Qs	36.76	ℓ/d
Sbsi	*49.8*	mgCOD/ℓ
fus	*0.080*	mgCOD/mgCOD
fts	*0.105*	mgCOD/mgCOD

Plot Sbsi (Max OUR) Plateau:

Sbsi Plat	x-Sbsi
0	**24.7**
18	*24.7*

Plot SBCOD OUR Plateau:

SBCOD Plat	x-SBCOD
0	**20.9**
18	*20.9*

Plot GAE-Sbsi End Criteria:

Sbsi End (Time)	Range
8.97	0
8.97	*27.7*

ΔOUR =	3.8	mgO/ℓ

Figure B3(b)-18. SB 19 SQW System OUR

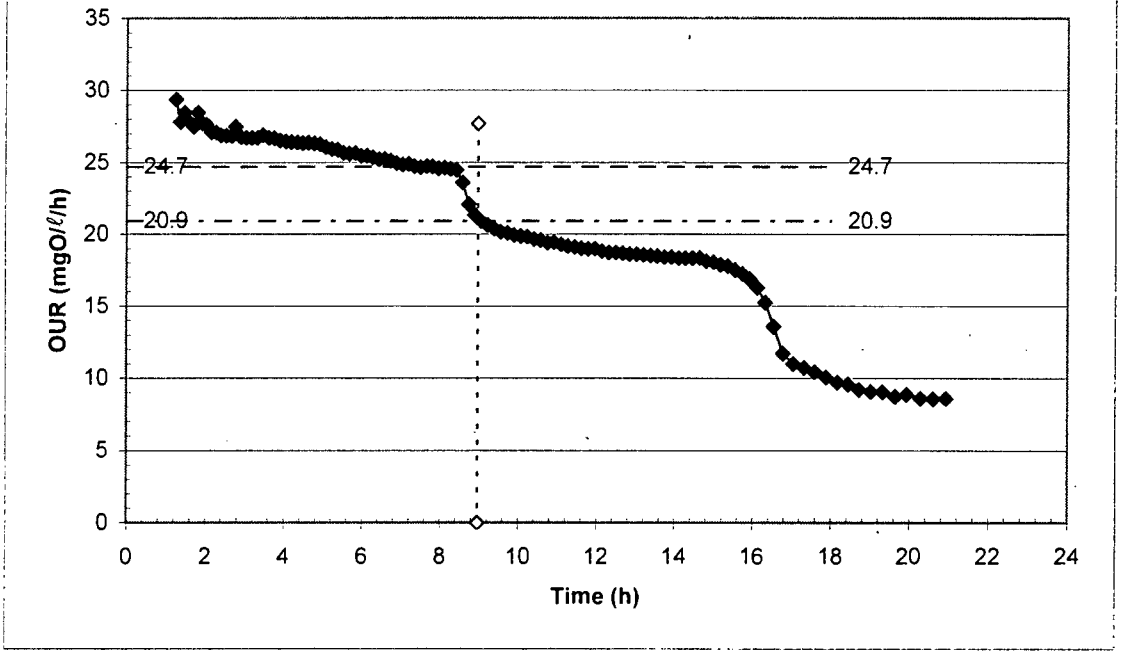

SB	Date	Day
19	13.09.02	299

Sbsi Drop (Time): 9.2

System Parameters:

Sti	477.6	mgCOD/ℓ
Suse	41.6	mgCOD/ℓ
Qs	36.56	ℓ/d
Sbsi	*40.8*	mgCOD/ℓ
fus	*0.087*	mgCOD/mgCOD
fts	*0.085*	mgCOD/mgCOD

Plot Sbsi (Max OUR) Plateau:

Sbsi Plat	x-Sbsi
0	22.6
18	*22.6*

Plot SBCOD OUR Plateau:

SBCOD Plat	x-SBCOD
0	19.5
18	*19.5*

Plot GAE-Sbsi End Criteria:

Sbsi End (Time)	Range
9.75	0
9.75	*25.6*

ΔOUR = *3.1* mgO/ℓ

Figure B3(b)-19. SB 19 SQW System OUR

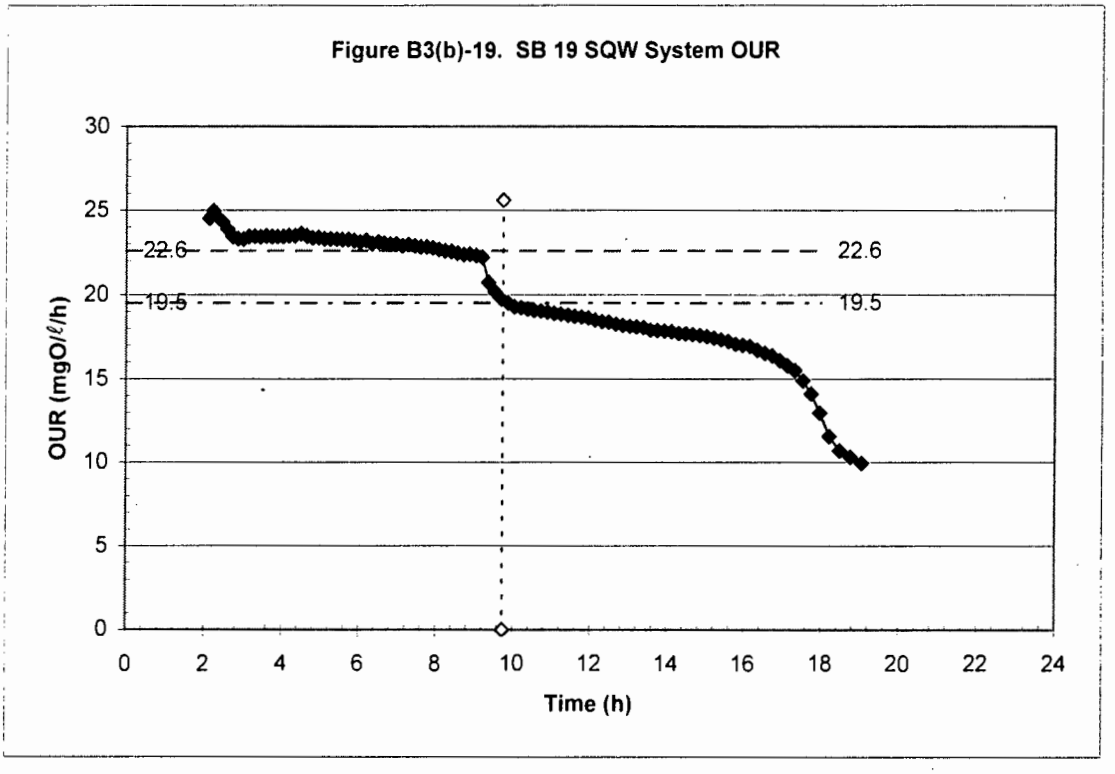

SB	Date	Day
19	14.9.02	300

Sbsi Drop (Time): 8.17

System Parameters:

Sti	490.8	mgCOD/ℓ
Suse	71	mgCOD/ℓ
Qs	35.51	ℓ/d
Sbsi	*52.2*	mgCOD/ℓ
fus	*0.145*	mgCOD/mgCOD
fts	*0.106*	mgCOD/mgCOD

Plot Sbsi (Max OUR) Plateau:

Sbsi Plat	x-Sbsi
0	25.55
18	*25.55*

Plot SBCOD OUR Plateau:

SBCOD Plat	x-SBCOD
0	21.7
18	*21.7*

Plot GAE-Sbsi End Criteria:

Sbsi End (Time)	Range
8.72	0
8.72	*28.55*

ΔOUR = *3.9* mgO/ℓ

Figure B3(b)-20. SB 19 SQW System OUR

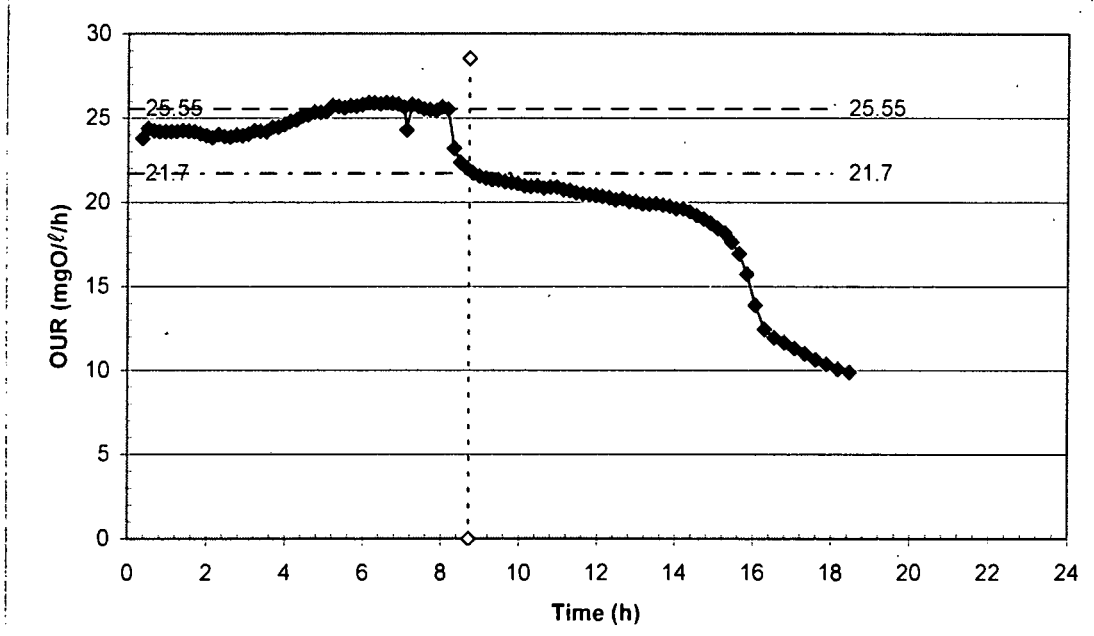

SB	Date	Day
19	15.09.02	301

Sbsi Drop (Time): **8.52**

System Parameters:

Sti	549.6	mgCOD/ℓ
Suse	67.9	mgCOD/ℓ
Qs	35.53	ℓ/d
Sbsi	*73.8*	mgCOD/ℓ
fus	*0.124*	mgCOD/mgCOD
fts	*0.134*	mgCOD/mgCOD

Plot Sbsi (Max OUR) Plateau:

Sbsi Plat	x-Sbsi
0	**28**
18	*28*

Plot SBCOD OUR Plateau:

SBCOD Plat	x-SBCOD
0	**22.55**
18	*22.55*

Plot GAE-Sbsi End Criteria:

Sbsi End (Time)	Range
9.07	0
9.07	*31*

ΔOUR = *5.5* mgO/ℓ

Figure B3(b)-21. SB 19 SQW System OUR

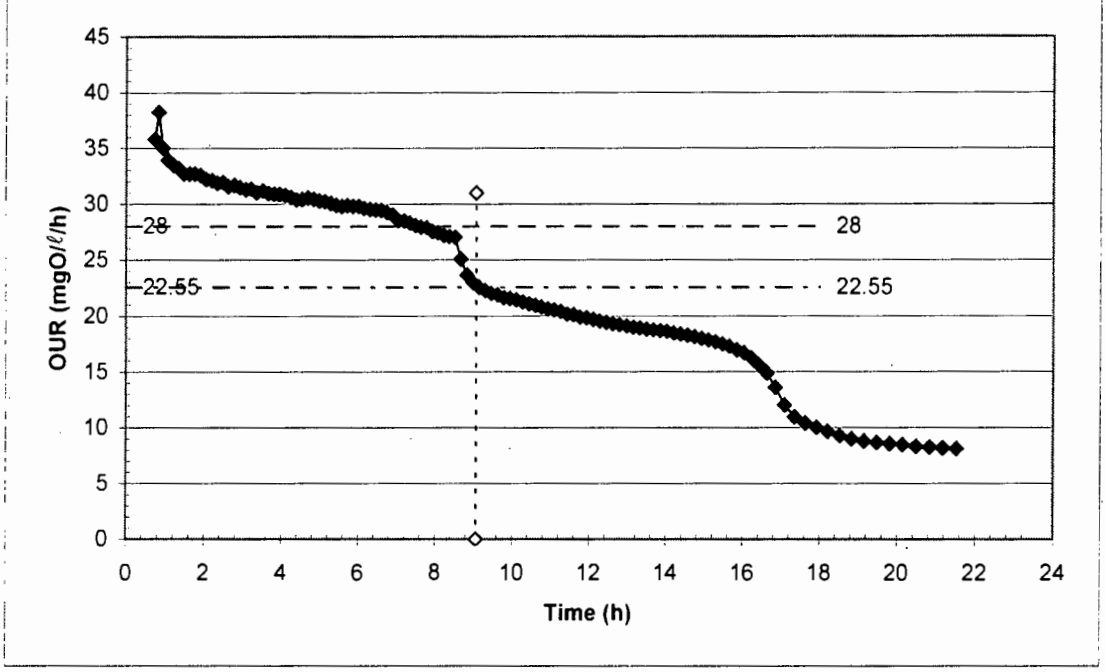

SB	Date	Day
20	16.09.02	302

Sbsi Drop (Time): **8.22**

System Parameters:

Sti	517.1	mgCOD/ℓ
Suse	50.7	mgCOD/ℓ
Qs	36.16	ℓ/d
Sbsi	*77.2*	mgCOD/ℓ
fus	*0.098*	mgCOD/mgCOD
fts	*0.149*	mgCOD/mgCOD

Plot Sbsi (Max OUR) Plateau:

Sbsi Plat	x-Sbsi
0	**30**
18	*30*

Plot SBCOD OUR Plateau:

SBCOD Plat	x-SBCOD
0	**24.2**
18	*24.2*

Plot GAE-Sbsi End Criteria:

Sbsi End (Time)	Range
8.77	0
8.77	*33*

ΔOUR = *5.8* mgO/ℓ

Figure B3(b)-22. SB 20 SQW System OUR

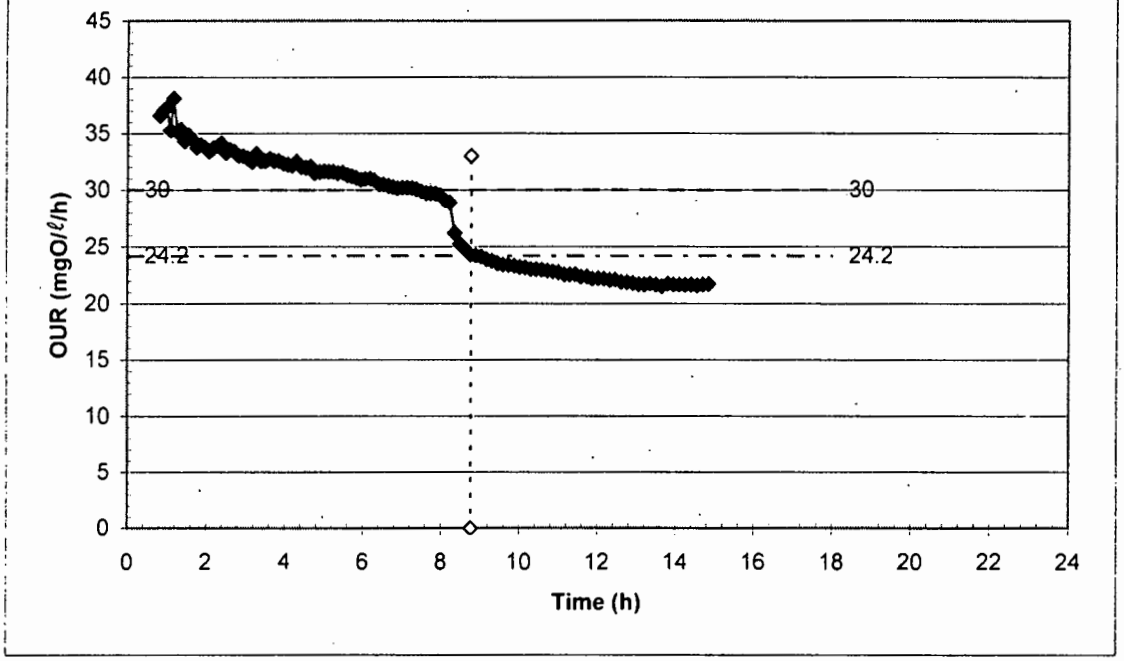

SB	Date	Day
20	17.09.02	303

Sbsi Drop (Time): **8.93**

System Parameters:

Sti	498.9	mgCOD/ℓ
Suse	43.6	mgCOD/ℓ
Qs	36.48	ℓ/d
Sbsi	*75.9*	mgCOD/ℓ
fus	*0.087*	mgCOD/mgCOD
fts	*0.152*	mgCOD/mgCOD

Plot Sbsi (Max OUR) Plateau:

Sbsi Plat	x-Sbsi
0	**29.4**
18	*29.4*

Plot SBCOD OUR Plateau:

SBCOD Plat	x-SBCOD
0	**23.65**
18	*23.65*

Plot GAE-Sbsi End Criteria:

Sbsi End (Time)	Range
9.48	0
9.48	*32.4*

ΔOUR = *5.8* mgO/ℓ

Figure B3(b)-23. SB 20 SQW System OUR

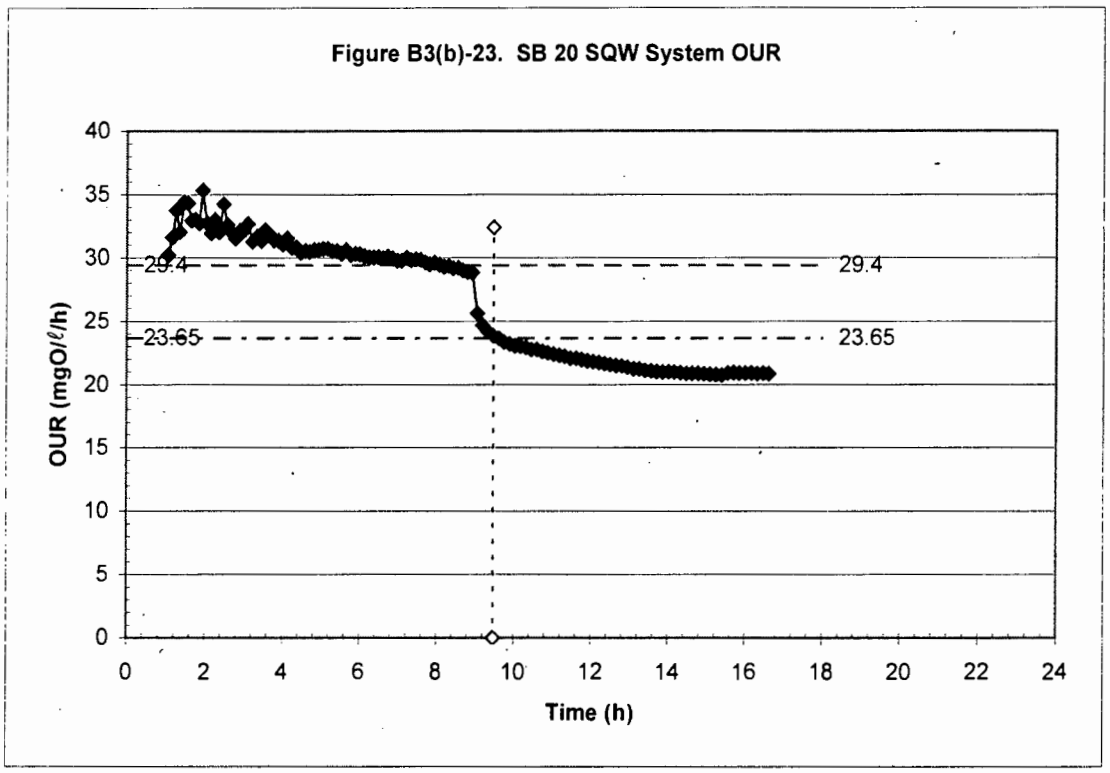

SB	Date	Day
20	18.09.02	304

Sbsi Drop (Time): 8.36

System Parameters:

Sti	497.9	mgCOD/ℓ
Suse	52.7	mgCOD/ℓ
Qs	36.24	ℓ/d
Sbsi	*70.4*	mgCOD/ℓ
fus	*0.106*	mgCOD/mgCOD
fts	*0.141*	mgCOD/mgCOD

Plot Sbsi (Max OUR) Plateau:

Sbsi Plat	x-Sbsi
0	27.7
18	27.7

Plot SBCOD OUR Plateau:

SBCOD Plat	x-SBCOD
0	22.4
18	*22.4*

Plot GAE-Sbsi End Criteria:

Sbsi End (Time)	Range
8.91	0
8.91	*30.7*

ΔOUR = *5.3* mgO/ℓ

Figure B3(b)-24. SB 20 SQW System OUR

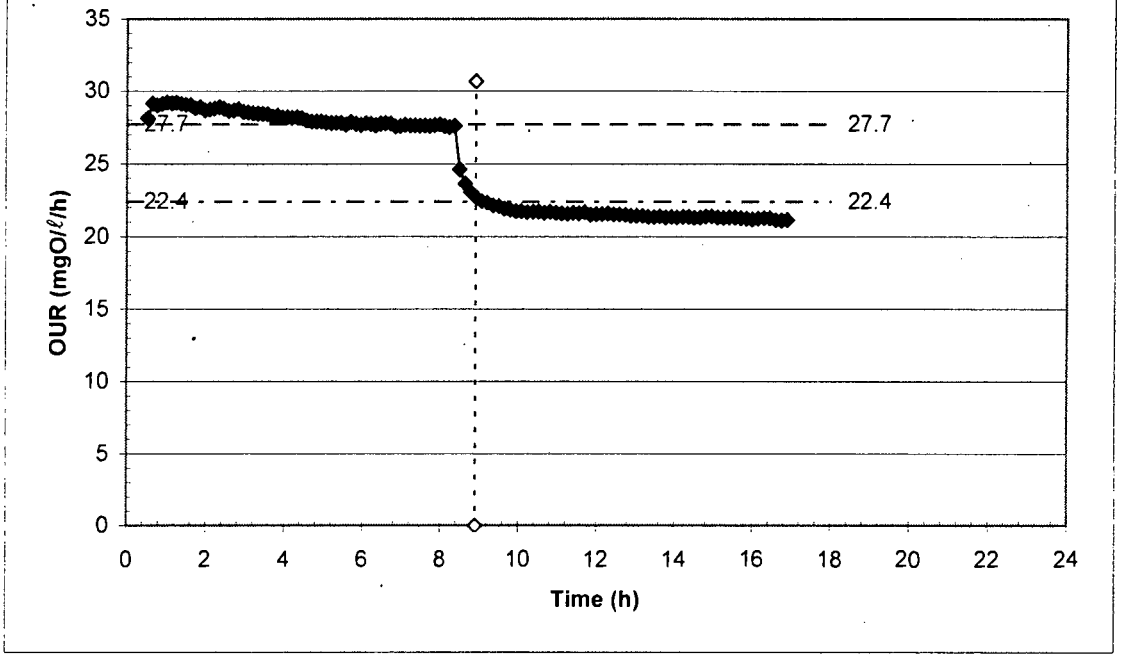

SB	Date	Day
20	19.09.02	305

Sbsi Drop (Time): 9.13

System Parameters:

Sti	467.5	mgCOD/ℓ
Suse	52.7	mgCOD/ℓ
Qs	35.7	ℓ/d
Sbsi	*68.8*	mgCOD/ℓ
fus	*0.113*	mgCOD/mgCOD
fts	*0.147*	mgCOD/mgCOD

Plot Sbsi (Max OUR) Plateau:

Sbsi Plat	x-Sbsi
0	33.3
18	33.3

Plot SBCOD OUR Plateau:

SBCOD Plat	x-SBCOD
0	28.2
18	*28.2*

Plot GAE-Sbsi End Criteria:

Sbsi End (Time)	Range
9.68	0
9.68	*36.3*

ΔOUR = *5.1* mgO/ℓ

Figure B3(b)-25. SB 20 SQW System OUR

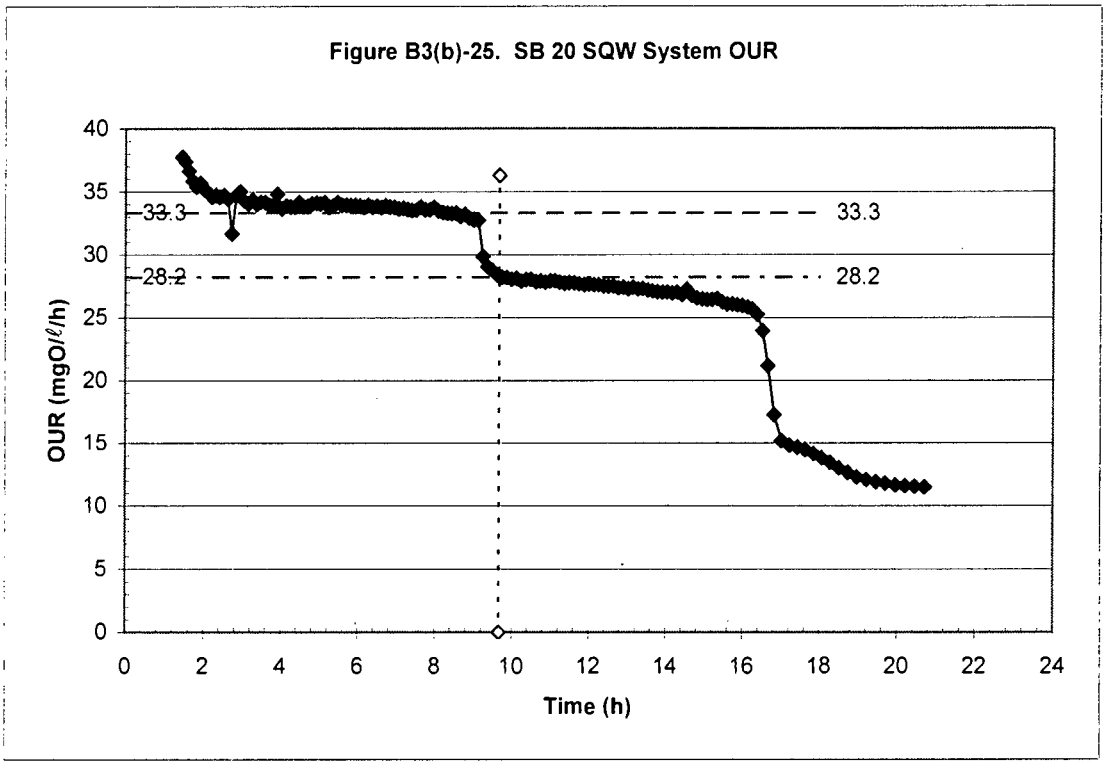

SB	Date	Day
20	20.09.02	306

Sbsi Drop (Time): 7.58

System Parameters:

Sti	495.9	mgCOD/ℓ
Suse	41.4	mgCOD/ℓ
Qs	36.52	ℓ/d
Sbsi	*69.9*	mgCOD/ℓ
fus	*0.083*	mgCOD/mgCOD
fts	*0.141*	mgCOD/mgCOD

Plot Sbsi (Max OUR) Plateau:

Sbsi Plat	x-Sbsi
0	31
18	*31*

Plot SBCOD OUR Plateau:

SBCOD Plat	x-SBCOD
0	25.7
18	*25.7*

Plot GAE-Sbsi End Criteria:

Sbsi End (Time)	Range
8.13	0
8.13	*34*

ΔOUR = *5.3* mgO/ℓ

Figure B3(b)-26. SB 20 SQW System OUR

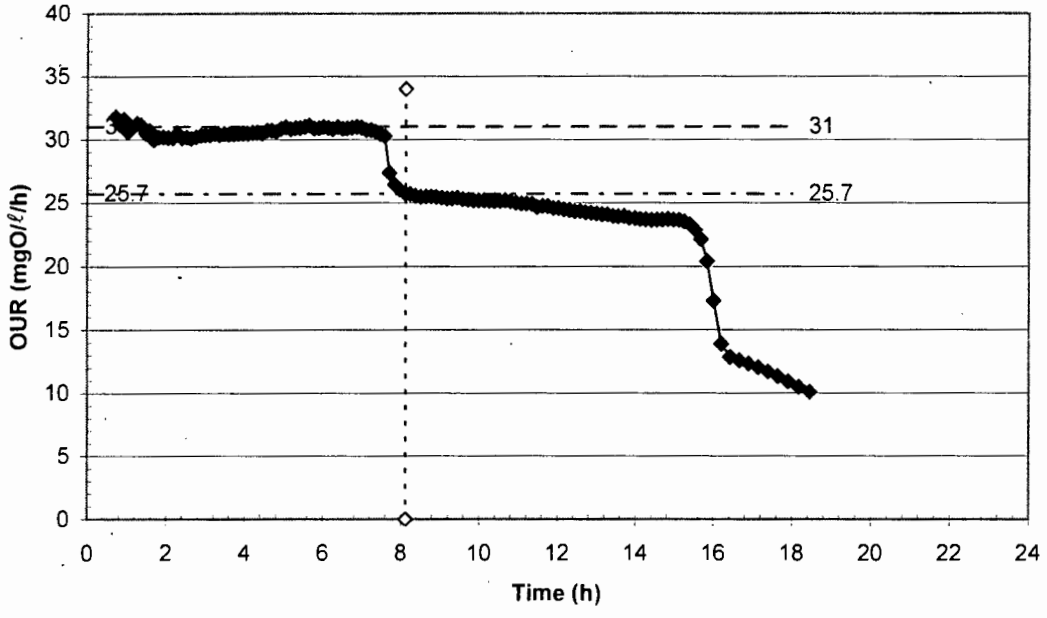

SB	Date	Day
20	21.09.02	307

Sbsi Drop (Time): 8.68

System Parameters:

Sti	479.8	mgCOD/ℓ
Suse	51.5	mgCOD/ℓ
Qs	36	ℓ/d
Sbsi	*56.2*	mgCOD/ℓ
fus	*0.107*	mgCOD/mgCOD
fts	*0.117*	mgCOD/mgCOD

Plot Sbsi (Max OUR) Plateau:

Sbsi Plat	x-Sbsi
0	31.7
18	31.7

Plot SBCOD OUR Plateau:

SBCOD Plat	x-SBCOD
0	27.5
18	27.5

Plot GAE-Sbsi End Criteria:

Sbsi End (Time)	Range
9.23	0
9.23	*34.7*

ΔOUR = *4.2* mgO/ℓ

Figure B3(b)-27. SB 20 SQW System OUR

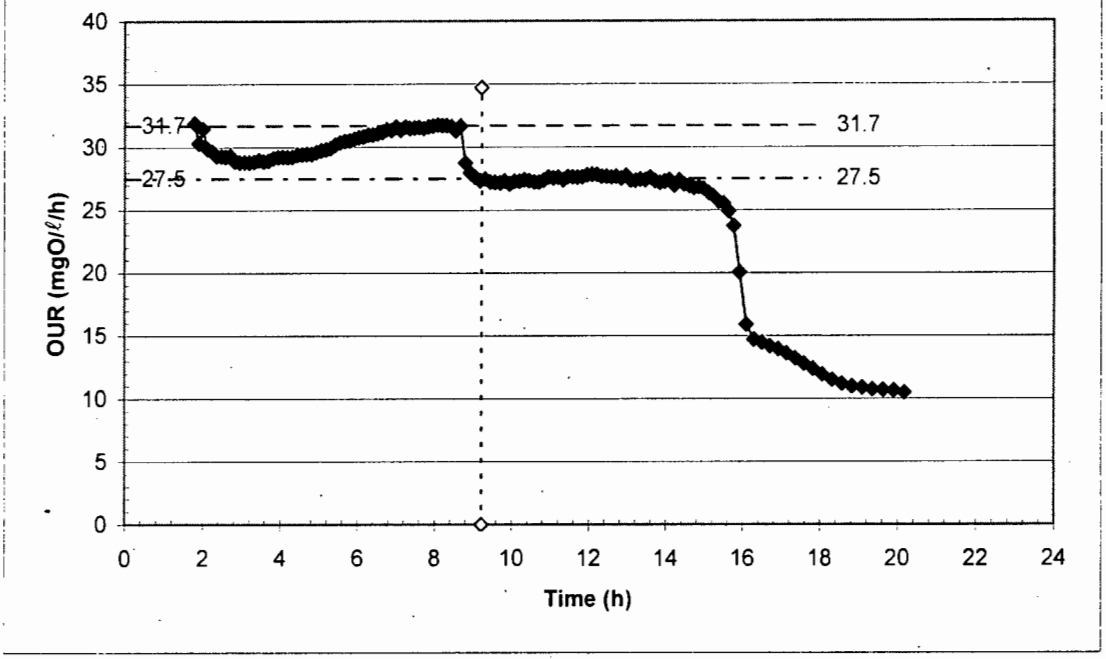

SB	Date	Day
20	22.09.02	308

Sbsi Drop (Time): 7.61

System Parameters:

Sti	462.6	mgCOD/ℓ
Suse	47.5	mgCOD/ℓ
Qs	35.64	ℓ/d
Sbsi	*73.6*	mgCOD/ℓ
fus	*0.103*	mgCOD/mgCOD
fts	*0.159*	mgCOD/mgCOD

Plot Sbsi (Max OUR) Plateau:

Sbsi Plat	x-Sbsi
0	32.2
18	*32.2*

Plot SBCOD OUR Plateau:

SBCOD Plat	x-SBCOD
0	26.75
18	*26.75*

Plot GAE-Sbsi End Criteria:

Sbsi End (Time)	Range
8.16	0
8.16	*35.2*

ΔOUR = *5.5* mgO/ℓ

Figure B3(b)-28. SB 20 SQW System OUR

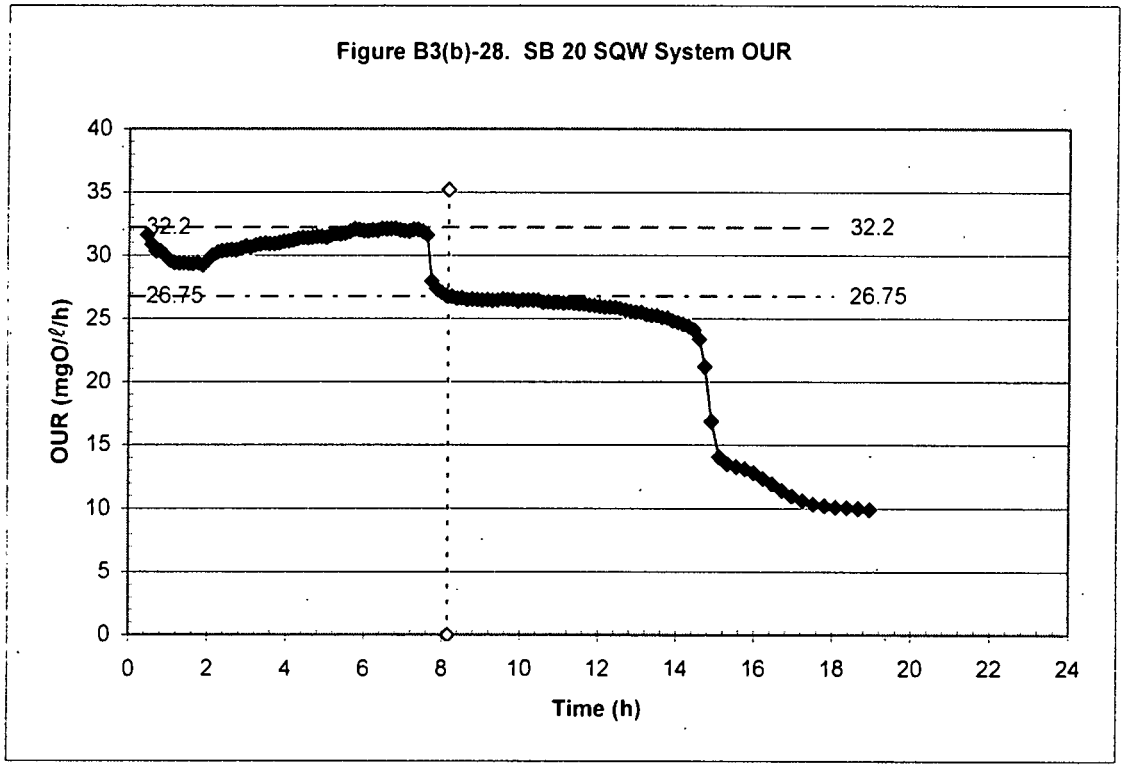

SB	Date	Day
20	23.09.02	309

Sbsi Drop (Time): 8.71

System Parameters:

Sti	631.3	mgCOD/ℓ
Suse	48.5	mgCOD/ℓ
Qs	35.49	ℓ/d
Sbsi	*67.8*	mgCOD/ℓ
fus	*0.077*	mgCOD/mgCOD
fts	***0.107***	mgCOD/mgCOD

Plot Sbsi (Max OUR) Plateau:

Sbsi Plat	x-Sbsi
0	33.5
18	33.5

Plot SBCOD OUR Plateau:

SBCOD Plat	x-SBCOD
0	28.5
18	28.5

Plot GAE-Sbsi End Criteria:

Sbsi End (Time)	Range
9.26	0
9.26	*36.5*

ΔOUR = *5.0* mgO/ℓ

Figure B3(b)-29. SB 20 SQW System OUR

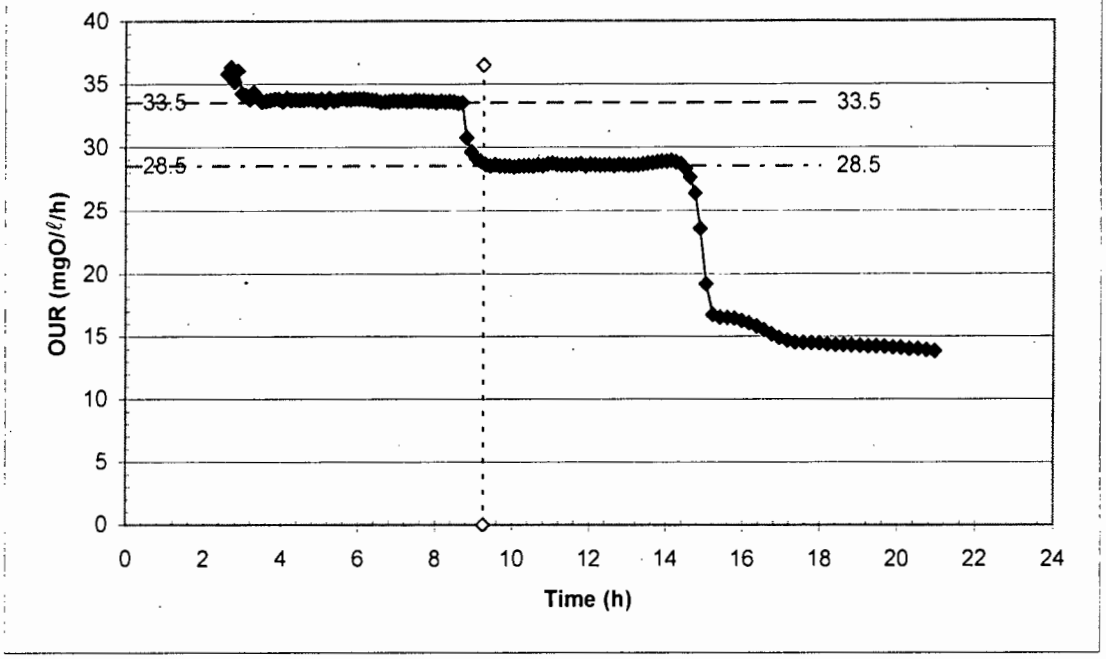

SB	Date	Day
20	24.09.02	310

Sbsi Drop (Time): 7.23

System Parameters:

Sti	472.7	mgCOD/ℓ
Suse	55.6	mgCOD/ℓ
Qs	34.7	ℓ/d
Sbsi	*83.2*	mgCOD/ℓ
fus	*0.118*	mgCOD/mgCOD
fts	*0.176*	mgCOD/mgCOD

Plot Sbsi (Max OUR) Plateau:

Sbsi Plat	x-Sbsi
0	32
18	*32*

Plot SBCOD OUR Plateau:

SBCOD Plat	x-SBCOD
0	26
18	*26*

Plot GAE-Sbsi End Criteria:

Sbsi End (Time)	Range
7.78	0
7.78	*35*

ΔOUR = *6.0* mgO/ℓ

Figure B3(b)-30. SB 20 SQW System OUR

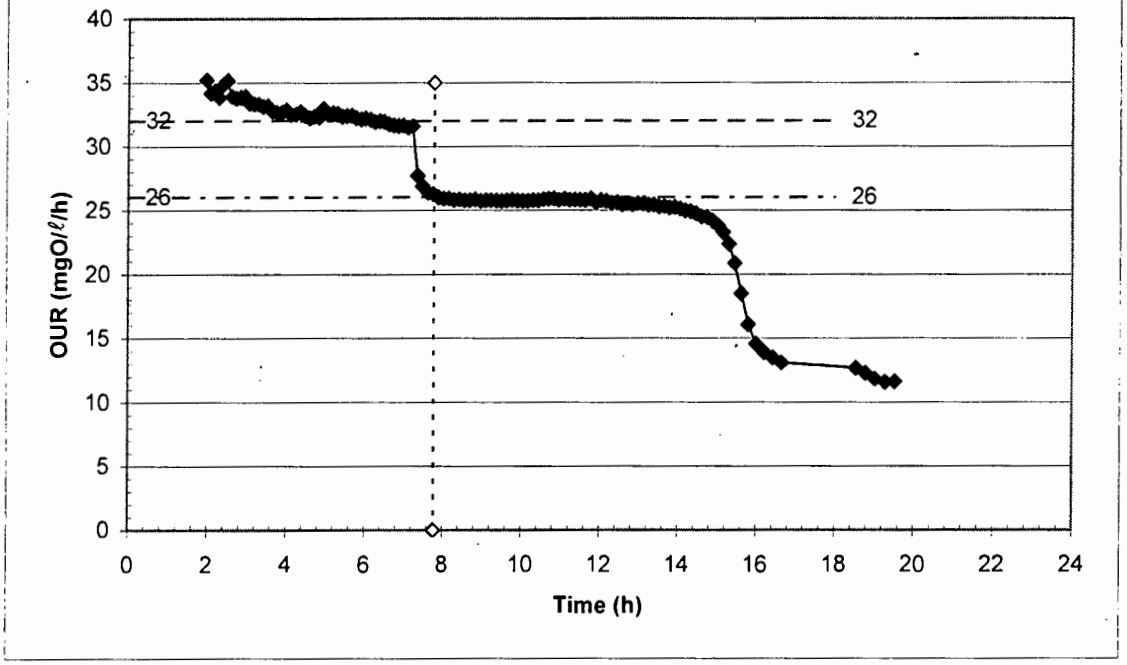

SB	Date	Day
20	25.09.02	311

Sbsi Drop (Time): 7.3

System Parameters:

Sti	490.9	mgCOD/ℓ
Suse	66.7	mgCOD/ℓ
Qs	35.04	ℓ/d
Sbsi	*74.2*	mgCOD/ℓ
fus	*0.136*	mgCOD/mgCOD
fts	*0.151*	mgCOD/mgCOD

Plot Sbsi (Max OUR) Plateau:

Sbsi Plat	x-Sbsi
0	33.6
18	*33.6*

Plot SBCOD OUR Plateau:

SBCOD Plat	x-SBCOD
0	28.2
18	*28.2*

Plot GAE-Sbsi End Criteria:

Sbsi End (Time)	Range
7.85	0
7.85	*36.6*

ΔOUR = *5.4* mgO/ℓ

Figure B3(b)-31. SB 20 SQW System OUR

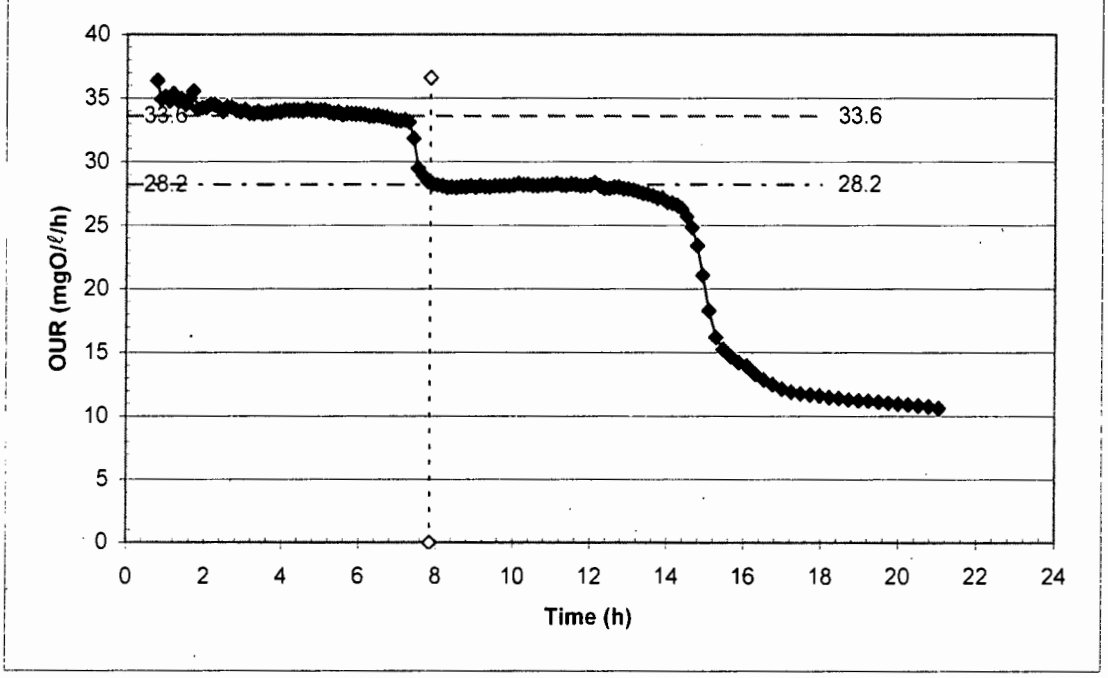

SB	Date	Day
20	26.09.02	312

Sbsi Drop (Time): 7.56

System Parameters:

Sti	481.8	mgCOD/ℓ
Suse	65.7	mgCOD/ℓ
Qs	35.07	ℓ/d
Sbsi	*64.5*	mgCOD/ℓ
fus	*0.136*	mgCOD/mgCOD
fts	*0.134*	mgCOD/mgCOD

Plot Sbsi (Max OUR) Plateau:

Sbsi Plat	x-Sbsi
0	33.6
18	*33.6*

Plot SBCOD OUR Plateau:

SBCOD Plat	x-SBCOD
0	28.9
18	*28.9*

Plot GAE-Sbsi End Criteria:

Sbsi End (Time)	Range
8.11	0
8.11	*36.6*

ΔOUR = *4.7* mgO/ℓ

Figure B3(b)-32. SB 20 SQW System OUR

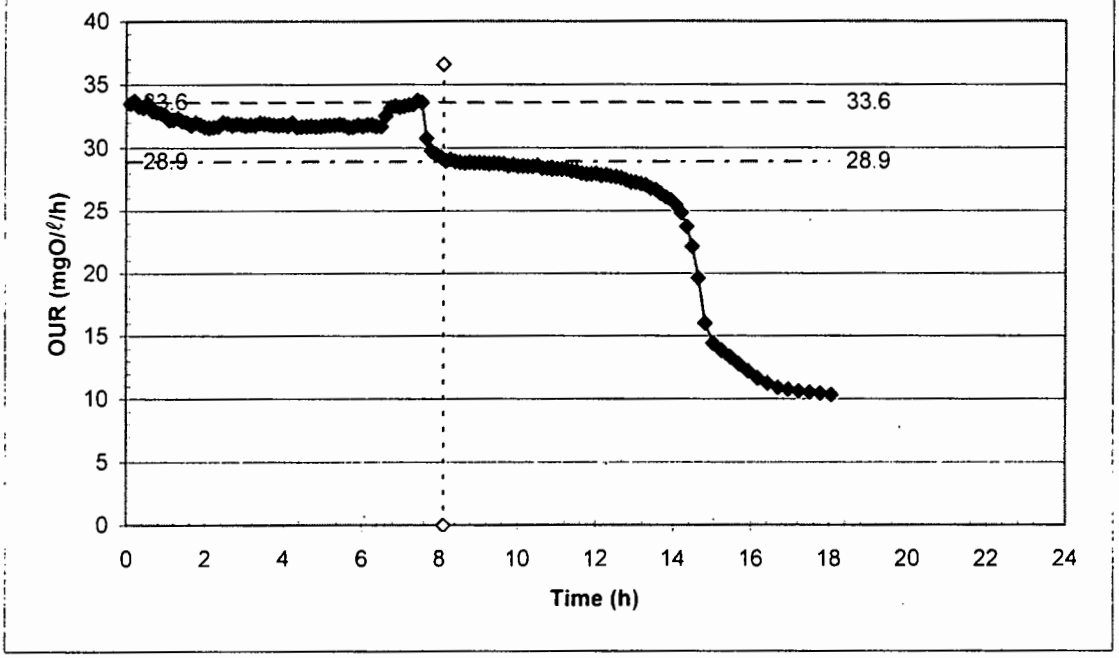

SB	Date	Day
20	27.09.02	313

Sbsi Drop (Time): 8.83

System Parameters:

Sti	452.5	mgCOD/ℓ
Suse	71.1	mgCOD/ℓ
Qs	34.06	ℓ/d
Sbsi	*59.4*	mgCOD/ℓ
fus	*0.157*	mgCOD/mgCOD
fts	*0.131*	mgCOD/mgCOD

Plot Sbsi (Max OUR) Plateau:

Sbsi Plat	x-Sbsi
0	30.8
18	*30.8*

Plot SBCOD OUR Plateau:

SBCOD Plat	x-SBCOD
0	26.6
18	*26.6*

Plot GAE-Sbsi End Criteria:

Sbsi End (Time)	Range
9.38	0
9.38	*33.8*

ΔOUR = *4.2* mgO/ℓ

Figure B3(b)-33. SB 20 SQW System OUR

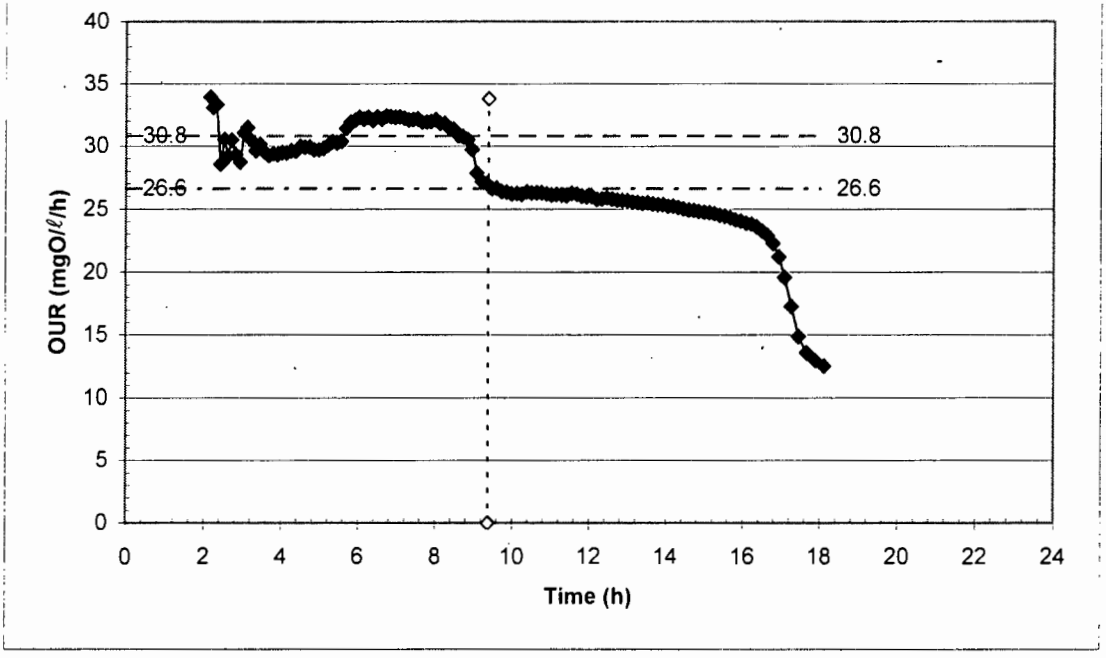

SB	Date	Day
20	28.09.02	314

Sbsi Drop (Time): **8.44**

System Parameters:

Sti	415.4	mgCOD/ℓ
Suse	62.1	mgCOD/ℓ
Qs	33.91	ℓ/d
Sbsi	*56.8*	mgCOD/ℓ
fus	*0.149*	mgCOD/mgCOD
fts	*0.137*	mgCOD/mgCOD

Plot Sbsi (Max OUR) Plateau:

Sbsi Plat	x-Sbsi
0	**28.1**
18	*28.1*

Plot SBCOD OUR Plateau:

SBCOD Plat	x-SBCOD
0	**24.1**
18	*24.1*

Plot GAE-Sbsi End Criteria:

Sbsi End (Time)	Range
8.99	0
8.99	*31.1*

ΔOUR = *4.0* mgO/ℓ

Figure B3(b)-34. SB 20 SQW System OUR

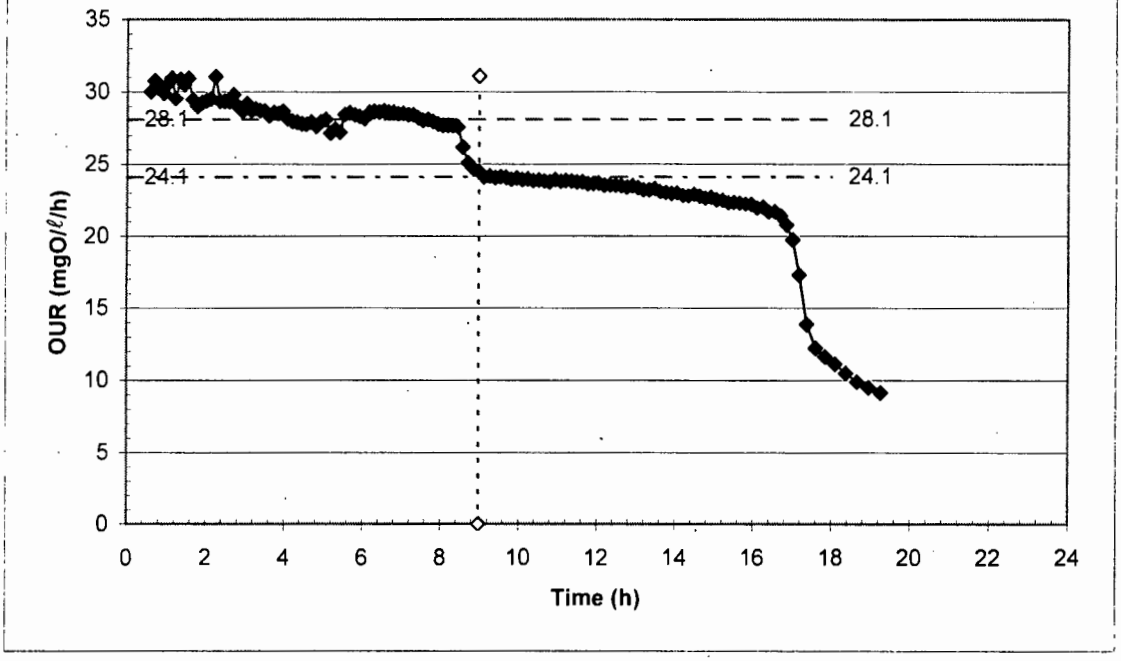

SB	Date	Day
21	30.9.02	316

Sbsi Drop (Time): 8.65

System Parameters:

Sti	503.5	mgCOD/ℓ
Suse	-	mgCOD/ℓ
Qs	35.83	ℓ/d
Sbsi	*66.9*	mgCOD/ℓ
fus	-	mgCOD/mgCOD
fts	*0.133*	mgCOD/mgCOD

Plot Sbsi (Max OUR) Plateau:

Sbsi Plat	XSbsi
0	33
18	*33*

Plot SBCOD OUR Plateau:

SBCOD Plat	XSBCOD
0	28.02
18	*28.02*

Plot GAE-Sbsi End Criteria:

Sbsi End (Time)	Range
9.2	0
9.2	35

ΔOUR = *4.98* mgO/ℓ

Figure B3(b)-35. SB 21 Sbsi System OUR

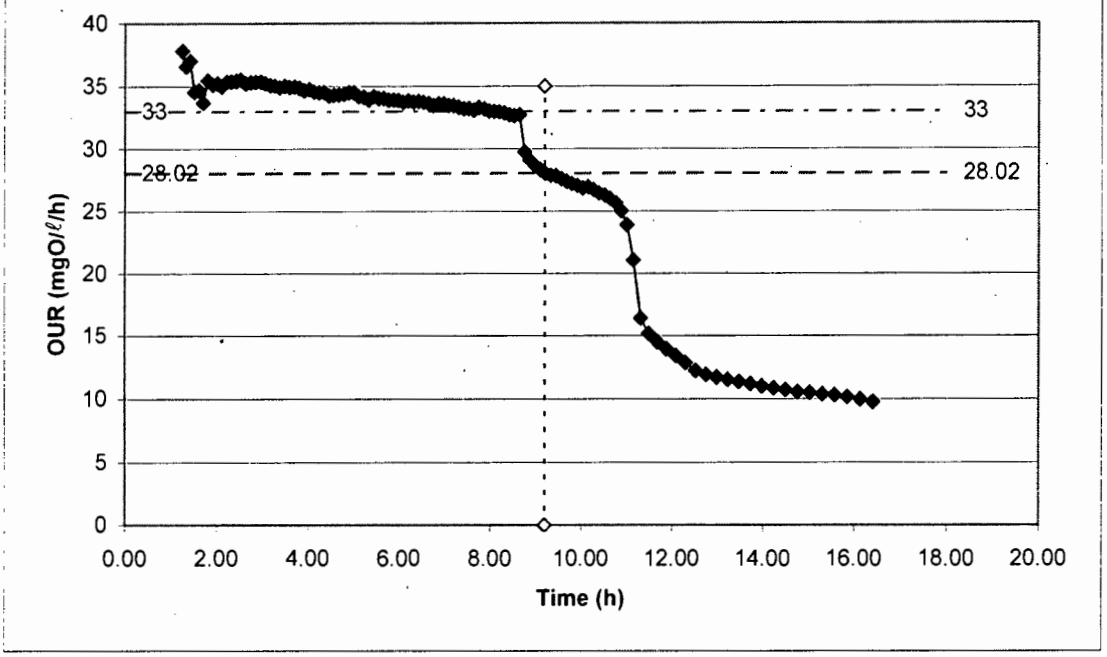

SB	Date	Day
21	1.10.02	317

Sbsi Drop (Time): 8.51

System Parameters:

Sti	496.5	mgCOD/ℓ
Suse	44	mgCOD/ℓ
Qs	35.21	ℓ/d
Sbsi	*68.4*	mgCOD/ℓ
fus	*0.089*	mgCOD/mgCOD
fts	*0.138*	mgCOD/mgCOD

Plot Sbsi (Max OUR) Plateau:

Sbsi Plat	XSbsi
0	29
18	*29*

Plot SBCOD OUR Plateau:

SBCOD Plat	XSBCOD
0	24
18	*24*

Plot GAE-Sbsi End Criteria:

Sbsi End (Time)	Range
9.06	0
9.06	*32*

ΔOUR = *5.0* mgO/ℓ

Figure B3(b)-36. SB 21 Sbsi System OUR

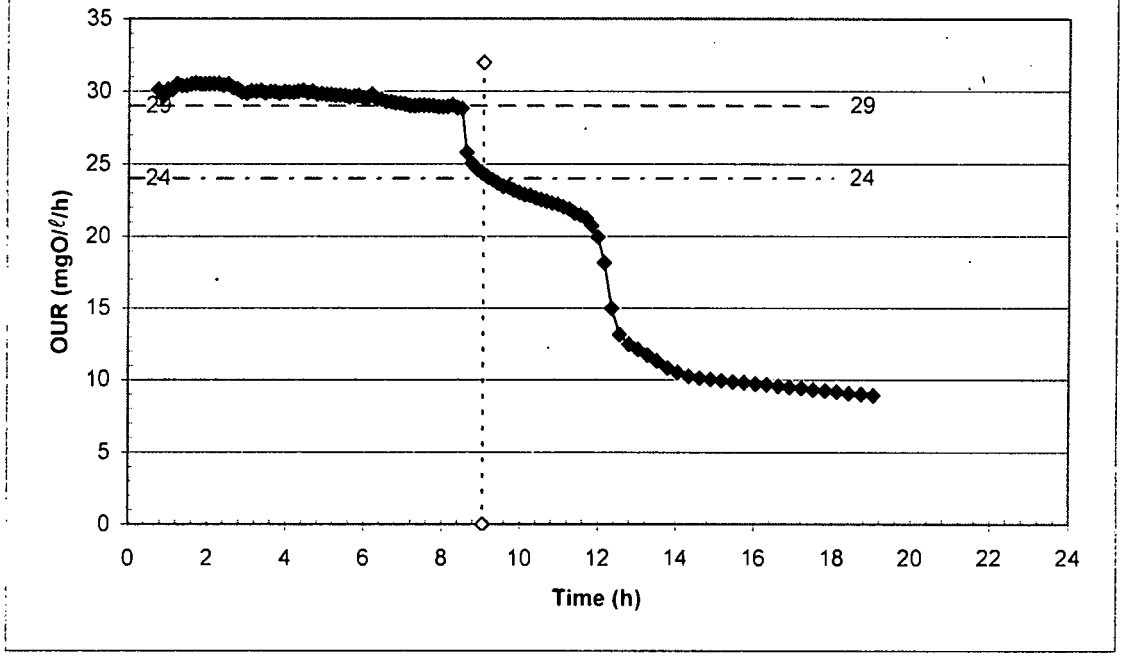

SB	Date	Day
21	2.10.02	318

Sbsi Drop (Time): **8.52**

System Parameters:

Sti	491.5	mgCOD/ℓ
Suse	52.1	mgCOD/ℓ
Qs	34.9	ℓ/d
Sbsi	*68.3*	mgCOD/ℓ
fus	*0.106*	mgCOD/mgCOD
fts	*0.139*	mgCOD/mgCOD

Plot Sbsi (Max OUR) Plateau:

Sbsi Plat	XSbsi
0	**32.2**
18	32.2

Plot SBCOD OUR Plateau:

SBCOD Plat	XSBCOD
0	**27.25**
18	*27.25*

Plot GAE-Sbsi End Criteria:

Sbsi End (Time)	Range
9.07	0
9.07	*35.2*

ΔOUR = *5.0* mgO/ℓ

Figure B3(b)-37. SB 21 Sbsi System OUR

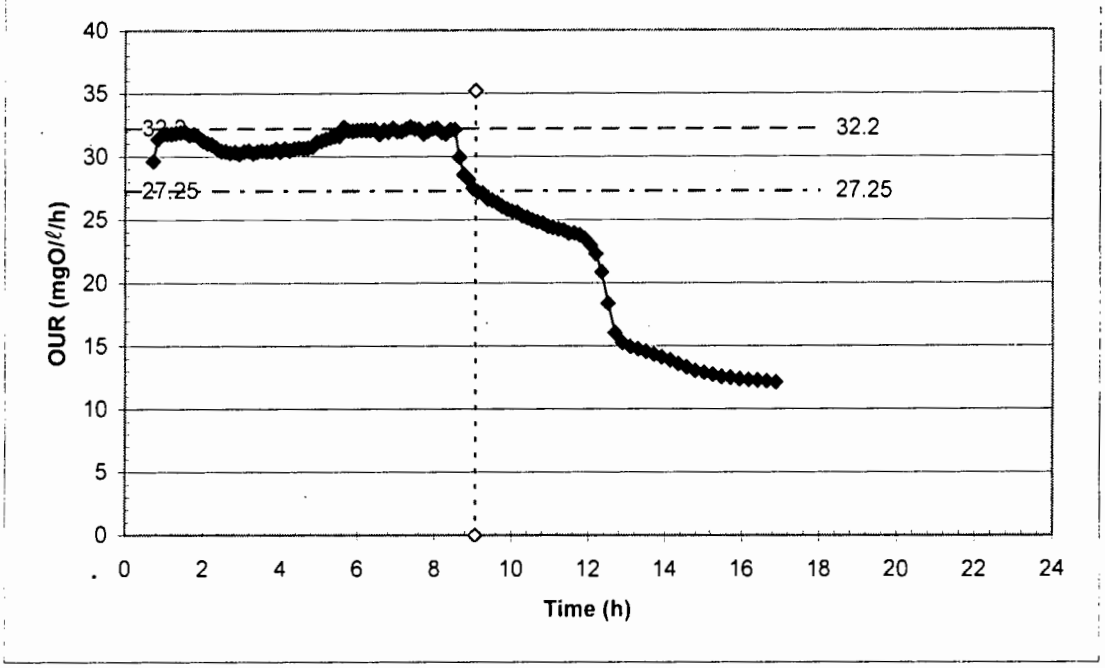

SB	Date	Day
21	3.10.02	319

Sbsi Drop (Time): 8.18

System Parameters:

Sti	501	mgCOD/ℓ
Suse	53.4	mgCOD/ℓ
Qs	36	ℓ/d
Sbsi	*69.5*	mgCOD/ℓ
fus	*0.107*	mgCOD/mgCOD
fts	*0.139*	mgCOD/mgCOD

Plot Sbsi (Max OUR) Plateau:

Sbsi Plat	XSbsi
0	28.7
18	28.7

Plot SBCOD OUR Plateau:

SBCOD Plat	XSBCOD
0	23.5
18	23.5

Plot GAE-Sbsi End Criteria:

Sbsi End (Time)	Range
8.73	0
8.73	*31.7*

ΔOUR = *5.2* mgO/ℓ

Figure B3(b)-38. SB 21 Sbsi System OUR

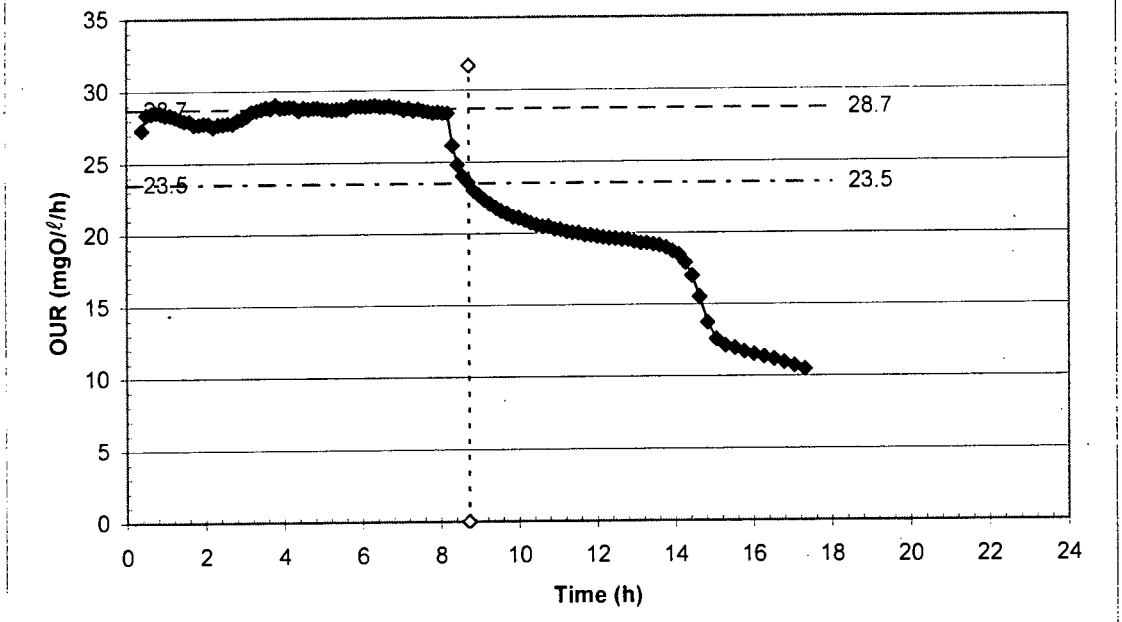

SB	Date	Day
21	4.10.02	320

Sbsi Drop (Time): 8.65

System Parameters:

Sti	510	mgCOD/ℓ
Suse	99.8	mgCOD/ℓ
Qs	36.16	ℓ/d
Sbsi	*66.6*	mgCOD/ℓ
fus	*0.196*	mgCOD/mgCOD
fts	*0.131*	mgCOD/mgCOD

Plot Sbsi (Max OUR) Plateau:

Sbsi Plat	XSbsi
0	28
18	28

Plot SBCOD OUR Plateau:

SBCOD Plat	XSBCOD
0	23
18	23

Plot GAE-Sbsi End Criteria:

Sbsi End (Time)	Range
9.2	0
9.2	*31*

ΔOUR = *5.0* mgO/ℓ

Figure B3(b)-39. SB 21 Sbsi System OUR

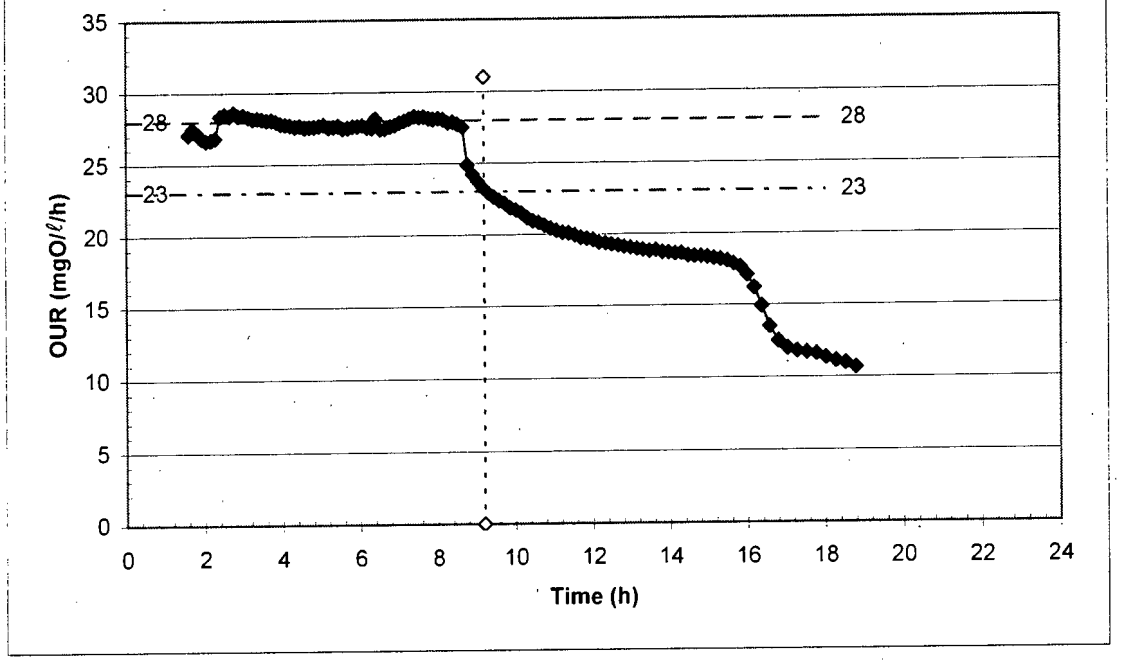

SB	Date	Day
21	6.10.02	322

Sbsi Drop (Time): 8.3

System Parameters:

Sti	508	mgCOD/ℓ
Suse	60.5	mgCOD/ℓ
Qs	36.16	ℓ/d
Sbsi	*59.9*	mgCOD/ℓ
fus	*0.119*	mgCOD/mgCOD
fts	*0.118*	mgCOD/mgCOD

Plot Sbsi (Max OUR) Plateau:

Sbsi Plat	XSbsi
0	25.75
18	*25.75*

Plot SBCOD OUR Plateau:

SBCOD Plat	XSBCOD
0	21.25
18	*21.25*

Plot GAE-Sbsi End Criteria:

Sbsi End (Time)	Range
8.85	0
8.85	*28.75*

ΔOUR = *4.5* mgO/ℓ

Figure B3(b)-40. SB 21 Sbsi System OUR

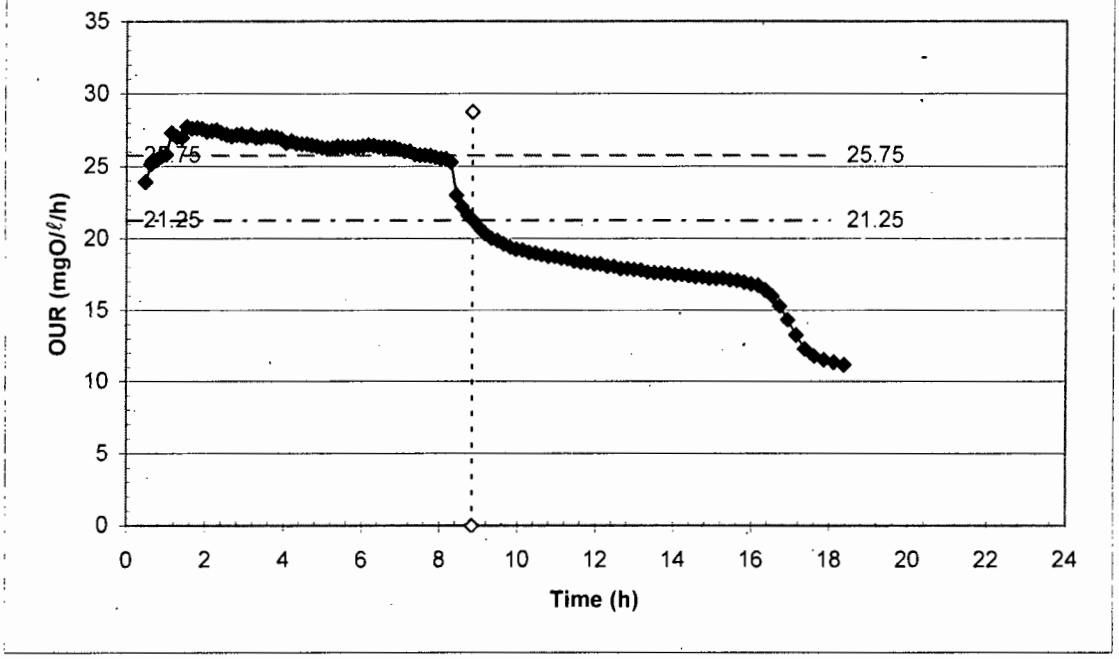

SB	Date	Day
21	7.10.02	323

Sbsi Drop (Time): 8.39

System Parameters:

Sti	472.8	mgCOD/ℓ
Suse	65	mgCOD/ℓ
Qs	36.96	ℓ/d
Sbsi	*62.5*	mgCOD/ℓ
fus	*0.137*	mgCOD/mgCOD
fts	*0.132*	mgCOD/mgCOD

Plot Sbsi (Max OUR) Plateau:

Sbsi Plat	XSbsi
0	26.6
18	*26.6*

Plot SBCOD OUR Plateau:

SBCOD Plat	XSBCOD
0	21.8
18	*21.8*

Plot GAE-Sbsi End Criteria:

Sbsi End (Time)	Range
8.94	0
8.94	29.6

ΔOUR = *4.8* mgO/ℓ

Figure B3(b)-41. SB 21 Sbsi System OUR

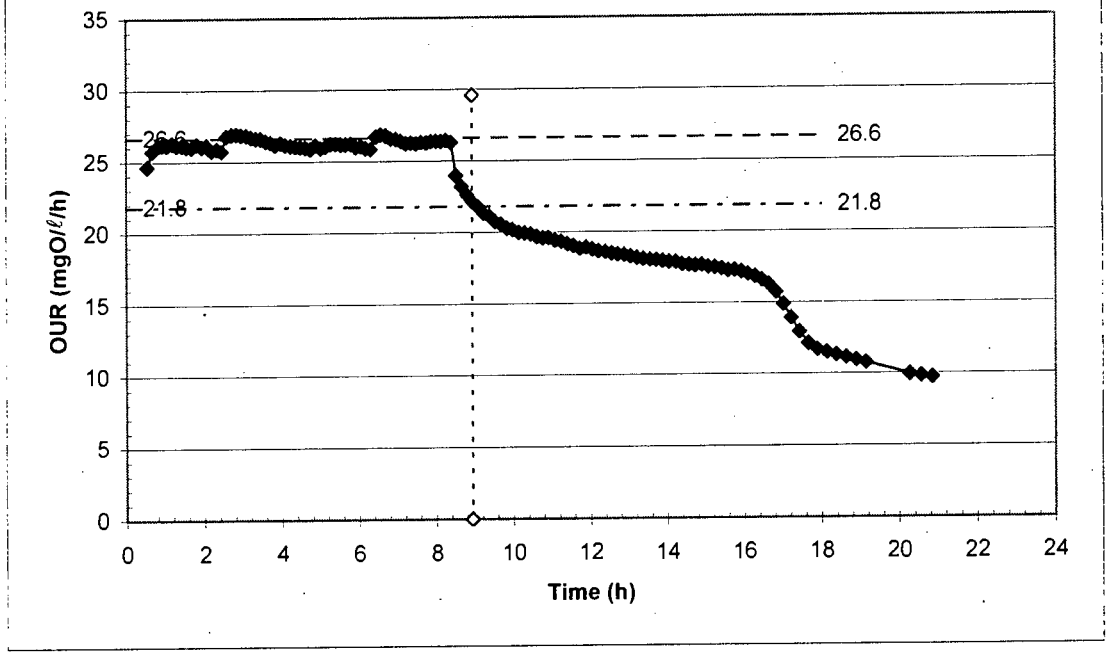

SB	Date	Day
21	8.10.02	324

Sbsi Drop (Time): **8.71**

System Parameters:

Sti	495.8	mgCOD/ℓ
Suse	73.2	mgCOD/ℓ
Qs	36.74	ℓ/d
Sbsi	*68.8*	mgCOD/ℓ
fus	*0.148*	mgCOD/mgCOD
fts	*0.139*	mgCOD/mgCOD

Plot Sbsi (Max OUR) Plateau:

Sbsi Plat	XSbsi
0	**25.45**
18	*25.45*

Plot SBCOD OUR Plateau:

SBCOD Plat	XSBCOD
0	**20.2**
18	*20.2*

Plot GAE-Sbsi End Criteria:

Sbsi End (Time)	Range
9.26	0
9.26	*28.45*

ΔOUR = *5.3* mgO/ℓ

Figure B3(b)-42. SB 21 Sbsi System OUR

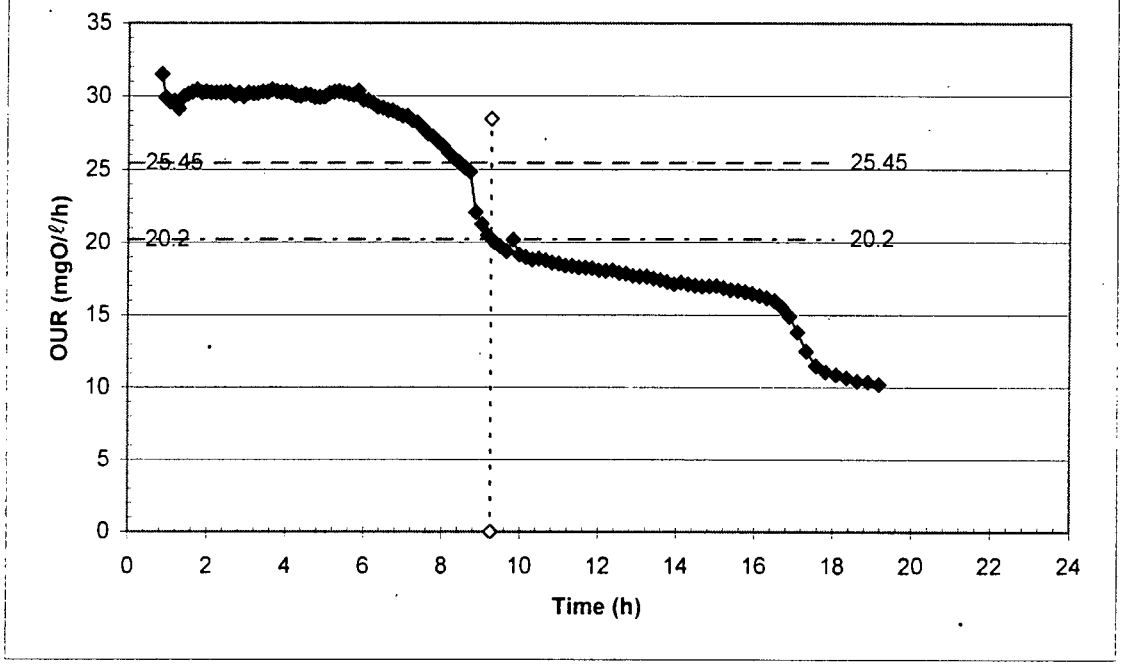

SB	Date	Day
21	9.10.02	325

Sbsi Drop (Time): 8.34

System Parameters:

Sti	495.8	mgCOD/ℓ
Suse	55.9	mgCOD/ℓ
Qs	37.28	ℓ/d
Sbsi	*43.3*	mgCOD/ℓ
fus	*0.113*	mgCOD/mgCOD
fts	*0.087*	mgCOD/mgCOD

Plot Sbsi (Max OUR) Plateau:

Sbsi Plat	XSbsi
0	27.75
18	27.75

Plot SBCOD OUR Plateau:

SBCOD Plat	XSBCOD
0	24.4
18	*24.4*

Plot GAE-Sbsi End Criteria:

Sbsi End (Time)	Range
8.89	0
8.89	*30.75*

ΔOUR = *3.4* mgO/ℓ

Figure B3(b)-43. SB 21 Sbsi System OUR

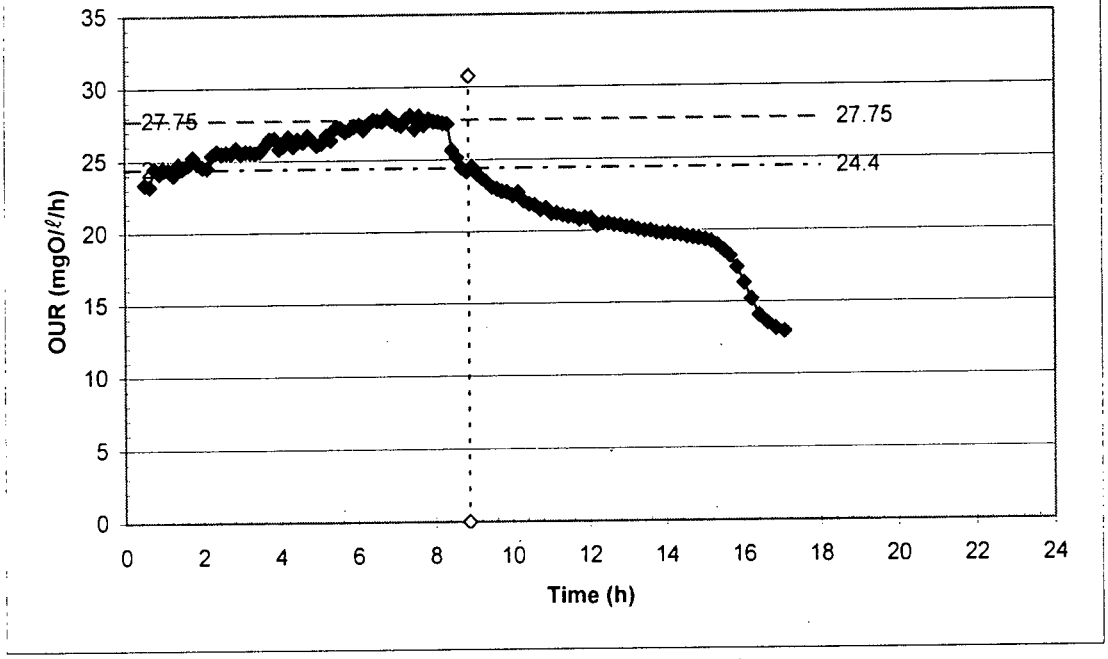

SB	Date	Day
21	10.10.02	326

Sbsi Drop (Time): **8.13**

System Parameters:

Sti	445	mgCOD/ℓ
Suse	44.7	mgCOD/ℓ
Qs	37.32	ℓ/d
Sbsi	*48.4*	mgCOD/ℓ
fus	*0.100*	mgCOD/mgCOD
fts	*0.109*	mgCOD/mgCOD

Plot Sbsi (Max OUR) Plateau:

Sbsi Plat	XSbsi
0	**27.6**
18	*27.6*

Plot SBCOD OUR Plateau:

SBCOD Plat	XSBCOD
0	**23.85**
18	*23.85*

Plot GAE-Sbsi End Criteria:

Sbsi End (Time)	Range
8.68	0
8.68	*30.6*

ΔOUR = *3.8* mgO/ℓ

Figure B3(b)-44. SB 21 Sbsi System OUR

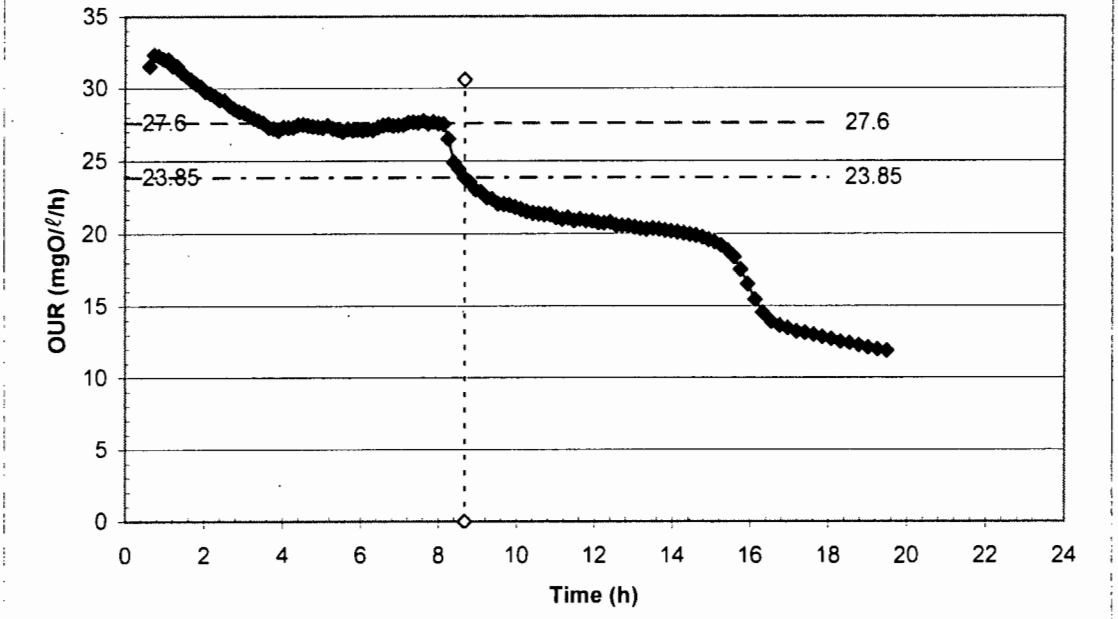

SB	Date	Day
21	13.10.02	329

Sbsi Drop (Time): 8.91

System Parameters:

Sti	485.6	mgCOD/ℓ
Suse	75.2	mgCOD/ℓ
Qs	31.76	ℓ/d
Sbsi	66.5	mgCOD/ℓ
fus	0.155	mgCOD/mgCOD
fts	0.137	mgCOD/mgCOD

Plot Sbsi (Max OUR) Plateau:

Sbsi Plat	XSbsi
0	25.29
18	25.29

Plot SBCOD OUR Plateau:

SBCOD Plat	XSBCOD
0	20.9
18	20.9

Plot GAE-Sbsi End Criteria:

Sbsi End (Time)	Range
9.46	0
9.46	28.29

ΔOUR = 4.4 mgO/ℓ

Figure B3(b)-45. SB 21 Sbsi System OUR

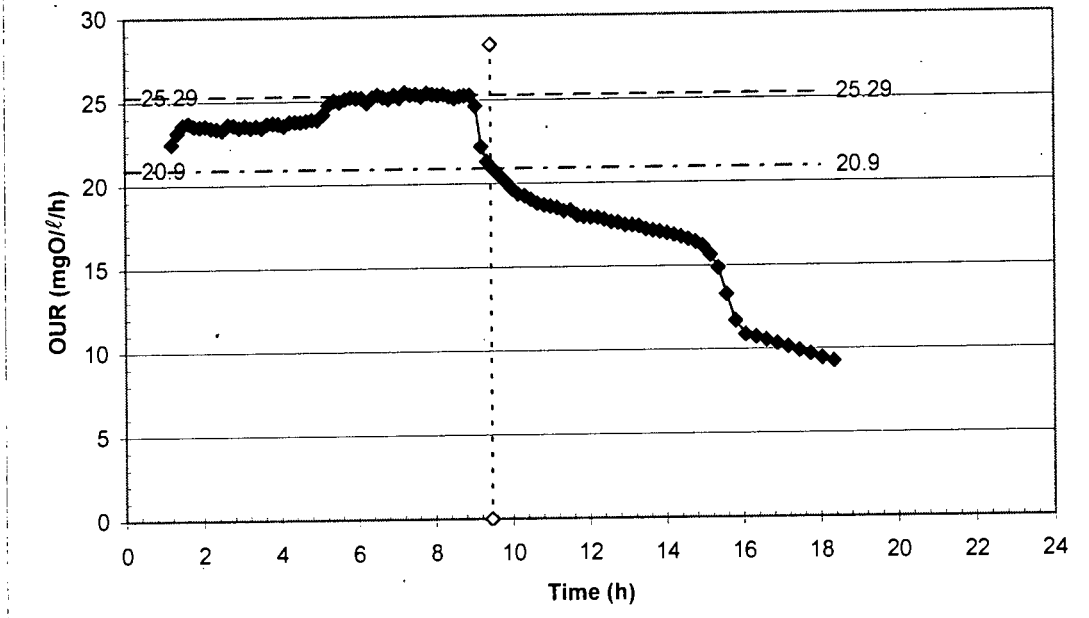

SB	Date	Day
21	16.10.02	332

Sbsi Drop (Time): **7.64**

System Parameters:

Sti	446	mgCOD/ℓ
Suse	48	mgCOD/ℓ
Qs	38.9	ℓ/d
Sbsi	*78.0*	mgCOD/ℓ
fus	*0.108*	mgCOD/mgCOD
fts	*0.175*	mgCOD/mgCOD

Plot Sbsi (Max OUR) Plateau:

Sbsi Plat	XSbsi
0	**30**
18	*30*

Plot SBCOD OUR Plateau:

SBCOD Plat	XSBCOD
0	**23.7**
18	*23.7*

Plot GAE-Sbsi End Criteria:

Sbsi End (Time)	Range
8.19	0
8.19	*33*

ΔOUR = *6.3* mgO/ℓ

Figure B3(b)-46. SB 21 Sbsi System OUR

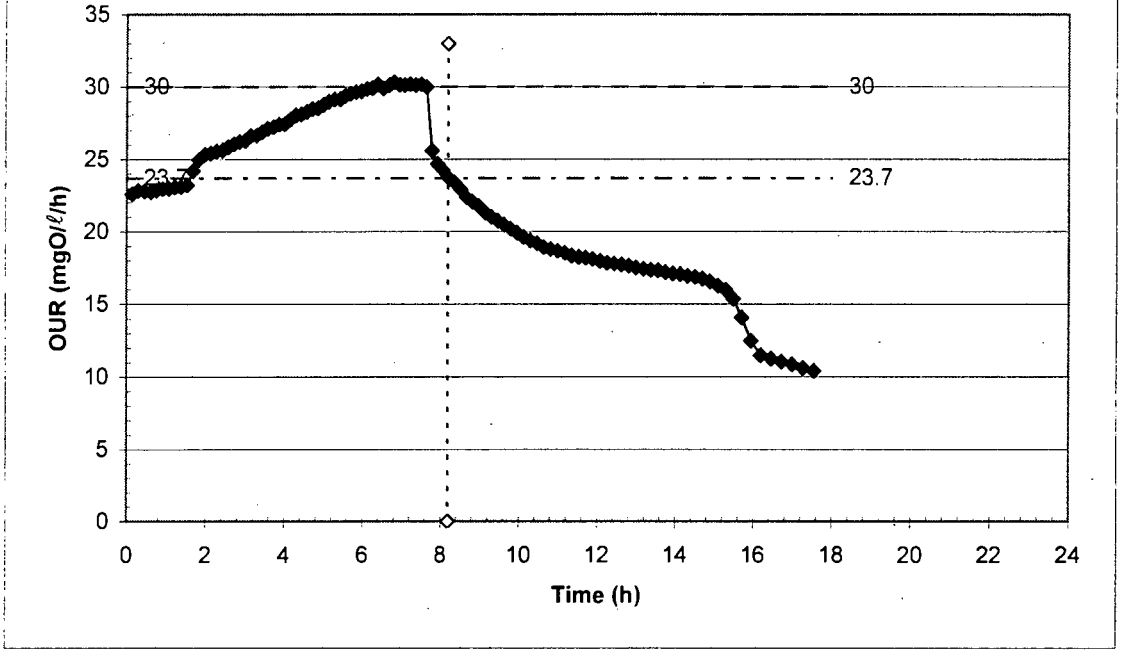

SB	Date	Day
22	17.10.02	333

Sbsi Drop (Time): 8.8

System Parameters:

Sti	535	mgCOD/ℓ
Suse		mgCOD/ℓ
Qs	36.88	ℓ/d
Sbsi	*95.2*	mgCOD/ℓ
fus		mgCOD/mgCOD
fts	*0.178*	mgCOD/mgCOD

Plot Sbsi (Max OUR) Plateau:

Sbsi Plat	XSbsi
0	31.4
18	*31.4*

Plot SBCOD OUR Plateau:

SBCOD Plat	XSBCOD
0	24.11
18	*24.11*

Plot GAE-Sbsi End Criteria:

Sbsi End (Time)	Range
9.35	0
9.35	*34.4*

ΔOUR = *7.3* mgO/ℓ

Figure B3(b)-47. SB 22 Sbsi System OUR

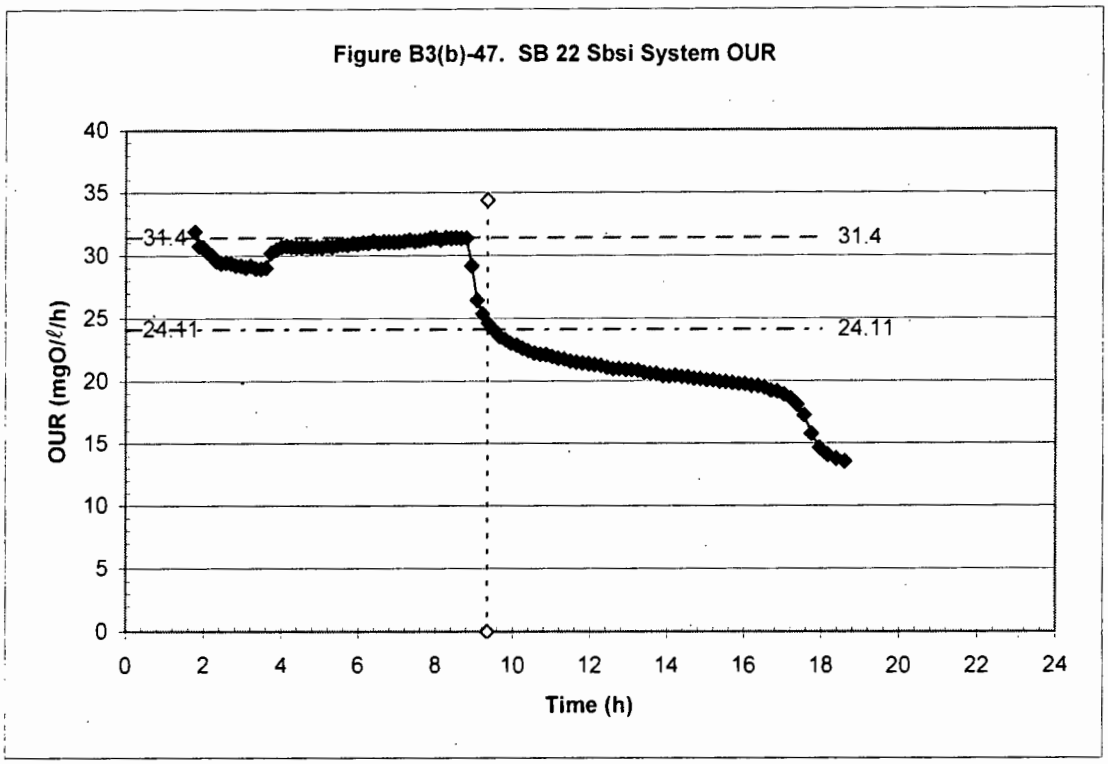

SB	Date	Day
22	18.10.02	334

Sbsi Drop (Time): 9.1

System Parameters:

Sti	481	mgCOD/ℓ
Suse		mgCOD/ℓ
Qs	38.56	ℓ/d
Sbsi	*108.0*	mgCOD/ℓ
fus		mgCOD/mgCOD
fts	*0.225*	mgCOD/mgCOD

Plot Sbsi (Max OUR) Plateau:

Sbsi Plat	XSbsi
0	37
18	37

Plot SBCOD OUR Plateau:

SBCOD Plat	XSBCOD
0	28.35
18	*28.35*

Plot GAE-Sbsi End Criteria:

Sbsi End (Time)	Range
9.65	0
9.65	*40*

ΔOUR = *8.7* mgO/ℓ

Figure B3(b)-48. SB 22 Sbsi System OUR

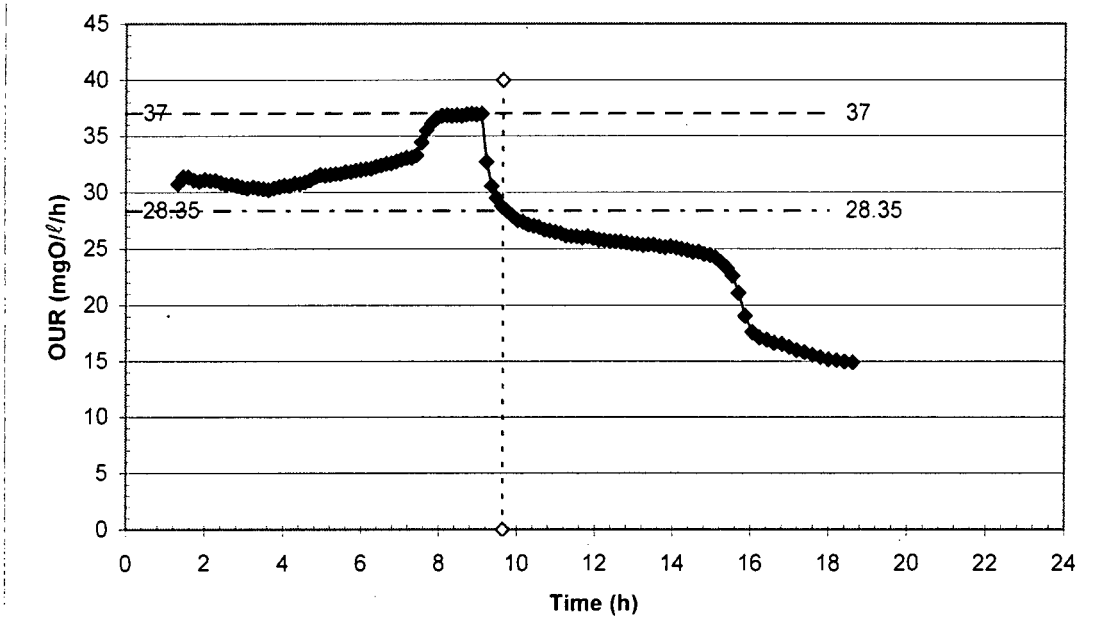

SB	Date	Day
22	19.10.02	335

Sbsi Drop (Time): 8.33

System Parameters:

Sti	506	mgCOD/ℓ
Suse	52	mgCOD/ℓ
Qs	38.56	ℓ/d
Sbsi	*101.1*	mgCOD/ℓ
fus	*0.103*	mgCOD/mgCOD
fts	*0.200*	mgCOD/mgCOD

Plot Sbsi (Max OUR) Plateau:

Sbsi Plat	XSbsi
0	33.5
18	33.5

Plot SBCOD OUR Plateau:

SBCOD Plat	XSBCOD
0	25.4
18	*25.4*

Plot GAE-Sbsi End Criteria:

Sbsi End (Time)	Range
8.88	0
8.88	*36.5*

ΔOUR = *8.1* mgO/ℓ

Figure B3(b)-49. SB 22 Sbsi System OUR

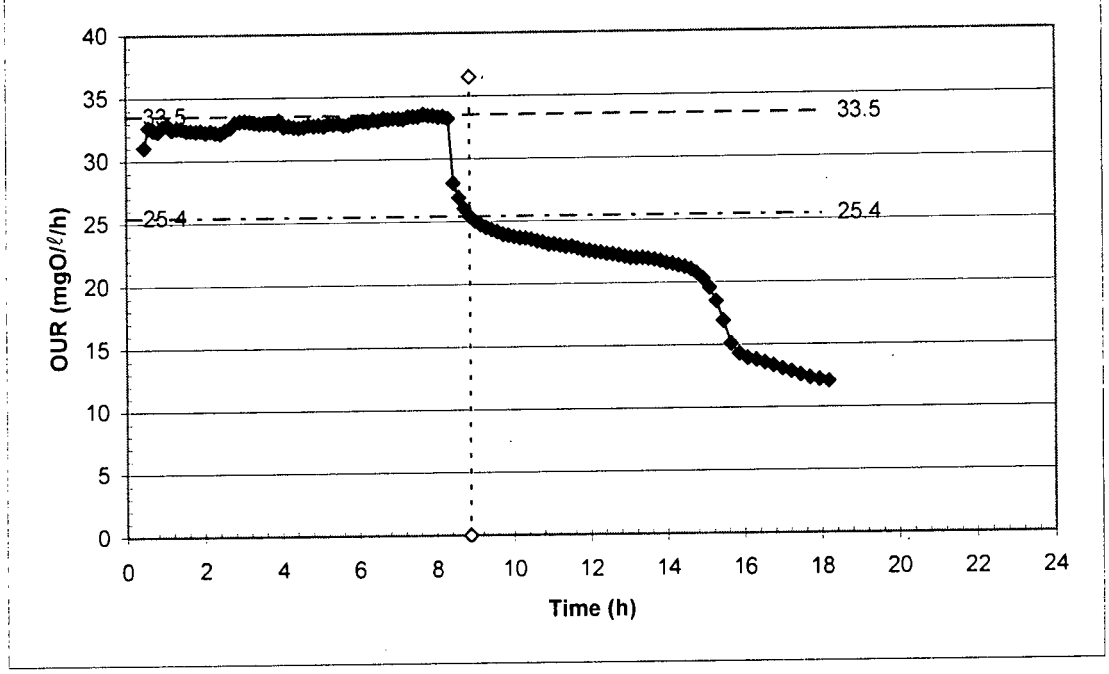

SB	Date	Day
22	23.10.02	339

Sbsi Drop (Time): 7.14

System Parameters:

Sti	492.5	mgCOD/ℓ
Suse	56.3	mgCOD/ℓ
Qs	32.8	ℓ/d
Sbsi	*99.8*	mgCOD/ℓ
fus	*0.114*	mgCOD/mgCOD
fts	*0.203*	mgCOD/mgCOD

Plot Sbsi (Max OUR) Plateau:

Sbsi Plat	XSbsi
0	31.5
18	*31.5*

Plot SBCOD OUR Plateau:

SBCOD Plat	XSBCOD
0	24.7
18	*24.7*

Plot GAE-Sbsi End Criteria:

Sbsi End (Time)	Range
7.69	0
7.69	*34.5*

ΔOUR = *6.8* mgO/ℓ

Figure B3(b)-50. SB 22 Sbsi System OUR

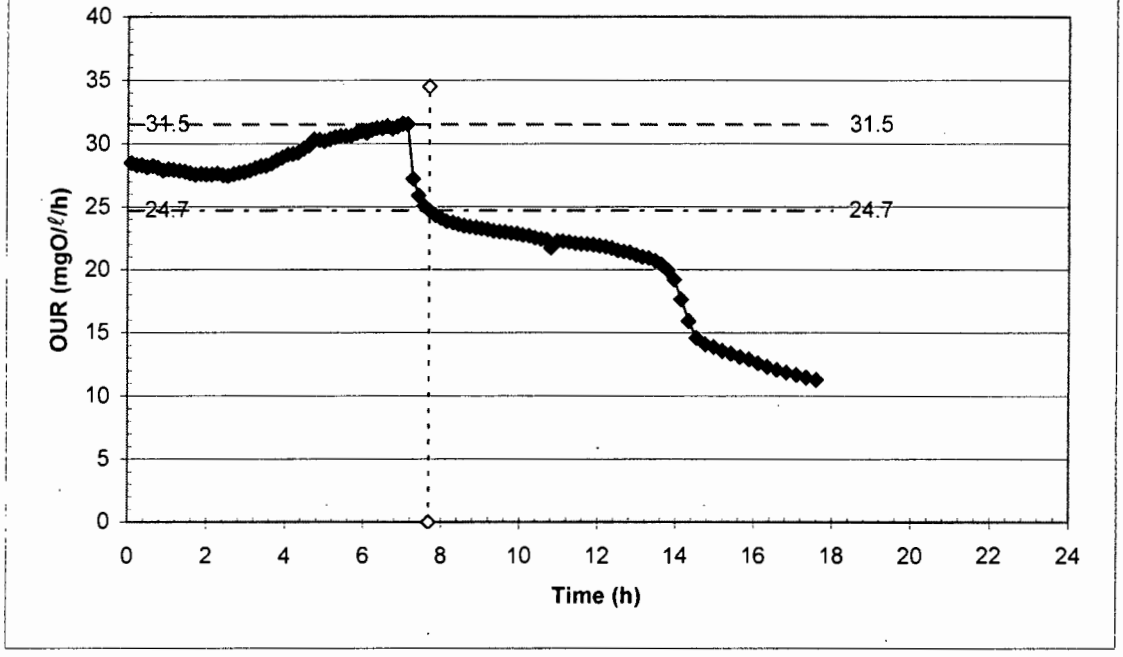

SB	Date	Day
22	24.10.02	340

Sbsi Drop (Time): 8.28

System Parameters:

Sti	522.2	mgCOD/ℓ
Suse	61.4	mgCOD/ℓ
Qs	35.82	ℓ/d
Sbsi	*104.4*	mgCOD/ℓ
fus	*0.118*	mgCOD/mgCOD
fts	*0.200*	mgCOD/mgCOD

Plot Sbsi (Max OUR) Plateau:

Sbsi Plat	XSbsi
0	31.95
18	*31.95*

Plot SBCOD OUR Plateau:

SBCOD Plat	XSBCOD
0	24.18
18	*24.18*

Plot GAE-Sbsi End Criteria:

Sbsi End (Time)	Range
8.83	0
8.83	*34.95*

ΔOUR = *7.8* mgO/ℓ

Figure B3(b)-51. SB 22 Sbsi System OUR

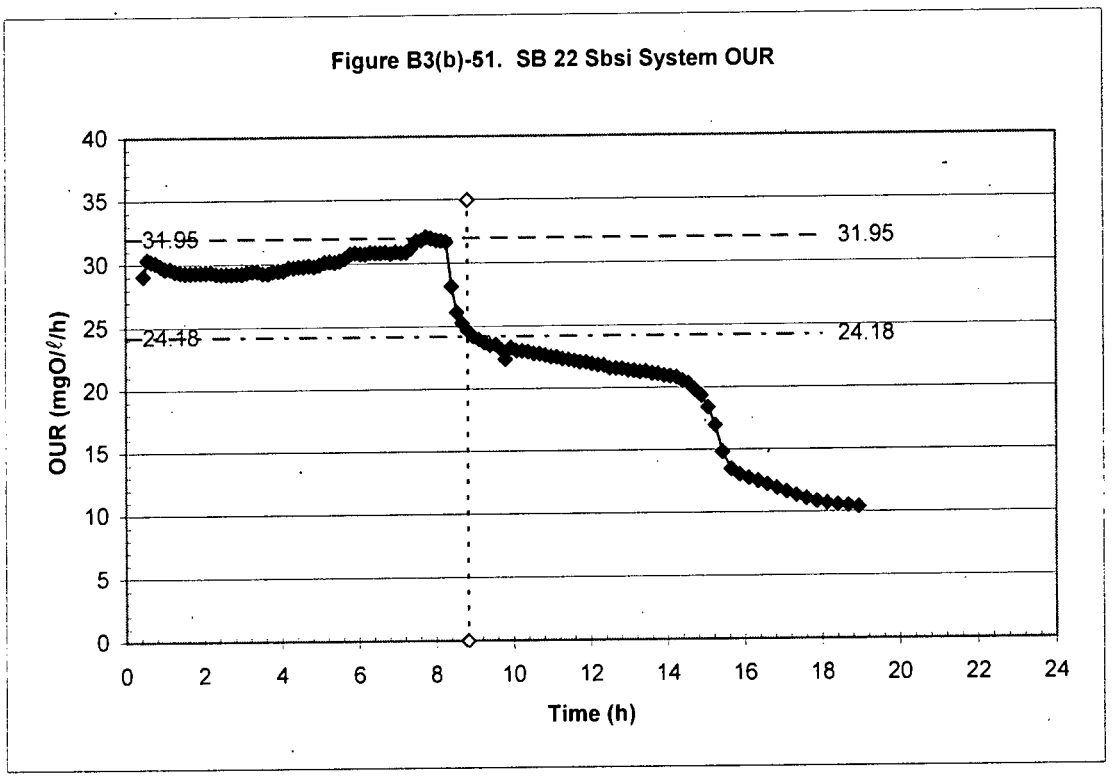

SB	Date	Day
22	25.10.02	341

Sbsi Drop (Time): 8.73

System Parameters:

Sti	528.4	mgCOD/ℓ
Suse	53.2	mgCOD/ℓ
Qs	35.87	ℓ/d
Sbsi	*82.5*	mgCOD/ℓ
fus	*0.101*	mgCOD/mgCOD
fts	*0.156*	mgCOD/mgCOD

Plot Sbsi (Max OUR) Plateau:

Sbsi Plat	XSbsi
0	28.15
18	*28.15*

Plot SBCOD OUR Plateau:

SBCOD Plat	XSBCOD
0	22
18	22

Plot GAE-Sbsi End Criteria:

Sbsi End (Time)	Range
9.28	0
9.28	*31.15*

ΔOUR = 6.2 mgO/ℓ

Figure B3(b)-52. SB 22 Sbsi System OUR

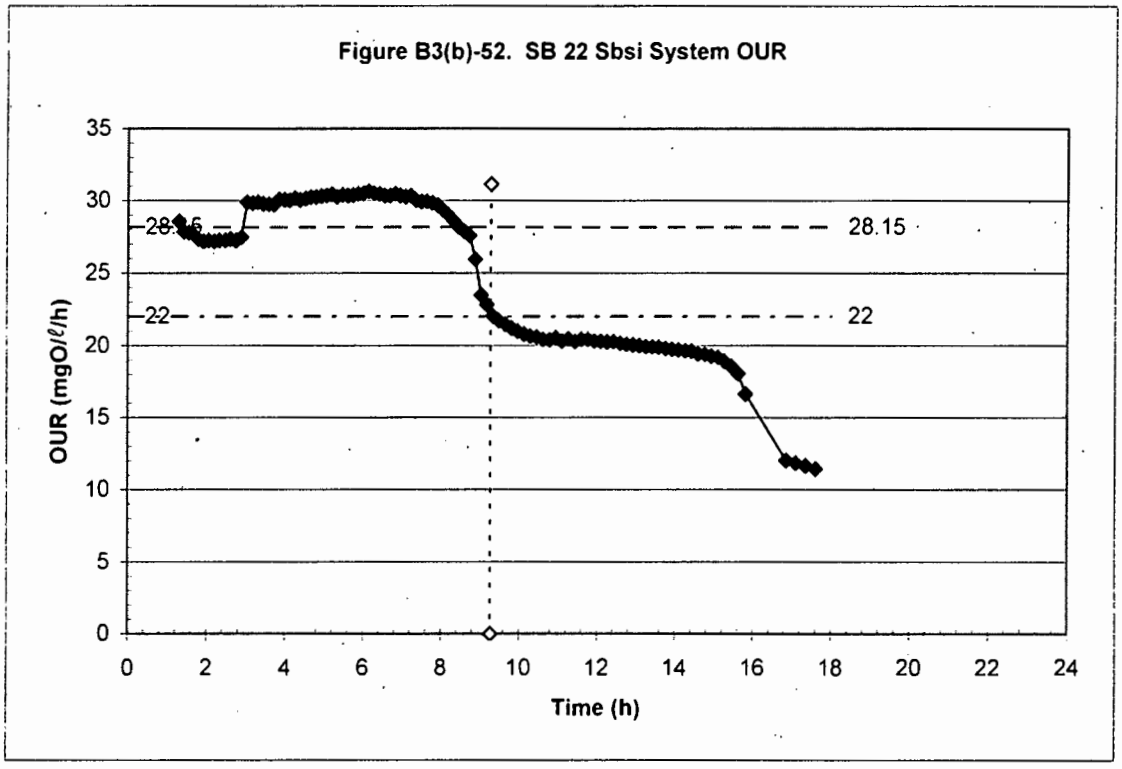

SB	Date	Day
22	26.10.02	332

Sbsi Drop (Time): **8.8**

System Parameters:

Sti	532.5	mgCOD/ℓ
Suse	59.4	mgCOD/ℓ
Qs	36	ℓ/d
Sbsi	*79.8*	mgCOD/ℓ
fus	*0.112*	mgCOD/mgCOD
fts	*0.150*	mgCOD/mgCOD

Plot Sbsi (Max OUR) Plateau:

Sbsi Plat	XSbsi
0	**29.1**
18	*29.1*

Plot SBCOD OUR Plateau:

SBCOD Plat	XSBCOD
0	**23.13**
18	*23.13*

Plot GAE-Sbsi End Criteria:

Sbsi End (Time)	Range
9.35	0
9.35	*32.1*

ΔOUR = *6.0* mgO/ℓ

Figure B3(b)-53. SB 22 Sbsi System OUR

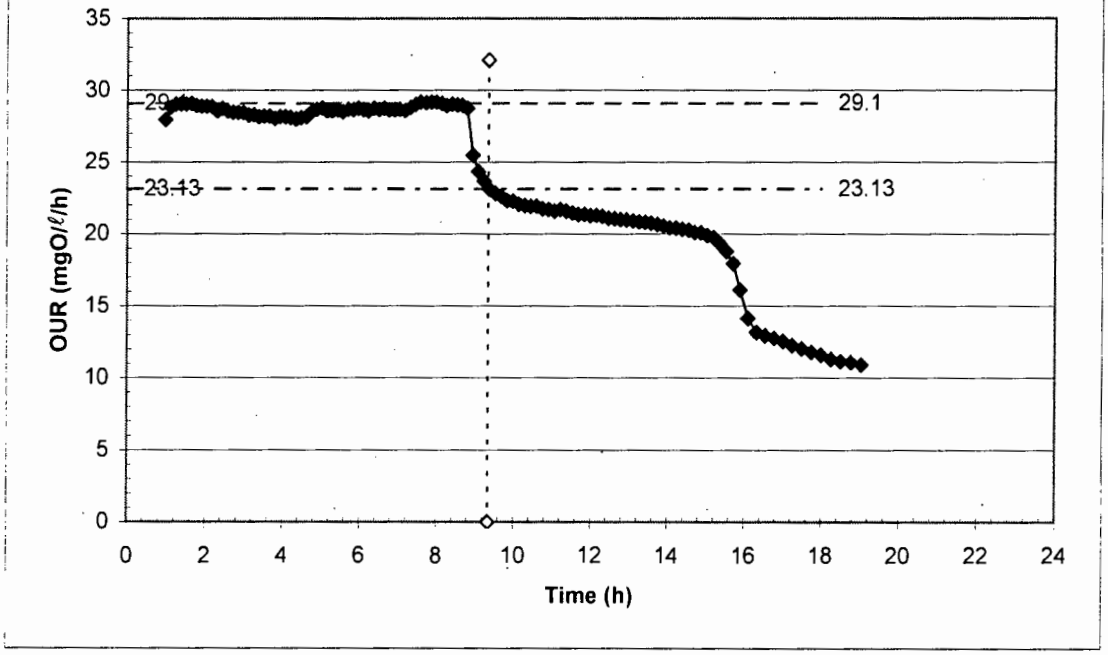

SB	Date	Day
22	28.10.02	344

Sbsi Drop (Time): **8.72**

System Parameters:

Sti	486.4	mgCOD/ℓ
Suse	75.8	mgCOD/ℓ
Qs	35.28	ℓ/d
Sbsi	*74.5*	mgCOD/ℓ
fus	*0.156*	mgCOD/mgCOD
fts	*0.153*	mgCOD/mgCOD

Plot Sbsi (Max OUR) Plateau:

Sbsi Plat	XSbsi
0	**31.36**
18	*31.36*

Plot SBCOD OUR Plateau:

SBCOD Plat	XSBCOD
0	**25.9**
18	*25.9*

Plot GAE-Sbsi End Criteria:

Sbsi End (Time)	Range
9.27	0
9.27	*34.36*

ΔOUR = *5.5* mgO/ℓ

Figure B3(b)-54. SB 22 Sbsi System OUR

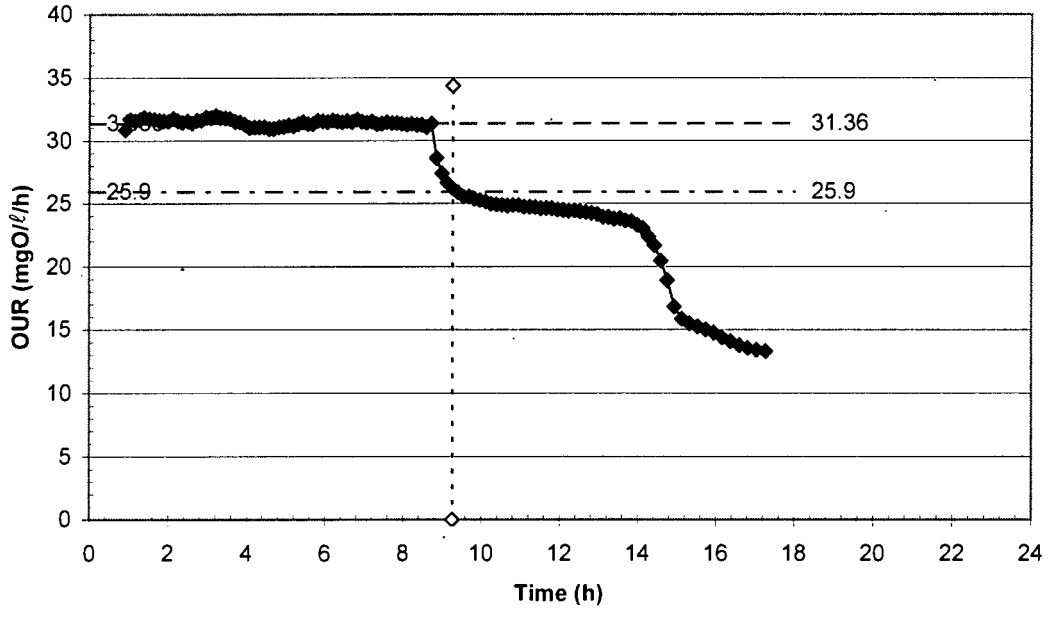

SB	Date	Day
22	29.10.02	345

Sbsi Drop (Time): 8.18

System Parameters:

Sti	501.8	mgCOD/ℓ
Suse	57.3	mgCOD/ℓ
Qs	36.52	ℓ/d
Sbsi	77.8	mgCOD/ℓ
fus	0.114	mgCOD/mgCOD
fts	0.155	mgCOD/mgCOD

Plot Sbsi (Max OUR) Plateau:

Sbsi Plat	XSbsi
0	30.4
18	30.4

Plot SBCOD OUR Plateau:

SBCOD Plat	XSBCOD
0	24.5
18	24.5

Plot GAE-Sbsi End Criteria:

Sbsi End (Time)	Range
8.73	0
8.73	33.4

ΔOUR = 5.9 mgO/ℓ

Figure B3(b)-55. SB 22 Sbsi System OUR

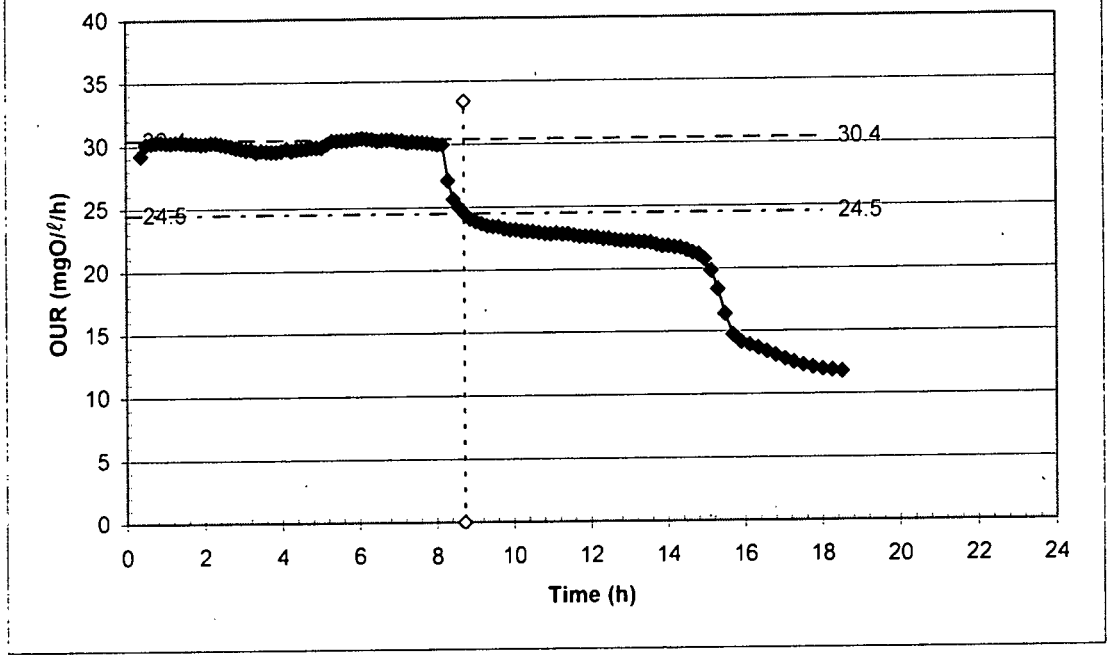

SB	Date	Day
23	3.11.02	350

Sbsi Drop (Time): 7.64

System Parameters:

Sti	520.2	mgCOD/ℓ
Suse	74.9	mgCOD/ℓ
Qs	36.08	ℓ/d
Sbsi	*84.1*	mgCOD/ℓ
fus	*0.144*	mgCOD/mgCOD
fts	*0.162*	mgCOD/mgCOD

Plot Sbsi (Max OUR) Plateau:

Sbsi Plat	XSbsi
0	30
18	*30*

Plot SBCOD OUR Plateau:

SBCOD Plat	XSBCOD
0	23.7
18	*23.7*

Plot GAE-Sbsi End Criteria:

Sbsi End (Time)	Range
8.19	0
8.19	*33*

ΔOUR = *6.3* mgO/ℓ

Figure B3(b)-56. SB 23 Sbsi System OUR

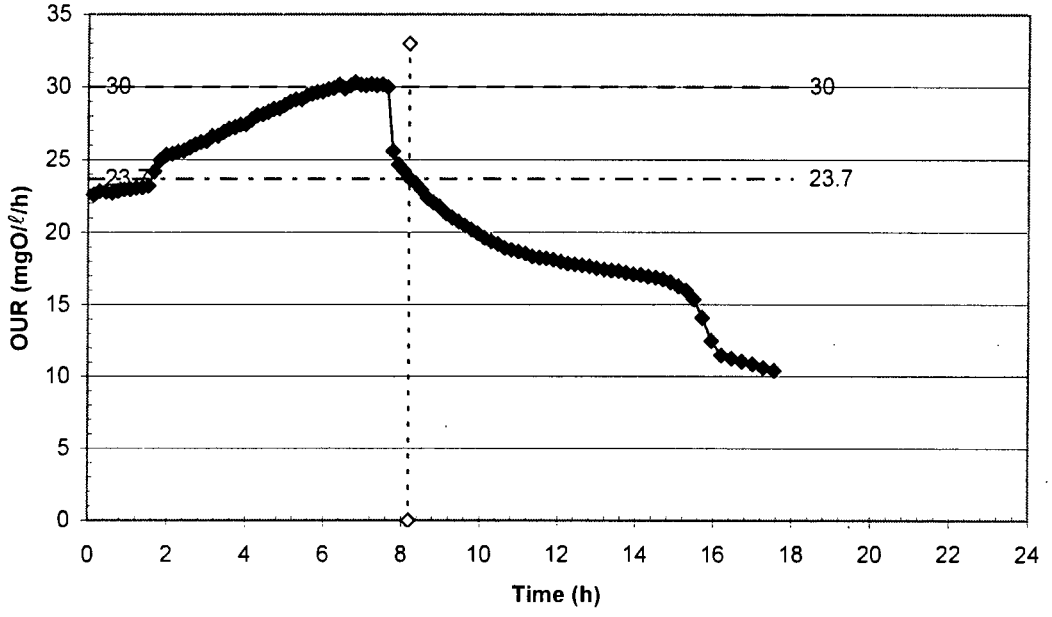

SB	Date	Day
23	4.11.02	351

Sbsi Drop (Time): **8.64**

System Parameters:

Sti	507.9	mgCOD/ℓ
Suse	67.7	mgCOD/ℓ
Qs	35.66	ℓ/d
Sbsi	*73.6*	mgCOD/ℓ
fus	*0.133*	mgCOD/mgCOD
fts	*0.145*	mgCOD/mgCOD

Plot Sbsi (Max OUR) Plateau:

Sbsi Plat	XSbsi
0	**28**
18	*28*

Plot SBCOD OUR Plateau:

SBCOD Plat	XSBCOD
0	**22.55**
18	*22.55*

Plot GAE-Sbsi End Criteria:

Sbsi End (Time)	Range
9.19	0
9.19	*31*

ΔOUR = *5.5* mgO/ℓ

Figure B3(b)-57. SB 23 Sbsi System OUR

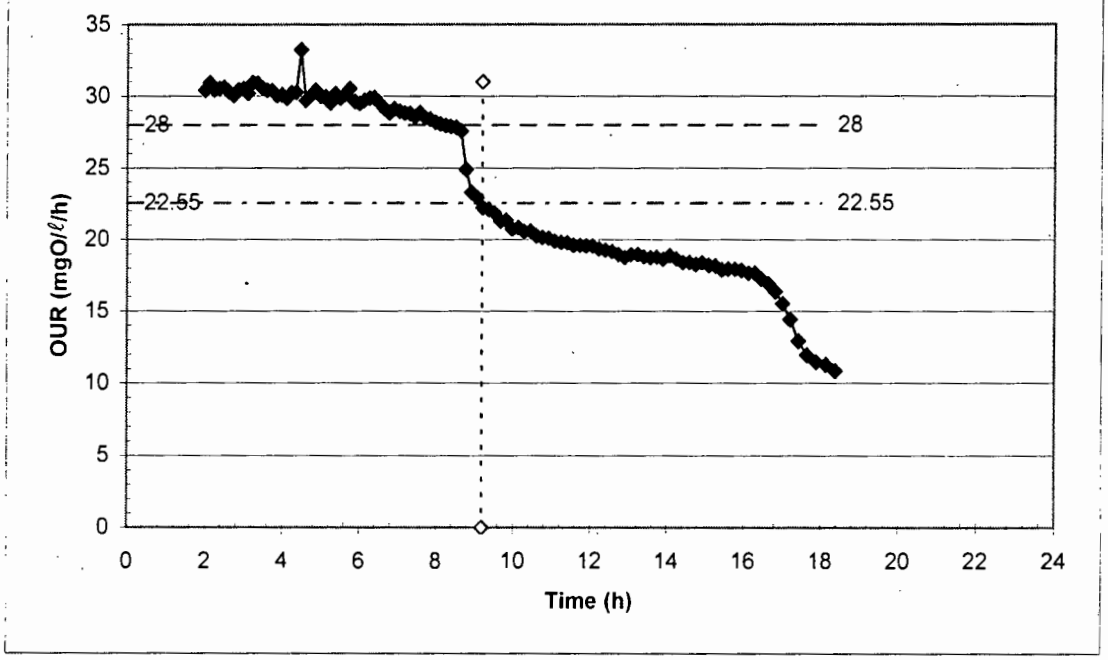

SB	Date	Day
23	5.11.02	352

Sbsi Drop (Time): 8.74

System Parameters:

Sti	510.9	mgCOD/ℓ
Suse	60.5	mgCOD/ℓ
Qs	35.92	ℓ/d
Sbsi	*71.0*	mgCOD/ℓ
fus	*0.118*	mgCOD/mgCOD
fts	*0.139*	mgCOD/mgCOD

Plot Sbsi (Max OUR) Plateau:

Sbsi Plat	XSbsi
0	26.75
18	*26.75*

Plot SBCOD OUR Plateau:

SBCOD Plat	XSBCOD
0	21.45
18	*21.45*

Plot GAE-Sbsi End Criteria:

Sbsi End (Time)	Range
9.29	0
9.29	*29.75*

ΔOUR = *5.3* mgO/ℓ

Figure B3(b)-58. SB 23 Sbsi System OUR

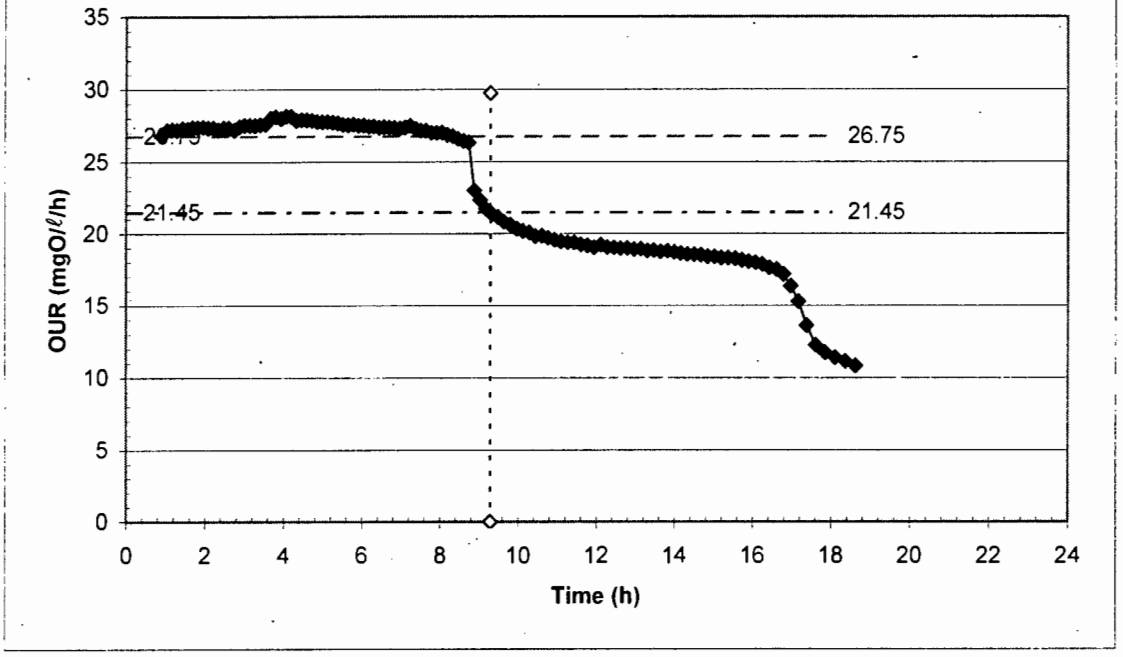

SB	Date	Day
23	6.11.02	353

Sbsi Drop (Time): 8.64

Plot Sbsi (Max OUR) Plateau:

Sbsi Plat	XSbsi
0	27.75
18	27.75

System Parameters:

Sti	521.2	mgCOD/ℓ
Suse	60.5	mgCOD/ℓ
Qs	36.22	ℓ/d
Sbsi	*65.1*	mgCOD/ℓ
fus	*0.116*	mgCOD/mgCOD
fts	*0.125*	mgCOD/mgCOD

Plot SBCOD OUR Plateau:

SBCOD Plat	XSBCOD
0	22.85
18	*22.85*

Plot GAE-Sbsi End Criteria:

Sbsi End (Time)	Range
9.19	0
9.19	*30.75*

ΔOUR = *4.9* mgO/ℓ

Figure B3(b)-59. SB 23 Sbsi System OUR

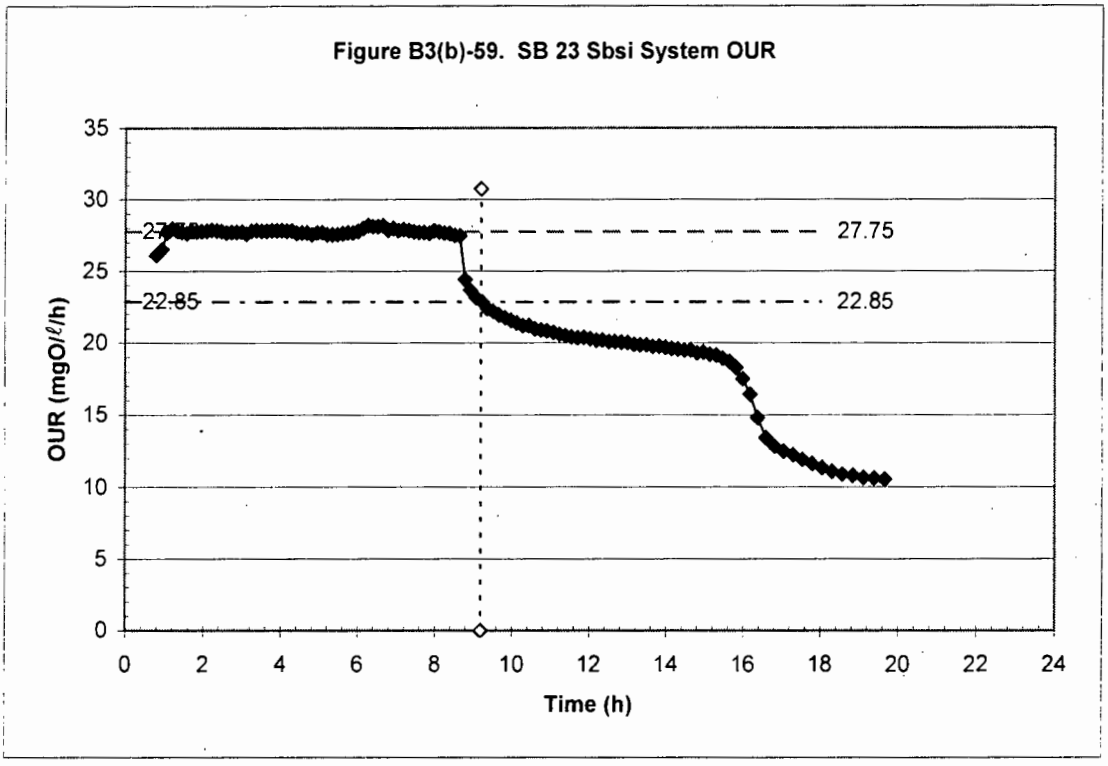

SB	Date	Day
23	7.11.02	354

Sbsi Drop (Time): 8.47

System Parameters:

Sti	474	mgCOD/ℓ
Suse	55.4	mgCOD/ℓ
Qs	35.96	ℓ/d
Sbsi	*61.3*	mgCOD/ℓ
fus	*0.117*	mgCOD/mgCOD
fts	*0.129*	mgCOD/mgCOD

Plot Sbsi (Max OUR) Plateau:

Sbsi Plat	XSbsi
0	28
18	*28*

Plot SBCOD OUR Plateau:

SBCOD Plat	XSBCOD
0	23.42
18	*23.42*

Plot GAE-Sbsi End Criteria:

Sbsi End (Time)	Range
9.02	0
9.02	*31*

ΔOUR = *4.6* mgO/ℓ

Figure B3(b)-60. SB 23 Sbsi System OUR

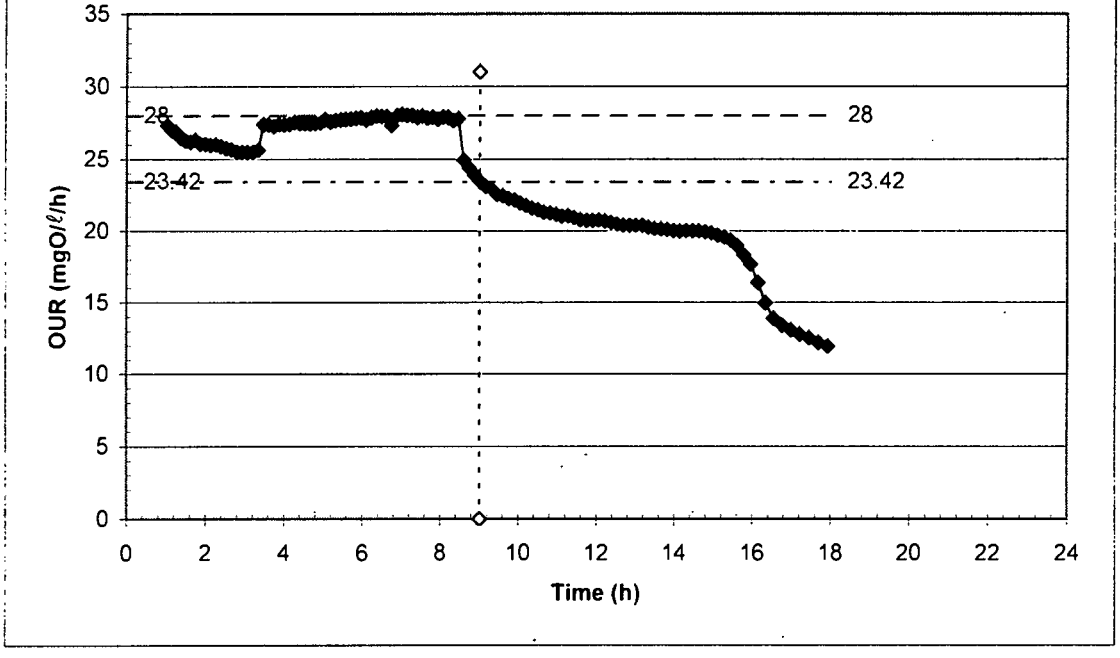

SB	Date	Day
23	8.11.02	355

Sbsi Drop (Time): **8.55**

System Parameters:

Sti	512	mgCOD/ℓ
Suse	62.6	mgCOD/ℓ
Qs	35.7	ℓ/d
Sbsi	*63.4*	mgCOD/ℓ
fus	*0.122*	mgCOD/mgCOD
fts	*0.124*	mgCOD/mgCOD

Plot Sbsi (Max OUR) Plateau:

Sbsi Plat	XSbsi
0	**29.5**
18	*29.5*

Plot SBCOD OUR Plateau:

SBCOD Plat	XSBCOD
0	**24.8**
18	*24.8*

Plot GAE-Sbsi End Criteria:

Sbsi End (Time)	Range
9.1	0
9.1	*32.5*

ΔOUR = *4.7* mgO/ℓ

Figure B3(b)-61. SB 23 Sbsi System OUR

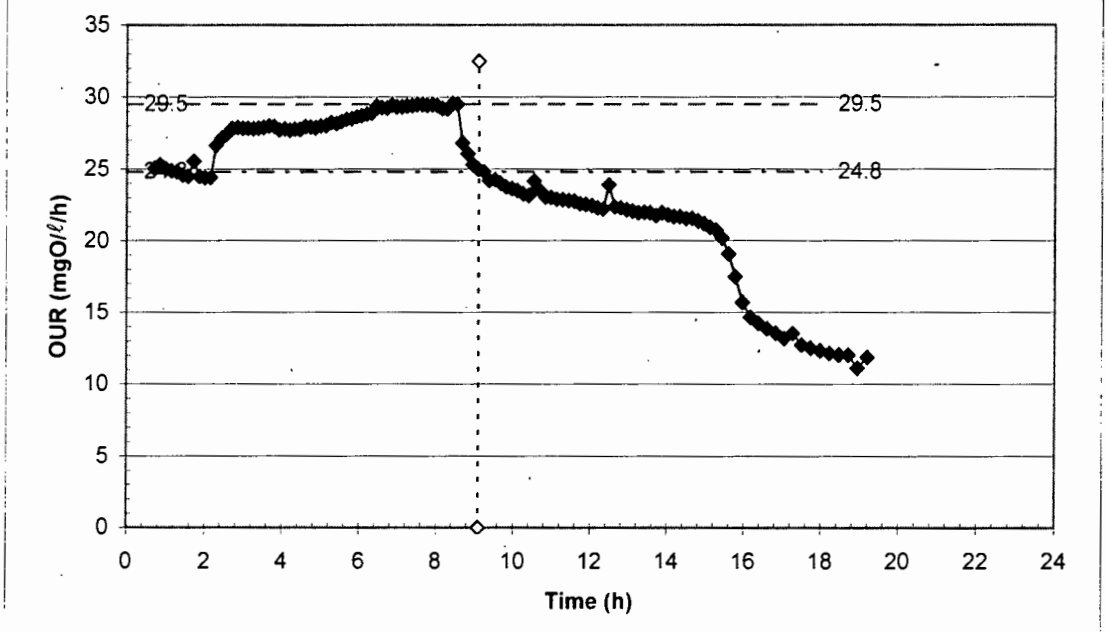

SB	Date	Day
23	9.11.02	3.56

Sbsi Drop (Time): 8.29

System Parameters:

Sti	472	mgCOD/ℓ
Suse	47.2	mgCOD/ℓ
Qs	36.16	ℓ/d
Sbsi	*74.6*	mgCOD/ℓ
fus	*0.100*	mgCOD/mgCOD
fts	*0.158*	mgCOD/mgCOD

Plot Sbsi (Max OUR) Plateau:

Sbsi Plat	XSbsi
0	28.5
18	*28.5*

Plot SBCOD OUR Plateau:

SBCOD Plat	XSBCOD
0	22.9
18	*22.9*

Plot GAE-Sbsi End Criteria:

Sbsi End (Time)	Range
8.84	0
8.84	*31.5*

ΔOUR = *5.6* mgO/ℓ

Figure B3(b)-62. SB 23 Sbsi System OUR

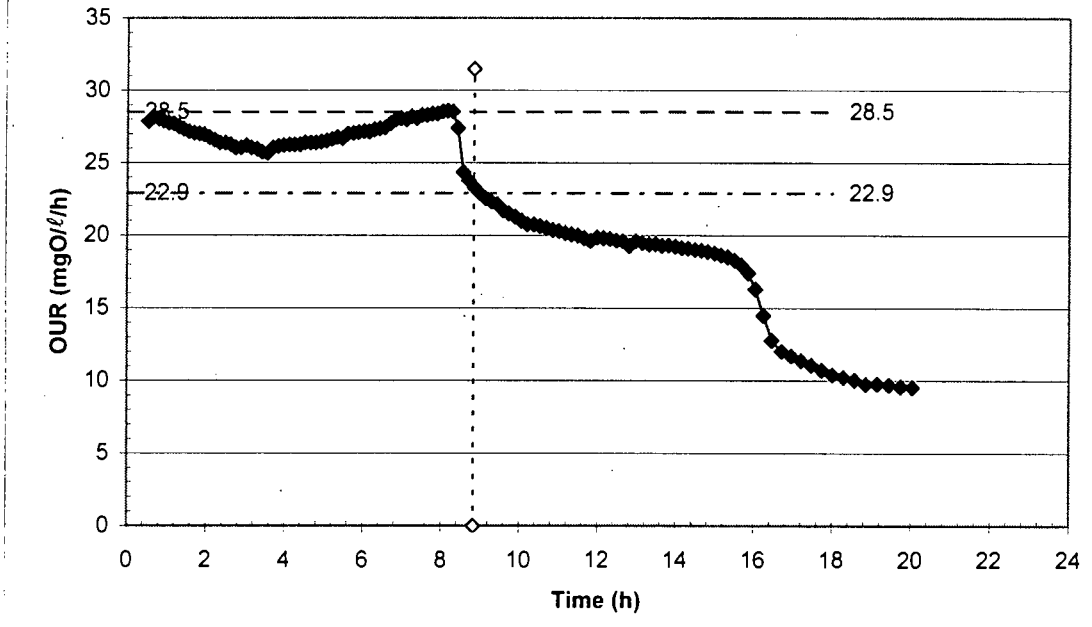

SB	Date	Day
23	10.11.02	357

Sbsi Drop (Time): 7.28

Plot Sbsi (Max OUR) Plateau:

Sbsi Plat	XSbsi
0	25.5
18	*25.5*

System Parameters:

Sti	515	mgCOD/ℓ
Suse	48.2	mgCOD/ℓ
Qs	36.1	ℓ/d
Sbsi	*67.3*	mgCOD/ℓ
fus	*0.094*	mgCOD/mgCOD
fts	*0.131*	mgCOD/mgCOD

Plot SBCOD OUR Plateau:

SBCOD Plat	XSBCOD
0	20.45
18	*20.45*

Plot GAE-Sbsi End Criteria:

Sbsi End (Time)	Range
7.83	0
7.83	*28.5*

ΔOUR = *5.1* mgO/ℓ

Figure B3(b)-63. SB 23 Sbsi System OUR

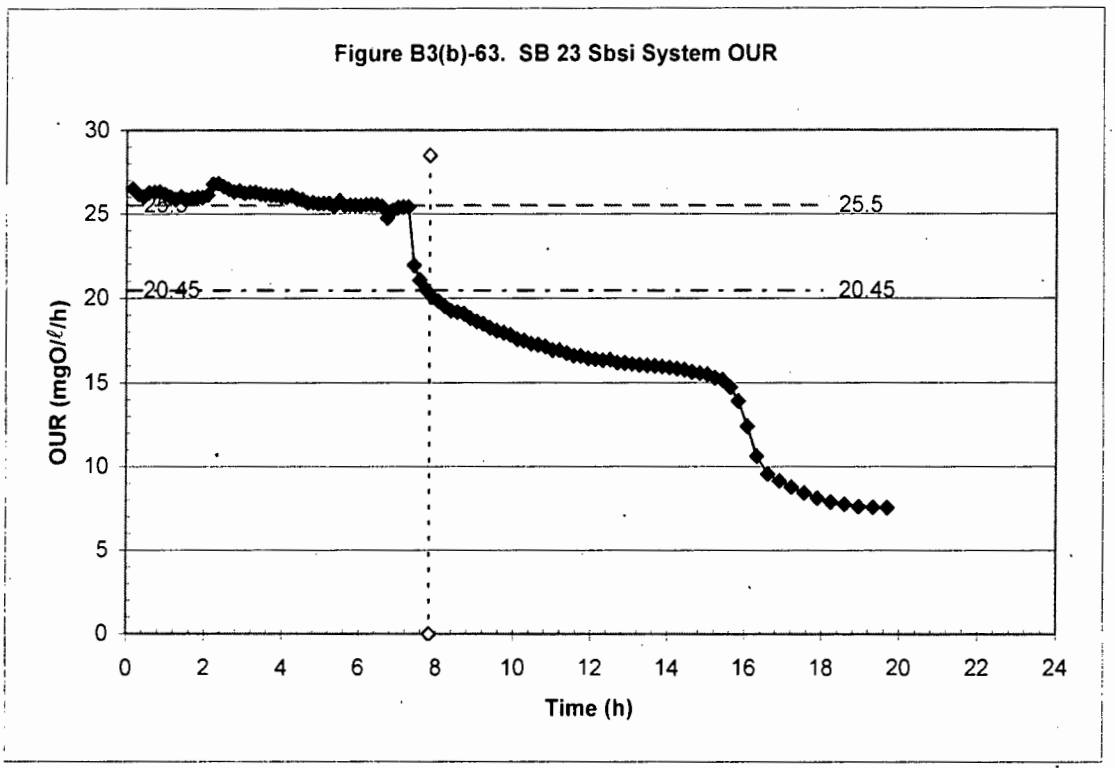

SB	Date	Day
23	11.11.02	358

Sbsi Drop (Time): **8.28**

System Parameters:

Sti	500.7	mgCOD/ℓ
Suse	55.4	mgCOD/ℓ
Qs	35.78	ℓ/d
Sbsi	*78.0*	mgCOD/ℓ
fus	*0.111*	mgCOD/mgCOD
fts	*0.156*	mgCOD/mgCOD

Plot Sbsi (Max OUR) Plateau:

Sbsi Plat	XSbsi
0	**27.2**
18	*27.2*

Plot SBCOD OUR Plateau:

SBCOD Plat	XSBCOD
0	**21.4**
18	*21.4*

Plot GAE-Sbsi End Criteria:

Sbsi End (Time)	Range
8.83	0
8.83	*30.2*

ΔOUR = *5.8* mgO/ℓ

Figure B3(b)-64. SB 23 Sbsi System OUR

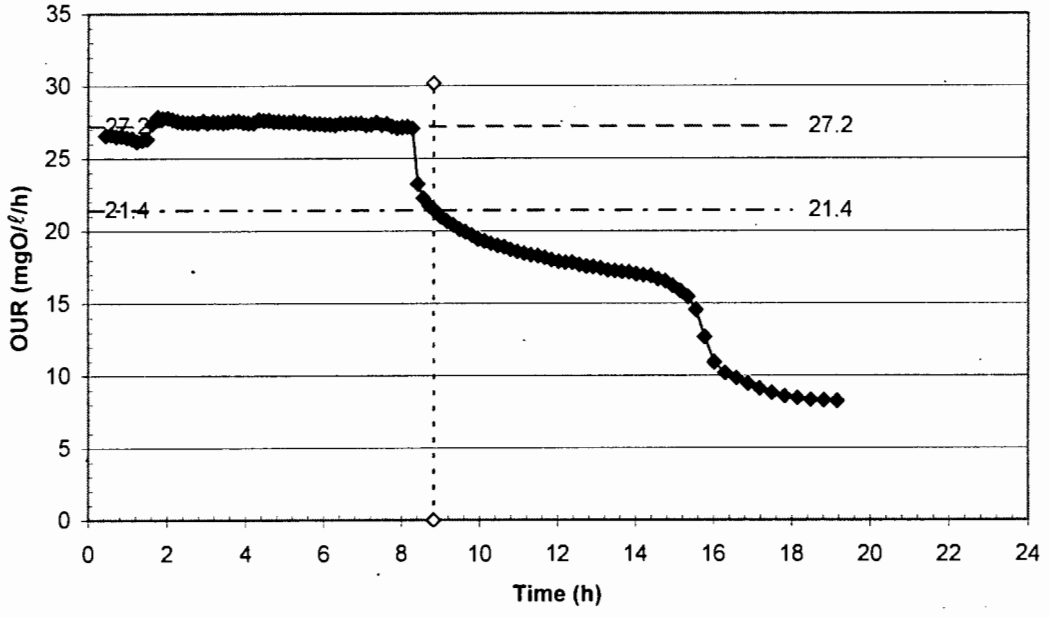

SB	Date	Day
23	12.11.02	359

Sbsi Drop (Time): 8.42

System Parameters:

Sti	481.2	mgCOD/ℓ
Suse	50.3	mgCOD/ℓ
Qs	34.62	ℓ/d
Sbsi	*78.3*	mgCOD/ℓ
fus	*0.105*	mgCOD/mgCOD
fts	*0.163*	mgCOD/mgCOD

Plot Sbsi (Max OUR) Plateau:

Sbsi Plat	XSbsi
0	28.36
18	28.36

Plot SBCOD OUR Plateau:

SBCOD Plat	XSBCOD
0	22.73
18	*22.73*

Plot GAE-Sbsi End Criteria:

Sbsi End (Time)	Range
8.97	0
8.97	*31.36*

ΔOUR = *5.6* mgO/ℓ

Figure B3(b)-65. SB 23 Sbsi System OUR

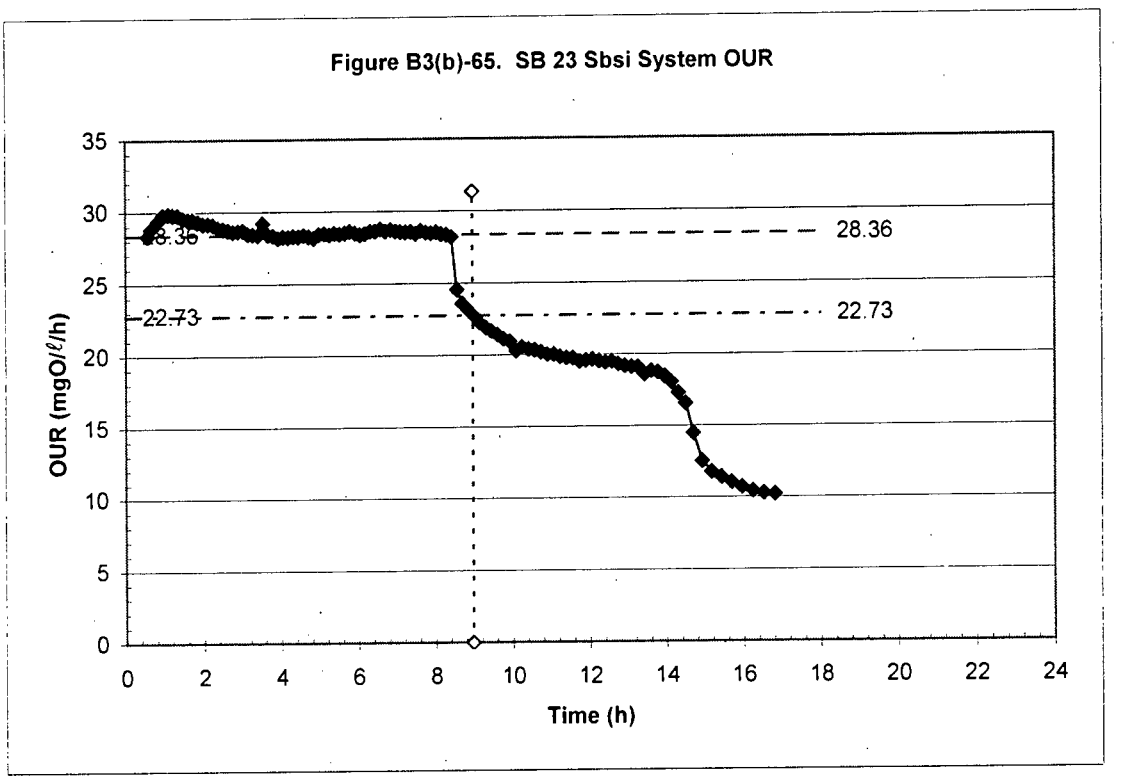

SB	Date	Day
23	13.11.02	360

Sbsi Drop (Time): 8.95

System Parameters:

Sti	457	mgCOD/ℓ
Suse	47.2	mgCOD/ℓ
Qs	35.4	ℓ/d
Sbsi	*71.4*	mgCOD/ℓ
fus	*0.103*	mgCOD/mgCOD
fts	*0.156*	mgCOD/mgCOD

Plot Sbsi (Max OUR) Plateau:

Sbsi Plat	XSbsi
0	27
18	*27*

Plot SBCOD OUR Plateau:

SBCOD Plat	XSBCOD
0	21.75
18	*21.75*

Plot GAE-Sbsi End Criteria:

Sbsi End (Time)	Range
9.5	0
9.5	*30*

ΔOUR = *5.3* mgO/ℓ

Figure B3(b)-66. SB 23 Sbsi System OUR

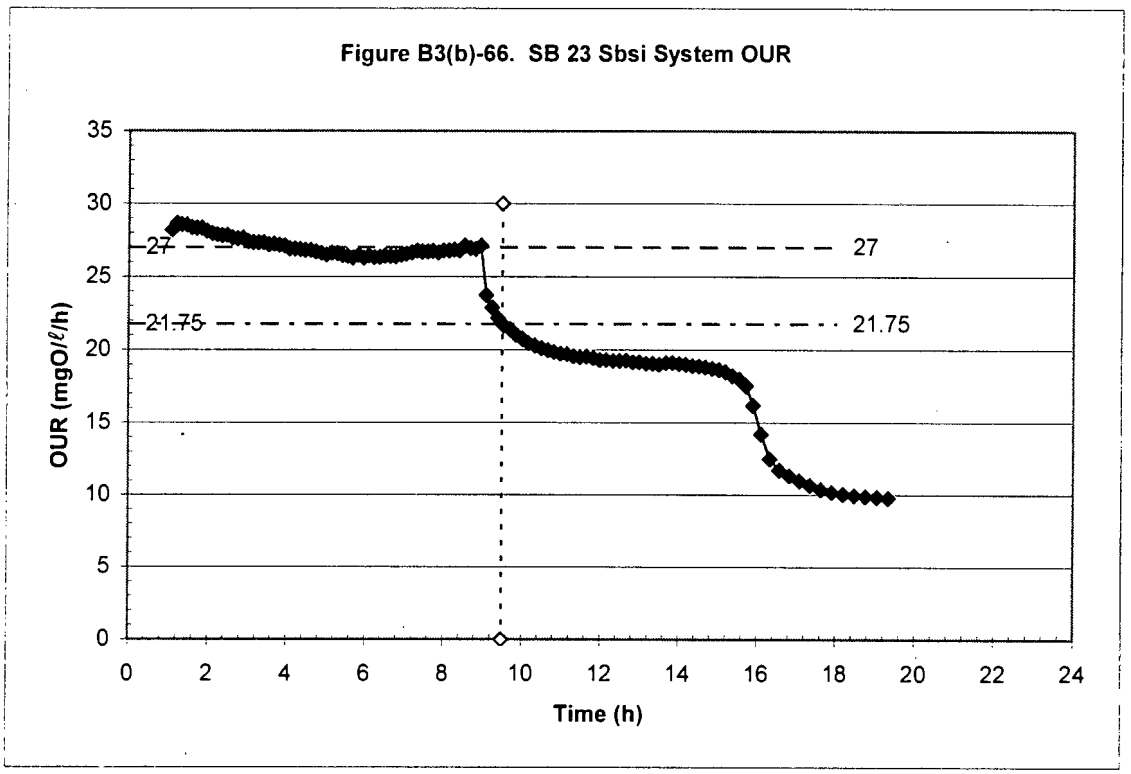

SB	Date	Day
23	14.11.02	361

Sbsi Drop (Time): **8.24**

System Parameters:

Sti	460.8	mgCOD/ℓ
Suse	47.2	mgCOD/ℓ
Qs	35.42	ℓ/d
Sbsi	*86.3*	mgCOD/ℓ
fus	*0.102*	mgCOD/mgCOD
fts	*0.187*	mgCOD/mgCOD

Plot Sbsi (Max OUR) Plateau:

Sbsi Plat	XSbsi
0	**28.6**
18	*28.6*

Plot SBCOD OUR Plateau:

SBCOD Plat	XSBCOD
0	**22.25**
18	*22.25*

Plot GAE-Sbsi End Criteria:

Sbsi End (Time)	Range
8.79	0
8.79	*31.6*

ΔOUR = *6.4* mgO/ℓ

Figure B3(b)-67. SB 23 Sbsi System OUR

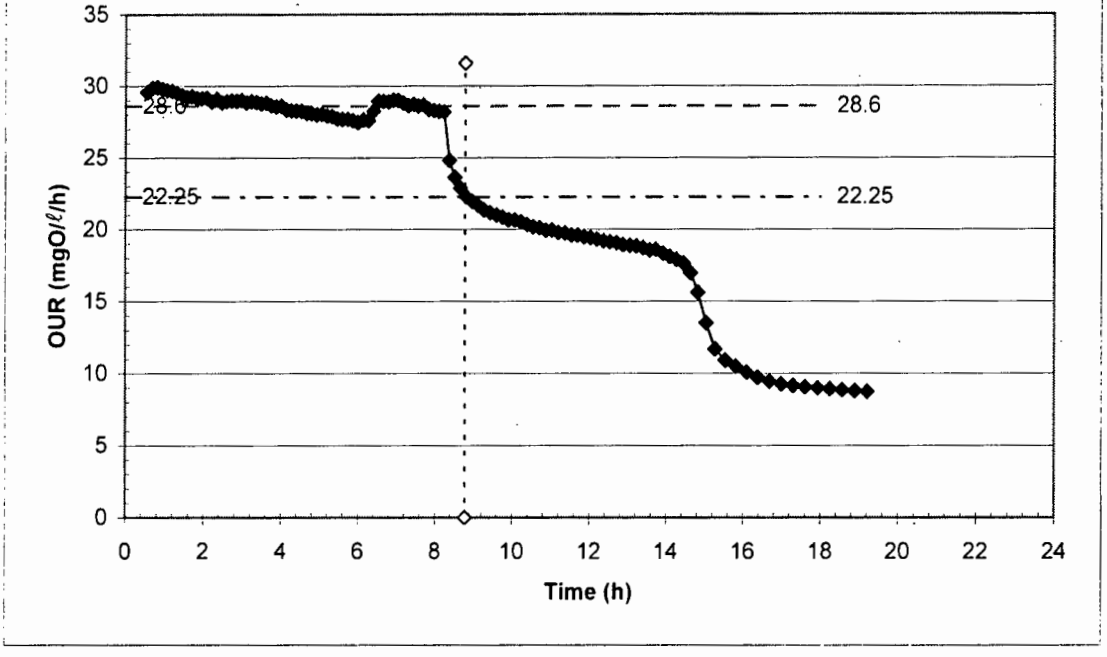

SB	Date	Day
23	15.11.02	362

Sbsi Drop (Time): **7.86**

System Parameters:

Sti	468.9	mgCOD/ℓ
Suse	51.2	mgCOD/ℓ
Qs	35.46	ℓ/d
Sbsi	*63.8*	mgCOD/ℓ
fus	*0.109*	mgCOD/mgCOD
fts	*0.136*	mgCOD/mgCOD

Plot Sbsi (Max OUR) Plateau:

Sbsi Plat	XSbsi
0	**28.5**
18	*28.5*

Plot SBCOD OUR Plateau:

SBCOD Plat	XSBCOD
0	**23.8**
18	*23.8*

Plot GAE-Sbsi End Criteria:

Sbsi End (Time)	Range
8.41	0
8.41	*31.5*

ΔOUR = *4.7* mgO/ℓ

Figure B3(b)-68. SB 23 Sbsi System OUR

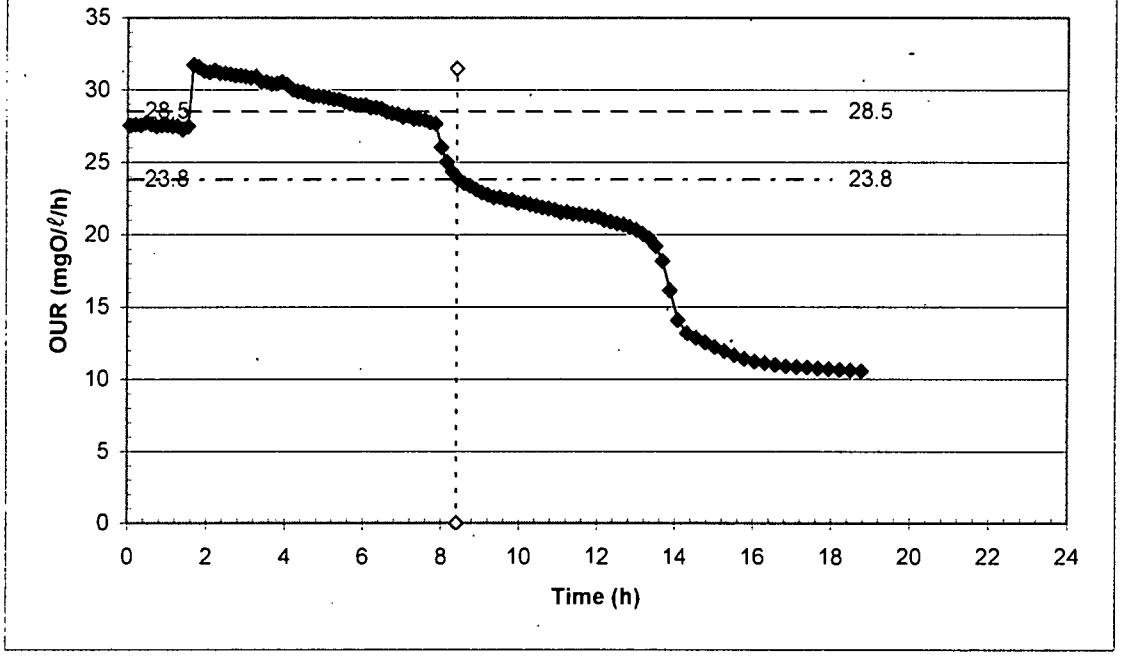

SB	Date	Day
23	16.11.02	363

Sbsi Drop (Time): 8.68

Plot Sbsi (Max OUR) Plateau:

Sbsi Plat	XSbsi
0	30.45
18	30.45

System Parameters:

Sti	453.8	mgCOD/ℓ
Suse	50.2	mgCOD/ℓ
Qs	35.56	ℓ/d
Sbsi	*51.4*	mgCOD/ℓ
fus	*0.111*	mgCOD/mgCOD
fts	*0.113*	mgCOD/mgCOD

Plot SBCOD OUR Plateau:

SBCOD Plat	XSBCOD
0	26.65
18	*26.65*

Plot GAE-Sbsi End Criteria:

Sbsi End (Time)	Range
9.23	0
9.23	*33.45*

ΔOUR = *3.8* mgO/ℓ

Figure B3(b)-69. SB 23 Sbsi System OUR

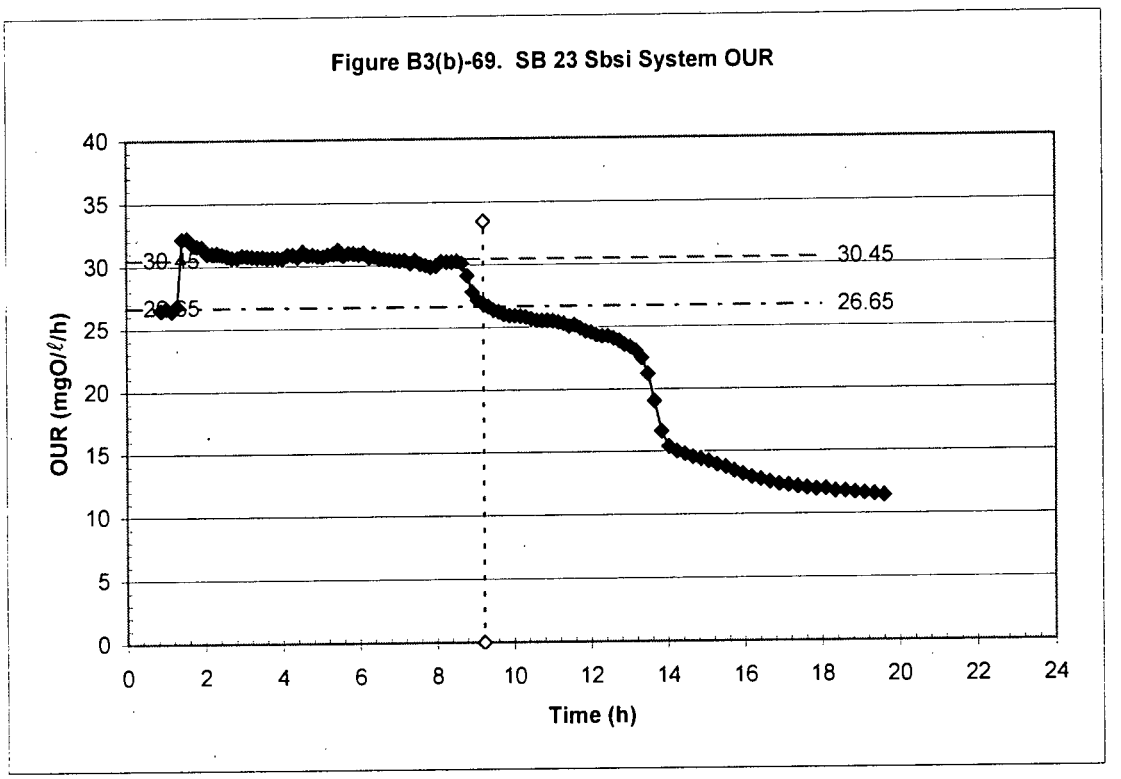

SB	Date	Day
23	17.11.02	364

Sbsi Drop (Time): 8.91

System Parameters:

Sti	445.8	mgCOD/ℓ
Suse	51.2	mgCOD/ℓ
Qs	35.72	ℓ/d
Sbsi	*54.6*	mgCOD/ℓ
fus	*0.115*	mgCOD/mgCOD
fts	*0.122*	mgCOD/mgCOD

Plot Sbsi (Max OUR) Plateau:

Sbsi Plat	XSbsi
0	30.4
18	*30.4*

Plot SBCOD OUR Plateau:

SBCOD Plat	XSBCOD
0	26.35
18	*26.35*

Plot GAE-Sbsi End Criteria:

Sbsi End (Time)	Range
9.46	0
9.46	*33.4*

ΔOUR = *4.1* mgO/ℓ

Figure B3(b)-70. SB 23 Sbsi System OUR

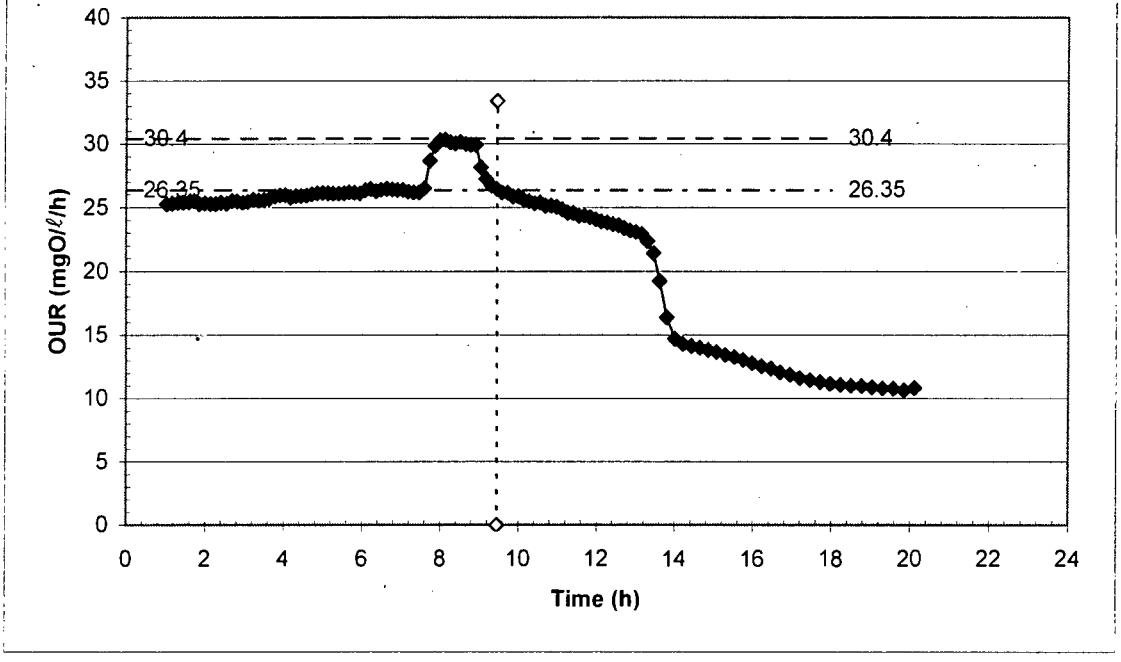

SB	Date	Day
23b	18.11.02	365

Sbsi Drop (Time): 7.86

System Parameters:

Sti	480.9	mgCOD/ℓ
Suse		mgCOD/ℓ
Qs	35.3	ℓ/d
Sbsi	*94.8*	mgCOD/ℓ
fus		mgCOD/mgCOD
fts	*0.197*	mgCOD/mgCOD

Plot Sbsi (Max OUR) Plateau:

Sbsi Plat	XSbsi
0	30.9
18	*30.9*

Plot SBCOD OUR Plateau:

SBCOD Plat	XSBCOD
0	23.95
18	*23.95*

Plot GAE-Sbsi End Criteria:

Sbsi End (Time)	Range
8.41	0
8.41	*33.9*

ΔOUR = *7.0* mgO/ℓ

Figure B3(b)-71. SB 23 Sbsi System OUR

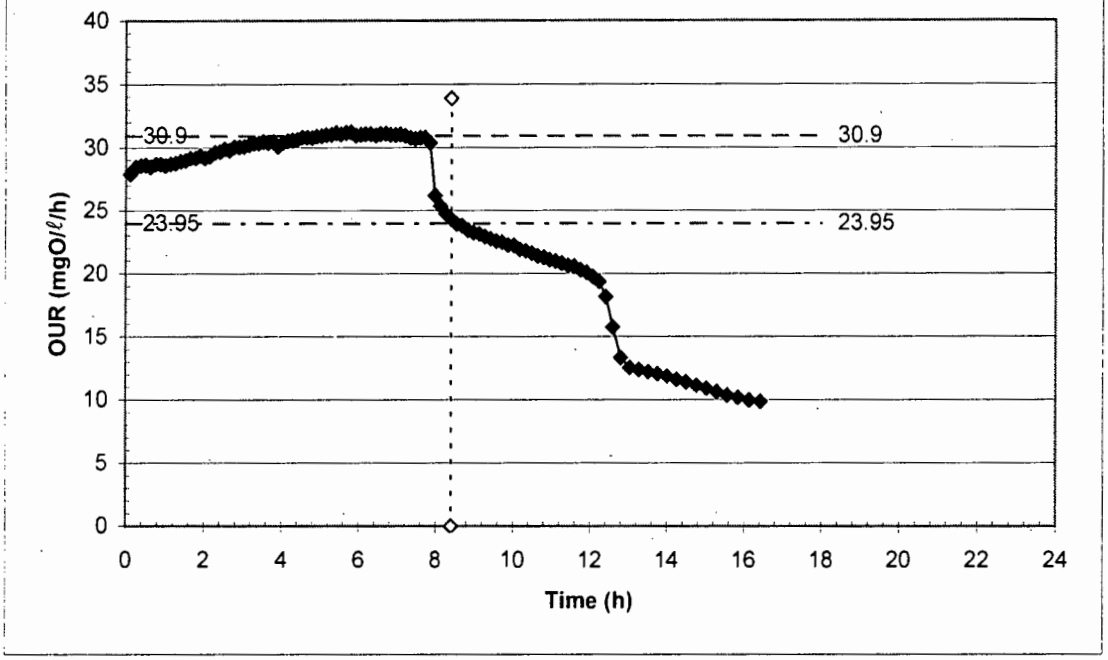

SB	Date	Day
23b	19.11.02	366

Sbsi Drop (Time): 8.86

System Parameters:

Sti		mgCOD/ℓ
Suse		mgCOD/ℓ
Qs	34.96	ℓ/d
Sbsi	*74.4*	mgCOD/ℓ
fus		mgCOD/mgCOD
fts		mgCOD/mgCOD

Plot Sbsi (Max OUR) Plateau:

Sbsi Plat	XSbsi
0	27.4
18	*27.4*

Plot SBCOD OUR Plateau:

SBCOD Plat	XSBCOD
0	22
18	*22*

Plot GAE-Sbsi End Criteria:

Sbsi End (Time)	Range
9.41	0
9.41	*30.4*

ΔOUR = *5.4* mgO/ℓ

Figure B3(b)-72. SB 23b Sbsi System OUR

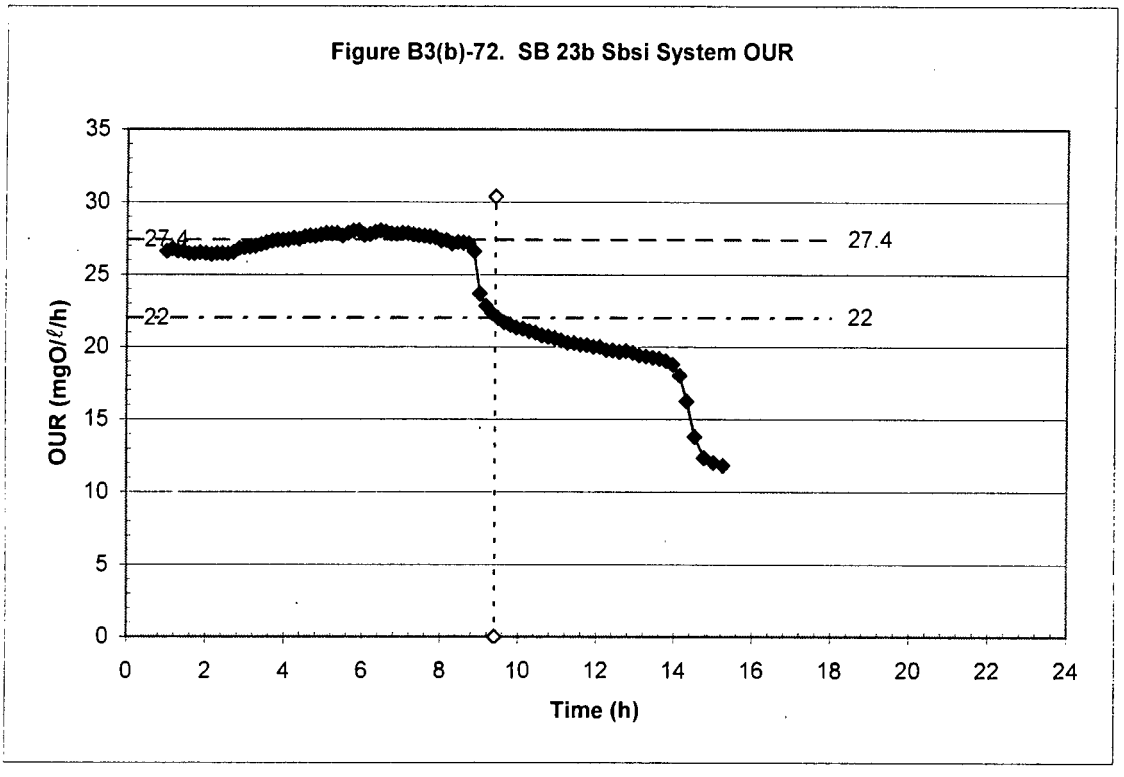

SB	Date	Day
24	21.11.02	368

Sbsi Drop (Time): **6.55**

System Parameters:

Sti	537.1	mgCOD/ℓ
Suse		mgCOD/ℓ
Qs	35	ℓ/d
Sbsi	*53.6*	mgCOD/ℓ
fus		mgCOD/mgCOD
fts	*0.100*	mgCOD/mgCOD

Plot Sbsi (Max OUR) Plateau:

Sbsi Plat	XSbsi
0	**28.1**
18	*28.1*

Plot SBCOD OUR Plateau:

SBCOD Plat	XSBCOD
0	**24.2**
18	*24.2*

Plot GAE-Sbsi End Criteria:

Sbsi End (Time)	Range
7.1	0
7.1	*31.1*

ΔOUR = *3.9* mgO/ℓ

Figure B3(b)-73. SB 24 Sbsi System OUR

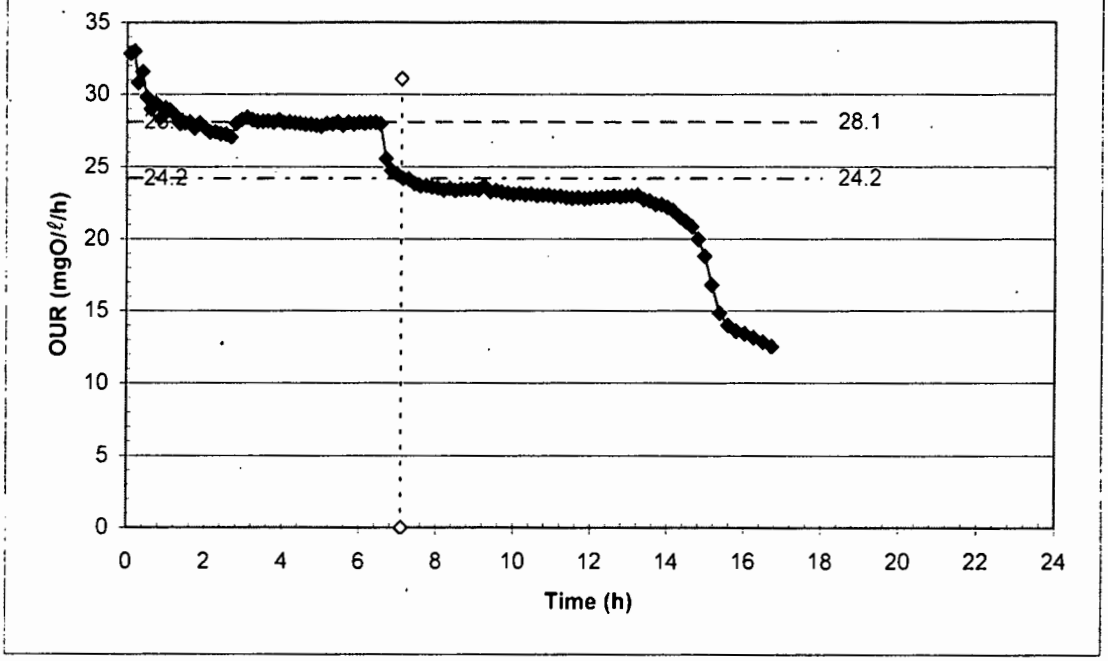

SB	Date	Day
24	22.11.02	369

Sbsi Drop (Time): **7.54**

System Parameters:

Sti	450.8	mgCOD/ℓ
Suse	53.2	mgCOD/ℓ
Qs	35.3	ℓ/d
Sbsi	*66.1*	mgCOD/ℓ
fus	*0.118*	mgCOD/mgCOD
fts	*0.147*	mgCOD/mgCOD

Plot Sbsi (Max OUR) Plateau:

Sbsi Plat	XSbsi
0	**30.1**
18	*30.1*

Plot SBCOD OUR Plateau:

SBCOD Plat	XSBCOD
0	**25.25**
18	*25.25*

Plot GAE-Sbsi End Criteria:

Sbsi End (Time)	Range
8.09	0
8.09	*33.1*

ΔOUR = *4.9* mgO/ℓ

Figure B3(b)-74. SB 24 Sbsi System OUR

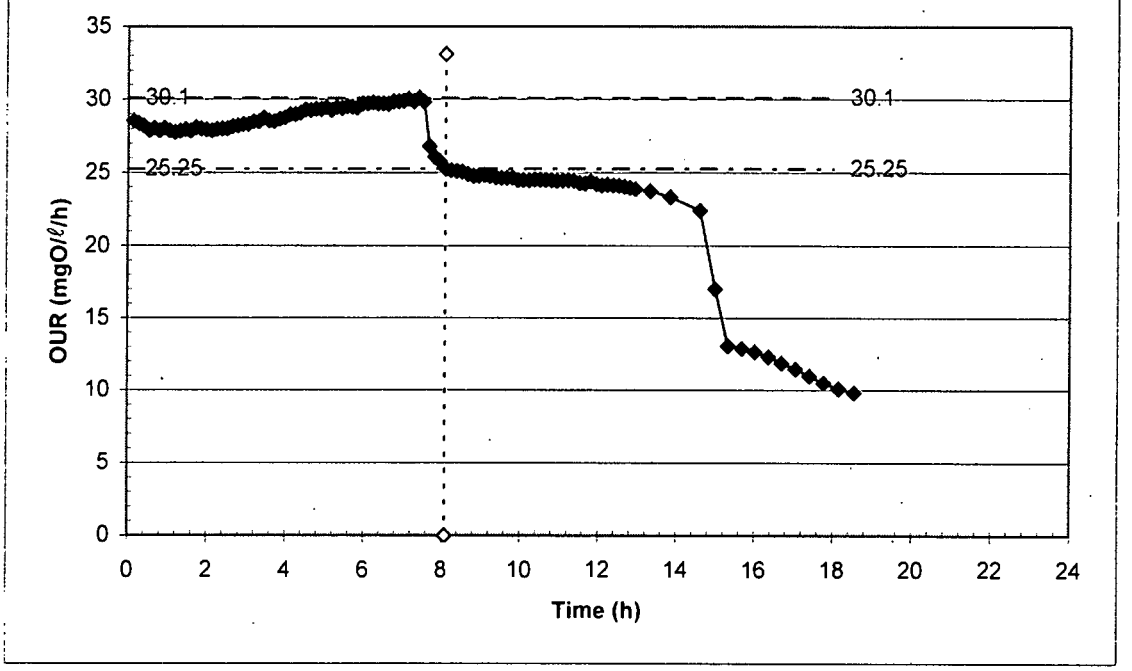

SB	Date	Day
24	23.11.02	370

Sbsi Drop (Time): 8.48

System Parameters:

Sti	480.9	mgCOD/ℓ
Suse	35.1	mgCOD/ℓ
Qs	35.32	ℓ/d
Sbsi	*69.9*	mgCOD/ℓ
fus	*0.073*	mgCOD/mgCOD
fts	*0.145*	mgCOD/mgCOD

Plot Sbsi (Max OUR) Plateau:

Sbsi Plat	XSbsi
0	30.1
18	*30.1*

Plot SBCOD OUR Plateau:

SBCOD Plat	XSBCOD
0	24.97
18	*24.97*

Plot GAE-Sbsi End Criteria:

Sbsi End (Time)	Range
9.03	0
9.03	*33.1*

ΔOUR = *5.1* mgO/ℓ

Figure B3(b)-75. SB 24 Sbsi System OUR

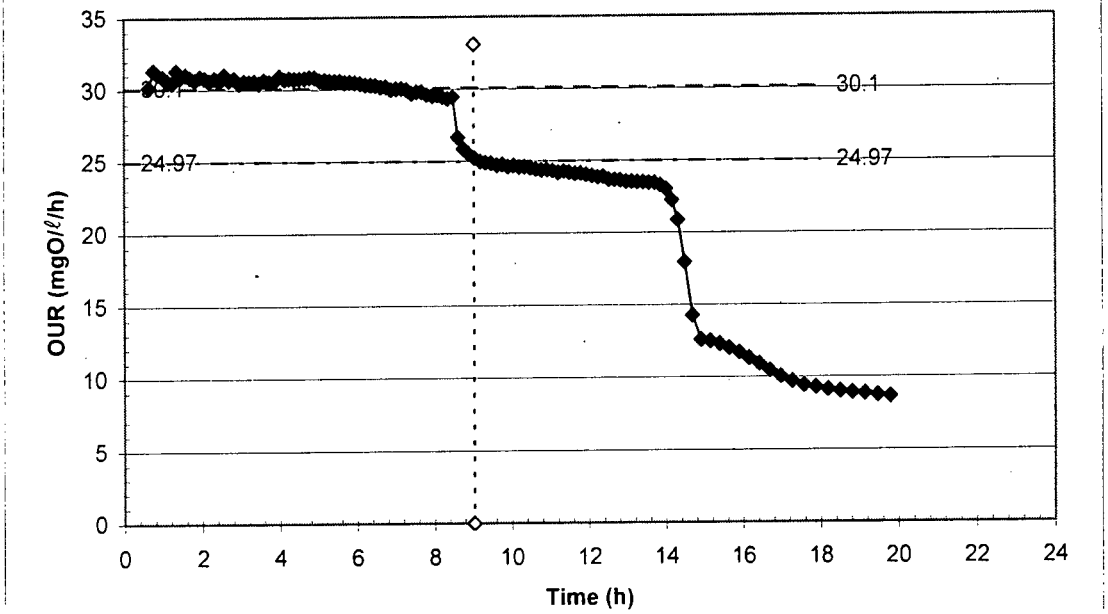

SB	Date	Day
24	24.11.02	371

Sbsi Drop (Time): **6.36**

System Parameters:

Sti	459.8	mgCOD/ℓ
Suse	51.2	mgCOD/ℓ
Qs	34.84	ℓ/d
Sbsi	*49.1*	mgCOD/ℓ
fus	*0.111*	mgCOD/mgCOD
fts	*0.107*	mgCOD/mgCOD

Plot Sbsi (Max OUR) Plateau:

Sbsi Plat	XSbsi
0	**25**
18	25

Plot SBCOD OUR Plateau:

SBCOD Plat	XSBCOD
0	**21.45**
18	*21.45*

Plot GAE-Sbsi End Criteria:

Sbsi End (Time)	Range
6.91	0
6.91	*28*

ΔOUR = *3.6* mgO/ℓ

Figure B3(b)-76. SB 24 Sbsi System OUR

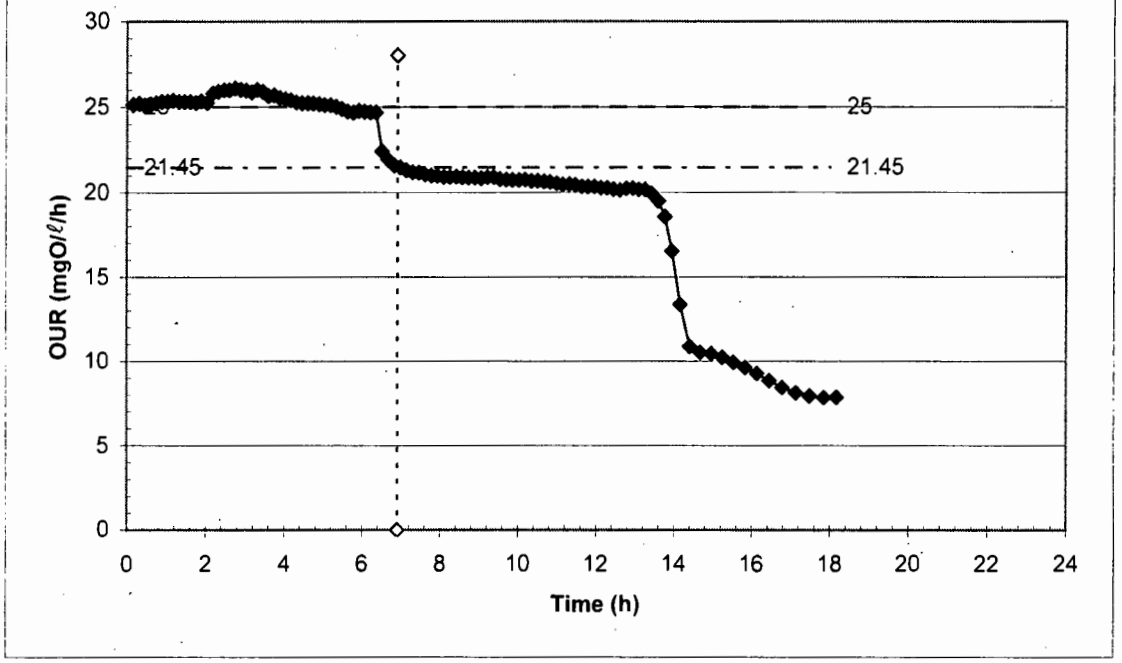

SB	Date	Day
24	25.11.02	372

Sbsi Drop (Time): 9.05

System Parameters:

Sti	380.5	mgCOD/ℓ
Suse	42.2	mgCOD/ℓ
Qs	34.54	ℓ/d
Sbsi	*57.1*	mgCOD/ℓ
fus	*0.111*	mgCOD/mgCOD
fts	*0.150*	mgCOD/mgCOD

Plot Sbsi (Max OUR) Plateau:

Sbsi Plat	XSbsi
0	31.5
18	31.5

Plot SBCOD OUR Plateau:

SBCOD Plat	XSBCOD
0	27.4
18	27.4

Plot GAE-Sbsi End Criteria:

Sbsi End (Time)	Range
9.6	0
9.6	*34.5*

ΔOUR = *4.1* mgO/ℓ

Figure B3(b)-77. SB 24 Sbsi System OUR

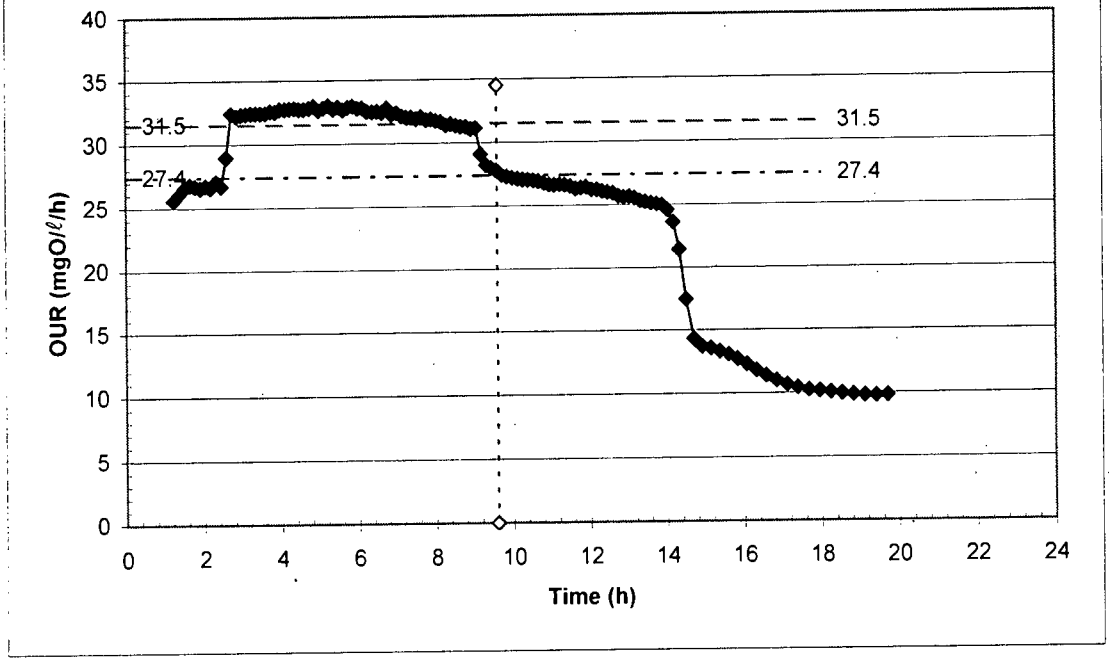

SB	Date	Day
24	26.11.02	373

Sbsi Drop (Time): 8.68

System Parameters:

Sti	473.8	mgCOD/ℓ
Suse	60.5	mgCOD/ℓ
Qs	34.5	ℓ/d
Sbsi	*58.6*	mgCOD/ℓ
fus	*0.128*	mgCOD/mgCOD
fts	*0.124*	mgCOD/mgCOD

Plot SBCOD OUR Plateau:

SBCOD Plat	XSBCOD
0	24.7
18	24.7

Plot GAE-Sbsi End Criteria:

Sbsi End (Time)	Range
9.23	0
9.23	*31.9*

ΔOUR = 4.2 mgO/ℓ

Figure B3(b)-78. SB 24 Sbsi System OUR

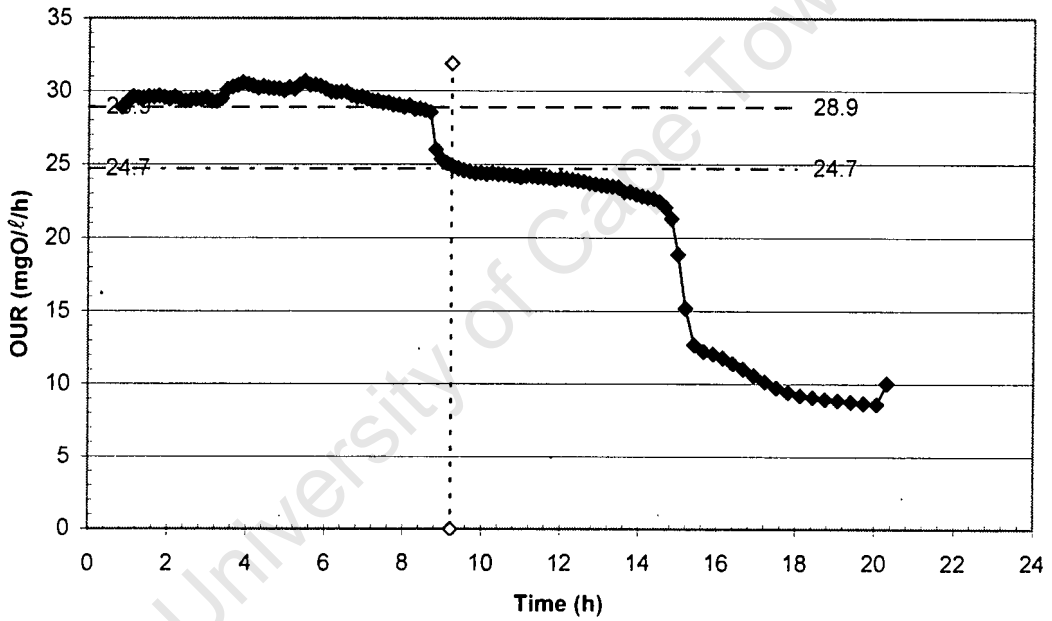

SB	Date	Day
24	28.11.02	375

Sbsi Drop (Time): 8.76

System Parameters:

Sti	506	mgCOD/ℓ
Suse	39.3	mgCOD/ℓ
Qs	32.32	ℓ/d
Sbsi	*70.0*	mgCOD/ℓ
fus	*0.078*	mgCOD/mgCOD
fts	*0.138*	mgCOD/mgCOD

Plot Sbsi (Max OUR) Plateau:

Sbsi Plat	XSbsi
0	34.3
18	*34.3*

Plot SBCOD OUR Plateau:

SBCOD Plat	XSBCOD
0	29.6
18	*29.6*

Plot GAE-Sbsi End Criteria:

Sbsi End (Time)	Range
9.31	0
9.31	*37.3*

ΔOUR = *4.7* mgO/ℓ

Figure B3(b)-79. SB 24 Sbsi System OUR

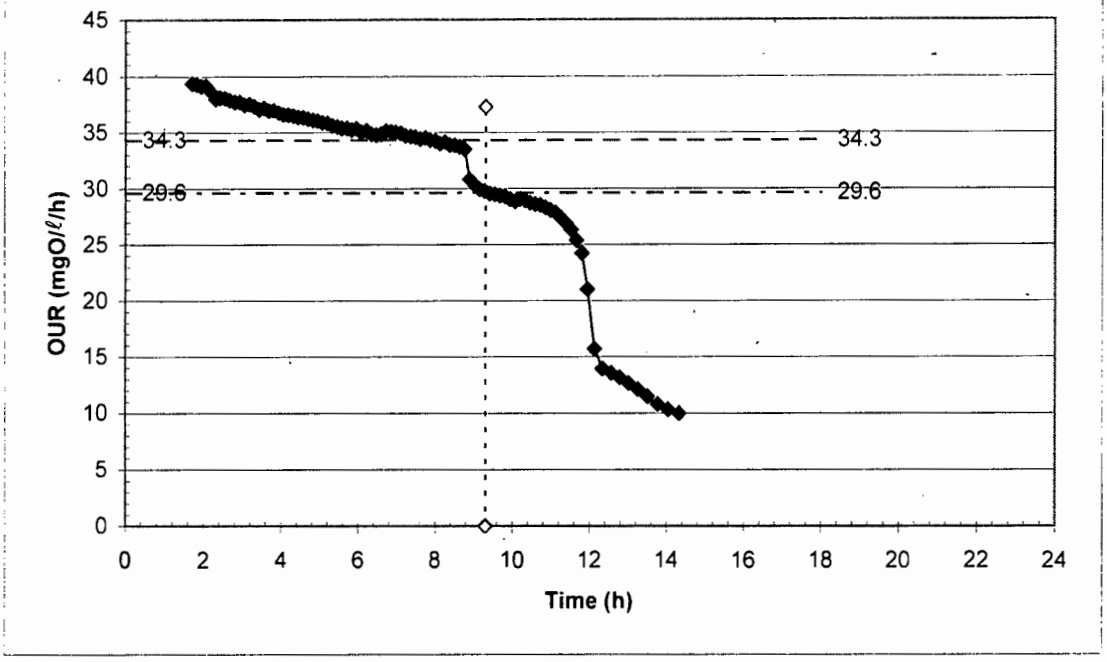

SB	Date	Day
24	29.11.02	376

Sbsi Drop (Time): 8.95

System Parameters:

Sti	479.8	mgCOD/ℓ
Suse	59.5	mgCOD/ℓ
Qs	35.78	ℓ/d
Sbsi	*59.9*	mgCOD/ℓ
fus	*0.124*	mgCOD/mgCOD
fts	*0.125*	mgCOD/mgCOD

Plot Sbsi (Max OUR) Plateau:

Sbsi Plat	XSbsi
0	34
18	*34*

Plot SBCOD OUR Plateau:

SBCOD Plat	XSBCOD
0	29.55
18	*29.55*

Plot GAE-Sbsi End Criteria:

Sbsi End (Time)	Range
9.5	0
9.5	*37*

ΔOUR = *4.5* mgO/ℓ

Figure B3(b)-80. SB 24 Sbsi System OUR

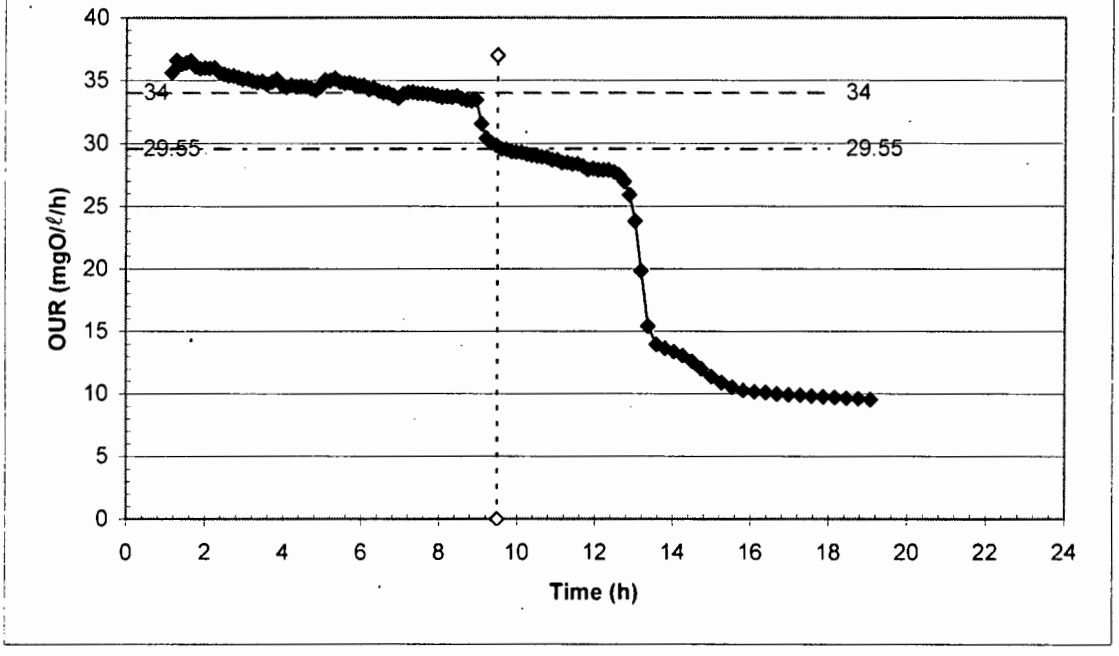

SB	Date	Day
24	30.11.02	377

Sbsi Drop (Time): **8.68**

System Parameters:

Sti	477.8	mgCOD/ℓ
Suse	63.5	mgCOD/ℓ
Qs	36.58	ℓ/d
Sbsi	*57.9*	mgCOD/ℓ
fus	*0.133*	mgCOD/mgCOD
fts	*0.121*	mgCOD/mgCOD

Plot Sbsi (Max OUR) Plateau:

Sbsi Plat	XSbsi
0	**34.4**
18	*34.4*

Plot SBCOD OUR Plateau:

SBCOD Plat	XSBCOD
0	**30**
18	*30*

Plot GAE-Sbsi End Criteria:

Sbsi End (Time)	Range
9.23	0
9.23	*37.4*

ΔOUR = *4.4* mgO/ℓ

Figure B3(b)-81. SB 24 Sbsi System OUR

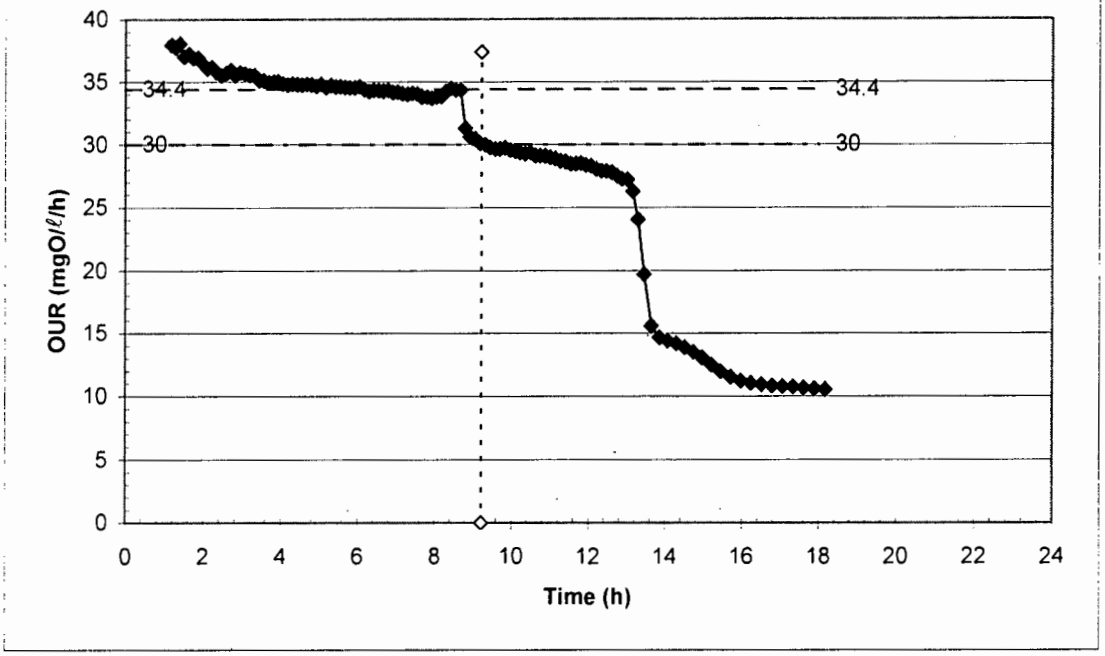

SB	Date	Day
24	01.12.02	378

Sbsi Drop (Time): **9.07**

System Parameters:

Sti	463.7	mgCOD/ℓ
Suse	55.4	mgCOD/ℓ
Qs	36.84	ℓ/d
Sbsi	*71.4*	mgCOD/ℓ
fus	*0.119*	mgCOD/mgCOD
fts	*0.154*	mgCOD/mgCOD

Plot Sbsi (Max OUR) Plateau:

Sbsi Plat	XSbsi
0	**34**
18	*34*

Plot SBCOD OUR Plateau:

SBCOD Plat	XSBCOD
0	**28.54**
18	*28.54*

Plot GAE-Sbsi End Criteria:

Sbsi End (Time)	Range
9.62	0
9.62	*37*

ΔOUR = *5.5* mgO/ℓ

Figure B3(b)-82. SB 24 Sbsi System OUR

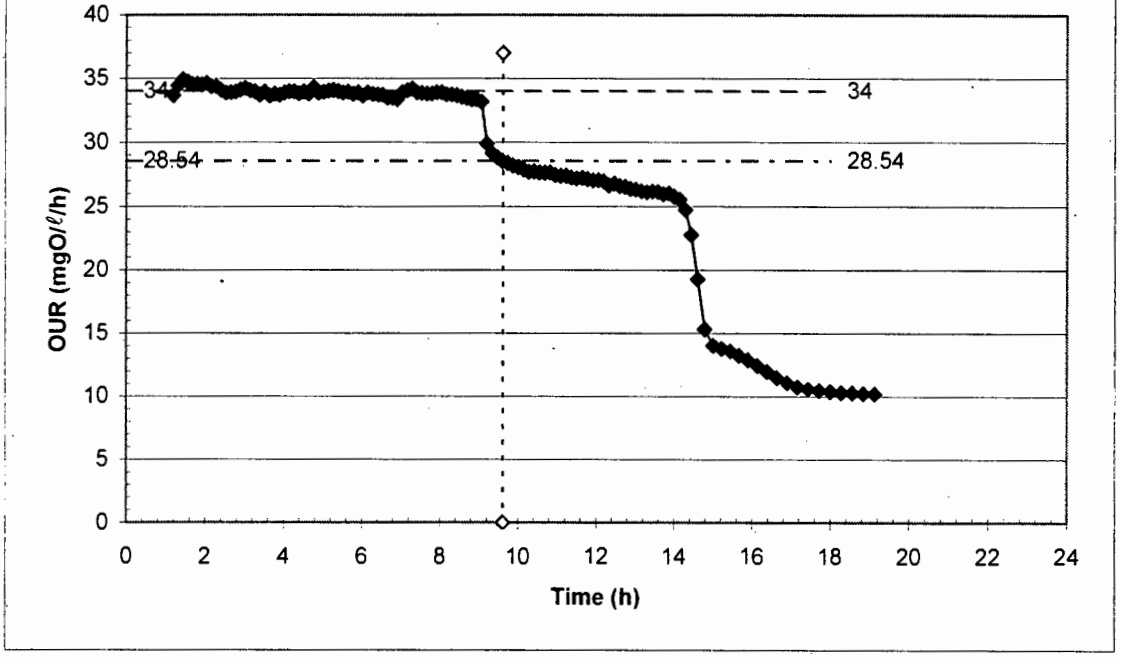

SB	Date	Day
24	02.12.02	379

Sbsi Drop (Time): 8.07

System Parameters:

Sti	502	mgCOD/ℓ
Suse	40.3	mgCOD/ℓ
Qs	37.34	ℓ/d
Sbsi	*61.2*	mgCOD/ℓ
fus	*0.080*	mgCOD/mgCOD
fts	*0.122*	mgCOD/mgCOD

Plot Sbsi (Max OUR) Plateau:

Sbsi Plat	XSbsi
0	36
18	36

Plot SBCOD OUR Plateau:

SBCOD Plat	XSBCOD
0	31.25
18	*31.25*

Plot GAE-Sbsi End Criteria:

Sbsi End (Time)	Range
8.62	0
8.62	*39*

ΔOUR = *4.8* mgO/ℓ

Figure B3(b)-83. SB 24 Sbsi System OUR

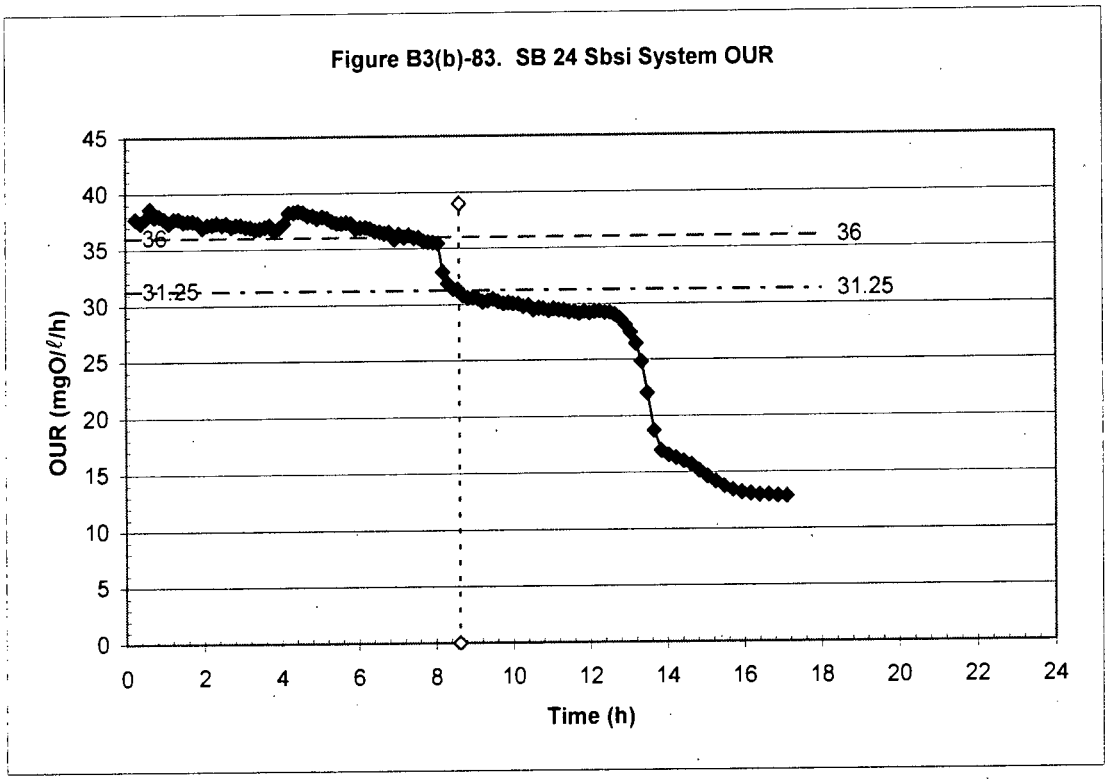

SB	Date	Day
24	03.12.02	380

Sbsi Drop (Time): 8.888

System Parameters:

Sti	483.8	mgCOD/ℓ
Suse	57.5	mgCOD/ℓ
Qs	37.96	ℓ/d
Sbsi	*63.7*	mgCOD/ℓ
fus	*0.119*	mgCOD/mgCOD
fts	*0.132*	mgCOD/mgCOD

Plot Sbsi (Max OUR) Plateau:

Sbsi Plat	XSbsi
0	37.4
18	*37.4*

Plot SBCOD OUR Plateau:

SBCOD Plat	XSBCOD
0	32.375
18	*32.375*

Plot GAE-Sbsi End Criteria:

Sbsi End (Time)	Range
9.438	0
9.438	*40.4*

ΔOUR = *5.0* mgO/ℓ

Figure B3(b)-84. SB 24 Sbsi System OUR

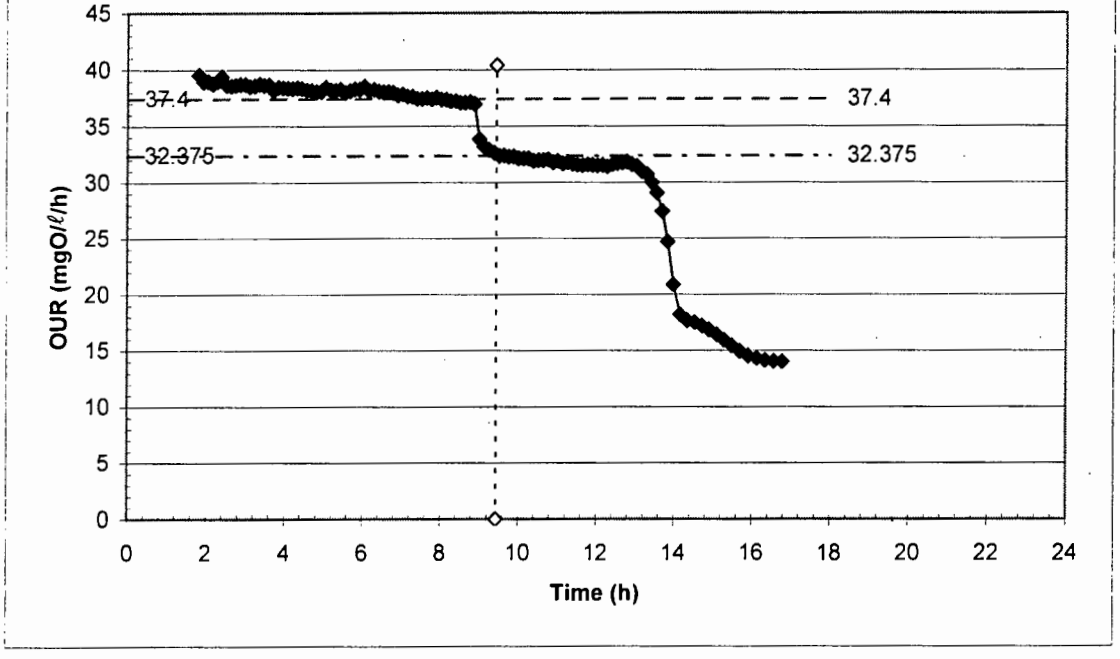

SB	Date	Day
24	04.12.02	381

Sbsi Drop (Time): **9.01**

System Parameters:

Sti	491.9	mgCOD/ℓ
Suse	50.4	mgCOD/ℓ
Qs	36.58	ℓ/d
Sbsi	*67.8*	mgCOD/ℓ
fus	*0.102*	mgCOD/mgCOD
fts	*0.138*	mgCOD/mgCOD

Plot Sbsi (Max OUR) Plateau:

Sbsi Plat	XSbsi
0	**36.25**
18	*36.25*

Plot SBCOD OUR Plateau:

SBCOD Plat	XSBCOD
0	**31.1**
18	*31.1*

Plot GAE-Sbsi End Criteria:

Sbsi End (Time)	Range
9.56	0
9.56	*39.25*

ΔOUR = *5.2* mgO/ℓ

Figure B3(b)-85. SB 24 Sbsi System OUR

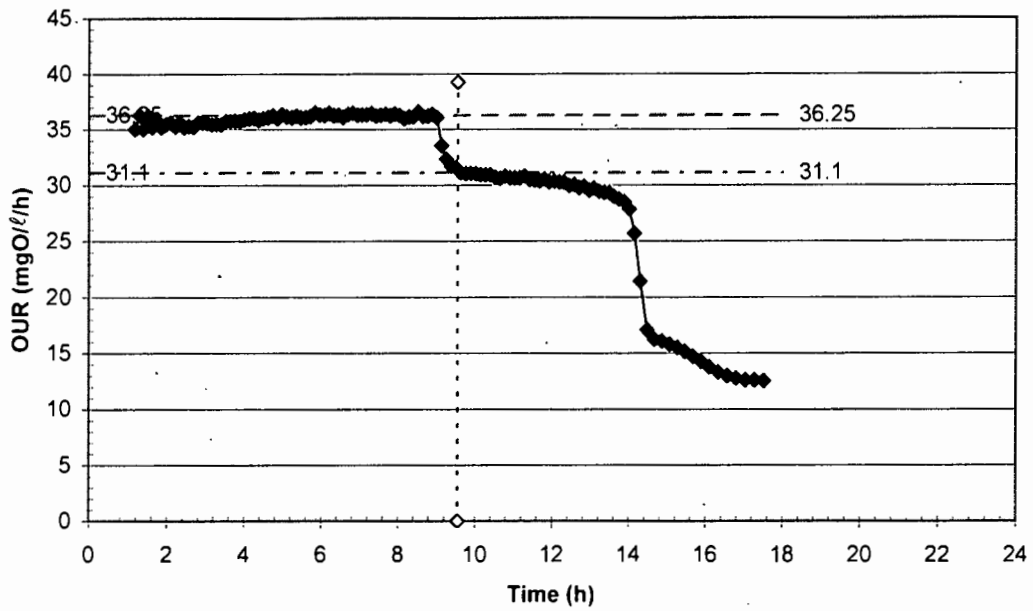

SB	Date	Day
24	05.12.02	382

Sbsi Drop (Time): **7.93**

System Parameters:

Sti	528.2	mgCOD/ℓ
Suse	49.4	mgCOD/ℓ
Qs	36.2	ℓ/d
Sbsi	*69.0*	mgCOD/ℓ
fus	*0.094*	mgCOD/mgCOD
fts	*0.131*	mgCOD/mgCOD

Plot Sbsi (Max OUR) Plateau:

Sbsi Plat	XSbsi
0	**40.75**
18	*40.75*

Plot SBCOD OUR Plateau:

SBCOD Plat	XSBCOD
0	**35.56**
18	*35.56*

Plot GAE-Sbsi End Criteria:

Sbsi End (Time)	Range
8.48	0
8.48	*43.75*

ΔOUR = *5.2* mgO/ℓ

Figure B3(b)-86. SB 24 Sbsi System OUR

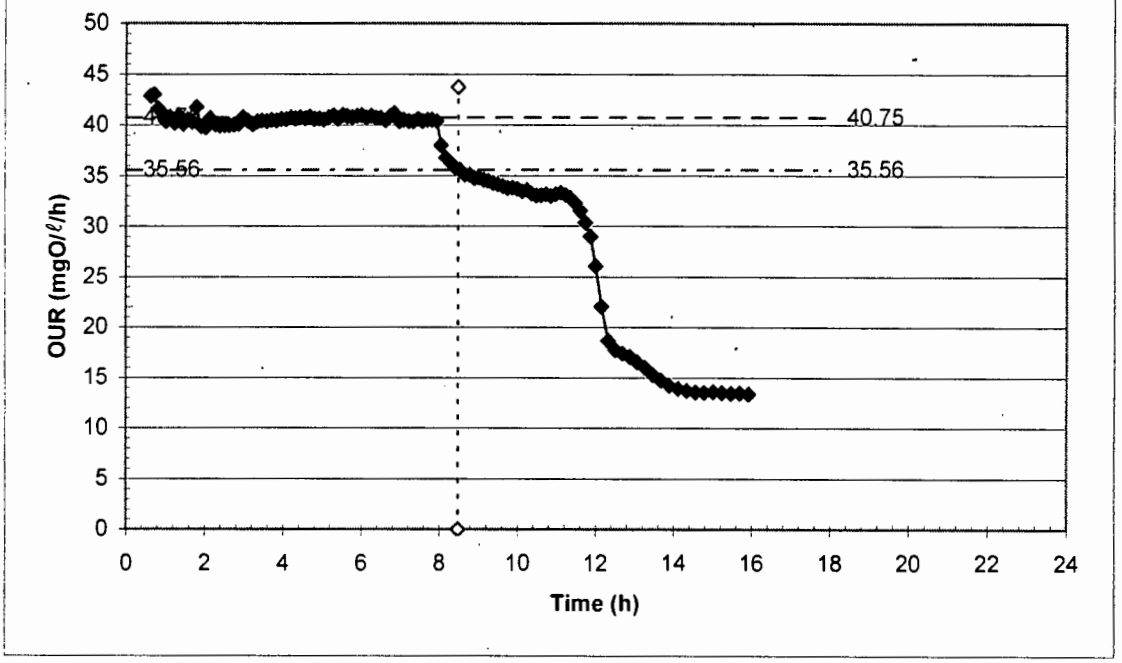

SB	Date	Day
24	06.12.02	383

Sbsi Drop (Time): 8.83

System Parameters:

Sti	528.2	mgCOD/ℓ
Suse	49.4	mgCOD/ℓ
Qs	36.2	ℓ/d
Sbsi	*65.6*	mgCOD/ℓ
fus	*0.094*	mgCOD/mgCOD
fts	*0.124*	mgCOD/mgCOD

Plot Sbsi (Max OUR) Plateau:

Sbsi Plat	XSbsi
0	42.75
18	42.75

Plot SBCOD OUR Plateau:

SBCOD Plat	XSBCOD
0	37.82
18	37.82

Plot GAE-Sbsi End Criteria:

Sbsi End (Time)	Range
9.38	0
9.38	*45.75*

ΔOUR = *4.9* mgO/ℓ

Figure B3(b)-87. SB 24 Sbsi System OUR

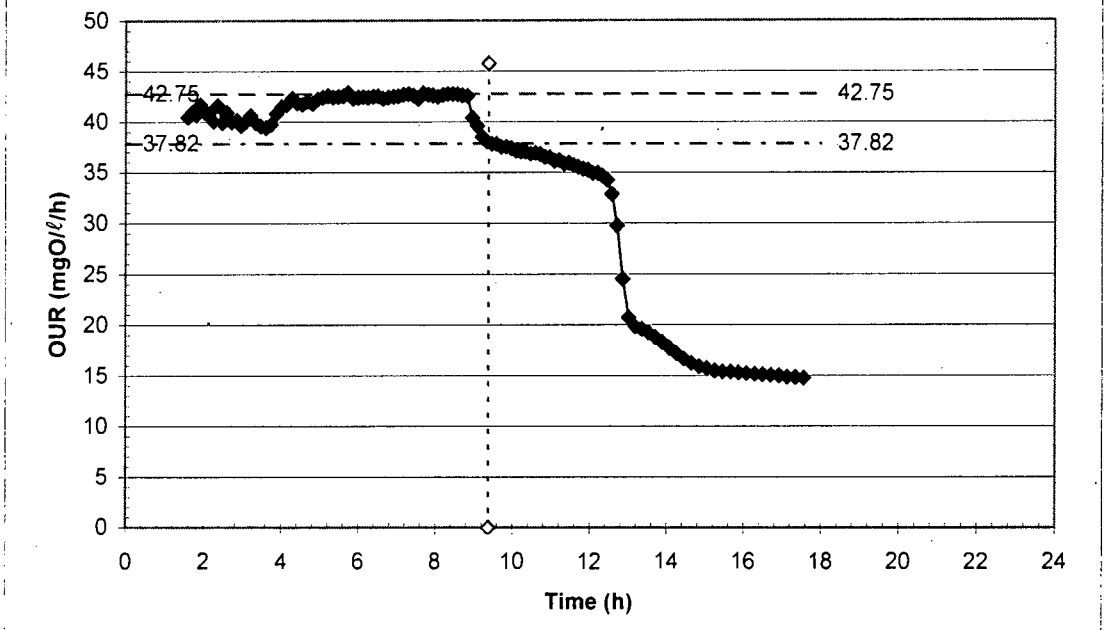

SB	Date	Day
25	8.12.02	385

Sbsi Drop (Time): **8.59**

System Parameters:

Sti	509	mgCOD/ℓ
Suse	59.5	mgCOD/ℓ
Qs	32.4	ℓ/d
Sbsi	*130.0*	mgCOD/ℓ
fus	*0.117*	mgCOD/mgCOD
fts	*0.255*	mgCOD/mgCOD

Plot Sbsi (Max OUR) Plateau:

Sbsi Plat	x-Sbsi
0	**40.5**
18	*40.5*

Plot SBCOD OUR Plateau:

SBCOD Plat	x-SBCOD
0	**31.75**
18	*31.75*

Plot GAE-Sbsi End Criteria:

Sbsi End (Time)	Range
9.14	0
9.14	*43.5*

ΔOUR = *8.8* mgO/ℓ

Figure B3(b)-88. SB 25 SQW System OUR

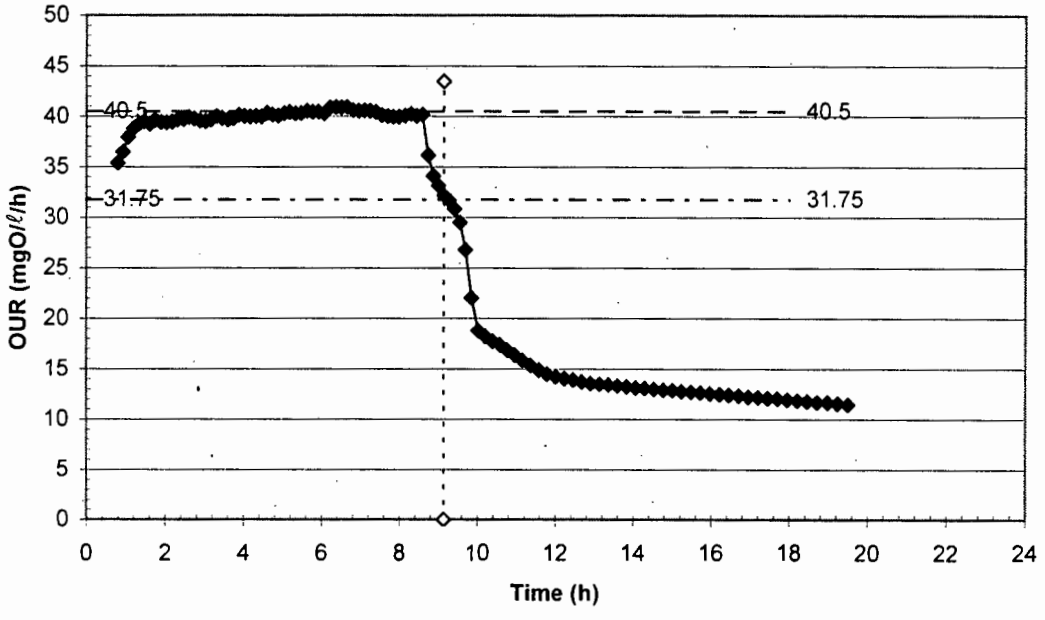

SB	Date	Day
25	9.12.02	386

Sbsi Drop (Time): 9.09

System Parameters:

Sti	494	mgCOD/ℓ
Suse	58	mgCOD/ℓ
Qs	34.9	ℓ/d
Sbsi	*113.8*	mgCOD/ℓ
fus	*0.117*	mgCOD/mgCOD
fts	*0.230*	mgCOD/mgCOD

Plot Sbsi (Max OUR) Plateau:

Sbsi Plat	x-Sbsi
0	35.75
18	35.75

Plot SBCOD OUR Plateau:

SBCOD Plat	x-SBCOD
0	27.5
18	27.5

Plot GAE-Sbsi End Criteria:

Sbsi End (Time)	Range
9.64	0
9.64	*38.75*

ΔOUR = *8.3* mgO/ℓ

Figure B3(b)-89. SB 25 SQW System OUR

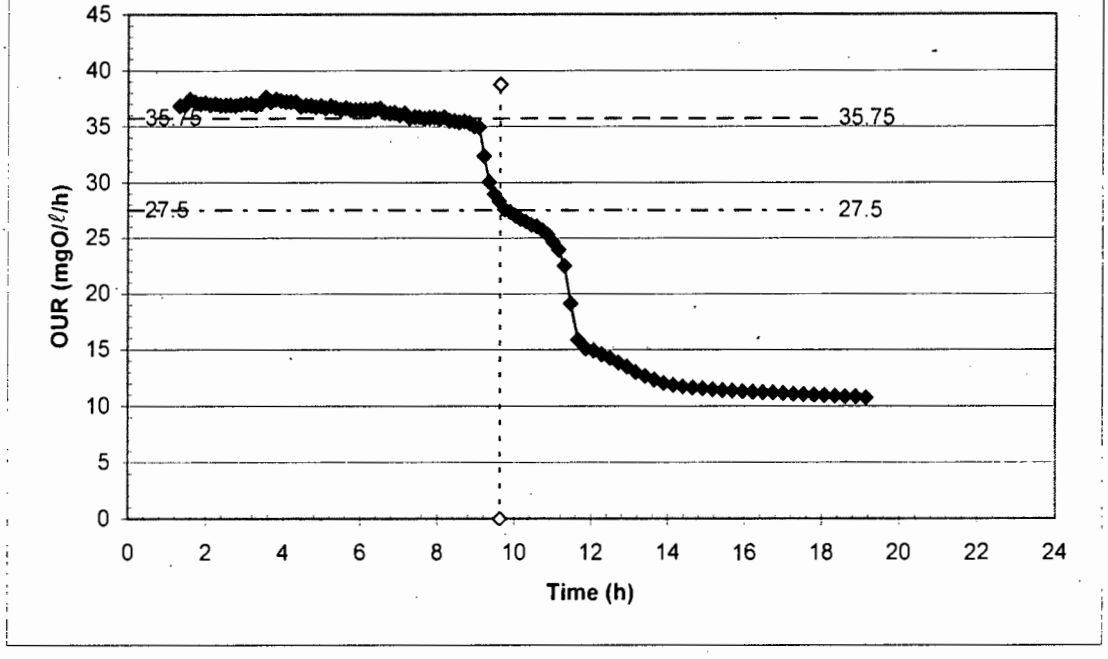

SB	Date	Day
25	10.12.02	387

Sbsi Drop (Time): 7.81

System Parameters:

Sti	449	mgCOD/ℓ
Suse	82	mgCOD/ℓ
Qs	35.4	ℓ/d
Sbsi	*106.8*	mgCOD/ℓ
fus	*0.183*	mgCOD/mgCOD
fts	*0.238*	mgCOD/mgCOD

Plot Sbsi (Max OUR) Plateau:

Sbsi Plat	x-Sbsi
0	33.6
18	*33.6*

Plot SBCOD OUR Plateau:

SBCOD Plat	x-SBCOD
0	25.75
18	*25.75*

Plot GAE-Sbsi End Criteria:

Sbsi End (Time)	Range
8.36	0
8.36	*36.6*

ΔOUR = *7.9* mgO/ℓ

Figure B3(b)-90. SB 25 SQW System OUR

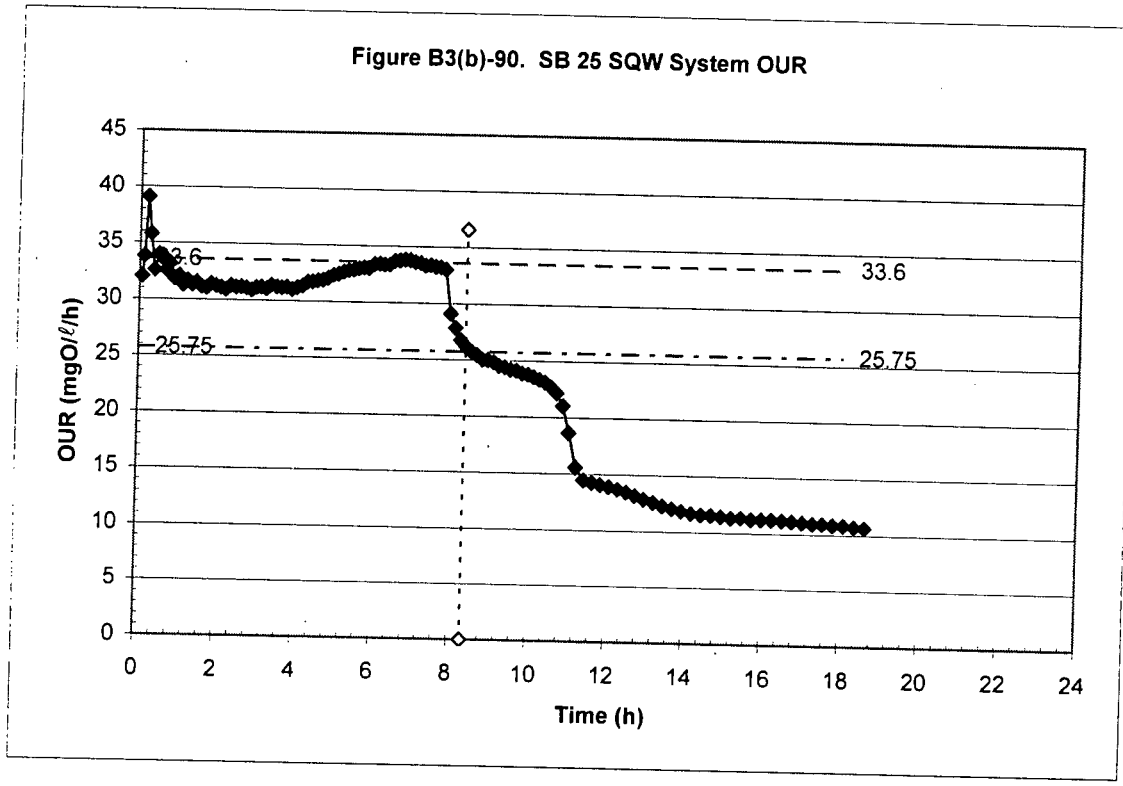

SB	Date	Day
25	11.12.02	388

Sbsi Drop (Time): 8.82

System Parameters:

Sti	538	mgCOD/ℓ
Suse	88	mgCOD/ℓ
Qs	35.69	ℓ/d
Sbsi	*101.8*	mgCOD/ℓ
fus	*0.164*	mgCOD/mgCOD
fts	*0.189*	mgCOD/mgCOD

Plot Sbsi (Max OUR) Plateau:

Sbsi Plat	x-Sbsi
0	34.5
18	*34.5*

Plot SBCOD OUR Plateau:

SBCOD Plat	x-SBCOD
0	26.95
18	*26.95*

Plot GAE-Sbsi End Criteria:

Sbsi End (Time)	Range
9.37	0
9.37	*37.5*

ΔOUR = *7.6* mgO/ℓ

Figure B3(b)-91. SB 25 SQW System OUR

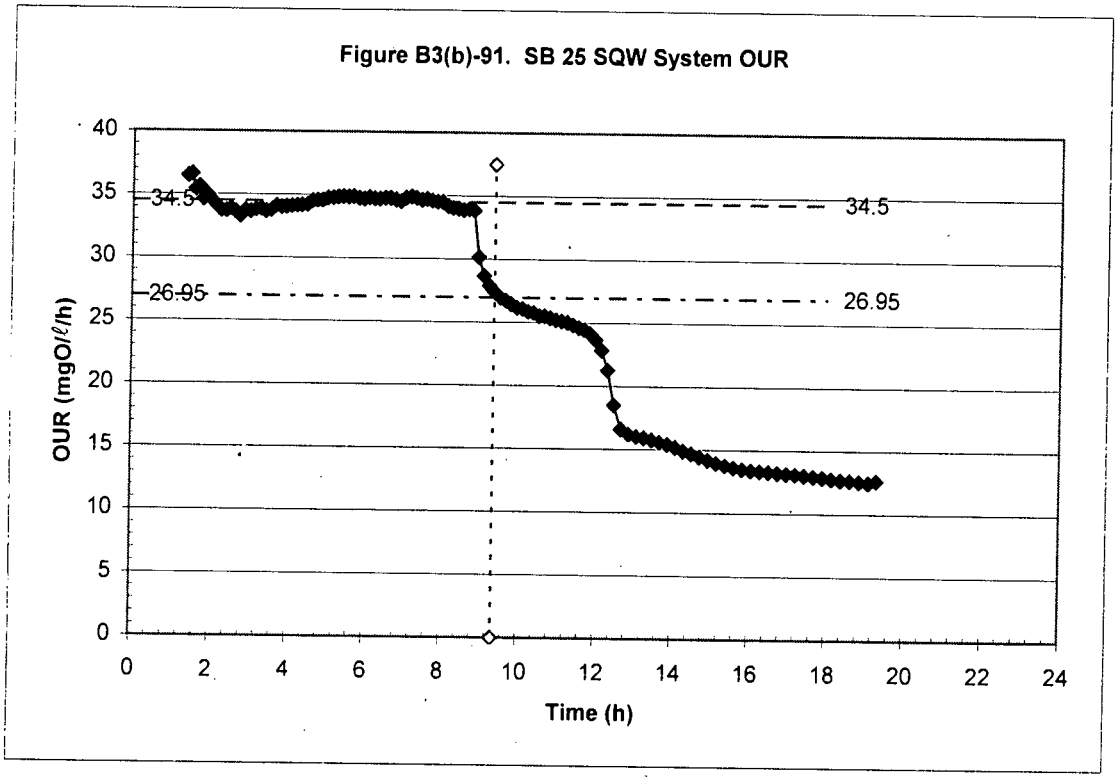

SB	Date	Day
25	12.12.02	389

Sbsi Drop (Time): 8.39

System Parameters:

Sti	528	mgCOD/ℓ
Suse	72	mgCOD/ℓ
Qs	36.06	ℓ/d
Sbsi	*90.8*	mgCOD/ℓ
fus	*0.136*	mgCOD/mgCOD
fts	*0.172*	mgCOD/mgCOD

Plot Sbsi (Max OUR) Plateau:

Sbsi Plat	x-Sbsi
0	30.6
18	*30.6*

Plot SBCOD OUR Plateau:

SBCOD Plat	x-SBCOD
0	23.8
18	*23.8*

Plot GAE-Sbsi End Criteria:

Sbsi End (Time)	Range
8.94	0
8.94	*33.6*

ΔOUR = *6.8* mgO/ℓ

Figure B3(b)-92. SB 25 SQW System OUR

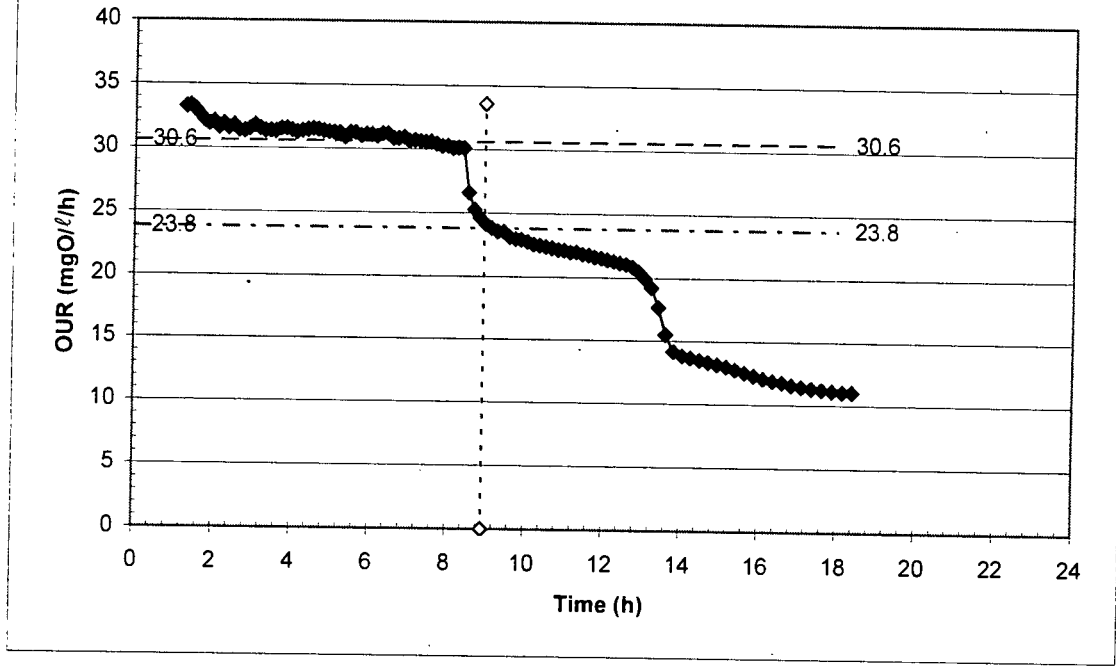

SB	Date	Day
25	13.12.02	390

Sbsi Drop (Time): **8.89**

System Parameters:

Sti	515	mgCOD/ℓ
Suse	59	mgCOD/ℓ
Qs	34.3	ℓ/d
Sbsi	*94.7*	mgCOD/ℓ
fus	*0.115*	mgCOD/mgCOD
fts	*0.184*	mgCOD/mgCOD

Plot Sbsi (Max OUR) Plateau:

Sbsi Plat	x-Sbsi
0	**30.75**
18	*30.75*

Plot SBCOD OUR Plateau:

SBCOD Plat	x-SBCOD
0	**24**
18	*24*

Plot GAE-Sbsi End Criteria:

Sbsi End (Time)	Range
9.44	0
9.44	*33.75*

ΔOUR = *6.8* mgO/ℓ

Figure B3(b)-93. SB 25 SQW System OUR

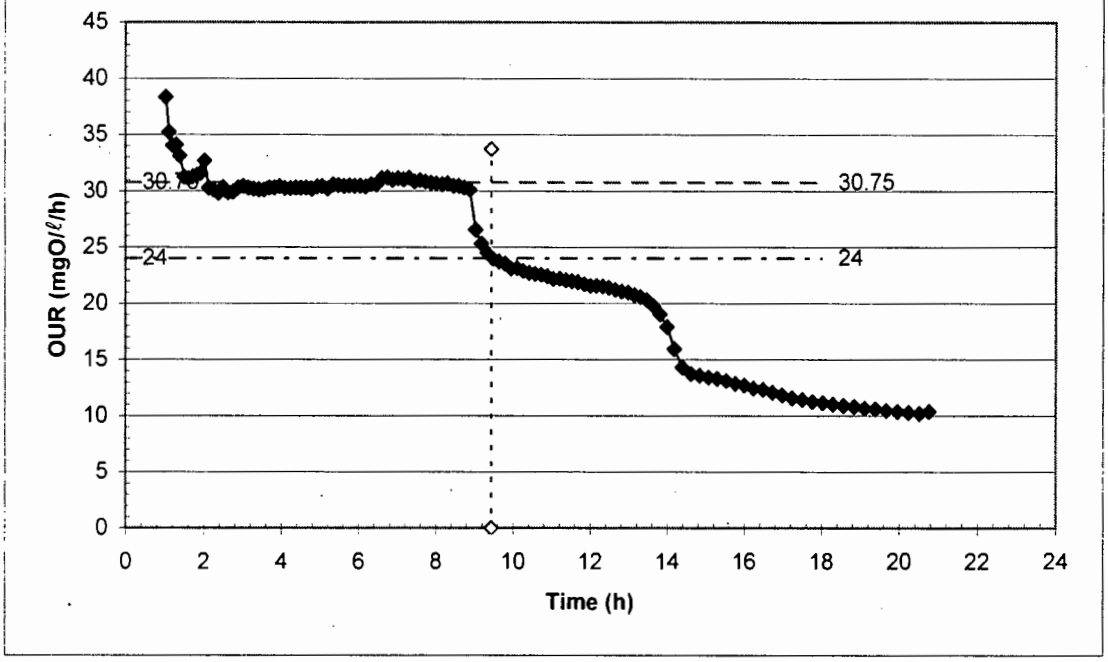

SB	Date	Day
25	14.12.02	391

Sbsi Drop (Time): 7.75

System Parameters:

Sti	519	mgCOD/ℓ
Suse	65	mgCOD/ℓ
Qs	34.3	ℓ/d
Sbsi	*88.4*	mgCOD/ℓ
fus	*0.125*	mgCOD/mgCOD
fts	*0.170*	mgCOD/mgCOD

Plot Sbsi (Max OUR) Plateau:

Sbsi Plat	x-Sbsi
0	31.95
18	*31.95*

Plot SBCOD OUR Plateau:

SBCOD Plat	x-SBCOD
0	25.65
18	*25.65*

Plot GAE-Sbsi End Criteria:

Sbsi End (Time)	Range
8.3	0
8.3	*34.95*

ΔOUR = *6.3* mgO/ℓ

Figure B3(b)-94. SB 25 SQW System OUR

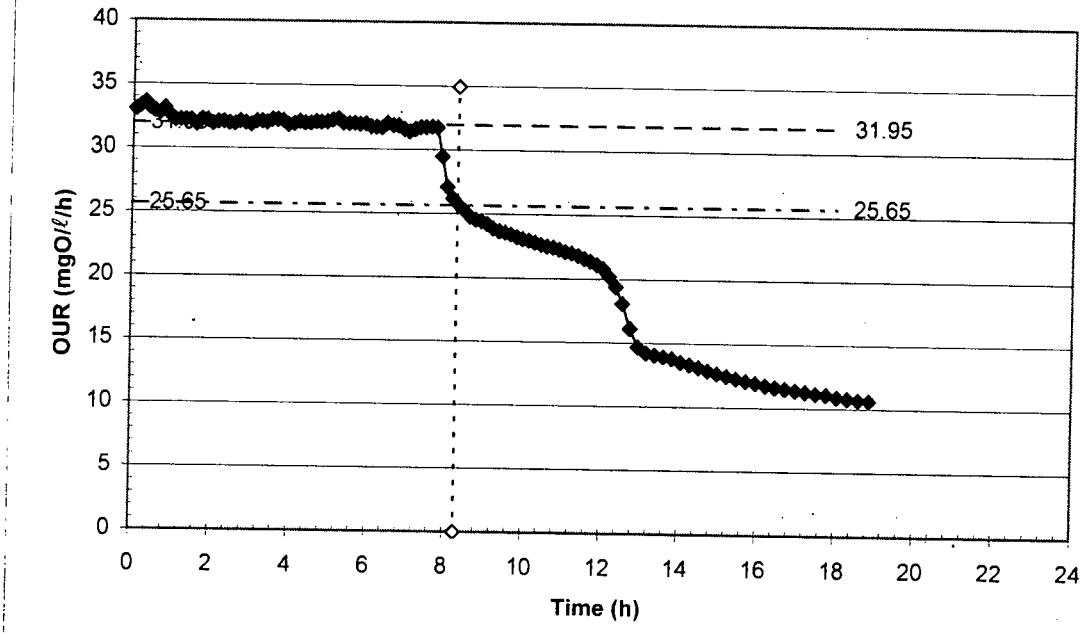

SB	Date	Day
25	15.12.02	392

Sbsi Drop (Time): 8.01

System Parameters:

Sti	498	mgCOD/ℓ
Suse	60	mgCOD/ℓ
Qs	32.6	ℓ/d
Sbsi	*100.4*	mgCOD/ℓ
fus	*0.120*	mgCOD/mgCOD
fts	*0.202*	mgCOD/mgCOD

Plot Sbsi (Max OUR) Plateau:

Sbsi Plat	x-Sbsi
0	30.4
18	30.4

Plot SBCOD OUR Plateau:

SBCOD Plat	x-SBCOD
0	23.6
18	*23.6*

Plot GAE-Sbsi End Criteria:

Sbsi End (Time)	Range
8.56	0
8.56	*33.4*

ΔOUR = *6.8* mgO/ℓ

Figure B3(b)-95. SB 25 SQW System OUR

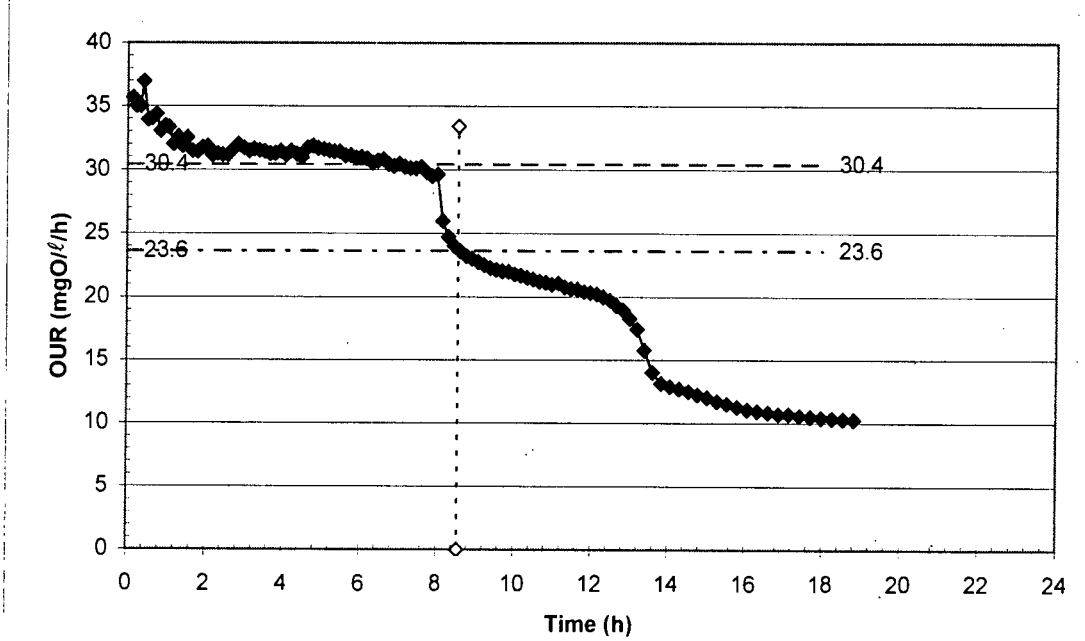

SB	Date	Day
25	17.12.02	394

Sbsi Drop (Time): 8.55

System Parameters:

Sti	491	mgCOD/ℓ
Suse	57	mgCOD/ℓ
Qs	36.82	ℓ/d
Sbsi	*82.4*	mgCOD/ℓ
fus	*0.116*	mgCOD/mgCOD
fts	*0.168*	mgCOD/mgCOD

Plot Sbsi (Max OUR) Plateau:

Sbsi Plat	x-Sbsi
0	27.7
18	*27.7*

Plot SBCOD OUR Plateau:

SBCOD Plat	x-SBCOD
0	21.4
18	*21.4*

Plot GAE-Sbsi End Criteria:

Sbsi End (Time)	Range
9.1	0
9.1	*30.7*

ΔOUR = *6.3* mgO/ℓ

Figure B3(b)-96. SB 25 SQW System OUR

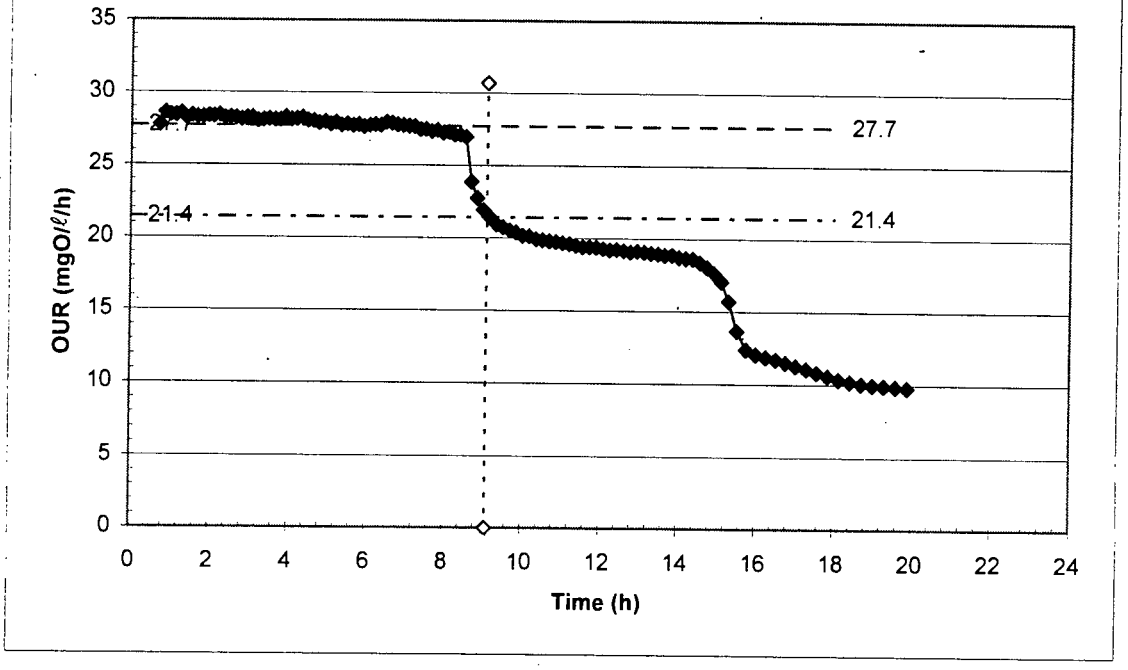

SB	Date	Day
25	18.12.02	395

Sbsi Drop (Time): 8.5

System Parameters:

Sti	512.1	mgCOD/ℓ
Suse	48.7	mgCOD/ℓ
Qs	37.68	ℓ/d
Sbsi	*76.7*	mgCOD/ℓ
fus	*0.095*	mgCOD/mgCOD
fts	*0.150*	mgCOD/mgCOD

Plot Sbsi (Max OUR) Plateau:

Sbsi Plat	x-Sbsi
0	28.7
18	*28.7*

Plot SBCOD OUR Plateau:

SBCOD Plat	x-SBCOD
0	22.7
18	22.7

Plot GAE-Sbsi End Criteria:

Sbsi End (Time)	Range
9.05	0
9.05	*31.7*

ΔOUR = *6.0* mgO/ℓ

Figure B3(b)-97. SB 25 SQW System OUR

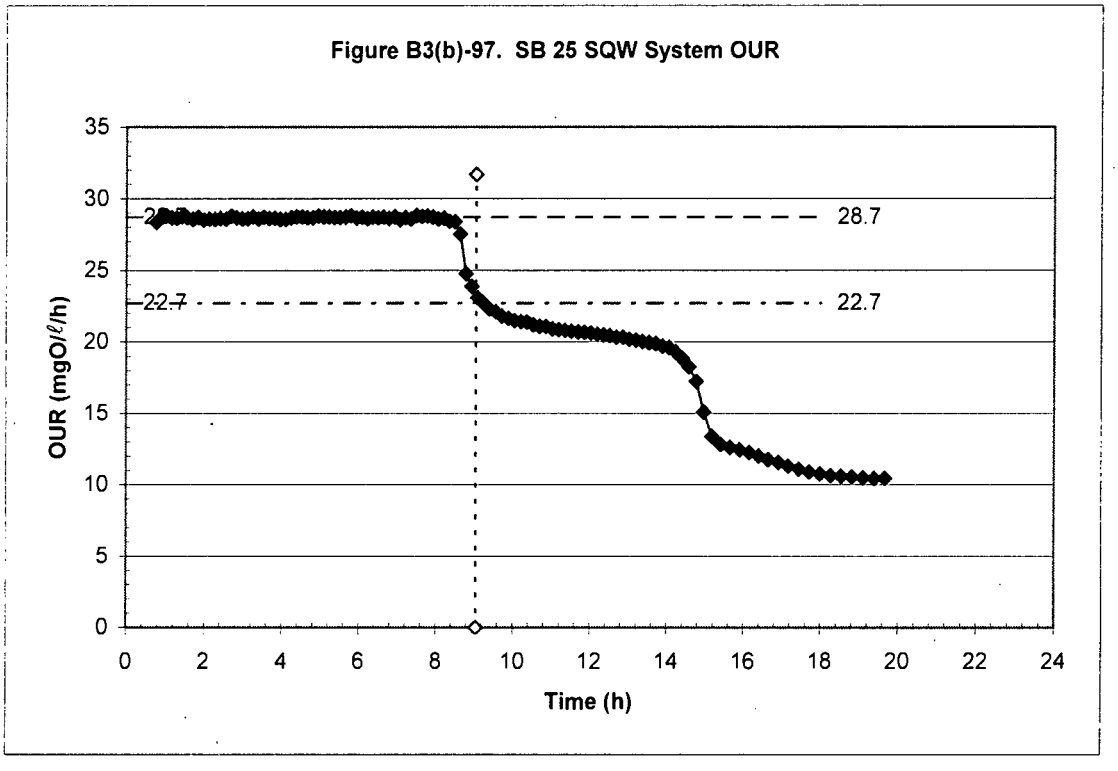

APPENDIX C

AEROBIC AND ANOXIC (DENITRIFICATION) BATCH TEST DATA AND ANALYSIS

TABLE OF CONTENTS

APPENDIX C-1

INDEPENDENT RBCOD ESTIMATION BY FLOCCULATION-FILTRATION IN PERIOD I

TABLE OF CONTENTS

APPENDIX C-1

INDEPENDENT RBCOD ESTIMATION BY FLOCCULATION-FILTRATION IN PERIOD I

As discussed previously (Chapters 1, 2 and 3), RBCOD is an essential parameter in this research. Although not explicitly required to estimate $Y_{H,NO}$ from equivalent aerobic and anoxic batch tests, provided $Y_{H,AE}$ is known, the RBCOD concentration is required to determine $Y_{H,NO}$ and $Y_{H,AE}$ directly and independantly. In Period I, independent estimation of the wastewater RBCOD fraction was by the flocculation-filtration (FF) method described in Section 3.8.1, Chapter 3 (Mbewe *et al.*, 1995), using the fraction unbiodegradable soluble COD (f_{us}) obtained in a long sludge age UCT activated sludge system operated concurrently on the same sewage. Analysis of the COD data for the UCT system is contained in this *Appendix* and presented below.

C1.1 UCT SYSTEM UNBIODEGRADABLE SOLUBLE COD FRACTION

Accepting each sewage batch as a steady-state period, daily measurements of the filtered effluent and total influent COD (S_{use} and S_{ti} respectively) were analysed for consistency within the 95% confidence interval; i.e., each value outside the interval range mean ± 1.96*sample standard deviation, was rejected as nonrepresentative of steady-state performance during that sewage batch (steady-state) period. All remaining measurements were considered valid and averaged to represent the "average" COD value for that sewage batch. The corresponding average unbiodegradable soluble COD fraction with respect to total COD (f_{us}), was calculated from the sewage batch averages of valid daily measurements by Eq.(C1.1):

$$f_{us} = S_{use}/S_{ti} \qquad \text{(C1.1)}$$

While a comprehensive listing of daily COD data for the UCT system is appended, a summary of the steady-state averages are presented in Table C1.1 below.

Table C1.1: UCT System: Sewage batch (SB) average (AVG) influent (S_{ti}), 0.45 μm filtered effluent (S_{use}) and fraction unbiodegradable soluble with respect to total (f_{us}) COD; also shown are sample standard deviations (SSD) and number of samples (N).

	S_{ti} (mgCOD/ℓ)			S_{use} (mgCOD/ℓ)			fus
SB	AVG	SSD	N	AVG	SSD	N	AVG
1	663.1	159.4	11	37.4	8.1	9	0.056
2	697.9	55.6	10	25.8	9.4	9	0.037
3	673.1	103.6	7	35.7	14.0	7	0.053
4	653.1	63.7	9	39.4	9.1	8	0.060
6	690.6	67.8	10	42.4	11.6	10	0.061
8	696.8	29.8	7	38.3	6.6	7	0.055
9	590.2	47.3	5	35.2	13.8	5	0.060
10	735.0	51.6	3	34.4	9.1	3	0.047
12	754.9	27.3	2	45.7	12.9	2	0.061

The sewage batch (steady-state) averages for f_{us} are plotted in a linearized probability graph below to check for normality (Fig. C1.1).

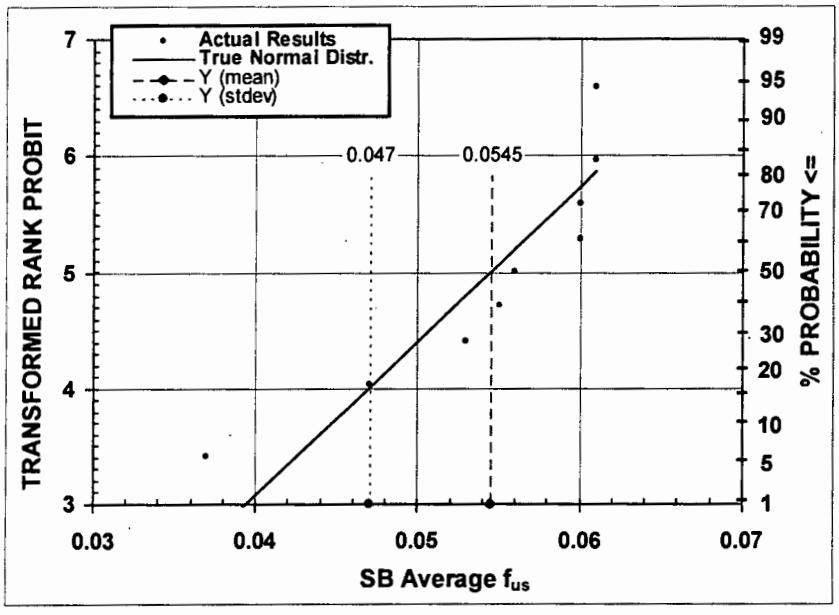

Fig. C1.1: UCT System: Linearized probability plot of average (steady-state) unbiodegradable soluble COD fraction (f_{us}) in influent wastewater.

One outlier was identified (SB 2, f_{us} = 0.037) and rejected, and the data replotted in Fig. C1.2.

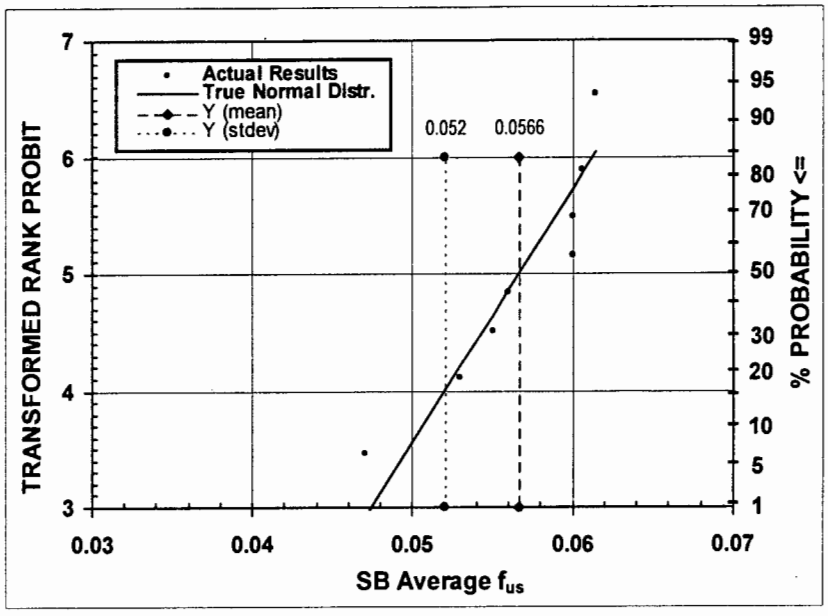

Fig. C1.2: UCT System: Revised (excluding outliers) probability plot of average (steady-state) influent unbiodegradable soluble COD fraction (f_{us}).

Although the f_{us} data for the UCT system plotted in Fig. C1.2 exhibits some curvature, the linear fit to the true normal is reasonable and gives a mean $f_{us} = 0.057 \pm 0.005$ for Mitchells Plain raw wastewater. This average is significantly lower than the 0.096 obtained with the Modified Ludzack-Ettinger (MLE) system described in Section 3.10, Chapter 3, as well as those observed by Cronje (2000), $f_{us} = 0.085$, Ubisi *et al.* (1997a,b), $f_{us} = 0.09$ and Mbewe *et al.* (1995), $f_{us} = 0.074$ also for Mitchells Plain raw wastewater. It is similar, however, to those observed by Lee (2002), $f_{us} = 0.04$ and by Beeharry *et al.* (2001), $f_{us} = 0.05$, also using Mitchells Plain raw wastewater. Of interest is the fact that Cronje (2000), Ubisi *et al.* (1997a,b) and Mbewe *et al.* (1995) were feeding an influent COD concentration of 500 ± 50 mgCOD/ℓ to their parent systems, as was the case for the MLE system in this study (Section 3.10, Chapter 3); whereas, both Lee (2002) and Beeharry *et al.* (2001) fed influent COD concentrations of 750 ± 50 mgCOD/ℓ, as was the case for the UCT system here. Thus, despite that the f_{us} values would be expected to be the same, given that the influent wastewater being treated was the same, the higher influent COD concentration apparently gave a lower f_{us}. This observation would imply that the concentration of the wastewater used as feed to the laboratory scale systems has an influence on the f_{us} values obtained. The f_{us} values obtained here by the UCT system are, however, within the range of typical values expected of South African domestic sewage (0.04 – 0.10, WRC, 1984).

C1.2 FLOC-FILTERED RBCOD ESTIMATION

Similarly accepting each sewage batch as a steady-state period, daily measurements of the floc-filtered influent COD (COD_{FF}) were analysed for consistency within the 95% confidence interval; i.e., each value outside the interval range mean ± 1.96*sample standard deviation, was rejected as nonrepresentative of steady-state performance during that sewage batch (steady-state) period. All remaining measurements were

considered valid and averaged to represent the "average" COD_{FF} value for that sewage batch. The corresponding average floc-filtered RBCOD ($S_{bsi,FF}$, $RBCOD_{FF}$) fraction with respect to total COD ($f_{ts,FF}$), was calculated from the sewage batch averages for COD_{FF}, total influent COD (S_{ti}) and f_{us} (Section C1.1) by Eqs.(C1.2) and (C1.3) below, and are summarised in Table C1.2:

$$S_{bsi,FF} \equiv RBCOD_{FF} = COD_{FF} - f_{us}*S_{ti} \quad (C1.2)$$

$$\Rightarrow f_{ts,FF} = S_{bsi,FF}/S_{ti} \quad (C1.3)$$

Table C1.2: UCT System: Sewage batch (SB) average (AVG) influent (S_{ti}), floc-filtered influent (COD_{FF}), fraction RBCOD (fts_{FF}) and unbiodegradable soluble with respect to total (f_{us}) COD, and RBCOD concentration ($Sbsi_{FF}$); also shown are sample standard deviations (SSD) and number of samples (N).

	S_{ti} (mgCOD/ℓ)			COD_{FF} (mgCOD/ℓ)			fus	$Sbsi_{FF}$	fts_{FF}
SB	AVG	SSD	N	AVG	SSD	N	AVG	mgCOD/ℓ	AVG
1	663.1	159.4	11				0.056		
2	697.9	55.6	10				0.037		
3	673.1	103.6	7	113.4	8.9	6	0.053	77.7	0.115
4	653.1	63.7	9	164.0	27.7	9	0.060	124.7	0.191
6	690.6	67.8	10	177.1	27.2	10	0.061	134.6	0.195
8	696.8	29.8	7	143.8	15.6	7	0.055	105.5	0.151
9	590.2	47.3	5	116.5	8.5	5	0.060	81.3	0.138
10	735.0	51.6	3	169.9	24.8	2	0.047	135.6	0.184
12	754.9	27.3	2				0.061		

The average $f_{ts,FF}$ values for each sewage batch (Table C1.2) are plotted in a linearized probability graph (Fig. C1.3) to check for normality.

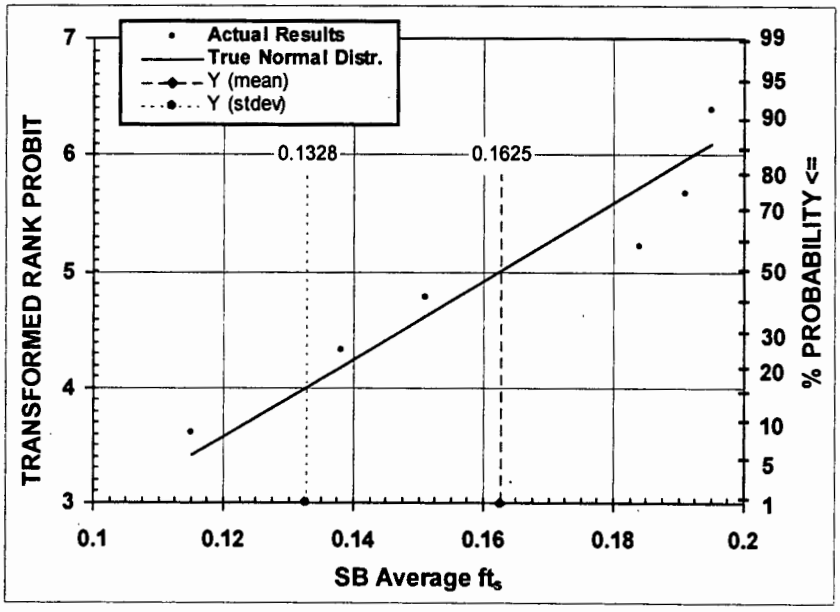

Fig.C1.3: UCT System: Linearized probability plot of average (steady-state) influent wastewater $RBCOD_{FF}$ fraction with respect to total COD ($f_{ts,FF}$).

No outliers were identified and the linear fit to the true normal is reasonable, indicating a normal distribution. The mean $f_{ts,FF}$ = 0.163 and sample standard deviation is 0.03 (range 0.133 – 0.193).

Daily $f_{ts,FF}$ estimates are similarly plotted in Fig. C1.4 (excluding one outlier, 12/1/02 $f_{ts,FF}$ = 0.248), which also shows normal distribution for the data. The mean $f_{ts,FF}$ = 0.163 and sample standard deviation of 0.04 (range 0.12 – 0.20) are practically identical to those obtained in Fig. C1.3 for the sewage batch averages. Hence, the mean $f_{ts,FF}$ = 0.163 ± 0.03 (range 0.133 – 0.193) is accepted for Mitchells Plain raw wastewater. This value compares well with the average $f_{ts,FF}$ = 0.18 ± 0.02 (range 0.14 – 0.23) determined by Mbewe *et al.* (1995), also for Mitchells Plain raw wastewater.

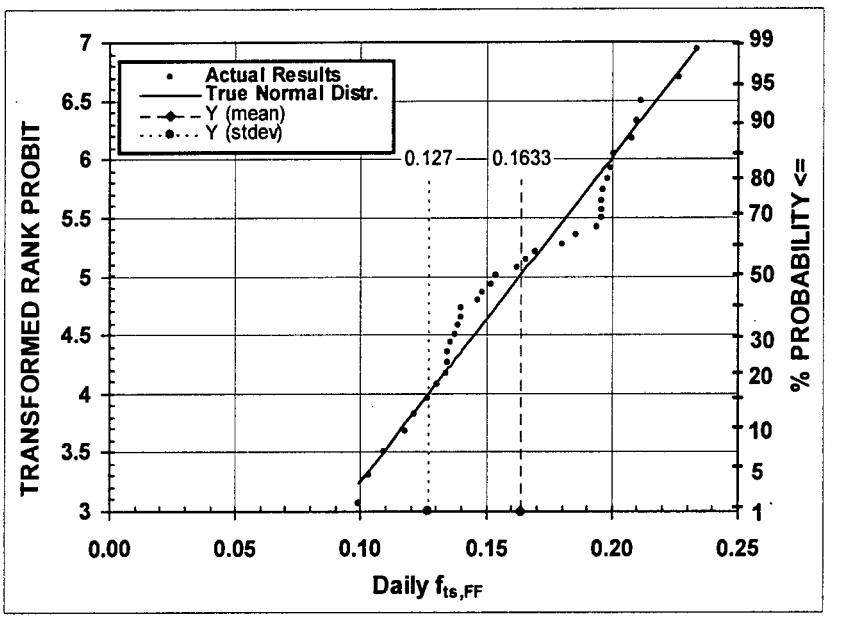

Fig. C1.4: UCT System: Linearized probability plot of daily estimates of the influent wastewater $RBCOD_{FF}$ fraction with respect to total COD ($f_{ts,FF}$).

Table C1.3. UCT System: Diluted influent (I), floc-filtered influent (FFI), 0.45 μm filtered effluent (FE), aerobic reactor (AE), RBCOD (Sbsi) and unfiltered effluent (UE) COD, all as mgCOD/ℓ; fractions unbiodegradable soluble (fus) and RBCOD in influent feed. *(Note: Outliers are boxed and reject from the analyses).*

SB	Day	Date	I	FFI	AE	UE	FE	fus	Sbsi	fts
1	1	19.11.01	793.2		3453.8	68.3	73.3	0.092		
	2	20.11.01	674.7		3152.6	100.4				
	3	21.11.01	457.8		3724.8	39.2	31.1	0.068		
	4	22.11.01	919.7		3584.3	44.2	38.2	0.041		
	5	23.11.01	500.0		3594.3	53.2	49.2	0.098		
	6	24.11.01	720.9		3634.5	70.3	52.2	0.072		
	7	25.11.01	921.3		3477.6	106.8	29.2	0.032		
	8	26.11.01	572.5		3427.2	115.9	32.3	0.056		
	9	27.11.01	572.5		3558.2	49.4	33.3	0.058		
	10	28.11.01	546.3		3427.2	72.6	33.3	0.061		
	11	29.11.01	614.9		3538.1	47.4	38.3	0.062		
		AVG	*663.1*		*3542.0*	*69.8*	*37.4*	*0.064*		
		STDEV	*159.4*		*97.2*	*26.9*	*8.1*	*0.020*		
		Count	*11*		*10*	*11*	*9*	*10*		
2	16	4.12.01	703.6		3175.2	22.2				
	17	5.12.01	647.1		3124.8	52.4	12.1	0.019		
	19	7.12.01	770.0		3040.0	31.0	23.0	0.030		
	20	8.12.01	644.0		3060.0	57.0	23.0	0.036		
	21	9.12.01	600.0		3140.0	13.0	13.0	0.022		
	22	10.12.01	692.0		3380.0	58.0	30.0	0.043		
	23	11.12.01	698.0		3490.0	61.0	34.0	0.049		
	24	12.12.01	776.0		3380.0	37.0	32.0	0.041		
	25	13.12.01	718.0		3490.0	42.0	25.0	0.035		
	26	14.12.01	729.8		3598.6	60.5	40.3	0.055		
		AVG	*697.9*		*3287.9*	*43.4*	*25.8*	*0.037*		
		STDEV	*55.6*		*202.7*	*17.2*	*9.4*	*0.012*		
		Count	*10*		*10*	*10*	*9*	*9*		
3	34	22.12.01	866.9	171.36	4626.7	52.4	44.4	0.051	127.0	0.147
	35	23.12.01	586.7	117.94	3860.6	61.5	57.5	0.098	60.5	0.103
	36	24.12.01	741.9	109.87	3880.8	15.1	13.1	0.018	96.8	0.130
	37	25.12.01	580.6	114.91	3719.5	50.4	34.3	0.059	80.6	0.139
	38	26.12.01	659.2	97.78	3931.2	11.1	32.3	0.049	65.5	0.099
	46	3.1.02	679.4	123.98	3830.4	45.4	41.3	0.061	82.7	0.122
	47	4.1.02	596.7	115.92	4092.5	33.3	27.2	0.046	88.7	0.149
		AVG	*673.1*	*113.4*	*3885.8*	*38.4*	*35.7*	*0.054*	*86.0*	*0.127*
		STDEV	*103.6*	*8.9*	*123.4*	*19.3*	*14.0*	*0.024*	*22.0*	*0.020*
		Count	*7*	*6*	*6*	*7*	*7*	*7*	*7*	*7*
4	52	9.1.02	718.2	186.50	2916.5	39.7	35.7	0.050	150.8	0.210
	53	10.1.02	615.0	120.03	2460.2	60.5				
	54	11.1.02	716.2	177.57	2847.0	99.2	36.7	0.051	140.9	0.197
	55	12.1.02	571.4	169.63	3065.3	29.8	27.8	0.049	141.9	0.248
	56	13.1.02	638.8	164.67	2896.6	53.6	39.7	0.062	125.0	0.196
	59	16.1.02	722.0	201.00	3080.0	78.0	58.0	0.080	143.0	0.198
	60	17.1.02	700.0	174.00	3310.0	60.0	37.0	0.053	137.0	0.196
	61	18.1.02	636.0	164.00	3510.0	48.0	46.0	0.072	118.0	0.186
	62	19.1.02	560.0	119.00	3530.0	26.0	34.0	0.061	85.0	0.152
		AVG	*653.1*	*164.0*	*3068.4*	*55.0*	*39.4*	*0.060*	*136.6*	*0.190*
		STDEV	*63.7*	*27.7*	*342.4*	*23.2*	*9.1*	*0.012*	*11.3*	*0.018*
		Count	*9*	*9*	*9*	*9*	*8*	*8*	*7*	*7*

6	89	16.2.02	750.0	188.00	2870.0	127.0	32.0	0.043	156.0	0.208
	90	17.2.02	650.0	194.00	3030.0	96.0	42.0	0.065	152.0	0.234
	91	18.2.02	780.0	174.00	2880.0	90.0	42.0	0.054	132.0	0.169
	92	19.2.02	719.7	222.77	2933.3	63.5	45.4	0.063	177.4	0.246
	93	20.2.02	774.1	193.54	3024.0	61.5	39.3	0.051	154.2	0.199
	94	21.2.02	667.3	191.52	3185.3	82.7	40.3	0.060	151.2	0.227
	95	22.2.02	717.7	164.30	2782.1	9.1	20.2	0.028	144.1	0.201
	107	6.3.02	602.8	170.35	3084.5	48.4	53.4	0.089	116.9	0.194
	108	7.3.02	653.2	129.02	3346.6	58.5	46.4	0.071	82.7	0.127
	111	8.3.02	590.7	143.14	3558.2	37.3	63.5	0.108	79.6	0.135
		AVG	*690.6*	*177.1*	*3015.1*	*67.4*	*42.4*	*0.058*	*134.6*	*0.194*
		STDEV	*67.8*	*27.2*	*174.7*	*33.2*	*11.6*	*0.017*	*32.3*	*0.040*
		Count	*10*	*10*	*9*	*10*	*10*	*9*	*10*	*10*
8	121	19.3.02	672.0	137.63	3440.8	38.5	47.6	0.071	90.1	0.134
	122	20.3.02	694.2	142.69	3653.3	67.8	45.5	0.066	97.2	0.140
	123	21.3.02	672.0	127.51	3623.0	32.4	36.4	0.054	91.1	0.136
	124	22.3.02	676.0	127.51	3501.5	45.5	34.4	0.051	93.1	0.138
	125	23.3.02	734.7	164.96	3643.2	41.5	32.4	0.044	132.6	0.180
	126	24.3.02	742.8	141.68	4058.1	98.2	41.5	0.056	100.2	0.135
	127	25.3.02	686.1	164.96	3572.4	29.3	30.4	0.044	134.6	0.196
		AVG	*696.8*	*143.8*	*3572.4*	*50.5*	*38.3*	*0.055*	*105.5*	*0.151*
		STDEV	*29.8*	*15.6*	*85.4*	*24.5*	*6.6*	*0.010*	*19.5*	*0.026*
		Count	*7*	*7*	*6*	*7*	*7*	*7*	*7*	*7*
9	132	30.3.02	556.8	101.60	3911.6	40.6	35.9	0.064	65.7	0.118
	134	1.4.02	577.1	119.89	3728.7	30.5	56.9	0.099	63.0	0.109
	135	2.4.02	547.6	120.67	3427.3	28.4	36.5	0.067	84.2	0.154
	136	3.4.02	665.2	117.62	3589.6	32.4	24.3	0.037	93.3	0.140
	138	5.4.02	604.3	122.69	3599.7	62.9	22.3	0.037	100.4	0.166
		AVG	*590.2*	*116.5*	*3651.4*	*39.0*	*35.2*	*0.061*	*81.3*	*0.137*
		STDEV	*47.3*	*8.5*	*180.5*	*14.1*	*13.8*	*0.026*	*16.5*	*0.024*
		Count	*5*	*5*	*5*	*5*	*5*	*5*	*5*	*5*
10	150	17.4.02	788.4	152.40		26.4	24.4	0.031	128.0	0.162
	151	18.4.02	685.4	187.49	3850.6	66.5	42.3	0.062	145.2	0.212
	159	26.4.02				72.7	36.4			
	161	28.4.02	731.2							
		AVG	*735.0*	*169.9*	*3850.6*	*55.2*	*34.4*	*0.046*	*136.6*	*0.187*
		STDEV	*51.6*	*24.8*		*25.1*	*9.1*	*0.022*	*12.1*	*0.035*
		Count	*3*	*2*	*1*	*3*	*3*	*2*	*2*	*2*
12	191	28.5.02	774.2				54.9	0.071		
	192	29.5.02	735.6				36.6	0.050		
		AVG	*754.9*				*45.7*	*0.060*		
		STDEV	*27.3*				*12.9*	*0.015*		
		Count	*2*				*2*	*2*		

APPENDIX C-2

AEROBIC BATCH TEST DATA

ML	SB	Date	ABT
LML	4	17.01.02	1

Plot end RBCOD:

t	End
7.169	0
7.169	20

Input SBCOD OUR:

9.3 mgO/L/h

Plot SBCOD OUR:

SBCODx	SBCODy
0	*9.3*
24	*9.3*

Batch Test Composition: V_{BT} 3 ℓ

V_{ww}	2.7	ℓ	V_{ML}	0.3	ℓ
S_{ti}	480	mgCOD/ℓ	X_v	3347	mgVSS/ℓ
$S_{ti,BT}$	432	mgCOD/ℓ	LR	1.291	mgCOD/mgVSS

Define RBCOD Area Sum:

OU = *NA* mgO/ℓ

S_{bsi} =	*NA*	mgCOD/ℓ
f_{ts} =	*NA*	

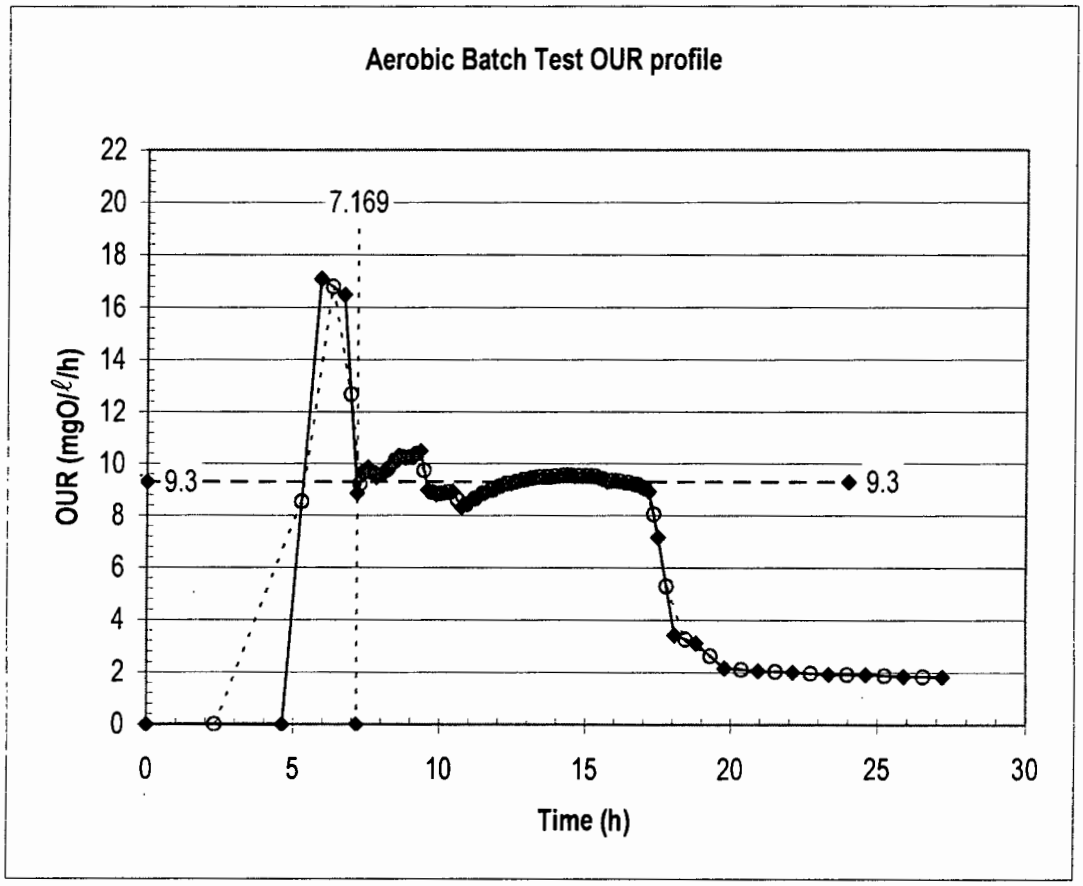

Plot end RBCOD:

t	End
1.711	0
1.711	22.5

Input SBCOD OUR:

12.5 mgO/L/h

Plot SBCOD OUR:

SBCODx	SBCODy
0	*12.5*
24	*12.5*

ML	SB	Date	ABT
LML	4	22.01.02	2

Batch Test Composition: V_{BT} 3 ℓ

V_{WW}	2.7	ℓ	V_{ML}	0.3	ℓ
S_{ti}	528	mgCOD/ℓ	X_v	3188	mgVSS/ℓ
$S_{ti,BT}$	475.2	mgCOD/ℓ	LR	1.491	mgCOD/mgVSS

Define RBCOD Area Sum:

OU = 7.2 mgO/ℓ

S_{bsi} =	21.88	mgCOD/ℓ
f_{ts} =	0.046	

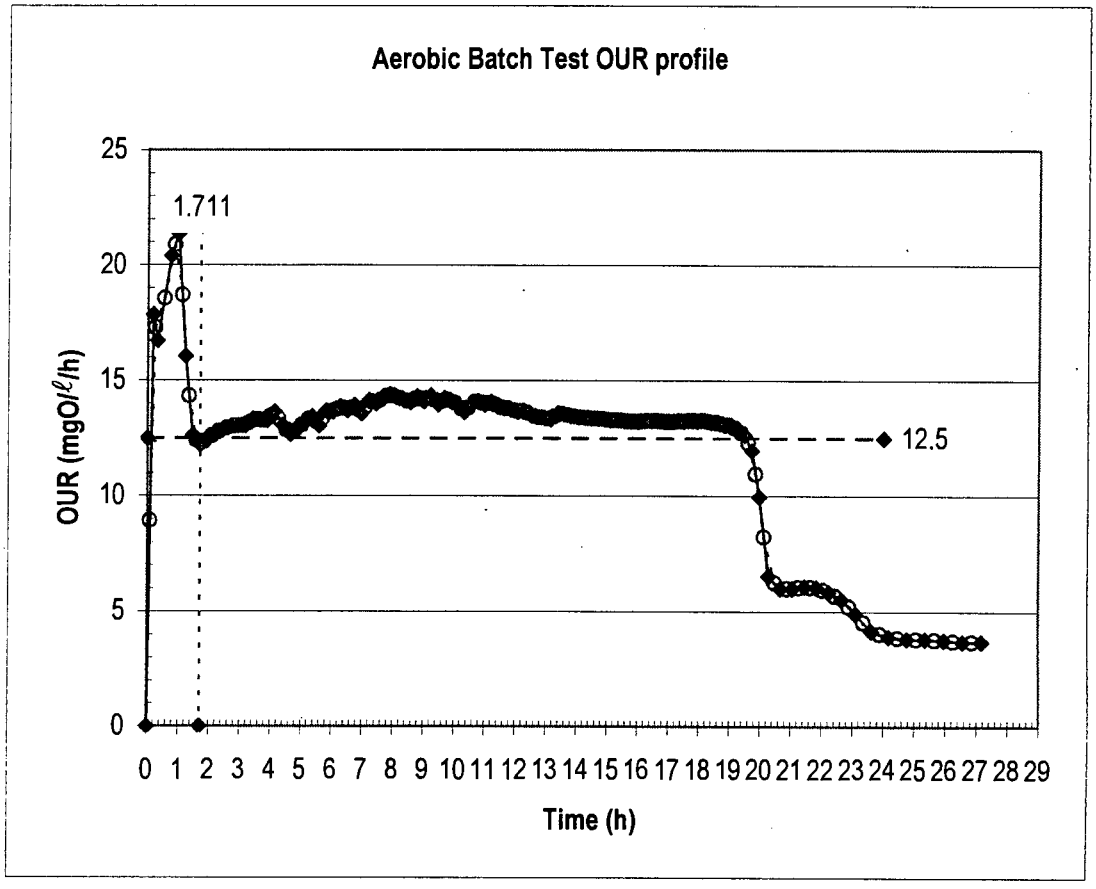

Plot end RBCOD:

t	End
3.969	0
3.969	13

Input SBCOD OUR:

NA mgO/ℓ/h

Plot SBCOD OUR:

SBCODx	SBCODy
0	*NA*
24	*NA*

ML	SB	Date	ABT
LML	6	24.02.02	3

Batch Test Composition: V_{BT} 3 ℓ

V_{WW}	2.7	ℓ	V_{ML}	0.3	ℓ
S_{ti}	245	mgCOD/ℓ	X_v	2497	mgVSS/ℓ
$S_{ti,BT}$	220.5	mgCOD/ℓ	LR	0.883	mgCOD/mgVSS

Define RBCOD Area Sum:

OU = **5.1** mgO/ℓ

S_{bsi} =	15.48	mgCOD/ℓ
f_{ts} =	0.070	

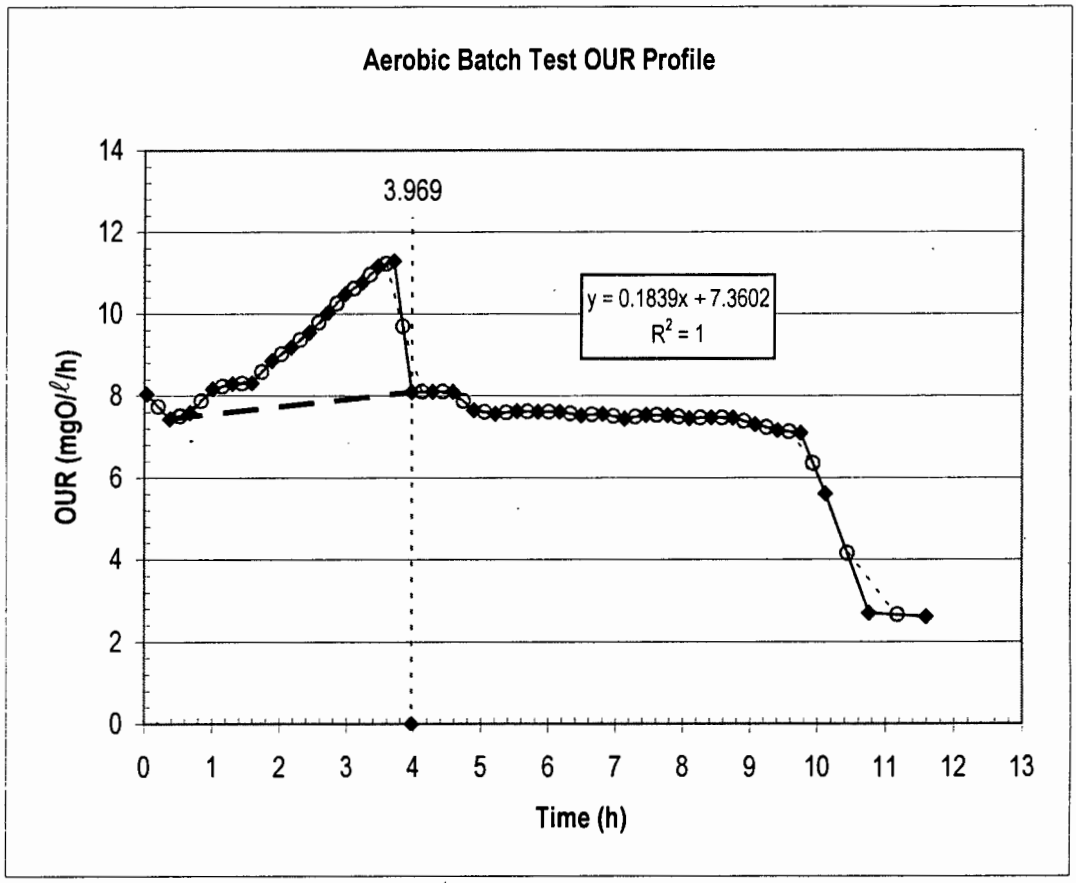

Plot end RBCOD:

t	End
2.955	0
2.955	13

ML	SB	Date	ABT
LML	6	25.02.02	4

Input SBCOD OUR:

8.875 mgO/L/h

Plot SBCOD OUR:

SBCODx	SBCODy
0	*8.875*
12	*8.875*

Batch Test Composition: V_{BT} 3 ℓ

V_{ww}	2.55	ℓ	V_{ML}	0.45	ℓ
S_{ti}	224	mgCOD/ℓ	X_v	2424	mgVSS/ℓ
$S_{ti,BT}$	190.4	mgCOD/ℓ	LR	0.524	mgCOD/mgVSS

Define RBCOD Area Sum:

OU = 4.4 mgO/ℓ

S_{bsi} =	13.20	mgCOD/ℓ
f_{ts} =	0.069	

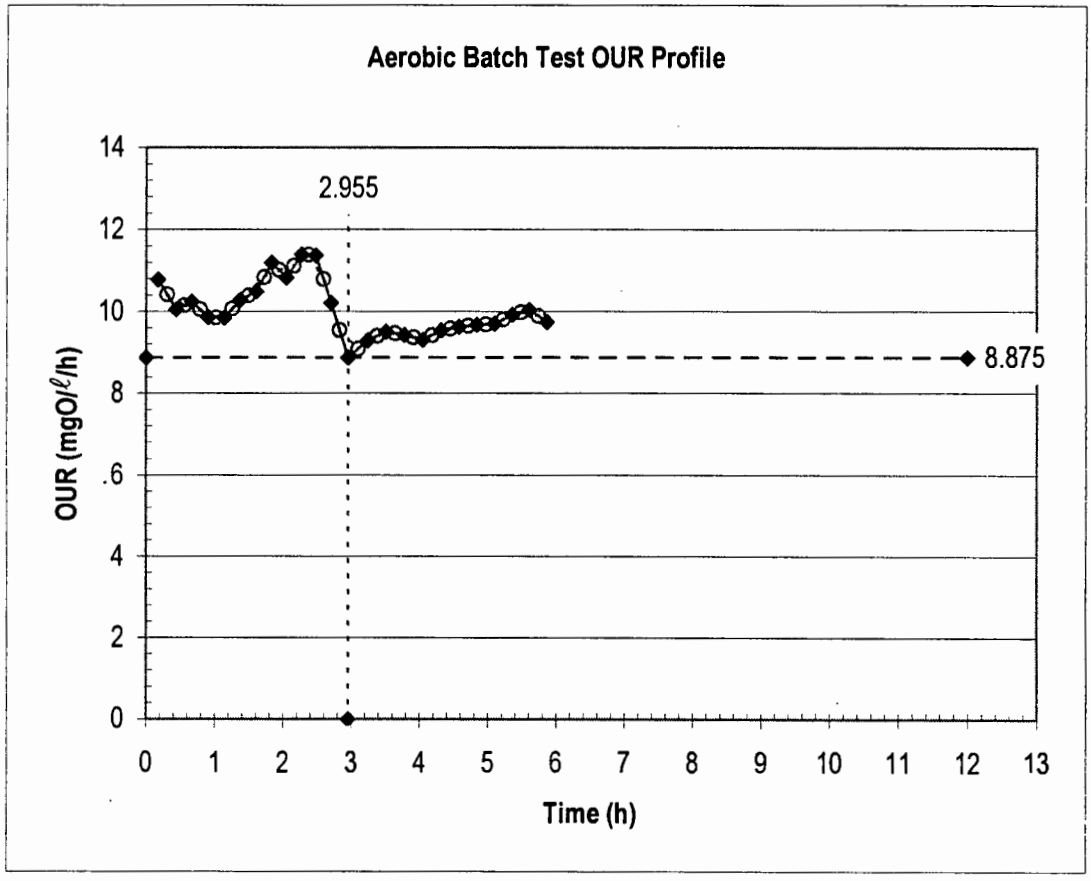

ML	SB	Date	ABT
LML	6	26.02.02	5

Plot end RBCOD:

t	End
2.090	0
2.090	22.5

Input SBCOD OUR:

14.5 mgO/L/h

Plot SBCOD OUR:

SBCODx	SBCODy
0	*14.5*
14	*14.5*

Batch Test Composition:

V_{WW}	0.815	ℓ	V_{ML}	0.685	ℓ
S_{ti}	528	mgCOD/ℓ	X_v	3188	mgVSS/ℓ
$S_{ti,BT}$	143.44	mgCOD/ℓ	LR	0.197	mgCOD/mgVSS

V_{BT} 3 ℓ

Define RBCOD Area Sum:

OU = 7.3 mgO/ℓ

S_{bsi} =	22.02	mgCOD/ℓ
f_{ts} =	0.154	

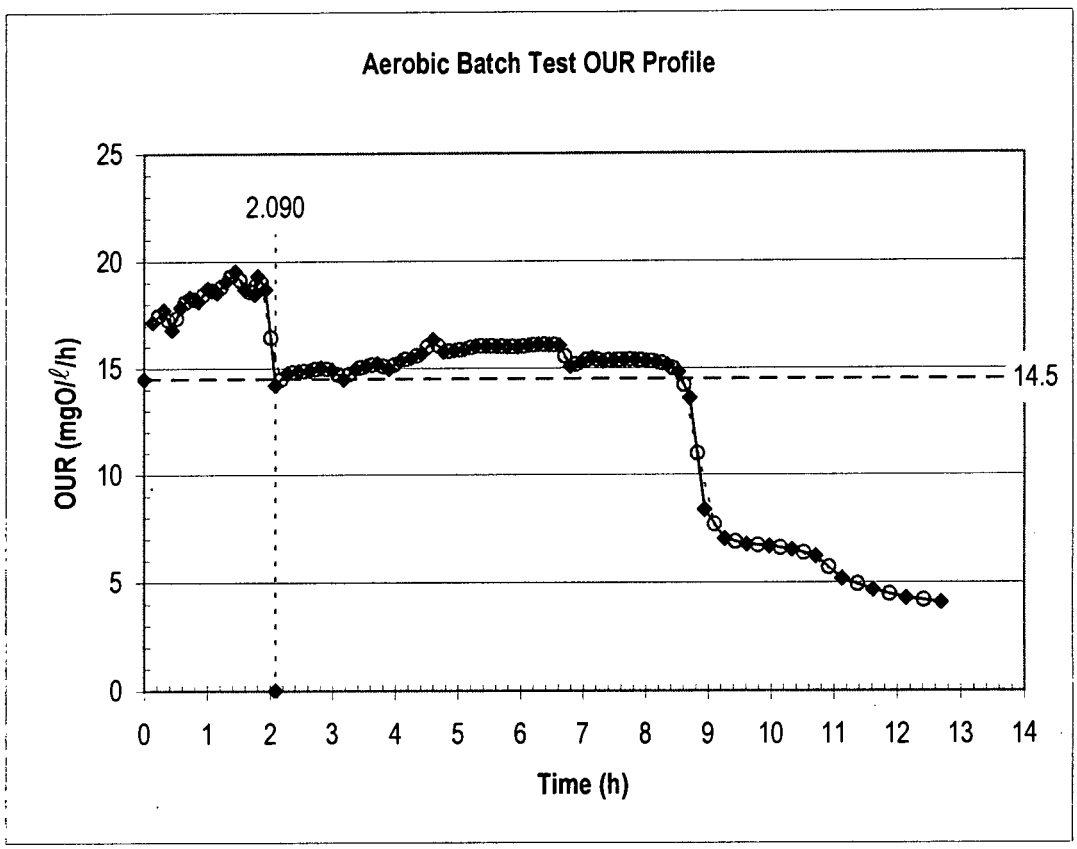

ML	SB	Date	ABT
LML	6	27.02.02	6

Plot end RBCOD:

t	End
2.230	0
2.230	35

Input SBCOD OUR:

22.5 mgO/L/h

Plot SBCOD OUR:

SBCODx	SBCODy
0	*22.5*
16	*22.5*

Batch Test Composition: V_{BT} 3 ℓ

V_{ww}	1.63	ℓ	V_{ML}	1.37	ℓ
S_{ti}	980	mgCOD/ℓ	X_v	2587	mgVSS/ℓ
$S_{ti,BT}$	532.47	mgCOD/ℓ	LR	0.451	mgCOD/mgVSS

Define RBCOD Area Sum:

OU = 13.0 mgO/ℓ

S_{bsi} =	39.35	mgCOD/ℓ
f_{ts} =	0.074	

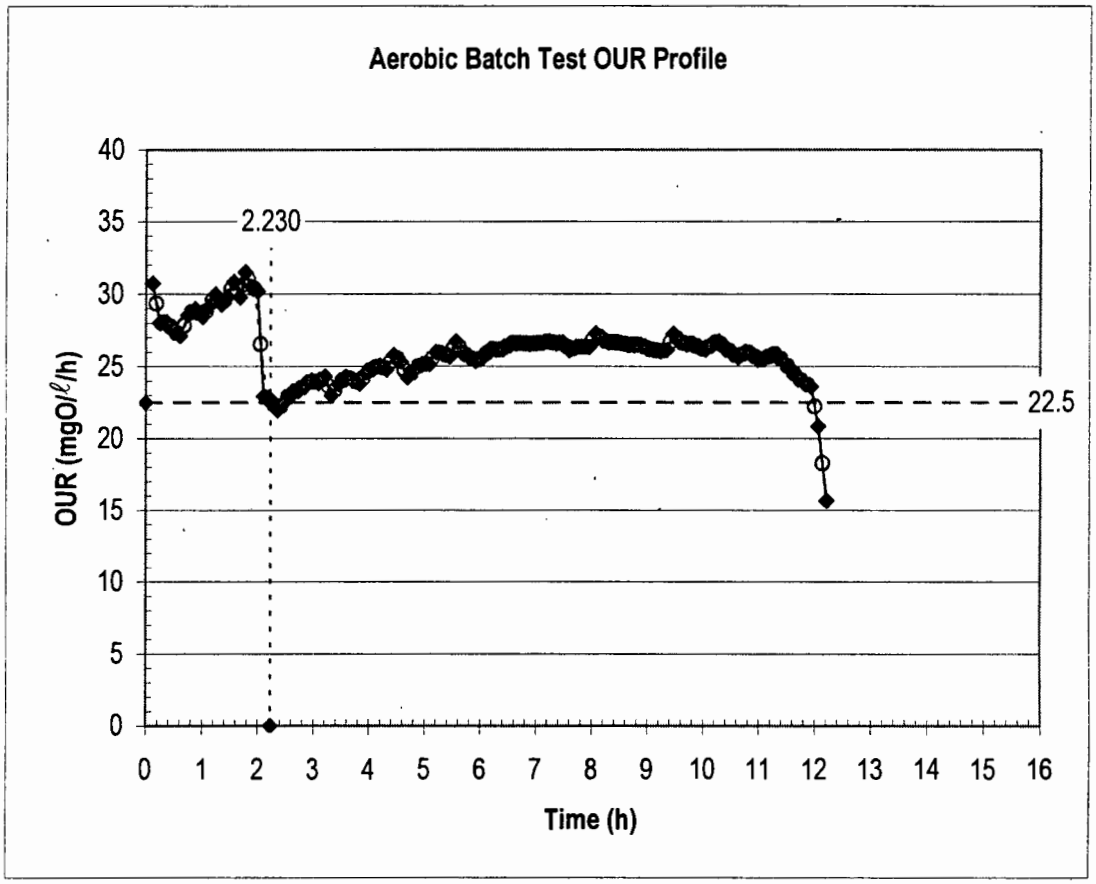

ML	SB	Date	ABT
LML	6	7.3.02	7

Plot end RBCOD:

t	End
1.123	0
1.123	*56*

Input SBCOD OUR:

33.9 mgO/L/h

Plot SBCOD OUR:

SBCODx	SBCODy
0	*33.9*
16	*33.9*

Batch Test Composition: V_{BT} 3 ℓ

V_{WW}	2	ℓ	V_{ML}	1	ℓ
S_{ti}	871	mgCOD/ℓ	X_v	4288	mgVSS/ℓ
$S_{ti,BT}$	580.67	mgCOD/ℓ	LR	0.406	mgCOD/mgVSS

Define RBCOD Area Sum:

OU = 9.8 mgO/ℓ

S_{bsi} =	29.79	mgCOD/ℓ
f_{ts} =	0.051	

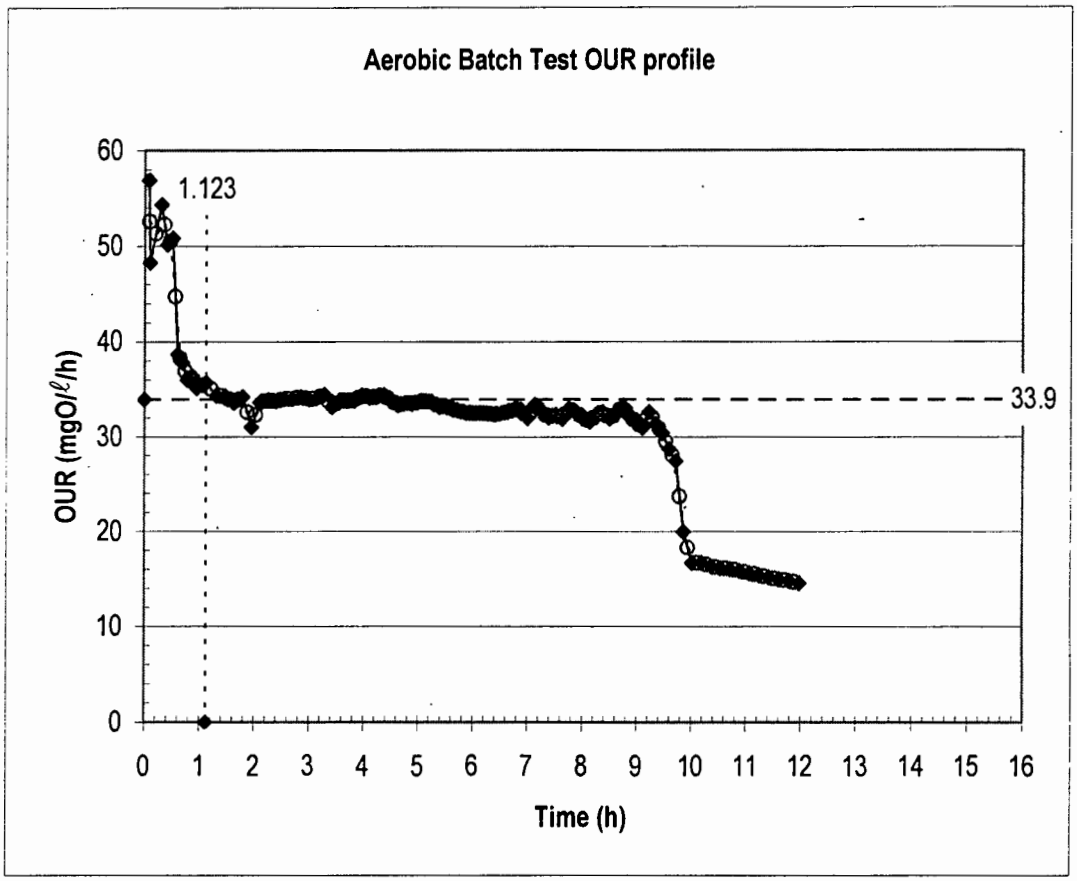

ML	SB	Date	ABT
LML	9	4.4.02	8

Plot end RBCOD:

t	End
2.219	0
2.219	*42.5*

Input SBCOD OUR:

24.5 mgO/ℓ/h

Plot SBCOD OUR:

SBCODx	SBCODy
0	*24.5*
12	*24.5*

Batch Test Composition: V_{BT} 3 ℓ

V_{WW}	2	ℓ	V_{ML}	1	ℓ
S_{ti}	892.5	mgCOD/ℓ	X_v	4109	mgVSS/ℓ
$S_{ti,BT}$	595	mgCOD/ℓ	LR	0.434	mgCOD/mgVSS

Define RBCOD Area Sum:

OU = 20.3 mgO/ℓ

S_{bsi} =	61.65	mgCOD/ℓ
f_{ts} =	0.104	

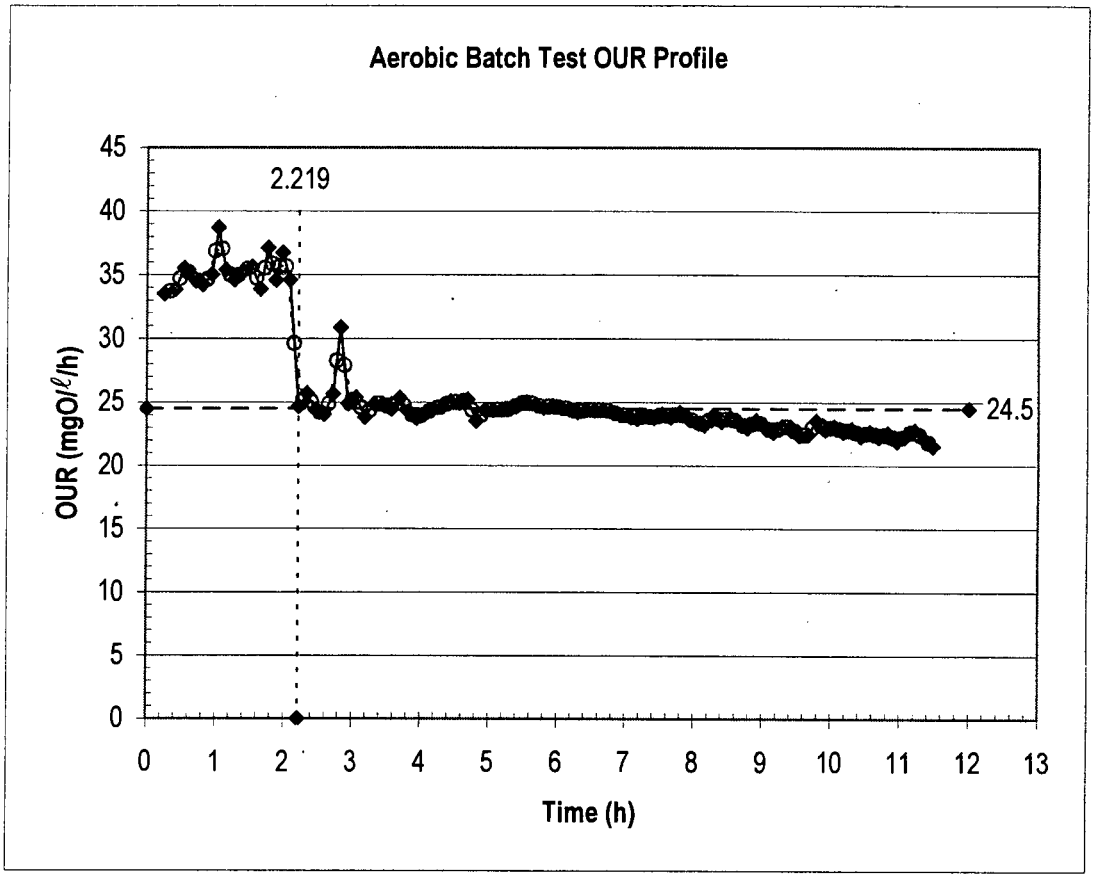

ML	SB	Date	ABT
LML	9	9.4.02	9

Plot end RBCOD:

t	End
3.855	0
3.855	47

Input SBCOD OUR:

NA mgO/ℓ/h

Plot SBCOD OUR:

SBCODx	SBCODy
0	*NA*
24	*NA*

Batch Test Composition: V_{BT} 3 ℓ

V_{WW}	2	ℓ	V_{ML}	1	ℓ
S_{ti}	917.5	mgCOD/ℓ	X_v	4061	mgVSS/ℓ
$S_{ti,BT}$	611.67	mgCOD/ℓ	LR	0.452	mgCOD/mgVSS

Define RBCOD Area Sum:

OU = **24.8** mgO/ℓ

S_{bsi} =	75.11	mgCOD/ℓ
f_{ts} =	0.123	

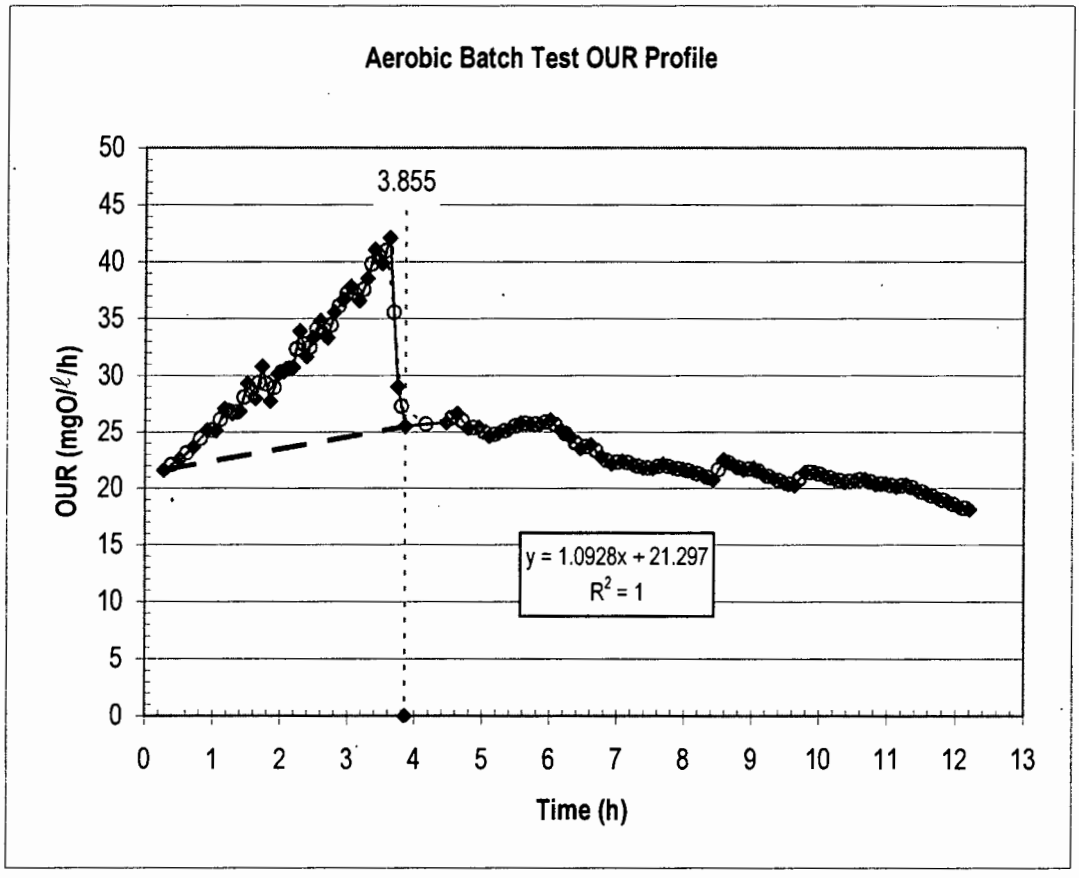

ML	SB	Date	ABT
LML	9	15.4.02	10

Plot end RBCOD:

t	End
1.554	0
1.554	56

Input SBCOD OUR:

29 mgO/L/h

Plot SBCOD OUR:

SBCODx	SBCODy
0	*29*
14	*29*

Batch Test Composition:

V_{WW}	2	ℓ	V_{ML}	1	ℓ
S_{ti}	845.3	mgCOD/ℓ	X_v	4153	mgVSS/ℓ
$S_{ti,BT}$	563.53	mgCOD/ℓ	LR	0.407	mgCOD/mgVSS

V_{BT} 3 ℓ

Define RBCOD Area Sum:

OU = 14.2 mgO/ℓ

S_{bsi} =	43.13	mgCOD/ℓ
f_{ts} =	0.077	

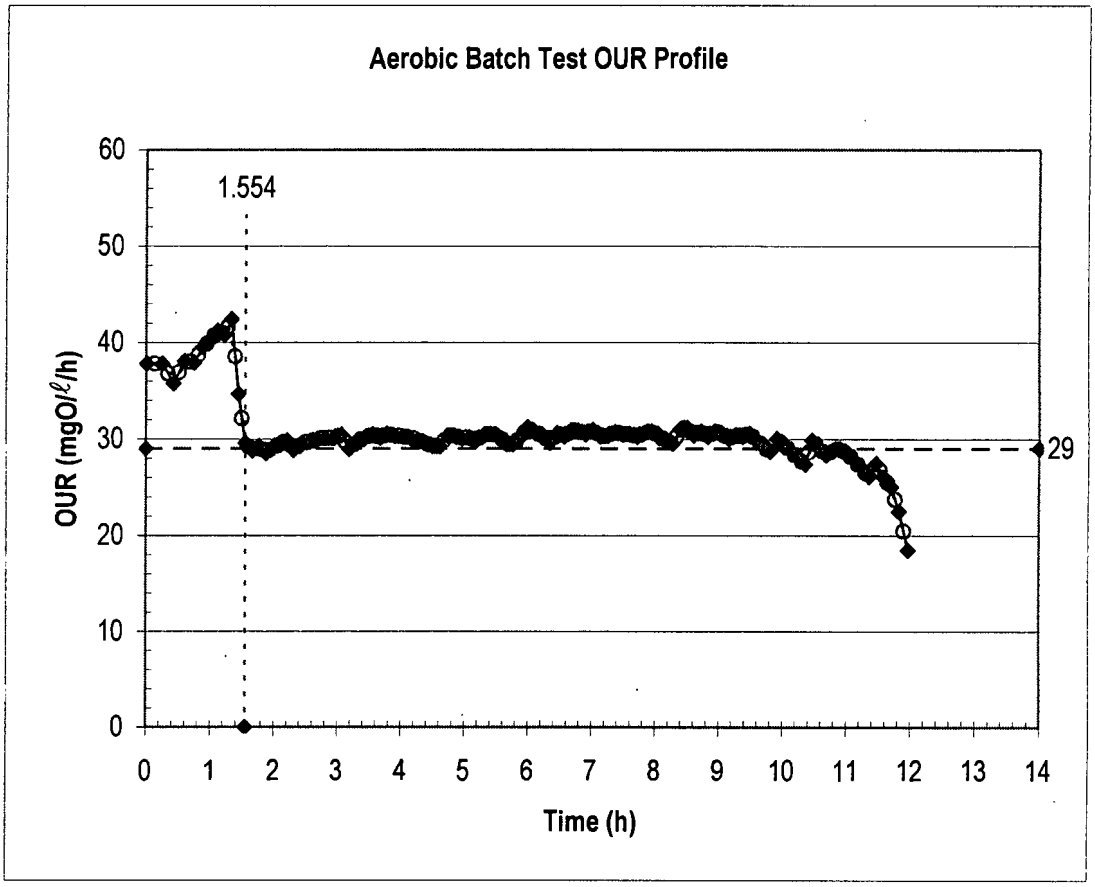

ML	SB	Date	ABT
LML	9	17.4.02	11

Plot end RBCOD:

t	End
1.617	0
1.617	37.5

Input SBCOD OUR:

23.5 mgO/L/h

Plot SBCOD OUR:

SBCODx	SBCODy
0	*23.5*
16	*23.5*

Batch Test Composition: V_{BT} 3 ℓ

V_{WW}	2	ℓ	V_{ML}	1	ℓ
S_{ti}	853.6	mgCOD/ℓ	X_v	4311	mgVSS/ℓ
$S_{ti,BT}$	569.07	mgCOD/ℓ	LR	0.396	mgCOD/mgVSS

Define RBCOD Area Sum:

OU = 9.8 mgO/ℓ

S_{bsi} =	29.59	mgCOD/ℓ
f_{ts} =	0.052	

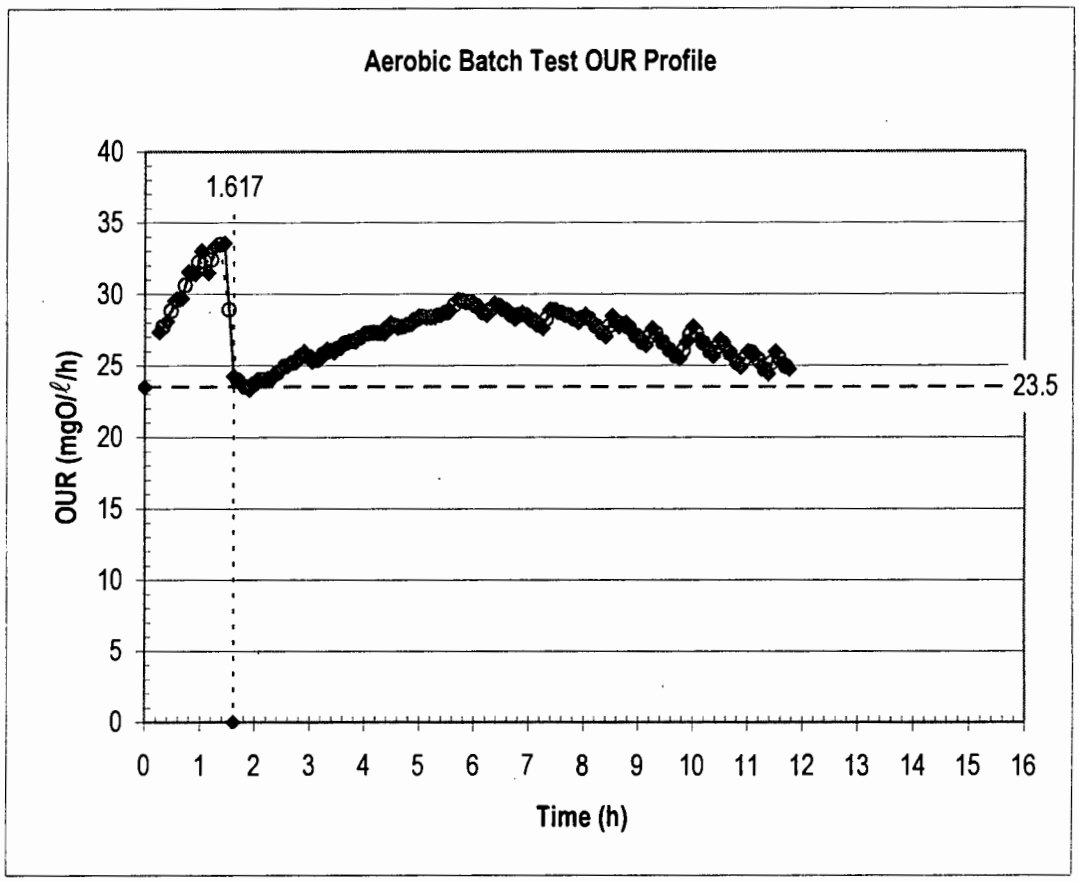

Plot end RBCOD:

t	End
1.913	0
1.913	55

Input SBCOD OUR:

34.25 mgO/ℓ/h

Plot SBCOD OUR:

SBCODx	SBCODy
0	*34.25*
12	*34.25*

ML	SB	Date	ABT
LML	10	24.4.02	12

Batch Test Composition: V_{BT} 3 ℓ

V_{WW}	2	ℓ	V_{ML}	1	ℓ
S_{ti}	1038.4	mgCOD/ℓ	X_v	4053	mgVSS/ℓ
$S_{ti,BT}$	692.27	mgCOD/ℓ	LR	0.512	mgCOD/mgVSS

Define RBCOD Area Sum:

OU = 17.8 mgO/ℓ

S_{bsi} =	53.89	mgCOD/ℓ
f_{ts} =	0.078	

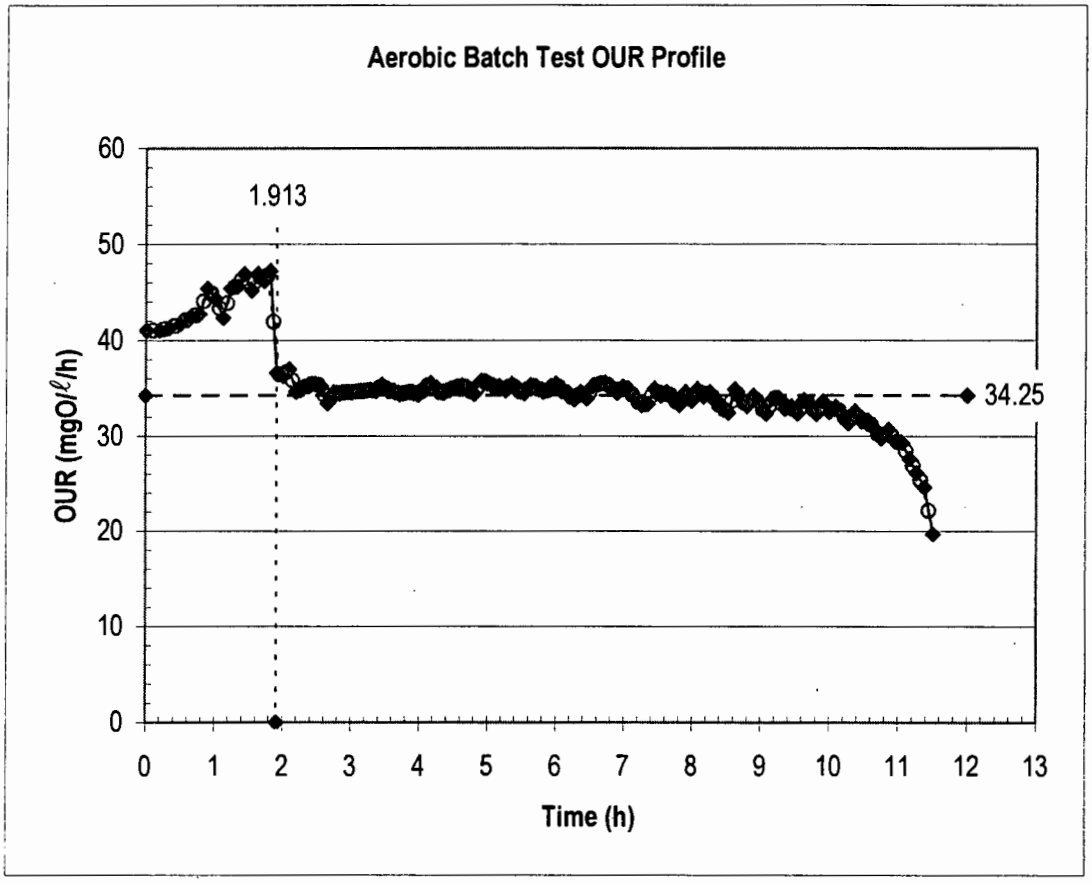

ML	SB	Date	ABT
LML	10	26.4.02	13

Plot end RBCOD:

t	End
2.708	0
2.708	37.5

Input SBCOD OUR:

23.3 mgO/L/h

Plot SBCOD OUR:

SBCODx	SBCODy
0	*23.3*
13	*23.3*

Batch Test Composition:

V_{BT}	3	ℓ			
V_{ww}	2	ℓ	V_{ML}	1	ℓ
S_{ti}	1179.4	mgCOD/ℓ	X_v	4034	mgVSS/ℓ
$S_{ti,BT}$	786.27	mgCOD/ℓ	LR	0.585	mgCOD/mgVSS

Define RBCOD Area Sum:

OU = 15.4 mgO/ℓ

S_{bsi} =	46.74	mgCOD/ℓ
f_{ts} =	0.059	

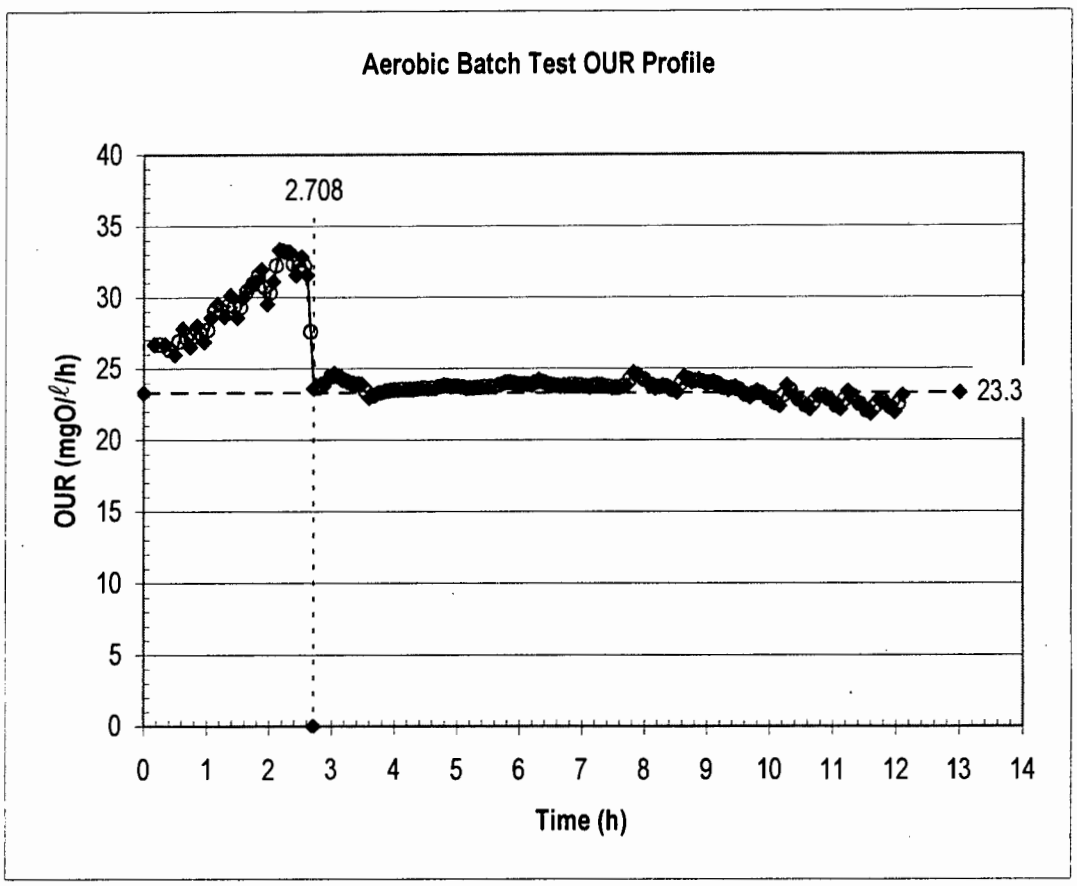

ML	SB	Date	ABT
MPP	11	29.4.02	14

Plot end RBCOD:

t	End
1.134	0
1.134	40

Input SBCOD OUR: 18.5 mgO/ℓh

Plot SBCOD OUR:

SBCODx	SBCODy
0	*18.5*
12	*18.5*

Batch Test Composition: V_{BT} 3 ℓ

V_{WW}	2	ℓ	V_{ML}	1	ℓ
S_{ti}	1090.8	mgCOD/ℓ	X_v	3102	mgVSS/ℓ
$S_{ti,BT}$	727.2	mgCOD/ℓ	LR	0.703	mgCOD/mgVSS

Define RBCOD Area Sum:

OU = 16.0 mgO/ℓ

S_{bsi} =	48.37	mgCOD/ℓ
f_{ts} =	0.067	

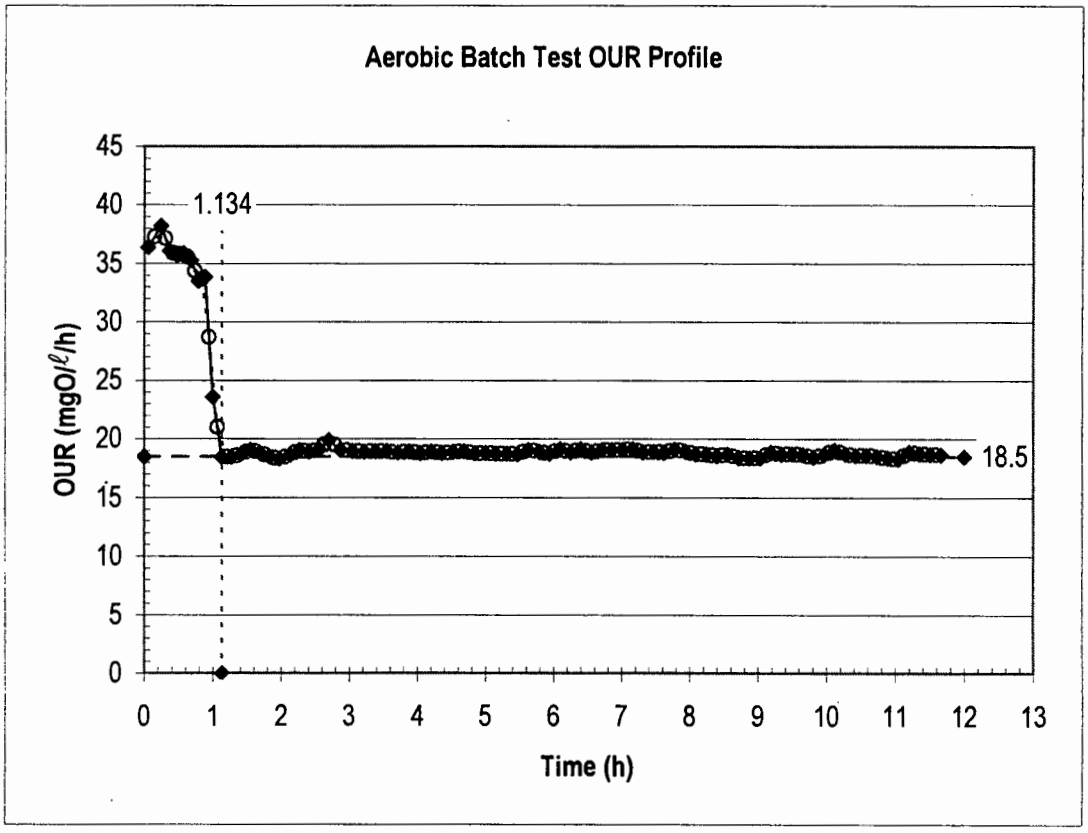

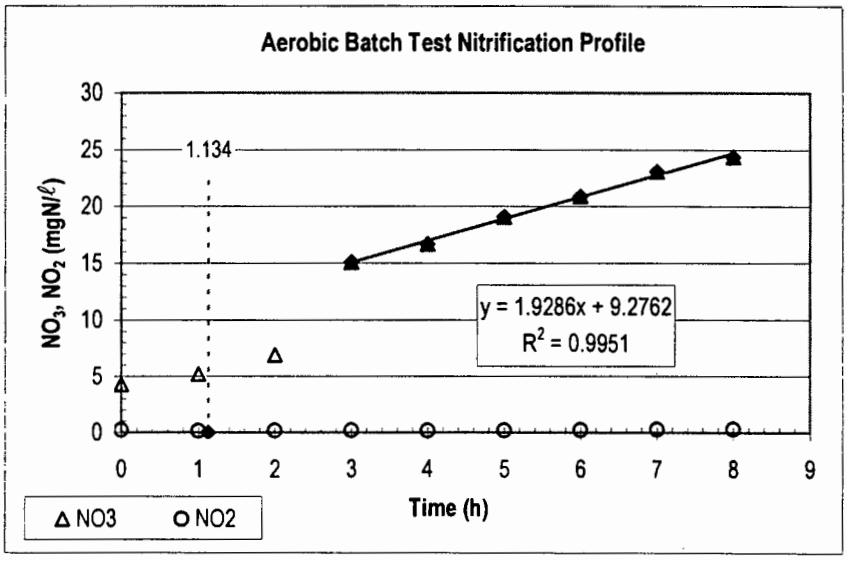

Plot end RBCOD:

t	End
1.134	0
1.134	25

Linear fit:

m =	1.9286
c =	9.2762
R^2 =	0.9951

Note: Dilution effects (Lee, 2002, p.4.48) caused step change at t=3; slopefrom upper portion only.

ML	SB	Date	ABT
MPP	11	2.5.02	15

Plot end RBCOD:

t	End
1.090	0
1.090	*40*

Input SBCOD OUR: 19.45 mgO/L/h

Plot SBCOD OUR:

SBCODx	SBCODy
0	*19.45*
12	*19.45*

Batch Test Composition: V_{BT} 3 ℓ

V_{WW}	2	ℓ	V_{ML}	1	ℓ
S_{ti}	1151.2	mgCOD/ℓ	X_v	2921	mgVSS/ℓ
$S_{ti,BT}$	767.47	mgCOD/ℓ	LR	0.788	mgCOD/mgVSS

Define RBCOD Area Sum:

OU = 15.5 mgO/ℓ

S_{bsi} =	46.92	mgCOD/ℓ
f_{ts} =	0.061	

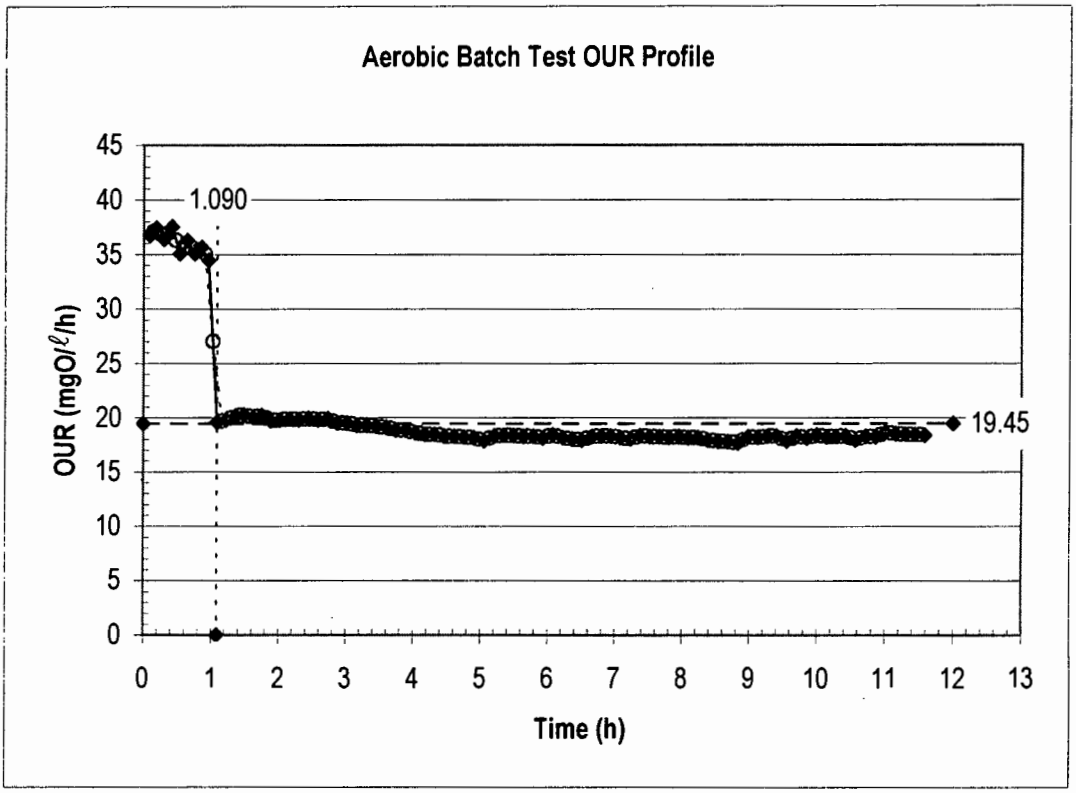

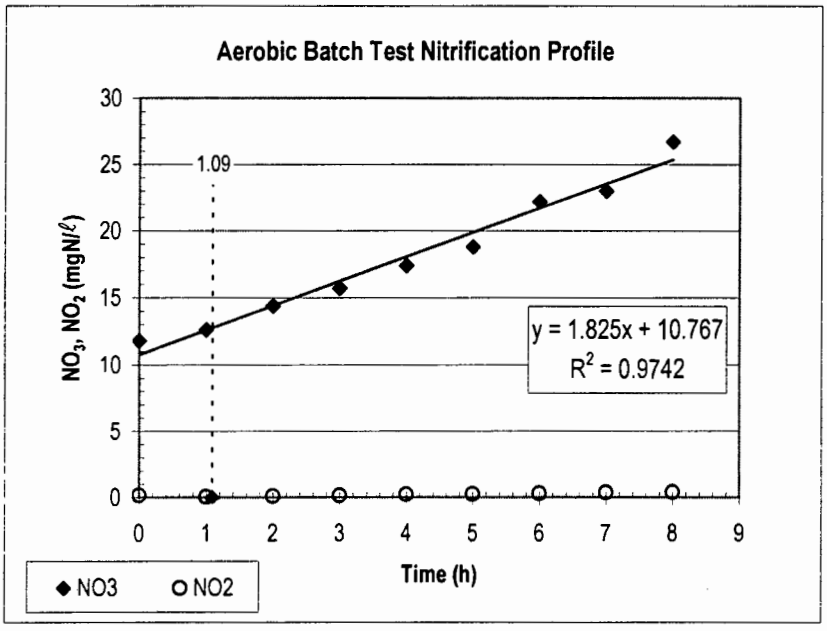

Plot end RBCOD:

t	End
1.090	0
1.09	25

Linear fit:

m =	1.825
c =	10.767
R^2 =	0.9742

Plot end RBCOD:

t	End
1.015	0
1.015	45

ML	SB	Date	ABT
MPP	11	3.5.02	16

Input SBCOD OUR: 21.45 mgO/L/h

Plot SBCOD OUR:

SBCODx	SBCODy
0	*21.45*
14	*21.45*

Batch Test Composition: V_{BT} 3 ℓ

V_{ww}	2	ℓ	V_{ML}	1	ℓ
S_{ti}	1151.2	mgCOD/ℓ	X_v	2887	mgVSS/ℓ
$S_{ti,BT}$	767.47	mgCOD/ℓ	LR	0.798	mgCOD/mgVSS

Define RBCOD Area Sum:

OU = 15.0 mgO/ℓ

S_{bsi} =	45.33	mgCOD/ℓ
f_{ts} =	0.059	

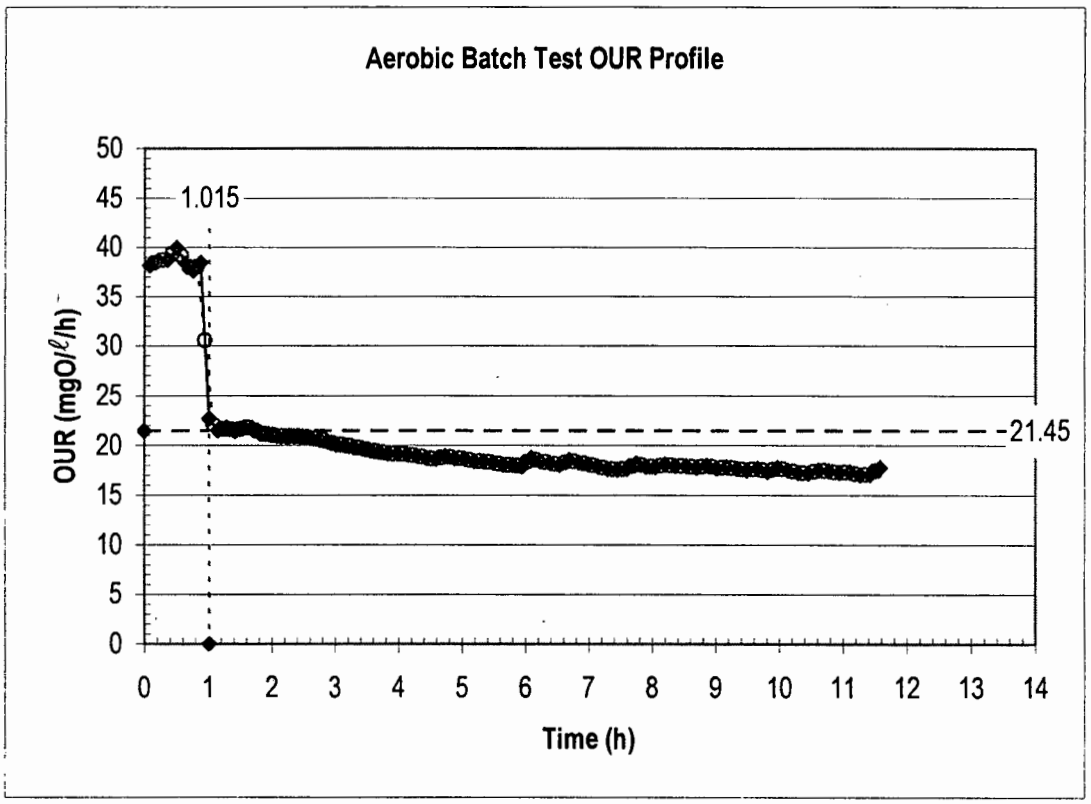

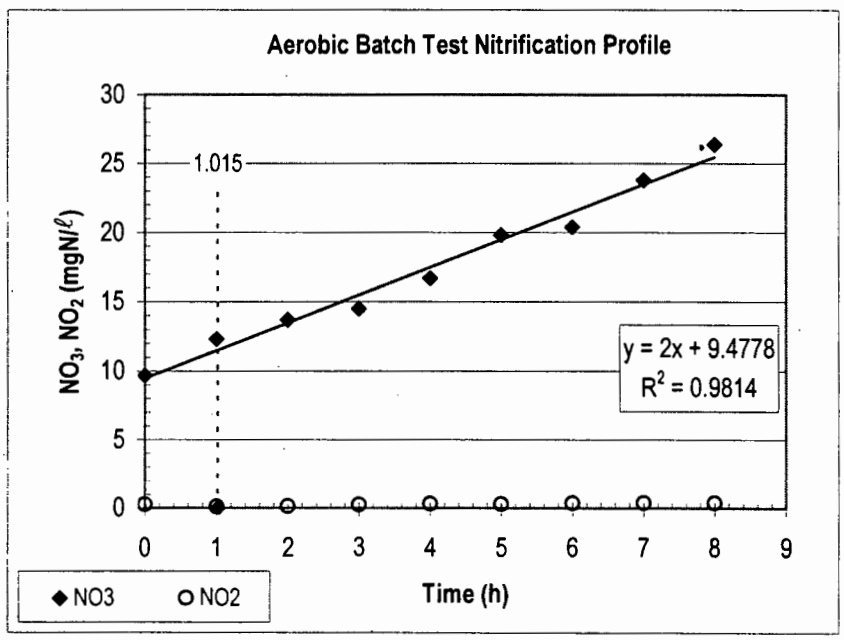

Plot end RBCOD:

t	End
1.015	0
1.0147	25

Linear fit:	
m =	2
c =	9.4778
R^2 =	0.9814

ML	SB	Date	ABT
MPP	11	4.5.02	17

Plot end RBCOD:

t	End
1.220	0
1.220	45

Input SBCOD OUR:

20.25 mgO/L/h

Plot SBCOD OUR:

SBCODx	SBCODy
0	*20.25*
16	*20.25*

Batch Test Composition: V_{BT} 3 ℓ

V_{WW}	2	ℓ	V_{ML}	1	ℓ
S_{ti}	853.6	mgCOD/ℓ	X_v	4311	mgVSS/ℓ
$S_{ti,BT}$	569.07	mgCOD/ℓ	LR	0.396	mgCOD/mgVSS

Define RBCOD Area Sum:

OU = 16.3 mgO/ℓ

S_{bsi} =	49.30	mgCOD/ℓ
f_{ts} =	0.087	

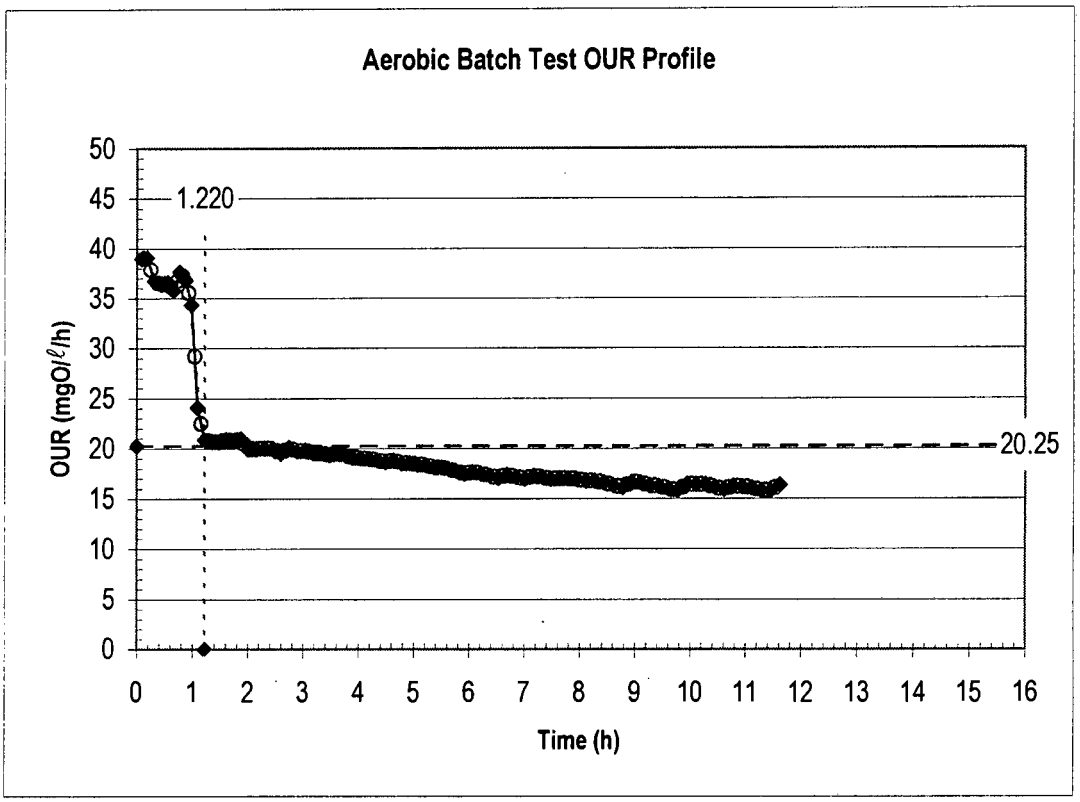

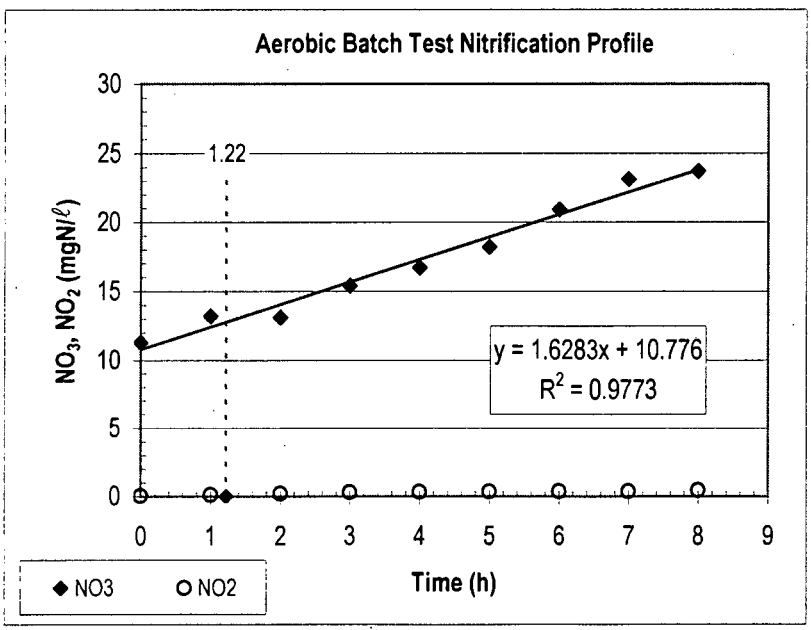

Plot end RBCOD:

t	End
1.220	0
1.22	25

Linear fit:	
m =	1.6283
c =	10.776
R^2 =	0.9773

ML	SB	Date	ABT
MPP	11	5.5.02	18

Plot end RBCOD:

t	End
1.155	0
1.155	45

Input SBCOD OUR:

20.8 mgO/L/h

Plot SBCOD OUR:

SBCODx	SBCODy
0	*20.8*
16	*20.8*

Batch Test Composition:

V_{BT} 3 ℓ

V_{WW}	2	ℓ	V_{ML}	1	ℓ
S_{ti}	1172	mgCOD/ℓ	X_v	2724	mgVSS/ℓ
$S_{ti,BT}$	781.33	mgCOD/ℓ	LR	0.860	mgCOD/mgVSS

Define RBCOD Area Sum:

OU = 16.3 mgO/ℓ

S_{bsi} =	49.25	mgCOD/ℓ
f_{ts} =	0.063	

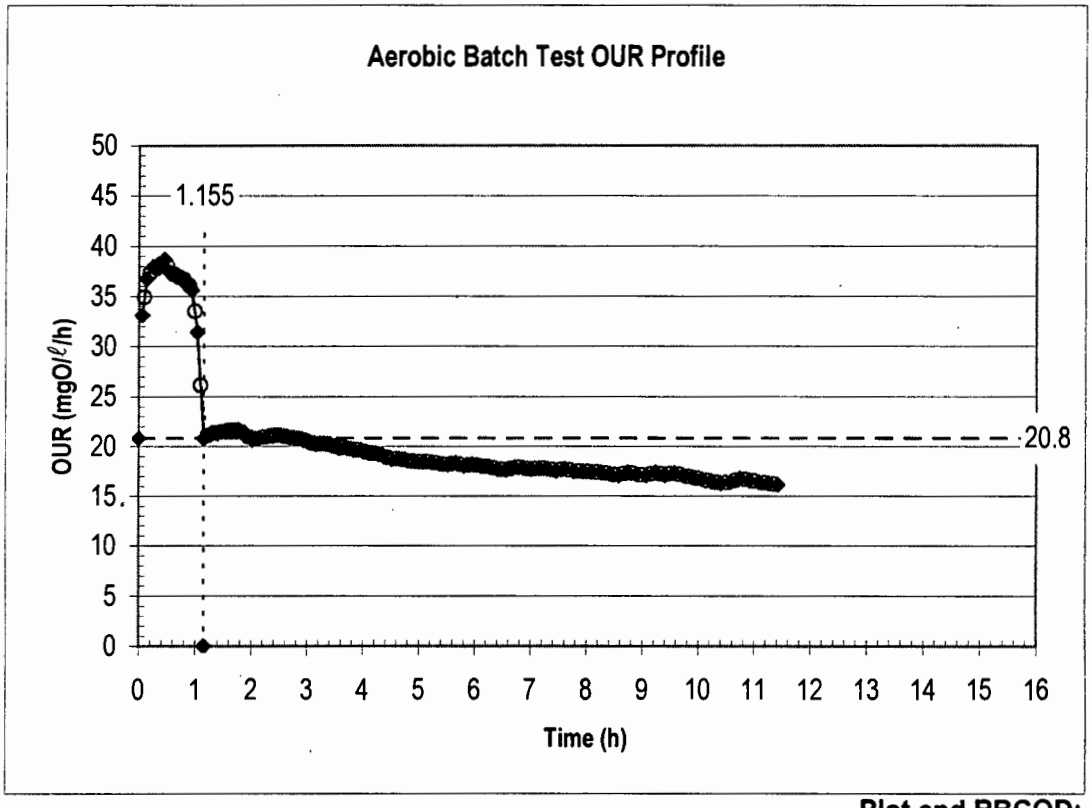

Plot end RBCOD:

t	End
1.155	0
1.1553	25

Linear fit:

m =	1.5333
c =	12.278
R^2 =	0.9856

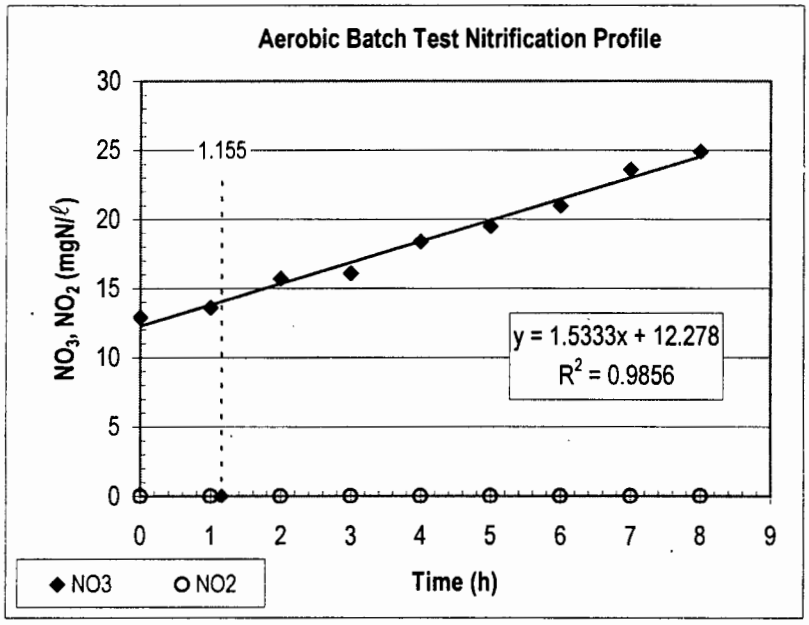

ML	SB	Date	ABT
MPP	*NS*	11.5.02	19

Plot end RBCOD:

t	End
1.219	0
1.219	35

Input SBCOD OUR:

12.9 mgO/L/h

Plot SBCOD OUR:

SBCODx	SBCODy
0	*12.9*
12	*12.9*

Batch Test Composition: V_{BT} 3 ℓ

V_{ww}	2	ℓ	V_{ML}	1	ℓ
S_{ti}	1154	mgCOD/ℓ	X_v	1520	mgVSS/ℓ
$S_{ti,BT}$	769.33	mgCOD/ℓ	LR	1.518	mgCOD/mgVSS

Define RBCOD Area Sum:

OU = 17.2 mgO/ℓ

S_{bsi} =	52.16	mgCOD/ℓ
f_{ts} =	0.068	

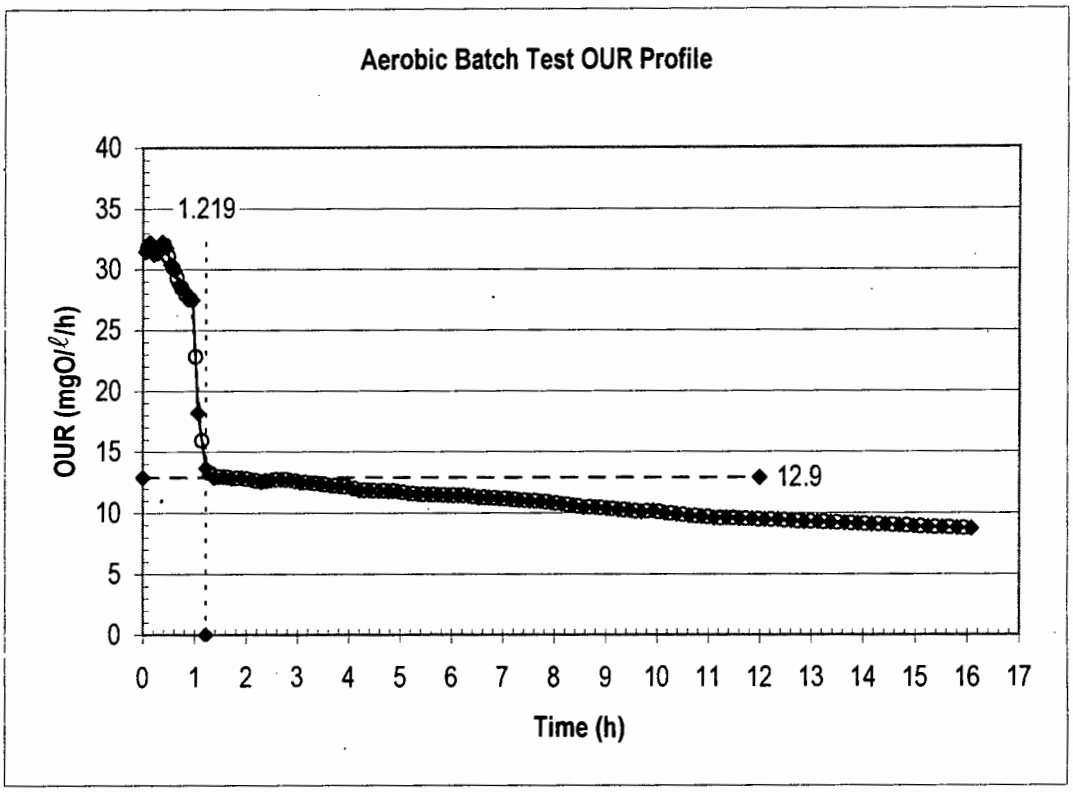

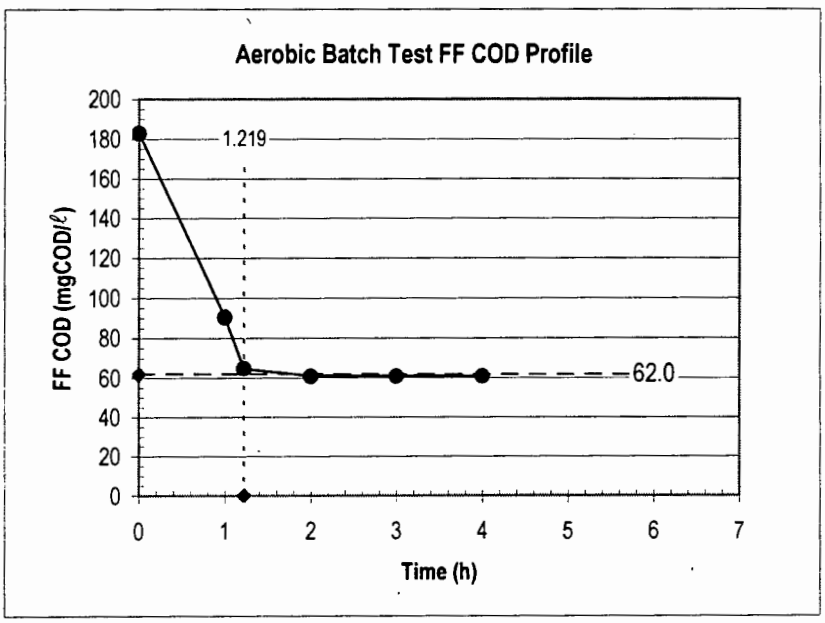

Plot end RBCOD:

t	End
1.219	0
1.21883	180

Plot FFE's:

t	FFE
0	182.9
1	90.4
1.22	65
2	61
3	61
4	61
Avg	*62.0*

Plot Avg FFE:

t	Avg
0	*62.0*
6	*62.0*

ML	SB	Date	ABT
MPP	12	16.5.02	20

Plot end RBCOD:

t	End
0.904	0
0.904	50

Input SBCOD OUR:

21.7 mgO/L/h

Plot SBCOD OUR:

SBCODx	SBCODy
0	*21.7*
14	*21.7*

Batch Test Composition:

V_{BT}	3	ℓ			
V_{ww}	2	ℓ	V_{ML}	1	ℓ
S_{ti}	1337.2	mgCOD/ℓ	X_v	2529	mgVSS/ℓ
$S_{ti,BT}$	891.47	mgCOD/ℓ	LR	1.057	mgCOD/mgVSS

Define RBCOD Area Sum:

OU = 15.9 mgO/ℓ

S_{bsi} =	48.09	mgCOD/ℓ
f_{ts} =	0.054	

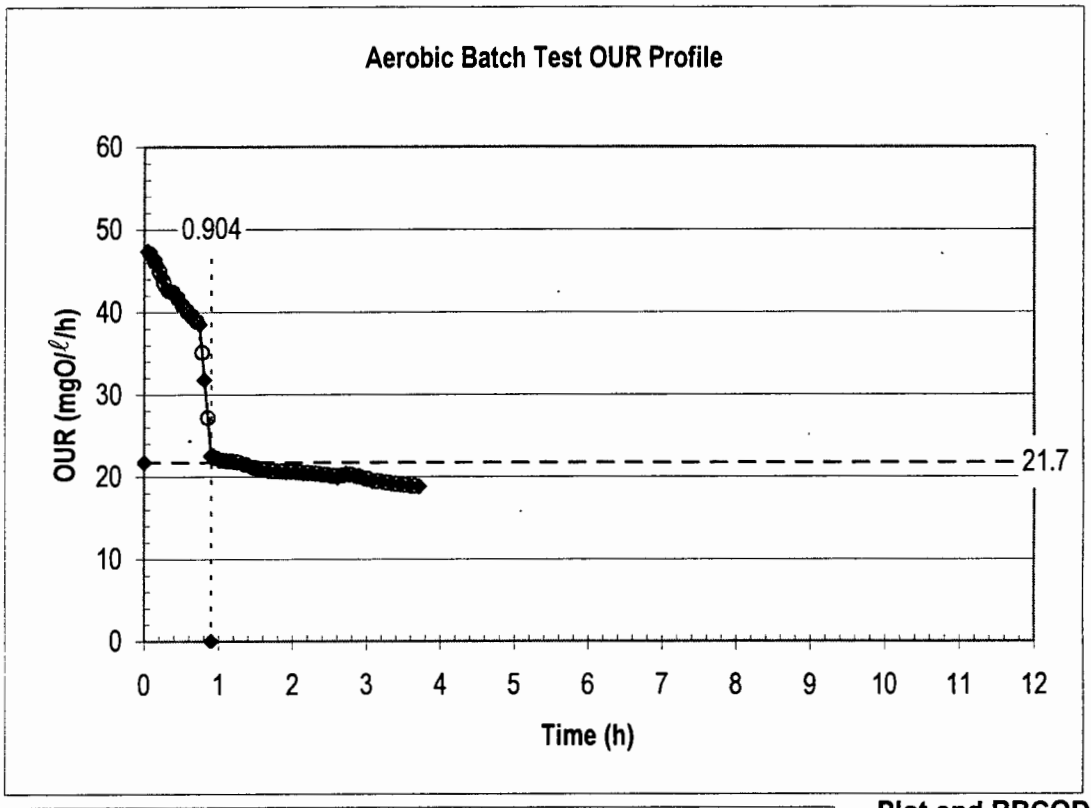

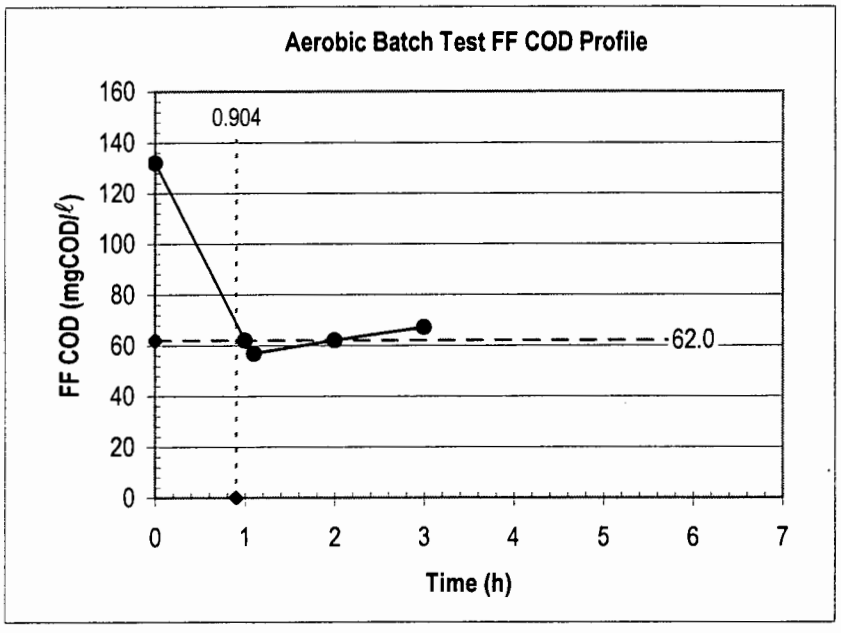

Plot end RBCOD:

t	End
0.904	0
0.90367	150

Plot FFE's:

t	FFE
0	132.1
1	62
1.1	56.9
2	62
3	67.1
4	
Avg	*62.0*

Plot Avg FFE:

t	Avg
0	*62.0*
6	*62.0*

ML	SB	Date	ABT
LML	13	3.6.02	21

Plot end RBCOD:

t	End
1.935	0
1.935	60

Input SBCOD OUR:

41.1 mgO/L/h

Plot SBCOD OUR:

SBCODx	SBCODy
0	*41.1*
16	*41.1*

Batch Test Composition:

V_{WW}	1.333	ℓ	V_{ML}	0.667	ℓ
S_{ti}	967.2	mgCOD/ℓ	X_v	5468	mgVSS/ℓ
$S_{ti,BT}$	429.76	mgCOD/ℓ	LR	0.354	mgCOD/mgVSS

V_{BT} 3 ℓ

Define RBCOD Area Sum:

OU = 15.7 mgO/ℓ

S_{bsi} =	47.56	mgCOD/ℓ
f_{ts} =	0.111	

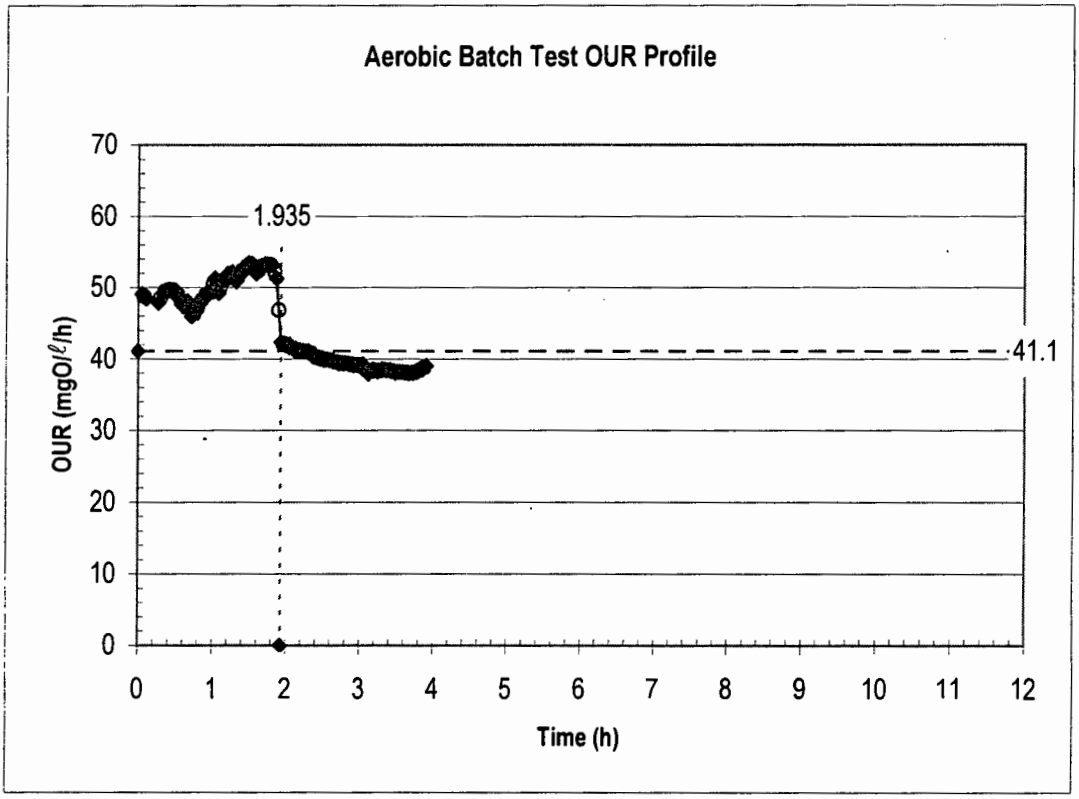

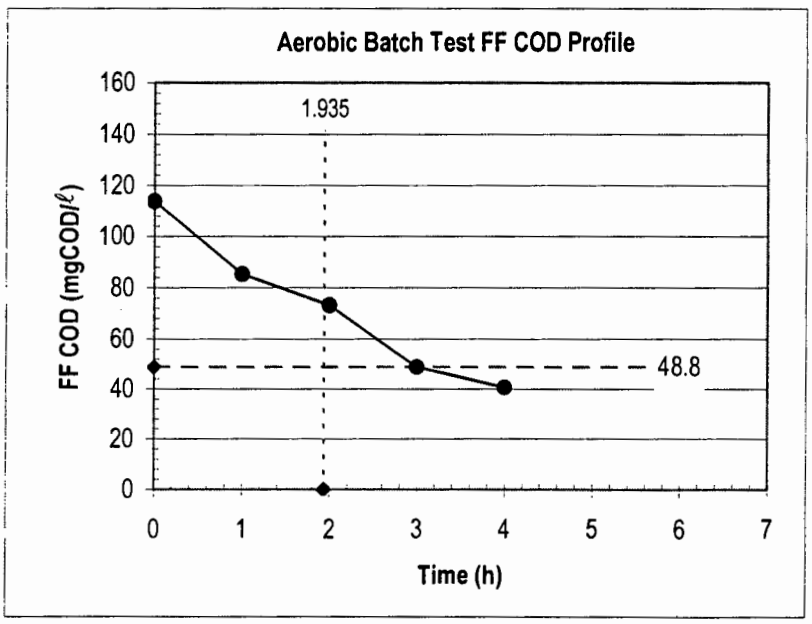

Plot end RBCOD:

t	End
1.935	0
1.93517	150

Plot FFE's:

t	FFE
0	113.8
1	85.3
2	73.2
3	48.8
4	40.6
Avg	*48.8*

Plot Avg FFE:

t	Avg
0	*48.8*
6	*48.8*

ML	SB	Date	ABT
MPP	13	4.6.02	22

Plot end RBCOD:

t	End
1.050	0
1.050	45

Input SBCOD OUR:

19.95 mgO/L/h

Plot SBCOD OUR:

SBCODx	SBCODy
0	*19.95*
16	*19.95*

Batch Test Composition:

V_{WW}	2	ℓ	V_{ML}	1	ℓ
S_{ti}	1209	mgCOD/ℓ	X_v	2161	mgVSS/ℓ
$S_{ti,BT}$	806	mgCOD/ℓ	LR	1.119	mgCOD/mgVSS

V_{BT} 3 ℓ

Define RBCOD Area Sum:

OU = *15.6* mgO/ℓ

S_{bsi} = *47.37* mgCOD/ℓ

f_{ts} = *0.059*

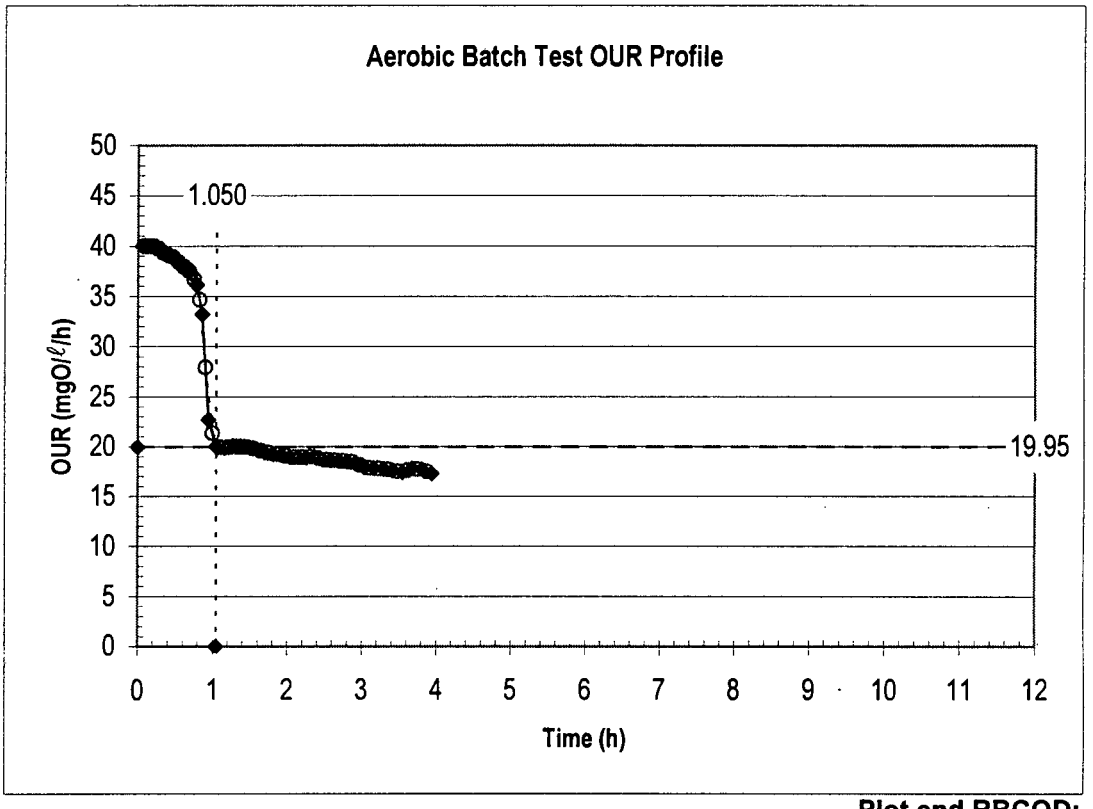

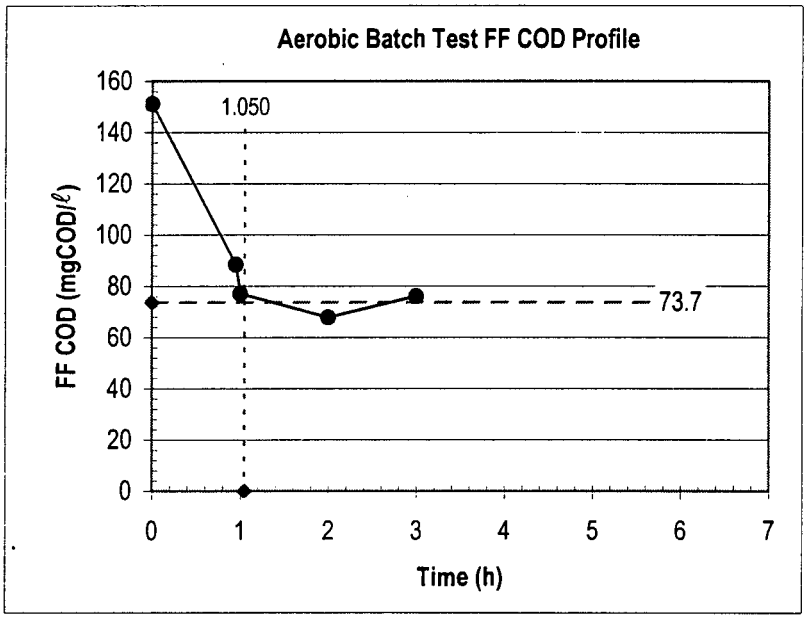

Plot end RBCOD:

t	End
1.050	0
1.05017	150

Plot FFE's:

t	FFE
0	151.1
0.95	88.4
1	77.1
2	67.8
3	76.1
4	
Avg	*73.7*

Plot Avg FFE:

t	Avg
0	*73.7*
6	*73.7*

ML	SB	Date	ABT
SQW	18	26.8.02	23

Plot end RBCOD:

t	End
1.823	0
1.823	35

Input SBCOD OUR:

21.7 mgO/L/h

Plot SBCOD OUR:

SBCODx	SBCODy
0	*21.7*
6	*21.7*

Batch Test Composition: V_{BT} 3 ℓ

V_{WW}	1.39	ℓ	V_{ML}	1.61	ℓ
S_{ti}	1139.8	mgCOD/ℓ	X_v	1059	mgVSS/ℓ
$S_{ti,BT}$	528.11	mgCOD/ℓ	LR	0.929	mgCOD/mgVSS

Define RBCOD Area Sum:

OU = 10.5 mgO/ℓ

S_{bsi} =	31.84	mgCOD/ℓ
f_{ts} =	0.060	

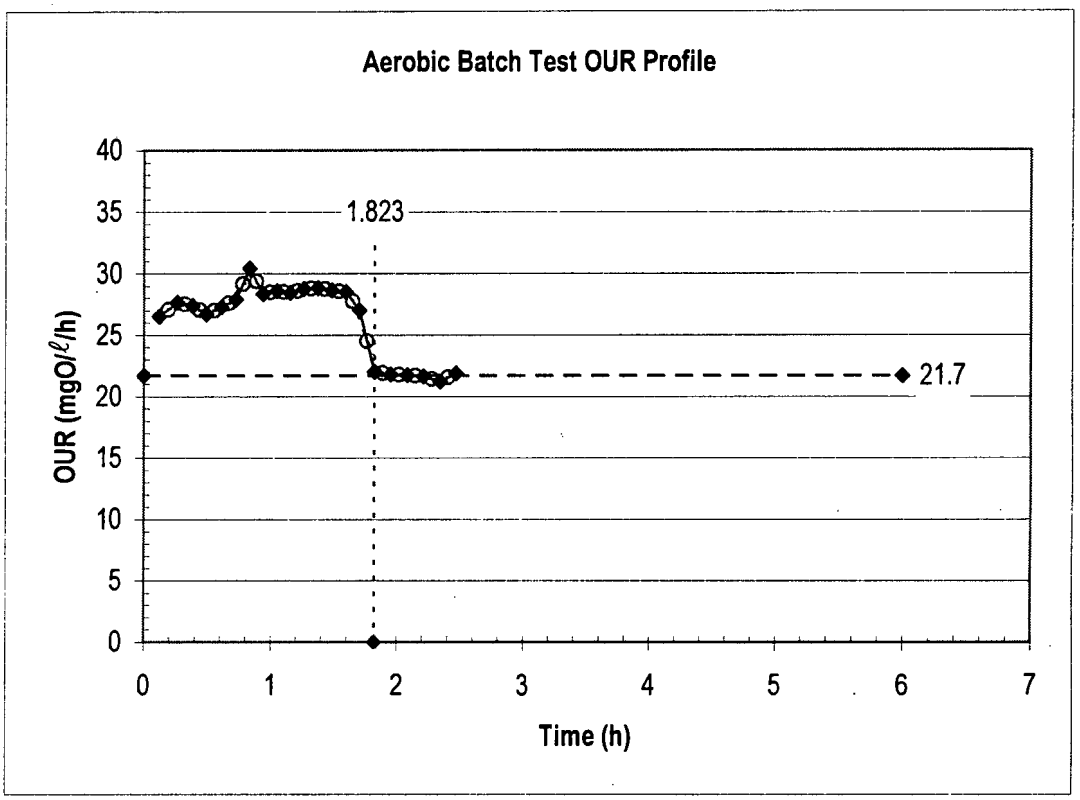

Plot end RBCOD:

t	End
1.596	0
1.596	50

Plot SBCOD OUR:

X_{SBCOD}	Y_{SBCOD}
0	33
3	*33*

Wastewater:

			ML	SB	Date	ABT
			SQW	18	27.8.02	24
V_{BT}	3	ℓ				
V_{WW}	2	ℓ	V_{ML}	1	ℓ	
S_{ti}	1352	mgCOD/ℓ	X_v	5236	mgVSS/ℓ	
$S_{ti,BT}$	901.3	mgCOD/ℓ	LR	0.516	mgCOD/mgVSS	
Define RBCOD Area Sum:			S_{bsi} =	45.88	mgCOD/ℓ	
OU =	**15.1**	mgO/ℓ	f_{ts} =	0.051		

Ac COD	2853.6	mgCOD/ℓ

	Ac1	Ac2
V_{Ac} (mℓ)	100	
V_{BT} (ℓ)	3	
$[Ac_{COD}]_{BT}$	95.12	
OU (mgO/ℓ)	**25.75**	
$Y_{H,AE\ (COD)}$	0.729	

Plot Ac Baselines:

t	Ac1	
4.170	31.035	-0.7042
5.946	29.785	33.972

t	Ac2
0	33
3	*33*

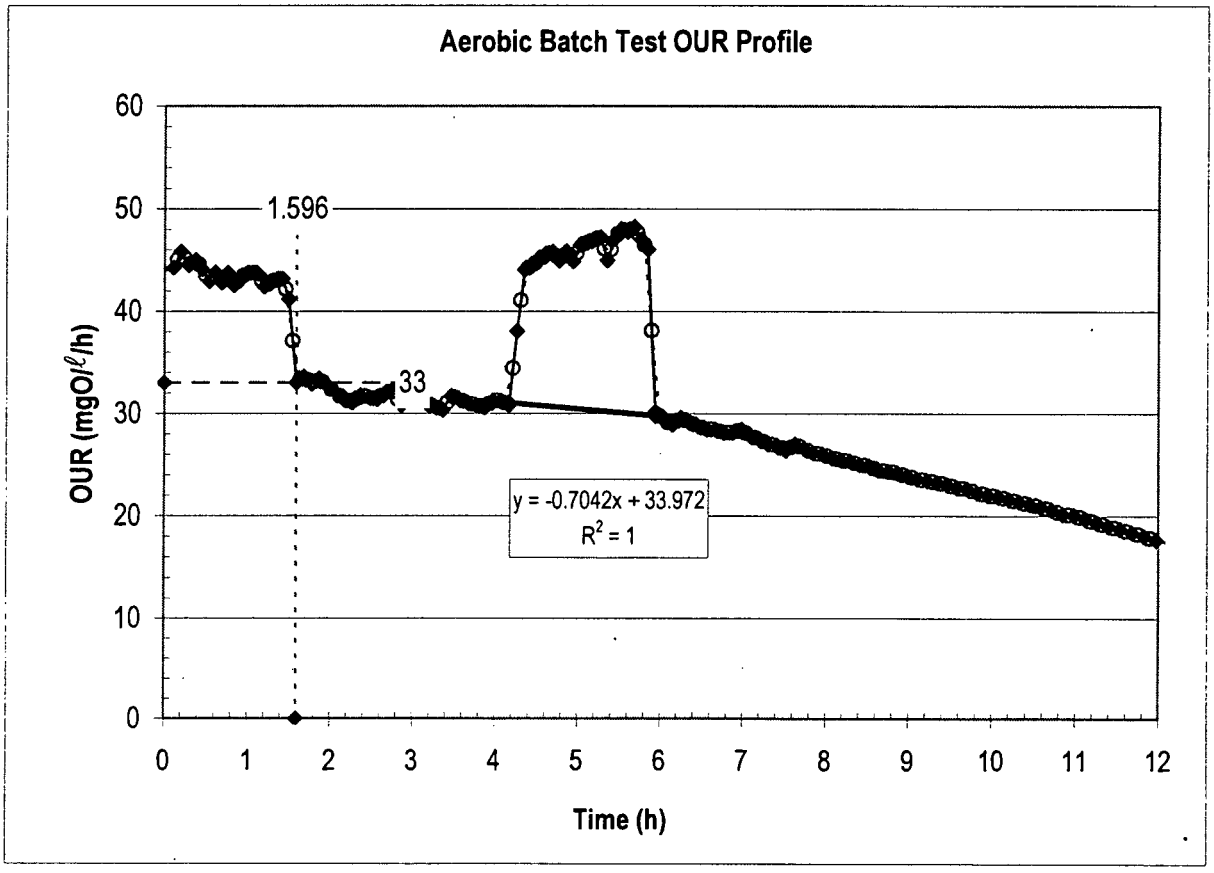

Plot end RBCOD:

t	End
3.008	0
3.008	40

Plot SBCOD OUR:

X_{SBCOD}	Y_{SBCOD}
0	16.65
8	*16.65*

	ML	SB	Date	ABT
	MLE	19	13.9.02	25

Wastwater:

V_{BT}	3	ℓ			
V_{WW}	2	ℓ	V_{ML}	1	ℓ
S_{ti}	1028.2	mgCOD/ℓ	X_v	2199	mgVSS/ℓ
$S_{ti,BT}$	685.5	mgCOD/ℓ	LR	0.935	mgCOD/mgVSS
Define RBCOD Area Sum:			S_{bsi} =	61.35	mgCOD/ℓ
OU =	**20.2**	mgO/ℓ	f_{ts} =	0.090	

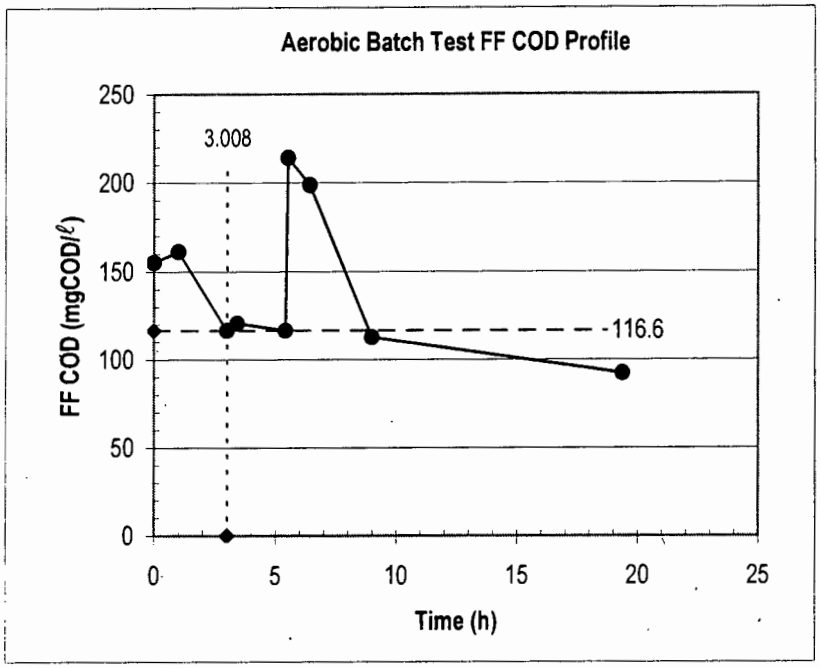

Ac COD	2993.2	mgCOD/ℓ

	Ac1	Ac2
V_{Ac} (mℓ)	75	
V_{BT} (ℓ)	2.357	
$[Ac_{COD}]_{BT}$	95.24	
OU (mgO/ℓ)	**44.31**	
$Y_{H,AE\ (COD)}$	0.535	

Plot Ac Baselines:

t	Ac1	
5.344	19.66	1.5276
8.669	24.74	11.497
t	**Ac2**	
5.646	29.8	
9.277	21.25	

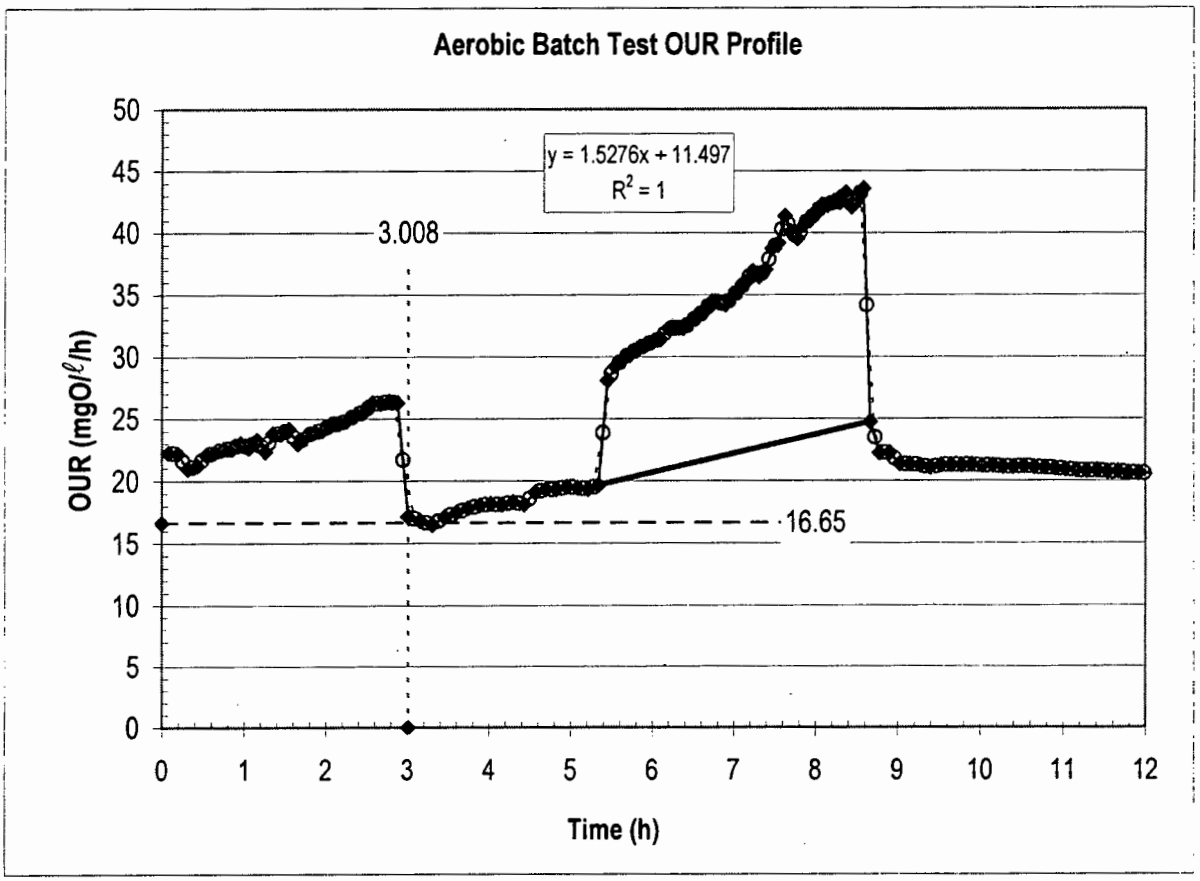

Plot end RBCOD:

t	End
2.230	0
2.230	55

Plot SBCOD OUR:

X_{SBCOD}	Y_{SBCOD}
0	27.6
3.5	*27.6*

	ML	SB	Date	ABT
	MLE	20	15.9.02	26

Wastwater:

V_{BT}	3	ℓ			
V_{WW}	2	ℓ	V_{ML}	1	ℓ
S_{ti}	955.2	mgCOD/ℓ	X_v	2505	mgVSS/ℓ
$S_{ti,BT}$	636.8	mgCOD/ℓ	LR	0.763	mgCOD/mgVSS
Define RBCOD Area Sum:			S_{bsi} =	47.85	mgCOD/ℓ
OU =	**15.8**	mgO/ℓ	f_{ts} =	0.075	

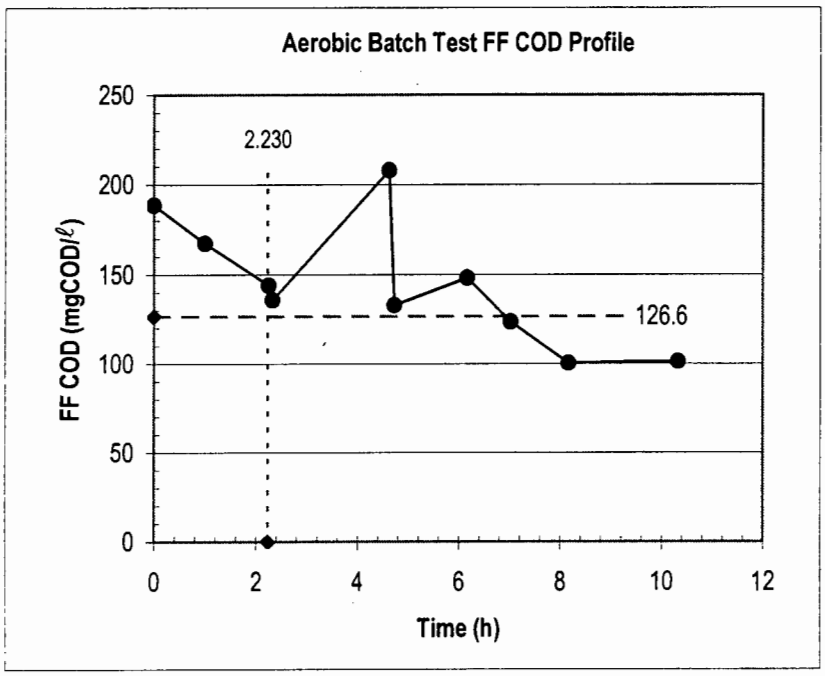

Ac COD	3037.9	mgCOD/ℓ

	Ac1	Ac2
V_{Ac} (mℓ)	75	50
V_{BT} (ℓ)	2.31	1.74
$[Ac_{COD}]_{BT}$	98.63	87.30
OU (mgO/ℓ)	**31.32**	**23.61**
$Y_{H,AE\ (COD)}$	0.682	0.730

Plot Ac Baselines:

t	Ac1	
4.617	29.05	0.2899
7.032	29.75	27.712
t	**Ac2**	
8.080	28.2	0.0709
9.632	28.31	27.627

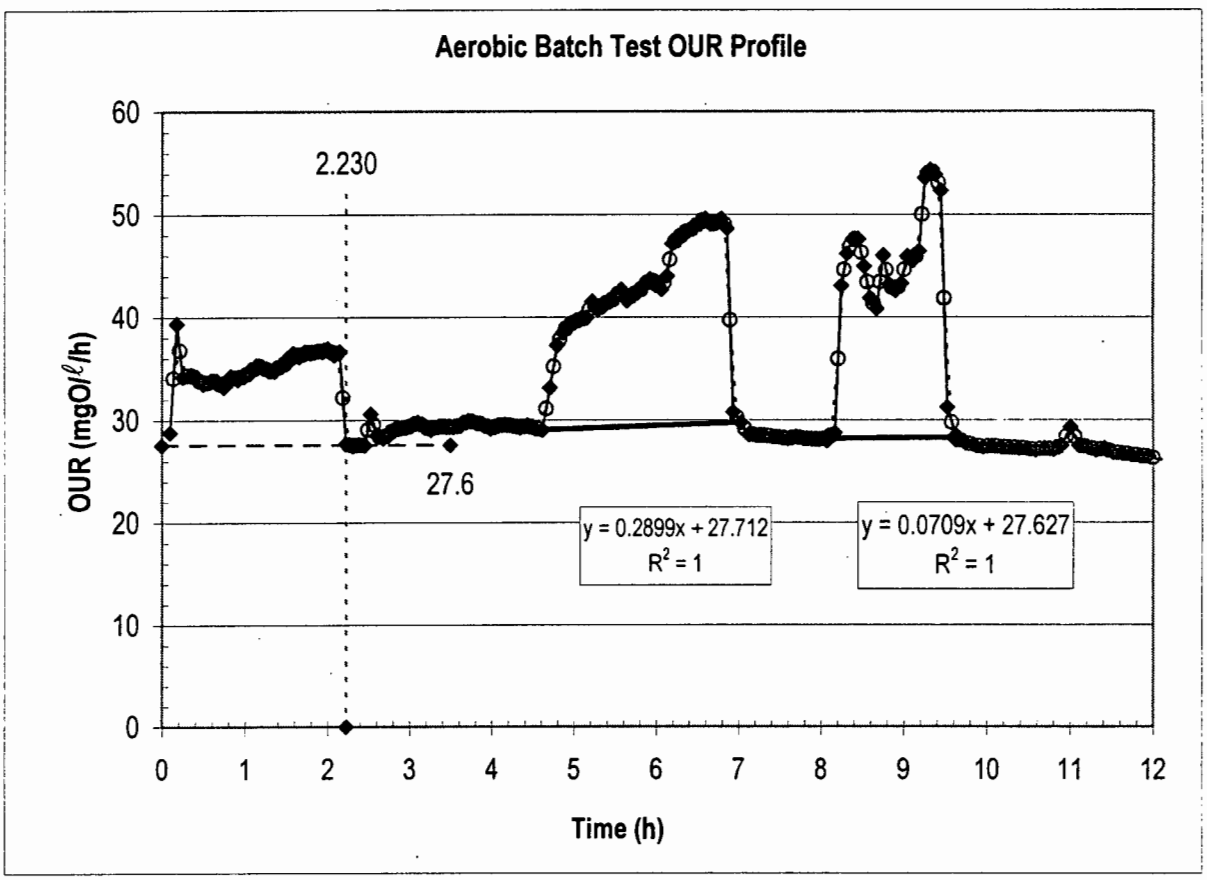

Plot end RBCOD:

t	End
1.777	0
1.777	*75*

Plot SBCOD OUR:

X_{SBCOD}	Y_{SBCOD}
0	45.5
2.5	*45.5*

	ML	SB	Date	ABT
	MLE	20	22.9.02	27

Wastwater:

V_{BT}	3	ℓ			
V_{WW}	2	ℓ	V_{ML}	1	ℓ
S_{ti}	1127.2	mgCOD/ℓ	X_v	3751	mgVSS/ℓ
$S_{ti,BT}$	751.5	mgCOD/ℓ	LR	0.601	mgCOD/mgVSS
Define RBCOD Area Sum:			S_{bsi} =	66.34	mgCOD/ℓ
OU =	**21.9**	mgO/ℓ	f_{ts} =	0.088	

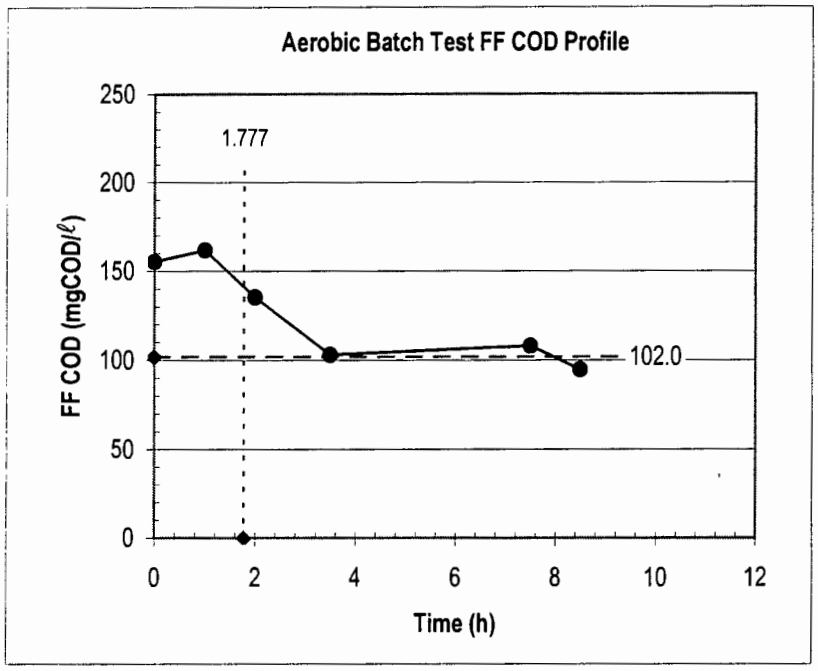

Ac COD	2852.2	mgCOD/ℓ

	Ac1	Ac2
V_{Ac} (mℓ)	75	50
V_{BT} (ℓ)	2.425	2.475
$[Ac_{COD}]_{BT}$	88.21	57.62
OU (mgO/ℓ)	**24.66**	**16.37**
$Y_{H,AE\ (COD)}$	0.720	0.716

Plot Ac Baselines:

t	Ac1	
3.544	45.58	0.2552
5.385	46.05	44.676
t	**Ac2**	
5.971	47.01	-0.1082
6.987	46.9	47.656

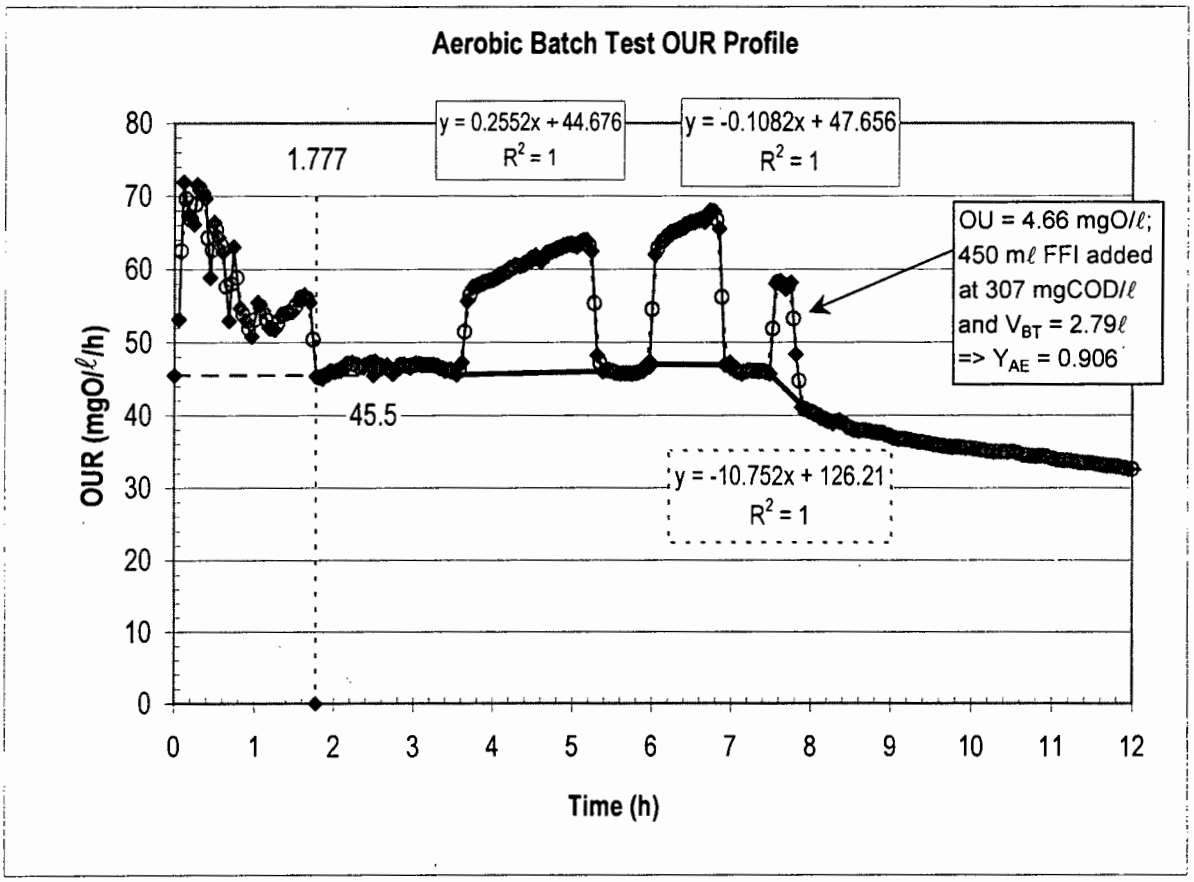

Plot end RBCOD:

t	End
1.609	0
1.609	*75*

Plot SBCOD OUR:

X_{SBCOD}	Y_{SBCOD}
0	49.5
2.5	*49.5*

	ML	SB	Date	ABT
Wastwater:	SQW	20	27.9.02	28

V_{BT}	3	ℓ			
V_{WW}	2	ℓ	V_{ML}	1	ℓ
S_{ti}	1113.2	mgCOD/ℓ	X_v	3076	mgVSS/ℓ
$S_{ti,BT}$	742.1	mgCOD/ℓ	LR	0.724	mgCOD/mgVSS
Define RBCOD Area Sum:			S_{bsi} =	70.56	mgCOD/ℓ
OU =	**23.3**	mgO/ℓ	f_{ts} =	0.095	

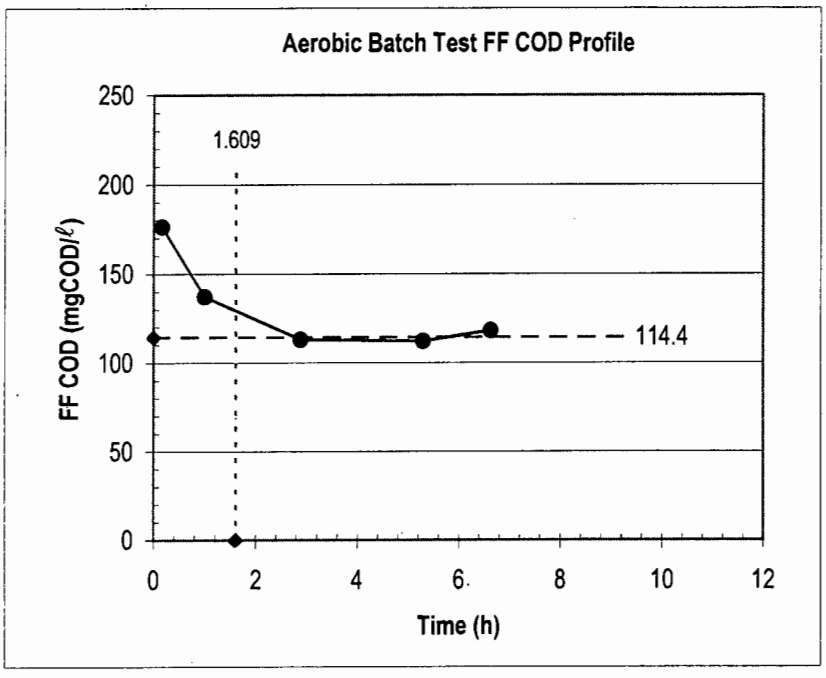

Ac COD	2946.9	mgCOD/ℓ

	Ac1	Ac2
V_{Ac} (mℓ)	75	50
V_{BT} (ℓ)	2.52	2.42
$[Ac_{COD}]_{BT}$	87.71	60.89
OU (mgO/ℓ)	**31.30**	**19.11**
$Y_{H,AE\ (COD)}$	0.643	0.686

Plot Ac Baselines:

t	Ac1	
3.341	45.62	0.2768
5.021	40.66	39.006
t	**Ac2**	
5.326	40.48	-2.9533
6.193	40.72	55.487

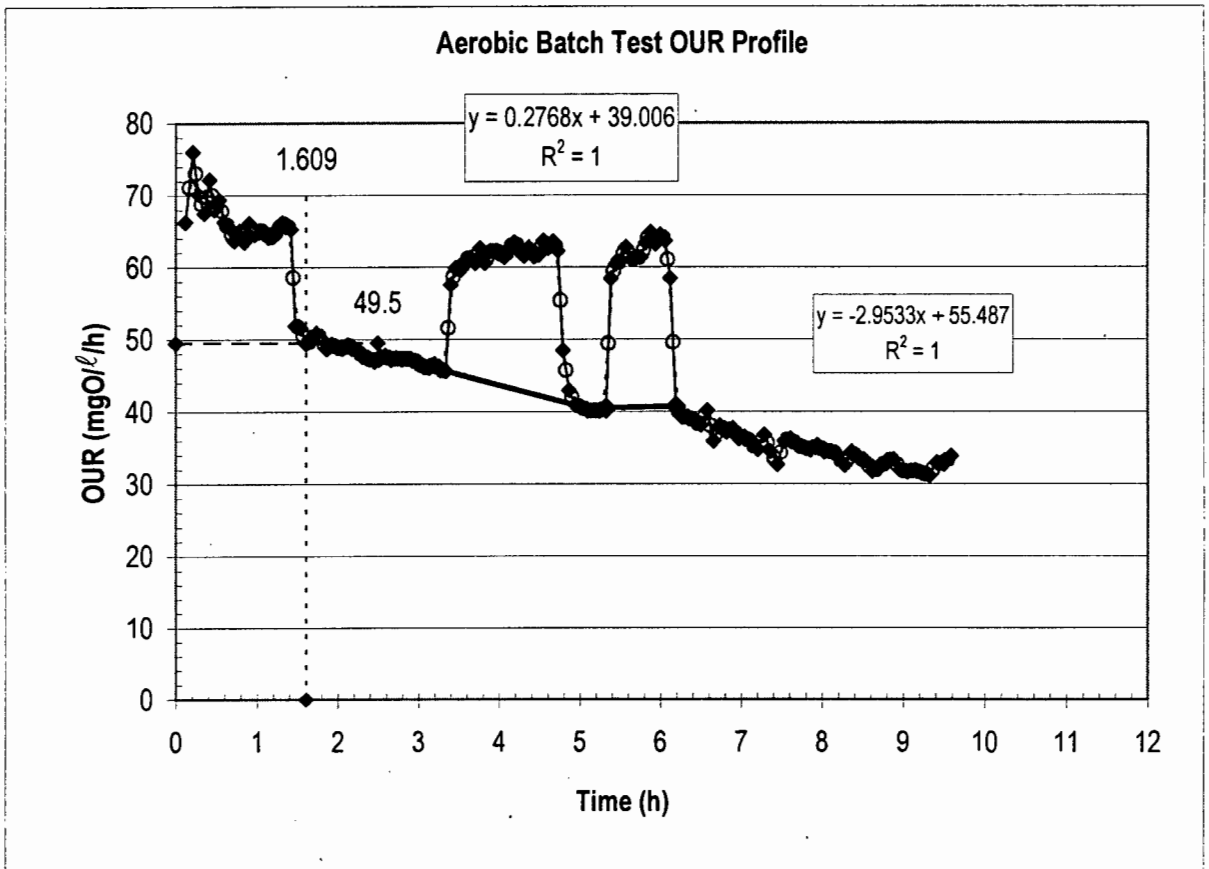

Plot end RBCOD:

t	End
1.584	0
1.584	80

Plot SBCOD OUR:

X_{SBCOD}	Y_{SBCOD}
0	45.8
8	*45.8*

	ML	SB	Date	ABT
	SQW	20	29.2.02	29

Wastwater:

V_{BT}	3	ℓ			
V_{WW}	2	ℓ	V_{ML}	1	ℓ
S_{ti}	1053	mgCOD/ℓ	X_v	2777	mgVSS/ℓ
$S_{ti,BT}$	702.0	mgCOD/ℓ	LR	0.758	mgCOD/mgVSS
Define RBCOD Area Sum:			S_{bsi} =	66.58	mgCOD/ℓ
OU =	**22.0**	mgO/ℓ	f_{ts} =	0.095	

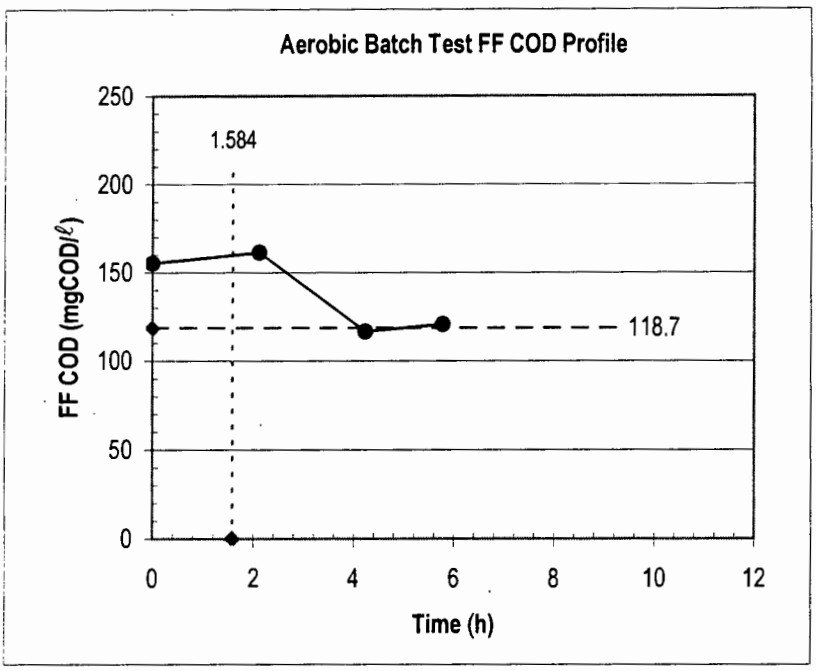

Ac COD	3019	mgCOD/ℓ
	Ac1	**Ac2**
V_{Ac} (mℓ)	75	25
V_{BT} (ℓ)	2.75	2.635
$[Ac_{COD}]_{BT}$	82.34	28.64
OU (mgO/ℓ)	**25.63**	**9.26**
$Y_{H,AE\ (COD)}$	0.689	0.677

Plot Ac Baselines:

t	Ac1	
2.134	45.12	-1
3.794	43.46	47.254
t	**Ac2**	
4.238	42.11	-0.8252
4.856	41.6	45.607

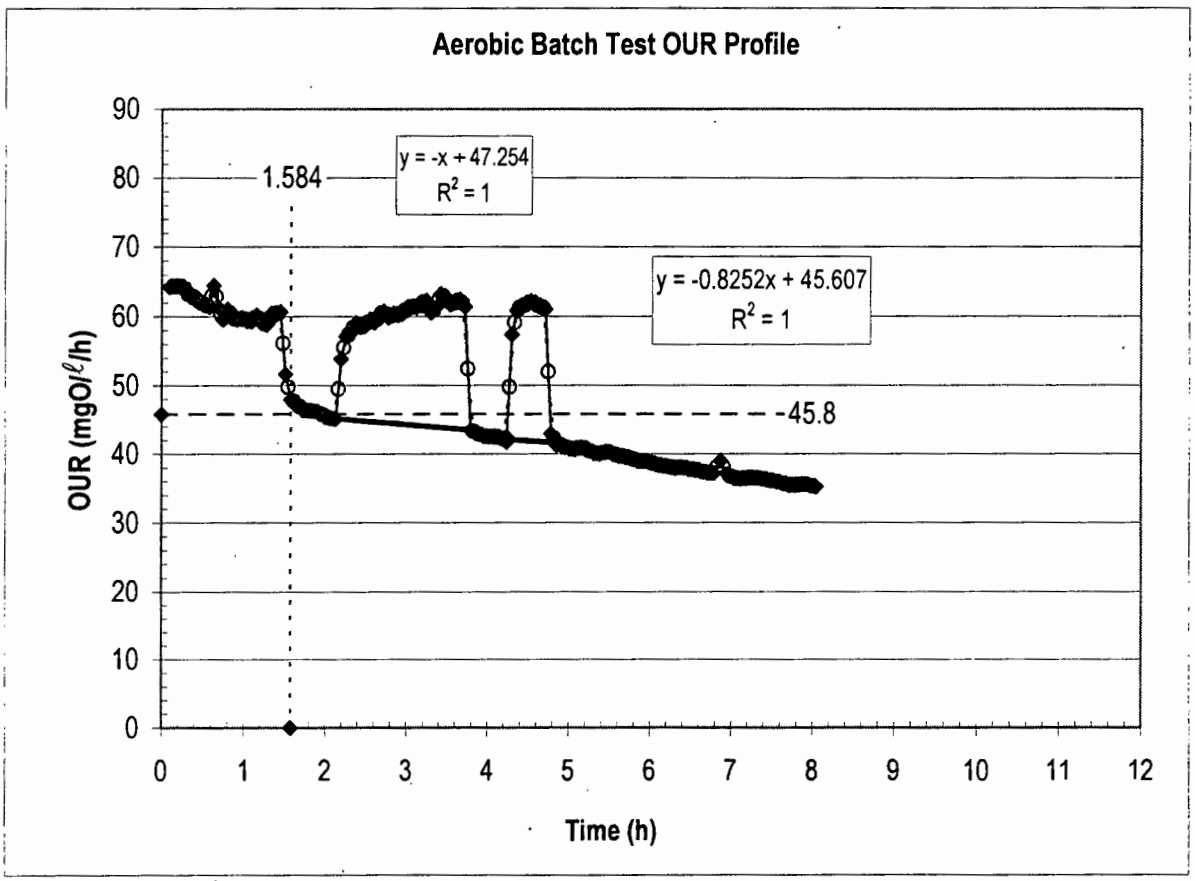

Plot end RBCOD:

t	End
2.995	0
2.995	45

Plot SBCOD OUR:

X_{SBCOD}	Y_{SBCOD}
0	NA
3.5	NA

	ML	SB	Date	ABT
	MLE	21	2.10.02	30

Wastwater:

V_{BT}	3	ℓ			
V_{WW}	2	ℓ	V_{ML}	1	ℓ
S_{ti}	1165.2	mgCOD/ℓ	X_v	2823	mgVSS/ℓ
$S_{ti,BT}$	776.8	mgCOD/ℓ	LR	0.826	mgCOD/mgVSS
Define RBCOD Area Sum:			S_{bsi} =	41.94	mgCOD/ℓ
OU =	**13.8**	mgO/ℓ	f_{ts} =	0.054	

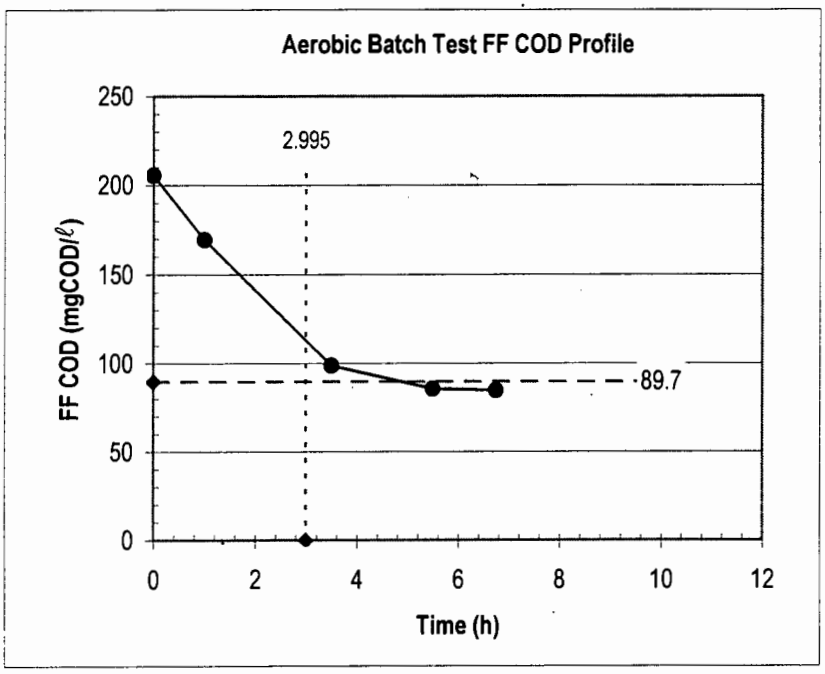

Ac COD	2790.1	mgCOD/ℓ

	Ac1	Ac2
V_{Ac} (mℓ)	50	25
V_{BT} (ℓ)	2.57	2.455
$[Ac_{COD}]_{BT}$	54.28	28.41
OU (mgO/ℓ)	**18.79**	**9.88**
$Y_{H,AE\ (COD)}$	0.654	0.652

Plot Ac Baselines:

t	Ac1	
3.522	30.53	-0.5339
5.208	29.63	32.41
t	**Ac2**	
5.525	30.97	-0.0782
6.293	30.91	31.402

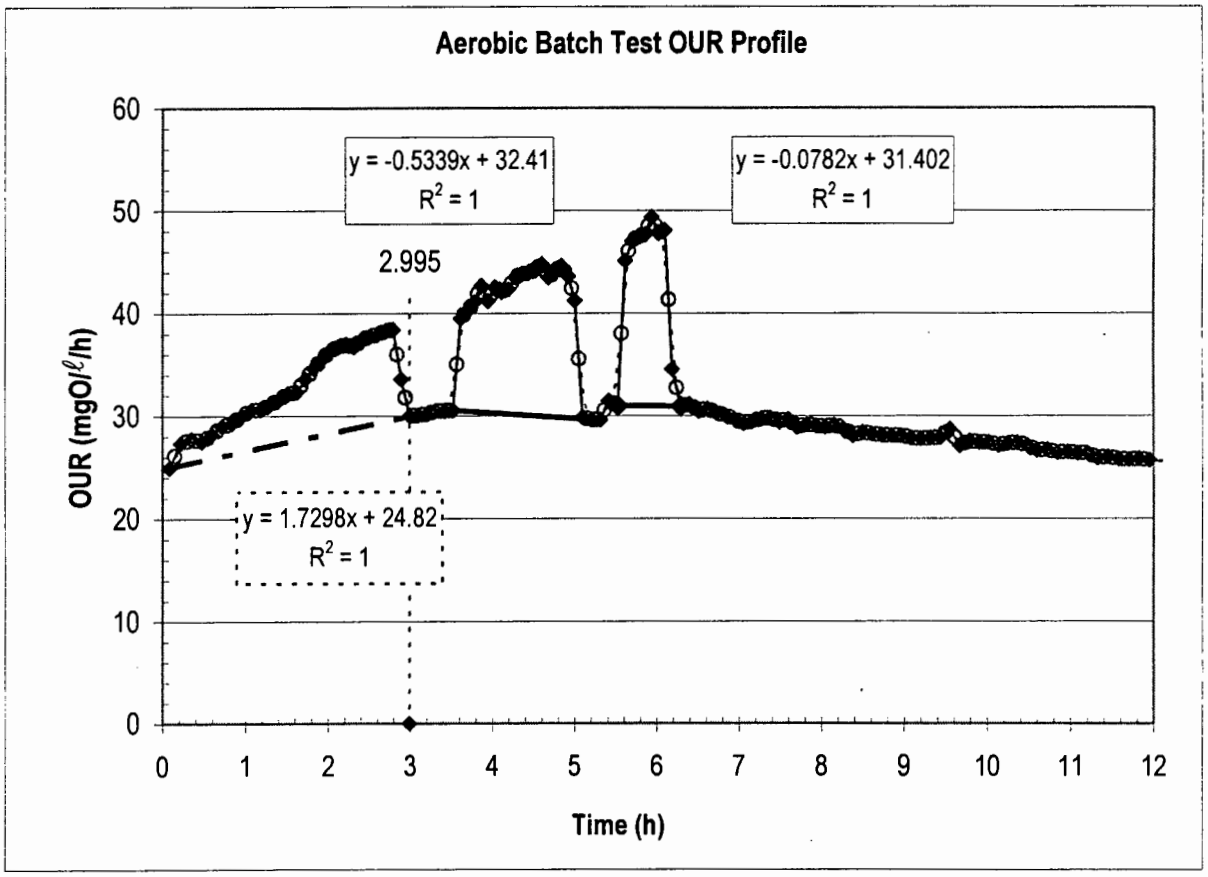

Plot end RBCOD:

t	End
2.700	0
2.700	45

Plot SBCOD OUR:

X_{SBCOD}	Y_{SBCOD}
0	NA
3.5	*NA*

	ML	SB	Date	ABT
	MLE	21	4.10.02	31

Wastewater:

V_{BT}	3	ℓ			
V_{WW}	2	ℓ	V_{ML}	1	ℓ
S_{ti}	1187.4	mgCOD/ℓ	X_v	2803	mgVSS/ℓ
$S_{ti,BT}$	791.6	mgCOD/ℓ	LR	0.847	mgCOD/mgVSS
Define RBCOD Area Sum:			S_{bsi} =	42.48	mgCOD/ℓ
OU =	**14.0**	mgO/ℓ	f_{ts} =	0.054	

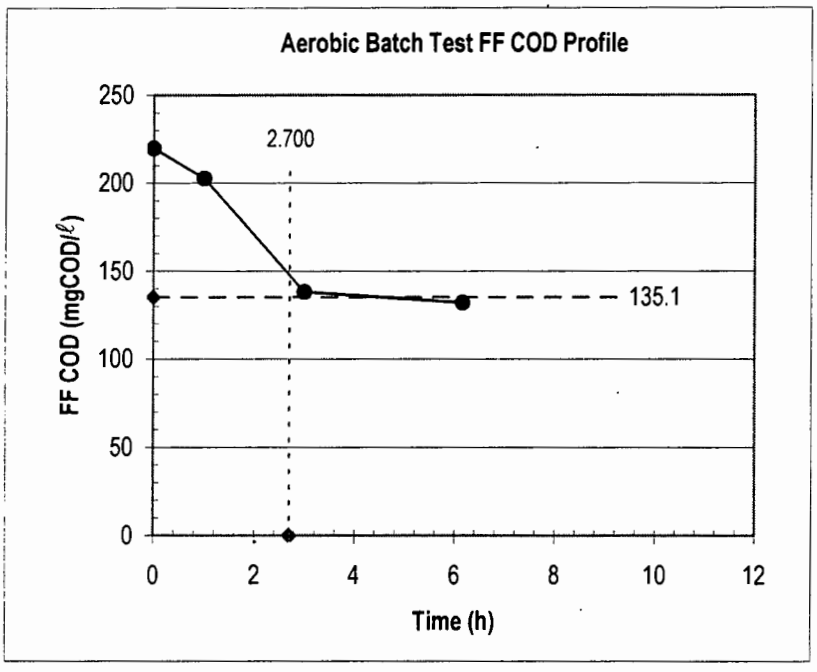

Ac COD	2752.5	mgCOD/ℓ

	Ac1	Ac2
V_{Ac} (mℓ)	50	25
V_{BT} (ℓ)	2.57	2.595
$[Ac_{COD}]_{BT}$	53.55	26.52
OU (mgO/ℓ)	**18.02**	**9.36**
$Y_{H,AE\ (COD)}$	0.663	0.647

Plot Ac Baselines:

t	Ac1	
3.239	28.8	0.9102
4.722	30.15	25.852
t	**Ac2**	
5.131	29.78	0.5931
5.873	30.22	26.737

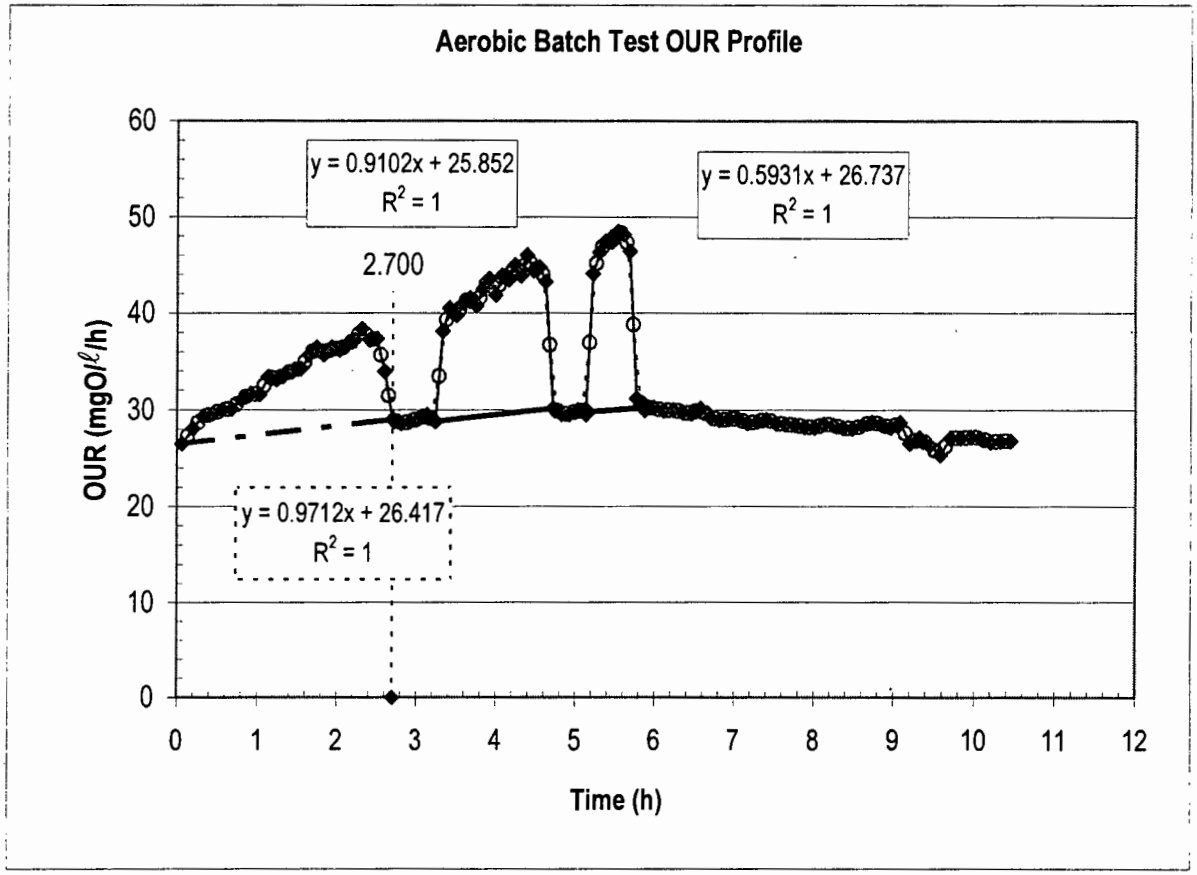

Plot end RBCOD:

t	End
1.850	0
1.850	70

Plot SBCOD OUR:

X_{SBCOD}	Y_{SBCOD}
0	37.55
2	*37.55*

	ML	SB	Date	ABT
	MLE	21	7.10.02	32

Wastwater:

V_{BT}	3	ℓ			
V_{WW}	2	ℓ	V_{ML}	1	ℓ
S_{ti}	1158.2	mgCOD/ℓ	X_v	4127	mgVSS/ℓ
$S_{ti,BT}$	772.1	mgCOD/ℓ	LR	0.561	mgCOD/mgVSS
Define RBCOD Area Sum:			S_{bsi} =	39.87	mgCOD/ℓ
OU =	**13.2**	mgO/ℓ	f_{ts} =	0.052	

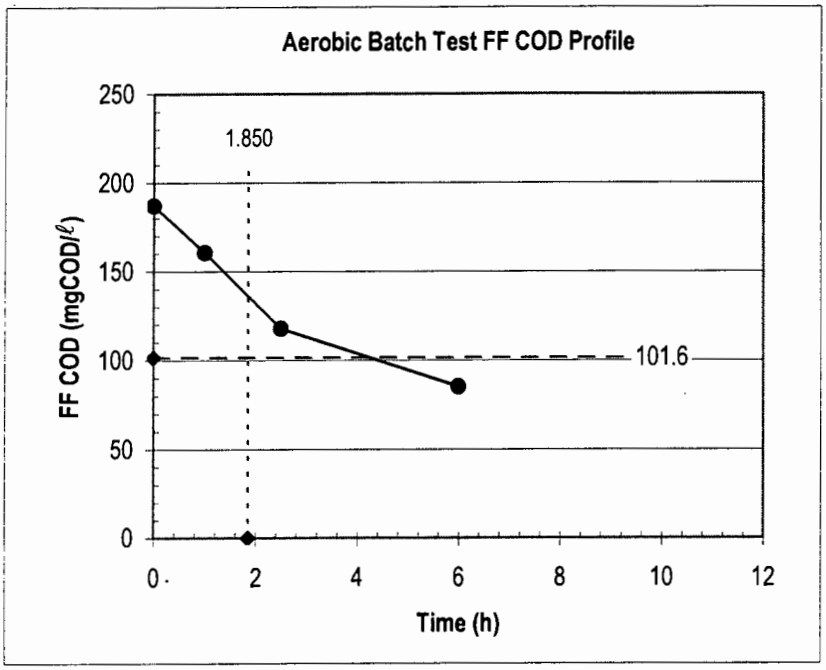

Ac COD	2706.6	mgCOD/ℓ
	Ac1	**Ac2**
V_{Ac} (mℓ)	75	50
V_{BT} (ℓ)	2.64	2.69
$[Ac_{COD}]_{BT}$	76.89	50.31
OU (mgO/ℓ)	**22.91**	**15.63**
$Y_{H,AE\ (COD)}$	0.702	0.689

Plot Ac Baselines:

t	Ac1	
2.465	37.13	3.0954
4.148	42.34	29.499
t	**Ac2**	
4.644	43.44	1.1856
5.564	44.53	37.934

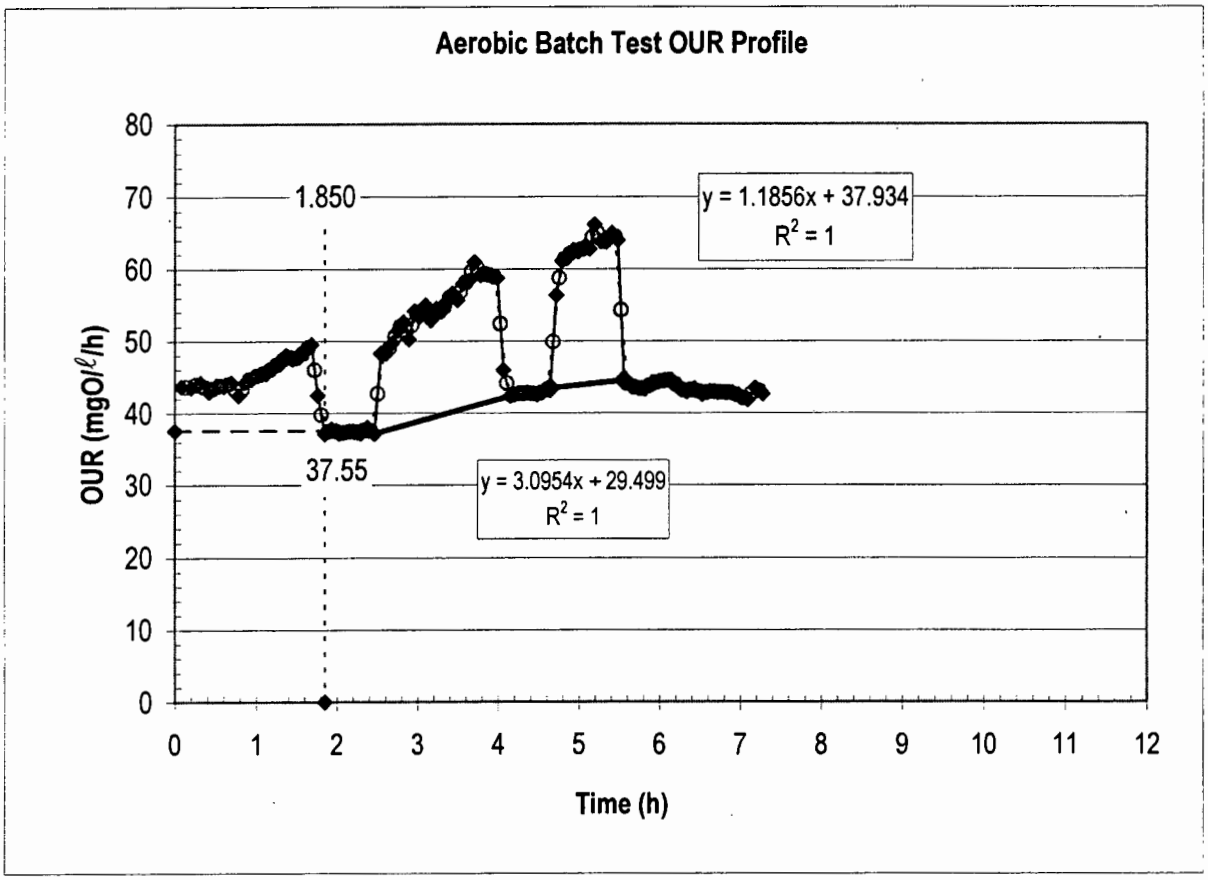

Plot end RBCOD:

t	End
1.996	0
1.996	60

Plot SBCOD OUR:

X_{SBCOD}	Y_{SBCOD}
0	33.75
2.5	*33.75*

ML	SB	Date	ABT
MLE	21	8.10.02	33

Wastwater:

V_{BT} 3 ℓ

V_{WW}	2	ℓ	V_{ML}	1	ℓ
S_{ti}	1162.3	mgCOD/ℓ	X_v	3628	mgVSS/ℓ
$S_{ti,BT}$	774.9	mgCOD/ℓ	LR	0.641	mgCOD/mgVSS
Define RBCOD Area Sum:			S_{bsi} =	44.77	mgCOD/ℓ
OU =	**14.8**	mgO/ℓ	f_{ts} =	0.058	

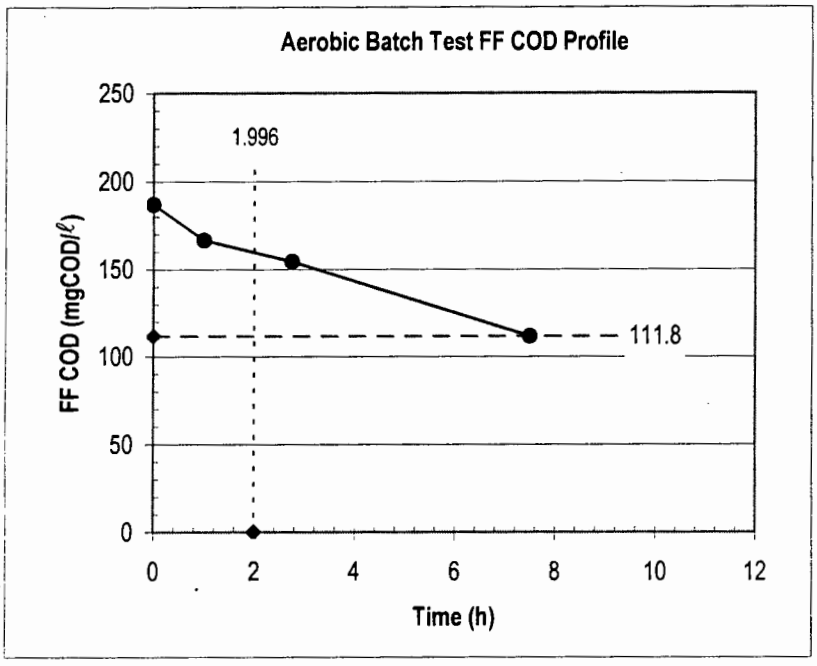

Ac COD	2783.8	mgCOD/ℓ

	Ac1	Ac2
V_{Ac} (mℓ)	75	50
V_{BT} (ℓ)	2.6	2.65
$[Ac_{COD}]_{BT}$	80.30	52.52
OU (mgO/ℓ)	**23.87**	**16.90**
$Y_{H,AE\ (COD)}$	0.703	0.678

Plot Ac Baselines:

t	Ac1	
2.748	33.45	1.1773
4.591	35.62	30.215
t	**Ac2**	
5.642	35.36	0.2797
6.786	35.68	33.782

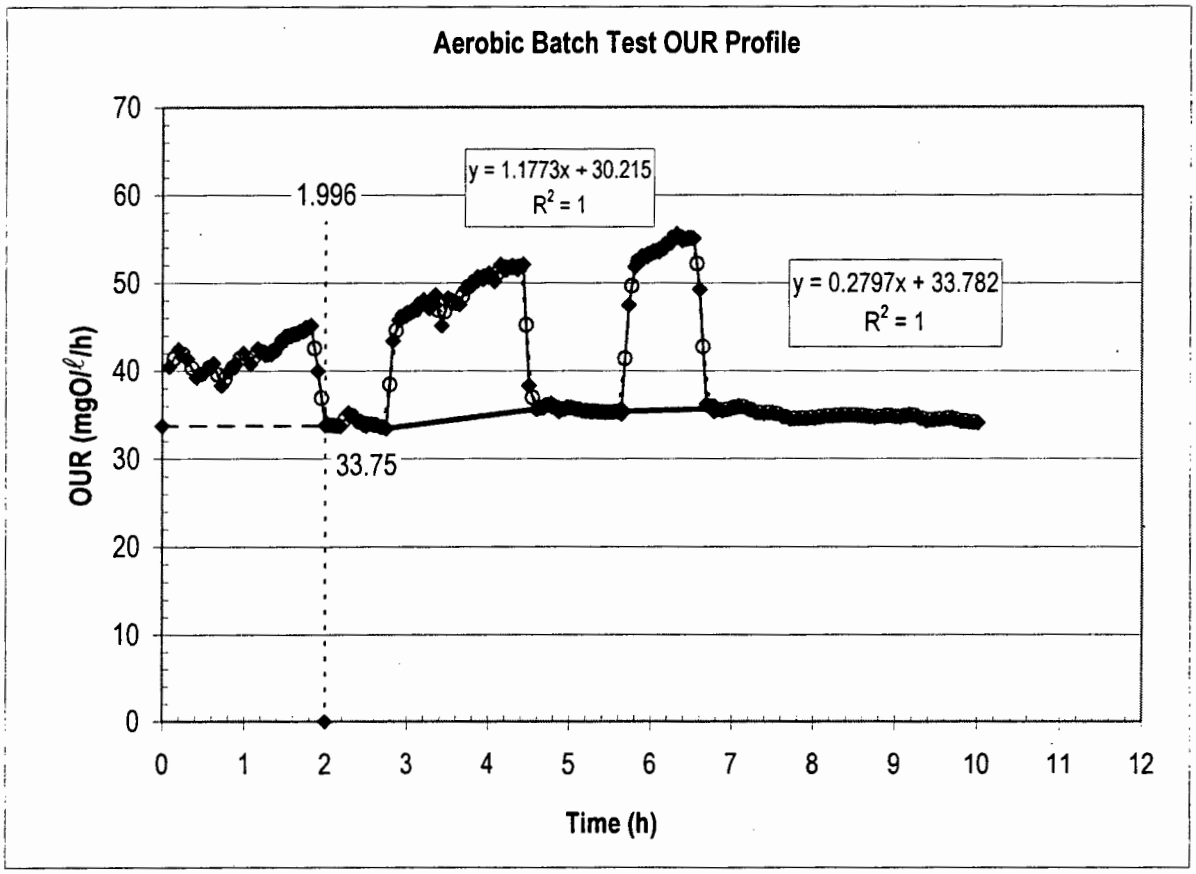

Plot end RBCOD:

t	End
2.108	0
2.108	55

Plot SBCOD OUR:

X_{SBCOD}	Y_{SBCOD}
0	31.2
2.75	*31.2*

	ML	SB	Date	ABT
	MLE	21	10.10.02	34

Wastwater:

V_{BT}	3	ℓ			
V_{WW}	2	ℓ	V_{ML}	1	ℓ
S_{ti}	1150.1	mgCOD/ℓ	X_v	3282	mgVSS/ℓ
$S_{ti,BT}$	766.7	mgCOD/ℓ	LR	0.701	mgCOD/mgVSS
Define RBCOD Area Sum:			S_{bsi} =	37.84	mgCOD/ℓ
OU =	**12.5**	mgO/ℓ	f_{ts} =	0.049	

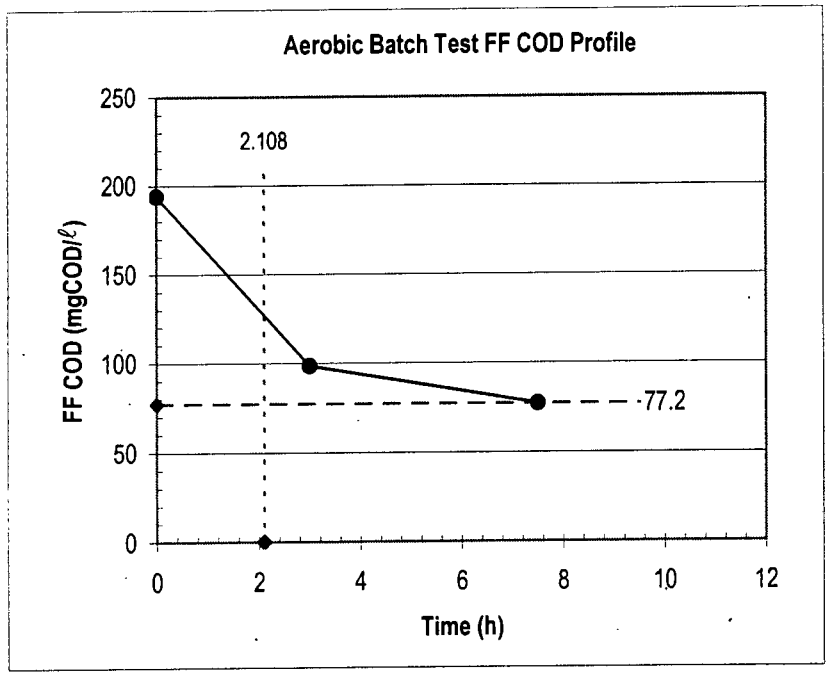

Ac COD	2812.3	mgCOD/ℓ

	Ac1	Ac2
V_{Ac} (mℓ)	75	50
V_{BT} (ℓ)	2.695	2.745
$[Ac_{COD}]_{BT}$	78.26	51.23
OU (mgO/ℓ)	**24.04**	**16.03**
$Y_{H,AE\ (COD)}$	0.693	0.687

Plot Ac Baselines:

t	Ac1	
3.399	32.82	2.5923
5.120	37.28	24.009
t	**Ac2**	
5.849	37.4	1.4252
6.769	38.71	29.064

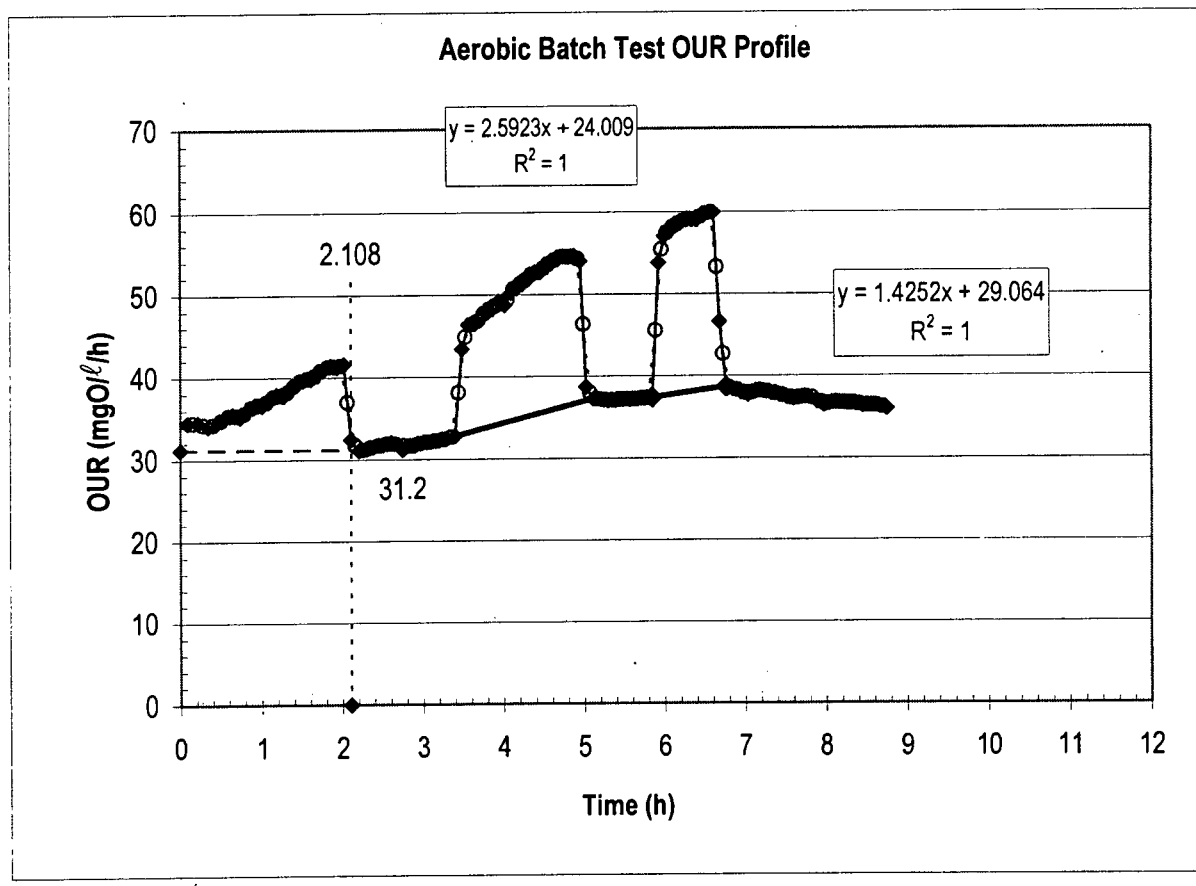

Plot end RBCOD:

t	End
2.334	0
2.334	50

Plot SBCOD OUR:

X_{SBCOD}	Y_{SBCOD}
0	28.5
2.75	*28.5*

Wastewater:

			ML	SB	Date	ABT
			MLE	22	25.10.02	35

V_{BT}	3	ℓ			
V_{WW}	2	ℓ	V_{ML}	1	ℓ
S_{ti}	1144.8	mgCOD/ℓ	X_v	2930	mgVSS/ℓ
$S_{ti,BT}$	763.2	mgCOD/ℓ	LR	0.781	mgCOD/mgVSS
Define RBCOD Area Sum:			S_{bsi} =	73.67	mgCOD/ℓ
OU =	**24.3**	mgO/ℓ	f_{ts} =	0.097	

Ac COD	2412.5	mgCOD/ℓ

	Ac1	Ac2
V_{Ac} (mℓ)	75	50
V_{BT} (ℓ)	3.115	3.165
$[Ac_{COD}]_{BT}$	58.09	38.11
OU (mgO/ℓ)	**20.82**	**12.09**
$Y_{H,AE\ (COD)}$	0.642	0.683

Plot Ac Baselines:

t	Ac1	
3.678	27.5	-0.7012
5.446	26.26	30.079
t	**Ac2**	
6.580	25.76	2.3914
7.609	28.22	10.024

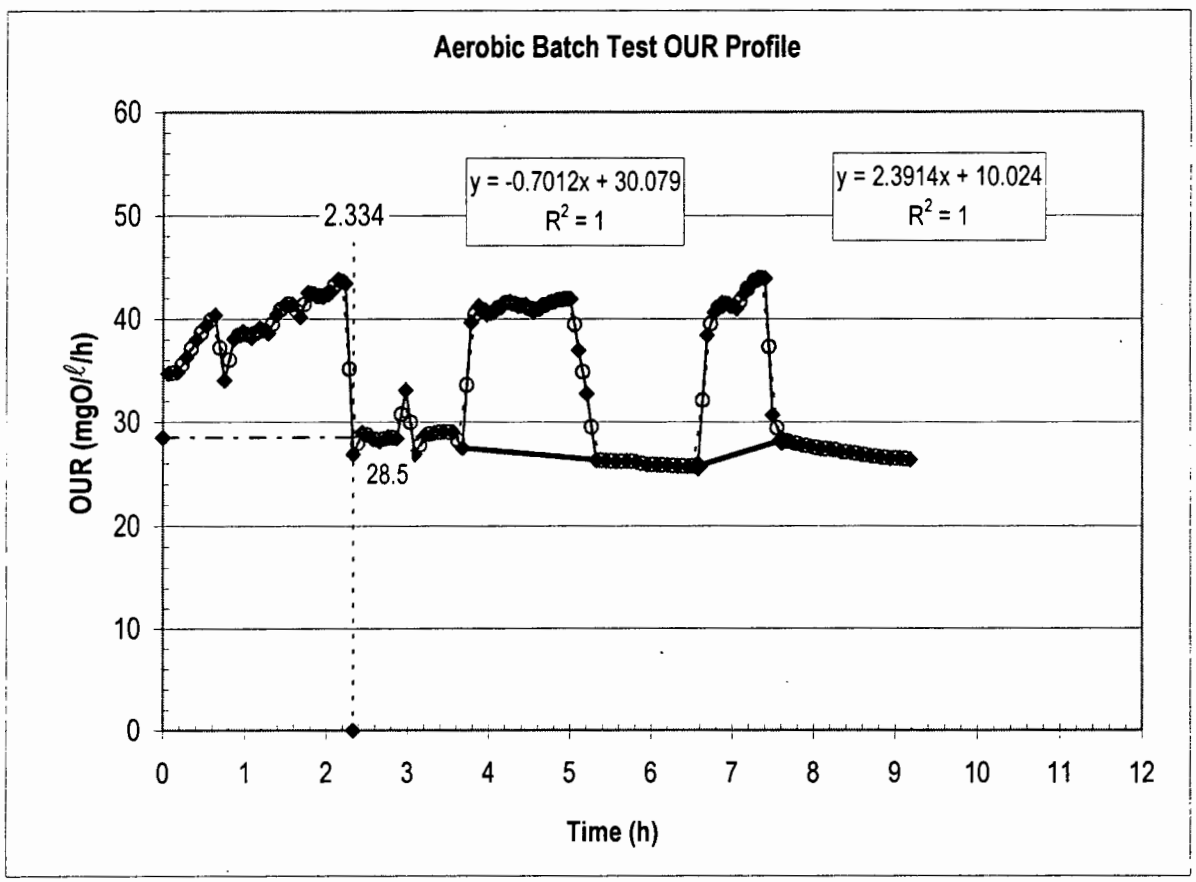

Plot end RBCOD:

t	End
2.277	0
2.277	55

Plot SBCOD OUR:

X_{SBCOD}	Y_{SBCOD}
0	32.64
2.75	32.64

	ML	SB	Date	ABT
	MLE	22	26.10.02	36

Wastwater:

V_{BT}	3	ℓ			
V_{WW}	2	ℓ	V_{ML}	1	ℓ
S_{ti}	1124.4	mgCOD/ℓ	X_v	3261	mgVSS/ℓ
$S_{ti,BT}$	749.6	mgCOD/ℓ	LR	0.690	mgCOD/mgVSS
Define RBCOD Area Sum:			S_{bsi} =	79.22	mgCOD/ℓ
OU =	**26.1**	mgO/ℓ	f_{ts} =	0.106	

Ac COD	2445.3	mgCOD/ℓ

	Ac1	Ac2
V_{Ac} (mℓ)	75	50
V_{BT} (ℓ)	3.115	3.165
$[Ac_{COD}]_{BT}$	58.88	38.63
OU (mgO/ℓ)	**19.20**	**12.03**
$Y_{H,AE\ (COD)}$	0.674	0.689

Plot Ac Baselines:

t	Ac1	
3.361	33.94	0.7749
4.729	35	31.336
t	**Ac2**	
5.446	35.04	2.2978
6.342	37.1	22.527

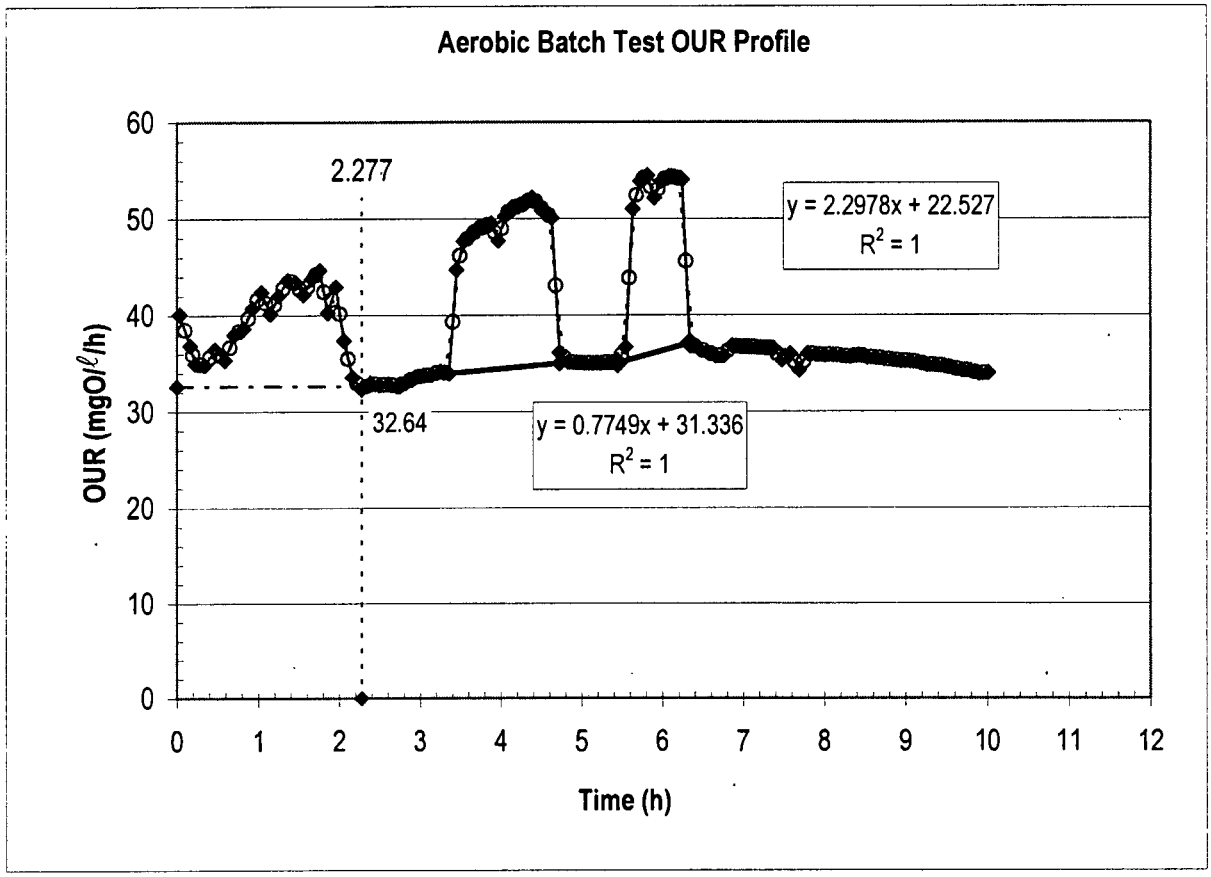

Plot end RBCOD:

t	End
3.040	0
3.040	45

Plot SBCOD OUR:

X_{SBCOD}	Y_{SBCOD}
0	NA
2	*NA*

	ML	SB	Date	ABT
Wastewater:	MLE	22	27.10.02	37

V_{BT}	3	ℓ			
V_{WW}	2	ℓ	V_{ML}	1	ℓ
S_{ti}	1110	mgCOD/ℓ	X_v	2153	mgVSS/ℓ
$S_{ti,BT}$	740.0	mgCOD/ℓ	LR	1.031	mgCOD/mgVSS
Define RBCOD Area Sum:			S_{bsi} =	24.09	mgCOD/ℓ
OU =	**8.0**	mgO/ℓ	f_{ts} =	0.033	

Ac COD	2416.6	mgCOD/ℓ

	Ac1	Ac2
V_{Ac} (mℓ)	75	50
V_{BT} (ℓ)	3.115	3.165
$[Ac_{COD}]_{BT}$	58.18	38.18
OU (mgO/ℓ)	**21.93**	**16.25**
$Y_{H,AE\ (COD)}$	0.623	0.574

Plot Ac Baselines:

t	Ac1	
3.601	26.82	-1.3982
5.453	24.23	31.855
t	**Ac2**	
6.086	26.25	0.3314
7.143	26.6	24.233

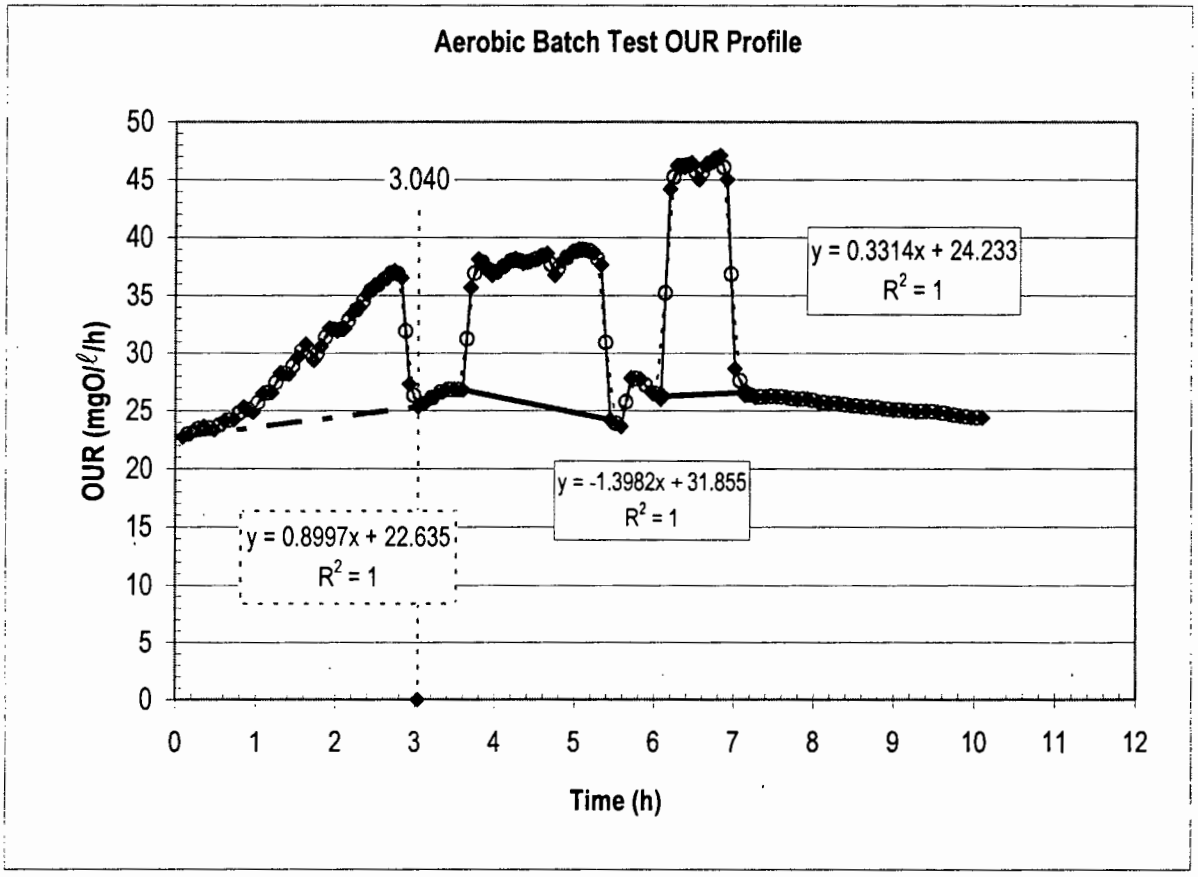

Plot end RBCOD:

t	End
2.155	0
2.155	55

Plot SBCOD OUR:

X_{SBCOD}	Y_{SBCOD}
0	36.4
12	*36.4*

	ML	SB	Date	ABT
Wastewater:	MLE	23	4.11.02	38

V_{BT}	3	ℓ			
V_{WW}	2	ℓ	V_{ML}	1	ℓ
S_{ti}	1143	mgCOD/ℓ	X_v	3078	mgVSS/ℓ
$S_{ti,BT}$	762.0	mgCOD/ℓ	LR	0.743	mgCOD/mgVSS
Define RBCOD Area Sum:			S_{bsi} =	47.71	mgCOD/ℓ
OU =	**15.7**	mgO/ℓ	f_{ts} =	0.063	

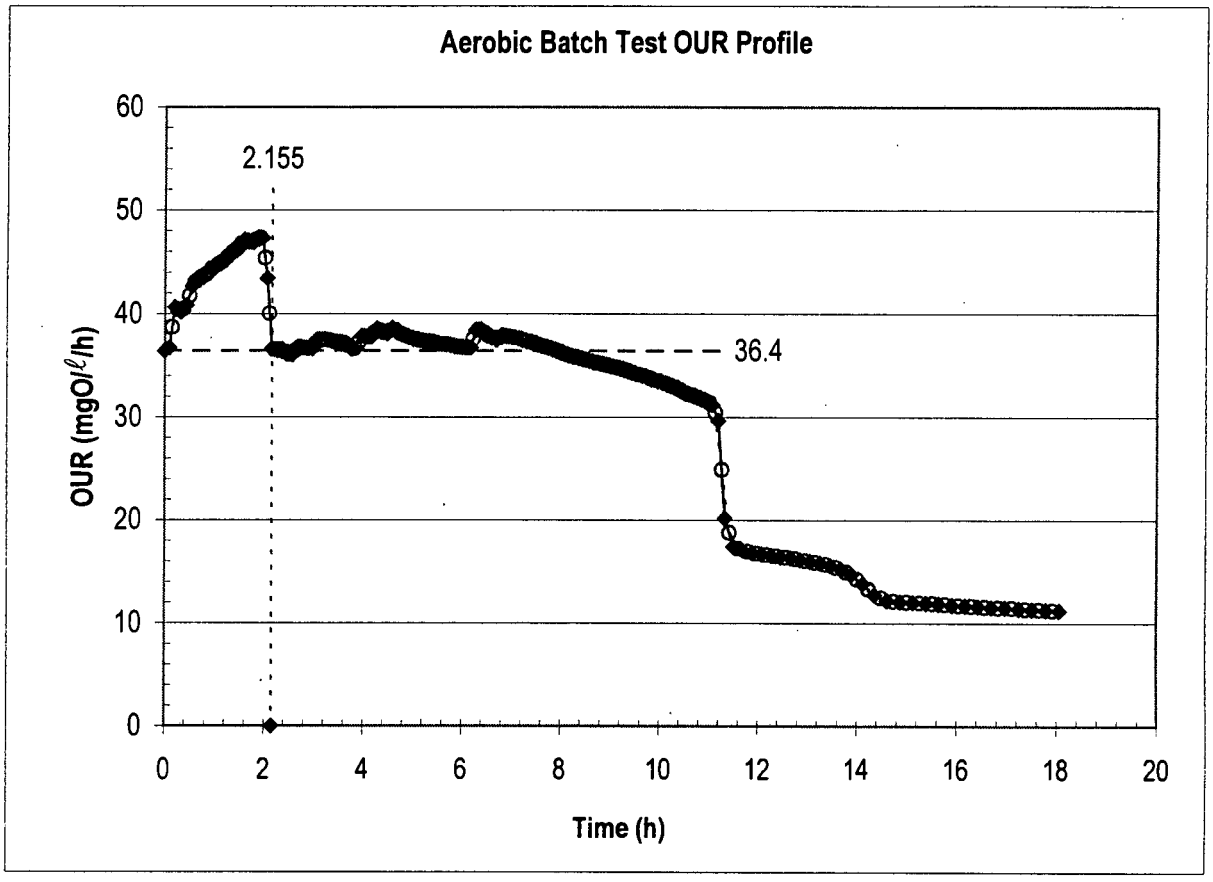

Plot end RBCOD:

t	End
2.117	0
2.117	55

Plot SBCOD OUR:

X_{SBCOD}	Y_{SBCOD}
0	36.375
2.5	*36.375*

Wastewater Batch Test:

	ML	SB	Date	ABT
	MLE	23	6.11.02	39

V_{BT}	3	ℓ			
V_{WW}	2	ℓ	V_{ML}	1	ℓ
S_{ti}	1188.1	mgCOD/ℓ	X_v	3595	mgVSS/ℓ
$S_{ti,BT}$	792.1	mgCOD/ℓ	LR	0.661	mgCOD/mgVSS
Define RBCOD Area Sum:			S_{bsi} =	36.15	mgCOD/ℓ
OU =	**11.9**	mgO/ℓ	f_{ts} =	0.046	

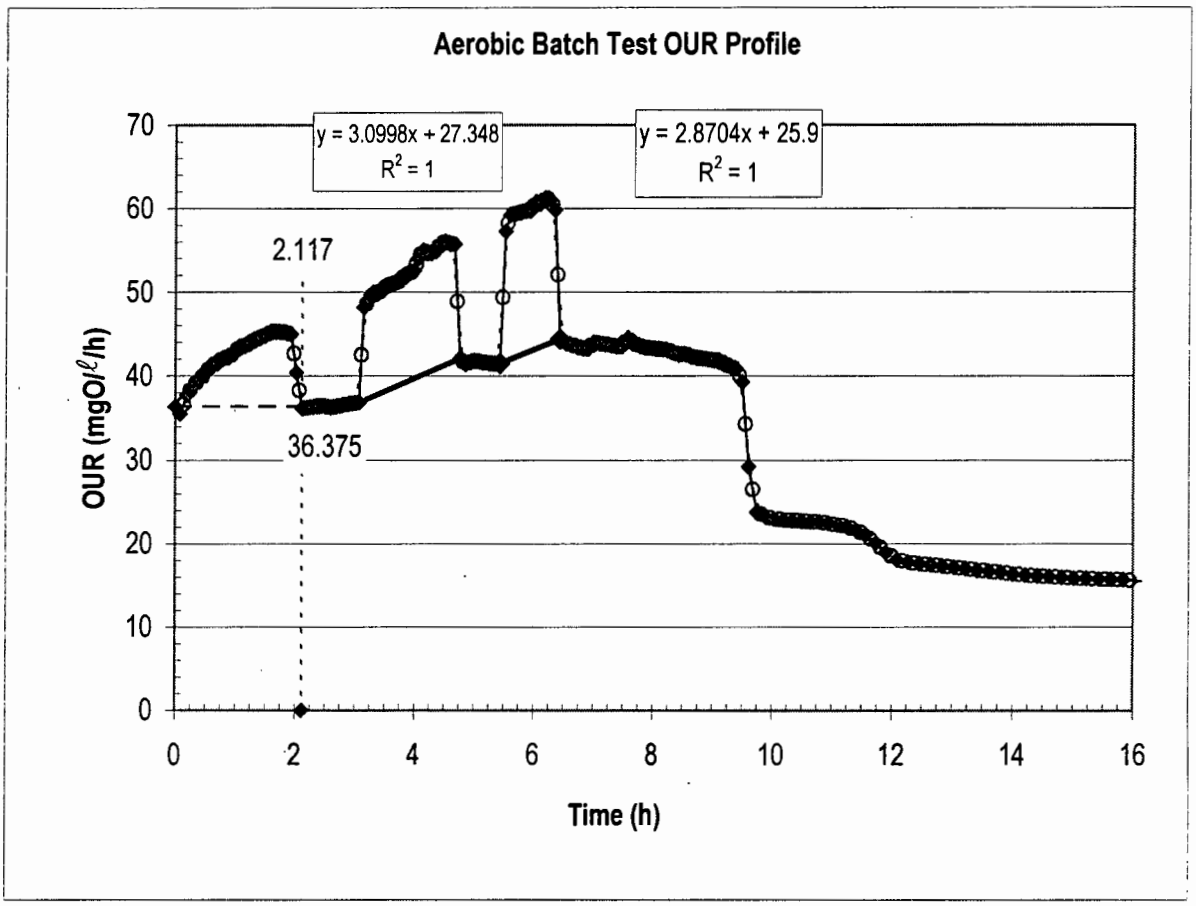

Acetate Addition:

Ac COD	2919.9	mgCOD/ℓ
	Ac1	**Ac2**
V_{Ac} (mℓ)	75	50
V_{BT} (ℓ)	2.86	2.86
$[Ac_{COD}]_{BT}$	76.57	51.05
OU (mgO/ℓ)	**20.52**	**15.16**
$Y_{H,AE\ (COD)}$	0.732	0.703

Plot Ac Baselines:

t	Ac1		
3.069	36.86	3.0998	mAc1
4.762	42.11	27.348	cAc1
t	**Ac2**		
5.435	41.5	2.8704	mAc2
6.442	44.39	25.9	cAc2

Plot end RBCOD:

t	End
3.069	0
3.069	45

Plot SBCOD OUR:

X_{SBCOD}	Y_{SBCOD}
0	28.5
3.75	*28.5*

Wastwater:

			ML	SB	Date	ABT
			MLE	23	7.11.02	40

V_{BT}	3	ℓ			
V_{WW}	2	ℓ	V_{ML}	1	ℓ
S_{ti}	1116.3	mgCOD/ℓ	X_v	2303	mgVSS/ℓ
$S_{ti,BT}$	744.2	mgCOD/ℓ	LR	0.969	mgCOD/mgVSS
Define RBCOD Area Sum:			S_{bsi} =	38.68	mgCOD/ℓ
OU =	**12.8**	mgO/ℓ	f_{ts} =	0.052	

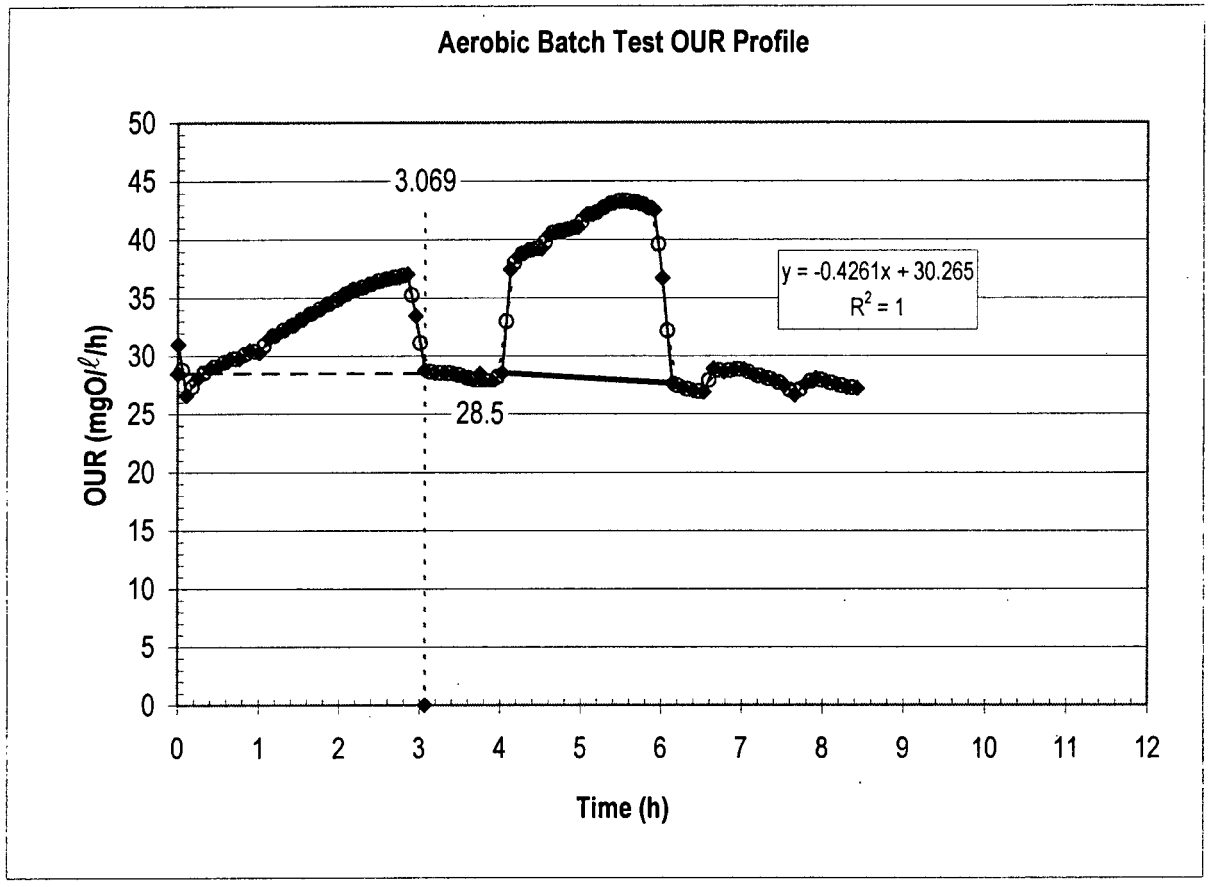

Acetate Addition:

Ac COD	2963.1	mgCOD/ℓ
	Ac1	**Ac2**
V_{Ac} (mℓ)	75	
V_{BT} (ℓ)	2.85	
$[Ac_{COD}]_{BT}$	77.98	
OU (mgO/ℓ)	**25.93**	
$Y_{H,AE\ (COD)}$	0.667	

Plot Ac Baselines:

t	Ac1		
4.025	28.55	-0.4261	mAc1
6.137	27.65	30.265	cAc1
t	**Ac2**		
			mAc2
			cAc2

APPENDIX C-3

ANOXIC (DENITRIFICATION) BATCH TEST DATA

SB	Date	DBT
4	17.1.02	1

Batch Test Composition:

			V_{BT}	3	ℓ
V_{WW}	2.7	ℓ	V_{ML}	0.3	ℓ
S_{ti}	480	mgCOD/ℓ	X_v	3347	mgVSS/ℓ
$S_{ti,BT}$	432.0	mgCOD/ℓ	LR	1.291	mgCOD/mgVSS

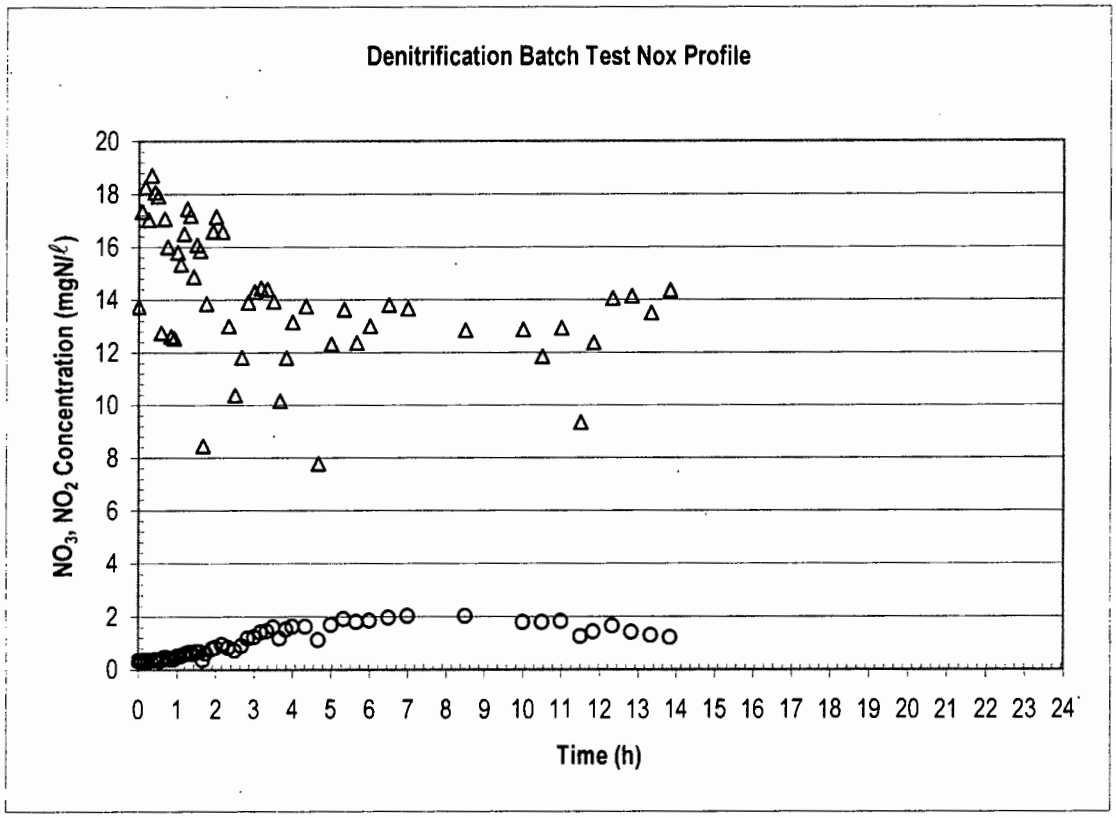

SB	Date	DBT
4	22.1.02	2

Batch Test Composition:

			V_{BT}	3	ℓ
V_{WW}	2.7	ℓ	V_{ML}	0.3	ℓ
S_{ti}	528	mgCOD/ℓ	X_v	3188	mgVSS/ℓ
$S_{ti,BT}$	475.2	mgCOD/ℓ	LR	1.491	mgCOD/mgVSS

Plot K1 End Time:

End Time	Y (K1 End)
1.9	0.00
1.9	*25.00*

Plot K1-NO2 Max:

X Range	Y (NO2)
0	4.8
12.5	*4.8*

Define NU (mgNO$_3$-N/ℓ):

	Y-int
K1	26.926
K2	20.468
ΔNO_3	6.458

NO_2-Corrected NU = **3.578** mgN/ℓ

S_{bsi} (0.67) =	31.01	mgCOD/ℓ
f_{ts} =	0.065	

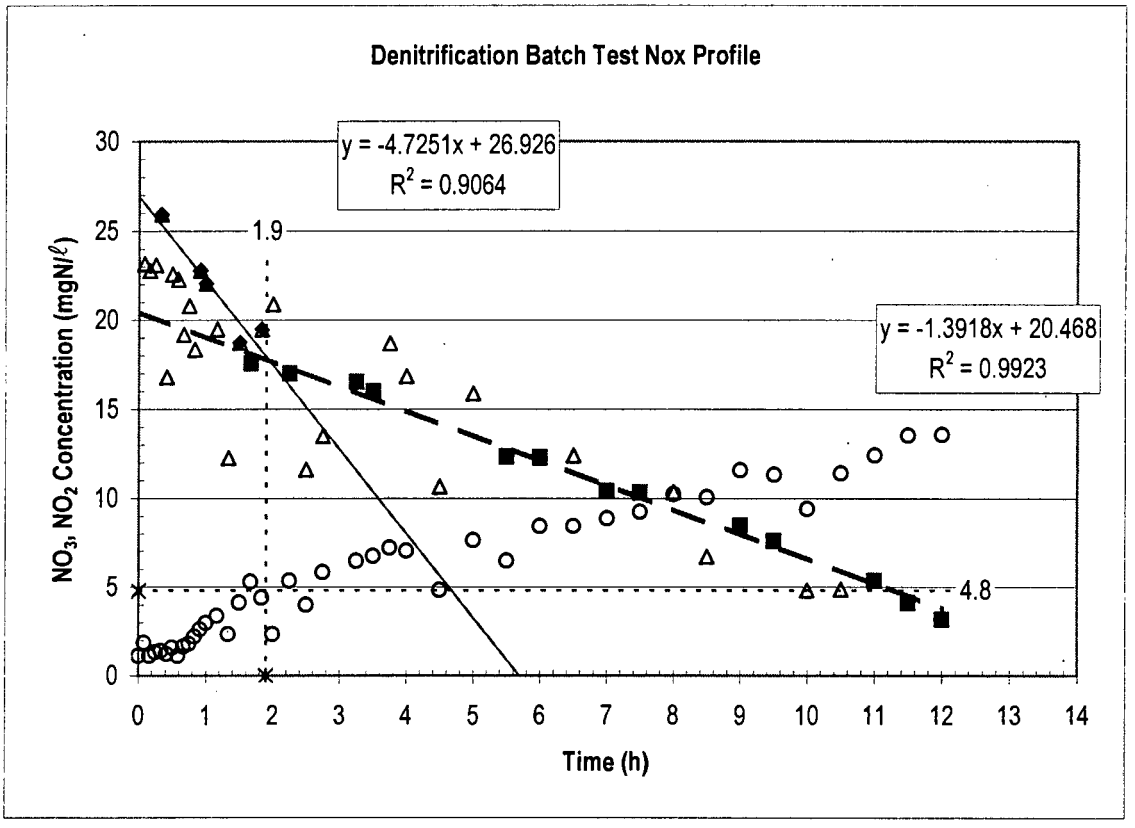

SB	Date	DBT
6	24.2.02	3

Batch Test Composition:

			V_{BT}	3	ℓ
V_{WW}	2.7	ℓ	V_{ML}	0.3	ℓ
S_{ti}	245	mgCOD/ℓ	X_v	2497	mgVSS/ℓ
$S_{ti,BT}$	220.5	mgCOD/ℓ	LR	0.883	mgCOD/mgVSS

Plot K1 End Time:

End Time	Y (K1 End)
1.1	0.00
1.1	12.00

Plot K1-NO2 Max:

X Range	Y (NO2)
0	0.95
6	*0.95*

Define NU (mgNO$_3$-N/ℓ):

	Y-int
K1	13.359
K2	10.542
ΔNO_3	2.817

NO_2-Corrected NU = **2.247** mgN/ℓ

S_{bsi} (0.67) =	19.47	mgCOD/ℓ
f_{ts} =	0.088	

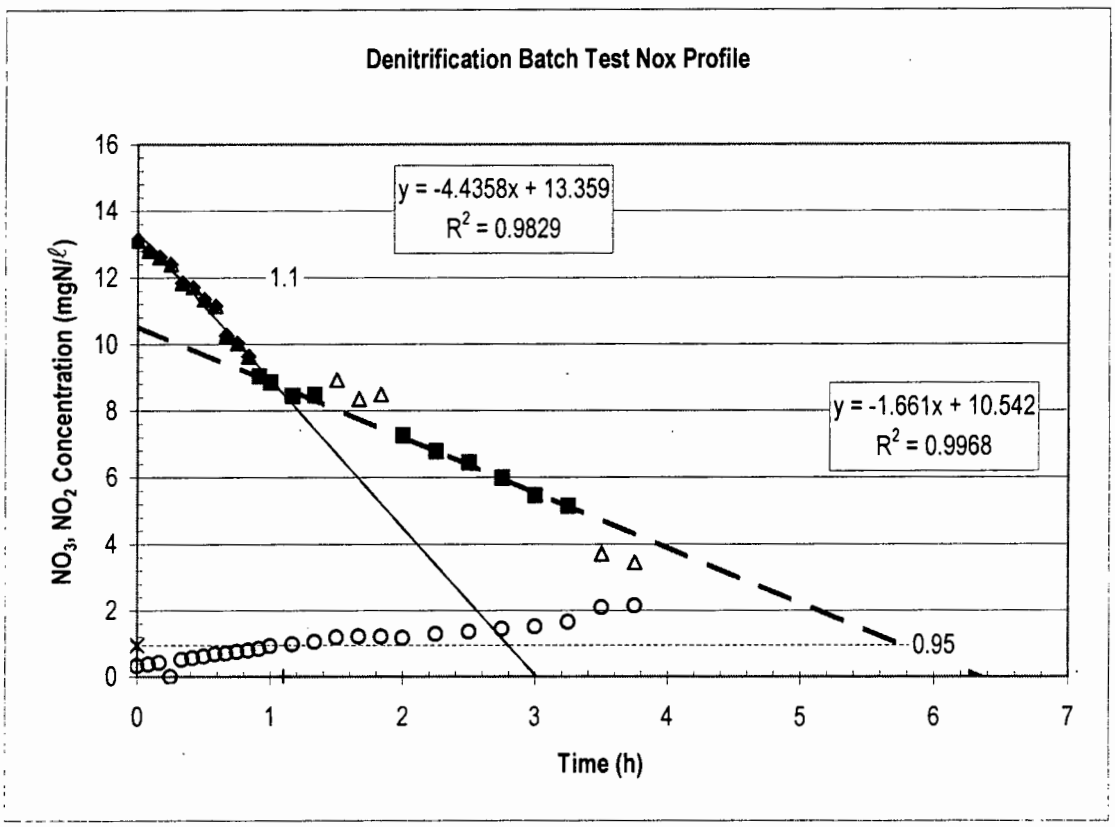

SB	Date	DBT
6	25.2.02	4

Batch Test Composition:

V_{WW}	2.55	ℓ	V_{BT}	3	ℓ
S_{ti}	1072	mgCOD/ℓ	V_{ML}	0.45	ℓ
$S_{ti,BT}$	911.2	mgCOD/ℓ	X_v	2424	mgVSS/ℓ
			LR	2.506	mgCOD/mgVSS

Plot K1 End Time:

End Time	Y (K1 End)
0.9	0.00
0.9	15.00

Plot K1-NO2 Max:

X Range	Y (NO2)
0	1.6
7.5	*1.6*

Define NU (mgNO$_3$-N/ℓ):

	Y-int
K1	15.864
K2	12.346
ΔNO$_3$	*3.518*

NO_2-Corrected NU = **2.558** mgN/ℓ

S_{bsi} (0.67) =	22.17	mgCOD/ℓ
f_{ts} =	0.024	

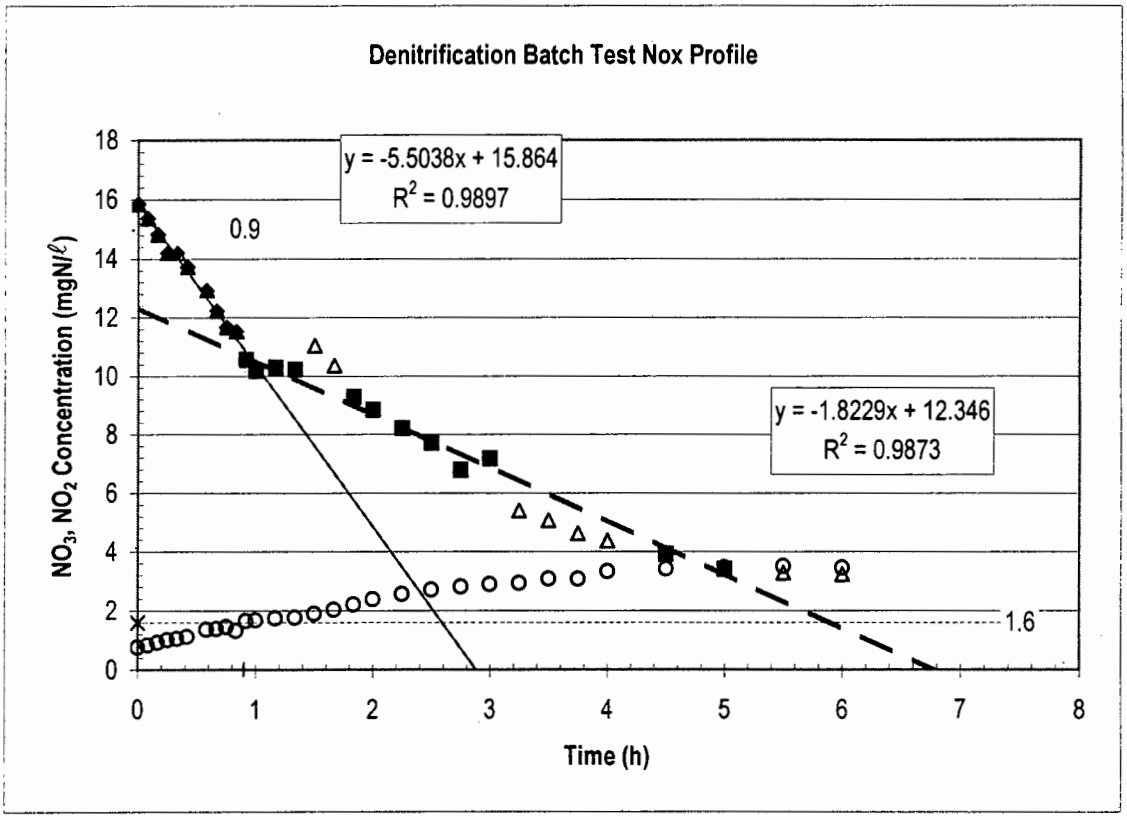

SB	Date	DBT
6	26.2.02	5

Batch Test Composition:

V_{WW}	0.815	ℓ	V_{ML}	0.685	ℓ
S_{ti}	1072	mgCOD/ℓ	X_v	2505	mgVSS/ℓ
$S_{ti,BT}$	291.2	mgCOD/ℓ	LR	0.509	mgCOD/mgVSS

V_{BT} 3 ℓ

Plot K1 End Time:

End Time	Y (K1 End)

Plot K1-NO2 Max:

X Range	Y (NO2)

Define NU (mgNO$_3$-N/ℓ):

Y-int

K1

K2

ΔNO_3

NO_2-Corrected NU = mgN/ℓ

S_{bsi} (0.67) =	mgCOD/ℓ
f_{ts} =	

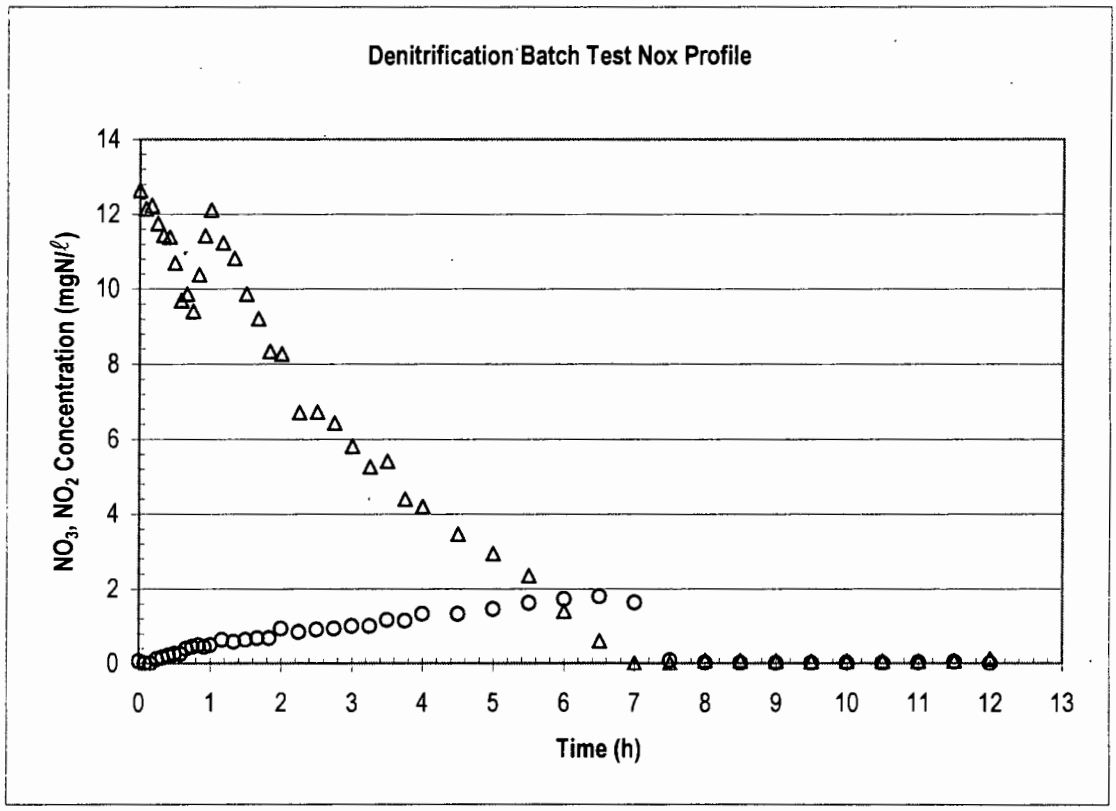

SB	Date	DBT
6	27.2.02	6

Batch Test Composition:

			V_{BT}	3	ℓ
V_{WW}	1.63	ℓ	V_{ML}	1.37	ℓ
S_{ti}	980	mgCOD/ℓ	X_v	2587	mgVSS/ℓ
$S_{ti,BT}$	532.5	mgCOD/ℓ	LR	0.451	mgCOD/mgVSS

Plot K1 End Time:

End Time	Y (K1 End)
0	0.00
0	0.00

Plot K1-NO2 Max:

X Range	Y (NO2)
0	0
12	*0*

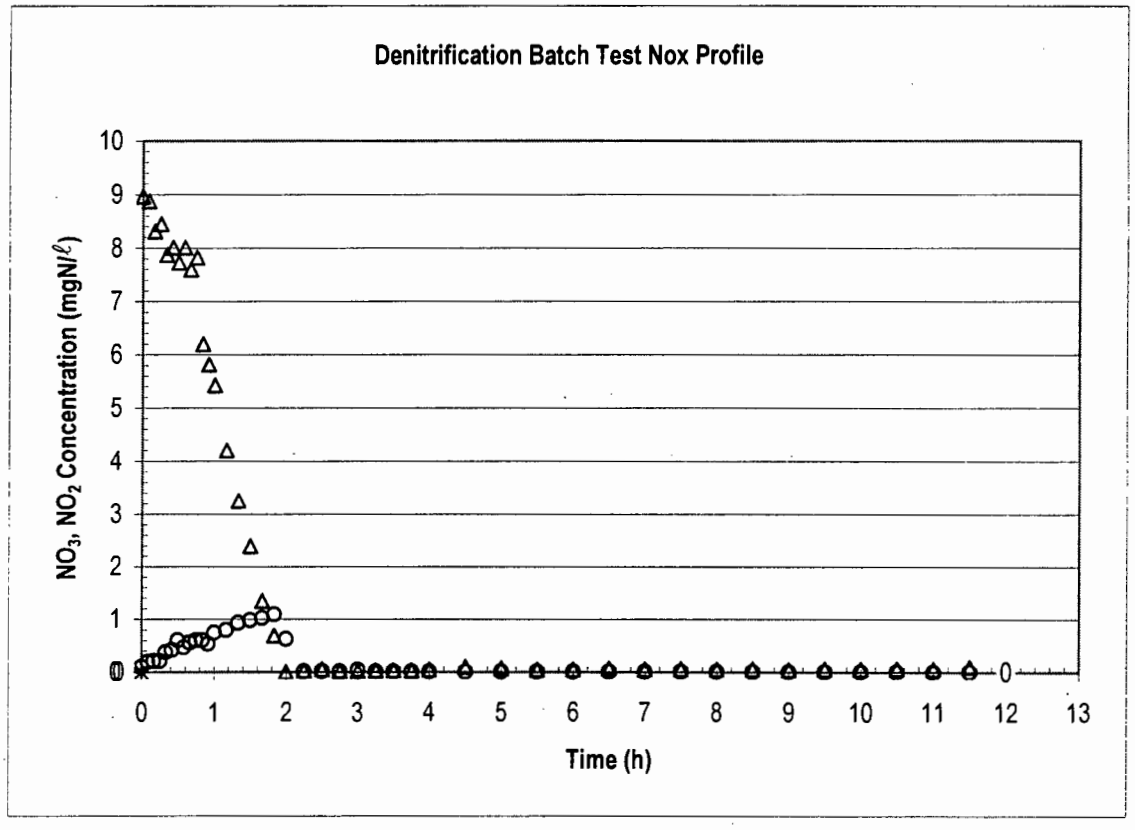

SB	Date	DBT
6	7.3.02	7

Batch Test Composition:

			V_{BT}	3	ℓ
V_{WW}	2	ℓ	V_{ML}	1	ℓ
S_{ti}	871	mgCOD/ℓ	X_v	4288	mgVSS/ℓ
$S_{ti,BT}$	580.7	mgCOD/ℓ	LR	0.406	mgCOD/mgVSS

Plot K1 End Time:

End Time	Y (K1 End)
0	0.00
0	0.00

Plot K1-NO2 Max:

X Range	Y (NO2)
0	0
12	*0*

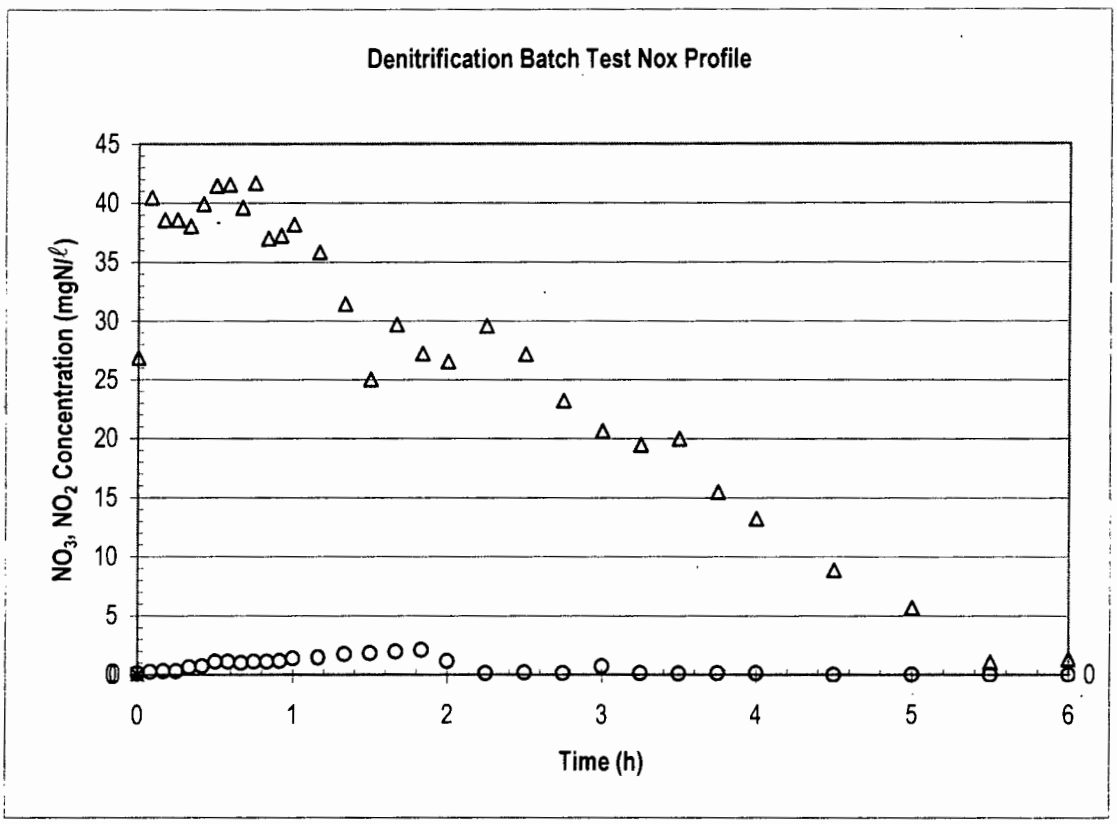

ML	SB	Date	DBT
LML	9	4.4.2	8

Batch Test Composition:

V_{WW}	2	ℓ	V_{ML}	1	ℓ
S_{ti}	892.5	mgCOD/ℓ	X_v	4109	mgVSS/ℓ
$S_{ti,BT}$	595.0	mgCOD/ℓ	LR	0.434	mgCOD/mgVSS

V_{BT} 3 ℓ

Plot K1 End Time:

End Time	Y (K1 End)

Plot K1-NO2 Max:

X Range	Y (NO2)

Define NU (mgNO$_3$-N/ℓ):

Y-int

K1

K2

ΔNO_3

NO_2-Corrected NU = mgN/ℓ

S_{bsi} (0.67) =	mgCOD/ℓ
f_{ts} =	

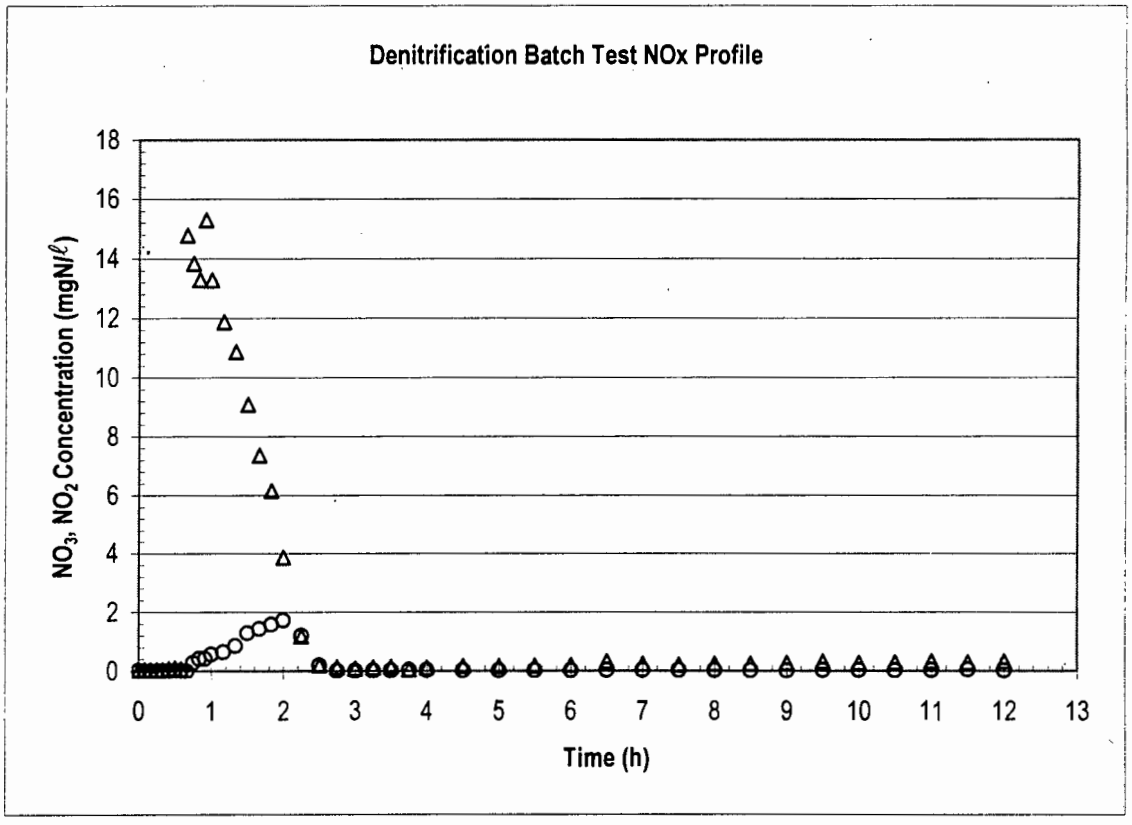

ML	SB	Date	DBT
LML	9	9.4.02	9

Batch Test Composition:

V_{WW}	2	ℓ	V_{ML}	1	ℓ
S_{ti}	917.5	mgCOD/ℓ	X_v	4061	mgVSS/ℓ
$S_{ti,BT}$	611.7	mgCOD/ℓ	LR	0.452	mgCOD/mgVSS
			V_{BT}	3	ℓ

Plot K1 End Time:

End Time	Y (K1 End)

Plot K1-NO2 Max:

X Range	Y (NO2)

Define NU (mgNO$_3$-N/ℓ):

	Y-int
K1	
K2	
ΔNO_3	

NO_2-Corrected NU = mgN/ℓ

S_{bsi} (0.67) =	mgCOD/ℓ
f_{ts} =	

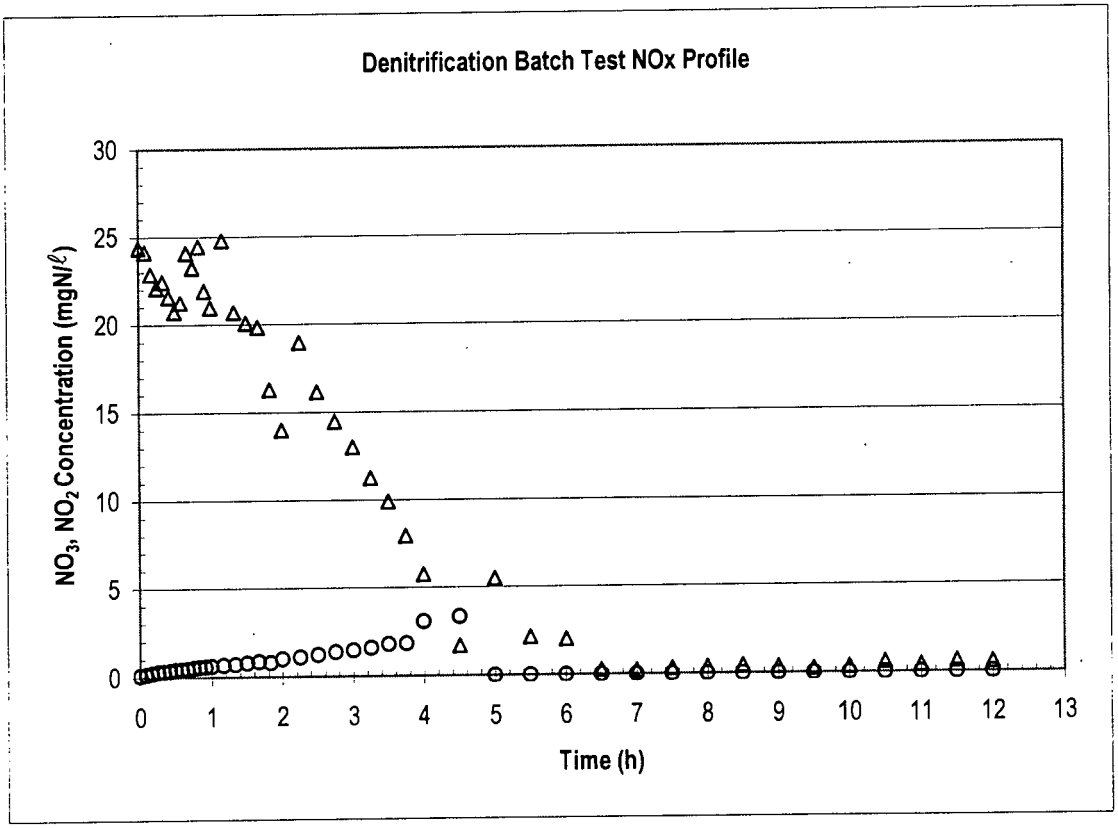

ML	SB	Date	DBT
LML	9	15.4.02	10

Batch Test Composition:

V_{WW}	2	ℓ	V_{ML}	1	ℓ
S_{ti}	845.3	mgCOD/ℓ	X_v	4153	mgVSS/ℓ
$S_{ti,BT}$	563.5	mgCOD/ℓ	LR	0.407	mgCOD/mgVSS

V_{BT} = 3 ℓ

Plot K1 End Time:

End Time	Y (K1 End)

Plot K1-NO2 Max:

X Range	Y (NO2)

Define NU (mgNO$_3$-N/ℓ):

Y-int

K1

K2

ΔNO_3

NO_2-Corrected NU = mgN/ℓ

S_{bsi} (0.67) =	mgCOD/ℓ
f_{ts} =	

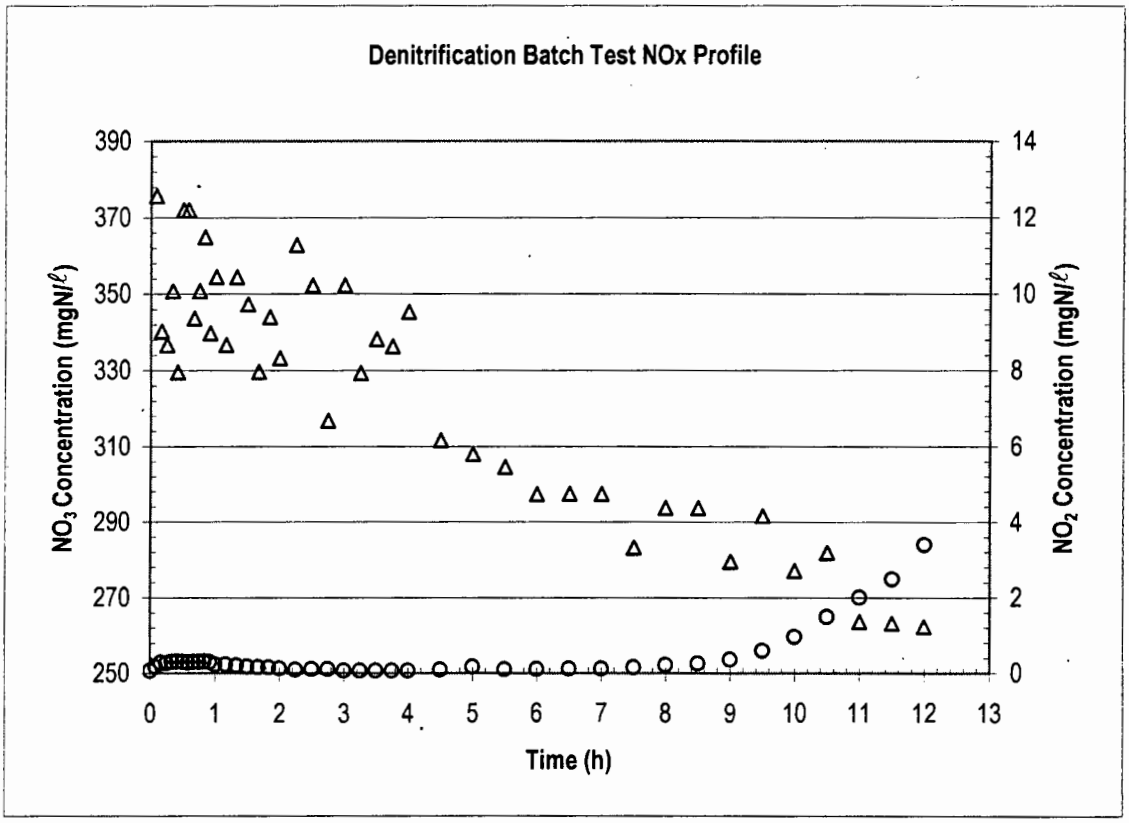

ML	SB	Date	DBT
LML	9	17.4.02	11

Batch Test Composition:

V_{WW}	2	ℓ	V_{ML}	1	ℓ
S_{ti}	853.6	mgCOD/ℓ	X_v	4311	mgVSS/ℓ
$S_{ti,BT}$	569.1	mgCOD/ℓ	LR	0.396	mgCOD/mgVSS

Plot K1 End Time:

End Time	Y (K1 End)

Plot K1-NO2 Max:

X Range	Y (NO2)

Define NU (mgNO$_3$-N/ℓ):

Y-int

K1

K2

ΔNO_3

NO_2-Corrected NU = mgN/ℓ

S_{bsi} (0.67) =	mgCOD/ℓ
f_{ts} =	

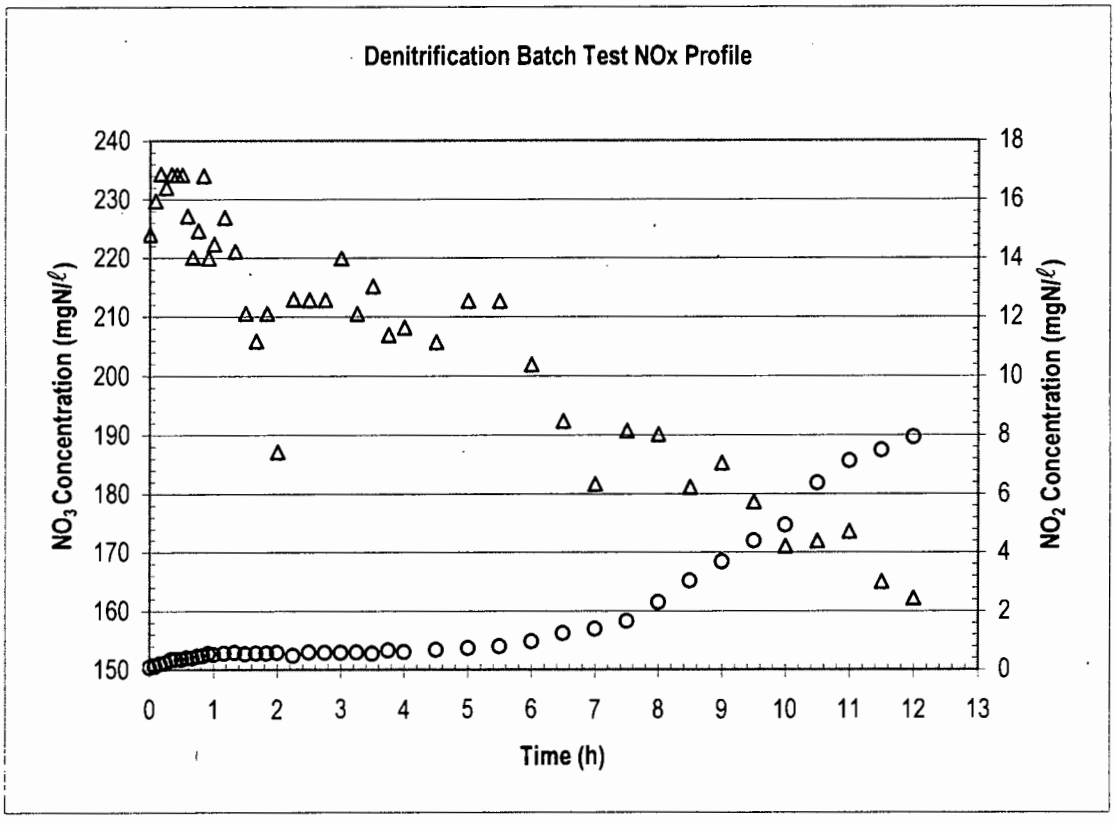

ML	SB	Date	DBT
LML	10	24.4.02	12

Batch Test Composition:

V_{WW}	2	ℓ	V_{ML}	1	ℓ
S_{ti}	1038.4	mgCOD/ℓ	X_v	4053	mgVSS/ℓ
$S_{ti,BT}$	692.3	mgCOD/ℓ	LR	0.512	mgCOD/mgVSS

V_{BT} 3 ℓ

Plot K1 End Time:

End Time	Y (K1 End)
2.1	0.00
2.1	50.00

Plot K1-NO2 Max:

X Range	Y (NO2)
0	0.75
12	*0.75*

Define NU (mgNO$_3$-N/ℓ):

	Y-int
K1	52.205
K2	43.461
ΔNO_3	8.744

NO_2-Corrected NU = **8.294** mgN/ℓ

S_{bsi} (0.67) =	71.88	mgCOD/ℓ
f_{ts} =	0.104	

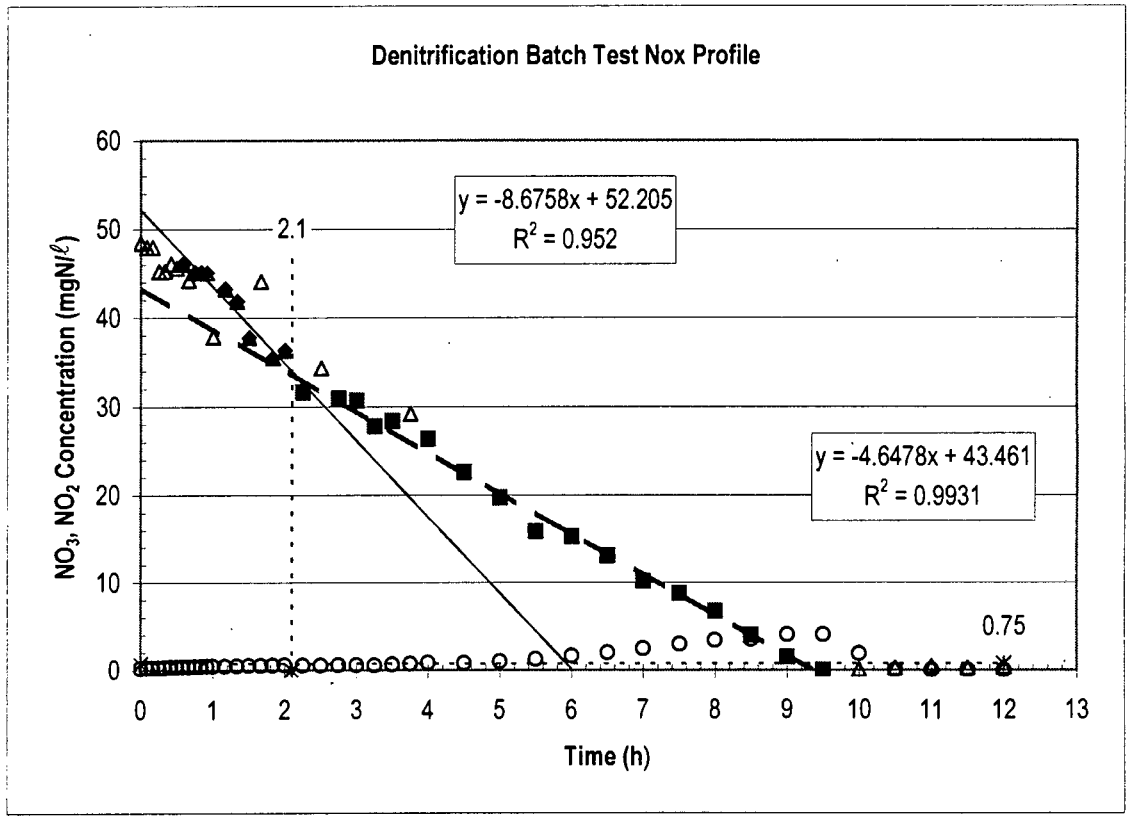

ML	SB	Date	DBT
LML	10	26.4.02	13

Batch Test Composition:

			V_{BT}	3	ℓ
V_{WW}	2	ℓ	V_{ML}	1	ℓ
S_{ti}	1179.4	mgCOD/ℓ	X_v	4034	mgVSS/ℓ
$S_{ti,BT}$	786.3	mgCOD/ℓ	LR	0.585	mgCOD/mgVSS

Plot K1 End Time:

End Time	Y (K1 End)
2.9	0.00
2.9	65.00

Plot K1-NO2 Max:

X Range	Y (NO2)
0	2.5
12	2.5

Define NU (mgNO$_3$-N/ℓ):

	Y-int
K1	75.381
K2	65.662
ΔNO$_3$	9.719

NO_2-Corrected NU = **8.219** mgN/ℓ

S_{bsi} (0.67) =	71.23	mgCOD/ℓ
f_{ts} =	0.091	

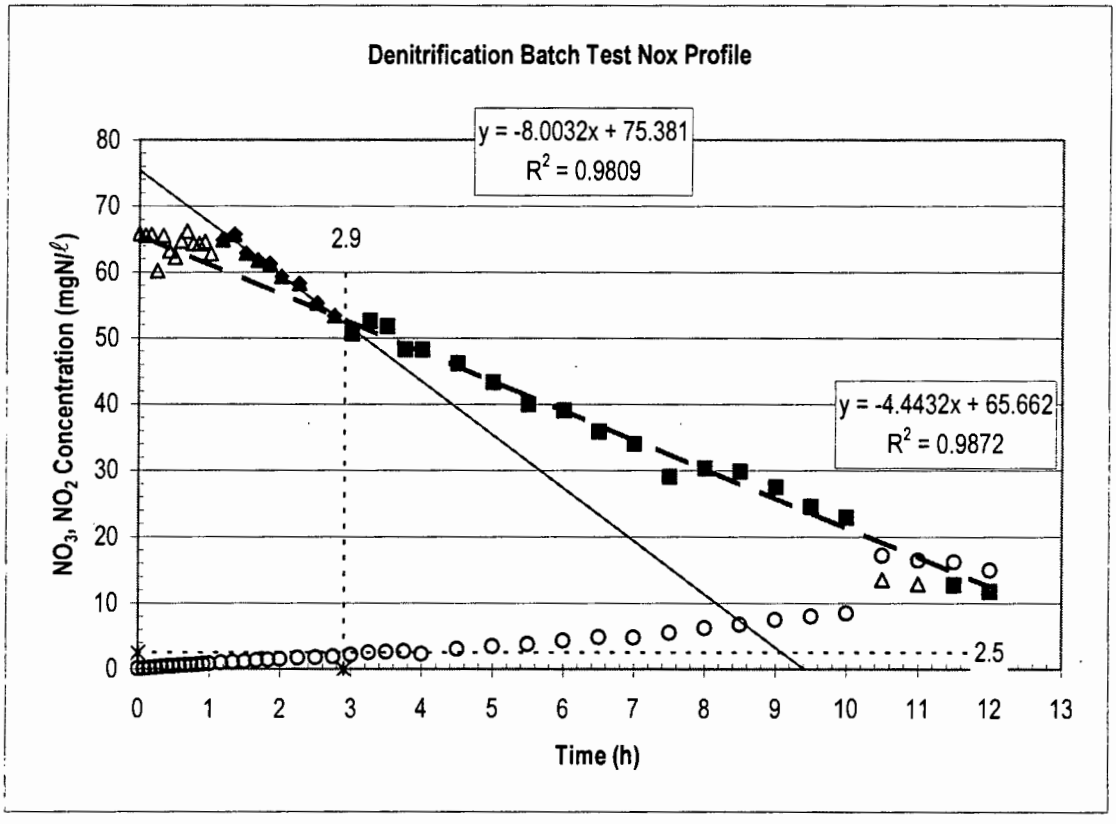

ML	SB	Date	DBT
MPP	11	29.4.02	14

Batch Test Composition:

			V_{BT}	3	ℓ
V_{WW}	2	ℓ	V_{ML}	1	ℓ
S_{ti}	1090.8	mgCOD/ℓ	X_v	3102	mgVSS/ℓ
$S_{ti,BT}$	727.2	mgCOD/ℓ	LR	0.703	mgCOD/mgVSS

Plot K1 End Time:

End Time	Y (K1 End)
1.35	0.00
1.35	70.00

Plot K1-NO2 Max:

X Range	Y (NO2)
0	3.16
12	*3.16*

Define NU (mgNO$_3$-N/ℓ):

	Y-int
K1	66.213
K2	55.914
ΔNO_3	10.299

NO_2-Corrected NU = **8.403** mgN/ℓ

S_{bsi} (0.67) =	72.83	mgCOD/ℓ
f_{ts} =	0.100	

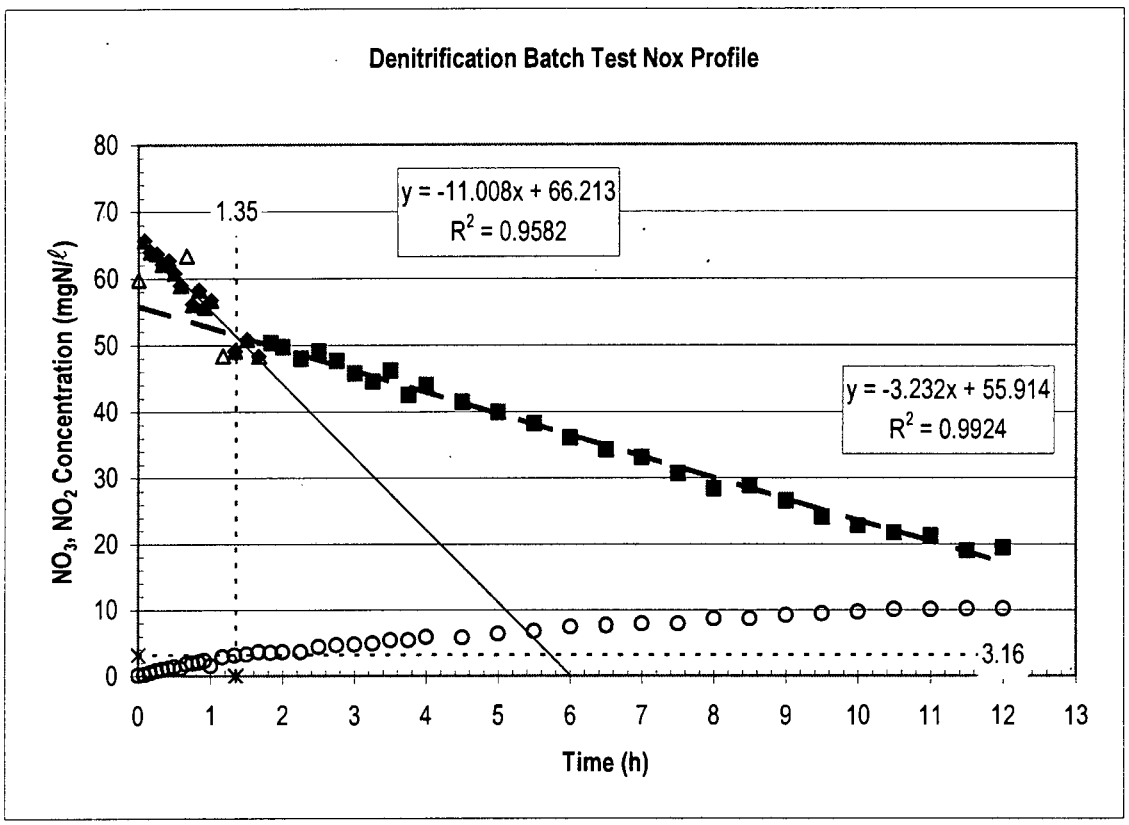

ML	SB	Date	DBT
MPP	11	2.5.02	15

Batch Test Composition:

V_{WW}	2	ℓ	V_{ML}	1	ℓ
S_{ti}	1151.2	mgCOD/ℓ	X_v	2921	mgVSS/ℓ
$S_{ti,BT}$	767.5	mgCOD/ℓ	LR	0.788	mgCOD/mgVSS

V_{BT} = 3 ℓ

Plot K1 End Time:

End Time	Y (K1 End)
2	0.00
2	30.00

Plot K1-NO2 Max:

X Range	Y (NO2)
0	3.8
12	3.8

Define NU (mgNO$_3$-N/ℓ):

	Y-int
K1	38.41
K2	29.297
ΔNO$_3$	9.113

NO_2-Corrected NU = **6.833** mgN/ℓ

S_{bsi} (0.67) =	59.22	mgCOD/ℓ
f_{ts} =	0.077	

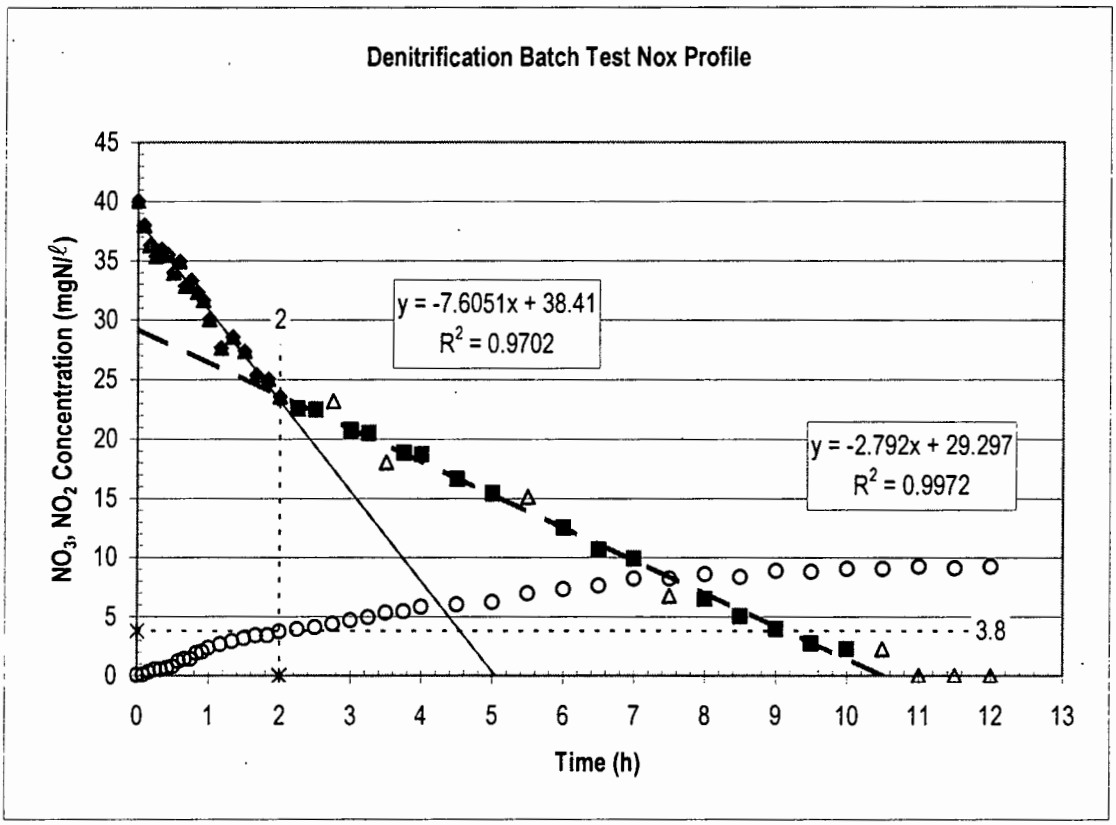

ML	SB	Date	DBT
MPP	11	3.5.02	16

Batch Test Composition:

			V_{BT}	3	ℓ
V_{WW}	2	ℓ	V_{ML}	1	ℓ
S_{ti}	1151.2	mgCOD/ℓ	X_v	2887	mgVSS/ℓ
$S_{ti,BT}$	767.5	mgCOD/ℓ	LR	0.798	mgCOD/mgVSS

Plot K1 End Time:

End Time	Y (K1 End)
1.65	0.00
1.65	35.00

Plot K1-NO2 Max:

X Range	Y (NO2)
0	3.93
12	*3.93*

Define NU (mgNO$_3$-N/ℓ):

	Y-int
K1	39.361
K2	29.414
ΔNO$_3$	9.947

NO_2-Corrected NU = **7.589** mgN/ℓ

S_{bsi} (0.67) =	65.77	mgCOD/ℓ
f_{ts} =	0.086	

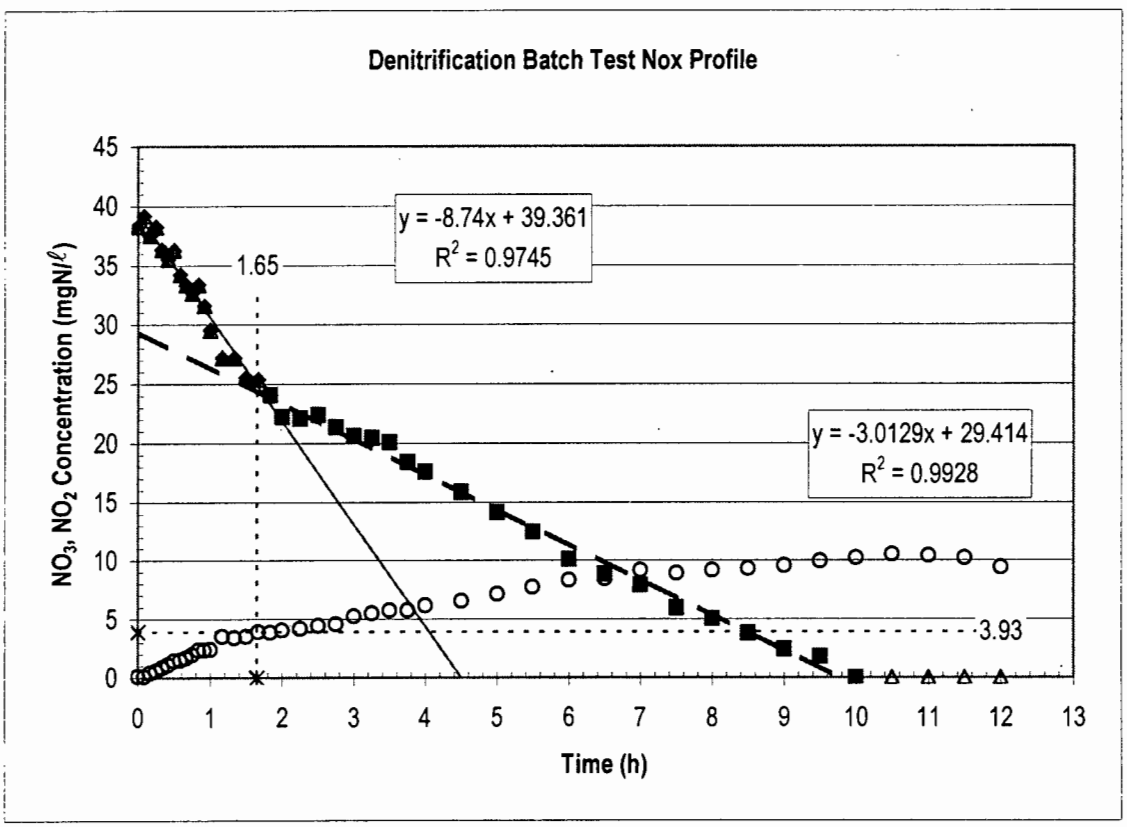

ML	SB	Date	DBT
MPP	11	4.5.02	17

Batch Test Composition:

V_{WW}	2	ℓ	V_{ML}	1	ℓ
S_{ti}	1126.8	mgCOD/ℓ	X_v	2844	mgVSS/ℓ
$S_{ti,BT}$	751.2	mgCOD/ℓ	LR	0.792	mgCOD/mgVSS

V_{BT} = 3 ℓ

Plot K1 End Time:

End Time	Y (K1 End)
2.1	0.00
2.1	35.00

Plot K1-NO2 Max:

X Range	Y (NO2)
0	4.1
12	*4.1*

Define NU (mgNO$_3$-N/ℓ):

	Y-int
K1	39.295
K2	31.603
ΔNO$_3$	7.692

NO_2-Corrected NU = **5.232** mgN/ℓ

S_{bsi} (0.67) =	45.34	mgCOD/ℓ
f_{ts} =	0.060	

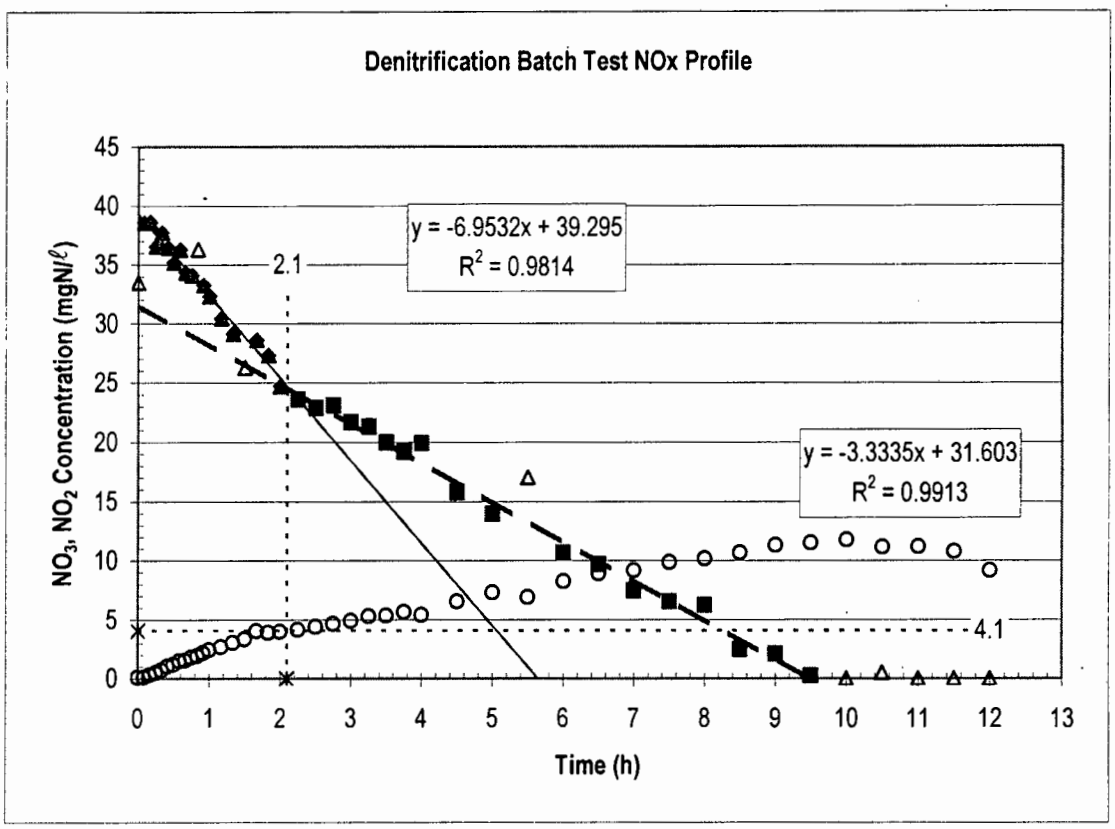

ML	SB	Date	DBT
MPP	11	5.5.02	18

Batch Test Composition:

			V_{BT}	3	ℓ
V_{WW}	2	ℓ	V_{ML}	1	ℓ
S_{ti}	1172	mgCOD/ℓ	X_v	2724	mgVSS/ℓ
$S_{ti,BT}$	781.3	mgCOD/ℓ	LR	0.860	mgCOD/mgVSS

Plot K1 End Time:

End Time	Y (K1 End)
1.65	0.00
1.65	35.00

Plot K1-NO2 Max:

X Range	Y (NO2)
0	4.3
12	*4.3*

Define NU (mgNO$_3$-N/ℓ):

	Y-int
K1	39.393
K2	31.183
ΔNO$_3$	8.21

NO_2-Corrected NU = **5.63** mgN/ℓ

S_{bsi} (0.67) =	48.79	mgCOD/ℓ
f_{ts} =	0.062	

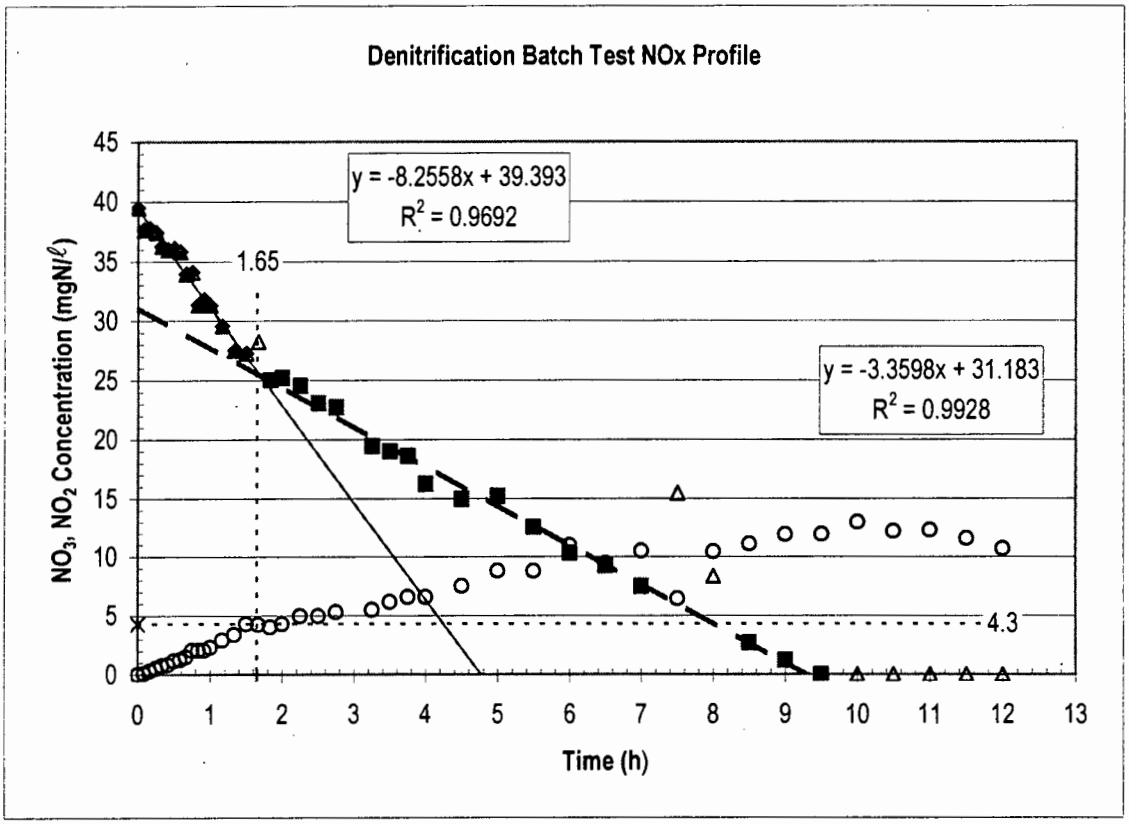

ML	SB	Date	DBT
MPP	NS	11.5.02	19

Batch Test Composition:

			V_{BT}	3	ℓ
V_{WW}	2	ℓ	V_{ML}	1	ℓ
S_{ti}	1446.8	mgCOD/ℓ	X_v	1520	mgVSS/ℓ
$S_{ti,BT}$	964.5	mgCOD/ℓ	LR	1.904	mgCOD/mgVSS

Plot K1 End Time:

End Time	Y (K1 End)
1.3	0.00
1.3	40.00

Plot K1-NO2 Max:

X Range	Y (NO2)
0	**1.4**
12	*1.4*

Define NU (mgNO$_3$-N/ℓ):

	Y-int
K1	41.347
K2	35.203
ΔNO_3	6.144

NO_2-Corrected NU = **5.304** mgN/ℓ

S_{bsi} (0.67) =	45.97	mgCOD/ℓ
f_{ts} =	0.048	

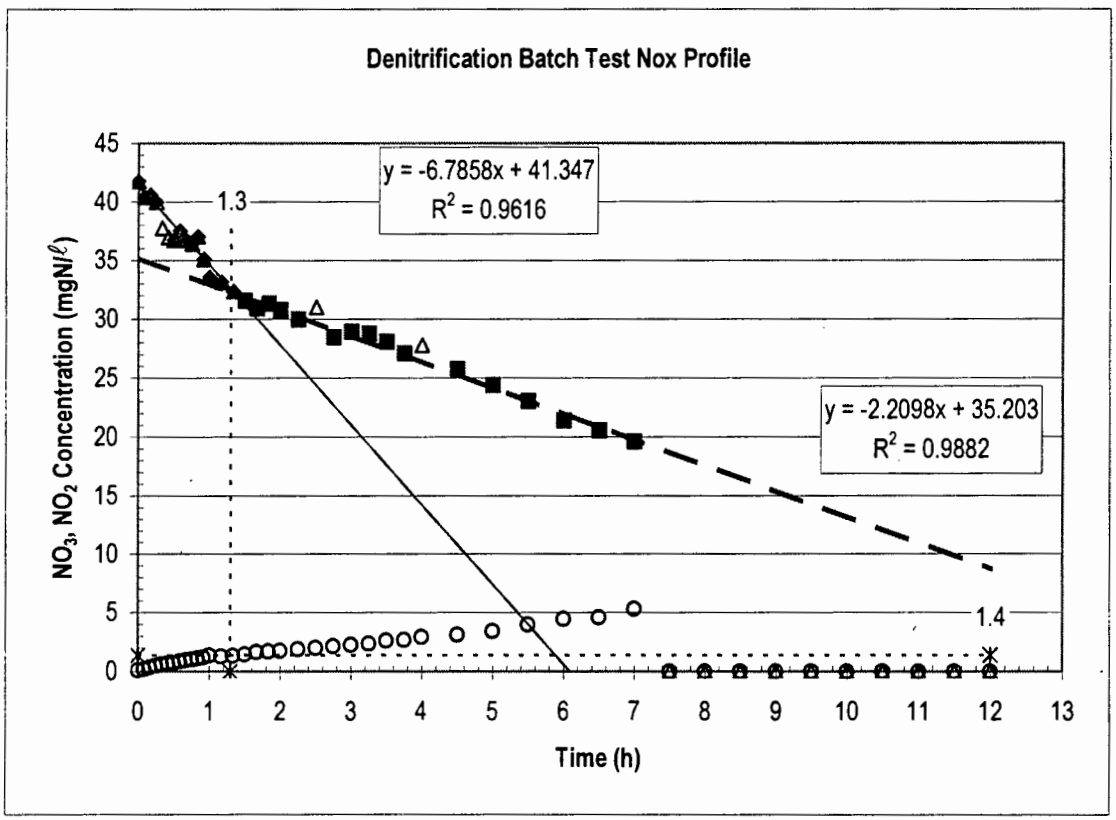

ML	SB	Date	DBT
MLE	18	28.8.02	20

Batch Test Composition:

V_{WW}	2	ℓ	V_{ML}	1	ℓ
S_{ti}	1206.4	mgCOD/ℓ	X_v	2451	mgVSS/ℓ
$S_{ti,BT}$	804.3	mgCOD/ℓ	LR	0.984	mgCOD/mgVSS

V_{BT} 3 ℓ

Plot K1 End Time:

End Time	Y (K1 End)

Plot K1-NO2 Max:

X Range	Y (NO2)

Define NU (mgNO$_3$-N/ℓ):

Y-int

K1

K2

ΔNO_3

NO_2-Corrected NU = mgN/ℓ

S_{bsi} (0.67) =	mgCOD/ℓ
f_{ts} =	

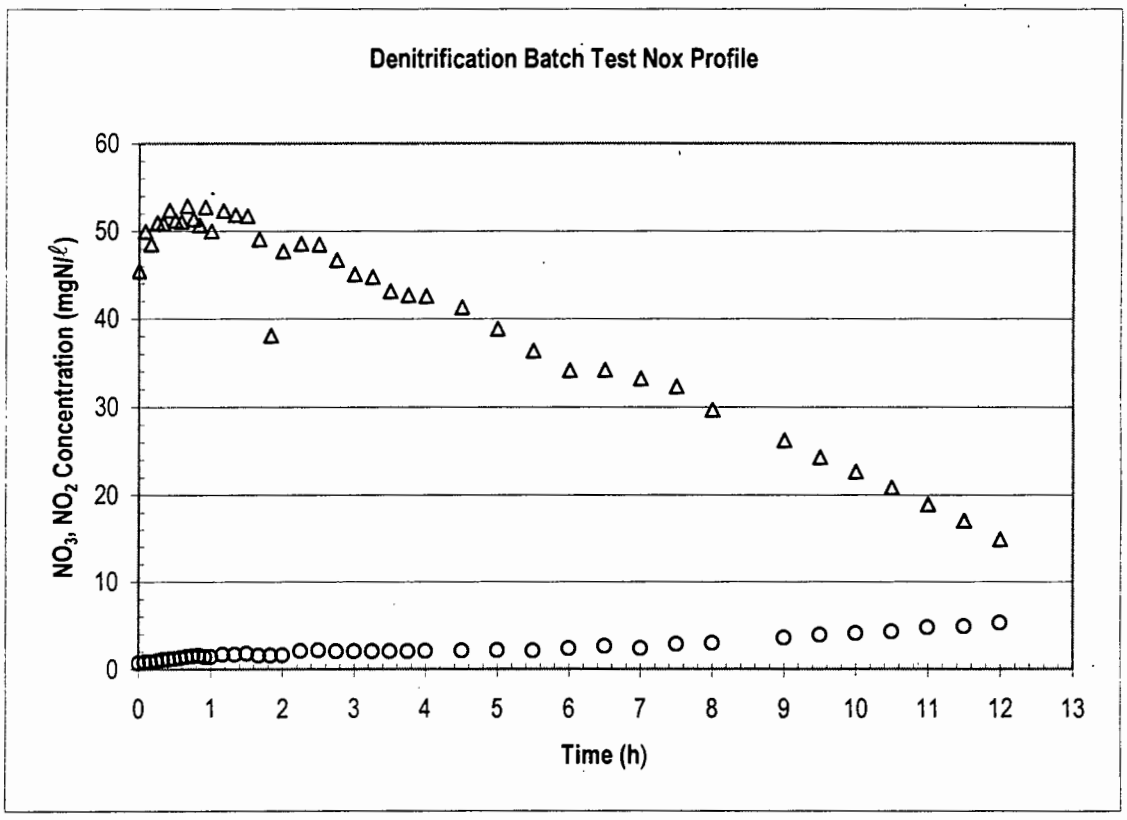

	ML	SB	Date	DBT
Batch Test Composition:	MLE	20	25.9.02	21

V_{BT} 3 ℓ

V_{WW}	2	ℓ	V_{ML}	1	ℓ
S_{ti}	1119.1	mgCOD/ℓ	X_v	4120	mgVSS/ℓ
$S_{ti,BT}$	746.1	mgCOD/ℓ	LR	0.543	mgCOD/mgVSS

Plot K1 End Time:

End Time	Y (K1 End)
1.85	0.00
1.85	55.00

Plot K1-NO2 Max:

X Range	Y (NO2)
0	**5.4**
12	*5.4*

Sbsi (0.67) mgCOD/ℓ 61.19

f_{ts} 0.082

Define NU (mgN/ℓ):

Y-int K1	Y-int K2	ΔNO_3	NO_2-Corrected NU (mgN/ℓ)
66.2	55.9	10.3	**7.06**

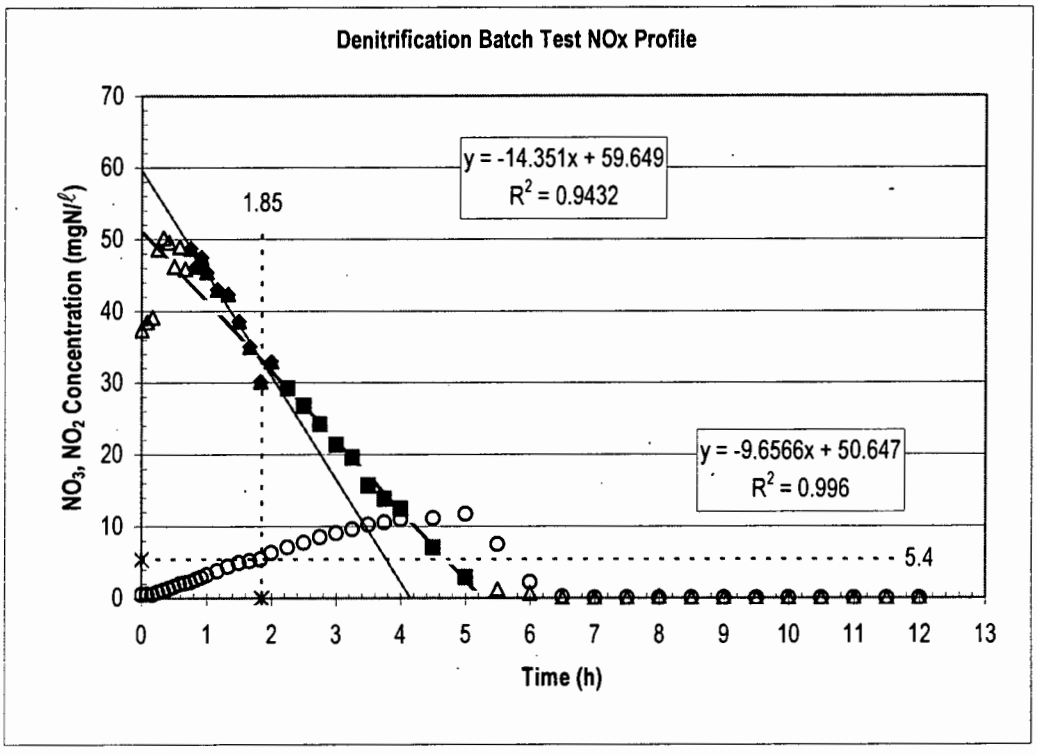

	ML	SB	Date	DBT
Batch Test Composition:	MLE	20	27.9.02	22

V_{BT} 3 ℓ

V_{WW}	2	ℓ	V_{ML}	1	ℓ
S_{ti}	1113.2	mgCOD/ℓ	X_v	3503	mgVSS/ℓ
$S_{ti,BT}$	742.1	mgCOD/ℓ	LR	0.636	mgCOD/mgVSS

Plot K1 End Time:

End Time	Y (K1 End)
2.5	0.00
2.5	70.00

Plot K1-NO2 Max:

X Range	Y (NO2)
0	**6.91**
12	*6.91*

Sbsi (0.67) 46.03 mgCOD/ℓ

f_{ts} 0.062

Define NU (mgN/ℓ):

Y-int K1	Y-int K2	ΔNO_3	NO_2-Corrected NU (mgN/ℓ)
74.491	65.034	9.457	**5.311**

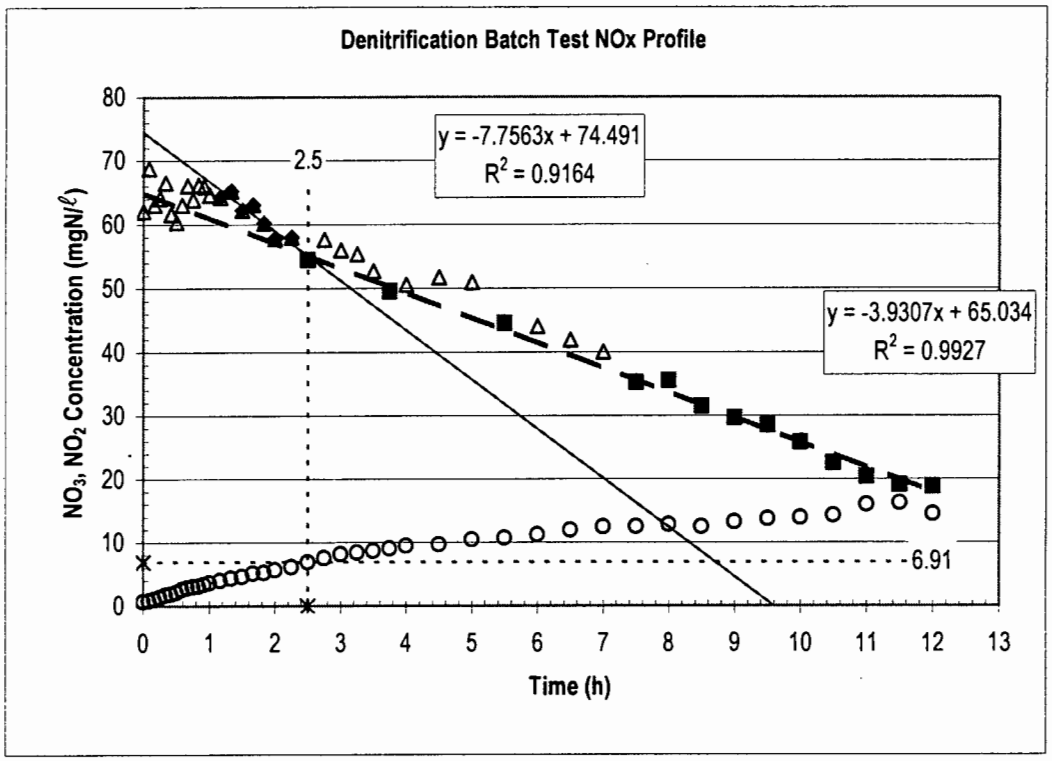

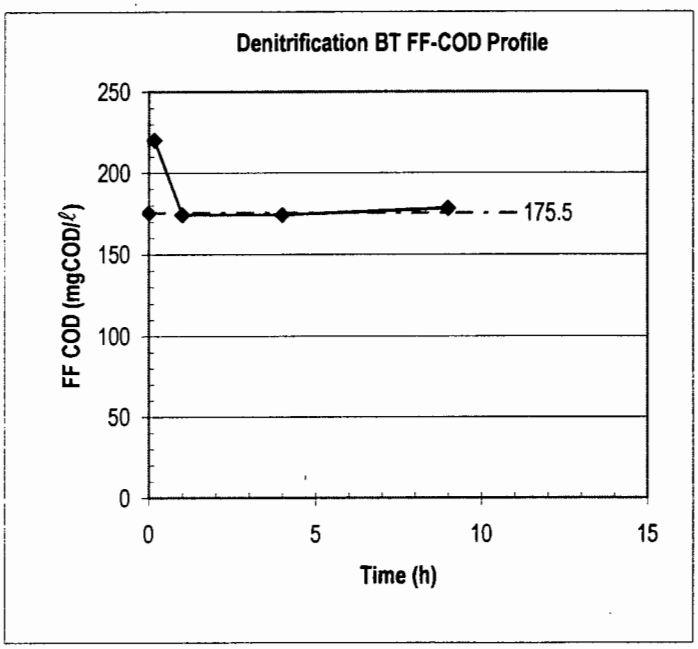

Plot FFE's:

t	FFE
0	
0.167	220.2
1	174.2
4	174.2
9	178.2
Avg	*175.5*

Plot Avg FFE:

t	Avg
0	*175.5*
12	*175.5*

	ML	SB	Date	DBT
Batch Test Composition:	MLE	20	29.9.02	23

V_{BT} 3 ℓ

V_{WW}	2	ℓ	V_{ML}	1	ℓ
S_{ti}	1053	mgCOD/ℓ	X_v	3093	mgVSS/ℓ
$S_{ti,BT}$	702.0	mgCOD/ℓ	LR	0.681	mgCOD/mgVSS

Plot K1 End Time:

End Time	Y (K1 End)
2.28	0.00
2.28	50.00

Plot K1-NO2 Max:

X Range	Y (NO2)
0	**4.49**
12	*4.49*

Sbsi (0.67) mgCOD/ℓ 106.49

f_{ts} 0.152

Define NU (mgN/ℓ):

Y-int K1	Y-int K2	ΔNO_3	NO_2-Corrected NU (mgN/ℓ)
54.438	39.457	14.981	**12.287**

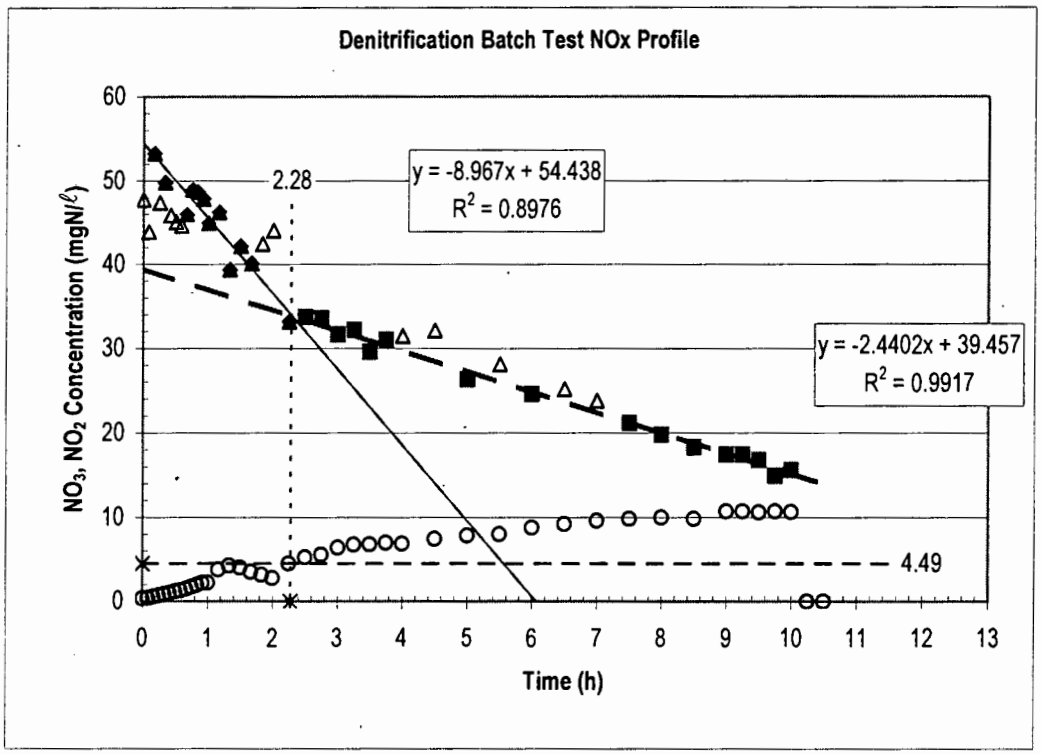

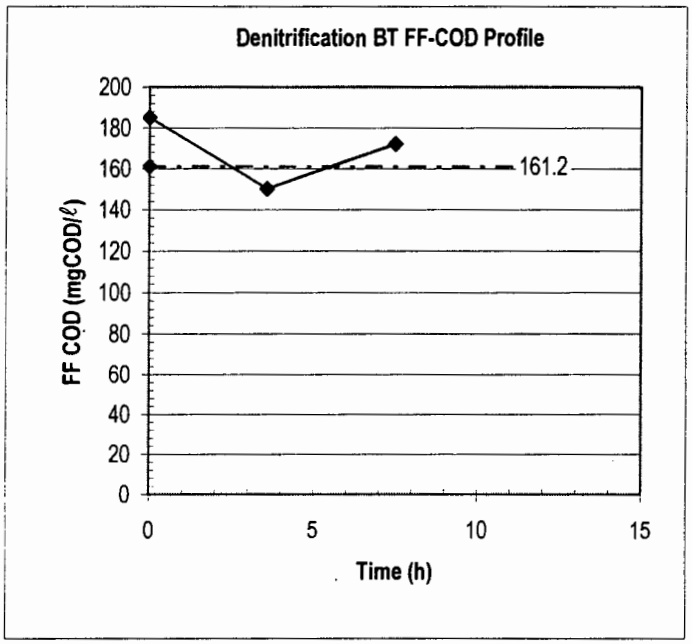

Plot FFE's:

t	FFE
0	185.2
3.583	150.2
7.5	172.2
Avg	*161.2*

Plot Avg FFE:

t	Avg
0	*161.2*
12	*161.2*

ML	SB	Date	DBT
MLE	21	1.10.02	24

Batch Test Composition:

V_{BT}	3	ℓ			
V_{WW}	2	ℓ	V_{ML}	1	ℓ
S_{ti}	1177.2	mgCOD/ℓ	X_v	4174	mgVSS/ℓ
$S_{ti,BT}$	784.8	mgCOD/ℓ	LR	0.564	mgCOD/mgVSS

Plot K1 End Time:

End Time	Y (K1 End)
	0.00
0	

Plot K1-NO2 Max:

X Range	Y (NO2)
0	
12	*0*

Sbsi (0.67) mgCOD/ℓ 0.00

f_{ts} 0.000

Define NU (mg N/ℓ):

Y-int K1	Y-int K2	ΔNO_3	NO_2-Corrected NU (mgN/ℓ)

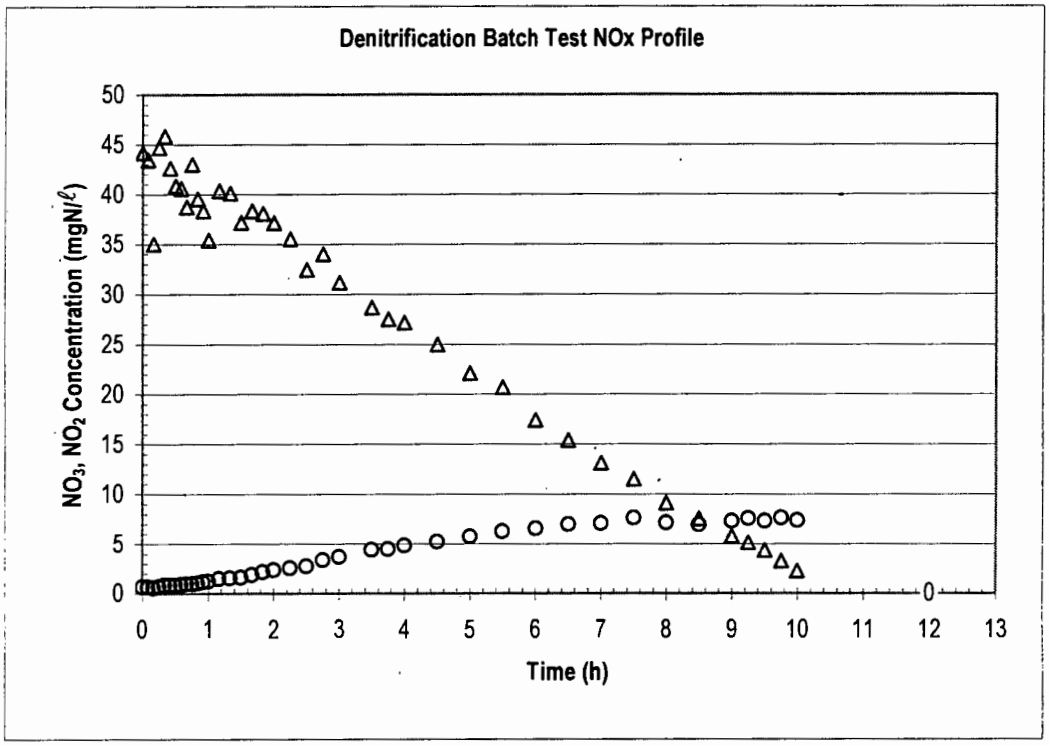

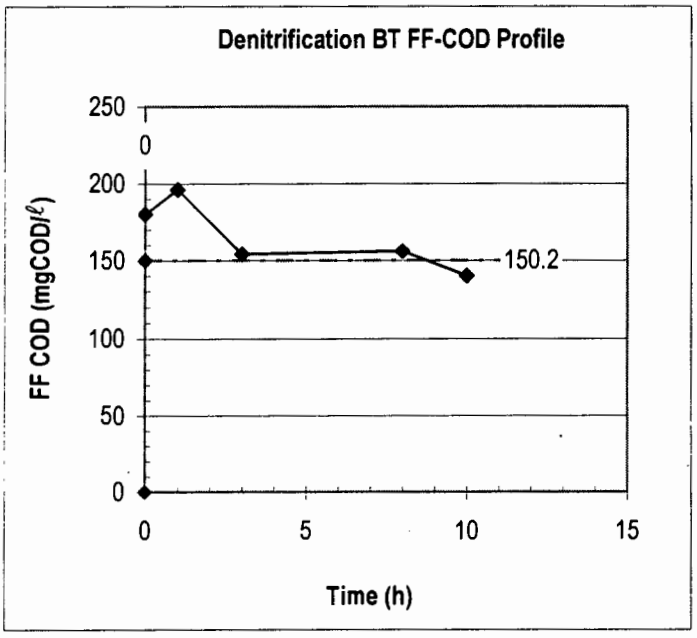

Plot FFE's:

t	FFE
0	180.2
1	196.2
3	154.2
8	156.2
10	140.1
Avg	*150.2*

Plot Avg FFE:

t	Avg
0	*150.2*
12	*150.2*

Plot K1 End Time:

End Time	Y (K1 End)
0	0.00
0	**225.00**

	ML	SB	Date	DBT
Batch Test Composition:	MLE	21	3.10.02	25

V_{BT} 3 ℓ

V_{WW}	2	ℓ	V_{ML}	1	ℓ
S_{ti}	1185.4	mgCOD/ℓ	X_v	3064	mgVSS/ℓ
$S_{ti,BT}$	790.3	mgCOD/ℓ	LR	0.774	mgCOD/mgVSS

Plot K1 End Time:

End Time	Y (K1 End)
	0.00
0	

Plot K1-NO2 Max:

X Range	Y (NO2)
0	
12	0

Sbsi (0.67) mgCOD/ℓ 0.00

f_{ts} 0.000

Define NU (mg N/ℓ):

Y-int K1	Y-int K2	ΔNO_3	NO_2-Corrected NU (mgN/ℓ)

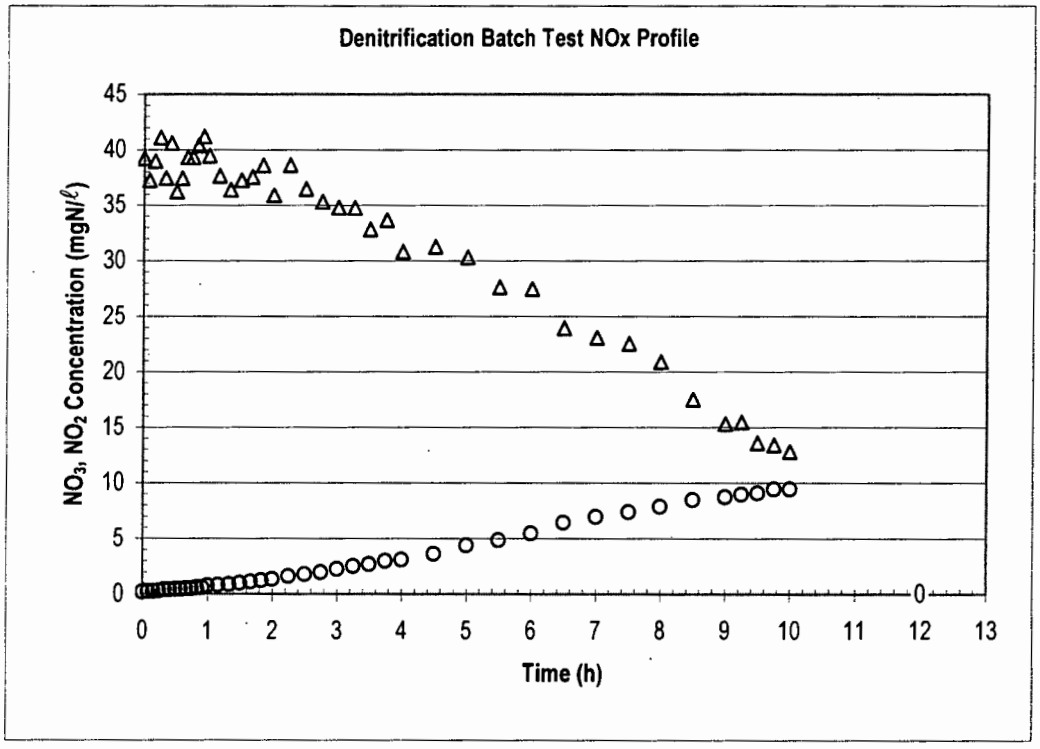

	ML	SB	Date	DBT
Batch Test Composition:	MLE	21	5.10.02	26

V_{BT} 3 ℓ

V_{WW}	2	ℓ	V_{ML}	1	ℓ
S_{ti}	1149.1	mgCOD/ℓ	X_v	2585	mgVSS/ℓ
$S_{ti,BT}$	766.1	mgCOD/ℓ	LR	0.889	mgCOD/mgVSS

Plot K1 End Time:

End Time	Y (K1 End)
	0.00
0	

Plot K1-NO2 Max:

X Range	Y (NO2)
0	
12	*0*

Sbsi (0.67) mgCOD/ℓ 0.00

f_{ts} 0.000

Define NU (mg N/ ℓ):

Y-int K1	Y-int K2	ΔNO_3	NO_2-Corrected NU (mgN/ℓ)

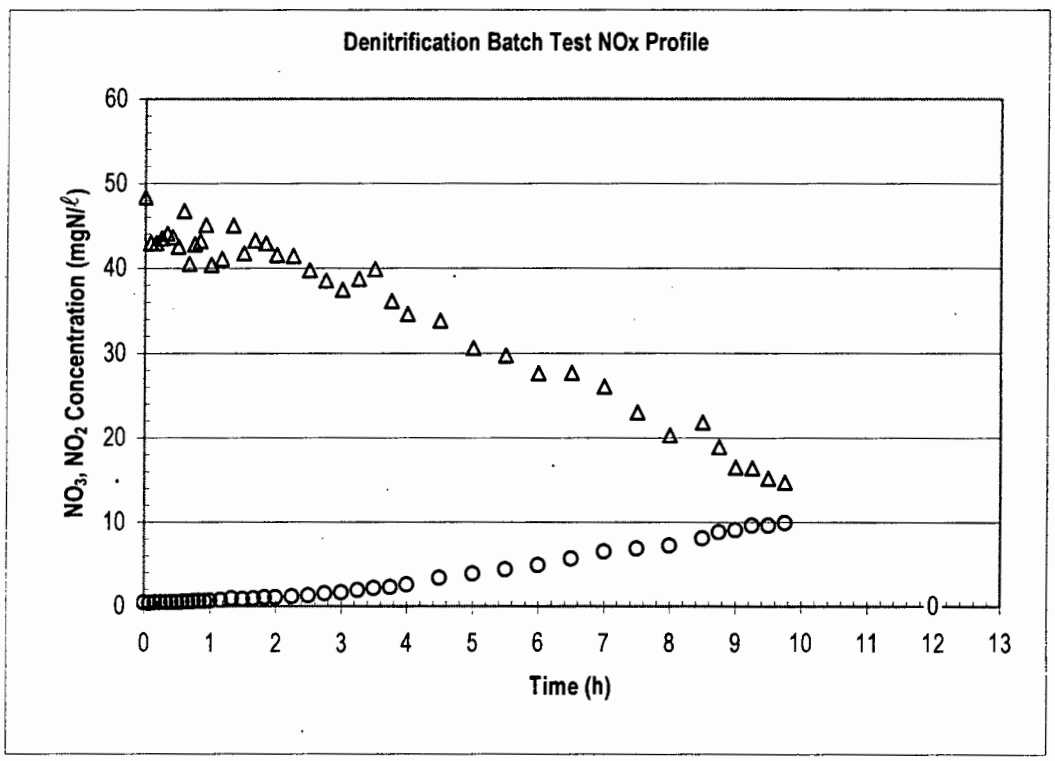

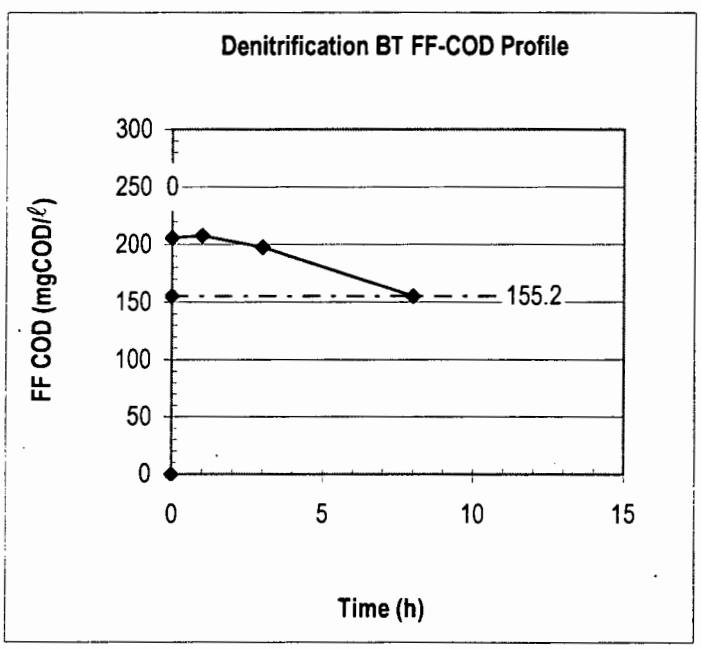

Plot FFE's:

t	FFE
0	205.6
1	207.6
3	197.6
8	155.2
Avg	*155.2*

Plot Avg FFE:

t	Avg
0	*155.2*
12	*155.2*

Plot K1 End Time:

End Time	Y (K1 End)
0	0.00
0	**250.00**

	ML	SB	Date	DBT
Batch Test Composition:	MLE	21	6.10.02	27

V_{BT} 3 ℓ

V_{WW}	2	ℓ	V_{ML}	1	ℓ
S_{ti}	1141.4	mgCOD/ℓ	X_v	4518	mgVSS/ℓ
$S_{ti,BT}$	760.9	mgCOD/ℓ	LR	0.505	mgCOD/mgVSS

Plot K1 End Time:

End Time	Y (K1 End)
3.25	0.00
3.25	*45.00*

Plot K1-NO2 Max:

X Range	Y (NO2)
0	1.1
12	*1.1*

Sbsi (0.67) mgCOD/ℓ 56.25

f_{ts} 0.074

Define NU (mg N/ℓ):

Y-int K1	Y-int K2	ΔNO_3	NO_2-Corrected NU (mgN/ℓ)
50.271	43.121	7.15	**6.49**

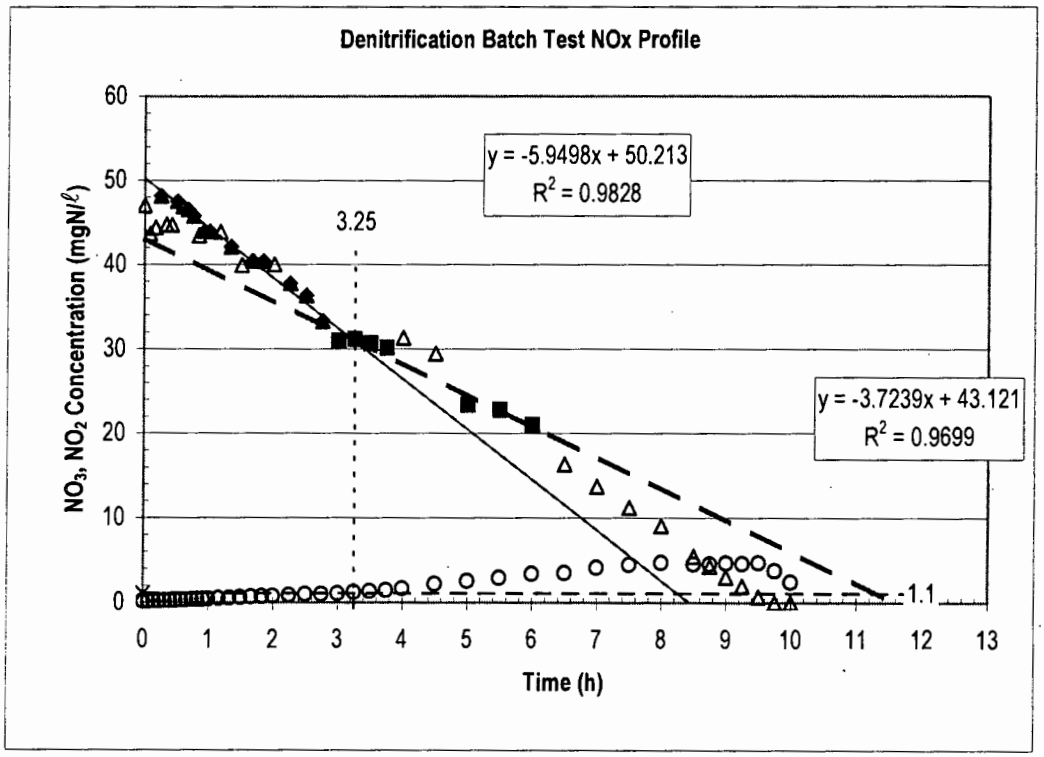

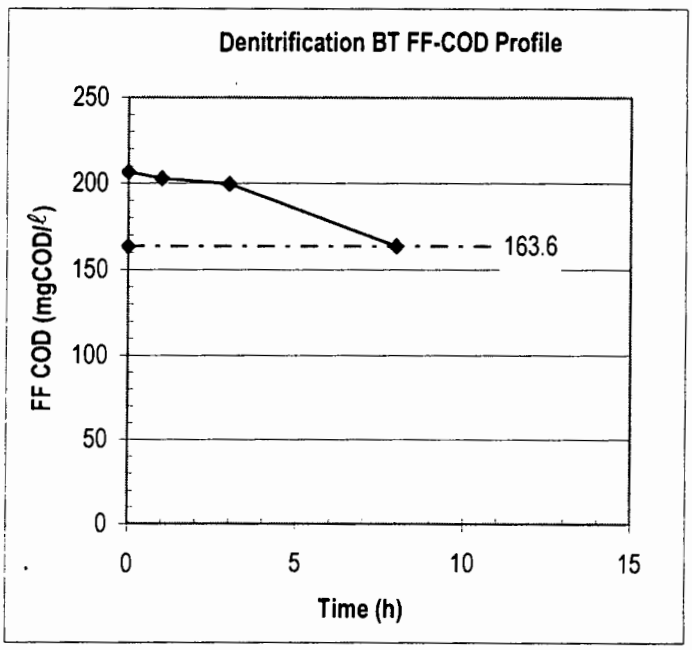

Plot FFE's:

t	FFE
0	206.6
1	202.6
3	199.6
8	163.6
Avg	*163.6*

Plot Avg FFE:

t	Avg
0	*163.6*
12	*163.6*

	ML	SB	Date	DBT
Batch Test Composition:	MLE	21	8.10.02	28

V_{BT} 3 ℓ

V_{WW}	2	ℓ	V_{ML}	1	ℓ
S_{ti}	1162.3	mgCOD/ℓ	X_v	4339	mgVSS/ℓ
$S_{ti,BT}$	774.9	mgCOD/ℓ	LR	0.536	mgCOD/mgVSS

Plot K1 End Time:

End Time	Y (K1 End)
3.75	0.00
3.75	50.00

Plot K1-NO2 Max:

X Range	Y (NO2)
0	2.3
12	*2.3*

Sbsi (0.67) mgCOD/ℓ 57.89

f_{ts} 0.075

Define NU (mg N/ ℓ):

Y-int K1	Y-int K2	ΔNO_3	NO_2-Corrected NU (mgN/ℓ)
50.313	42.253	8.06	**6.68**

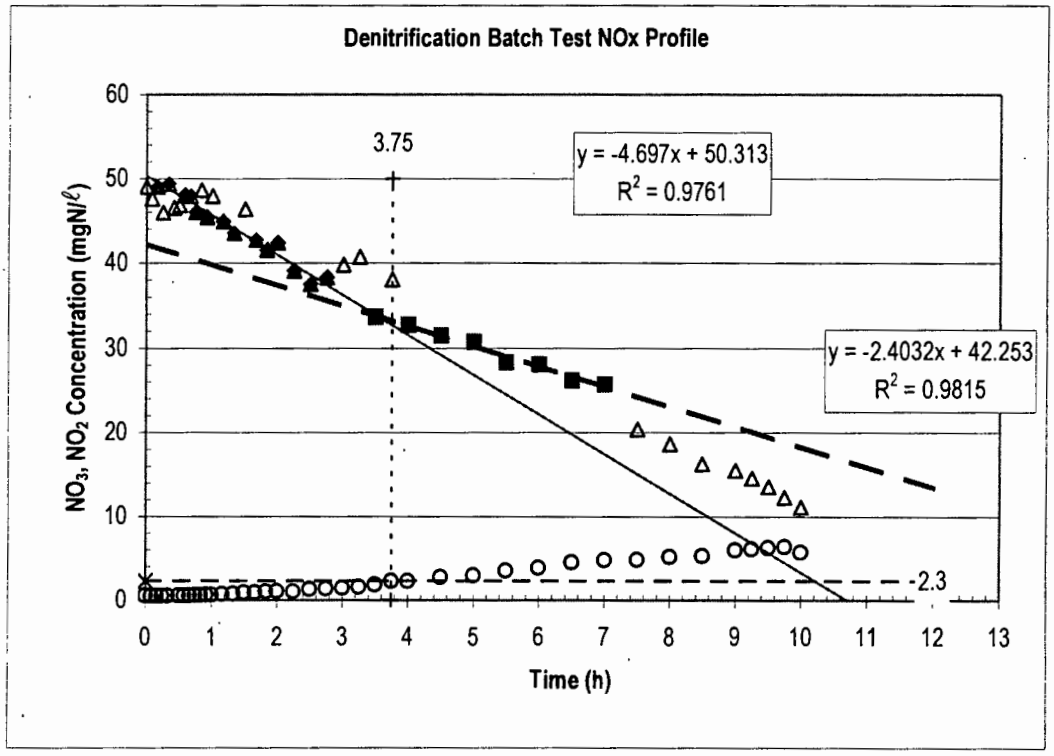

ML	SB	Date	DBT
MLE	21	10.10.02	29

Batch Test Composition:

V_{BT} 3 ℓ

V_{WW}	2	ℓ	V_{ML}	1	ℓ
S_{ti}	1150.1	mgCOD/ℓ	X_v	4417	mgVSS/ℓ
$S_{ti,BT}$	766.7	mgCOD/ℓ	LR	0.521	mgCOD/mgVSS

Plot K1 End Time:

End Time	Y (K1 End)
2.1	0.00
2.1	50.00

Plot K1-NO2 Max:

X Range	Y (NO2)
0	1.6
12	*1.6*

Sbsi (0.67) mgCOD/ℓ 54.28

f_{ts} 0.071

Define NU (mg N/ ℓ):

Y-int K1	Y-int K2	ΔNO_3	NO_2-Corrected NU (mgN/ℓ)
47.223	40	7.223	**6.263**

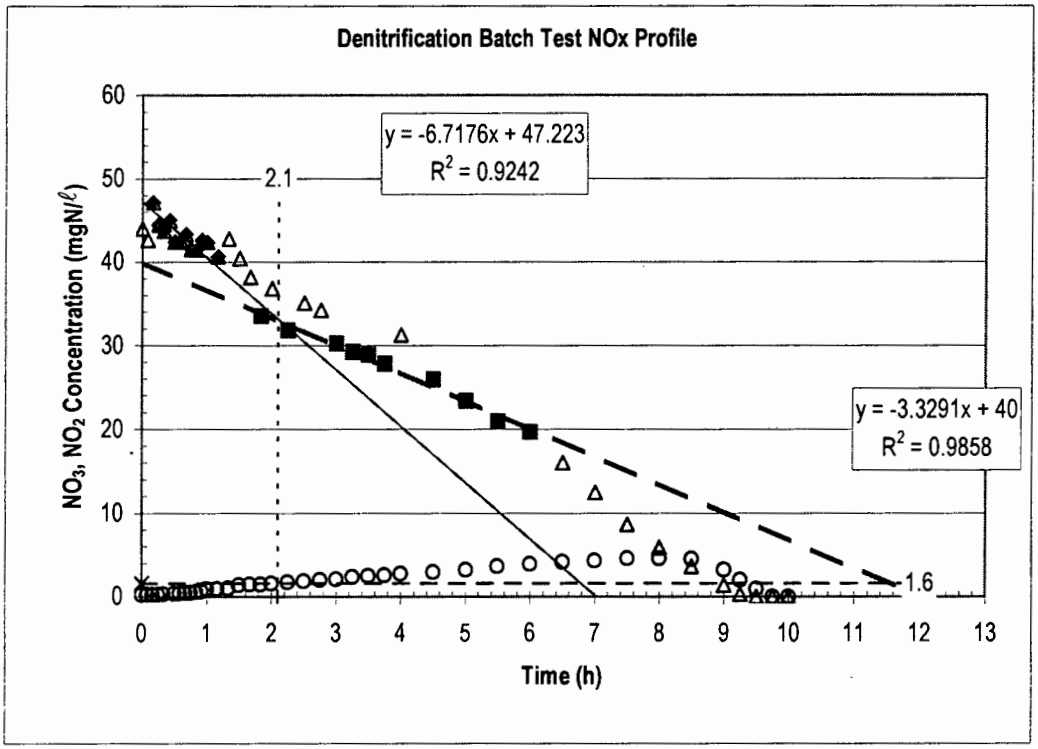

	ML	SB	Date	DBT
Batch Test Composition:	MLE	Acetate	11.10.02	30

V_{BT}	3	ℓ	$V_{BT,Ac(25)}$	2.41	ℓ
V_{Ac}	50	mℓ	V_{ML}	1	ℓ
Ac_{ti}	2605	mgCOD/ℓ	X_v	3282	mgVSS/ℓ
$Ac_{ti,BT}$	54.0	mgCOD/ℓ	LR	0.049	mgCOD/mgVSS

Plot K1 End Time:

End Time	Y (K1 End)
3	0.00
3	*87.50*

Plot K1-NO2 Max:

X Range	Y (NO2)
0	4.46
12	*4.46*

Sbsi (0.67) mgCOD/ℓ

f_{ts}

Define NU (mg N/ℓ):

Y-int K1	Y-int K2	ΔNO_3	NO_2-Corrected NU (mgN/ℓ)

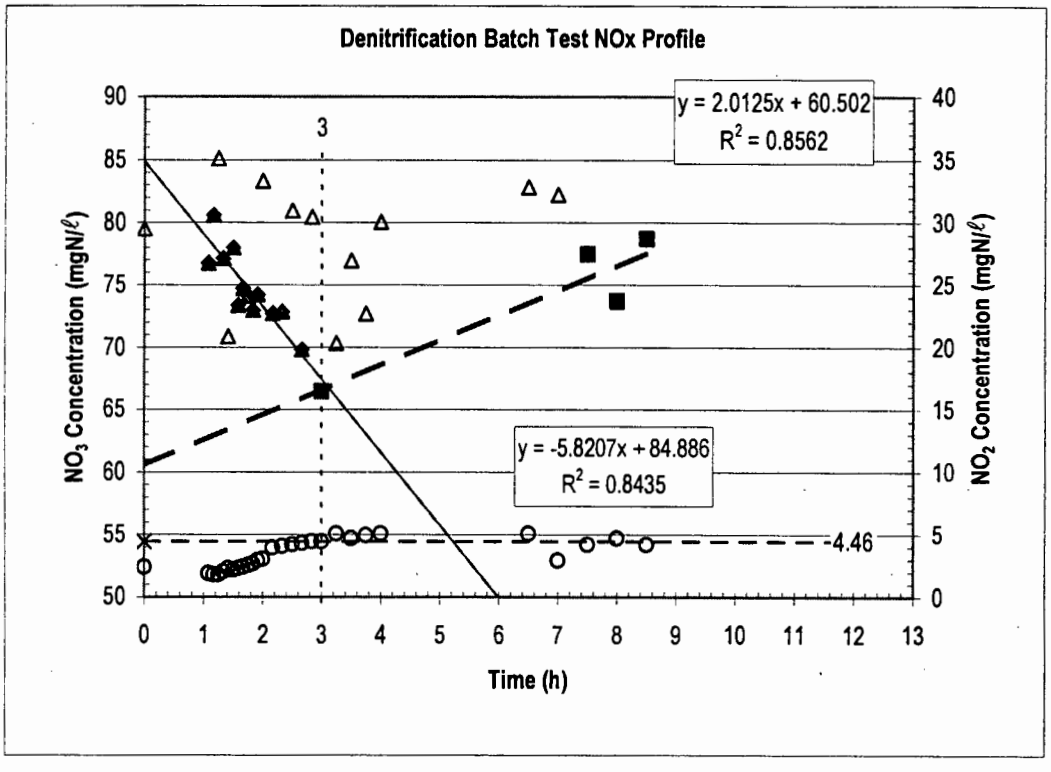

	ML	SB	Date	DBT
Batch Test Composition:	MLE	Acetate	12.10.02	31

V_{BT}	3	ℓ	$V_{BT,Ac(25)}$	2.64	ℓ
V_{Ac}	25	mℓ	V_{ML}	2	ℓ
Ac_{ti}	2389.6	mgCOD/ℓ	X_v	1932	mgVSS/ℓ
$Ac_{ti,BT}$	22.6	mgCOD/ℓ	LR	0.018	mgCOD/mgVSS

Plot K1 End Time:

End Time	Y (K1 End)
1.3	0.00
1.3	12.00

Plot K1-NO2 Max:

X Range	Y (NO2)
0	0.6
5.5	*0.6*

Sbsi (0.67) mgCOD/ℓ

f_{ts}

Define NU (mg N/ℓ):

Y-int K1	Y-int K2	ΔNO_3	NO_2-Corrected NU (mgN/ℓ)

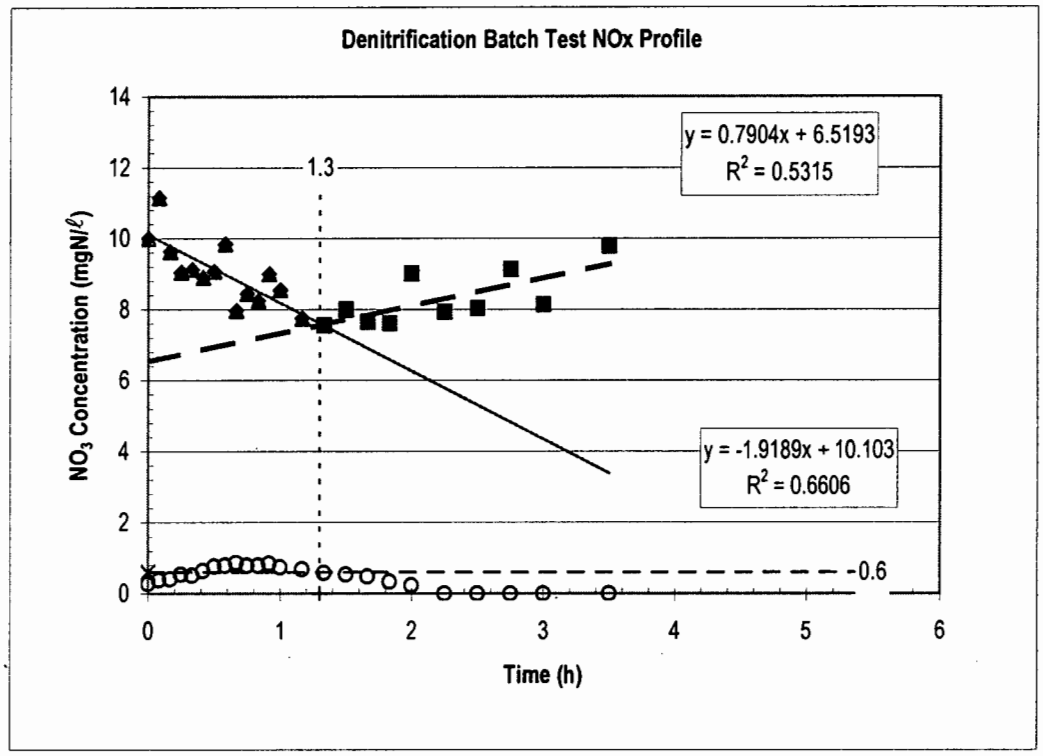

	ML	SB	Date	DBT
Batch Test Composition:	MLE	Acetate	13.10.02	32

V_{BT}	3	ℓ	$V_{BT,Ac(25)}$	2.63	ℓ
V_{Ac}	25	mℓ	V_{ML}	2	ℓ
Ac_{ti}	2389.6	mgCOD/ℓ	X_v	1938	mgVSS/ℓ
$Ac_{ti,BT}$	22.7	mgCOD/ℓ	LR	0.018	mgCOD/mgVSS

Plot K1 End Time:

End Time	Y (K1 End)
1.07	0.00
1.07	12.00

Plot K1-NO2 Max:

X Range	Y (NO2)
0	0.75
5.5	*0.75*

Sbsi (0.67) mgCOD/ℓ

f_{ts}

Define NU (mg N/ ℓ):

Y-int K1	Y-int K2	ΔNO_3	NO_2-Corrected NU (mgN/ℓ)

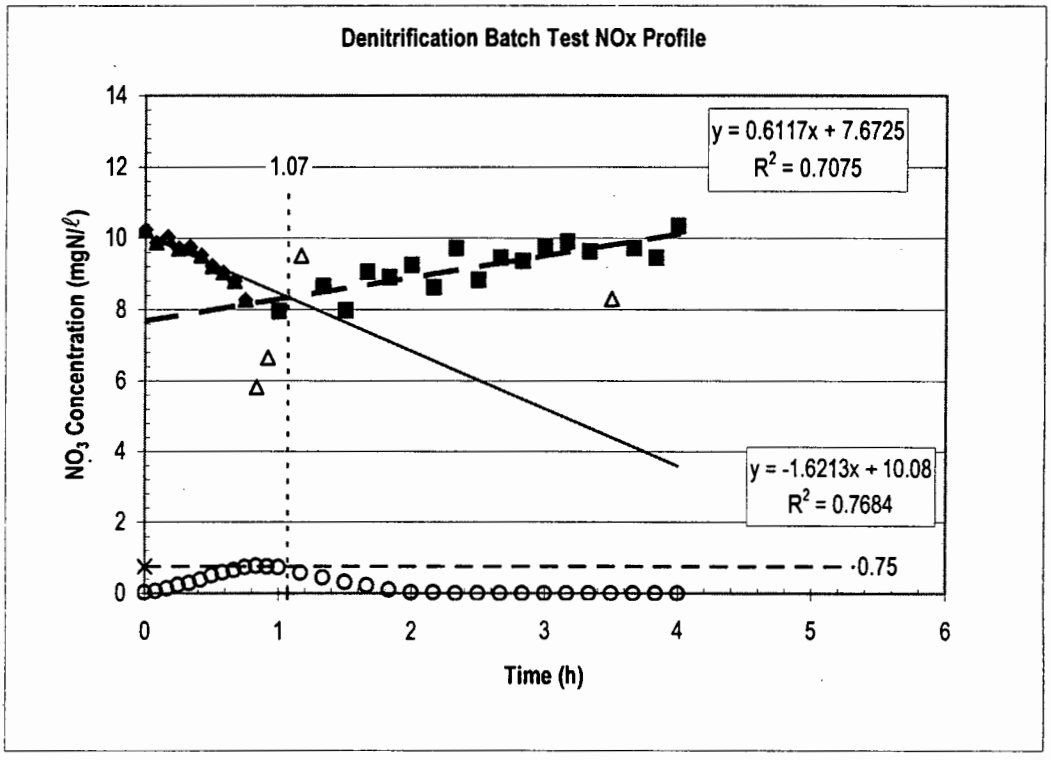

	ML	SB	Date	DBT
Batch Test Composition:	MLE	Acetate	14.10.02	33

V_{BT}	3	ℓ	$V_{BT,Ac(25)}$	2.85	ℓ
V_{Ac}	25	mℓ	V_{ML}	2	ℓ
Ac_{ti}	1763.5	mgCOD/ℓ	X_v	1926	mgVSS/ℓ
$Ac_{ti,BT}$	15.5	mgCOD/ℓ	LR	0.012	mgCOD/mgVSS

Plot K1 End Time:

End Time	Y (K1 End)
0.64	0.00
0.64	10.00

Plot K1-NO2 Max:

X Range	Y (NO2)
0	0.65
5.5	*0.65*

Sbsi (0.67) mgCOD/ℓ

f_{ts}

Define NU (mg N/ℓ):

Y-int K1	Y-int K2	ΔNO_3	NO_2-Corrected NU (mgN/ℓ)

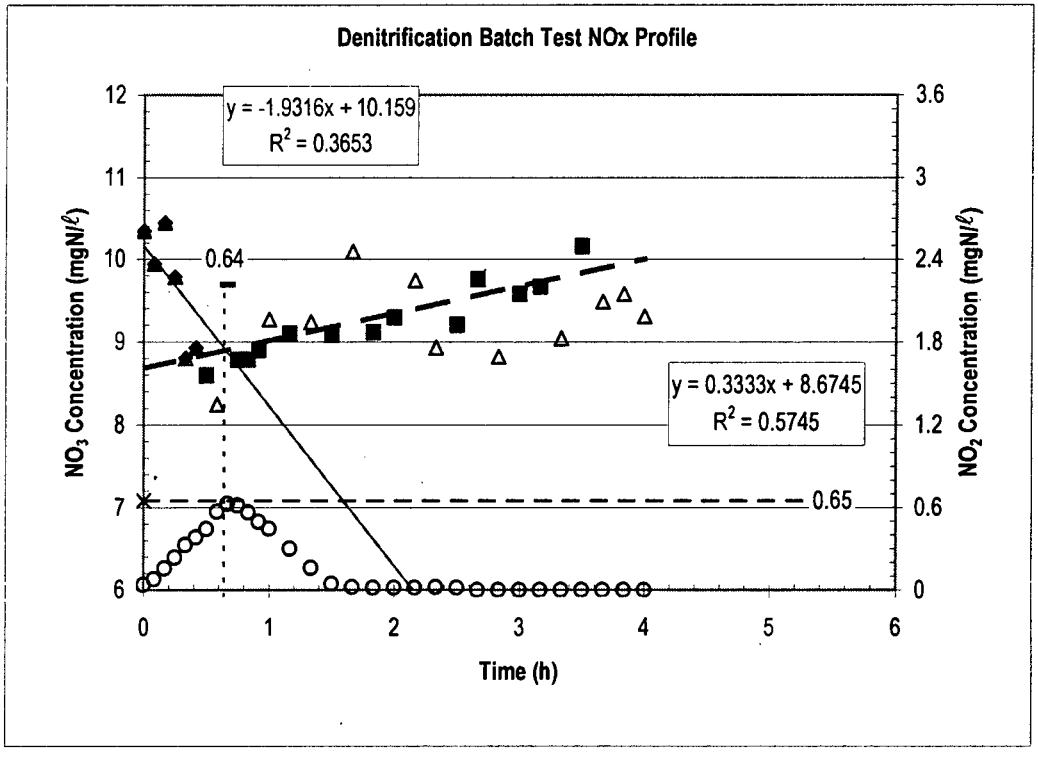

	ML	SB	Date	DBT
Batch Test Composition:	MLE	22	24.10.02	34

V_{BT} 3 ℓ

V_{WW}	2	ℓ	V_{ML}	1	ℓ
S_{ti}	1118.2	mgCOD/ℓ	X_v	2285	mgVSS/ℓ
$S_{ti,BT}$	745.5	mgCOD/ℓ	LR	0.979	mgCOD/mgVSS

Plot K1 End Time:

End Time	Y (K1 End)
5	0.00
5	35.00

Plot K1-NO2 Max:

X Range	Y (NO2)
0	**0**
12	*0*

Sbsi (0.67) mgCOD/ℓ 91.10

f_{ts} 0.122

Define NU (mgN/ℓ):

Y-int K1	Y-int K2	ΔNO_3	NO_2-Corrected NU (mgN/ℓ)
39.855	29.343	10.512	**10.512**

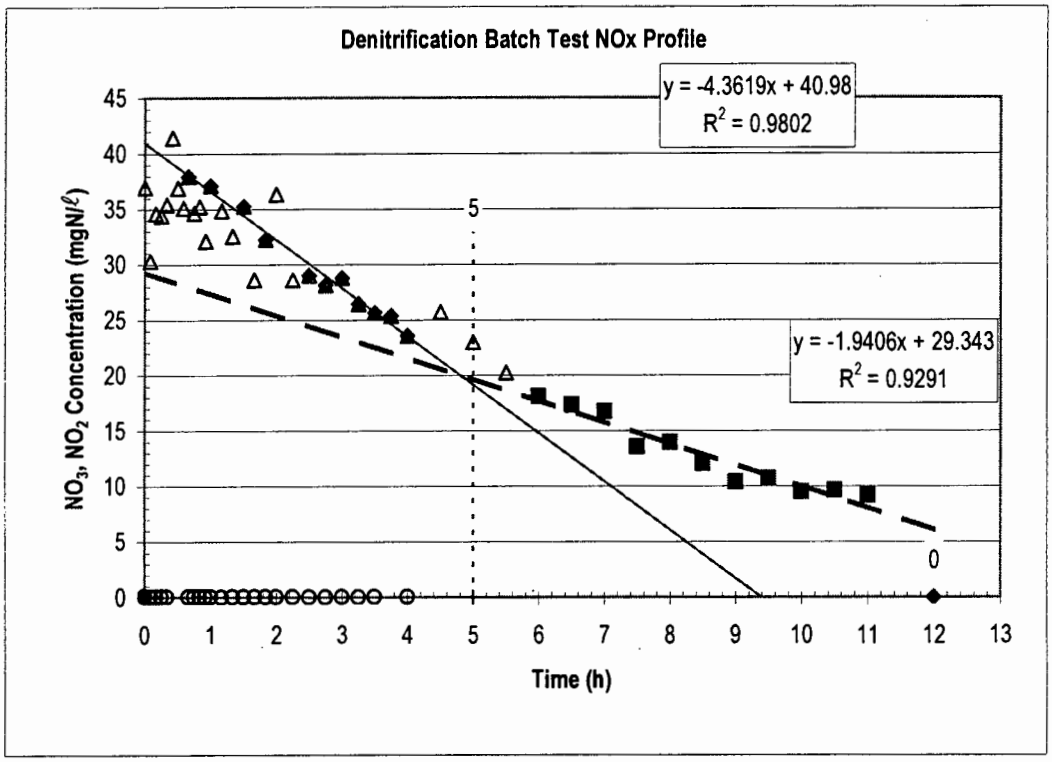

NOTE:

NO3 and NO2 concentrations determined by ion chromatography; concentrations reported in mgNO3/l and mgNO2/l units, respectively - a correction factor is applied to convert IC values to "equivalent" Auto-Analyzer values in mgN/l units, based on IC values obtained for standard NO3 and NO2 solutions; i.e.: NO3: AA equivalent (as mgN/ℓ) = 0.2534*IC (as mgNO3/ℓ)
NO2: AA equivalent (as mgN/ℓ) = 0.2591*IC (as mgNO3/ℓ)

STANDARD VALUES:

Standard NO3 (mgN/ℓ)	Standard NO2 (mgN/ℓ)	IC - NO3 mgNO3/ℓ	mgN/ℓ	IC - NO2 mgNO2/ℓ	mgN/ℓ
0.25	0.1	1.060	0.239	0.040	0.009
0.5	0.2	1.830	0.413	0.910	0.205
0.75	0.3	2.740	0.619	1.070	0.242
1	0.4	3.860	0.872	1.490	0.336
1.25	0.5	7.780	1.757	1.860	0.420
1.5	0.6	6.010	1.357	2.300	0.519
1.75	0.7	6.720	1.517	2.780	0.628
2	0.8	8.120	1.834	4.270	0.964

	ML	SB	Date	DBT
Batch Test Composition:	MLE	23	5.11.02	35

V_{BT} 3 ℓ

V_{WW}	2	ℓ	V_{ML}	1	ℓ
S_{ti}	1140.9	mgCOD/ℓ	X_v	3450	mgVSS/ℓ
$S_{ti,BT}$	760.6	mgCOD/ℓ	LR	0.661	mgCOD/mgVSS

Plot K1 End Time:

End Time	Y (K1 End)
3.83	0.00
3.83	25.00

Plot K1-NO2 Max:

X Range	Y (NO2)
0	**1**
12	*1*

Sbsi (0.67) mgCOD/ℓ 67.92

f_{ts} 0.089

Define NU (mgN/ℓ):

Y-int K1	Y-int K2	ΔNO_3	NO_2-Corrected NU (mgN/ℓ)
33.855	25.418	8.437	**7.837**

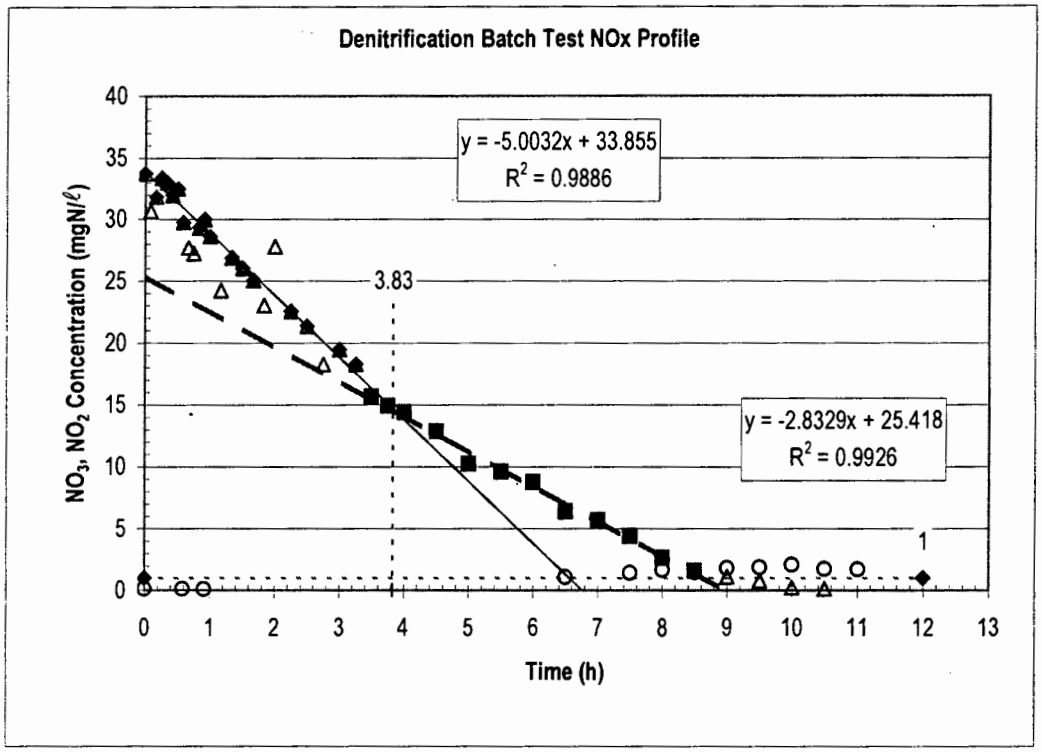

NOTE:

NO3 and NO2 concentrations determined by ion chromatography; concentrations reported in mgNO3/l and mgNO2/l units, respectively - a correction factor is applied to convert IC values to "equivalent" Auto-Analyzer values in mgN/l units, based on IC values obtained for standard NO3 and NO2 solutions; i.e.: NO3: AA equivalent (as mgN/ℓ) = 0.2534*IC (as mgNO3/ℓ)
NO2: AA equivalent (as mgN/ℓ) = 0.2591*IC (as mgNO3/ℓ)

STANDARD VALUES:

Standard NO3 (mgN/ℓ)	Standard NO2 (mgN/ℓ)	IC - NO3 mgNO3/ℓ	mgN/ℓ	IC - NO2 mgNO2/ℓ	mgN/ℓ
0.25	0.1	1.060	0.239	0.040	0.009
0.5	0.2	1.830	0.413	0.910	0.205
0.75	0.3	2.740	0.619	1.070	0.242
1	0.4	3.860	0.872	1.490	0.336
1.25	0.5	7.780	1.757	1.860	0.420
1.5	0.6	6.010	1.357	2.300	0.519
1.75	0.7	6.720	1.517	2.780	0.628
2	0.8	8.120	1.834	4.270	0.964

	ML	SB	Date	DBT
Batch Test Composition:	MLE	23	11.11.02	36

V_{BT} 3 ℓ

V_{WW}	2	ℓ	V_{ML}	1	ℓ
S_{ti}	1120.4	mgCOD/ℓ	X_v	3920	mgVSS/ℓ
$S_{ti,BT}$	746.9	mgCOD/ℓ	LR	0.572	mgCOD/mgVSS

Plot K1 End Time: **Plot K1-NO2 Max:** Sbsi (0.67) mgCOD/ℓ

End Time	Y (K1 End)	X Range	Y (NO2)	58.70
3.5	0.00	0	**0.05**	f_{ts}
3.5	22.50	12	*0.05*	0.079

Define NU (mgN/ℓ):

Y-int K1	Y-int K2	ΔNO_3	NO_2-Corrected NU (mgN/ℓ)
28.363	21.56	6.803	**6.773**

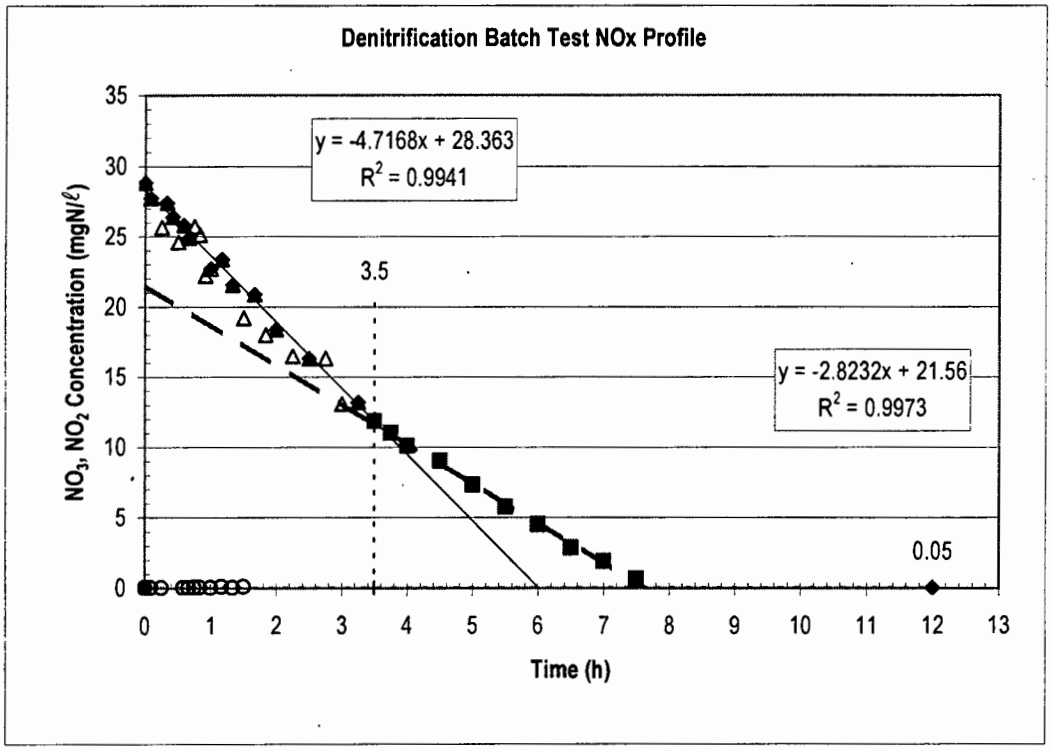

NOTE:

NO3 and NO2 concentrations determined by ion chromatography; concentrations reported in mgNO3/l and mgNO2/l units, respectively - a correction factor is applied to convert IC values to "equivalent" Auto-Analyzer values in mgN/l units, based on IC values obtained for standard NO3 and NO2 solutions; i.e.: NO3: AA equivalent (as mgN/ℓ) = 0.2534*IC (as mgNO3/ℓ)
NO2: AA equivalent (as mgN/ℓ) = 0.2591*IC (as mgNO3/ℓ)

STANDARD VALUES:

Standard NO3 (mgN/ℓ)	Standard NO2 (mgN/ℓ)	IC - NO3 mgNO3/ℓ	mgN/ℓ	IC - NO2 mgNO2/ℓ	mgN/ℓ
0.25	0.1	1.060	0.239	0.040	0.009
0.5	0.2	1.830	0.413	0.910	0.205
0.75	0.3	2.740	0.619	1.070	0.242
1	0.4	3.860	0.872	1.490	0.336
1.25	0.5	7.780	1.757	1.860	0.420
1.5	0.6	6.010	1.357	2.300	0.519
1.75	0.7	6.720	1.517	2.780	0.628
2	0.8	8.120	1.834	4.270	0.964

	ML	SB	Date	DBT
Batch Test Composition:	MLE	23	17.11.02	37

V_{BT} 3 ℓ

V_{WW}	2	ℓ	V_{ML}	1	ℓ
S_{ti}	971.9	mgCOD/ℓ	X_v	3462	mgVSS/ℓ
$S_{ti,BT}$	647.9	mgCOD/ℓ	LR	0.561	mgCOD/mgVSS

Plot K1 End Time:

End Time	Y (K1 End)
5.25	0.00
5.25	25.00

Plot K1-NO2 Max:

X Range	Y (NO2)
0	**1.1**
12	*1.1*

Sbsi (0.67) mgCOD/ℓ 71.08

f_{ts} 0.110

Define NU (mgN/ℓ):

Y-int K1	Y-int K2	ΔNO_3	NO_2-Corrected NU (mgN/ℓ)
35.727	26.865	8.862	**8.202**

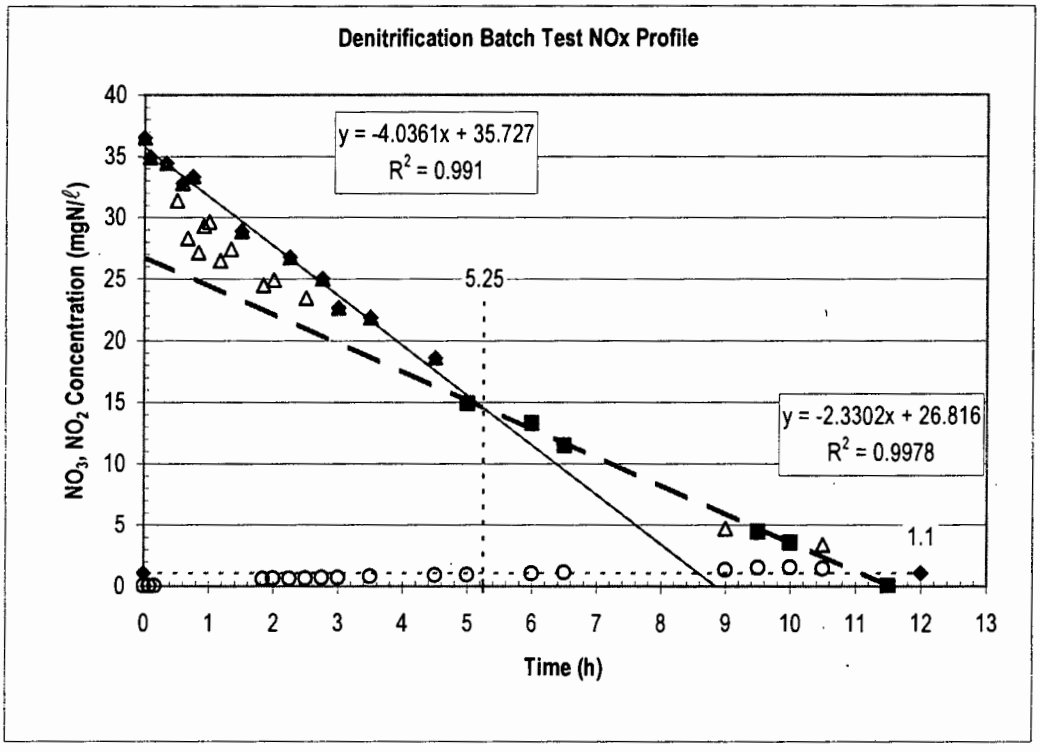

NOTE:

NO3 and NO2 concentrations determined by ion chromatography; concentrations reported in mgNO3/l and mgNO2/l units, respectively - a correction factor is applied to convert IC values to "equivalent" Auto-Analyzer values in mgN/l units, based on IC values obtained for standard NO3 and NO2 solutions; i.e.: NO3: AA equivalent (as mgN/ℓ) = 0.2534*IC (as mgNO3/ℓ)
NO2: AA equivalent (as mgN/ℓ) = 0.2591*IC (as mgNO3/ℓ)

STANDARD VALUES:

Standard NO3 (mgN/ℓ)	Standard NO2 (mgN/ℓ)	IC - NO3 mgNO3/ℓ	mgN/ℓ	IC - NO2 mgNO2/ℓ	mgN/ℓ
0.25	0.1	1.060	0.239	0.040	0.009
0.5	0.2	1.830	0.413	0.910	0.205
0.75	0.3	2.740	0.619	1.070	0.242
1	0.4	3.860	0.872	1.490	0.336
1.25	0.5	7.780	1.757	1.860	0.420
1.5	0.6	6.010	1.357	2.300	0.519
1.75	0.7	6.720	1.517	2.780	0.628
2	0.8	8.120	1.834	4.270	0.964

	ML	SB	Date	DBT
Batch Test Composition:	MLE	Acetate	7.12.02	38

V_{BT} 2.875 ℓ

V_{Ac}	25	mℓ	V_{ML}	3	ℓ
Ac_{ti}	1967.6	mgCOD/ℓ	X_v	1589	mgVSS/ℓ
$Ac_{ti,BT}$	17.1	mgCOD/ℓ	LR	0.011	mgCOD/mgVSS

Plot K1 End Time:

End Time	Y (K1 End)
1.55	0.00
1.55	43.00

Plot K1-NO2 Max:

X Range	Y (NO2)
0	**1.95**
3.25	*1.95*

Define NU (mgN/ℓ):

Y-int K1	Y-int K2	ΔNO_3	NO_2-Corrected NU (mgN/ℓ)	$Y_{H,NO}$ (COD/COD)
40.407	36.635	3.772	**2.602**	**0.565**

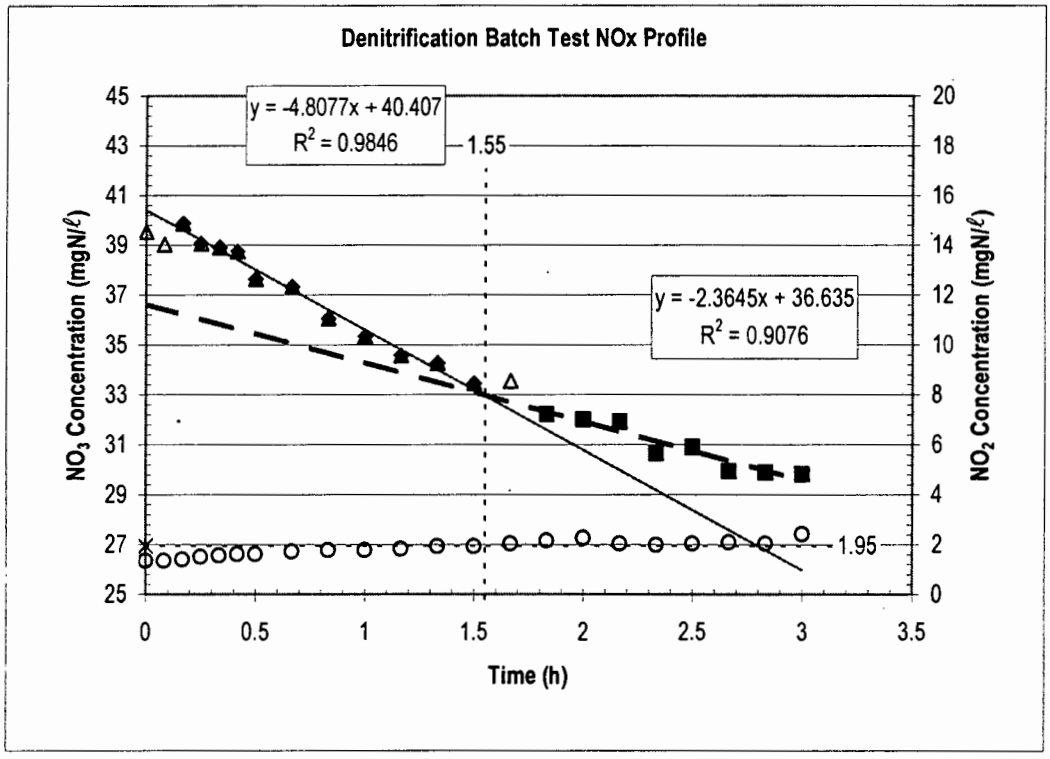

	ML	SB	Date	DBT
Batch Test Composition:	MLE	Acetate	8.12.02	39

V_{BT} 2.94 ℓ

V_{Ac}	25	mℓ	V_{ML}	3	ℓ
Ac_{ti}	2201.5	mgCOD/ℓ	X_v	1479	mgVSS/ℓ
$Ac_{ti,BT}$	18.7	mgCOD/ℓ	LR	0.013	mgCOD/mgVSS

Plot K1 End Time:

End Time	Y (K1 End)
0.825	0.00
0.825	43.50

Plot K1-NO2 Max:

X Range	Y (NO2)
0	**1.18**
3.25	*1.18*

Define NU (mgN/ℓ):

Y-int K1	Y-int K2	ΔNO_3	NO_2-Corrected NU (mgN/ℓ)	$Y_{H,NO}$ (COD/COD)
45.268	41.537	3.731	**3.023**	**0.538**

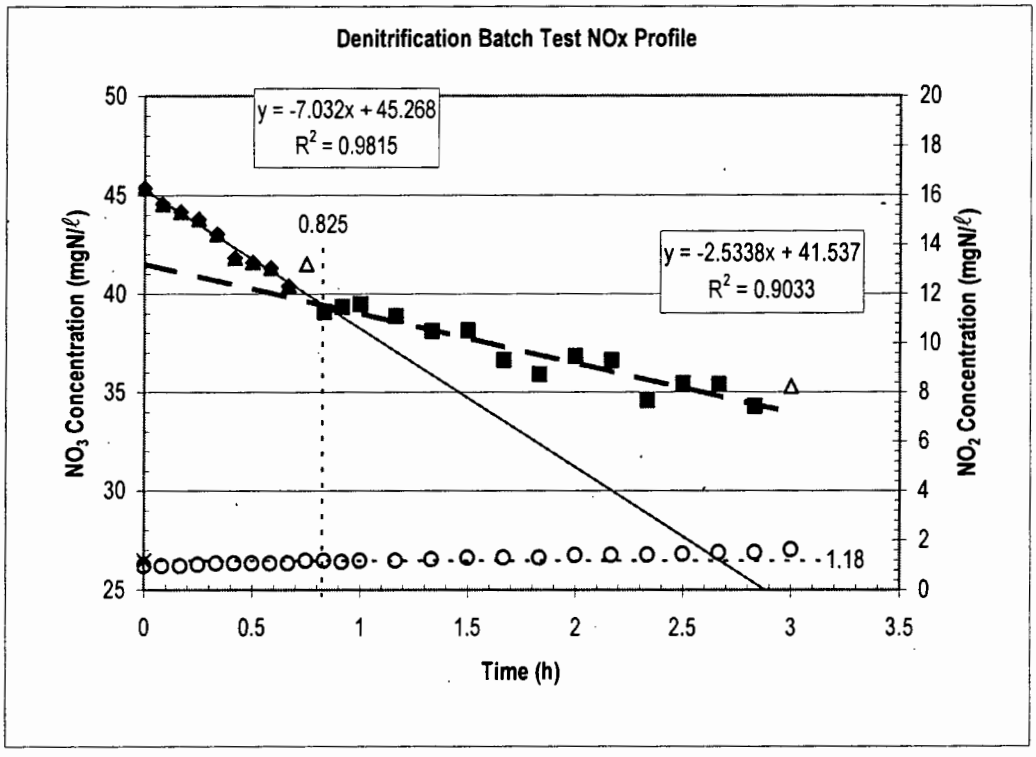

	ML	SB	Date	DBT
Batch Test Composition (a):	MLE	Acetate	10.12.02	40(a)

V_{BT} 2.96 ℓ

V_{Ac}	25	mℓ	V_{ML}	3	ℓ
Ac_{ti}	2224	mgCOD/ℓ	X_v	1573	mgVSS/ℓ
$Ac_{ti,BT}$	18.8	mgCOD/ℓ	LR	0.012	mgCOD/mgVSS

Plot K1 End Time:

End Time	Y (K1 End)
0.7	0.00
0.7	40.00

Plot K1-NO2 Max:

X Range	Y (NO2)
0	**0.81**
3.25	*0.81*

Define NU (mgN/ℓ):

Y-int K1	Y-int K2	ΔNO_3	NO_2-Corrected NU (mgN/ℓ)	$Y_{H,NO}$ (COD/COD)
39.327	36.383	2.944	**2.458**	**0.626**

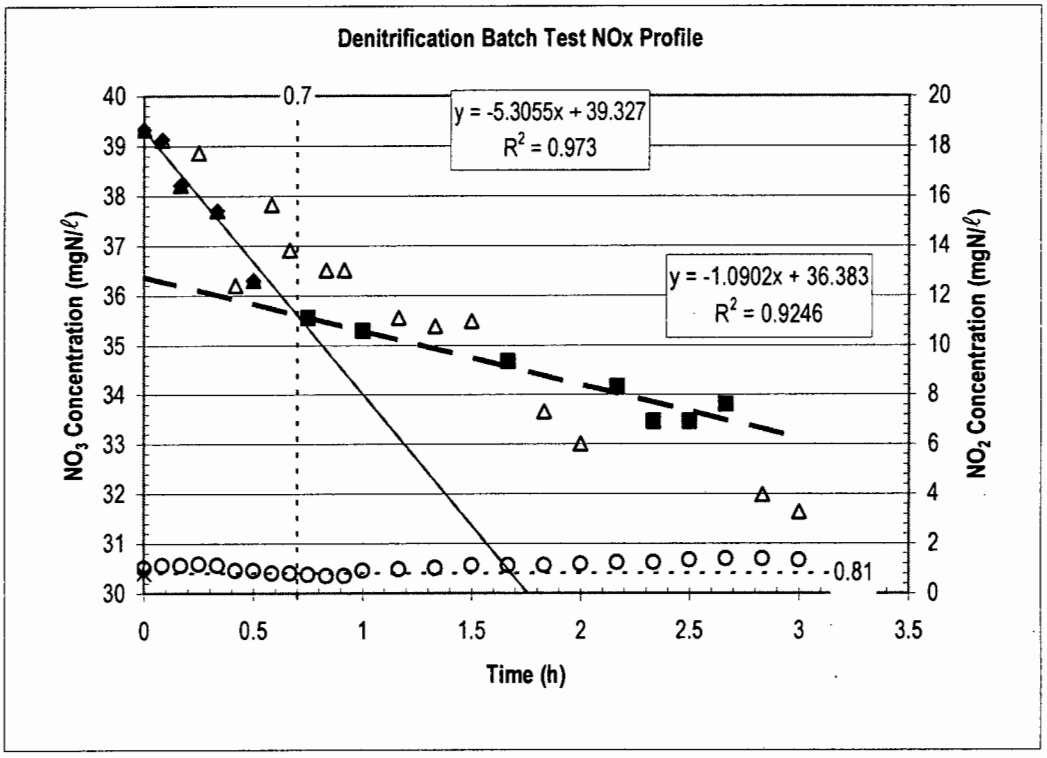

C3.40(b)

	ML	SB	Date	DBT
Batch Test Composition (a):	MLE	Acetate	10.12.02	40(b)

V_{BT}	2.465	ℓ			
V_{Ac}	25	mℓ	V_{ML}	3	ℓ
Ac_{ti}	2224	mgCOD/ℓ	X_v	1573	mgVSS/ℓ
$Ac_{ti,BT}$	22.6	mgCOD/ℓ	LR	0.014	mgCOD/mgVSS

Plot K1 End Time:

End Time	Y (K1 End)
0.71	0.00
0.71	33.00

Plot K1-NO2 Max:

X Range	Y (NO2)
0	**1.12**
3.25	*1.12*

	Y-int
K1	32.051
K2	28.756
ΔNO_3	3.295
NO_2-Corrected NU (mgN/ℓ)	**2.623**
$Y_{H,NO}$ (mgCOD/mgCOD)	**0.667**

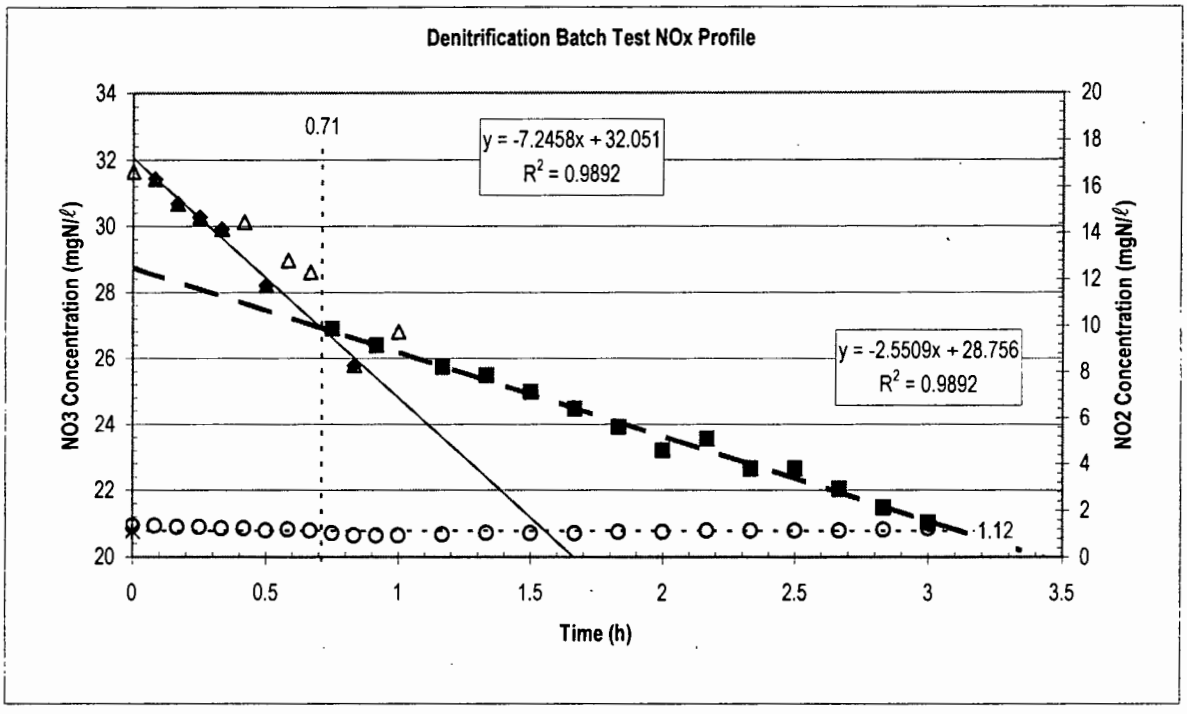

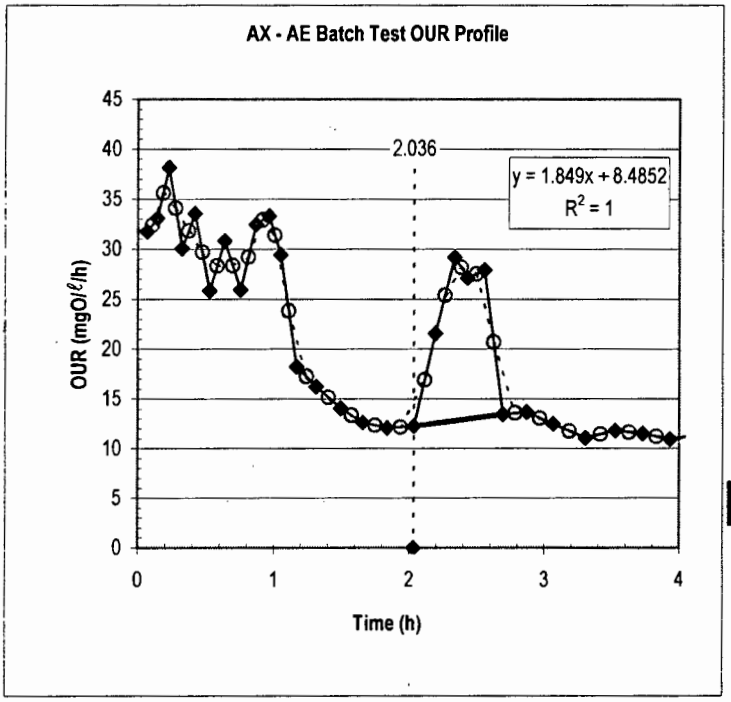

Ac COD	2224	mgCOD/ℓ
	Ac1	
V_{Ac} (mℓ)	25	
V_{BT} (ℓ)	1.95	
$[Ac_{COD}]_{BT}$	28.51	
OU (mgO/ℓ)	**6.55**	
$Y_{H,AE\ (COD)}$	**0.770**	

Plot Ac Baselines:

t	Ac1	
2.036	12.25	1.849
2.696	13.47	8.4852

$Y_{H,NO}$:$Y_{H,AE}$ Ratio	**0.866**

	ML	SB	Date	DBT
Batch Test Composition (a):	MLE	Acetate	10.12.02	40 a & b

V_{BT} ℓ

V_{Ac}	mℓ	V_{ML}	ℓ
Ac_{ti}	mgCOD/ℓ	X_v	mgVSS/ℓ
$Ac_{ti,BT}$	mgCOD/ℓ	LR	mgCOD/mgVSS

Plot K1 End Time:

End Time	Y (K1 End)
0.7	20.00
0.7	40.00

Plot K1-NO2 Max:

X Range	Y (NO2)
0	**0.9**
2	*0.9*

Batch Test Composition (b):

V_{BT} ℓ

V_{Ac}	mℓ	V_{ML}	ℓ
Ac_{ti}	mgCOD/ℓ	X_v	mgVSS/ℓ
$Ac_{ti,BT}$	mgCOD/ℓ	LR	mgCOD/mgVSS

Plot K1 End Time:

End Time	Y (K1 End)
3.88	20.00
3.88	32.50

Plot K1-NO2 Max:

X Range	Y (NO2)
0	**1.13**
7.5	*1.13*

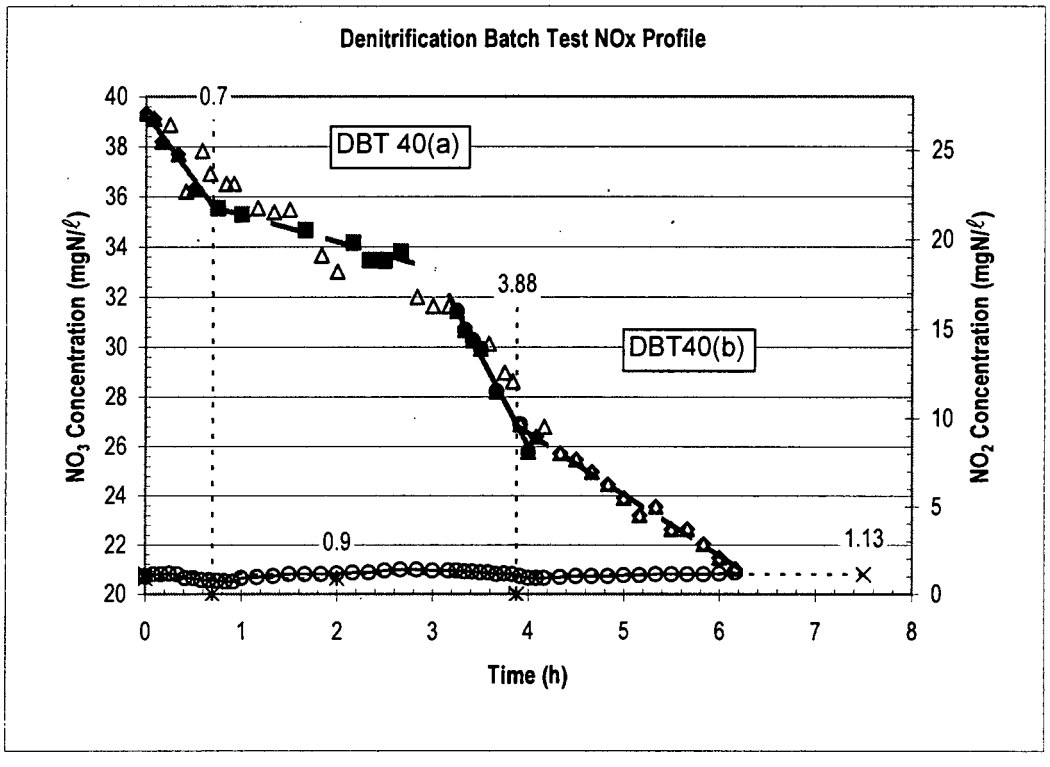

	ML	SB	Date	DBT
Batch Test Composition (a):	MLE	Acetate	14.12.02	41

V_{BT}	3	ℓ			
V_{Ac}	25	mℓ	V_{ML}	3	ℓ
Ac_{ti}	2540	mgCOD/ℓ	X_v	1302	mgVSS/ℓ
$Ac_{ti,BT}$	21.2	mgCOD/ℓ	LR	0.016	mgCOD/mgVSS

Plot K1 End Time:

End Time	Y (K1 End)
0.8	0.00
0.8	45.00

Plot K1-NO2 Max:

X Range	Y (NO2)
0	**1.06**
3.25	*1.06*

	Y-int
K1	43.674
K2	40.138
ΔNO_3	3.536
NO_2-Corrected NU (mgN/ℓ)	**2.900**
$Y_{H,NO}$ (mgCOD/mgCOD)	**0.608**

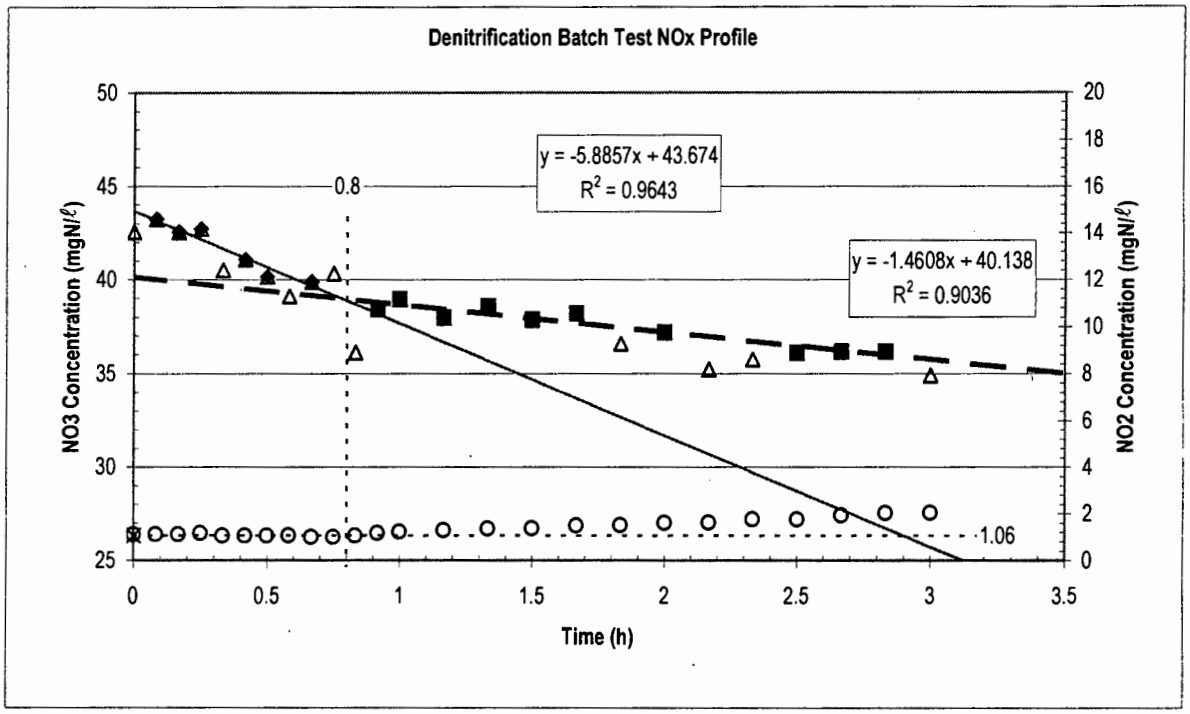

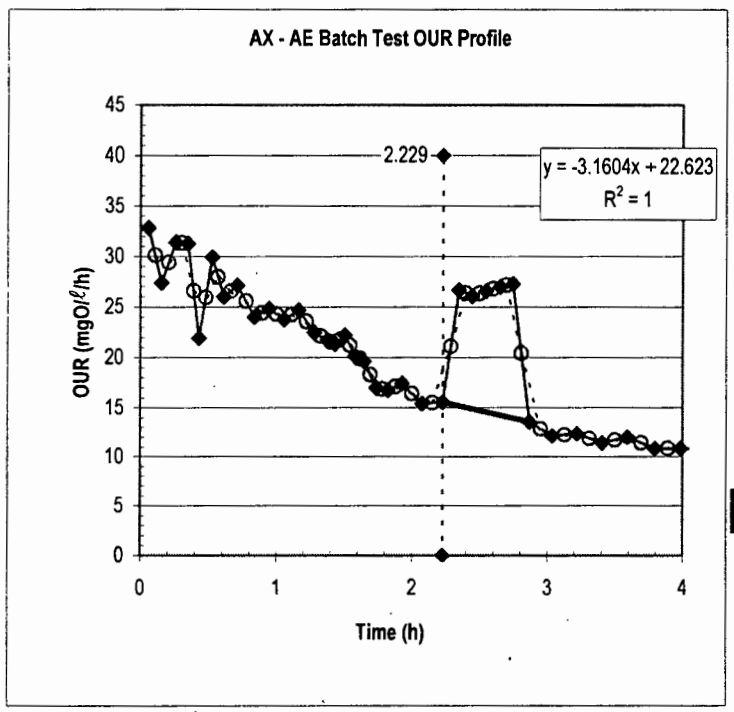

Ac COD	2540	mgCOD/ℓ
	Ac1	
V_{Ac} (mℓ)	25	
V_{BT} (ℓ)	2.49	
$[Ac_{COD}]_{BT}$	25.50	
OU (mgO/ℓ)	**6.70**	
$Y_{H,AE\ (COD)}$	**0.737**	

Plot Ac Baselines:

t	Ac1	
2.229	15.58	-3.1604
2.868	13.56	22.623

$Y_{H,NO}$:$Y_{H,AE}$ Ratio	**0.825**

	ML	SB	Date	DBT
Batch Test Composition (a):	MLE	Acetate	16.12.02	42

V_{BT}	3	ℓ			
V_{Ac}	25	mℓ	V_{ML}	3	ℓ
Ac_{ti}	2556	mgCOD/ℓ	X_v	1485	mgVSS/ℓ
$Ac_{ti,BT}$	21.3	mgCOD/ℓ	LR	0.014	mgCOD/mgVSS

Plot K1 End Time:

End Time	Y (K1 End)
1.18	0.00
1.18	30.00

Plot K1-NO2 Max:

X Range	Y (NO2)
0	**1.45**
3.25	*1.45*

	Y-int
K1	31.955
K2	28.015
ΔNO_3	3.940
NO_2-Corrected NU (mgN/ℓ)	**3.070**
$Y_{H,NO}$ (mgCOD/mgCOD)	**0.588**

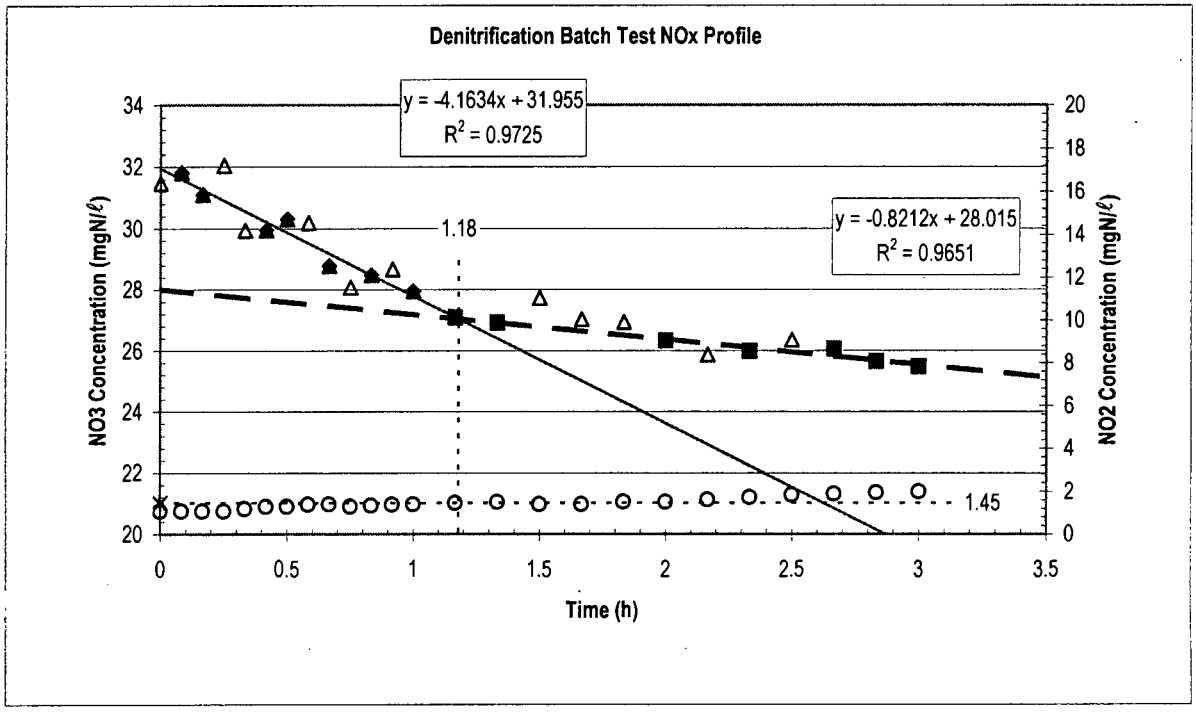

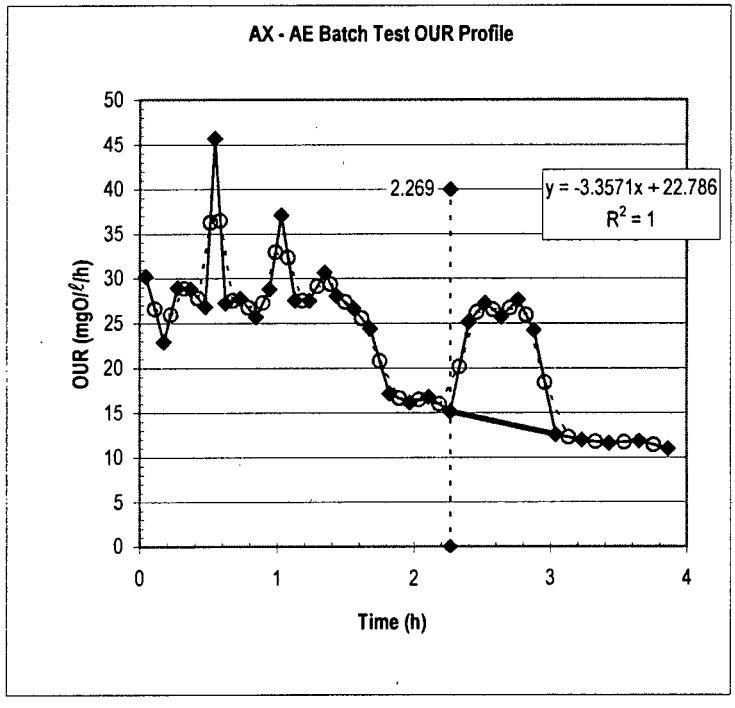

Ac COD	2556	mgCOD/ℓ
	Ac1	
V_{Ac} (mℓ)	25	
V_{BT} (ℓ)	2.49	
$[Ac_{COD}]_{BT}$	25.66	
OU (mgO/ℓ)	**7.72**	
$Y_{H,AE\ (COD)}$	**0.699**	

Plot Ac Baselines:

t	Ac1	
2.269	15.17	-3.357
3.040	12.58	22.786

$Y_{H,NO}$:$Y_{H,AE}$ Ratio	**0.840**

APPENDIX D

CONCENTRATED SODIUM ACETATE STOCK SOLUTION AND STATISTICAL F- AND STUDENT t-TESTS

TABLE OF CONTENTS

APPENDIX D-1

CALCULATION OF THEORETICAL COD AND CORRESPONDING CONCENTRATION OF SODIUM ACETATE STOCK SOLUTION REQUIRED

APPENDIX D-1

CALCULATION OF THEORETICAL COD AND CORRESPONDING CONCENTRATION OF SODIUM ACETATE STOCK SOLUTION REQUIRED

A concentrated sodium acetate stock solution was used for adding known quantities of artificial readily biodegradable (RB)COD to aerobic and anoxic batch tests, for direct determination of the ordinary heterotrophic organism (OHO) aerobic ($Y_{H,AE}$) and anoxic ($Y_{H,NO}$) cell yields. The theoretical COD calculation and corresponding acetate solution concentration are described below.

D1.1 ACETATE STOCK SOLUTION THEORETICAL COD AND CONCENTRATION

A concentrated stock solution of sodium acetate (CH_3COONa) was prepared by dissolving 3.908g sodium acetate (CH_3COONa) in 1ℓ of distilled water, to achieve a target theoretical COD ("$COD_{Th.}$") of 3000 mgCOD/ℓ in the stock solution. The theoretical COD of the solution is estimated as follows: Accepting that sodium acetate ("Ac", CH_3COONa) ionises in water to form acetic acid (CH_3COO^-), the theoretical chemical oxidation reactions indicate that 1 mole of acetate (CH_3COOH) requires ("demands") 2 moles of oxygen (O_2), i.e.:

$$CH_3COONa \rightarrow CH_3COO^- + Na^+$$
$$CH_3COO^- + H^+ \rightarrow CH_3COOH$$

where:

$$CH_3COOH + 2H_2O \rightarrow 2CO_2 + 8H^+ + 8e^-$$
$$2O_2 + 8H^+ + 8e^- \rightarrow 4H_2O$$
$$\Rightarrow \quad CH_3COOH + 2O_2 \rightarrow 2CO_2 + 2H_2O$$

Therefore, given the molecular weights (in g/mol) for CH_3COOH = 60, O_2 = 32, CH_3COO^- = 59 and CH_3COONa = 82:

$\Rightarrow$ 1 mole CH_3COOH has a (theoretical) oxygen demand of 2 moles O_2; which, equivalently can be expressed as:

$\Rightarrow$ $1mol*60g.mol^{-1}$ Ac requires $2mol*32g.mol^{-1}$ $COD_{Th.}$

$\Rightarrow$ $COD_{Th.} = (64/60)*mgAc/\ell \equiv \underline{1.067*mgAc/\ell}$

Therefore, for an acetate solution with a target $COD_{Th.}$ of 3000 mgCOD/ℓ, a solution of 3000/1.067 = 2812 mgAc/ℓ is required; which is equivalent to a sodium acetate solution of 2812/(59/82) = 3908 mgCH_3COONa/ℓ.

APPENDIX D-2

STATISTICAL F- AND STUDENT t-TESTS APPLIED TO ANOXIC YIELD ESTIMATES OBTAINED IN PERIOD I WITH SEWAGE BATCH 11

APPENDIX D-2

STATISTICAL F- AND STUDENT t-TESTS APPLIED TO ANOXIC YIELD ESTIMATES OBTAINED IN PERIOD I WITH SEWAGE BATCH 11

To determine whether or not two data sets originate from two different data populations, the Student t-Test is used to compare the means of the two populations (Underhill and Bradfield, 1996): if the means are equal, then the two data sets originate from the same population and can be pooled (grouped); however, if the means are not equal, then the two data sets originate from different populations and must be treated separately. The application of the Student t-Test to two apparent data sets observed for anoxic yield ($Y_{H,NO}$) estimates using sewage batch (SB) 11 in Period I, is analysed here.

D2.1 F-TEST: TESTING THE ASSUMPTION THAT THE TWO APPARENT DATA SETS IN SEWAGE BATCH 11 HAVE EQUAL VARIANCE

In the Student t-Test it is assumed that the variances of the two populations are equal; this assumption must be tested using the F-Test, see Underhill and Bradfield (1996) for detailed descriptions of the F- and t-Test methods.

The two apparent data sets observed in the $Y_{H,NO}$ estimations using sewage batch (SB) 11 are shown in Fig. D2-1 below.

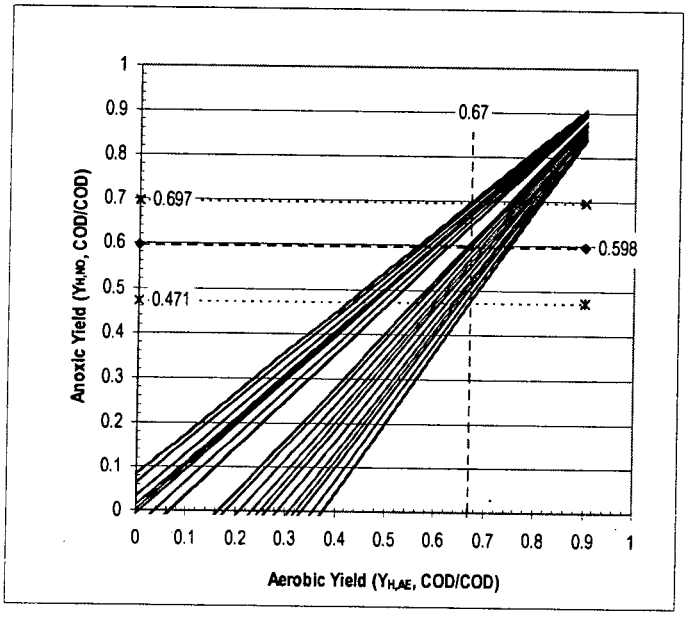

Fig. D2-1: Period I: Plot of $Y_{H,NO}$ in terms of $Y_{H,AE}$ for OU-NU combinations from respective aerobic and anoxic batch tests using sewage batch (SB) 11.

The two data sets are separated by calculating $Y_{H,NO}$ for each aerobic-anoxic batch test ("ABT-DBT", i.e. OU and NU respectively) combination, with respect to the "standard" aerobic yield value of $Y_{H,AE}$ = 0.67 mgCOD/mgCOD. These $Y_{H,NO}$ estimates are then ranked in ascending order while retaining the corresponding ABT-DBT index for each. By inspection, data set one is selected for all $Y_{H,NO}$ estimates ≤ 0.604 mgCOD/mgCOD, while data set 2 comprises the remainder, i.e. $Y_{H,NO}$ > 0.604 mgCOD/mgCOD; the two data sets, "1" and "2" respectively, are described in Table D2-1.

Table D2-1: Sewage batch (SB) 11 data analysis: Two data sets (1 and 2) separated by ranking $Y_{H,NO}$ estimates for each ABT-DBT (i.e. OU and NU respectively) combination using $Y_{H,AE}$ = 0.67 mgCOD/mgCOD. Also shown are: sample standard deviation (SSD), sample mean, number of data (N) and sample degrees of freedom (Deg. f).

SB 11: DATA SET 1		**SB 11: DATA SET 2**	
ABT-DBT Combination	**$Y_{H,NO}$ (mgCOD/mgCOD)**	**ABT-DBT Combination**	**$Y_{H,NO}$ (mgCOD/mgCOD)**
16-14	0.471	16-18	0.646
15-14	0.488	15-18	0.657
14-14	0.504	14-18	0.668
17-14	0.513	16-17	0.671
18-14	0.513	17-18	0.674
16-16	0.523	18-18	0.674
15-16	0.538	15-17	0.681
14-16	0.552	14-17	0.691
17-16	0.561	17-17	0.697
18-16	0.561	18-17	0.697
16-15	0.570		
15-15	0.584		
14-15	0.597		
17-15	0.604		
18-15	0.604		
SSD1	0.042484	**SSD2**	0.0167345
N1	15	**N2**	10
Deg. f1	14	**Deg. f2**	9
Mean1	0.546	**Mean2**	0.676

In the F-Test, for data sets "1" and "2" above, we are testing the null hypothesis ("H_0") $\sigma_1^2 = \sigma_2^2$ against the alternative hypothesis ("H_1") $\sigma_1^2 \neq \sigma_2^2$, where σ is the population standard deviation, approximated for each corresponding data set ("sample") by the *sample* standard deviation (SSD), and σ^2 is the population variance; correspondingly, approximated by SSD^2. The test statistic (F) is given by the ratio:

$$F = \frac{SSD_1^2}{SSD_2^2} \tag{D2.1}$$

By definition F is always positive, so that when H_0 is true (i.e. $\sigma_1^2 = \sigma_2^2$), we expect F ~1, and conversely, when H_0 is false (i.e. $\sigma_1^2 \neq \sigma_2^2$), we expect F to be either too large or too small (close to zero). The rejection region is obtained from published F-tables, and H_0 is rejected (i.e. false) if the observed F-value ("F_{obs}") exceeds the published (tabulated) F-table ("F_{tab}") value.

For the two data sets identified in Table D2-1 above, the observed and tabled F-values, at the 5% significance level (95% of the data), are given by F_{obs} and $F^{\text{significance level, \%}}_{\text{Deg. f1, Deg. f2}}$ ($\equiv F_{tab}$) respectively, i.e.:

$$F_{obs} = \frac{SSD_1^2}{SSD_2^2} = \frac{0.0425^2}{0.0167^2} = 6.445 \tag{D2.2}$$

and:

$$F_{14,9}^{0.025} = 3.43 = \text{"}F_{tab}\text{"} \tag{D2.3}$$

Since $F_{obs} = 6.445$ is $> F_{tab} = 3.43 \Rightarrow H_o$ is rejected; i.e. the population variances corresponding to data sets 1 and 2 are not equal (i.e. $\sigma_1^2 \neq \sigma_2^2$), and consequently, the Student t-Test cannot be used. In such cases, i.e. when the population variances cannot be assumed to be equal, an "approximate" t-Test that approximates the t-distribution, can be used (Underhill and Bradfield, 1996).

D2.2 THE APPROXIMATE t-TEST: COMPARING THE POPULATION MEANS OF DATA SETS 1 AND 2

In the approximate t-Test (as in the normal t-Test), for data sets "1" and "2", we are testing the null hypothesis (H_0) $\mu_1 = \mu_2$ against the alternative hypothesis (H_1) $\mu_1 \neq \mu_2$, where μ is the mean of the respective data populations, approximated by "Mean" for the corresponding data sets in Table D2-1. The test statistic for the approximate t-Test is given by "t*" below, where N is the number of data points in the respective data sets (other variables are as defined previously).

$$t^* = \frac{(Mean_1 - Mean_2) - (\mu_1 - \mu_2)}{\sqrt{\frac{SSD_1^2}{N_1} + \frac{SSD_2^2}{N_2}}} \tag{D2.4}$$

Since the population variances cannot be pooled as in the normal t-Test, instead the degrees of freedom (Deg.f*) are adjusted ("lumped") according to Eq.(D2.5); non-integer estimates are rounded to the nearest integer. The value for the test statistic is then obtained by interpolation from published t-Test tables (i.e. "t_{tab}"), using the adjusted degrees of freedom.

$$\text{Deg.f}^* = \left\{ \frac{\left(\frac{SSD_1^2}{N_1} + \frac{SSD_2^2}{N_2} \right)^2}{\frac{\left(\frac{SSD_1^2}{N_1} \right)^2}{N_1 + 1} + \frac{\left(\frac{SSD_2^2}{N_2} \right)^2}{N_2 + 1}} \right\} - 2 \qquad \text{(D2.5)}$$

For the two data sets identified in Table D2-1 above, the observed and published t-values, at the 5% significance level (95% of the data), are t_{obs} and $t_{Deg.f^*}^{significancelevel,\%}$ ($\equiv t_{tab}$) respectively, where:

$$t_{obs} \equiv t^* = -3.07$$

and:

$$\text{Deg.f}^* = 20.5 \approx 21$$
$$\Rightarrow t_{21}^{0.025} = 2.08 = \text{“}t_{tab}\text{”}$$

Since $t_{obs} = -3.07$ is outside the interval $t_{tab} = \pm 2.08$ (i.e. $t_{obs} = -3.07$ is < -2.08), $\Rightarrow H_o$ is rejected, i.e. the population means corresponding to data sets 1 and 2 are not equal (i.e. $\mu_1 \neq \mu_2$), and consequently, the two data sets in Table D2-1 originate from different data populations and must, therefore, be analysed separately.

D2.3 RESULT OF F- AND t-TEST ANALYSES ON SEWAGE BATCH 11 DATA

Reviewing the data in Table D2-1, it is apparent that all the $Y_{H,NO}$ estimates in data set 2 are formed by OU-NU combinations corresponding with the NU from DBT 17 and 18. It is reasonable to assume, therefore, that DBT 17 and 18 were each influenced by a single dominant factor, and, therefore, cannot be accepted as representative of the same batch test conditions as the other batch tests also using SB 11. Consequently, DBT 17 and 18 were rejected from further analysis. Also, since the aerobic and anoxic batch tests in Period I were performed in parallel on the same day, composed of the same wastewater and mixed-liquor samples, it was assumed that ABT 17 and 18 were subject to the same influences and conditions as DBT 17 and 18; therefore, the corresponding aerobic batch tests, ABT 17 and 18, were also rejected from further analysis. On this basis, the $Y_{H,NO}$ estimates from corresponding OU-NU combinations with SB 11 are re-analysed, excluding ABT and DBT 17 and 18.

F- AND t-TEST ANALYSES FOR TWO APPARENT DATA SETS IN $Y_{H,NO}$ wrt $Y_{H,AE}$ = 0.67 COD/COD FOR SEWAGE BATCH 11, PERIOD I.

Un-sorted data:	
OU-NU	$Y_{H,NO}$
14-14	0.504
14-15	0.597
14-16	0.552
14-17	0.691
14-18	0.668
15-14	0.488
15-15	0.584
15-16	0.538
15-17	0.681
15-18	0.657
16-14	0.471
16-15	0.570
16-16	0.523
16-17	0.671
16-18	0.646
17-14	0.513
17-15	0.604
17-16	0.561
17-17	0.697
17-18	0.674
18-14	0.513
18-15	0.604
18-16	0.561
18-17	0.697
18-18	0.674
Avg	0.598
Stdev	0.073382
Upper	0.741469
Lower	0.453812
Count	25

Sorted data	
OU-NU	$Y_{H,NO}$
16-14	*0.471*
15-14	*0.488*
14-14	*0.504*
17-14	*0.513*
18-14	*0.513*
16-16	*0.523*
15-16	*0.538*
14-16	*0.552*
17-16	*0.561*
18-16	*0.561*
16-15	*0.570*
15-15	*0.584*
14-15	*0.597*
17-15	*0.604*
18-15	*0.604*
16-18	0.646
15-18	0.657
14-18	0.668
16-17	0.671
17-18	0.674
18-18	0.674
15-17	0.681
14-17	0.691
17-17	0.697
18-17	0.697
Avg	0.598
Stdev	0.073382
Upper	0.741469
Lower	0.453812
Count	25

Data Set 1	
OU-NU	$Y_{H,NO}$
16-14	*0.471*
15-14	*0.488*
14-14	*0.504*
17-14	*0.513*
18-14	*0.513*
16-16	*0.523*
15-16	*0.538*
14-16	*0.552*
17-16	*0.561*
18-16	*0.561*
16-15	*0.570*
15-15	*0.584*
14-15	*0.597*
17-15	*0.604*
18-15	*0.604*
SSD1	0.042484
count1	15
deg f1	14
Mean1	0.546

Data Set 2	
OU-NU	$Y_{H,NO}$
16-18	0.646
15-18	0.657
14-18	0.668
16-17	0.671
17-18	0.674
18-18	0.674
15-17	0.681
14-17	0.691
17-17	0.697
18-17	0.697
SSD2	0.0167345
count2	10
def f2	9
Mean2	0.676

F-test to check if two sample sets have same variances:

degf-numerator 14
degf-denominator 9
Ftable(2.5%) 3.43 Enter Table value here:
Fobs 6.4449762

Reject F-test Ho!
i.e. Fobs > Ftable => var1 <> var2 => cannot pool SSD's,
=> Must use approx. t-Test!

Normal t-Test to check if two sample sets have the same mean:

pooled var. = 0.0141952
pooled SSD = 0.1191437
pooled degf ("n") = 21.00
t-table(n, 2.5%) = 2.08 Enter Table value here:
tobs = -2.673324

Reject t-Test Ho! tobs<-t-table
=> Mean1 <> Mean2 Different Data Populations!

Approximate t-Test (by approximating the deg f):

degfapprox = 21 20.54
t-table(n, 2.5%) = 2.08 Enter Table value here:
approx. tobs = -3.07017

Reject t-Test Ho! tobs<-t-table
=> Mean1 <> Mean2 Different Data Populations!

APPENDIX E

EVALUATION OF EXPERIMENTAL DATA BY OTHER INVESTIGATIONS

TABLE OF CONTENTS

APPENDIX E-1

EXPERIMENTAL DATA BY WILSON, DAVID E. (1976)

ML	SB	Date	WSS No.
W	W	Jul-76	7

Influent RBCOD Concentration:

Avg f_{ts}	0.086	CFWWTP	S_{ti}	465	mgCOD/ℓ
a-Recycle	5	ratio a:Q_i	$S_{ti,BT}$	6.67	mgCOD/ℓ

Define NU ($mgNO_3$-N/ℓ):

	Y-int			
K1	6.8865			
K2	5.7014	$Y_{H,NO}$ =	**0.491**	mgCOD/mgCOD
ΔNO_3	1.19	$Y_{H,NO}$:$Y_{H,AE}$ =	**0.734**	($Y_{H,AE}$ = 0.67 COD/COD)

Plot K1 End Time:

End Time	Y (K1 End)
4.125	0.00
4.125	6.25

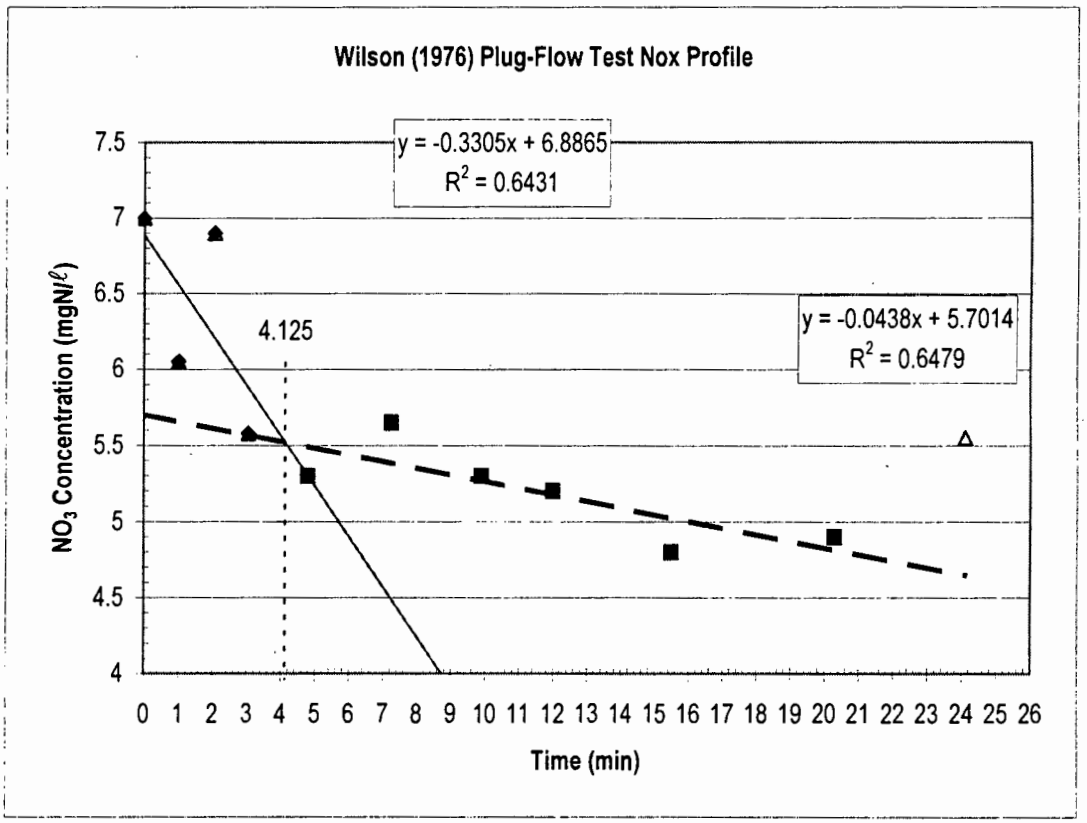

ML	SB	Date	WSS No.
W	W	Jul-76	1

Influent RBCOD Concentration:

Avg f_{ts}	0.086	CFWWTP	S_{ti}	480	mgCOD/ℓ
a-Recycle	5	ratio a:Q_i	$S_{ti,BT}$	6.88	mgCOD/ℓ

Define NU (mgNO$_3$-N/ℓ):

	Y-int
K1	9.3675
K2	8.4569
ΔNO_3	0.91

$Y_{H,NO}$ = **0.621** mgCOD/mgCOD

$Y_{H,NO}$:$Y_{H,AE}$ = **0.928** ($Y_{H,AE}$ = 0.67 COD/COD)

Plot K1 End Time:

End Time	Y (K1 End)
6.55	0.00
6.55	9.00

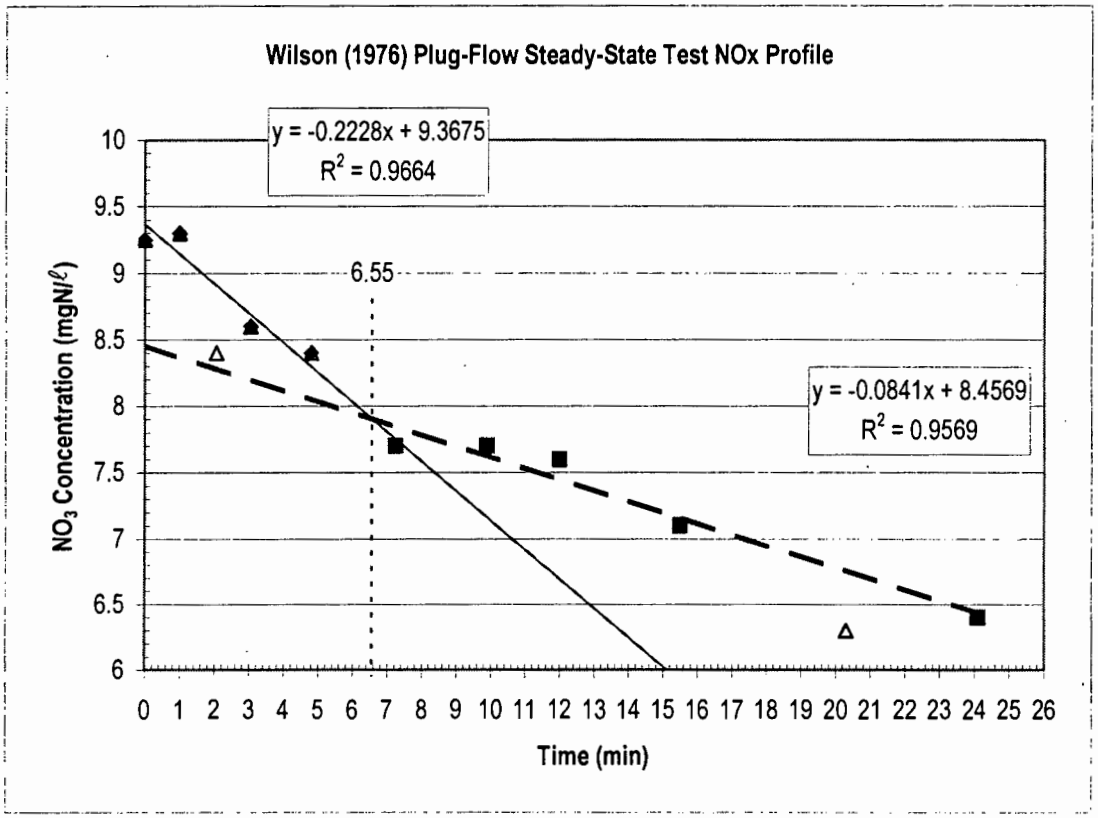

ML	SB	Date	WSS No.
W	W	Jul-76	2

Influent RBCOD Concentration:

Avg f_{ts}	0.086	CFWWTP	S_{ti}	427	mgCOD/ℓ
a-Recycle	5	ratio a:Q_i	$S_{ti,BT}$	6.12	mgCOD/ℓ

Define NU (mgNO$_3$-N/ℓ):

	Y-int			
K1	7.5426			
K2	6.3727	$Y_{H,NO}$ =	**0.453**	mgCOD/mgCOD
ΔNO_3	1.17	$Y_{H,NO}$:$Y_{H,AE}$ =	**0.677**	($Y_{H,AE}$ = 0.67 COD/COD)

Plot K1 End Time:

End Time	Y (K1 End)
10.55	0.00
10.55	7.25

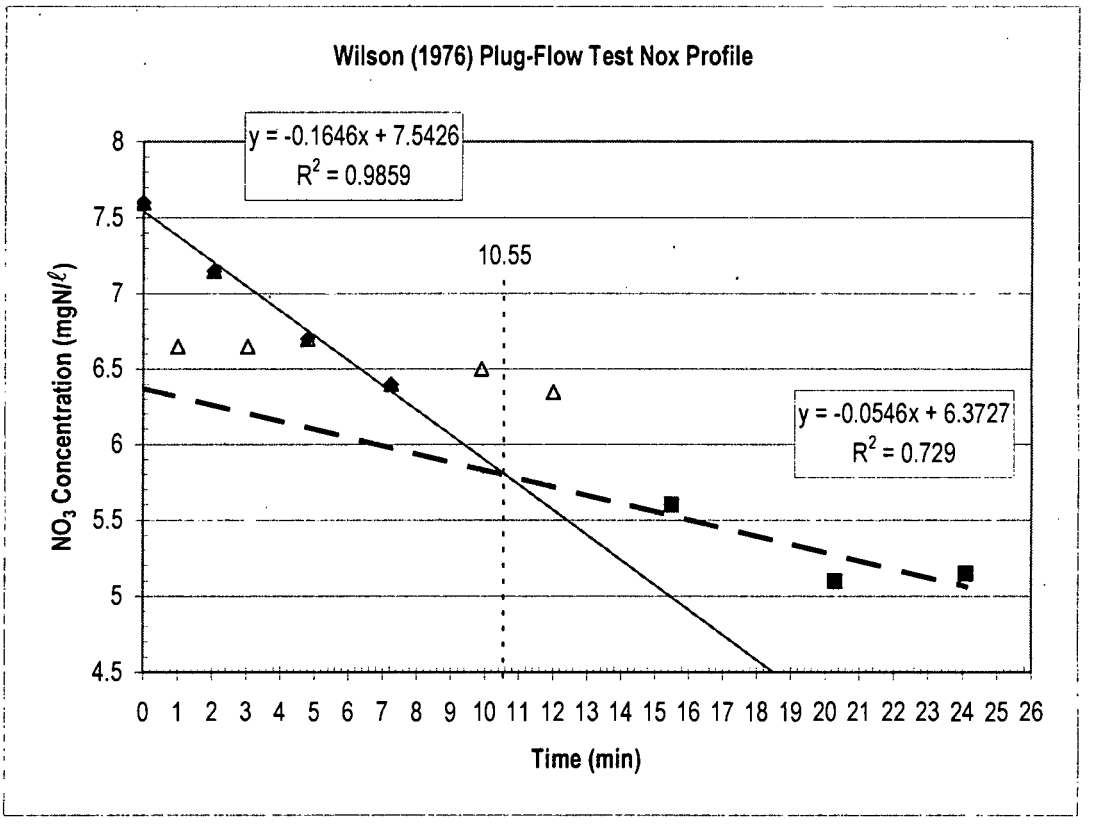

ML	SB	Date	WSS No.
W	W	Jul-76	3

Influent RBCOD Concentration:

Avg f_{ts}	0.086	CFWWTP	S_{ti}	440	mgCOD/ℓ
a-Recycle	5	ratio a:Q_i	$S_{ti;BT}$	6.31	mgCOD/ℓ

Define NU (mgNO$_3$-N/ℓ):

	Y-int
K1	6.1774
K2	4.4326
ΔNO_3	1.74

$Y_{H,NO}$ = **0.209** mgCOD/mgCOD

$Y_{H,NO}$:$Y_{H,AE}$ = **0.312** ($Y_{H,AE}$ = 0.67 COD/COD)

Plot K1 End Time:

End Time	Y (K1 End)
4.7	0.00
4.7	5.50

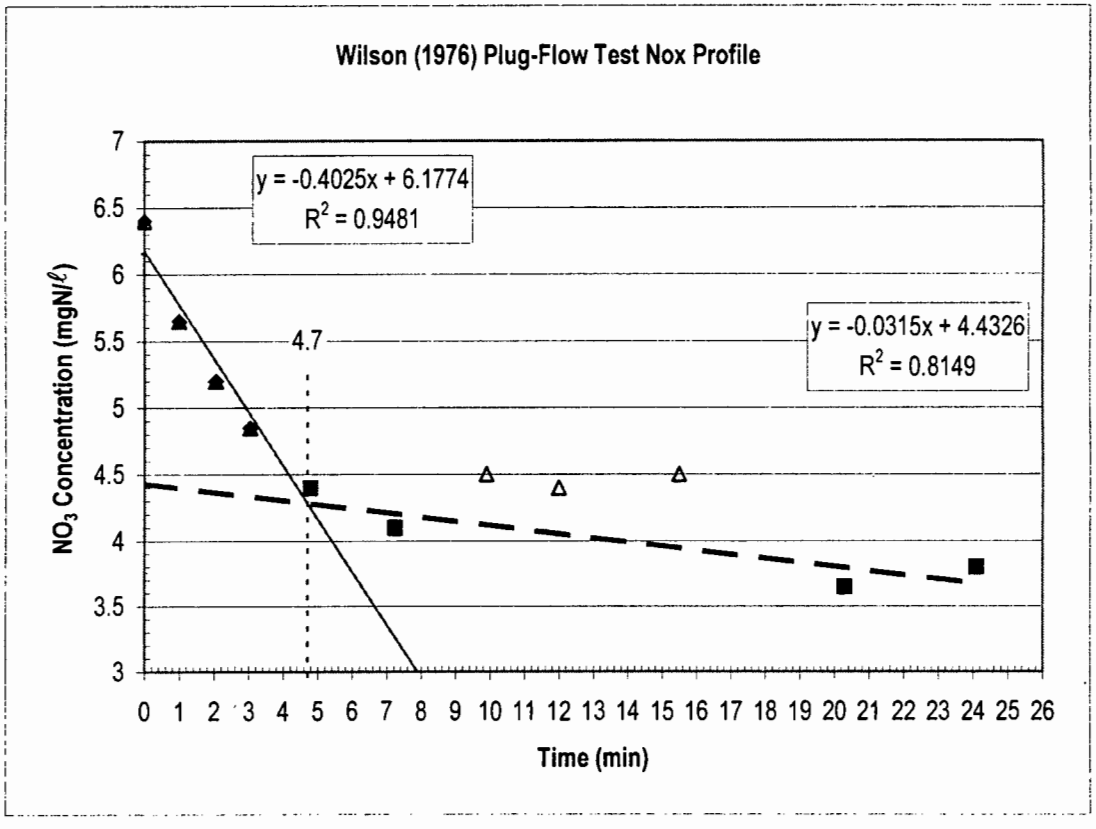

ML	SB	Date	WSS No.
W	W	Jul-76	4

Influent RBCOD Concentration:

Avg f_{ts}	0.086	CFWWTP	S_{ti}	458	mgCOD/ℓ
a-Recycle	5	ratio a:Q_i	$S_{ti,BT}$	6.56	mgCOD/ℓ

Define NU (mgNO$_3$-N/ℓ):

	Y-int
K1	6.5825
K2	4.8736
ΔNO$_3$	1.71

$Y_{H,NO}$ = **0.255** mgCOD/mgCOD

$Y_{H,NO}$:$Y_{H,AE}$ = **0.381** ($Y_{H,AE}$ = 0.67 COD/COD)

Plot K1 End Time:

End Time	Y (K1 End)
4.8	0.00
4.8	5.50

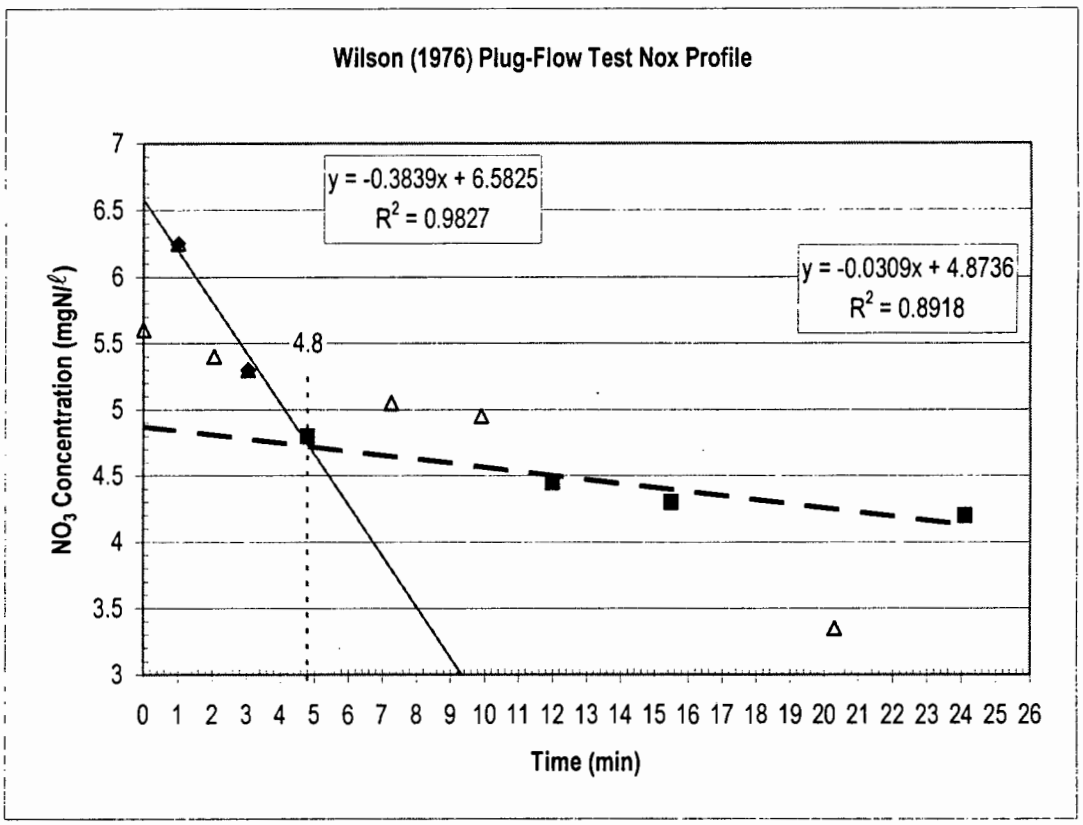

ML	SB	Date	WSS No.
W	W	Jul-76	5

Influent RBCOD Concentration:

Avg f_{ts}	0.086	CFWWTP	S_{ti}	480	mgCOD/ℓ
a-Recycle	5	ratio a:Q_i	$S_{ti,BT}$	6.88	mgCOD/ℓ

Define NU (mgNO$_3$-N/ℓ):

	Y-int			
K1	8.5526			
K2	7.9249	$Y_{H,NO}$ =	**0.739**	mgCOD/mgCOD
ΔNO_3	0.63	$Y_{H,NO}$:$Y_{H,AE}$ =	**1.103**	($Y_{H,AE}$ = 0.67 COD/COD)

Plot K1 End Time:

End Time	Y (K1 End)
3.05	0.00
3.05	8.50

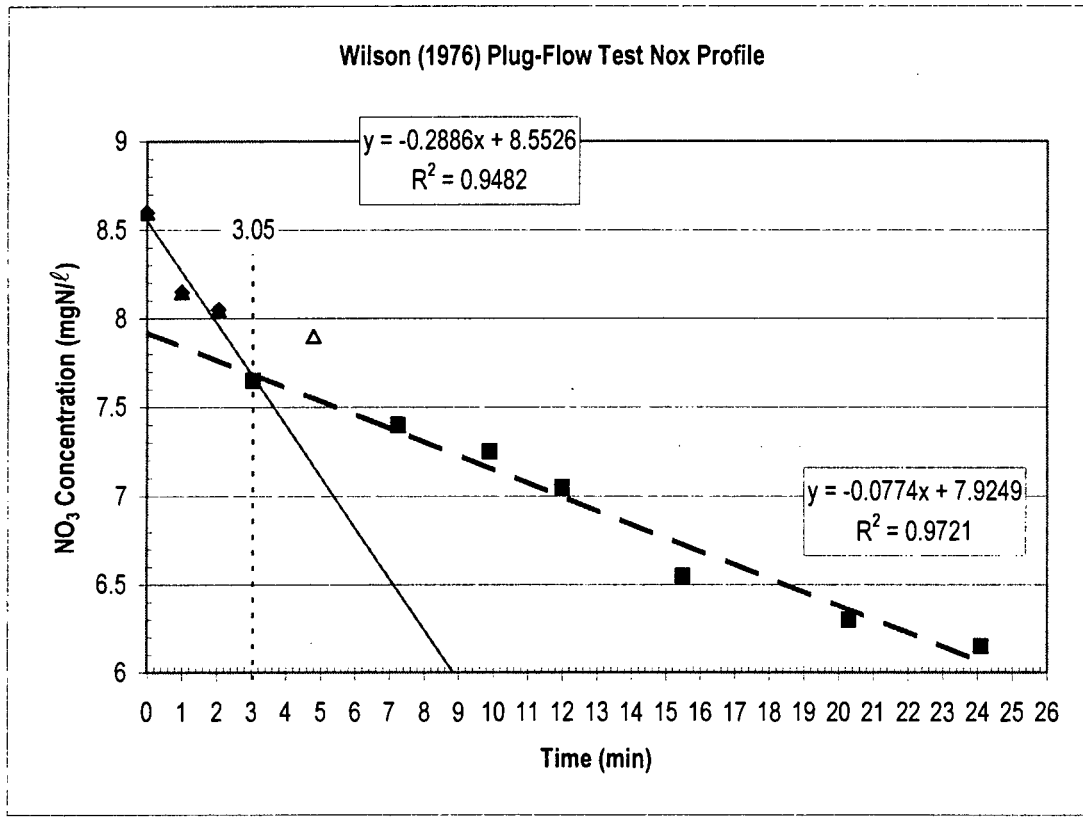

ML	SB	Date	WSS No.
W	W	Jul-76	6

Influent RBCOD Concentration:

Avg f_{ts}	0.086	CFWWTP	S_{ti}	433	mgCOD/ℓ
a-Recycle	5	ratio a:Q_i	$S_{ti,BT}$	6.21	mgCOD/ℓ

Define NU (mgNO$_3$-N/ℓ):

	Y-int			
K1	6.0181			
K2	4.6455	$Y_{H,NO}$ =	**0.367**	mgCOD/mgCOD
ΔNO_3	1.37	$Y_{H,NO}$:$Y_{H,AE}$ =	**0.548**	($Y_{H,AE}$ = 0.67 COD/COD)

Plot K1 End Time:

End Time	Y (K1 End)
9.85	0.00
9.85	5.50

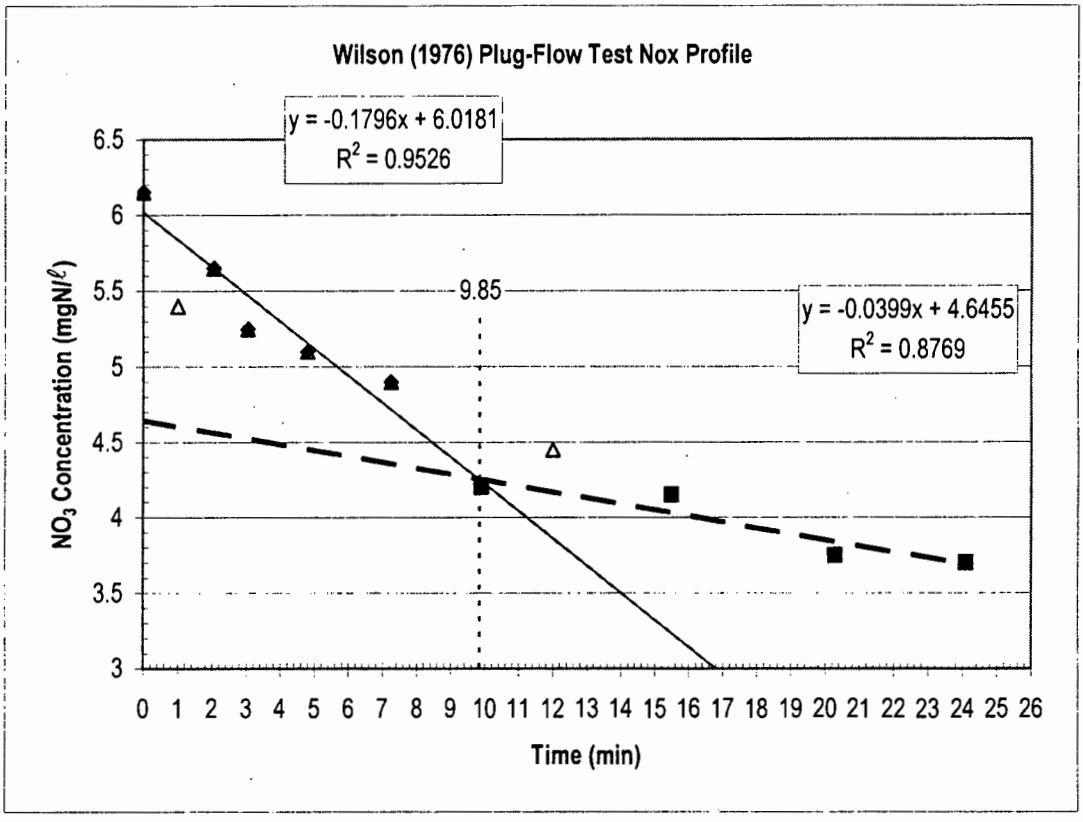

ML	SB	Date	WSS No.
W	W	Jul-76	8

Influent RBCOD Concentration:

Avg f_{ts}	0.086	CFWWTP	S_{ti}	433	mgCOD/ℓ
a-Recycle	5	ratio a:Q_i	$S_{ti,BT}$	6.21	mgCOD/ℓ

Define NU (mgNO_3-N/ℓ):

	Y-int
K1	6.2598
K2	4.9675
ΔNO_3	1.29

$Y_{H,NO}$ = **0.404** mgCOD/mgCOD

$Y_{H,NO}$:$Y_{H,AE}$ = **0.604** ($Y_{H,AE}$ = 0.67 COD/COD)

Plot K1 End Time:

End Time	Y (K1 End)
11.25	0.00
11.25	5.50

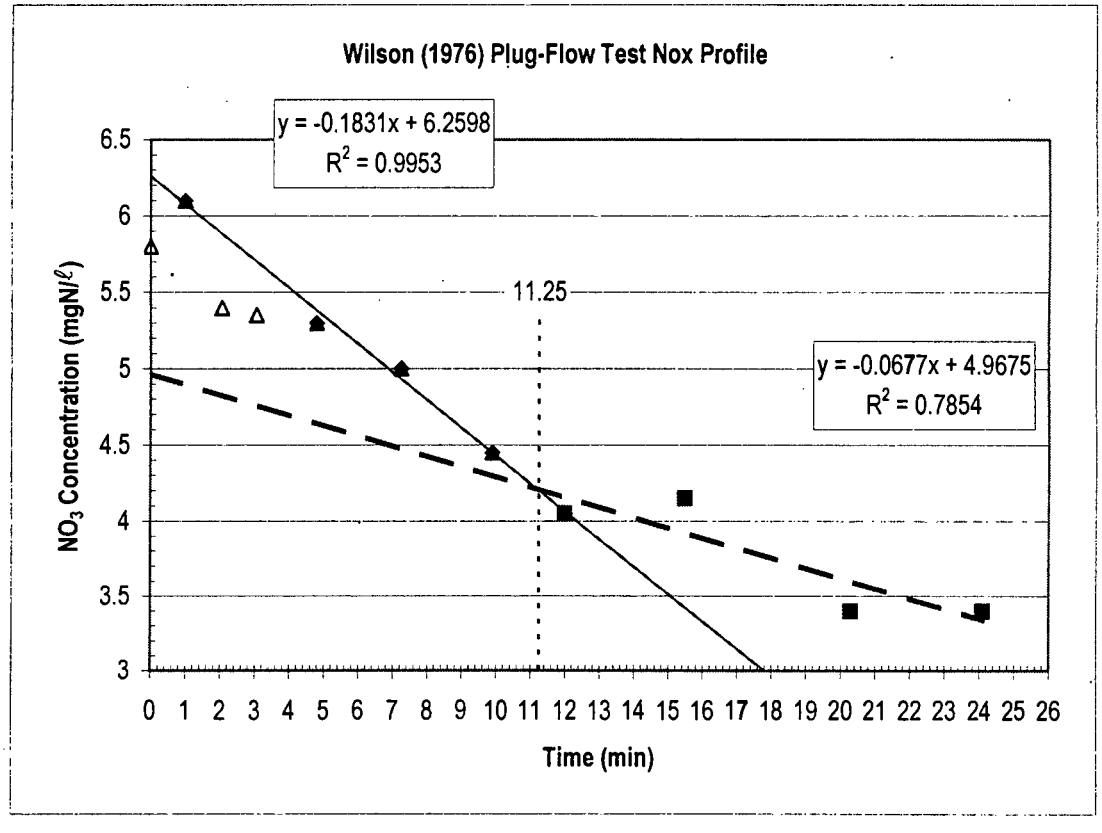

ML	SB	Date	WSS No.
W	W	Jul-76	9

Influent RBCOD Concentration:

Avg f_{ts}	0.086	CFWWTP	S_{ti}	450	mgCOD/ℓ
a-Recycle	5	ratio a:Q_i	$S_{ti,BT}$	6.45	mgCOD/ℓ

Define NU ($mgNO_3$-N/ℓ):

	Y-int
K1	8.5937
K2	7.9878
ΔNO_3	0.61

$Y_{H,NO}$ = **0.731** mgCOD/mgCOD

$Y_{H,NO}$:$Y_{H,AE}$ = **1.092** ($Y_{H,AE}$ = 0.67 COD/COD)

Plot K1 End Time:

End Time	Y (K1 End)
3.25	0.00
3.25	8.50

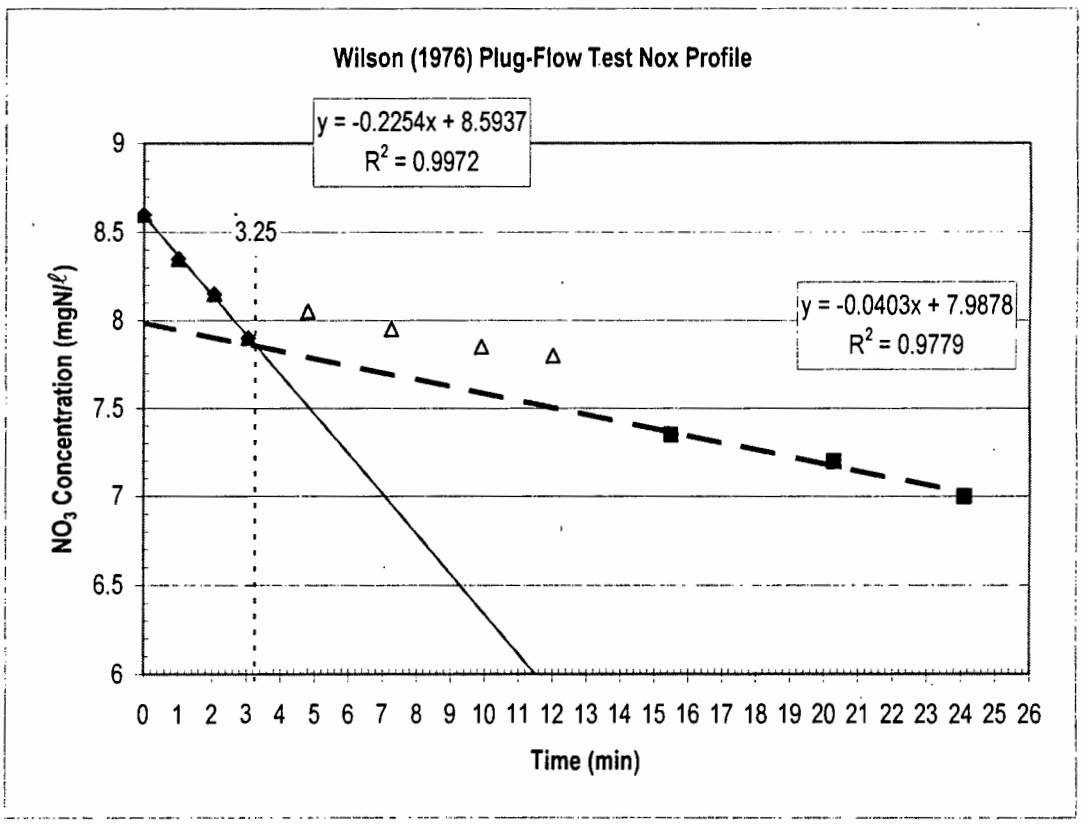

ML	SB	Date	WSS No.
W	W	Jul-76	10

Influent RBCOD Concentration:

Avg f_{ts}	0.086	CFWWTP	S_{ti}	465	mgCOD/ℓ
a-Recycle	5	ratio a:Q_i	$S_{ti,BT}$	6.67	mgCOD/ℓ

Define NU (mgNO$_3$-N/ℓ):

	Y-int
K1	7.173
K2	5.6545
ΔNO_3	1.52

$Y_{H,NO}$ =	**0.348**	mgCOD/mgCOD
$Y_{H,NO}$:$Y_{H,AE}$ =	**0.520**	($Y_{H,AE}$ = 0.67 COD/COD)

Plot K1 End Time:

End Time	Y (K1 End)
2.9	0.00
2.9	8.00

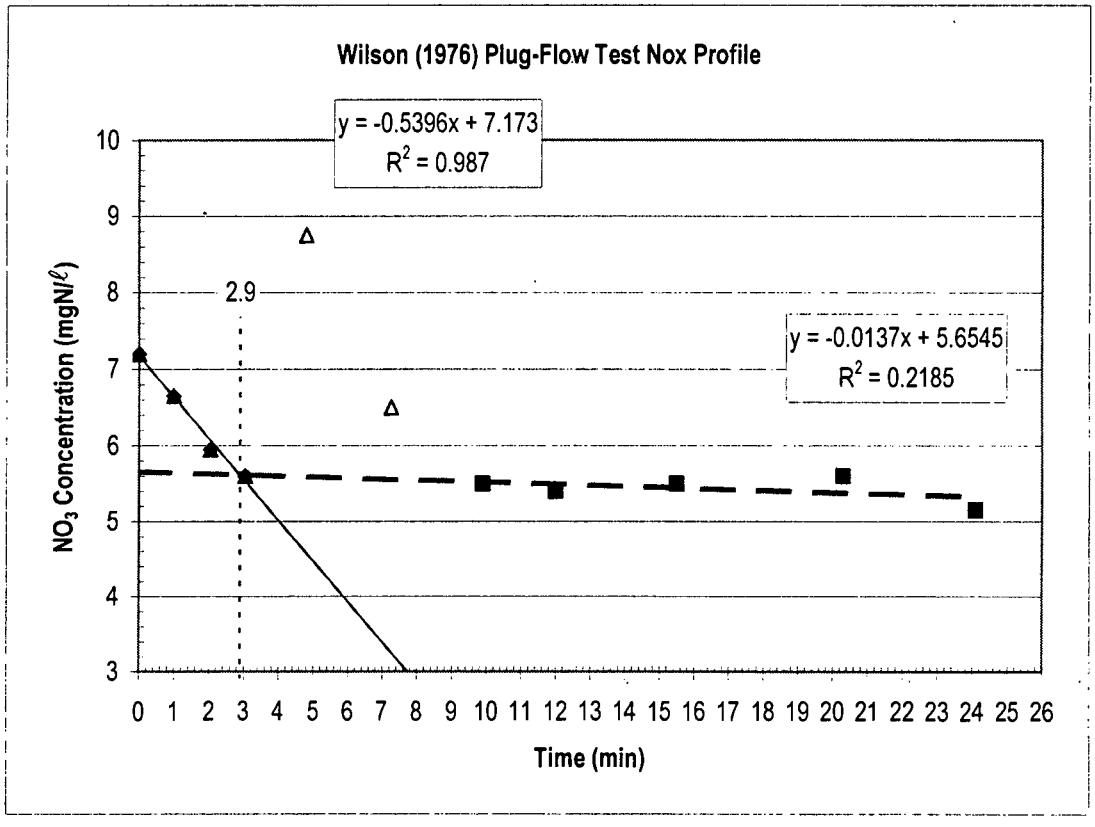

APPENDIX E-2

EXPERIMENTAL DATA BY KETLEY *et al.* (1991)

APPENDIX E-2

EXPERIMENTAL DATA BY KETLEY *et al.* (1991)

The following Tables E2-1 and 2 summarise the test conditions for the corresponding anoxic and aerobic batch tests (respectively) performed by Ketley *et al.* (1991) reassessed in this investigation to derive anoxic yield ($Y_{H,NO}$) estimates. The corresponding nitrate concentration – time curves and oxygen utilization rate (OUR) profiles are presented in Figs. E2-1 and 2 below. Tables E2-1 and 2, and Figs. E2-1 and 2 are reproduced from Tables 3.10 and 3.11, and Figs. 3.16 and 3.18 in Ketley *et al.* (1991), respectively.

Table E2-1. Ketley *et al.* (1991): Batch test conditions for anoxic batch tests ANBT 1 and ANBT 2 performed on day 42 (excerpted from Table 3.10, Ketley *et al.*, 1991); where "ML" = mixed-liquor.

Batch Test Conditions	ANBT 1	ANBT 2
Day	42	42
Parent System ML	ANOX 2	ANOX 3
VSS (mg/ℓ)	1166	1250
AVSS (mg/ℓ)	414	448
Loading Rate (mgCOD/mgVSS)	305	298

Note: The AVSS was calculated accepting an active biomass fraction of f_{av} = 0.40 mgAVSS/mgVSS determined from the steady-state theory (WRC, 1984) applied to the experimental data obtained in the investigation.

Table E2-1. Ketley *et al.* (1991): Batch test conditions for aerobic batch tests ABT 1 and ABT 2 performed on day 42 (excerpted from Table 3.11, Ketley *et al.*, 1991); "ML" = mixed-liquor.

Batch Test Conditions	ABT 2	ABT 3
Day	42	42
Parent System ML	ANOX 2	ANOX 3
VSS (mg/ℓ)	1166	1250
AVSS (mg/ℓ)	414	448
Loading Rate (mgCOD/mgVSS)	413	360

Note: The AVSS was calculated accepting an active biomass fraction of f_{av} = 0.40 mgAVSS/mgVSS determined from the steady-state theory (WRC, 1984) applied to the experimental data obtained in the investigation.

Fig. E2-1a,b. Ketley *et al.* (1991): Nitrate concentration – time curves measured during anoxic batch tests (a) ANBT 1 and (b) ANBT 2 performed on day 42 (reproduced from Fig. 3.16, Ketley *et al.*, 1991).

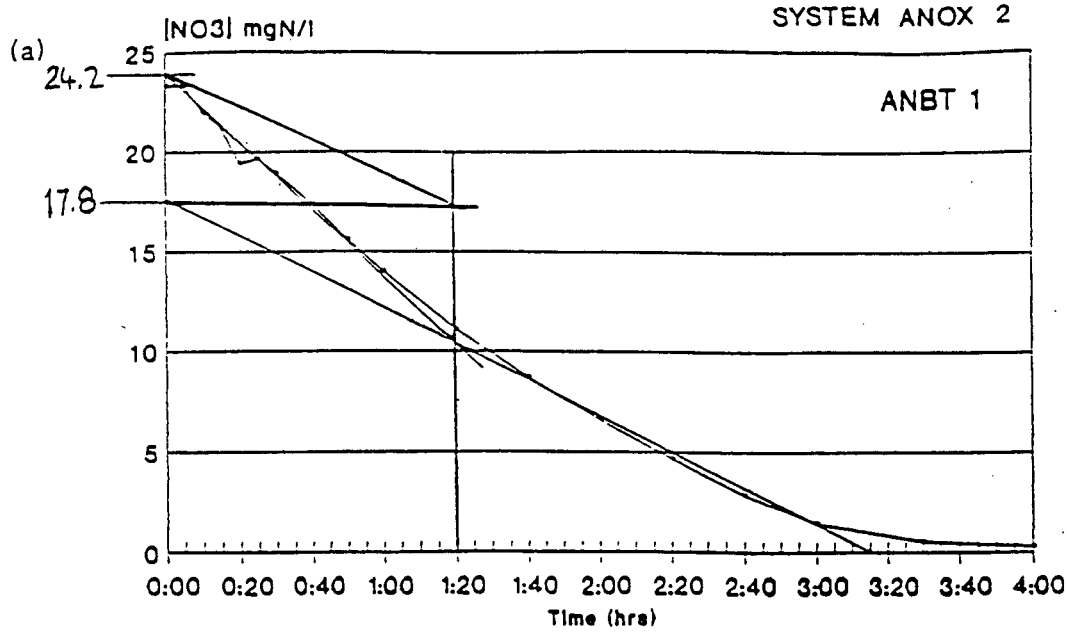

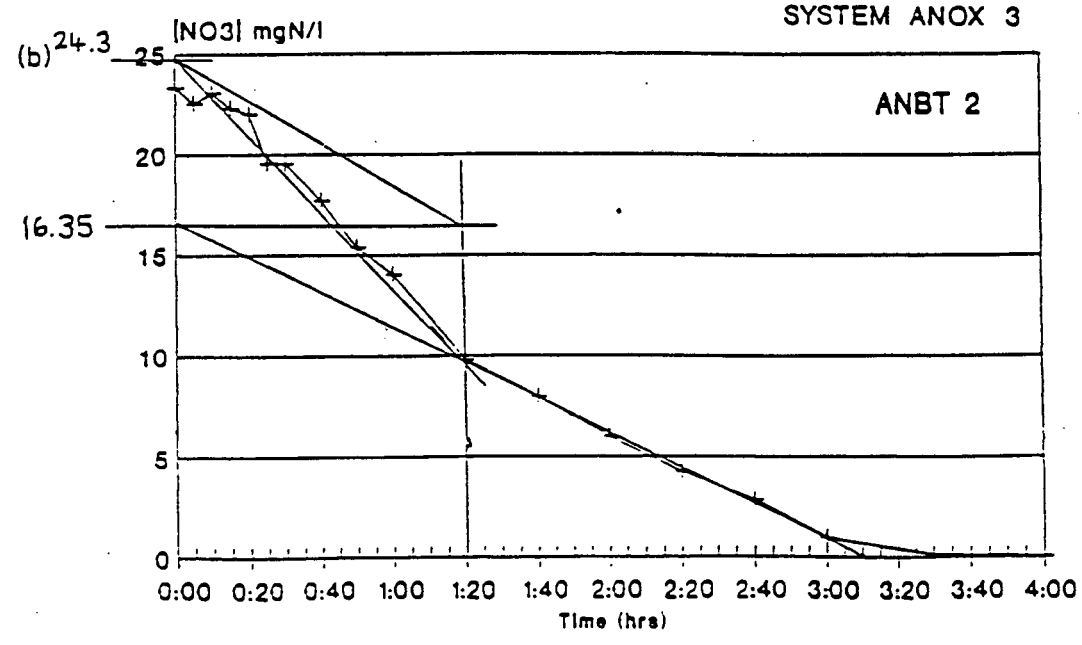

Fig. E2-2a,b. Ketley *et al.* (1991): OUR profiles measured during aerobic batch tests (a) ABT 2 and (b) ABT 3 performed on day 42 (reproduced from Fig. 3.18, Ketley *et al.*, 1991).

3.52

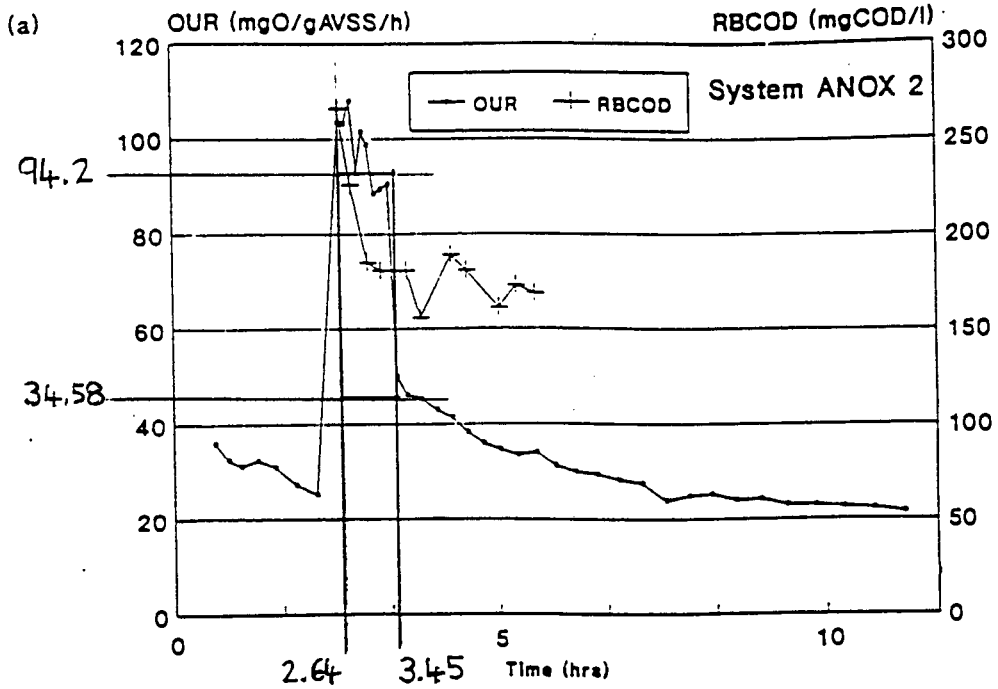

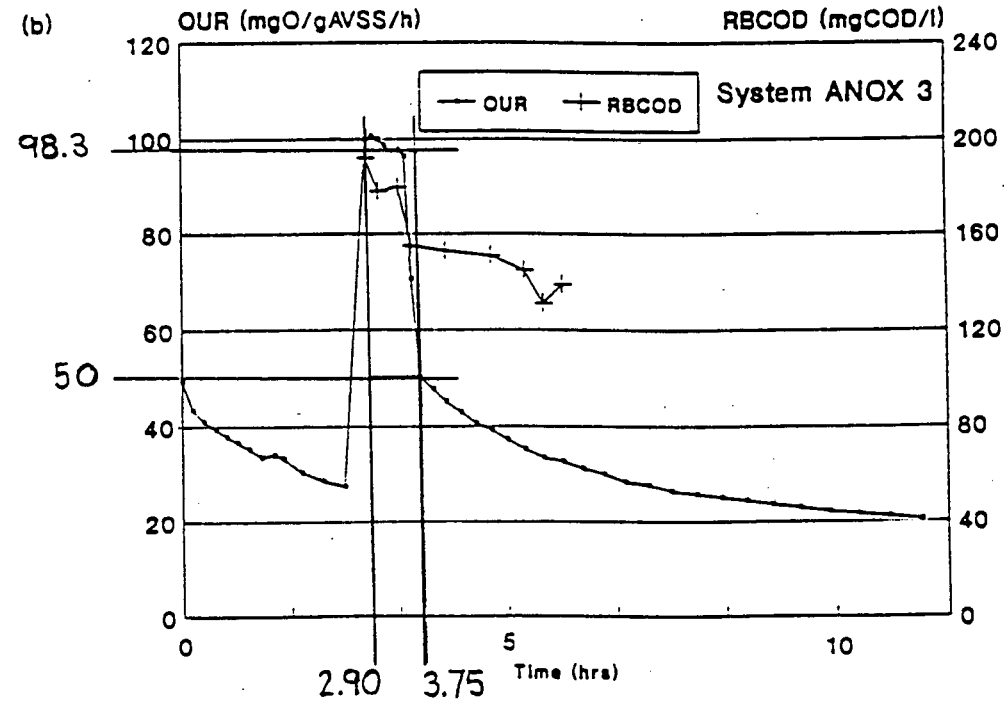

APPENDIX E-3

EXPERIMENTAL DATA BY EKAMA *et al.* (1996)

F- AND t-TEST ANALYSES FOR TWO APPARENT DATA SETS IN $Y_{H,NO}$ wrt $Y_{H,AE}$ = 0.67 COD/COD FOR EKAMA *et al.* (1996).

Un-sorted data:	
OU-NU	$Y_{H,NO}$
1-1	0.589
1-2	0.434
1-3	0.563
2-1	0.595
2-2	0.443
2-3	0.570
3-1	0.610
3-1	0.463
3-3	0.585
4-1	0.481
4-3	0.449
5-1	0.638
5-2	0.502
5-3	0.615
Avg	0.538
Stdev	0.072638
Upper	0.680762
Lower	0.396023
Count	14

Sorted data	
OU-NU	$Y_{H,NO}$
1-2	*0.434*
2-2	*0.443*
4-3	*0.449*
3-1	*0.463*
4-1	*0.481*
5-2	*0.502*
1-3	0.563
2-3	0.570
3-3	0.585
1-1	0.589
2-1	0.595
3-1	0.610
5-3	0.615
5-1	0.638
Avg	0.538
Stdev	0.072638
Upper	0.680762
Lower	0.396023
Count	14

Data Set 1	
OU-NU	$Y_{H,NO}$
1-2	*0.434*
2-2	*0.443*
4-3	*0.449*
3-1	*0.463*
4-1	*0.481*
5-2	*0.502*
SSD1	0.025571
count1	6
deg f1	5
Mean1	0.462

Data Set 2	
OU-NU	$Y_{H,NO}$
1-3	0.563
2-3	0.570
3-3	0.585
1-1	0.589
2-1	0.595
3-1	0.610
5-3	0.615
5-1	0.638
SSD2	0.0246858
count2	8
def f2	7
Mean2	0.596

F-test to check if two sample sets have same variances:

degf-numerator 5
degf-denominator 7
Ftable(2.5%) 6.85 Enter Table value here:
Fobs 1.0730029

Accept F-test Ho!
i.e. Fobs < Ftable => var1 = var2 => can pool SSD's,
=> normal t-Test OK.

Normal t-Test to check if two sample sets have the same mean:

pooled var. = 0.0290726
pooled SSD = 0.1705068
pooled degf ("n") = 10.00
t-table(n, 2.5%) = **2.228** Enter Table value here:
tobs = -1.4491771

Accept t-Test Ho! -t-table< tobs< +t-table
=> Mean1 = Mean2 OK => Same Data Population!

Table E3-1. Oxygen and nitrate utilization data from Ekama et al. (1996)

Aerobic Profile	OU (mgO/ℓ)	Anoxic Profile	NU (mgN/ℓ)
1	36.7	1	16
2	37.3	2	22
3	38.7	3	17
4	29.1		
5	41.7		

APPENDIX F

CONSTRUCTION AND INTERPRETATION OF STATISTICAL PLOTS FOR DATA ANALYSIS

TABLE OF CONTENTS

APPENDIX F

CONSTRUCTION AND INTERPRETATION OF STATISTICAL PLOTS

F.1 INTRODUCTION

Data from different tests could not be compared directly on a daily basis because of the variability in results from all the tests, due to variations in multitude of factors that influence the data. Therefore a graphical approach was used to evaluate the data (Velz, 1950), to interpret the trends and compare the results between two test methods.

For a particular batch of wastewater, the data obtained from the different test methods were statistically analysed using a graphical procedure, to determine the mean, sample standard deviation, and standard deviation of the mean for the data set. This information then could be used to evaluate whether the difference between the means from two data sets is statistically significant at a selected confidence level, or not.

F.2 CONSTRUCTION OF STATISTICAL PLOT

The experimental data is plotted using the procedure below:

- Arrange the data (n in number) in order of ascending magnitude.
- Assign a serial number "m" to each of the values (1, 2, 3, 4 .....n)
- Compute the y-axis plotting the position of each serial value, as the probability equal to or less than from the expression [m/(n + 1)]. The x-axis plotting position is the actual value for the data.
- The probability curve is linearized and plotted; for this investigation the transformed rank probability method (Scientific Tables, 1975) was used to linearize the probability curve, see Fig. F1. Alternatively, probability paper can be used on which the y-axis has been linearized.

F.3 INTERPRETATION OF THE STATISTICAL PLOT

The data plotted can give an indication of whether the data is normally distributed or not:

- If a straight line can be fitted to the plot it indicates that the data have a normal distribution.
- If a straight line cannot be fitted to the plot, the data are not normally distributed.

If the data are normally distributed it indicates that a multitude of factors have each had an independent small influence on the measurements; if the data are not normally distributed it indicates that one factor has had a dominating influence.

From the above, provided a straight line can be fitted to the distribution (i.e. the data are normally distributed), it is possible to determine graphically (refer to Fig. F1):

- The mean of the data plotted – this is determined as the x-value where the straight line of the distribution intercepts a vertical line extended from y = 5.

- The standard deviation of the sample, which provides a measure of the variation of the data – this is the difference between the mean (i.e. the x-value that gives y = 5) and the x-value that gives y = 4 (or y = 6).

F.4 TEST FOR STATISTICAL SIGNIFICANCE OF THE DIFFERENCES BETWEEN TWO MEAN VALUES

Visual comparison of two data (or data sets) is a common method of appraisal, to determine whether they differ. However, observed differences or similarities may not be significant as these may arise solely by chance. Statistics defines the expected variations due to chance, to determine whether the observed differences between two data have arisen by chance alone or are significant. In the graphical method, by plotting of two or more series of data on the same probability plot, a quick visual appraisal of similarities and differences can be obtained. To test whether the visual differences in the two series of data are statistically significant, a mathematical significant test is done as follows:

- Plot the two or more distributions to test for normality as described above.

- If normal, obtain the mean (m) and the sample standard deviation (σ) of each series.

- Compute standard deviation of each mean:
  SD(mean) = $(\sigma/\sqrt{n})$
  where n = number of data points.

- Compute the standard deviation of the difference between the two means:
  SD(difference) = $\sqrt{\{(\text{SD mean1})^2 = (\text{SD mean2})^2\}}$

- Compute the absolute value (i.e. positive) of the difference between the two means:
  mean(difference) = $|\text{mean1} - \text{mean2}|$

- Decide upon a confidence level for the test for significance, 95% certainty or 99% or any other level desired.

- Apply the test for statistical significance of the difference.

For example, if 95% is selected as the confidence level, subtract from the difference between the two means [SD(difference)], i.e. [mean(difference) – 2 • SD(difference)] - if positive number is obtained it can be concluded that the difference between the two means is statistically significant at the selected level of confidence; if a negative value is obtained, then the difference between the two means was by chance alone, and it can be concluded that the apparent difference between the two means is **NOT** statistically significant.

F.5 ILLUSTRATION BY AN EXAMPLE

An example plot is given in Fig. F-1.

The mean of a set of values from an experiment is read off from the statistical graph as the value of x that gives y = 5, in this case:

from the graph the mean = 0.534 mgCOD/mgCOD

The standard deviation of a set of values is calculated from the difference between the x-value that gives y = 5 and the x-value that gives y = 4 (OR, from the difference between the x-value that gives y = 5 and the x-value that gives y = 4), as shown in Fig. F-1; from the graph:

the x-value at y = 4 = 0.493 mgCOD/mgCOD
$\therefore$ the standard deviation (σ) = 0.534 – 0.493 = 0.041 mgCOD/mgCOD

The standard deviation of the mean is the standard deviation divided by the square root of the number of values in the data set. In this case:-

number data in set (n) = 18
$\therefore$ SD mean = $0.041/\sqrt{(18)}$ = 0.0096 mgCOD/mgCOD

Say a second set of 10 data is analyzed as above to give:

mean = 0.519 mgCOD/mgCOD
and standard deviation (σ) = 0.039 mgCOD/mgCOD

Standard deviation of the mean is calculated:

SD mean = $0.039/\sqrt{(10)}$ = 0.01233 mgCOD/mgCOD

Now, comparing the data from the two sets:

SD(difference) = $\sqrt{\{0.041^2 + 0.039^2\}}$
= 0.000245 mgCOD/mgCOD

mean(difference) = $|0.534 - 0.519|$ = 0.015 mgCOD/mgCOD

Selecting a 95% confidence interval:

Test = mean(difference) – 2 • SD(difference)
= 0.015 – 2 • 0.000245
= **0.0145**

Since the resultant value is positive, it can be concluded that the two means are significantly different at the 95% confidence interval.

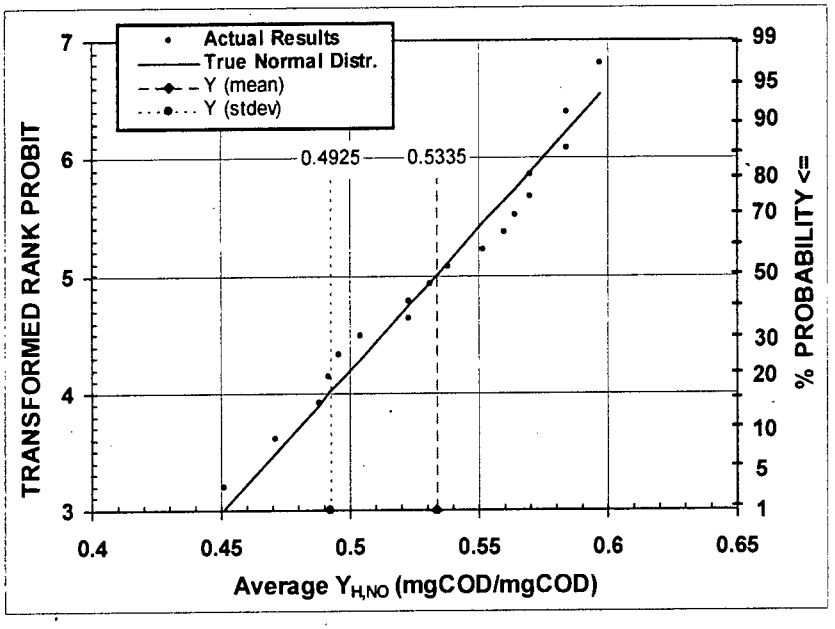

Fig. F-1: Example of a linearized probability graph (after Fig. 5.8, Chapter 5: Statistical plot of all $Y_{H,NO}$ estimates corresponding to $Y_{H,AE}$ = 0.67 mgCOD/mgCOD determined in Period I).